ICAMS 2018

Under the Patronage of the Ministry of Research and Innovation

ADVANCED MATERIALS
AND SYSTEMS

Proceedings of the 7th International Conference

October 18th - 20th, 2018

Bucharest, ROMANIA

Luminiţa ALBU
Viorica DESELNICU

EDITORS

THE 7th INTERNATIONAL CONFERENCE ON ADVANCED MATERIALS AND SYSTEMS

Bucharest, ROMANIA
October 18th-20th, 2018

Disclaimer

This book contains full papers approved by the Scientific Committee. Authors are responsible for the content and accuracy. Opinions expressed may not necessarily reflect the position of the International Scientific Committee of ICAMS. Information in the ICAMS 2018 Conference Proceedings is subject to change without notice. No part of this book may be reproduced or transmitted in any form or by any means, electronic or mechanical, for any purpose, without the express written permission of the International Scientific Committee of ICAMS.

CONFERENCE COMMITTEE

Luminita ALBU, INCDTP-ICPI, RO
Carmen GHITULEASA, INCDTP, RO
Alina POPESCU, INCDTP, RO
Lucretia MIU, INCDTP-ICPI, RO
Viorica DESELNICU, INCDTP-ICPI, RO
Laurentia ALEXANDRESCU, INCDTP-ICPI, RO
Behzat Oral BITLISLI, Ege University, Bornova, TR
Aura MIHAI, "Gheorghe Asachi" Technical Univ. of Iasi, RO
Dmitriy SHALBUEV, East Siberia State Univ. of Techn.&Manag., RU
Huseyin ATA KARAVANA, Ege University, Bornova, TR
Stelian MAIER, "Gheorghe Asachi" Technical Univ. of Iasi, RO
Viacheslav BARSUKOV, Kiev Nat. Univ. of Techn&Design, UA
Nizami DURAN, Mustafa Kemal University, Antakya, TR
Dimosthenis PAPAKONSTANTINOU, CRE.THI.DEV, GR
Ana-Maria VASILESCU, INCDTP-ICPI, RO
Gheorghe COARA, INCDTP-ICPI, RO
Carmen GAIDAU, INCDTP-ICPI, RO
Boguslaw WOZNIAK, Institute of Leather Industry, PL
Edyta GRZESIAK, Institute of Leather Industry, PL
Margareta FLORESCU, Bucharest Academy of Economic Studies, RO
Madalina Georgiana ALBU KAYA, INCDTP-ICPI, RO
Mihaela GHICA, "Carol Davila" Univ. of Medicine&Pharmacy, RO
Gustavo GONZALEZ-QUIJANO, Secretary General, COTANCE, BE
Gurbuz GULUMSER, Ege University, Bornova, TR
Altan AFSAR, Ege University, Bornova, TR
Bahri BASARAN, Ege University, Bornova, TR
Arife Candas ADIGUZEL ZENGIN, Ege University, Bornova, TR

Alpaslan KAYA, Mustafa Kemal University, Antakya, TR
Minodora LECA, University of Bucharest, RO
Alcino MARTINHO, CTIC, PT
Carmen ARIAS CASTELLANO, General Secretary, CEC, BE
Keyong TANG, Zhengzhou University, CN
Aurelia MEGHEA, "Politehnica" University Bucharest, RO
Elena BADEA, University of Craiova and INCDTP-ICPI, RO
Mehmet METE MUTLU, Ege University, Bornova, TR
Wuyong CHEN, Sichuan University, CN
Georgios PANAGIARIS, Technological Education Institute, GR
Victoriya PLAVAN, Kiev Nat. Univ. of Techn&Design, UA
Irina TITORENCU, "N. Simionescu" I.C.B.P., RO
Gabriel ZAINESCU, INCDTP-ICPI, RO
Ding ZHIWEN, CLFIR Institute, CN
Dana DESELNICU, "Politehnica" University Bucharest, RO
Gheorghe MILITARU, "Politehnica" University Bucharest, RO
Anca PURCAREA, "Politehnica" University Bucharest, RO

ORGANIZING COMMITTEE

Dr. Luminita Albu, Chair, Director INCDTP - Leather and Footwear Research Institute Division (ICPI), RO
Dr. Carmen Ghituleasa, Co-Chair, General Director**,** National Research and Development Institute for Textile and Leather, RO
Dr. Lucretia Miu, Co-Chair, Scientific Secretary, INCDTP - Leather and Footwear Research Institute Division, RO
Dr. Viorica Deselnicu, INCDTP-ICPI, RO
Ioana Pivniceru, INCDTP-ICPI, RO
Dana Gurau, INCDTP-ICPI, RO
Dr. Bogdan Hanchevici, INCDTP-ICPI, RO
Dr. Ciprian Chelaru, INCDTP-ICPI, RO

UNDER THE PATRONAGE OF:

MINISTERUL CERCETĂRII ȘI INOVĂRII

MINISTRY OF RESEARCH AND INNOVATION

ORGANIZED BY:

NATIONAL RESEARCH & DEVELOPMENT INSTITUTE FOR
TEXTILE AND LEATHER (INCDTP), BUCHAREST, ROMANIA

DIVISION LEATHER & FOOTWEAR RESEARCH INSTITUTE
(ICPI) BUCHAREST, ROMANIA

PARTNERS

EAST SIBERIA STATE
UNIVERSITY OF
TECHNOLOGY &
MANAGEMENT, ULAN-
UDE, RUSSIA

LEATHER ENGINEERING
DEPARTMENT
EGE UNIVERSITY, TURKEY

MUSTAFA KEMAL
UNIVERSITY, ANTAKYA-
HATAY, TURKEY

CHINA LEATHER &
FOOTWEAR RESEARCH
INSTITUTE, CHINA

"POLITEHNICA"
UNIVERSITY
BUCHAREST, ROMANIA

"GH. ASACHI" TECHNICAL
UNIVERSITY OF IASI,
ROMANIA

BUCHAREST ACADEMY
OF ECONOMIC STUDIES,
ROMANIA

"ITA TEXCONF " ROMANIAN
ENTITY WITHIN INNOVATION
& LEATHER TECHNOLOGICAL
TRANSFER

CONFEDERATION OF NATIONAL
ASSOCIATIONS OF TANNERS AND
DRESSERS OF THE EUROPEAN
COMMUNITY

SFERA FACTOR
THE ROMANIAN LEATHER
MANUFACTURERS
ORGANIZATION

ROMANIAN LEATHER & FUR
PRODUCERS ASSOCIATION

FOREWORD

ICAMS 2018 is offering the framework for presenting the latest results in research, focusing on the field of Materials Science and Innovative Technologies, which records an impressive dynamics and is recognized as a current national and European priority.

The conference provides the opportunity for exchanging ideas and experience with researchers, scientists and experts at international level, and for developing new scientific contributions.

The ICAMS 2018 international event, organised by the National Institute for Research and Development for Textiles and Leather - Division Leather and Footwear Institute (INCDTP-ICPI) under the patronage of the Romanian Ministry for Research and Innovation (MCI), took place in Bucharest on 18-20 October 2018. ICAMS 2018 brought together different stakeholders and provided a platform for a better understanding of the European innovation ecosystem while raising awareness of the actions needed to enable synergies and drawing lessons for future actions.

The 7th edition of ICAMS marked 100 Years from the Great Union through a special session to celebrate and promote Romanian heritage and cultural identity by presenting papers on the protection and conservation of the national heritage of leather and parchment objects.

Around 130 participants joined the event from several academic and research institutions, public and private sectors, as well as Managing Authorities. Participants presented their experience on research, innovation, policies and the creation of synergies. All these inputs offered insightful elements for discussion in the different participatory sessions throughout the event.

The conference topics include, but are not limited to:

1. **Advanced Functional Materials & Biomaterials**
2. **Nanotechnology and Nanomaterials**
3. **Emerging Techniques**
4. **Smart Materials**
5. **Materials Engineering and Performance**
6. **Materials Processing and Product Manufacturing**
7. **Modelling and Simulation**
8. **Materials Characterization**
9. **Non-destructive Testing**
10. **Advanced Materials & Systems Innovation**
11. **Towards a Circular Economy**

We would like to thank all the participants, the International Scientific Committee and all the sponsors that made this scientific event possible. ICAMS Conference has already become a tradition, contributing to the advancement of Materials Science in academic, social and business environments worldwide.

EDITORS,

Dr. Luminița Albu
Director, INCDTP – Division: Leather and Footwear Research Institute (ICPI), RO

Dr. Viorica Deselnicu
INCDTP – Division: Leather and Footwear Research Institute (ICPI), RO

CONTENTS

I. ADVANCED FUNCTIONAL MATERIALS & BIOMATERIALS

II. NANOTECHNOLOGY AND NANOMATERIALS

III. EMERGING TECHNIQUES

IV. SMART MATERIALS

V. MATERIALS ENGINEERING AND PERFORMANCE

VI. MATERIALS PROCESSING AND PRODUCT MANUFACTURING

xvi

IX. NON-DESTRUCTIVE TESTING

X. ADVANCED MATERIALS & SYSTEMS INNOVATION

SPECIAL SESSION. TOWARDS A CIRCULAR ECONOMY

I.

ADVANCED FUNCTIONAL MATERIALS & BIOMATERIALS

ANTIBACTERIAL POLYMERIC NANOCOMPOSITES WITH MATRIX OF PET AND TIO$_2$ FUNCTIONALIZED NANOPARTICLES WITH APPLICATION IN MEDICAL AND FOOD INDUSTRY

LAURENŢIA ALEXANDRESCU, MARIA SÖNMEZ, MIHAI GEORGESCU,
DANIELA STELESCU, DANA GURĂU

INCDTP - Division: Leather and Footwear Research Institute, 93 Ion Minulescu St., 031215, sector 3, Bucharest, Romania, laurentia.alexandrescu@icpi.ro, laura_alexandrescu@yahoo.com

Thermoplastic polyesters represent an important class of polymers used in a variety of products and applications, one of which is poly (ethylene terephthalate) (PET). Currently, PET is the most cost-effective polyester. PET can be processed in a variety of domestic and industrial shapes and products by melt processing techniques such as spinning, extrusion, injection, blowing, thermoforming. Polymer composite materials are systems consisting of one or more discontinuous phases dispersed in a continuous phase. In this paper, elastomeric nanocompound materials were selected, due to performance properties such as: antimicrobial, resistance to aggressive chemical agents, mechanical properties, especially hardness which, depending on the degree of plastification, can present values from very low to high 30 -100°Sh D, thermal, impermeability, resilience, low density, elasticity, thermostability, processability, impact resistance etc. The new compounds produced by a simple and efficient technology for obtaining polyethylene terephthalate (PET) composite, TiO$_2$ functionalized nanoparticles, provide flexibility in adapting superficial chemistry and molecular structure to the polymer / nanoparticle interface. These nanomorphic molecules form the "molecular bridges" between individually dispersed compounding agents and the continuous phase polymer matrix resulting in a maximized performance of the composite material by optimized interface compatibility and bonding.

Keywords: nanocomposites; functionalized nanoparticles; antibacterial.

INTRODUCTION

Thermoplastic polyesters represent an important class of polymers used in a variety of products and applications, one of which is poly (ethylene terephthalate) (PET). Currently, PET is the most cost-effective polyester and used of about 95 % of the total consumption worldwide, the approximately 25 million tons per year (Fakirov, 2002; Johnson, 2005; Bartolome, 2012). PET has applications in various fields: fiber for clothing, bottles and jars for packaging, the textile component in the tires, safety belts, bags, technical, including non-woven textile, audio/video tapes, medical objects, etc. One of the main reasons for the widespread use of PET is the possibility of obtaining in a single polymerization plant several types of products with a different degree of polymerization. PET can be processed in a variety of domestic and industrial forms and products by melt processing techniques such as filler, extrusion, injection, blowing, thermoforming (Chand, 2008; Tsai, 2013). The polyethylene terephthalate (PET) was used more than 50 years in medical and food devices. Current PET applications include implanted sutures, surgical meshes, vascular grafts, sleeves for heart valves, and percutaneous components for access devices, bottles, food packaging boxes, disposable glasses, and so on. The notable characteristics of PET are bioscience, promoting tissue ingestion, a well-characterized biotic response, and a long history of human implantation (Tayel, 2011; Mekonnen, 2013).

Polymeric composite materials are systems that consist of one or several discontinued phases, dispersed in a continuous phase. Thus, at least two different materials, which are completely immiscible, are mixed to form a composite. Additionally, additives such as compatibilizers, plasticizers, pigments, temperature

stabilizers and UV radiation, nanoparticles are additionally added to improve certain properties. The type and geometry of the discontinuous phase of the composite gives enhanced properties, such as high specific strength, stiffness and hardness, antimicrobial, etc. (Deng, 2012).

There are different types of nanoparticles which may be incorporated in the polymeric matrix, selected according to their properties and their application. ZnO found various applications in everyday life, such as the rubber and plastic industry, medical packaging, cosmetics, medical devices (Saehana *et al*., 2013), dentistry, and orthopedics, antibacterial coating (Arenas *et al*., 2013), the textile industry (Bazant *et al*., 2014; Alexandrescu *et al*., 2017), etc. Antibacterial activity has been proven on various bacterial strains (*Staphylococcus aureus, Staphylococcus epidermidis, E. coli, Listeria monocytogenes, Bacillus subtilis, Pseudomonas fluorescens, Pseudomonas aeruginosa, Salmonella enteritidis, Salmonella typhimurium* etc.) (Stegarus and Lengyel, 2017). The particles normally have a higher surface / volume ratio, which ensures more efficient antibacterial activity. Its role is particularly important in terms of antimicrobial and UV protection. The properties of composite materials depend on the compatibility method. For this purpose, the external surface of the nanoparticles can be functionalized with different agents, the most common functionalizing agents being organo-functional siloxanes or sodium oleate. Functioning agents are used to improve adhesion between the polymer matrix and nanoparticles, protect surfaces against internal stresses that can cause cracks, stabilize the interface layer, improve wetting and increase hydrophobicity.

EXPERIMENTAL

Materials

All composites contain the same components: polyethylene terephtate recycled Green Tech company in Buzau, with the following characteristics: Melt Flow Index (260°C/10 kg), and 44,4 g/10 min; melt temperature-Vicat, 201°C and density-1,33 g/cm3 and EPDM - Ethylene-Propylene Diene-Monomer, was purchased from Du Pont - NORDEL IP-3745 P, with the following characteristics: ethylene content - 70%, polypropylene content -30% and density-0,88 g/cm³. Other components: TiO₂, white powder, with particle size of 21 Nm, molecular mass - 79,87 g/mol, the specific area 23 m²/g, density – 4.26 g/ml and concentration - 99.5%, functionalized with PDMS, polydimethylsiloxane, produced by Sigma-Aldrich, plasticizer - dipropyl heptyl phthalate produced by Bayer, stabilizer - calcium stearate, antioxidant - Irganox 1010, the last two components from the company Ciba Geigy.

Method

PET, TiO₂ functionalized with PDMS, plasticizer - dipropyl heptyl phthalate, calcium stearate, EPDM and antioxidant -Irganox 1010 were mechanically mixed in a Brabender Plasti-Corder PLE-360 at 30-100 rotations/min, for 3 min. at 230°C to melt the plastomer, mixed for 5 min. at 248°C and 2 min. at 210°C for homogenisation. The total processing time was 10 minutes. Table 1 shows tested formulations. Continue mixing at a speed of 100-110 revolutions per minute and 248°C for 3 minutes until the ingredients are embedded and the mixture is uniform. Remove the composition from the

mixer and press into specimen molds for physico-mechanical, chemical and microbiological characterizations.

Table 1. Polymeric composites based on PET, plasticized 10% with dipropyl heptyl phthalate and TiO_2 nanoparticles functionalized with PDMS

Compound	E1	E21	E22	E23
PET	285	285	285	285
TiO2/PDMS	-	3	9	21
Dipropyl heptyl phthalate	10	10	10	10
Calcium stearate	3	3	3	3
EPDM	15	15	15	15
Irganox 1010	3	3	3	3

The Brabender mixing diagrams, figures 1 and 2, show that the mixing chamber temperature increases by only 3°C from 248 to 251°C for control sample E1, with a maximum torque of 56 N / mm at 190s. When adding nanoparticles, both the mixing force increases (65 N/mm-E21, and 90N/mm-E23) and the time it takes to reach maximum change. Decreasing proportionally with the amount of TiO_2 added in the mixture, from 180s to 170 s (E21 and E22), higher than the control and 260s-E23.
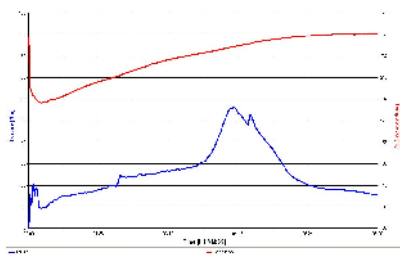
Figure 1. Brabender mixing diagram for control sample E1 polymeric composite based on PET plastified with 10% dipropyl heptyl phthalate –DPHP
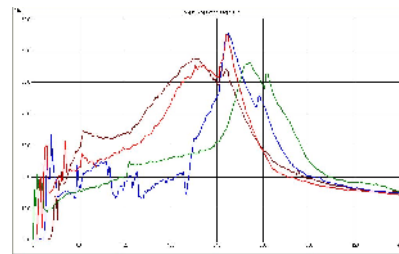
Figure 2. Brabender mixing diagram for polymeric composite based on PET plastified with 10% dipropyl heptyl phthalate –DPHP and 1, 3, and 7 % TiO2 nanoparticles

Testing Methods

Tensile strength tests of the samples were carried out according to SR ISO 37:2012 using a Schopper Tensile Testing machine 1445, at a constant crosshead speed of 500 ± 5 mm/min.

Hardness of the samples was measured by Shore "D" Durometer according to SR ISO 7619-1:2011.

Melt flow index. Samples were tested using a Melt Flow Index device – Haake that displays values for the melt volume rate (MVR – cm^3/10min) as well as melt flow rate (MFR- g/10min). Working temperature (chamber temperature up to 350°C), 2 heating areas, operating according to ISO 1133 standard.

Shock resistance tests were conducted using an INSTRON equipment with pendulum hammer, which can carry out Izod or Charpy tests with a wide range of testing capacity (0.7-27.847 J), according to STAS 7310-87.

FT-IT spectroscopy was done using the FT-IR 4200 JASCO, Herschel series instrument, equipped with ATR having diamond crystal and sapphire head within the spectrometric range 2000-530 cm^{-1}.

RESULTS AND DISCUSSION

The polymer structures obtained, in initial state and after accelerated ageing were characterized in terms of their physical-mechanical properties, and results are presented in table 2. Analyzing the values of physical-mechanical tests reveals the following:

Hardness of the control sample is 82°Sh D, when the nanoparticles are added, it increases by several units up to 85°Sh D. This is demonstrated by the fact that the hardness increases with the amount of filler in the mixture.

Table 2. Physico-mechanical characteristics for polymeric composites based on PET, plasticized 10% with dipropyl heptyl phthalate and TiO$_2$ nanoparticles functionalized with PDMS

Mixtures Normal	E1	E21	E22	E23
Hardness 0Sh D SR ISO 7619-1:2011	82	83	83	85
Tensile strength, N /mm^2 SR ISO 37:2012	6,6	7,4	8,7	9,0
Density, g /cm^3 SR ISO 2781:2010	1,02	1,02	1,02	1,02
Izod shock resistance, [KJ/m^2] STAS 7310-87	1,46	1,70	1,82	2,02
Melt flow index - 230°C,5 Kg, g/10min	27,2	26,7	26,4	25,8
Elongation at break, % SR ISO 37:2012	1,47	1,60	1,69	1,78

Tensile strength ranges from 6.6 to 9.0 N/mm^2, higher values show PET/TiO$_2$ composites and increase proportionally with the amount of nanoscale filler.

Elongation at break shows high values compared to rigid materials, and increases proportionally with the amount of nanoparticles introduced into the composite. Similar to tensile strength, higher values show for TiO$_2$ nanoparticle composites.

To estimate the fragility of polymeric nanocomposite, they were tested by the Izod Impact Resistance Method (SR EN 179-2: 2010). The values are small, the control is at the limit of fragility, and by the addition of functionalised nanoparticles, increases with approx. 3-5%.

In order to establish technological parameters for the processing composites in finished products, tests were carried out for melt flow index at 245°C and a force of 10 kg. The values of the flow indices are small and close to the control sample, with a decrease of approx. 3% and are in the range: 27.2-control sample and 23.7-26.7. Values decrease when adding ZnO and TiO$_2$ nanofillers into composites.

FT-IT spectroscopy. IR spectrum represents the radiant energy absorption curve in the IR domain by the sample molecule, depending on the wave length or radiation frequency. The infrared domain of the electromagnetic radiation is between 0.8 and 200 μm. IR domain for usual organic chemistry is between 2.5 and 25 μm. The structural determinations were carried out on an IR molecular absorption spectrometer with double beam, in the range of 4000-600 cm^{-1}, using 4200 FT-IR equipped with ATR diamond crystal and sapphire head. The solid state samples were set in the ATR and the equipment recorded the transmittance spectra of the sample and then compared it with the background spectra previously recorded. The recorded spectra of the samples were compared with the pure elastomer spectrum. After the tests were carried out, the following were found:
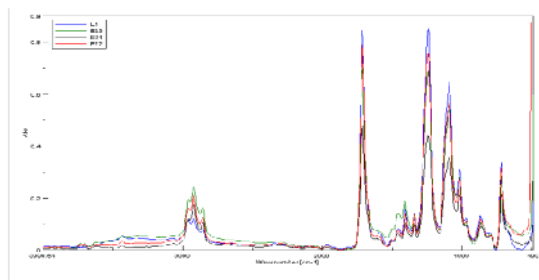
Figure 3. Composites based on PET / EPDM / DPHF and / or reinforced with 1, 3 and 7% TiO$_2$/PDMS nanoparticles

If analyzing blends based on polyethylene terephthalate (PET) / 5% ethylene propylene diene terpolymer (EPDM) plasticized with 10% dipropyl heptyl phthalate reinforced with 1, 3 and 7% of TiO$_2$ nanoparticles surface functionalized with PDMS (Figure 3), can be identified, both PET functional groups and EPDMs at different wavelengths.

Thus, the main characteristic bands assigned to PET are: the carbonyl group C = O (derived from the terephthalic acid ester) at 1712 cm^{-1}, the asymmetric C-C-O group at 1241 cm^{-1} and the stretch at 1091 cm^{-1}, C-H vibration bond (pendulum) from the aromatic structure to 721 cm^{-1}. The presence of the EPDM can be identified based on the presence of the two intense peaks occurring at approximately 2920 and 2851 cm^{-1} and are assigned to the stretching vibrations of asymmetric and symmetric CH3 groups.

Numerous other peaks can be identified at 721 cm^{-1}, the deformation vibration pattern of the CH2 (rotation), 1343 cm^{-1}- characteristic for the deformation vibration of the CH2 bond outside the plane (pendulum) and the 1463 cm^{-1}deformation vibration of the of the CH$_3$(shear) bond. The vinyl -C = C group derived from the EPDM structure can be observed around 988 cm^{-1}, and the one assigned to the RR'C-CH$_2$ group can be identified at about 865 cm^{-1}.

As can be seen from Figure 3, if the mixture consists of PET / EPDM / plasticizer (E1) or PET / EPDM / plasticizer / 1% TiO$_2$-PDMS (E21) the carbonyl group-specific bands are very intense and are not affected by their presence. In contrast, when higher than 3 and 7% of TiO$_2$ / PDMS nanoparticles are used, the intensity of the carbonyl group decreases considerably, probably due to the fact that these carbonyl groups come from the plasticizer and during the processing of the mixture under the influence of temperature and screws speed this is adsorbed into the nanoparticle structure.

Also, a decrease in the intensity of the asymmetric C-C-O group from PET at 1241 cm^{-1} is observed, as the ZnO / PDMS nanoparticles amount increase, probably due to specific interactions that occur between the components in the mixture.

CONCLUSION

The paper presents the study of the new nanostructured polymer composites based on chemically functionalized nanoparticles dispersed in the plastomer matrix. Hybrid TiO₂ nanoparticles (filler) dispersed in PET matrix resulted lead to a high performance polymeric material with multi-functional antibacterial, and polymorphic processing properties. The materials are adapted for biomedical and food applications and have been subjected to physico-mechanical and spectrometric tests. Prototypes of biomedical applications will be obtain from nanocomposites, and will be microbiological tested for a further examination.

REFERENCES

Alexandrescu, L. *et al*. (2017), "Polymer nanocomposites PE/PE-g-MA/EPDM/nanoZnO and TiO2 dynamically crosslinked with sulfur and accelerators", *Proceeding 2nd International Conference on Structural Integrity*, https://doi.org/10.1016/j.prostr.2017.07.040.

Arenas, M.A. *et al*. (2013), "Doped TiO2 anodic layers of enhanced antibacterial properties", *Colloids and Surfaces B-Biointerfaces*, 1(105), 106-112, https://doi.org/10.1016/j.colsurfb.2012.12.051.

Bartolome, L. and Muhammad, I. (2012), *Material Recycling - Trends and Perspectives*, Edited by Dr. Dimitris Achilias (Ed.), ISBN: 978-953-51-0327-1.

Bazant, P. *et al*. (2014), "Microwawe-Assisted synthesis of Ag/ZnO Hybrid Filler, Preparation, and Characterization of AntibacterialPoly(vinyl chloride) Composites Made from the Same", *Polymer Composites*, 35, 19-26, https://doi.org/10.1002/pc.22629.

Chand, N. and Fahim, M. (2008), *Tribology of natural fiber polymer composites*. Chapter 1, 1-58, Woodhead Publishing and CRC Press, https://doi.org/10.1533/9781845695057.

Deng, Z.Y. (2012), "Mechanical Properties Research on Concrete Block Doped Nano-TiO2 under the Conditions of Common Conservation", *Innovation in Civil Engineering, Architecture and Sustainable Infrastructure*, 238, 9-12.

Fakirov, S. (2002), *Handbook of Thermoplastic Polymers: Homopolymers, Copolymers, Blends, and Composites*, WILEY-VCH Verlag GmbH, Weinheim, ISBN: 3-527-30113-5.

Johnson, T. (1999), "Outlook for man-made fibers to 2005/2010", *Chem Fibers Intern*, 49, 455-459.

Mekonnen, T. and Mussone, P. (2013), "Progress in bio-based plastics and plasticizing modifications", *J. Mater. Chem. A*, 1, 13379–13398, https://doi.org/10.1039/c3ta12555f.

Saehana, S. *et al*. (2013), "Dye-Sensitized Solar Cells (DSSC) from Black Rice and its Performance Improvement by Depositing Interconnected Copper (Copper Bridge) into the Space between TiO₂ Nanoparticles", *Nanotechnology Applications in Energy and Environment*, 737, 43-53.

Stegarus, D.I and Lengyel, E. (2017), "The antimicrobial effect of essential oil upon certain nosocomial bacteria", *International Multidisciplinary Scientific GeoConference Surveying Geology and Mining Ecology Management, SGEM*, 17(61), 1089-1096, https://doi.org/10.5593/sgem2017/61/S25.142.

Tayel, A.A. *et al*. (2011), "Antibacterial Action of Zinc Oxide Nanoparticles against Foodborne Pathogens", *Journal of Food Safety*, 31(2), 211-218, https://doi.org/10.1111/j.1745-4565.2010.00287.x.

Tsai, M.T. *et al*. (2013), "Characterization and antibacterial performance of bioactive Ti-Zn-O coatings deposited on titanium implants", *Thin Solid Films*, 15(528), 143-150, https://doi.org/10.1016/j.tsf.2012.05.093.

POLYAMIDE/POLYPROPYLENE/GRAPHITE NANOCOMPOSITES WITH FUNCTIONAL COMPATIBILIZERS

LAURENŢIA ALEXANDRESCU[1], MARIA SÖNMEZ[1], MIHAI GEORGESCU[1], ANTON FICAI[2], ROXANA TRUŞCĂ[2], DANA GURĂU[1], LIGIAN TUDOROIU[3]

[1] INCDTP - Division: Leather and Footwear Research Institute, 93 Ion Minulescu St., 031215, sector 3, Bucharest, Romania, laurentia.alexandrescu@icpi.ro, laura_alexandrescu@yahoo.com

[2] Faculty of Applied Chemistry and Materials Science, University POLITEHNICA of Bucharest, 1 Polizu St., 011061, Bucharest, Romania

[3] SC RONERA SA, 3 Serelor St., Bascov, Arges, 117045, Romania

Bipolymeric composites are widely used to make new materials with predefined properties. Polyamide / Polypropylene (PA/PP) based compounds are often subjects of research because both components are relatively cheap, have useful and good properties, and can be processed by melt blending and extrusion-injection technologies, which are time-saving and environment-friendly technologies due to the possibility of reusing the material. Compatibility of binary polymeric compounds can be accomplished by adding a grafted copolymer, the segments of which have physical or chemical affinity with the two immiscible homopolymers. In this paper, maleic anhydride grafted polypropylene (PP-g-MA) was used. Composites having nanofiller are considered as a new generation of composite materials due to their unique properties. To increase the impact resistance of polymer composites (PA / PP-g-MA / PP) dispersion of graphite nanoparticles (nanoG) in polymeric mass was achieved. In addition to the PA / PP-g-MA / PP / nanoG bipolymer nanocomposite obtaining methodology, the combined effects of graphite treatment and compatibiliser polymer (PP-g-MA) on the structure and properties of the composites were studied. A number of optimal receptions have been developed in different technological conditions. Experimental composites have been physico-mechanically characterized by standardized methods specific to plastics and microscopic analysis -SEM.

Keywords: nanocomposites; polyamide; graphite.

INTRODUCTION

Bipolymeric composites are widely used to make new materials with predefined properties. Polyamide / Polypropylene (PA/PP) based compounds are often subjects of research because both components are relatively cheap, have useful and good properties, and can be processed by melt blending and extrusion-injection technologies, which are time-saving and environment-friendly technologies due to the possibility of reusing the material. Compatibility of binary polymeric compounds can be accomplished by adding a grafted copolymer, the segments of which have physical or chemical affinity with the two immiscible homopolymers. Various types of PA based nano blend composite have been studied by numerous researchers. PA nanocomposites obtained by thermoplastic-thermoplastic blending (both functionalized and simple): PA6/PP (Chen *et al*., 2006; Suter *et al*., 2007; Brune and Bicerano, 2002; Balandin, 2008), PA6/polyimide/organoclay (Ward and Sweeney, 2004); PA6/thermotropic liquid crystalline polymer/organoclay (Das *et al*., 2013); Nylon 66/Nylon 6/organoclay (Paul and Robertson, 2008); PA6/acrylonitrile- butadiene-styrene (ABS) (Lonjon *et al*., 2013); PA6/low density polyethylene (LDPE)/nanoclay (Biswas and Ray, 2001); PA6/polymethyl methacrylate (PMMA) (Lonjon *et al*., 2013); PA6/polystyrene (PS) (Hyunwoo *et al*., 2010) PA6/PS/nanosilica (Biswas and Ray, 2001). Nanocomposites have been considered a stimulating way for creating a new type of high performance material that combines the advantages of polymers and nanoparticles. Polymer nanocomposites are multiphase

materials, which consist of a polymer or copolymer having nanoparticles or nanofillers (with dimension of 1–50 nm) dispersed in the polymer matrix, significantly affecting different physical properties. Recently, graphite has emerged as the most promising nanofiller, due to its extraordinary physical properties, which has opened a new class of polymeric nanomaterials (Sandeep *et al.*, 2017).

In this paper graphite nanoparticles were selected for PA/PP composites reinforcement. A big challenge in developing polymer/graphite composites with high efficiency is achieving the individual graphene sheets within a polymer matrix in order to have a better dispersion and strong interfacial interactions, in order to decrease percolation threshold in graphite sheets loading and enhancing the graphite-polymer matrix interface (Bhattacharya, 2016) Graphite is a material with high chemical inertia, which leads to low compatibility with many organic or inorganic matrices. To eliminate this disadvantage, graphite nanoparticles are subjected to superficial oxidation, in which case adhesion improves by increasing surface polarity, or treated with an acid, thus improving the mechanical anchoring effect due to increased surface roughness (Alexandrescu *et al.*, 2017).

EXPERIMENTAL

Materials

All composites contain the same two polymer components: the polyamide elastomer PA6 (POLIMID B AV NATURALE – Poliblend Engineering Polymers Italy), with the following characteristics: specific weight, $1.40 g/cm^3$; impact resistance, $1.4 KJ/m^2$; Mt = 215-230°C, and polypropylene PP (Triplen 949- MOL Petrochemicals Group), with the following characteristics: impact resistance $4 KJ/m^2$, flex module-1.2 Mpa, specific weight $0.89-0.91 g/cm^3$, Mp 160-1850°C. Other components: compatibilizer: maleic anhydride grafted polypropylene PP-g-MA, viscosity of 330000 cps and an acidity index of 43.1 mg KOH/g, manufactured by Sigma Aldrich, and the graphite powders (C) 0520BX- Skyspring Nanomaterials USA with average particle size 3-4 nm.

Method

Polyamide, polypropylene, PP-g-MA, and graphite were mechanically mixed in a Brabender Plasti-Corder PLE-360 at 10-120 rotations/min, for 3 min. at 230°C to melt the plastomer, mixed for 5 min. at 240°C, and 2 min. at 210°C for homogenisation. The total processing time was 10 minutes. Table 1 shows tested formulations.

Table 1. Control – PA, and PA/PP-gMA/PP/G polymer nanocomposite formulations with varying G amounts (GPP1-0,1%; GPP2-0,5%; GPP3-1%; GPP4-2%; GPP5-3%)

Compound	GPP0	GPP1	GPP2	GPP3	GPP4	GPP5
Polyamide	270	270	270	270	270	270
Polypropylene	30	30	30	30	30	30
Polypropylene graft methylmetacrylate	9	9	9	9	9	9
Graphite nanoparticles	-	0,3	1,5	3	6	9
Molybdenum bisulphite	0,6	0,6	0,6	0,6	0,6	0,6
Total	309,6	310,1	311,1	312,6	315.6	318,6

The Brabender mixing diagrams, figures 1 and 2, show that the temperature in the chamber drops from 220 to 213°C at higher percentages of graphite (starts at 260°C, decreases to about 220°C with a peak of 216°C at the end in the case of the 0.15 G percentage and a lower one at 240°C in the case of 3% G percentage), and there are minor time changes in mixing forces, the maximum force is 0,8 min. in the case of 0.1% G percentage and 1.5 min. in the case of maximum percentage of 5% and its value exceeds 105 Nm for GPP01 and decreases of 85 Nm with a larger mixing area between 70-175s.
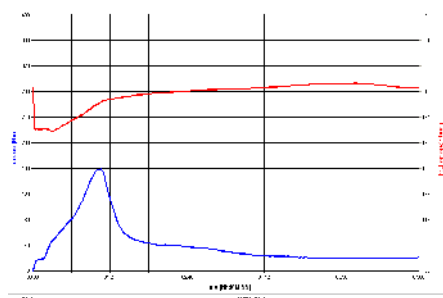
Figure 1. Brabender mixing diagram for composite GPP01
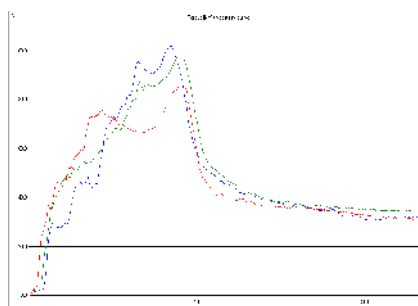
Figure 2. Brabender mixing diagram for composites GPP1(-), GPP3(-) and GPP5(-)

Testing Methods

1.   **Tensile strength tests** of the samples were carried out according to SR ISO 37:2012 using a Schopper Tensile Testing machine 1445, at a constant crosshead speed of 500 ± 5 mm/min.
2.   **Hardness** of the samples was measured by Shore "D" Durometer according to SR ISO 7619-1:2011.
3.   **Melt flow index.** Samples were tested using a Melt Flow Index device – Haake that displays values for the melt volume rate (MVR – cm^3/10min) as well as melt flow rate (MFR- g/10min). Working temperature (chamber temperature up to 350°C), 2 heating areas, operating according to ISO 1133 standard,
4.   **Shock resistance** tests were conducted using an INSTRON equipment with pendulum hammer, which can carry out Izod or Charpy tests with a wide range of testing capacity (0.7-27.847 J), according to STAS 7310-87.
5.   **SEM**. Films obtained from fracture of specimens used for physico-mechanical testing of nanocomposites GPP01, GPP1-GPP5 were cryogenically fractured and their cross sections were analyzed by SEM, using an ESEM QUANTA 200 instrument operating in low vacuum, equipped with LFD detector.

RESULTS AND DISCUSSION

The polymer structures obtained, in initial state and after accelerated ageing were characterized in terms of their physical-mechanical properties, and results are presented in table 2. Analyzing the values of physical-mechanical tests reveals the following:
-   *Hardness* of PA/PP-g-MA/PP/G polymer nanocomposites increases proportionally with the amount of graphite compared to that of polyamide (PA - 80°Sh) and PA/PP-g-

MA/PP composite -blank (GPP01-79°Sh). The higher value is given by the composite with 3% oxidized graphite (GPP5-80°Sh).

Table 2. Physical-mechanical characteristics of polymeric PA/PP-g-MA/PP/G composites

Formulations	GPP01	GPP1	GPP2	GPP3	GPP4	GPP5
			NORMAL STATE			
Hardness 0Sh D SR ISO 7619-1:2011	79	78	78	78	79	80
Tensile strength, N /mm2 SR ISO 37:2012	44,5	28,5	33,9	46,6	37,2	37,5
Density, g /cm3 SR ISO 2781:2010	1,13	1,14	1,14	1,14	1,15	1,15
Izod shock resistance, [KJ/m2] STAS 7310-87	4,11	4,22	5,19	5,81	6,42	5,93
Melt flow index - 230°C pressure of 5 Kg, g/10min	41,9	38,6	41,5	42,4	41,8	40,9
		ACCELERATED AGEING 2000 X 168 h SR ISO 188 : 2007				
Hardness 0Sh D SR ISO 7619-1:2011	80	77	77	77	78	79
Tensile strength, N /mm2 SR ISO 37:2012	43,8	16,8	20,1	32,6	34,2	35,7

- Similar to hardness, the value of tensile strength of nanocomposites increases compared to the value specific to polyamide (PA – 30.5 N /mm^2) and PA/PP-g-MA/PP composite -blank (GPP01-44.5 N /mm^2), the higher value is that of sample GPP3-46,6 N /mm^2 (1% G). The percentages of 2 and 3% graphene oxide added to the composite leads to an increase in tensile strength values, but lower than values obtained for samples with G below 1%.
- Density increases proportionally with amount of graphite added to the mixture.
- In order to test resistance to high temperature, accelerated ageing tests were conducted on the samples conditioned at 200°C for 168h. The analysis of obtained values shows very small changes, the samples were not damaged and did not modify their shape.
- In order to estimate the resistance of brittleness of polymer nanocomposites, they were tested by Izod shock resistance method (STAS 7310-87). This determination is the most important one due to the fact that one of the requirements of polymer nanocomposites is shock resistance optimization, for use in heavy impact conditions. PA value is 2.5 KJ/m^2 and GPP01-4,11 (compound PA/PP-g-MA/PP). All nanocomposites tested have increased values compared to the control sample PA and GPP01, ranging between 4.22 and 6.42 KJ/m^2. Increased values were obtained for samples GPP3 (PA/PP-g-MA/PP/G-1% G) – 5.19 KJ/m^2 and GPP5 (PA/PP-g-MA/PP/G-1,5% G) –6.42 KJ/m^2. Graphite concentrations higher than 1,5% lead to decreases in shock resistance values. This leads to the conclusion that percentages in the 0.1-1,5% range lead to maximum values of physical-mechanical parameters.
- In order to establish the technological parameters for processing GPP1-GPP5 polymeric architectures in finished products, tests were carried out to determine the melt flow index at temperatures of 230°C and a pressure force of 10 kg. The analysis

of the obtained values (Table 2) show an increased flow compared to GPP01 (41,9 g / 10min) for the samples: GPP1 (0.1% G) -38,6; g/10min, GPP2 (0.5% G) 41,5 g/10 min and GPP3 (1% G) 42,4 g / 10 min. The other samples, with concentrations above 1% G in the composite, GPP4-2% G and G5-3% G have flow values below the control sample value, which demonstrates that higher graphite concentrations in the nanocomposite have a positive influence on the flow of the material in the injection process, the value is GPP4 41,8 g/10 min and GPP5 40,9 g/10 min.

- SEM image of the cross section of the fracture obtained from GPP01 compound, presented in Figure 3, emphasize a lamellar structure. On the other hand, the SEM images of cross sections of the fracture obtained from the other tree samples (GPP1, GPP3 and GPP5), shown in the Figures 4-6, in which the nanocomposites with rates differ from G, have completely different aspects: they show a biphasic type morphology consisting in spheroid particles distributed within a matrix with less evident lamellar morphology. The number of particles increases directly with the amount of G of the nanocompound.
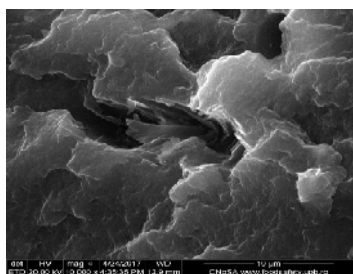
Figure 3. SEM image for sample GPP01
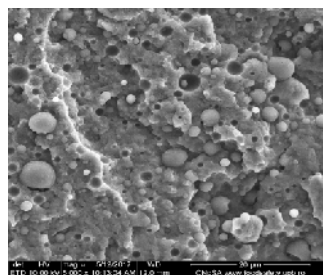
Figure 4. SEM image for sample GPP1
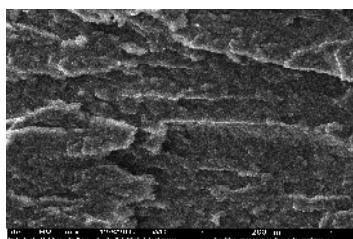
Figure 5. SEM image for sample GPP3
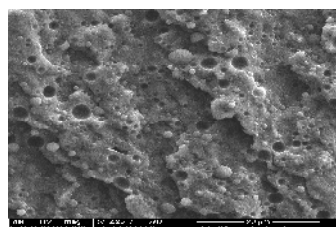
Figure 6. SEM image for sample GPP5

CONCLUSION

- The paper presents the study of the new nanostructured polymer composites from polyamide/oxidized graphite nanoparticles-PA/G to manufacture, by injection, bearing seals, contact plates, and other components for the railway industry, with shock resistance higher than 5-8 kJ/m², wear resistance below 100 mm³, resistance to temperatures from -40 to $+240^0$C, resistance to impact and to outdoor applications, with temperatures ranging from -40 to $+60^0$C, in rain, snow or sunshine.

- Polyamide and graphite were mechanically mixed in a Brabender Plasti-Corder

PLE-360 at 10-120 rotations/min for 2 min. at 230°C, melt the plastomer for 3 min. at 240°C, and 2 min. at 200°C for homogenisation.

- The nanocomposites polyamide/oxidized graphite were characterized by scanning electron microscopy (SEM) and physico-mechanical.

- Graphene concentrations higher than 1% lead to decreases in shock resistance values and tensile strength values. This leads to the conclusion that percentages in the 0.1-1% range lead to best values of physical-mechanical parameters.

REFERENCES

Alexandrescu, L. *et al*. (2017), "Polyamide/polypropylene/graphene oxide nanocomposites with functional compatibilizers: morpho-structural and physico-mechanical characterization", *Procedia Structural Integrity*, 5, 675-682, https://doi.org/10.1016/j.prostr.2017.07.042.

Balandin, A.A. *et al*. (2008), "Superior Thermal Conductivity of Single-Layer Graphene", *Nano Lett*, 8, 902–907, https://doi.org/10.1021/nl0731872.

Bhattacharya, M. (2016), "Polymer Nanocomposites—A Comparison between Carbon Nanotubes, Graphene, and Clay as Nanofillers", *Materials*, 9, 262-297.

Biswas, M. and Ray, S.S. (2001), "Recent progress in synthesis and evaluation of polymer-montmorillonite nanocomposites", *Adv Polym Sci*, 155, 167–221, https://doi.org/10.1007/3-540-44473-4_3.

Brune, D.A. and Bicerano, J. (2002), "Micromechanics of nanocomposites: Comparison of tensile and compressive elastic moduli, and prediction of effects of incomplete exfoliation and imperfect alignment on modulus", *Polymer*, 43, 369–387, https://doi.org/10.1016/S0032-3861(01)00543-2.

Chen, B. and Evans, J.R.G. (2006), "Elastic moduli of clay platelets", *Scripta Mater*, 54, 1581–1585, https://doi.org/10.1016/j.scriptamat.2006.01.018.

Das, P. *et al*. (2013), "Facile Access to Large-Scale, Self-Assembled, Nacre-Inspired, High-Performance Materials with Tunable Nanoscale Periodicities", *ACS Appl. Mater. Interfaces*, 5, 3738–3747, https://doi.org/10.1021/am400350q.

Hyunwoo, K., Ahmed, A. and Macosko, W. (2010), "Graphene/Polymer Nanocomposites", *Macromolecules*, 43(16), 6515–6530, https://doi.org/10.1021/ma100572e.

Lonjon, A. *et al*. (2013), "High electrically conductive composites of Polyamide 11 filled with silver nanowires: Nanocomposites processing, mechanical and electrical analysis", *Journal of Non-Crystalline Solids*, 376, 199–204, https://doi.org/10.1016/j.jnoncrysol.2013.05.020.

Paul, D.R. and Robeson, L.M. (2008), "Polymer Nanotechnology: Nanocomposites", *Polymer*, 49, 3187–3204, https://doi.org/10.1016/j.polymer.2008.04.017.

Sandeep, N. *et al*. (2017), "Polyolefin/graphene nanocomposites: a review", *RSC Adv.*, 7, 23615–23632, https://doi.org/10.1039/c6ra28392f.

Suter, J.L. *et al*. (2007), "Large-scale molecular dynamics study of montmorillonite clay: Emergence of undulatory fluctuations and determination of material properties", *J. Phys. Chem. C*, 111, 8248–8259, https://doi.org/10.1021/jp070294b.

Ward, I.M. and Sweeney, J. (2004), *An Introduction to the Mechanical Properties of Solid Polymers*, John Wiley: Sussex, UK.

Zhang, X. *et al*. (2017), "Effect of polyamide 6 on the morphology and electrical conductivity of carbon black-filled polypropylene composites", *R. Soc. Open sci*, 4, 170769, http://dx.doi.org/10.1098/rsos.170769.

INVESTIGATION OF THE ANTIVIRAL ACTIVITY OF *Ficus carica* L. LATEX AGAINST HSV-2

EMRAH AY, NİZAMİ DURAN

Microbiology & Clinical Microbiology Department, Medical Faculty, Hatay Mustafa Kemal University, Turkey, nizamduran@hotmail.com

Ficus carica L. has been widely used in the treatment of many diseases in folk medicine for centuries. It has been reported to have many pharmacological properties. In this study, we aimed to investigate the antiviral activities of *Ficus carica* L. latex against HSV-2 and its synergistic effects with acyclovir. In order to determine the presence of antiviral activity of *Ficus carica* latex samples, different concentrations of latex (1024, 512, 256, 128, 64, 32, 16, 8, 4, 2 and 1 μg/mL) were added into the culture medium. HSV-2 proliferation was detected by real-time PCR method. Acyclovir was selected as the control drug. Compared with acyclovir, *Ficus carica* effectively inhibits viral replication of HSV-2, although the antiviral activity of *Ficus carica* is statistically significantly lower than that of acyclovir. It has been determined that the antiviral activity of Ficus carica is increased due to the polysaccharide. The activity of *Ficus carica* against HSV-2 was confirmed by a significant decrease in the number of viral copies. It was determined that *Ficus carica* L. samples have important antiviral effects compared with acyclovir. In particular, the synergy produced by antiviral activity of *Ficus carica* and acyclovir combined had a stronger effect against HSV-2 than acyclovir alone.

Keywords: *Ficus carica* L. HSV-2, antiviral, acyclovir, synergistic

INTRODUCTION

Ficus carica L. has been widely used in the treatment of many diseases in folk medicine for centuries. It has been reported to have many pharmacological properties (Ronsted *et al*., 2008; Duenas *et al*., 2008; Jeong and Lachance 2001).

Herpes simplex virus (HSV) infections are a common clinical problem all over the world. Especially in immunocompromised patients, the infection is severe and progressive and leads to significant morbidity and mortality. Herpes simplex viruses (HSV) are the most common viral agents in humans (Jerome and Ashley, 2003).

Infection caused by HSV can occur in a wide spectrum ranging from asymptomatic infections to disseminated diseases resulting in death. Recurrent HSV infections lead to severe clinical manifestations, such as meningoencephalitis, pneumonia and hepatitis, especially in newborns and immunocompromised patients (Whitley and Roizman, 2001).

Increased acyclovir resistance is particularly noteworthy in herpes simplex viruses, especially in immunocompromised individuals. For this reason, effective new drug research in herpesviruses is extremely important. Fig is one of the most important fruit of the Mediterranean region with many pharmacological features.

In this study, we aimed to investigate the antiviral activities of *Ficus carica* L. latex against HSV-2 and its synergistic effects with acyclovir.

MATERIALS AND METHODS

In this study, viral cultures were carried out in HEp-2 cell line. Al proliferation experiments were performed in flat bottom microplates. We inoculated 1×10^5 cells per ml and RPMI 1640 medium with 10% fetal bovine serum into each culture plate. Firstly, the non-cytotoxic concentration of Ficus carica latex in the study was

determined in the HEp-2 cell line. In order to determine the presence of antiviral activity of *Ficus carica* latex samples, different concentrations of latex (1024, 512, 256, 128, 64, 32, 16, 8, 4, 2 and 1 µg/mL) were added into the culture medium. HSV-2 proliferation was detected by real-time PCR method. Acyclovir was selected as the control drug.

Ficus carica Latex

Ficus carica latex was obtained drop-by-drop through cutting young leaves and fruits of fig tree in Hatay district. Different concentrations of fig latex were provided including 12.5, 25, 50, 100, 200, 400 and 800 µg/ml. To determine the cytotoxicity of Ficus carica latex, HEp-2 cell line was used. For this purpose, the cell density was adjusted to. $2x10^4$ cells cultured with RMPI 1640 containing 10% fetal bovine serum and antibiotics (100 U/L penicillin and streptomycin). The culture plates were incubated at 37°C, with a saturated humidity and 5% CO_2.

DMSO

The cell number and viability of the cells were determined by trypan blue exclusion method with a hemocytometer. In the experiments DMSO (Sigma, USA) was used to dissolve the Ficus carica latex. To determine the non-toxic concentration of DMSO in the cells, HEp-2 cells were inoculated at a density of 1×10^5 cells/ml. Then, different concentrations of DMSO (4 %, 2 %, 1 %, and 0.5 %) were added to the cell cultures. After 72 hours of incubation, viable cells ratios were calculated.

Virus

The HEp-2 cell line was used for cytotoxicity tests. And also, all viral culture tests were carried out on HEp-2 cell lines. The cultivation of cell cultures was carried out in RPMI-1640 medium with 10% fetal bovine serum. The virus strains (HSV-2 virus) were obtained from Ankara University. Three different titers of HSV-2 were used in the experiments (1, 10, and 100x$TCID_{50}$; Tissue Culture of Infectious Dose). Incubation of all culture plates was performed in 5% carbon dioxide atmosphere at 37°C. Acyclovir (Sigma, USA) was selected as a control drug. Acyclovir was dissolved in bi-distillated water before use (1 mg/ml). Various concentrations of *Ficus carica* L. ranging from 1 to 1024 µg/ml were used in the experiments.

Viral quantification by real-time PCR

The real time PCR assay was performed according to the method of Readand and Kurtz, in 1999.

RESULTS

In the study, it was shown that 1% of DMSO did not affect cell proliferation, both by microscopic evaluation and by cell viability (Figure 1). *Ficus carica* L. was found to be toxic to HEp-2 cells at the level of 256 µg/ml (Figure 2). For this reason, antiviral effect studies were investigated at concentrations below 256 µg/ml. Compared with acyclovir; *Ficus carica* effectively inhibits viral replication of HSV-2, although the antiviral activity of *Ficus carica* is statistically significantly lower than that of acyclovir

(Figure 3). It has been determined that the antiviral activity of Ficus carica is increased due to the polysaccharide (Figure 4). The activity of *Ficus carica* against HSV-2 was confirmed by a significant decrease in the number of viral copies (Figure 5).
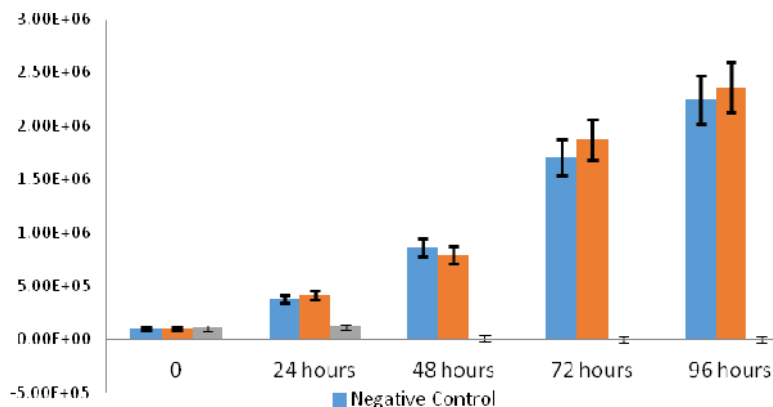
Figure 1. The effects on cell viability of the DMSO and Acyclovir compared with the control group
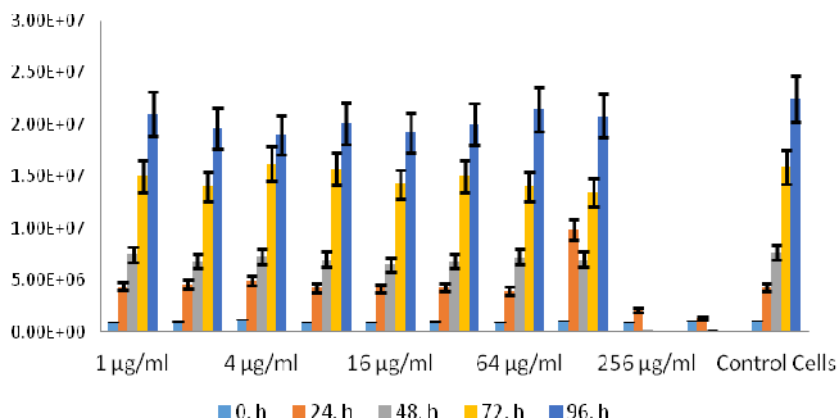
Figure 2. The effects of *Ficus carica* L. latex on cell viability of HEp-2 cells compared with control group cells
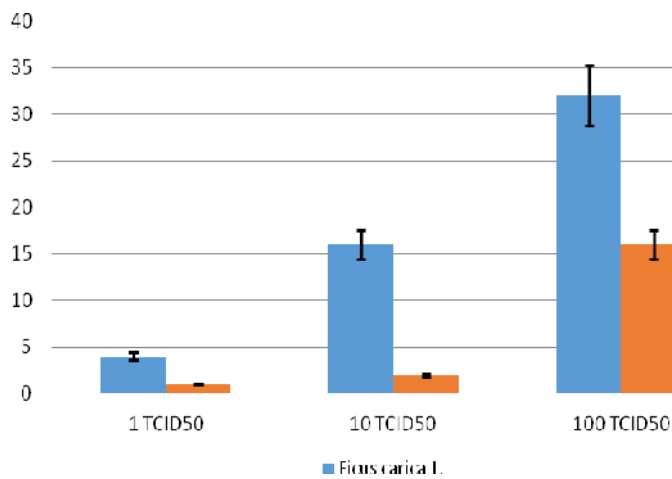
Figure 3. MIC values of *Ficus carica* L. and Acyclovir against some Herpes simplex virus type-2
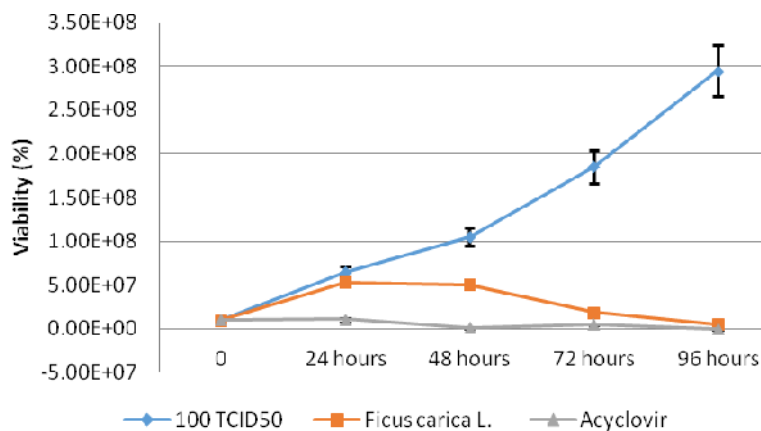
Figure 4. The effects of *Ficus carica* L. on HSV-2 replication as compared to the Acyclovir
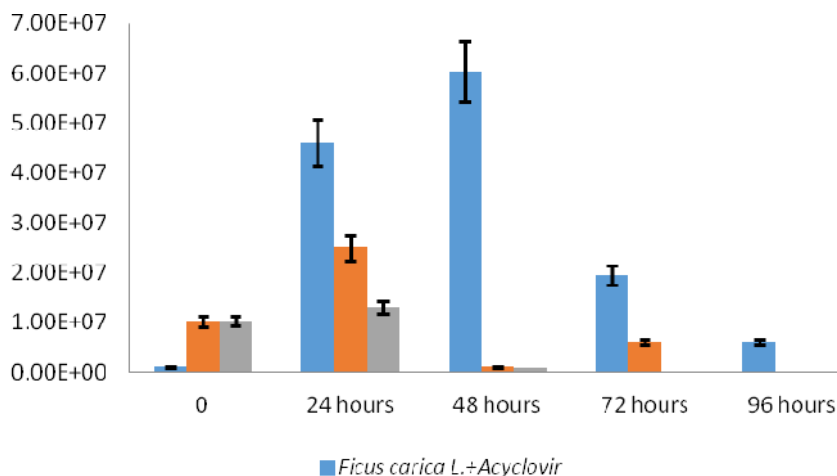
Figure 5. The synergistic effects of Ficus carica L. and Acyclovir on HSV-2 replication as compared to the Acyclovir

DISCUSSION AND CONCLUSION

It was determined that *Ficus carica* L. samples have important antiviral effects compared with acyclovir. In particular, the synergy produced by antiviral activity of *Ficus carica* and acyclovir combined had a stronger effect against HSV-2 than acyclovir alone.

REFERENCES

Dueñas, M. *et al*. (2008), "Anthocyanin composition in fig (*Ficus carica* L.)", *Journal of Food Composition and Analysis*, 21(2), 107-115, https://doi.org/10.1016/j.jfca.2007.09.002.
Jeong, W.S. and Lachance, P.A. (2001), "Phytosterols and fatty acids in fig (*Ficus carica* var. mission) fruit and tree components", *Food Chemistry and Toxicology*, 66, 278–281.
Jerome, K.R. and Ashley, R.L. (2003), "Herpes simplex viruses and herpes B virus", in: Murray, P.R. (ed.), *Manual of Clinical Microbiology*, 8thed., ASM Press, Washington DC, 1291-303.
Readand, S.J. and Kurtz, J.B. (1999), "Laboratory diagnosis of common viral infections of the central nervous system by using a single multiplex PCR screening assay", *J Clin Microbiol*, 37(5), 1352–55.
Rønsted, N. *et al*. (2008), "Phylogeny, biogeography, and ecology of *Ficus* section *Malvanthera* (Moraceae)", *Molecular Phylogenetics and Evolution*, 48(1), 12-22, https://doi.org/10.1016/j.ympev.2008.04.005.
Whitley, R.J. and Roizman, B. (2001), "Herpes simplex virus infections", *Lancet*, 357, 1513-8, https://doi.org/10.1016/S0140-6736(00)04638-9.

THE INFLUENCE OF ALKALINE HYDROLYSIS OF WOOL BY-PRODUCTS ON THE CHARACTERISTICS OF KERATIN HYDROLYSATES

MARIANA DANIELA BERECHET, CARMEN GAIDĂU, MIHAELA-DOINA NICULESCU, MARIA STANCA

INCDTP - Division: Leather and Footwear Research Institute, Bucharest, 031215, Romania, daniela.berechet@icpi.ro

Wool by-products represent an important bioresource for designing new biodegradable materials, alternative to synthetic products for regenerative medicine, cosmetic formulations, food package, fertilizers etc. Keratin is the main structural protein of wool, with highest concentration of cysteine as compared to other proteins. Research has been carried out on the physico-chemical properties of keratin hydrolysates obtained from wool by-products by using different concentrations of sodium hydroxide. The influence of sodium hydroxide concentrations from 8% to 25% on keratin hydrolysate characteristics was shown by chemical analyses, SDS-PAGE electrophoresis, particle size and Zeta potential measurements. It was concluded that the alkaline hydrolyse allows efficient solubilisation of wool by-products and producing of keratin hydrolysates with different molecular weights and cysteine concentrations. The use of 10% sodium hydroxide allows to obtain keratin hydrolysates with high molecular weight and higher concentration of cysteine meanwhile 15% sodium hydroxide represents the threshold for low molecular hydrolysates and low cysteine concentrations. The experiments showed the thresholds for sodium hydroxide concentration related to different properties of keratin hydrolysates.

Keywords: wool by-products, keratin hydrolyzate, alkaline hydrolysis.

INTRODUCTION

At present, there is a particular interest in research on biodegradable materials obtained from renewable sources such as proteins, polysaccharides and lipids. The use of biodegradable materials is the most effective solution to solve environmental pollution problems generated by synthetic polymers from petroleum origin (Dou *et al.,* 2016; Moore *et al.,* 2006; Mauri and Anon, 2006).

Keratin is a group of insoluble, filamentous proteins, with high-sulfur content forming the bulk of epidermal appendages such as wool, claws, horns, beaks, and feathers (Wang *et al.,*2016). Keratin extracted from wool is a biopolymer with excellent properties that synthetic polymers cannot achieve (Cardamone, 2010).

The study of biological materials opens the way for discovering new materials by providing principles and mechanisms obtained from the micro and macro multifunctional natural design (Meyers *et al*., 2008; Meyers *et al*., 2012).

The research of the biochemistry, structure, physical and chemical properties of keratin and keratinised materials is important for the development of new advanced ecological materials and models based on keratin (Holkar *et al.,* 2018). Keratin based products showed bioactive properties in many pharmaceutical, medicine, cosmetic and agriculture products (Sundar *et al*., 2010). Bhavsar and coworkers obtained nitrogen rich product from raw wool hydrolyzed with superheated water in a semi-industrial reactor (Bhavsar *el al.,* 2016).

Keratin can be extracted using strong acid, alkali, high concentration of salt solutions or expensive enzymes. Recent methods use ionic liquids for keratin extraction from wool, feathers and hair with improved yield (Ji *et al*., 2016).

The paper presents the influence of sodium hydroxide concentration on keratin hydrolysate properties in view of designing different applications with improved ecological impact.

MATERIALS AND METHODS

Materials

The raw wool was purchased from sheep breeders, NaOH rotulis was purchased from Lach-Ner, Czech Republic, NH_3 (25% solution), Na_2CO_3 and the detergent were purchased from Chimreactiv, Romania.

Wool Degreasing and Hydrolysis

The raw wool was degreased in water in ratio 1:10 with 1% Na_2CO_3, 1% NH_3 and 1% detergent by shaking for 8 hours at 35°C in a FAVE drum. The alkaline hydrolysis of the degreased wool was made in a solution containing water in ratio 1:20 and NaOH at 80°C, by stirring for 3 hours, followed by decantation, filtration and separation (Fig.1). Five concentrations of NaOH: 8%, 10%, 15%, 20% and 25% were used and five keratin hydrolysates were obtained: KerNa8, KerNa10, KerNa15, KerNa20 and KerNa25. The solubilisation of wool was complete for alkaline hydrolysis processes with 10%, 15%, 20% and 25% NaOH and no waste wool was generated.
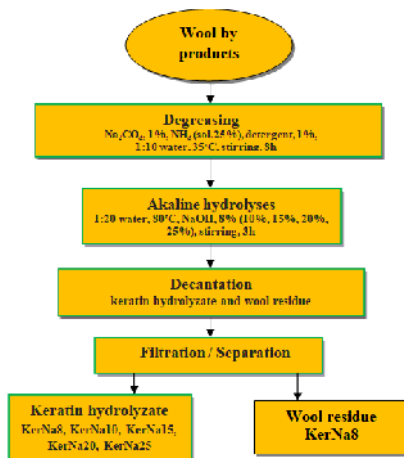
Figure 1. The flow chart for obtaining keratin hydrolysates

Keratin Hydrolysate Characterization

The obtained keratin hydrolysates (KerNa8, KerNa10, KerNa15, KerNa20 and KerNa25) were physically and chemically analyzed for: dry matter (SR EN ISO 4684:2006), ash (SR EN ISO 4047:2002), total nitrogen and protein (SR ISO 5397:1996), pH (STAS 8619/3:1990), aminic nitrogen (ICPI Method), cysteine and cystine sulfur (SR 13206:1994) content.

Sodium dodecyl sulfate-polyacrylamide gel electrophoresis (SDS-PAGE) was performed for molecular weight evaluation according to Laemmli's method (Laemmli, 1970) with a Vertical Dual-Gel Units (VWR Austria).

Particle size and Zeta potential of keratin hydrolysates were measured by using a Zetasizer Nano ZS (Malvern).

RESULTS AND DISCUSSION

The physical-chemical characteristics of keratin hydrolysates are presented in Table 1. The keratin hydrolysate obtained in the presence of 8% NaOH (KerNa8) is characterized by a significant percentage of protein content (79.86%), total nitrogen (14.18%) and highest concentration of cysteine (6.67%) and cystine sulfur (1.78).

It can be seen that the use of 15% sodium hydroxide substantially increase the aminic nitrogen concentration in correlation with keratin molecule breaking and cysteine and cystine sulphur decreasing. Table 1 shows that the wool hydrolyse with 10% sodium hydroxide can be a threshold for lower aminic nitrogen concentration (lower molecular weight) and higher cysteine and cystine sulphur concentration. The threshold for obtaining keratin hydrolysate with low molecular weight and low concentration of cysteine and cystine sulphur is represented by the wool hydrolysate with 15% sodium hydroxide.

Table 1. Physical-chemical characteristics of the keratin hydrolysates

No.	Characteristics, UM	KerNa8	KerNa10	KerNa15	KerNa20	KerNa25
1	Dry matter, %	4.16	4.31	5.16	4.68	5.22
2	Ash*, %	12.50	12.30	17.25	19.87	24.14
3	Total nitrogen*, %	14.18	14.62	13.18	13.03	11.30
4	Protein*, %	79.56	82.13	74.03	73.29	63.60
5	pH, units of pH	11.40	12.04	12.52	12.62	12.90
6	Aminic nitrogen**, %	0.60	0.93	2.09	2.04	1.81
7	Cysteine, %	6.67	5.74	2.38	1.03	-
8	Cystine Sulphur, %	1.78	1.53	0.63	0.27	-

*values reported on a dry matter basis, **value reported on protein basis

The physical-chemical analyses results are in agreement with SDS-PAGE electrophoresis. The bands for KerNa8 and KerNa10 are more prominent than the KerNa15, KerNa20 and KerNa25 bands (Fig.2) suggesting higher molecular weights, in agreement with lower values for aminic nitrogen (Table 1).
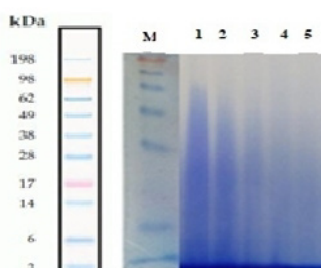
Figure 2. SDS-PAGE electrophoresis for keratin hydrolysate: M - marker, 1- KerNa8, 2 – KerNa10, 3 – NaKer15, 4 – KerNa20, 5 – KerNa25

The molecular weights of keratin hydrolysates range between 3 and 62 kDa for KerNa8 and KerNa10, between 3 and 38 kDa for KerNa15 and KerNa20 and between 3 and 28 kDa for KerNa25.

DLS analysis presented in Table 2 shows the tendency of increasing of low size population of particles with increase concentration of sodium hydroxide used for wool solubilisation. The third particle size population with lowest dimension appears in the case of the most hydrolysed product, KerNa25. The association tendency of protein polydispersions can explain higher particles sizes in the case of the most hydrolysed keratin (KerNa25). The stability of keratin hydrolysates ranges between -22.8 mV and -27 mV, values which are not very far from the stability value of $\pm$ 30 mV.

Table 2. Particle sizes and Zeta potential for keratin hydrolysate

No	Keratin hydrolysate	Particle populations (%) and size (nm)						Pdl	Zeta potential, mV
		Majority population 3		Majority population 2		Majority population 1			
		Size	%	Size	%	Size	%		
1	KerNa8	-	-	110.9	17.3	648.6	82.7	0.699	-25.2
2	KerNa10	-	-	146.6	24.5	631.1	75.5	0.872	-25.5
3	KerNa15	-	-	131.8	27.1	1027	72.9	1	-27.0
4	KerNa20	-	-	110.4	24.0	539.9	76.0	0.754	-26.4
5	KerNa25	51.80	7.7	189.0	31.6	714.5	60.7	0.675	-22.8

Five keratin hydrolysates were obtained using different concentrations of NaOH, following the technological steps shown in Fig 1. The five keratin hydrolysates are individualized by their physico-chemical characteristics. The total nitrogen values are similar for KerNa8 and KerNa10. From KerNa15 it was observed a small decrease in content of total nitrogen (Figure 3) in correlation with ash content increase. The chemical action of the alkaline medium is manifested on wool keratin by the unbinding of the electrovalences, the breaking of the cystine bridge and the hydrolysis of the peptide bonds. These changes are largely influenced by the pH value of the reaction medium, the working time and temperature (Ifrim, 1979).
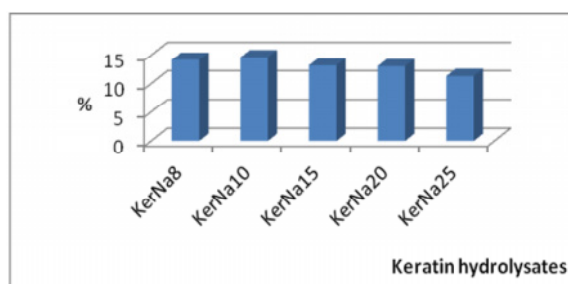
Figure 3. The influence of sodium hydroxide on the total nitrogen content of keratin hydrolysates

Research result has highlighted that alkaline-solubilized keratins are poorer in sulfur with increasing NaOH concentration, by decreasing cystine sulphur content from 1.78% in KerNa8 to 0.27% in KerNa20. Aminic nitrogen values (Fig. 4) increase from 0.6% for KerNa8 to 2.09% for KerNa15, showing that alkaline hydrolysis has been enhanced the keratin molecule breaking.
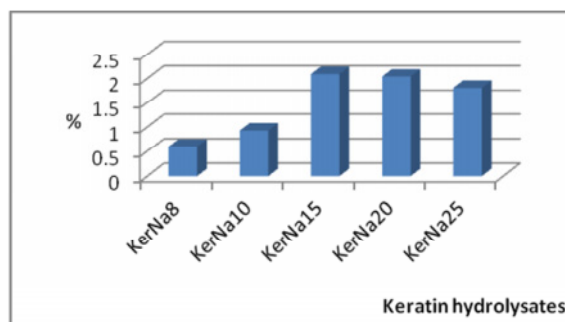
Figure 4. The influence of sodium hydroxide on aminic nitrogen content in keratin hydrolysates

Particle size measurement for the five obtained keratin hydrolysates confirms the chemical-physical analyses and SDS-PAGE electrophoresis results. In Figure 5 it can be seen the tendency of decreasing the share of high particle size and increasing of particle populations with low particle size.
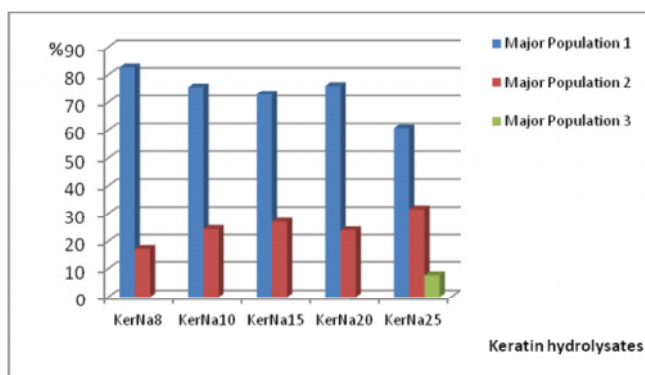
Figure 5. The influence of alkaline hydrolysis on particle size populations of keratin hydrolysates

CONCLUSIONS

The production of keratin hydrolysates from wool by-products represents an ecological route for designing new added values products: biodegradable food packages, organic biostimulants and fertilizers, biodegradable auxiliaries (flame retardants, tensides etc). The research results showed that the complete solubilisation of wool can be achieved by alkaline hydrolyse with sodium hydroxide starting with 10% concetration. Different keratin hydrolysates with high molecular weights and high

cysteine content can be obtained by using 8% sodium hydroxide in atmospheric conditions of reaction. The hydrolyse of wool with 15% of sodium hydroxide seems to be a threshold for getting low concentration of cysteine and low molecular weight keratin.

REFERENCES

Bhavsar, P. *et al*. (2016), "Superheated Water Hydrolysis of Waste Wool in a Semi-Industrial Reactor to Obtain Nitrogen Fertilizers", *ACS Sustainable Chem Eng*, 4, 6722-6731, https://doi.org/10.1021/acssuschemeng.6b01664.

Cardamone, J.M. (2010), "Investigating the microstructure of keratin extracted from wool: Peptide sequence (MALDI-TOF/TOF) and protein conformation (FTIR)", *Journal of Molecular Structure*, 969, 97–105, https://doi.org/10.1016/j.molstruc.2010.01.048.

Dou, Y. *et al*. (2016), "The Structure, Tensile Properties and Water Resistance of Hydrolyzed Feather Cheratin-Based bioplastics, *Chin J Chem Eng*, 24(3), 415-420, https://doi.org/10.1016/j.cjche.2015.11.007.

Holkar, C.R. *et al*. (2018), "Valorization of keratin based waste", *Process Safety and Environmental Protection*, 115, 85–98, https://doi.org/10.1016/j.psep.2017.08.045.

Ifrim, S. (1979), *Chemistry of Wool* (in Romanian), Editura Tehnica, Bucharest.

Ji, Y. *et al*. (2014), "Extraction of keratin with ionic liquids from poultry feather", *Separation and Purification Technology*, 132, 577–583, https://doi.org/10.1016/j.seppur.2014.05.049.

Laemmli, U.K. (1970), "Cleavage of structural proteins during the assembly of the head of bacteriophage T4", *Nature*, 227, 680-685, https://doi.org/10.1038/227680a0.

Mauri, A.N. and Anon, M.C. (2006), "Effect of solution pH on solubility and some structural properties of soybean protein isolate films", *J Sci Food Agric*, 86(7), 1064-1072, https://doi.org/10.1002/jsfa.2457.

Meyers, M.A. *et al*. (2008), "Biological materials: structure and mechanical properties', *Prog Mater Sci*, 53, 1–206, https://doi.org/10.1016/j.pmatsci.2007.05.002.

Meyers, M.A., McKittrick, J. and Chen, P.Y. (2013), "Structural biological materials: critical mechanics–materials connections", *Science*, 339(6121), 773–9, https://doi.org/10.1126/science.1220854.

Moore, G.R.P. *et al*. (2006), "Influence of the glycerol concentration on some physical properties of feather cheratin films", *Food Hydrocolloid*, 20(7), 975-982, https://doi.org/10.1016/j.foodhyd.2005.11.001.

Sundar, S., Kundu, J. and Kundu, S.C. (2010), "Biopolymeric nanoparticles", *Sci Technol Adv Mater*, 11, 014104, https://doi.org/10.1088/1468-6996/11/1/014104.

Wang, B. *et al*. (2016), "Keratin: Structure, mechanical properties, occurrence in biological organisms, and efforts at bioinspiration, *Progress in Materials Science*, 76, 229–318, https://doi.org/10.1016/j.pmatsci.2015.06.001.

POSTOPERATIVE PERITONEAL ADHESIONS PROPHYLAXY USING COLLAGEN-BASED BIOMATERIALS

SIMONA BOBIC[1,2], VLAD DENIS CONSTANTIN[1,2], MĂDĂLINA ALBU KAYA[5], ŞTEFANIA MARIN[3,5], ELENA DĂNILĂ[4,5], MIHAI DIMITRIU[1,2], BOGDAN SOCEA[1,2]

[1]"Carol Davila" University of Medicine and Pharmacy, Surgery Department, Bucharest, Romania

[2]"Sfântul Pantelimon" Emergency Clinical Hospital, Surgery Department, Bucharest, Romania

[3]Center of Surface Science and Nanotechnology, University Politehnica of Bucharest, Splaiul Independentei 313, Romania

[4]University Politehnica of Bucharest, Faculty of Applied Chemistry and Materials Science, Bucharest,1-7 Gheorghe POLIZU Str., 011061, Bucharest, Romania

[5]INCDTP - Division: Leather and Footwear Research Institute, Bucharest 031215, Romania, madalina.albu@icpi.ro

Corresponding author: Vlad Denis Constantin M.D. Ph.D., Professor of Surgery „Carol Davila" University of Medicine and Pharmacy Bucharest „Sfântul Pantelimon" Emergency Clinical Hospital Bucharest 340–342 Pantelimon Street, Bucharest, Romania e-mail: constantindenis@yahoo.com

Peritoneal adhesion occurs after abdominal, gynecological, and thoracic surgeries, determining important postsurgical complications such as infertility, chronic pelvic pain and intestinal obstruction, with difficulties of extensive adhesiolysis in future surgery. Antiadhesive barrier methods, providing physical separation between the injured site and the adjacent tissues, have been developed. Taking into account the fact that physical separation is only required during the critical time of wound healing of the damaged area, bioabsorbable polymers, available in the forms of solutions, gels, and sheets, have proved to be efficient. The study presents the characteristics and limitations of the currently available antiadhesive biomaterials, mentioning the recent investigations regarding the use of collagen-based biomaterial, that show promising performance, such as ease of handling and more effective reduction of adhesion.

Keywords: peritoneal adhesions, prevention, biomaterial, collagen

INTRODUCTION

Postoperative adhesion has been reported to be responsible for 60–70% of cases of small bowel obstruction (SBO) and 15–40% of infertilities, approximately 300000 hospital readmissions annually being related to the formation of postoperative adhesions in the USA, the annual financial expenditure for pertinent treatment exceeding $1.3 billion (Suzuki, 2012).

Strategies of prevention of adhesions can be grouped into four categories: general principles, surgical techniques, chemical agents and mechanical barriers. Antiadhesive materials are used as a physical barrier between an injured site and the adjacent tissues. Although several nonabsorbable synthetic materials such as silicone and PTFE have been shown to be effective, bioabsorbable materials are preferred because of the lack of necessity of a second surgical intervention for the removal of the nonabsorbable material. The purpose of the present study is to determine the efficiency of collagen-based biomaterials in preventing localized peritoneal postoperative adhesions, associating a review of literature related to the recent biomaterials used as antiadhesive methods.

MATERIAL AND METHOD

The study represents a single-center prospective, case-control, randomized controlled investigation of the safety and efficacy of collagen-based sponge in preventing the postoperative peritoneal adhesions.

The study group, who underwent an intra-abdominal surgical intervention followed up by intra-peritoneal application of collagen sponge, is compared to a control-group, with blinded evaluation of the therapeutic role of collagen sponge in reducing peritoneal adhesion formation and the need of laparotomy or laparoscopy for adhesiolysis, measuring the incidence, extent, severity and chronic abdominal pain.

30 patients with surgical indication to laparotomy (trauma, oncological or surgical emergencies), admitted at the General Surgery Department of the "Sfântul Pantelimon" Emergency Clinical Hospital, an academic hospital of the University of Medicine and Pharmacy "Carol Davila" in Bucharest, Romania, were organized into two groups, from January 1st 2015 to September 1st 2017, including a 8 months follow-up interval. 15 patients receiving traditional treatment were included in the control group, those from the study group having been received intraperitoneal application of collagen sponge before the abdominal closure.

The collagen-sponge samples were made of 50x50x3 mm, made of 2mg collagen fibers derived from equine tendon covered with 4, 3-6,7mg human fibrinogen, 1, 5-2,5 IU bovine thrombine, 0,055-0,087 Ph.Eur. bovine aprotinine and 7-26mcg riboflavine. The samples were applied in the peritoneal cavity, under sterile conditions, after lavage and cleaning of the surgical site, covering the peritoneal defect, 2-3 cm beyond the edges, before the abdominal closure.

Inclusion criteria were: age over 18 years and under 75 years old, the high risk for peritoneal adhesion formation (patients that needed open surgical intervention, like trauma, oncologic surgery or emergencies), no peritoneal faecal contamination or sepsis and no prior open surgical intervention. Exclusion criteria were: patients under 18 years or over 75 years old, requiring of a simultaneous intervention, pregnancy or participation in other clinical investigations.

Patients were treated, as well as written informed consents for each procedure adopted were collected, according to the usual clinical practice and to the ethical guidelines. Approval by the institutional review committee was obtained, since this study prospectively analyzed patients' data, regarding demographics, diagnosis, duration of hospital stays, complications and mortality. The analysis of the data was made using Microsoft Office Excel 2013 software.

RESULTS

Controls were recruited to match each case, with similar distribution of urban/rural and male/female variables. Regarding the surgical indication for laparotomy, 4 hemodynamically unstable trauma patients from the control group and 5 from the case group, with positive focused assessment with ultrasonography in trauma (FAST exam) or diagnostic peritoneal aspiration/lavage (DPA/DPL), underwent emergent abdominal surgical exploration in order to control life-threatening hemorrhage. The other indications for laparotomy were: 6 patients with mechanical small bowel obstruction (SBO) and 5 with large bowel obstruction (LBO) from the case group, 4 SBO subjects and 6 LBO subjects from the control group (Figure 1. The trauma / SBO /LBO cases that needed surgical intervention).
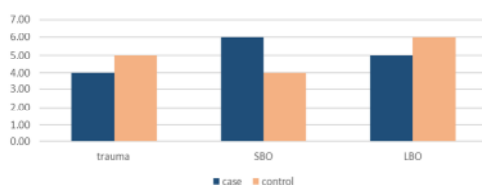
Figure 1. The trauma / SBO /LBO cases that needed surgical intervention

The average duration of the surgical intervention was 2h 45 min in the case group, versus 2h 30 min in the control group, with a mean interval of 10 min required for the intraperitoneal placement of the collagen-based sponge before the abdominal closure (figure 2).
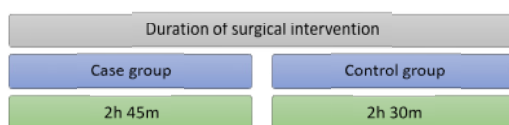
Figure 2. The average duration of the surgical intervention

The immediate postoperative complications taken into consideration in the present study were: ileus, SBO, fever, intraabdominal hematoma or abscess, seroma at the surgical wound and sepsis. In the case group 4 patients suffered prolonged ileus, 6 patients had fever for over 48 h, 1 with intraabdominal hematoma and 4 with seroma. In the control group the results were similar to the case group, with slightly reduced number of patients with ileus or fever (2 patients with prolonged ileus and 4 with fever for over 48 h), 3 intraabdominal hematoma and 6 patients with seroma. No cases of SBO, abscess or sepsis were recorded in both case and control groups (Figure 3).
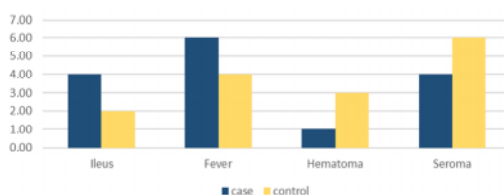
Figure 3. Case-control comparison of the immediate postoperative complications

The length of the hospital stay was an average of 12 days for the case group and 15 days for those from the control group. Evaluation of post-surgical adhesion by second-look laparoscopy was performed at 7 months after initial surgery. At the time of the evaluating laparoscopy, aspects regarding severity, distribution and histopathology of the peritoneal adhesions were analyzed based on the scores proposed by Coccolini *et al*., in 2013, Mazuji and Zhülke, 1965.

According to Coccolini and Mazuji scores, from the case group, 4 patients presented grade 1-3 peritoneal adhesions located, predominately, in the supramesocolic compartment, with no cases of grade 4 peritoneal adhesions. From the control group, 9 patients had grade 1-3 peritoneal adhesions located diffusely and 4 patients presented

grade 4 adhesions. 11 patients from the case group and 2 patients from the control group presented no peritoneal adhesions after 7 months (figure 4).
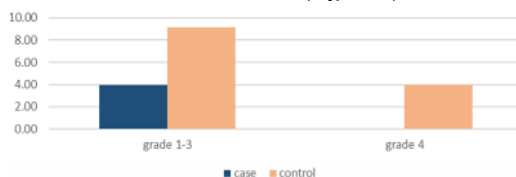
Figure 4. Type of peritoneal adhesion according to Coccolini and Mazuji scores, at the time of the evaluating laparoscopy

According to the histopathological analysis, 3 patients presented loose or firmer connective tissue, grade 1-3 according to Zuhlke scoring, and 1 with grade 4 adhesions, from the case-group, and 10 patients from the control group had grade 1-3, with 2 cases of grade 4 (figure 5).
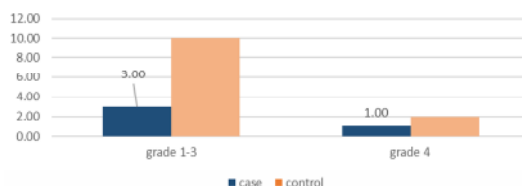
Figure 5. The histopathological analysis of the adhesions, according to Zuhlke classification, after 7 months

Late complications of the postoperative peritoneal adhesion syndrome are known to be infertility in women, chronic abdominal pain and intestinal obstruction. Among the patients from the case group, 3 suffered chronic abdominal pain, for 1 patient surgical reintervention being indicated for SBO. 5 patients from the control group presented chronic abdominal pain within the follow-up interval and 2 patients had SBO, for whom surgical reintervention was indicated. No fertility issues in women were observed, a possible reason being the 8 months interval of follow-up. (Figure 6. Late postoperative complications in the case and control groups).
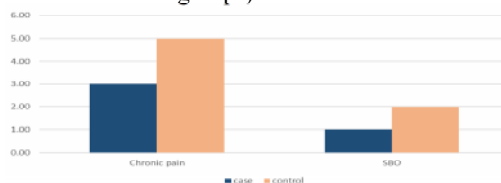
Figure 6. Late postoperative complications in the case and control groups

Thus, surgical re-intervention was indicated for 3 patients out of the total of 30 included in the present research, one from the case group and 2 from the control group. A significant reduction was observed in adhesion incidence and severity when the

collagen sponge was applied in the case groups, reducing the inflammation and the fibrosis processes.

DISCUSSION

The present study aimed to investigate the potential of a spongy sheet composed of 2mg collagen fibers derived from equine tendon covered with 4, 3-6,7mg human fibrinogen, 1, 5-2,5 IU bovine thrombine, 0,055-0,087 Ph.Eur. bovine aprotinine and 7-26mcg riboflavine, to reduce the rate of peritoneal adhesion formation in an in-vivo model.

Animal-derived and recombinant collagens, especially type I represent one of the most useful biomaterials available, being widely used for tissue engineering, cosmetic surgery, and drug delivery systems. They are used either in their native fibrillar form or after denaturation in variously fabricated forms, such as sponges, sheets, plugs, and pellets. Type I collagen sponges have been used in developing patellar tendons in rabbits under different culture conditions. Collagen sponge was combined with mesenchymal stem cells derived from bone-marrow, proving that the resulted neotissue reached about three-fourth of the mechanical properties of the normal tissue (Awad, 2003; Juncosa-Melvin, 2006; Juncosa-Melvin, 2007; Koide, 2007). Equine and bovine collagen type I was proposed and evaluated as 3D scaffolds for reestablishing the collagen fibrillar structure of the peritoneum or skin, such substitutes being, nowadays, commercialized extensively (e.g., Tutomesh from Tutoplast, Apligraf from Organogenesis, Inc. and OrCel from Ortec Int.) (Chung, 2007; Nair, 2007). The anti-adhesive efficacy of the spongy sheet of collagen-based biomaterial derived from equine tendones was evaluated in animal experiments using Sprague Dawley rats. Under anesthesia, a $1\,cm \times 2\,cm$ segment of peritoneum was superficially excised from walls, with the cecum being abraded by scraping with a scalpel blade over a $1\,cm \times 2\,cm$ area. A piece of spongy sheet of collagen was placed on the peritoneal defect, both defects being, consecutively, placed in contact, before the abdominal closure. 7 days after the surgical application of the collagen sponge, the peritoneal condition was evaluated, demonstrating the role of the biomaterial used in the study in facilitating the wound healing of surgically excised tissue and preventing surgically excised tissue from adhering to adjacent structures (Misato, 2014).

The feasibility of using collagen as biomaterials for engineering collagen (type I) tissues in peritoneum, tendon and skin can be ascertained, but, the use of animal-derived products may be compromised by possible allergic reactions and pathogen transmission. Because recombinant collagen does not undergo significant posttranslational modifications, the efficacy of the animal-derived collagen biomaterials may be decreased by the lack of biologic activities of native tissue.

Replicating the nanoscaled structures and the molecular components of native collagen fibrils shed light on the desired bioactivities of those novel biomaterials. Although only oversimplified replicas can be developed currently, they still represent advances in biomaterials engineering and cell biology, even though current application is still at the beginning. The application of biomaterials, such as animal-derived collagen, has provided further insight into biomaterial-cellular interactions, further refinement of current biotechnology being necessary for the evolution of tissue engineering in the future.

To promote further development of tissue engineering and clinical applicability of these products, it is important to optimize fabrication and application that provides satisfactory interaction and imitation of biologic functions.

CONCLUSIONS

Postsurgical adhesion syndrome represents a major health problem with impact on both quality of life and health-care costs. General intraoperative preventative practices such as use of starch-free gloves, avoidance of unnecessary peritoneal dissection, and avoidance of spillage of intestinal contents or gallstones may reduce the risk of adhesions, but the use of adhesion barriers is necessary in high-risk procedures. Equine and bovine collagen type I provides a 3D scaffold for reestablishing the collagen fibrillar structure of the peritoneum, representing an effcient method in the prevention of the postoperative peritoneal adhesions. Animal- derived collagen substitutes used in the prevention of the postoperative peritoneal adhesion syndrome are, nowadays, commercialized extensively. There is still no unequivocally effective adhesion-reducing barrier. Continuing research is needed for the development of more effective products for reduction of adhesions.

REFERENCES

Awad, H.A. *et al*. (2003), "Repair of patellar tendon injuries using a cell-collagen composite", *The Journal of Orthopaedic Research,* 21, 420–431, https://doi.org/10.1016/S0736-0266(02)00163-8.

Chung, H.J. and Park, T.G. (2007), "Surface engineered and drug releasing pre-fabricated scaffolds for tissue engineering", *Advance Drug Delivery Review*, 59, 249–262, https://doi.org/10.1016/j.addr.2007.03.015.

Coccolini, S. (2013), "Peritoneal adhesion index (PAI): proposal of a score for the "ignored iceberg" of medicine and surgery", *World Journal of Emergency Surgery*, 8, 6, https://doi.org/10.1186/1749-7922-8-6.

Johns, A. (2001), "Evidence-based prevention of post-operative adhesions", *Human Reproduction Update,* 7, 577–9, https://doi.org/10.1093/humupd/7.6.577.

Juncosa-Melvin, N. *et al*. (2007), "Mechanical stimulation increases collagen type I and collagen type III gene expression of stem cell-collagen sponge constructs for patellar tendon repair", *Tissue Engineering,* 13, 1219–1226, https://doi.org/10.1089/ten.2006.0339.

Juncosa-Melvin, N. *et al*. (2006), "Effects of mechanical stimulation on the biomechanics and histology of stem cell-collagen sponge constructs for rabbit patellar tendon repair", *Tissue Engineering,* 12, 2291–2300, https://doi.org/10.1089/ten.2006.12.2291.

Koide, T. (2007), "Designed triple-helical peptides as tools for collagen biochemistry and matrix engineering", *Philosophical transactions of the Royal Society of London. Series B, Biological sciences,* 362, 1281–1291, https://doi.org/10.1098/rstb.2007.2115.

Malinak, L.R. and Young, A. (1997), "Peritoneal closure: when and why", *Contemporary Obstetrics and Gynecology*, 42, 102–12.

MaZuJI, M. and FaDhLI, H.A. (1965), "Peritoneal adhesions; prevention with povidone and dextran", *Archives of Surgery,* 91, 872-874, https://doi.org/10.1001/archsurg.1965.01320180006002.

Misato, K. *et al*. (2014), "Development of anti-adhesive spongy sheet composed of hyaluronic acid and collagen containing epidermal growth factor", *Journal of Biomaterials Science, Polymer Edition,* 25, 13-12.

Nair, L.S. and Laurencin, C.T. (2007), "Biodegradable polymers as biomaterials", *Progress in Polymer Science,* 32, 762–798, https://doi.org/10.1016/j.progpolymsci.2007.05.017.

Suzuki, Y. and Ikada, Y. (2012), *Biomaterials for Surgical Operation*, Springer Science+Business Media, LLC.

Tulandi, T. and Al-Jaroudi, D. (2003), "Nonclosure of peritoneum: a reappraisal", *American Journal of Obstetrics and Gynecology*, 189(2), 609–12, https://doi.org/10.1067/S0002-9378(03)00299-0.

Ulandi, T. *et al*. (1988), "Closure of laparotomy incisions with or without peritoneal suturing and second-look laparoscopy", *American Journal of Obstetrics and Gynecology*, 158, 536–7, https://doi.org/10.1016/0002-9378(88)90020-8.

APPLICATION OF GAMMA IRRADIATION FOR THE FUNCTIONALIZATION OF TEXTILE MATERIALS

OVIDIU CĂPRARU[1], COSMIN HERMAN[1], BOGDAN LUNGU[1], IOANA STĂNCULESCU[1,2]

[1]*Horia Hulubei National Institute for Physics and Nuclear Engineering, Dept IRASM, 30 Reactorului Str, 077125 Magurele, Ilfov Romania*

[2]*University of Bucharest Dept of Physical Chemistry, Regina Elisabeta Bld 4-12, 030018 Bucharest Romania, istanculescu@nipne.ro*

This work focuses on the synthesis of multiple studies made on the investigation of gamma irradiation effects on textiles. Gamma radiation is used in the research for improved dyeing or to change the mechanical properties of textile and in some cases to reduce the ecological impact of the processing methods. One study researches the effects of gamma irradiation on specific composites such as silk with polypropylene and E-Glass with polypropylene and the changes of their mechanical properties, showing that the mechanical properties of the silk composite increase more compared to the E-Glass composite. The application of gamma irradiation in the process of dying polyester textiles can be used to reduce the dyeing temperature. Studies were made even on the effect of gamma irradiation only on dyes and the possibility that it can reduce wastewater production, resulting in the fact that gamma irradiation can result in the degradation and discoloration of dyes in water depending on the dose and dye used. In one study it was researched if gamma preirradiation can affect the growth of microorganism on the textiles for three different fibers. One study was made on reinforcement of synthetic fibers and compared the effect of e-beam radiation and gamma radiation. It resulted that the effects are similar while gamma radiation affects the mechanical properties more than e-beam.The synthesis of the literature review has lead to the development of a conceptual application model for gamma irradiation in the field of textiles.

Keywords: gamma irradiation, functionalization, textile.

INTRODUCTION

The textile industry is a major branch of the world's economy, some of its biggest producers and exporters being China, India and Italy. Textiles have been found to originate as early as the Neolithic period from evidence found in excavations, with some indication that weaving was known even in Paleolithic. Over time the materials and techniques evolved and become more sophisticated such as the creation of synthetic textiles.

Gamma radiation is an electromagnetic penetrative ionizing radiation produced during the radioactive decay of the atomic nucleus. One of the main results of gamma irradiation is the excitation of the electron resulting in ionization from which may result bond breaking, the effects being formation of excited states, short life radicals and finally formation of new bonds. Two of the main zones where it is used are industry and research. In industry it can be used for sterilization, DNA alteration in plants and structure and properties material modification. Research in using gamma irradiation for textiles concerns the optimization of textile dyeing, reducing the ecological impact and cultural heritage artifacts biological decontamination (Ahmad Bhatti *et al*., 2012; Bashar *et al*., 2018; Blouin and Arthur, 1958; Chirila *et al*., 2018; Colella *et al*., 2011; Geba *et al*., 2014; Machnowski *et al*., 2012; Millington, 2000; Shubhra and Alam, 2011; Takács *et al*., 2001; Takács *et al*., 2000).

This article objective is to review some of the more relevant research made in the usage of gamma radiation for textile functionalization and in the end to propose a conceptual model of the process variants.

Literature Review

In the Table 1 is given the synthesis of the case studies related to the application of gamma treatment to various textile materials.

Table 1. Textile material, irradiation dose and characterization tests performed and conclusions of literature research study

Materials	Dose (kGy)	Tests	Objective	Observations	References
Cotton+H$_2$O$_2$	5, 10, 15, 20	SEM	Exploitation of gamma radiation for the processing of cotton textiles	No impurities and smooth	Ahmad Bhatti et al., 2012
Grey Cotton	100		Effect of gamma irradiation on the mechanical properties and surface morphology	Longitudinal crack in the second cellular wall	Bashar et al., 2018
Cotton + Itodye Nat Pomegranate+ Iron alum	5, 10, 15, 20, 45		To improve the dyeing behavior of Itodye Nat Pomegranate	No observed structural changes	Blouin and Arthur, 1958
Cotton + NaOH	Unspecified directly		Effects of gamma irradiation and alkaline treatment on the structure of cotton cellulose	Changes in fibrils structure starts to be observed after irradiation with 300 kGy and treatment with 14% NaOH	Chirila et al., 2018
Grey Cotton	5, 10, 15, 20	FTIR	Exploitation of gamma radiation for the processing of cotton textiles	Peaks at 2918 and 2849 cm^{-1} are responsible for the presence of waxes	Ahmad Bhatti et al., 2012
Colored Cotton				Showed many peaks in 1100-1400 cm^{-1} region	
Colored Cotton	1000		Radiation induced deterioration of textile fibers and the potential impact of radiation damaged fibers on the results of the forensic analysis	Nothing different observed in FTIR	Colella et al., 2011
Cotton +NaOH/TMAH	Up to 300		The comparison of two types of alkalies on the crystalline structure of irradiated cotton	It was observed the transformation of cellulose I in cellulose II depending on the radiation dose and alkali treatment	Geba et al., 2014
Cotton	0.877, 8.77, 43.85, 87.7, 438.5, 877		Effects of gamma radiation on the physical and chemical properties of purified cotton in oxygen and nitrogen atmosphere	Relative unchanged FTIR spectra	Machnowski et al., 2012
	5, 10, 15, 20, 45		To improve the dyeing behavior of Itodye Nat Pomegranate	No important differences	Blouin and Arthur, 1958

	Up to 500		Effects of gamma irradiation and alkaline treatment on the structure of cotton cellulose	Increase absorbance at 1740 cm^{-1} as consequence of radiation degradation	Chirila et al., 2018
Cotton+H$_2$O$_2$	100	Mechanical tests	Exploitation of gamma radiation for the processing of cotton textiles	The bursting strength decreases with the H$_2$O$_2$ concentration	Ahmad Bhatti et al., 2012
Cotton	5, 10, 25, 100		Effect of gamma irradiation on the mechanical properties and surface morphology	Irradiation causes a decrease of the breaking force and elongation at break depending on the dose. Irradiation with doses between 5-25 kGy does not cause statistically significant differences	Bashar et al., 2018
	0.877, 8.77, 43.85, 87.7, 438.5, 877		Effects of gamma radiation on the physical and chemical properties of purified cotton in oxygen and nitrogen atmosphere	Decrease in tensile strength of the fibers	Machnowski et al., 2012
Cotton + Itodye Nat Pomegranate+ Iron alum	5, 10, 15, 20, 45		To improve the dyeing behavior of Itodye Nat Pomegranate	Lower tensile strength, pre-treatment with gamma radiation does not negatively influence elongation at break.	Blouin and Arthur, 1958
Cotton +NaOH/TMAH	Up to 300	XRD	The comparison of two types of alkaline on the crystalline structure of irradiated cotton	It was observed the transformation of cellulose I in cellulose II	Geba et al., 2014
Cotton +NaOH	Up to 500		Effects of gamma irradiation and alkaline treatment on the structure of cotton cellulose		Chirila et al., 2018
Cotton + Reactive Black-5	0.1, 0.2, 0.3, 0.4, 0.5, 0.6	Color strength	The improvement of color strength and fastness for Reactive Black-5 using high energy radiation	Color strength increases with radiation doze and temperature up to 60°C	Millington, 2000
Cotton + Itodye Nat Pomegranate	5, 10, 15, 20, 45		To improve the dyeing behavior of Itodye Nat Pomegranate	It's observed an increase in color strength with the dose	Blouin and Arthur, 1958
Colored Wool	1000		Radiation induced deterioration of textile fibers and the potential impact of radiation damaged fibers on the results of the forensic analysis	Nothing different observed in FTIR	Colella et al., 2011
Wool + Artificial ageing	10, 25	FTIR-ATR Mechani	To demonstrate that gamma irradiation does not destroy too much	Modification in the Amide I and II ratio Reduced breaking force and	Shubhra and Alam, 2011

		cal tests		elongation at break	
Wool	9.1, 25, 50, 100, 250, 500		To determine if gamma radiation can be used in the wool processing chain	At doses above 100 kGy the burst strength is reduced by 15%	Takács et al., 2001
Wool + Artificial ageing	10, 25	TG and DTG	To demonstrate that gamma irradiation does not destroy too much	Degradation starts at 230-234 ^{o}C with minor changes caused by radiation or ageing, irradiation up to 10 kGy does not have great influence on thermal stability	Shubhra and Alam, 2011
Wool	9.1, 25, 50, 100, 250, 500	Color changes	To determine if gamma radiation can be used in the wool processing chain	Color changes to pink-red for 25-250 kGy and yellow at 500 kGy	Takács et al., 2001
Silk	100	SEM	Effect of gamma irradiation on the mechanical properties and surface morphology	No visible difference compared to the control sample	Bashar et al., 2018
Silk	10, 25	FTIR	Determination of the optimal radiation dose for heritage textile decontamination	Modification in the Amide I and II ratio	Shubhra and Alam, 2011
Silk	5, 10, 25, 100	Mechanical Tests	Effect of gamma irradiation on the mechanical properties and surface morphology	Irradiation causes a decrease of the breaking force and elongation at break depending on the dose. Irradiation with doses between 5-25 kGy does not cause statistically significant differences	Bashar et al., 2018
Silk+Polypropylene	2.5, 5, 10		The comparison of gamma radiation effect on silk/PP and E-Glass/PP composites	Improved tensile, bending and impact properties, hardness unchanged until 5 kGy but changes at 10kGy	Takács et al., 2000
Silk	10, 25		Determination of the optimal radiation dose for heritage textile decontamination	Reduced breaking force and elongation at break	Shubhra and Alam, 2011
Silk	10, 25	TG and DTG		Both in air and nitrogen atmosphere thermal stability is lower, endothermic peak temperature slightly increased with dose, insignificant changes in thermal stability with dose	
Flax	100	SEM	Effect of gamma irradiation on the mechanical properties and surface morphology	No visible difference compared to the control sample	Bashar et al., 2018
Flax+ Itodye Nat Pomegranate+ Iron	5, 10, 15, 20, 45		To improve the dyeing behavior of Itodye Nat Pomegranate	Changes dependent on the dose can be observed	Blouin and Arthur, 1958

alum					
Flax	5, 10, 25, 100	Mechanical Tests	Effect of gamma irradiation on the mechanical properties and surface morphology	Irradiation causes a decrease of the breaking force and elongation at break depending on the dose. Irradiation with doses between 5-25 kGy does not cause statistically significant differences	Bashar *et al.*, 2018
Flax+ Itodye Nat Pomegranate+ Iron alum	5, 10, 15, 20, 45		To improve the dyeing behavior of Itodye Nat Pomegranate	Lower tensile strength, pre-treatment with gamma radiation does not negatively influence elongation at break.	Blouin and Arthur, 1958
	5, 10, 15, 20, 45	FTIR		No important differences but the crystallinity indices present an irregular variation	
	5, 10, 15, 20, 45	Color Strength		It's observed an increase in color strength with the dose	

As can be seen there are few studies and more research need to be done in the domain to create a real functional model for the treatment of textiles using gamma radiation. Nevertheless a simplified model is proposed in Fig. 1:
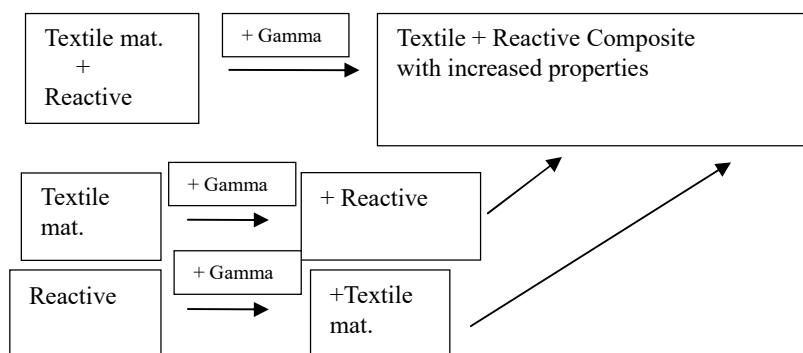
Figure 1. Conceptual model of textile materials functionalization by irradiation

Irradiation may be performed in dry or wet state at various dose ratios and at total absorbed doses in order to obtain the desired properties.

CONCLUSIONS

Our study revealed that the majority of the studies focus on the effect of gamma irradiation on natural textiles, the majority of experiments being done in air atmosphere. The main effect observed was that the mechanical properties slightly diminished while if there are dyes used the color strength is increased. Gamma irradiation can be used to increase mechanical properties if the textile is used in combination with various compounds. Research and development in the application of gamma irradiation to

textile materials is in the laboratory phase a lot of technological development needs to be done in order to be able to apply this green treatment method in industry.

REFERENCES

Ahmad Bhatti, I., Adeel, S., Nadeem, R. and Asghar, T. (2012), "Improvement of colour strength and colourfastness properties of gamma irradiated cotton using reactive black-5", *Radiation Physics and Chemistry*, 81(3), 264-266, https://doi.org/10.1016/j.carbpol.2014.11.023.

Bashar, M., Siddiquee, M. and Khan, M. (2018), *Preparation of cotton knitted fabric by gamma radiation: A new approach*, https://doi.org/10.1177/0040517512449045.

Blouin, F. and Arthur, J. (1958), "The Effects of Gamma Radiation on Cotton", *Textile Research Journal*, 28(3), 198-204, https://doi.org/10.1016/j.radphyschem.2017.12.017.

Chirila, L., Popescu, A., Cutrubinis, M., Stanculescu, I. and Moise, V. (2018), "The influence of gamma irradiation on natural dyeing properties of cotton and flax fabrics", *Radiation Physics and Chemistry*, 145, 97-103, https://doi.org/10.1016/S0969-806X(99)00409-0.

Colella, M., Parkinson, A., Evans, T., Robertson, J. and Roux, C. (2011), "The Effect of Ionizing Gamma Radiation on Natural and Synthetic Fibers and Its Implications for the Forensic Examination of Fiber Evidence", *Journal of Forensic Sciences*, 56(3), 591-605, https://doi.org/10.1111/j.1556-4029.2010.01654.x.

Geba, M., Lisa, G., Ursescu, C., Olaru, A., Spiridon, I., Leon, A. and Stanculescu, I. (2014), "Gamma irradiation of protein-based textiles for historical collections decontamination", *Journal of Thermal Analysis and Calorimetry*, 118(2), 977-985, https://doi.org/10.1163/15685670152622103.

Machnowski, W., Gutarowska, B., Perkowski, J. and Wrzosek, H. (2012), "Effects of gamma radiation on the mechanical properties of and susceptibility to biodegradation of natural fibers", *Textile Research Journal*, 83(1), 44-55, https://doi.org/10.1177/004051755802800302.

Millington, K. (2000), "Comparison of the effects of gamma and ultraviolet radiation on wool keratin", *Coloration Technology*, 116(9), 266-272, https://doi.org/10.1016/j.radphyschem.2011.10.019.

Shubhra, Q. and Alam, A. (2011), "Effect of gamma radiation on the mechanical properties of natural silk fiber and synthetic E-glass fiber reinforced polypropylene composites: A comparative study", *Radiation Physics and Chemistry*, 80(11), 1228-1232, https://doi.org/10.1007/s10973-014-3988-8.

Takács, E., Wojnárovits, L., Földváry, C., Borsa, J. and Sajó, I. (2001), "Radiation activation of cotton-cellulose prior to alkali treatment", *Research on Chemical Intermediates*, 27(7-8), 837-845, https://doi.org/10.1111/j.1478-4408.2000.tb00045.x.

Takács, E., Wojnárovits, L., Földváry, C., Hargittai, P., Borsa, J. and Sajó, I. (2000), "Effect of combined gamma-irradiation and alkali treatment on cotton–cellulose", *Radiation Physics and Chemistry*, 57(3-6), 399-403, https://doi.org/10.1016/j.radphyschem.2011.04.010.

FUNCTIONAL FINISHING OF TEXTILES USING BIOACTIVE AGENTS BASED ON NATURAL PRODUCTS

LAURA CHIRILĂ[1], ALINA POPESCU[1], LAURA CHIRIAC[1], RODICA ROXANA CONSTANTINESCU[2], ELENA-CORNELIA MITRAN[1], CIPRIAN CHELARU[2], MARIAN RAȘCOV[1]

[1]*The National Research and Development Institute for Textile and Leather, 16 Lucretiu Patrascanu Street, 030508, Bucharest, Romania, e-mail: certex@ns.certex.ro*

[2]*INCDTP - Division: Leather and Footwear Research Institute*, *93 Ion Minulescu Street, 031215, Bucharest, Romania, e-mail: icpi@icpi.ro*

There is nowadays an increasing vogue for so-called cosmetic textiles which are essentially garments that are designed to come into contact with the skin, which then transfer some active substances that may be used for cosmetic purposes. In order to obtain the textile materials with potential for use in the development of cosmetic textiles, this study approached the experimentation of deposition by padding and exhaustion of commercial rose microcapsules on knitted textile structures with different fiber compositions. The finished textile materials were characterized in terms of functionalization treatments durability, release of bioactive compounds in sweat solution and antibacterial activity, respectively. In order to identify the functionalization method which ensures the deposition of a high content of microcapsules on the knitted fabric surface, which implicitly leads to a high functional effect, solid-liquid and liquid-liquid extraction method for sample preparation and a gas chromatography with mass spectrometry detection (GC-MS) for identification of active compunds have been involved. SEM analysis was used to investigate the distribution of microcapsules on the textile materials surface, before and after 1 washing cycle and 9000 abrasion cycles. Antibacterial activity of treated samples has been evaluated before and after 1 washing cycle against the *Staphylococcus aureus* test strains.

Keywords: knitted textile materials, rose essential oil, GC-MS, SEM

INTRODUCTION

Health and beauty are an increasing vogue for everybody in this entire world. In recent years, cosmetic textiles take over as a rapidly growing and developing segment of functional textiles used in health and hygiene sectors, means new target groups and new markets for textile industry (Azizi *et al*., 2014). Microencapsulation technology is gaining wide acceptance in a broad range of industrial applications in markets such textiles, drug delivery systems, pesticides and agrochemicals, consumer care and adhesives. Some active substances which are used for cosmetic purpose are then introduced to the skin through friction or other trigger mechanisms, in particular to combat ageing effects in order to promote the younger look (Alonso *et al*., 2013).

Rose essential oil is especially great for dry or aging skin. Researchers have found that it contains several therapeutic compounds known to promote healing, especially antimicrobial and anti-inflammatory compounds. As a result, rose essential oil helps refine skin texture and tone, and can be helpful with managing skin conditions such as psoriasis and dermatitis.

In order to obtain the textile materials with potential for use in the development of cosmetic textiles, this study approached the experimentation of deposition by padding and exhaustion of commercial microcapsules with rose essential oil content on knitted textile structures with different fiber compositions.

EXPERIMENTAL PART

Materials

Deposition of microcapsules dispersions was performed on 100% cotton pique knitted fabric with the weight of 196 g/m^2 (Code V1) and 50% cotton / 50% polyester interlock knitted fabric with the weight of 178 g/m^2 (Code V2). For functionalization treatments, highly concentrated rose essential oil microcapsules slurry from Rudolf Duraner (Turkey) with 80% active content has been used. Binder ST from Rudolf Duraner (Turkey) has been used for the fixation of microcapsules on textile materials.

Functionalization Treatments

Prior to functionalization treatments the textile fabrics were subjected to preliminary preparation by hot alkaline treatment and bleaching.

Padding Method (P)

The deposition of microcapsules on the textile materials was performed in a single bath, on the laboratory padder (Roaches, UK) with 9.6 g/L microcapsule slurry and 2.4 g/L Binder ST, with a wet pick-up rate of 100 %. Drying of the impregnated textile materials was carried out at a temperature of 100°C for 2 minutes on the drying/ curing/ heat-setting/ vaporization unit, model TFO/S 500 mm (ROACHES, UK).

Exhaustion Method (E)

In the exhaustion method, the textile materials were treated with 1,6% microcapsule slurry (w/v) and 0,4% Binder ST (w/v) at MLR (material to liquor ratio) 1:20 for 20 minutes at 50°C. The pH=5 of the process bath was ajusted with CH_3COOH (60%). The treated textile materials were then squeezed and dried at 100°C for 2 minutes. For the functionalization treatments, the laboratory equipment Ugolini (Italy) has been used.

Methods

Durability to Washing

The samples treated with microcapsules have subjected to 1 wash cycle under the following conditions: 2g/L detergent containing no phosphate and bleaching agent, at a temperature of 40°C for 30 minutes. Samples were subsequently rinsed with cold water, freely dried horizontally and then analized by GC-MS method and SEM.

Durability to Abrasion

According to the SR EN ISO 12947-2/2017 standard, the treated fabrics were tested by the Martindale Abrasion Tester for 9000 abrasion cycles. The presence of the microcapsules after an abrasion test was observed by SEM.

Release of Active Compounds to Sweat (Acidic and Alkaline)

For the release assessment of bioactive compounds to sweat, the samples were immersed during 30 minutes in alkaline and acidic solutions. The identification of the main active compunds remained on the treated samples was performed by GC-MS.

Antibacterial Tests

The antibacterial activity of the treated samples was qualitatively assessed through agar diffusion method according with the SR EN ISO 20645:2004 standard, by using of cultures in liquid medium of ATCC 6538 *Staphylococcus aureus* test strains (Gram-positive). The samples were disposed on the culture medium in the middle of Petri plates, and after were incubated at 37°C for 24 h. In order to asses the durability of applied treatment the samples were also tested after 1 washing cycle.

Gas-Chromatography (GC-MS)

For GC-MS analysis, 0,3 g textile material were cut in small pieces and then extracted in 30 mL distilled water by agitation at 500 rpm, during for 10 minutes, after that the extracted solution was filtered. 30 mL ethyl acetate was added in the filtered solution and the solution was agitated for 3 minutes, while the organic phase was separated. Gas-Chromatography was carried out with an Agilent 6890N Gas-Chromatograph coupled with 5973N Mass Spectrometer (USA).

RESULTS AND DISCUSSION

Gas-Chromatography (GC-MS)

Retention time (Rt), CAS number and peaks area for the representative compounds identified on the functionalized samples are shown in Table 1.

Table 1. Main compounds indentified by GC-MS

Rt	CAS	Component	Area	Rt	CAS	Component	Area
		V1E				V1P	
6.46	1117-61-9	(R)-(+)-β-Citronellol	128655	6.46	1117-61-9	(R)-(+)-β-Citronellol	184020
6.98	624-15-7	Geraniol	51633	6.98	624-15-7	Geraniol	78645
11.71	90-17-5	Rose acetate	45069	11.71	90-17-5	Rose acetate	31432
13.21	110-27-0	Isopropyl myristate	95213	13.21	110-27-0	Isopropyl myristate	49388
-	-	-	-	9.09	97-53-0	Eugenol	21786
		V2E				V2P	
6.46	1117-61-9	(R)-(+)-β-Citronellol	117487	6.46	1117-61-9	(R)-(+)-β-Citronellol	162723
6.98	624-15-7	Geraniol	43716	6.98	624-15-7	Geraniol	68934
11.71	90-17-5	Rose acetate	32200	11.71	90-17-5	Rose acetate	37565
13.21	110-27-0	Isopropyl myristate	61312	13.21	110-27-0	Isopropyl myristate	52364

GS-MS analysis identified the main components of rose essential oil, such us: rose acetate, R)-(+)-β-Citronellol, geraniol, isopropyl myristate, and eugenol.

From the GC-MS data, a clear delimitation between the experimental variants and the most efficient solution in terms of immobilization of the microcapsules with rose essential oil on the surface of the textile materials cannot be made.

Functionalization Treatments Durability to Washing

Retention time (Rt), CAS number and peaks area for the representative compounds identified on the functionalized samples after 1 washing cycle and treatment with sweat (alkaline and acidic) solution are depicted in Table 2.

Table 2. Main compounds indentified on the samples after 1 washing cycle / treatment to sweat solution

Rt	CAS	Component	Area	Rt	CAS	Component	Area
				1 washing cycle			
		V1E				V1P	
11.71	90-17-5	Rose acetate	14069	11.71	90-17-5	Rose acetate	17202
13.21	110-27-0	Isopropyl myristate	17648	13.21	110-27-0	Isopropyl myristate	20947
		V2E				V2P	
11.71	90-17-5	Rose acetate	17653	11.71	90-17-5	Rose acetate	18370
13.21	110-27-0	Isopropyl myristate	33495	13.21	110-27-0	Isopropyl myristate	42800
				Release to sweat			
	Acidic perspiration				Alkaline perspiration		
		V1E					
-	-	-	-	6.45	1117-61-9	(R)-(+)-β-Citronellol	16223
11.71	90-17-5	Rose acetate	7125	11.71	90-17-5	Rose acetate	6195
-	-	-	-	13.21	110-27-0	Isopropyl myristate	3334
		V1P					
6.45	1117-61-9	(R)-(+)-β-Citronellol	19129	11.71	90-17-5	Rose acetate	5121
11.70	90-17-5	Rose acetate	5148	13.21	110-27-0	Isopropyl myristate	3558
		V2E					
6.46	1117-61-9	(R)-(+)-β-Citronellol	18581	11.71	90-17-5	Rose acetate	5812
11.71	90-17-5	Rose acetate	6020	-	-	-	-
		V2P					
11.70	90-17-5	Rose acetate	3580	11.70	90-17-5	Rose acetate	3483

Analyzing the data obtained after 1 washing cycle, it can be observed that (R)-(+)-β-citronellol and geraniol components were not been highlighted for all the samples, meaning that durability of the treatment is decreased. However, some of the main compounds have been identified, confirming that the microcapsules remained loaded after 1 washing cycle. The amount of rose acetate component decreased when the impregnated textile knitted fabrics were subjected to 1 washing cycle, the loss of this component ranging from 45% (V1P, V2E) to 69 % (V1E). Also, the isopropyl myristate component decrease after 1 washing cycle, the small decrease being around of 18 %, observed for the 50 % cotton / 50 polyester knitted fabric treated by padding method (V2P).

Regarding the release of active compounds to sweat solution, it can be noticed that the peak areas for compounds remained on the samples after treatment are substantially diminished, indicated the release tendency that occurs after treatment to sweat.

Electron Microscopy

SEM images obtained at a magnification of x 2000 for analyzed samples before and after 1 washing cycle and 9000 abrasion cycles are shown in Figure 1.

V1E   V1P   V1E   V2P

1 washing cycle

V1E   V1P   V2E   V2P

9000 abrasion cycles

V1E   V1P   V2E   V2P
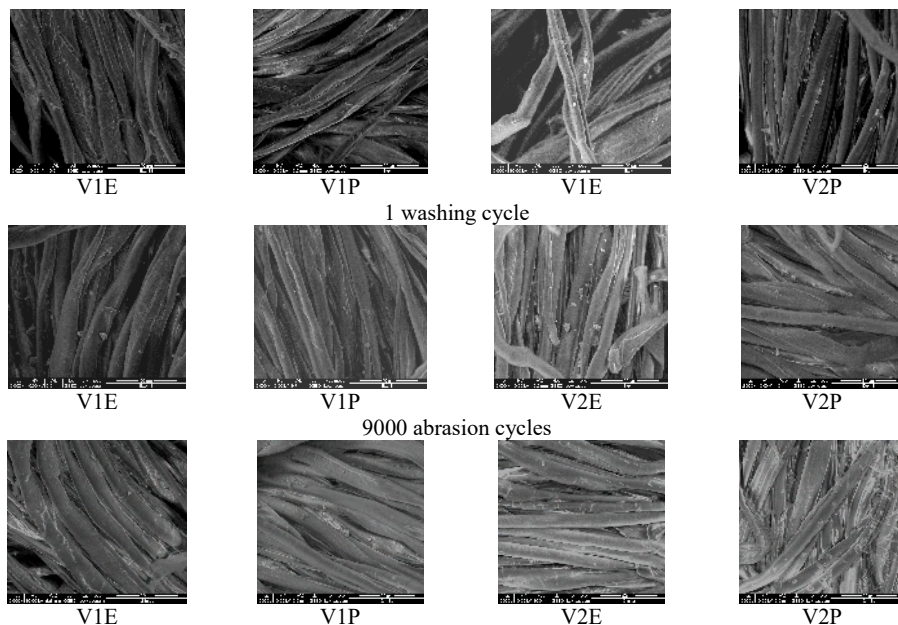
Figure 1. SEM images for the analyzed samples

SEM micrographs registered for the functionalized fabrics highlights that the microcapsules were successfully embedded in the textile materials structure. 1 washing cycle reveal that part of the microcapsules still adhered to the fibers surface and the washing operation did not cause any significant damages to the microcapsules. The amount of the microcapsules is significantly lower after 9000 abrasion cycles, only few microcapsules were still found adhering to the fiber surface.

Antibacterial Tests

Images of Petri plates after 48 h incubation are shown in Figure 2.

Control	Functionalized samples		1 washing cycle	
M1	V1E	V1P	V1E	V1P
M2	V2E	V2P	V2E	V2P
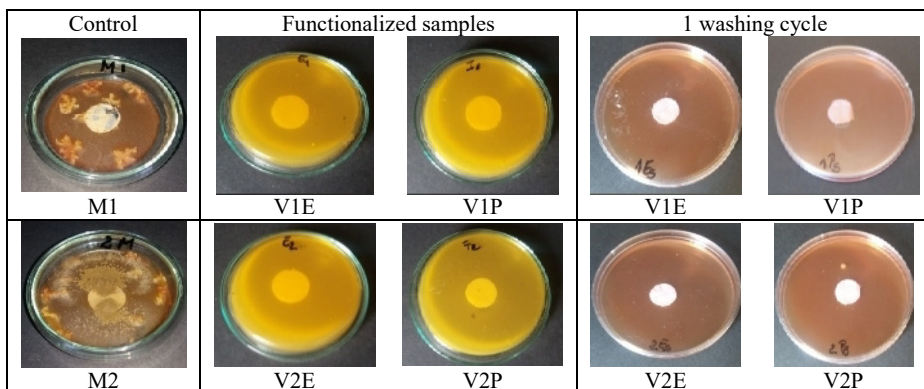
Figure 2. Images of Petri plates after 24 h incubation

It can be observed that the knitted fabrics before washing shows a good antibacterial effect against *S. aureus* (Figure 1), but after 1 washing cycle, the effect is reduced being evaluated at the efficacy limit (0 mm inhibition area and slight growth of bacteria).

CONCLUSIONS

The commercial microcapsules with rose essential oil content were embedded in the cotton and cotton/polyester knitted fabrics by using padding and exhaustion techniques. From the GC-MS data, a clear delimitation between the experimental variants and the most efficient solution in terms of immobilization of the microcapsules on the surface of the textile materials cannot be made. The peak areas for compounds remained on the samples after treatment to sweat solution are substantially diminished indicated the release tendency that occurs. The overall results confirmed that the functionalized treatments withstand 1 washing cycle, but the amount of the microcapsules is significantly lower after 9000 abrasion cycles. An antibacterial effect against the *Staphylococcus aureus* test strain is observed for all experimental variants, antibacterial activity decrease after 1 washing cycle.

REFERENCES

Azizi, N., Chevalier, Y., Majdoub, M. (2014), "Isosorbide-based microcapsules for cosmeto-textiles", *Industrial Crops and Products*, 52,150-157, https://doi.org/10.1016/j.indcrop.2013.10.027.
Alonso, C., Martí, M., Martínez V., Rubio L., Parra, J. L., Coderch L. (2013), "Antioxidant cosmeto-textiles: Skin assessment", *Eur J Pharm Biopharm*., 84, 192–199, https://doi.org/10.1016/j.ejpb.2012.12.004.

TISSUE ENGINEERING - COLLAGEN SPONGE DRESSING FOR CHRONIC WOUNDS

VLAD DENIS CONSTANTIN[1,2], ALEXANDRU CARÂP[1,2], SIMONA BOBIC[1,2], VLAD BUDU[1,2], MĂDĂLINA ALBU KAYA[5], ŞTEFANIA MARIN[3,5], MARIA MINODORA MARIN[4,5], BOGDAN SOCEA[1,2]

[1] ”Carol Davila" University of Medicine and Pharmacy, Surgery Department, Bucharest, Romania, Corresponding author: Bogdan Socea, constantindenis@yahoo.com

[2] "Sfântul Pantelimon" Emergency Clinical Hospital, Surgery Department, Bucharest, Romania

[3] University Politehnica of Bucharest, Center of Surface Science and Nanotechnology, Splaiul Independentei 313, Romania

[4] University Politehnica of Bucharest, Faculty of Applied Chemistry and Materials Science;

[5] INCDTP - Division: Leather and Footwear Research Institute, Bucharest 031215, Romania, madalina.albu@icpi.ro

The high number of available wound dressing materials as well as the scientific reports about the topic indicate that the problem of an ideal wound dressing is to be solved. For the last half of century many scientific reports about collagen as wound covering have been published, the benefits of collagen application as a wound dressing being proved. The aim of the present study is to demonstrate the efficiency of the collagen sponge on healing full thickness skin wounds. The study population was divided into two groups: control and experimental. In the control group, the wounds were treated conventionally, using gauze swabs, in the experimental group such wounds being covered with collagen sponge, the results being compared. The wounds from the control group healed in 50 days, covering the wounds with collagen sponge in the case-group shortening the healing process to 27 days. Not only the healing time was shortened but also the quality of the wound repair by dressing the wounds with collagen sponge was enhanced.

Keywords: chronic wounds, collagen sponge, dressing, biomaterial.

INTRODUCTION

There are a number of different collagen dressings commercially available, which employ a variety of carriers/combining agents such as gels, pastes, polymers, oxidized regenerated cellulose (ORC) and ethylene diamine tetraacetic acid (EDTA).

The collagen contained in these products may be derived from bovine, porcine, equine, or avian sources, in a purified form in order to render it nonantigenic. The collagen dressings vary in concentration and type of collagen contained, some of them comprising type I (native) collagen, whereas, other collagen dressings containing denatured collagen. Apart from collagen, these dressings may, also, contain ingredients, such as alginates and cellulose derivatives that can enhance absorbency, flexibility, and comfort, and help maintain a moist wound environment, many collagen dressings containing an antimicrobial agent to control pathogens within the wound. Collagen dressings have a variety of pore sizes and surface areas, as well. All of these attributes are meant to improve the wound management process. Collagen dressings typically require a secondary dressing, such as cotton gauze swabs, as used in the present study.

Recent research has shown that collagen-based dressings produce a significant increase in the fibroblast production, have a hydrophilic property that facilitates fibroblast permeation, enhance the deposition of oriented, organized collagen fibers by attracting fibroblasts and causing a directed migration of cells, promote the uptake and bioavailability of fibronectin, help preserve leukocytes, macrophages, fibroblasts, and epithelial cells, and maintain the chemical and thermostatic microenvironment of the wound.

Collagen dressings act by inhibiting or deactivating excess of matrix metalloproinases (MMPs), the excess of MMPs determining wound chronicity.

In chronic wounds, which do not heal within six weeks, there is a hyperactivity of the healing process, which is out of phase, non-progressive, and with a persistent, uncoordinated, mixed acute and chronic inflammatory response, the most common cause of the chronicity being infection, from increasing microbial colonization, inevitable in open wounds healing by secondary intention, to increasing contamination and clinically overt infection.

The use of collagen in wound management has not yet been unanimously accepted for widespread clinical use, as the studies on the subject only offer evidence for collagen as a dressing matrix and not as an active agent. Thus, the use of collagen-based products as wound dressings on a large scale still needs to be proved, even though there are many collagen biomaterials available on the market and the use of collagen materials as a scaffold in hernia and abdominal wound repair seems to be clinically and cost-effective.

MATERIAL AND METHOD

The study was conducted in the General Surgery Department "Sfântul Pantelimon" Emergency Hospital from Bucharest, Romania, between January 2015 to April 2017, including 10 patients with chronic postoperative wounds: 4 men and 6 women; age between 18 and 60 years with mean age 39 years and average body mass index 27.6kg/m2. The exclusion criteria were diabetes, smoking, and vascular diseases. All the patients had undergone surgical intervention with delayed healing of the postoperative wound. In all the patients, tubular drains were positioned. The suture was performed using Sentesorb or Monofilament. At the end of the procedure, in the operating room, a dressing with sterile cotton gauze and patch was put on the postoperative wound.

From the 10 patients included in the study, for whom the wound-healing process was delayed, due to local infection or seroma, for 5 of the randomly selected cases collagen sponge was applied on the affected wound, for the other 5 cases cotton gauze being used as dressing.

A sponge shaped device, constituted exclusively by lyophilized type I native heterologous equine collagen which transforms in a soft gel that allows contact with the entire wound bed, was used in the present study. The collagen sponge was cut to fit the size of the wound, being applied directly to the wound bed, covering the entire wound, without overlapping the edges of the wound. A secondary cotton dressing was used to cover the collagen sponge. Depending on the amount of exudate, was reapplied daily or at every 48 hours, being absorbed into the wound bed over time.

At each dressing change, surveys with a 10-point scale evaluation were used to assess nontraumatic removal level, ease of application, adhesion, and strength of the 2 treatment methods. All wounds were followed through to full closure.

The number of days necessary for wound healing, the number of infection cases, and wound-related complications, the wound location, the age of wound, co-morbidities and previous treatments were the variables analyzed by the present study. Costs of the medications were also taken into account. At the time of the wound closure patients answered a questionnaire with multiple-choice questions to assess comfort, pain at dressing change, pruritus, adhesion and strength of the dressing, and number of dressing changes.

The study was approved by the ethics committee of our institution and was performed in accordance with the ethical standards laid down in the 1964 Declaration of Helsinki and its later amendments.

RESULTS

Descriptive statistics of quality measures of the 2 dressings are summarized in table 1.

Table 1. Descriptive statistics of Quality Measures of the study paired samples. N represents the sample size of each group; all but the last variable is evaluated by the physician in a 10-point scale

Variable	N	Minimum	Maximum	Mean
Nontraumatic removal level				
Collagen sponge	5	4	9	6,6
Traditional dressing	5	1	5	3
Ease of application (higher-easier)				
Collagen sponge	5	4	9	6,2
Traditional dressing	5	1	5	2,8
Adhesion and strength (higher-better)				
Collagen sponge	5	4	9	6,8
Traditional dressing	5	1	5	2,6
Number of days for wound healing				
Collagen sponge	5	5	7	5,3
Traditional dressing	5	8	16	12

The results revealed significant differences between the two treatment methods for quality measures, the dressing change being about 3 to 4 points less traumatic on average and about 4 points easier on average with collagen sponge than with the control traditional dressing. The collagen sponge remained adherent to the wound in each of the patients in the24-48 hourse, the adhesion and strength being about 4 to 5 points better on average than with traditional dressing.

The number of days for wound healing exhibits a different distribution depending on the type of dressing used, as shown in table I, collagen sponge eliciting a statistically significant median acceleration (about 5–6 days less) for a complete healing compared with the control medication (figure 1, 2).
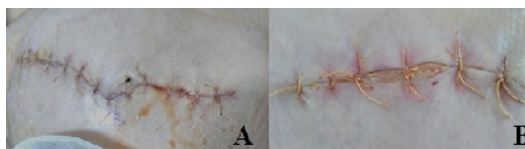
Figure 1. Postoperative wound seroma (A) with macroscopic aspect after collagen-sponge dressing (B)

Figure 2. Post-surgical excision of inguinal phlegmona wound- evolution under collagen-sponge dressing: day 1 (A), day 2 (B), day 3 (C), day 5 (D)

Statistical analysis revealed no significant differences between the risk of infection and wound-related complications between the 2 treatment methods, with 1 patient from the case-group and 2 subjects from the control-group presenting fever or wound-related complications (dehiscence).

The unitary cost of collagen-sponge dressing is 5 Euros, whereas the unitary cost of a traditional dressing is 30 cents. Collagen-sponge needs to be replaced daily or every 48 hours, while the traditional dressing twice a day or daily. In the present study, all the patients needed at least 3 replacements of collagen-sponge dressings, the total median expenditure with this medication being 15 Euros. Taking into account the time for a complete recovery and the number of required changes of the traditional dressing, a higher variability of costs with this medication was observed (table 2).

Table 2. Statistical description of the cost of a complete treatment with the traditional dressing (in Euros)

Cost	N	Minimum	Maximum	Median
Traditional dressing	5	5,4	11	8,36

A statistically significant median higher cost with Aquacel Surgical (about 6 euros more expensive for a complete medication treatment) compared with the control treatment cost of medication. We analyzed the data gathered from the questionnaires completed by the patients. All patients from the control group reported that the dressing change was painful (maximum scored), one patient from the case-group scoring the pain with the maximum value. All the patients reported more comfort during dressing application, a longer duration, and total atraumaticity during the dressing change with collagen sponge.

DISSCUSION

Adequate dressing material must be used, in accordance with the type of wound. Choosing the best option of wound dressing is determined by its properties, such as the capacity to provide or maintain moist environment, to enhance epidermal migration, to promote angiogenesis and connective tissue synthesis, to allow gas exchange between wounded tissue and environment, its ability to maintain appropriate tissue temperature to improve the blood flow to the wound bed, to provide protection against bacterial infection. The ideal dressing should be non-adherent to the wound and easy to remove after healing, providing debridement and enhancing leucocytes migration. Also, the wound dressing must be sterile, non-toxic and non-allergic.

Skin represents the ideal cover for wounds, a whole range of autologous skin graft techniques being available, from splitthickness skin grafts to complex pedicle or free microvascular myocutaneous flaps, the results being limited in the case of widespread skin loss. Nevertheless, the grafted wounds are at risk of failure or infection of both donor and recipient sites, with considerable subsequent morbidity. Several techniques have been designed to extend the area of split-thickness grafts, such as meshing, or to make harvest simpler and accessible, as in pinch grafting, but they still inflict an injury to healthy, intact skin (Horch, 2005).

Dermal allografts are still used, but they are progressively replaced by new tissue engineering technology, starting with the development of monolayer culture of keratinocytes, up to the use of collagen, hyaluronic acid or synthetic polymers as carriers of live, human-derived fibroblasts and keratinocytes (Horch, 2000)

Even freeze-dried cellular dressings with a carrier matrix have been shown to be effective in healing wounds of diverse origins Lost functional cells are, thus, replaced by artificial skin substitutes that can control the dysfunctional wound healing process compromised (Cavorsi, 2006).

While it is appreciated that the gold standard of complete healing has to be replaced by surrogates of healing rates using, for example, computerised planimetry, there is often too much emphasis on poor clinical assessments of presence of infection or inflammation, pain, handling of exudate, odour, numbers of dressing changes and dressing acceptability or tolerance, and inadequate 'add-on' attempts at cost-effectiveness (Feng, 1999; Fu, 2005; Gault, 1999).

The recently developed wound dressings are produced from biomaterials, derived generally from natural tissues or artificial sources such as collagen, hyaluronic acid, chitosan, alginate and elastin, which play an important role in healing process, their biocompatibility, biodegradability and non-toxic nature being demonstrated, sometimes incorporating growth factors and antimicrobials to enhance wound healing process (Barlett, 1981; Doillon, 1986; Ishihara, 2002).

Collagen, a major structural protein has been discussed by many researchers for their active role in natural healing process. Collagen initiates fibroblast formation and accelerates endothelial migration upon contact with wound tissue (Rao, 1995; Mian, 1992).

There have been several sources of collagen for use as a dermal matrix (table 3).

Table 3. Currently available acellular collagen and dermal matrix products for wound care

Permacol ®	Porcine dermis	Tissue Science Laboratories
Integra ®	Bovine tendon/synthetic polysiloxanne	Integra Lifesciences
Fibracol®	Collagen/alginate	Systagenix
Oasis®	Porcine small intestine submucosa	Cook Biotech
Biostep ®	Porcine collagen/alginate/CMC+/-Ag	Smith and Nephew
Catrix ®	Bovine cartilage (powder)	Lescarden
Matriderm®	Collagen/elastin	Suwelak
Decutastar®	Equine collagen	ADL
Septocoll E®	Collagen fleece/gentamicin	Biomet
AlloDerm®	Human cadaver de-epithelialised skin	LifeCell Corp
GraftJacket®	Human cadaver dermal matrix	Wright Medical Technology

The dermal skin substitute Integra® (Integra Life Sciences) is a bi-layer bovine collagen and polysiloxane dressing, used, mainly, for burn wounds. AlloDerm® (Life CellCorp), an acellular dermal matrix derived from cadaveric skin has also been widely used for burn management.

Adequate trials studying the use of collagen as dermal matrix, and other similar dressings, in different wound types other than burns are also awaited. The high costs limits introduction into wide clinical practice, extensive evidence being needed for their application. The application of biomaterials as skin substitutes vary from simple direct application as cell monolayers to polymer, or animal-derived collagen scaffolds.

From the results of our study, it was confirmed that collagen-sponge dressing represents a more comfortable method, easier to manage for the patient, durable, waterproof, and nontraumatic at dressing change, the use of collagen-sponge biomaterials being recommend in all the surgery procedures where the risk of wound dehiscence and maceration is high. There is a plethora of case reports and small patient series, which are supportive for the wide application of the collagen-based biomaterials, but these have a high risk of publication bias.

The limits of the present study are determined by the difficulty with the clinical studies and attempts at randomised controlled trials, being underpowered, with randomisation which is poor or not defined, comparing the dressing with an ineffective traditional therapy such as cotton gauze swabs, evaluations being unblinded and subjective, and therefore biased, high dropout rates ofen occurring so that assessment even up to 12 weeks represents a challenge for the rsearcher.

CONCLUSION

Collagen gives the skin its tensile strength contributing to the formation of the natural tissue matrix. Collagen sponge, a biodegradable material, plays an active part in normal physiological wound healing and new tissue formation, representing an attractive choice from a tissue biocompatibility and a toxicological point of view. Collagen sponge was proved to be comfortable and easier to manage for the patient, durable, waterproof, and nontraumatic at dressing change, making it the treatment of choice for the patients with high risk of wound complications. The high costs limits the introduction of collagen-based dressings into wide clinical practice, extensive evidence being needed in order to support their cost-effectivenes. There is no superior product that heals chronic wounds that fail to achieve complete healing, developing a dressing material that addresses the major interfering factors of normal healing process representing the major step in tissue engineering that will help patients and wound care practitioners largely.

REFERENCES

Barlett, R.H. (1981), "Skin substitutes", *Journal of Trauma*, 21, S731, https://doi.org/10.1097/00005373-198108001-00041.

Cavorsi, J. *et al*. (2006), "Best practice algorithms for the use of a bilayered living cell therapy (Apligraf) in the treatment of lower extremity ulcers", *Wound Repair and Regeneration*, 14, 102–9, https://doi.org/10.1111/j.1743-6109.2006.00098.x.

Doillon, C.J. and Silver, F.H. (1986), "Collagen-based wound dressing: Effect of hyaluronic acid and fibronectin on wound healing", *Biomaterials*, 7, 3-8, https://doi.org/10.1016/0142-9612(86)90080-3.

Feng, X. *et al*. (1999), "Fibrin and collagen differentially regulate human dermal microvascular endothelial cell integrins: stabilisation of alphav/beta3 mRNA Wuk by fibrin", *The Journal of Investigative Dermatology*, 113, 913–19, https://doi.org/10.1046/j.1523-1747.1999.00786.x.

Fu, X. *et al*. (2005), "Engineered growth factors and cutaneous wound healing: Success and possible questions in the past 10 years", *Wound Repair And Regeneration*, 13, 122–30, https://doi.org/10.1111/j.1067-1927.2005.130202.x.

Gault, S. (1999), "Scars and contractures", *Surgery*, 17, 73–5.

Gelfand, J.M. *et al*. (2002), "Surrogate endpoints for the treatment of venous leg ulcers", *The Journal of Investigative Dermatology*, 119, 1420–5, https://doi.org/10.1046/j.1523-1747.2002.19629.x.

Horch, R.E. *et al*. (2000), "Cultured human keratinocytes on type I collagen membranes to reconstitute the epidermis", *Tissue Engineering*, 6(1), 53–67, https://doi.org/10.1089/107632700320892.

Horch, R.E. *et al*. (2005), "Tissue engineering of cultured skin substitutes", *Journal of Cellular and Molecular Medicine*, 9, 592–608, https://doi.org/10.1111/j.1582-4934.2005.tb00491.x.

Ishihara, M. *et al*. (2002), "Photo crosslinkable chitosan as a dressing for wound occlusion and accelerator in healing process", *Biomaterials*, 23, 833-40, https://doi.org/10.1016/S0142-9612(01)00189-2.

Mian, M. *et al*. (1992), "Collagen as a pharmacological approach in wound healing", *International journal of tissue reactions*, 14, 1-9.

Rao, K.P. (1995), "Recent developments of collagen based materials for medical applications and drug delivery", *Journal of Biomaterials Science, Polymer Edition*, 7, 623-45.

ANTIMICROBIAL COMPOSITION FOR THE PROTECTION OF LEATHER, FURS AND LEATHER ARTICLES

VIORICA DESELNICU, CORINA CHIRILĂ

INCDTP - Division: Leather and Footwear Research Institute, 93 Ion Minulescu str., sector 3, RO-031215 Bucharest, viorica.deselnicu@icpi.ro

This work presents a composition based on essential oils for the protection of leather, furs and leather articles against fungi. The composition based on essential oils, such as: thyme oil, cinnamon oil, cloves oil, oregano oil, lavender oil in a proportion of 10 to 50% of the total composition. The composition was tested against *Trichophyton interdigitale* by applying by spraying of 5 -7 passes on the surface of sheepskins lining leather, furs or leather articles / shoes. The composition was effective 28 days for sheepskins lining leather and furs and 15 days for inside shoes, against *Trichophyton interdigitale.*

Keywords: essential oils, antifungal activity, lining leather, furs, shoes

INTRODUCTION

It is known that leather, fur and leather articles can be easily contaminated with various bacterial and fungal species (Chirila, 2014 a, b, c). These microorganisms can damage the material or be pathogenic to the wearer. Hides/skins and leather items are very sensitive to the destructive action of molds, while footwear linings may be contaminated with pathogenic bacteria or dermatophytes.

Among these microorganisms recall species: *Aspergillus niger, Aspergillius flavus, Trichoderma viridae, Penicillium glaucum, Penicillium cyclopium, Paecilomyces varioti, Candida albicans, Scopulariopsis brevicaulis* that develops on various leather items, degrading material.

Also, the warm and humid environment inside the shoe facilitates the development of various harmful microorganisms that can cause foot diseases. Pathogenic fungi that grow on the human skin include: *Trichophyton interdigitale, Trichophyton rubrum, Epidermophyton floccosum and Microsporum gypseum, Aspergillius niger, Aspergillius flavus.* These fungi cause *tinea pedis*, a condition known as "athlete's foot". These fungi are located between the toes, feet or nails, causing onychomycosis. "Athlete's foot" is very contagious and can easily be transmitted through footwear previously worn by infected people, as spores remain on the material with which the footwear is lined. By the same mechanism, the "athlete's foot" can recur after it has been removed by treatment. Disease prevention is more effective than treating them. Therefore, a lining material for footwear lined with antifungal / antimicrobial properties could prevent both the spread of fungal infections and the reinfection of the wearer.

For the protection of leather, fur, footwear and leather articles against microorganisms biocides are used (Deselnicu, V. *et al*., 2005; Deselnicu, V. *et al.*, 2007). Biocide act as oxidizing agents or by distorting or crosslinking proteins, through a number of mechanisms including inhibition of bacterial enzyme systems (Radwan *et al*., 2014). Biocides are part of chemicals potentially harmful to humans and the environment, therefore their production and marketing is regulated and monitored continuously by European directives and regulations of European Parliament and Council (Deselnicu, D.C., 2014; Deselnicu, D.C. *et al.,* 2014). There is no EU legislation in regulating specifically the content of chemicals in footwear and other leather products, but the use of chemicals is restricted by REACH (EC 1907/2006).

Attempts to use essential oils to obtain disinfectant solutions based on essential oils are known (Deselnicu, V. *et al*., 2016; Berechet *et al.* 2016 a, b; Chirila C. *et al.* 2016; Chirila C. *et al*., 2017; Stevi *et.al*., 2014). However, due to their hydrophobic nature, essential oils are not readily miscible with water. As a result, essential oil is often difficult to incorporate into an aqueous solution.

Thus, U.S. Pat. no. 5,403,587 (McCue *et al*., 1985) discloses an antimicrobial composition which uses both a solvent and a surfactant to facilitate the formation of a homogeneous aqueous mixture of essential oils. Although this disinfectant composition is more natural than others, it requires relatively high concentrations of solvent and synthetic surfactant, and its effectiveness is questioned.

U.S. Pat. 9,655,939 B2 (Reeve and Michael, 2017) describes an antifungic and/or antiviral composition effective against *Staphylococcus aureus* for application to the surface of any type of electrical device such as a computer, keyboard, mouse, television, MP3 player portable. The disadvantage of this composition is that it is used for non-porous surfaces and contains high concentrations of solvent.

WO Patent 2011156415 A2 (Barnhill, 2010) discloses a composition composed of three key elements: i) Ethyl alcohol (main component), ii) Essential oils (tea tree oil and peppermint oil) and iii) water which form a liquid sprayable mixture on susceptible surfaces of microbial infestation. The disadvantage of this invention is that it relates to the treatment of nonporous surfaces in hospitals, gymnasiums, hotels and care centers, which are sources of bacterial pathogens such as MRSA Staph aureus, non-MRSA Staph and Strept Group A that can survive for long periods of time.

Thus, there is a need for compositions and methods which are not limited to use on non-porous surfaces and which can be used on porous surfaces such as leather, furs, leather articles, shoes, etc..

This paper present a composition which relates to such a necessity, based on essential oils having synergistic antimicrobial properties, which can be applied on leather, furs, footwear, reducing /eliminating harmful microorganisms on the surfaces to which it is applied and ensuring that the color and dimensions of the surfaces on which it is applied are not modified.

MATERIALS AND METHODS

Materials

The antimicrobial composition contains essential oils in a total amount of about 10 to 50% of the total antimicrobial composition, as follows:

- Thyme Essential oil – the major compounds identified by gas chromatography were ca. of 57,35% and γ-terpinene approx. 32.43% (Berechet *et al*., 2016a).

- Cinnamon Essential oil (*Cinnamomum aromaticum*) the major compounds identified was cinamaldehyde, ca. 84.12% (Berechet *et al*., 2016b).

- Cloves Essential oil (*Eugenia caryophyllata*), the major compounds identified was eugenol with a 96.99% area (Berechet *et al*., 2016b).

- Oregano Essential oil (*Origanum vulgare*) the major compounds identified were tymol, ca. 64.41% and carvacrol approx. 27.62% (Berechet *et al*., 2016b).

- Lavender essential oil (*Lavandula angustifolia*) the major compounds identified were geraniol ca. 26,34%, camphor approx. 23.19% and eucalyptol ca. 20.82% (Berechet *et al*., 2016b).

The antimicrobial composition contain a mixture of essential oils that are solubilized or dispersed in water with a solubilizing or dispersing agent. The antimicrobial composition contain one or more non-toxic organic solvents that help disperse the oils in water and increase the rate of evaporation after application to the treated surfaces. The resulting essential oil solution or dispersion is a homogeneous mixture that allows for easy and efficient application of the composition on the treated surface by spraying.

Sheepskins for footwear linings
Woolen sheepskins for footwear uppers
6 pairs of women shoes with leather uppers
Biologic material: *Trichophyton interdigitale*

Methods

Antifungal activity against *Trichophyton interdigitale:* The tests were made following standard ASTM D4576–86 (1996) - Standard Test Method for Mold Growth Resistance of Wet Blue. Petri dishes were placed in thermo-hygrostat at 30°C temperature and were analized after 3, 7, 14, 21 and 28 days.

Optical microscopy images were captured using a Leica stereomicroscope S8AP0 model with optic fiber cold light source, L2, with three levels of intensity, and magnification 40X.

Treating materials: Composition was applied by spraying 5-7 passes on the surface of lining leather, fur or inside shoes.

RESULTS AND DISCUSSION

Antifungal Activity

Antifungal activity of essential oil composition against *Trichophyton interdigitale* have been tested on sheepskin leather for footwear lining (Table 1), furs (Table 2) and footwear (Figure 1).

Table 1. Antifungal activity of essential oil composition against *Trichophyton interdigitale* on sheepskin leather for lining
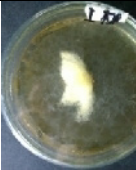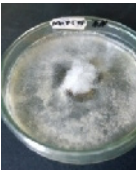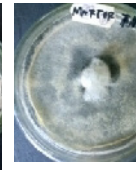
	3 days	7 days	14 days	21 days	28 days
Essential oil composition					
Grade	0	0	0	0	0
Control					
Grade	2	4	4	4	4

Table 2. Antifungal activity of essential oil composition against *Trichophyton interdigitale* on furs

	3 days	7 days	14 days	21 days	28 days
Essential oil composition					
Grade	0	0	0	0	0
Control					
Grade	4	5	5	5	5

At antifungal activity testing, a total inhibition of the development of *Trichophyton interdigitale* was found for a period of 28 days on skins and fur treated with the antifungal composition, as compared to the untreated control sample, which showed growth of fungi after 3 days.

The antifungal activity of the composition against *Trichophyton interdigitale* was also tested on wearing footwear by treating the shoe interior in the fingers area (left shoe), having as control untreated shoe (right shoe) (Figure 1). After 30 days of wearing shoes, samples were taken from the inside of the shoes in the fingers area and the antifungal activity of the treatment with essential oils based composition was tested.

a).   b).
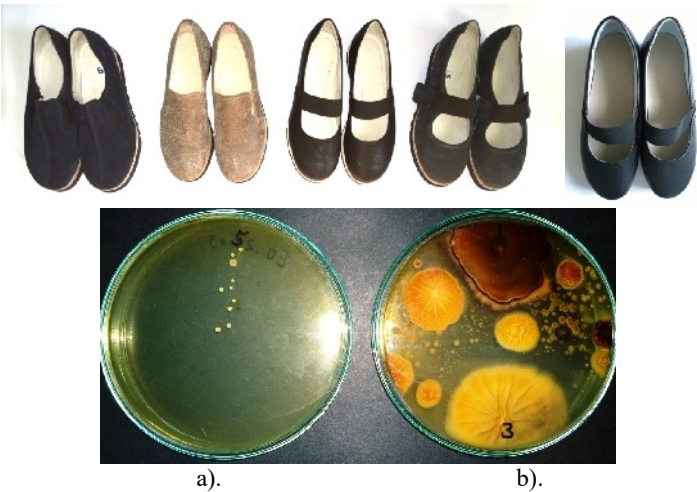
Figure 1. Antifungal activity of essential oil composition against *Trichophyton interdigitale* on the footwear: a) treated footwear and b) untreated footwear

Almost a total inhibition of fungi was observed through the treatment of the shoe interior. Untreated shoes were observed to have colonies of *Aspegillus flavus, Candida albicans, Penicillium* and *Trichophyton interdigitale* after 5 days (Figure 2).
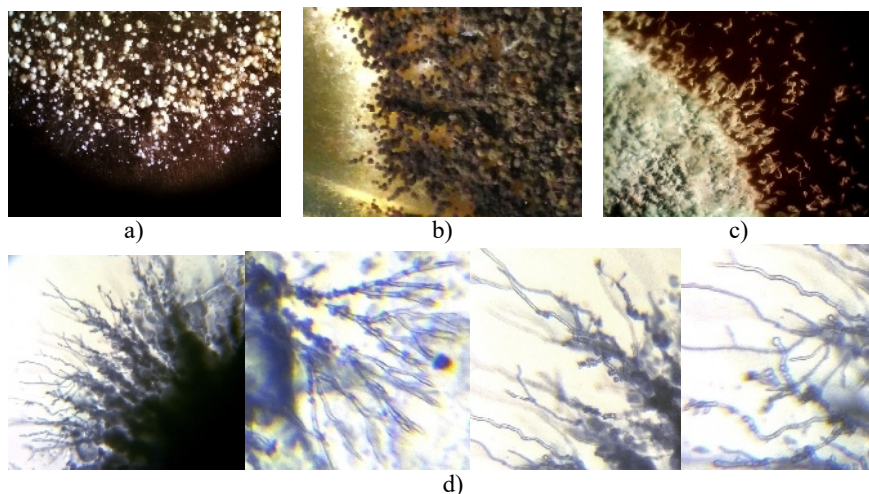
Figure 2. Fungi growth after 5 days on the untreated shoes: a) *Aspergillus flavus*; b) *Aspergillus niger;* c) *Penicilium;* d) *Trichophyton interdigitale*

The antimicrobial composition based on the essential oils has the following advantages: it is biodegradable; not toxic for people's health; ecofriendly for the environment; non-corrosive, has neutral pH; does not change the color of the material on which it is applied and preserves the integrity / dimensions of the treated materials; it is based on raw materials from renewable resources; easy application by spraying, moistening.

CONCLUSION

The antimicrobial compositions due to the presence of several essential oils having synergistic antimicrobial properties, significantly reduce/eliminate the harmful microorganisms on the surfaces to which they apply. This composition it is an alternative method for the protection of leather, furs and leather articles.

REFERENCES

Berechet, M.D., Chirila, C., Deselnicu, V. (2016a), "Antifungal activity of thyme essential oil on woolen sheepskins", *Proceedings of The 6th ICAMS 2016*, 203-208, 20-22 October 2016, Bucharest, https://doi.org/10.24264/icams-2016.II.2.

Berechet, M.D., Chirila, C., Deselnicu, V. (2016b), "Antifungal activity of some essential oils on cotton fabrics", *Proceedings of The 6th ICAMS 2016*, 197-202, 20-22 October 2016, Bucharest, https://doi.org/10.24264/icams-2016.II.1.

Chirila, C., Berechet, M.D., Deselnicu, V. (2016), "Thyme essential oil as natural leather preservative against fungi", *Proceedings of The 6th ICAMS 2016*, 227-232, 20-22 October 2016, Bucharest, https://doi.org/10.24264/icams-2016.II.6.

Chirila, C., Crudu, M., Deselnicu, V. (2014a), "Comparative study regarding resistance of wet-white and wet-blue leather to the growth of fungi", *Leather and Footwear Journal*, 14(2), 107-120, https://doi.org/10.24264/lfj.14.2.4.

Chirila, C., Crudu, M., Deselnicu, V. (2014b), "Study regarding the resistance to the growth of fungi of wet-white leather tanned with Titanium – Aluminum", *Proceedings of The 5th ICAMS 2014*, 23-25 October 2014, Bucharest, pp 31-36.

Chirila, C., Deselnicu, V., Berechet, M.D. (2017a), "Footwear protection against fungi using thyme essential oil", *Leather and Footwear Journal*, 17(3), 173-178, https://:doi.org/10.24264/lfj.17.3.7.

Chirila, C., Deselnicu, V., Berechet, M.D. (2017b), "Study regarding footwear protection against fungi with essential oils", *Proceedings of The 4th International Leather Engineering Congress: Innovative Aspects for Leather Industry*, October 19-20, 2017, Izmir, Turkey, 179-183, ISBN 978-605-338-222-5.

Chirila, C., Deselnicu, V., Crudu, M. (2014c), "Study regarding the resistance of wet-white leather organic tanned to the growth of fungi", *Proceedings of The 5th ICAMS 2014*, 23-25 October 2014, Bucharest, pp. 37.

Deselnicu, D.C. (2014), *Politici Europene pentru produse si relevanța lor pentru sectorul de încălțăminte,* (RO) ISBN: 978-973-720-555-1 (245pg), Agir Press.

Deselnicu, D.C. *et al.* (2014), "Sustainable consumption and production in the footwear sector", *Leather and Footwear Journal,* 14(3), 159-180, https://doi.org/10.24264/lfj.14.3.3.

Deselnicu, V. *et al.* (2005), "Impact of technological changes on increased health and comfort efficiency", *Proceedings of The 4th International Conference in Management of Technological Change*, book 1, pg. 87-92, Chania, Greece, 19-20 August.

Deselnicu, V. *et al.* (2007), "Antimicrobial and antifungal leathers for increasing the health and the comfort of the individuals", *CORTEP,* 18-21 Oct., Iassy, RO.

McCue *et al.* (1995), "Disinfectant and sanitizing compositions based on essential oils", U.S. Patent No. 5,403,587.

Niculescu, O., Leca, M., Moldovan, Z., Deselnicu, D.C. (2015), "Obtaining and characterizing of a product with antifungal properties based on essential oils and natural waxes for finishing natural leathers", *Revista de chimie (Bucharest)*, 66(11), 1733-1736.

Niculescu, O., Leca, M., Moldovan, Z., Deselnicu, D.C. (2015), "Research on Obtaining Products for Fragrance and Biological Protection on Natural Leathers and Furs", *Rev. Chim. (Bucharest)*, 66(12), 1956-1959.

Radwan, I.A. *et al.* (2014), "Effect of thyme, clove and cinnamon essential oils on Candida albicans and moulds isolated from different sources", *American journal of animal and veterinary sciences,* 9(4), 303-314, https://doi.org/10.3844/ajavsp.2014.303.314.

Reeve, R.A. and Michael, T.P.J. (2017), "Antimicrobial and/or antiviral composition and to methods for preparing and administering same", US Patent 9.655.939 B2.

Barnhill, S.D., Jr. (2010), "Antimicrobial composition and method for using same", WO Patent 2011156415 A2.

Stevi, T. *et al.* (2014), "Antifungal activity of selected essential oils against fungi isolated from medicinal plant", *Industrial Crops and Products*, 55, 116–122, https://doi.org/10.1016/j.indcrop.2014.02.011.

DICLOFENAC SPONGIOUS MATRICES BASED ON COLLAGEN AND ALGINATE FOR RELIEVING INJURY PAINS

ROXANA-DENISA DRĂGHICI[1], MARIA MINODORA MARIN[2,3], MIHAELA VIOLETA GHICA[4], MĂDĂLINA GEORGIANA ALBU KAYA[3], VALENTINA ANUȚA[4], CRISTINA DINU-PÎRVU[4], DURMUȘ ALPASLAN KAYA[5], GHEORGHE COARĂ[3], LUMINIȚA ALBU[3], CIPRIAN CHELARU[3]

[1]University Politehnica of Bucharest, Faculty of Medical Engineering, 1-7 Gheorghe Polizu Str., 011061, Bucharest, Romania, roxana.rene26@yahoo.com

[2]University Politehnica of Bucharest, Faculty of Applied Chemistry and Materials Science, Bucharest,1-7 Gheorghe Polizu Str., 011061, Bucharest, Romania

[3]INCDTP - Division: Leather and Footwear Research Institute, 93 Ion Minulescu Str., 031215, Bucharest, Romania, icpi@icpi.ro

[4]"Carol Davila" University of Medicine and Pharmacy, Faculty of Pharmacy, Physical and Colloidal Chemistry Department, 6 TraianVuia Str., 020956, Bucharest, Romania, mihaelaghica@yahoo.com

[5]Hatay Mustafa Kemal University, Faculty of Agriculture, Field Crops Department, 31034, Antakya-Hatay, Turkey

The sport injuries become more and more frequent so there is a need to discover new solutions for increasing the quality of life for people affected by such wounds. The aim of this study was to obtain a novel NSAID drug delivery system, topical diclofenac spongious matrices based on collagen and alginate for the treatment of injuries and relieving of pain. The samples were analyzed by flow analysis and after their freeze-drying were analyzed by FT-IR and in vitro release of sodium diclofenac.The results obtained from analyses confirmed that diclofenac spongious matrices based on collagen and alginate exhibit proper characteristics for the treatment of injuries and relieving of pain.

Keywords: diclofenac, collagen, alginate.

INTRODUCTION

The sport injuries have become more and more frequent so there is a need to discover new solutions for increasing the life quality of people affected by such wounds (Barbour *et al*., 2017).

The most widely recommended and used drug treatment for the pain associated with these sporting injuries are orally administered drugs, such as nonsteroidal anti-inflammatory drugs (NSAIDs) (Ong *et al*., 2007). Diclofenac is a member of the aryl alkanoic group of NSAIDs, synthesized by Ciba-Geigy in the 1960's. Development of pharmaceutical forms of diclofenac for application on the skin subsequently followed, and a variety of commercial preparations are currently available (Goh *et al*., 2014). The chemical name of diclofenac is (2-(2- [(2,6-dichlorophenyl) amino]phenyl) acetic acid) and it contains a phenylacetic acid group, a secondary amino group and a phenyl ring, with chlorine atoms at the two ortho positions. One recent study reported that the current use of any oral NSAID almost doubles the risk for endoscopically confirmed ulcer (Kok *et al*., 2018). Topically applied NSAIDs could act directly within the area of injury and reduce the inflammatory reaction without unwanted systemic activity (Mason *et al*., 2004). In the last few decades, wound dressings containing drugs gained popularity as an effective analgesic modality for injuries, owing this to advantages such as ease of application and reduced risk of dose dumping compared with cream and gel

forms of topical delivery. These advantages also lead to better patient compliance (Hsieh *et al.*, 2010).

Collagen, the most abundant protein in the human body, is an excellent material which can be used in applications such as topical drug delivery systems due to its high biocompatibility properties (Ramshaw *et al.*, 2014; Yu *et al.*, 2014). Another material suitable in these applications is alginate, extracted from brown seaweed. Alginate has a unique capability of high absorbency of water, biocompatibility, low toxicity, relatively low cost, and mild gelation by addition of divalent cations such as Ca^{2+} (Chiu, 2008).

The aim of this study was to obtain a novel NSAID drug delivery system, topical diclofenac spongious matrices based on collagen and alginate for the treatment of injuries and relieving of pain.

MATERIALS AND METHODS

Materials

The type I fibrillar collagen gel having a concentration of 2.54% (w/v) was extracted from calf hide using technology developed in our institute, Collagen Department (Albu, 2011). Alginic acid sodium salt from brown algae (Alg), Diclofenac Sodium (DFNa) were purchased from Sigma-Aldrich (Germany), and Glutaraldehyde (GA) from Merck (Germany).

Preparation of Collagen Hydrogels

The collagen gel with an initial concentration of 2.54% and acid pH was adjusted using 1M sodium hydroxide at pH 7.4 for better biocompatibility. The final concentration of the collagen gel used was 1% (w/v). Alginate and diclofenac were added in the collagen gels, in different proportions, according to the compositions shown in Table 1, and then the composite gels were cross-linked with 0.025% glutaraldehyde.

Table 1. Composition of collagen gels

code	COLL, %	DFNa, %	ALG,%	GA,%
CDA1	1	0.1	1.5	0.025
CDA2	1	0.1	2	0.025
CDA3	1	0.2	1.5	0.025
CDA4	1	0.2	2	0.025
CDA5	1	-	1.5	0.025
CDA6	1	-	2	0.025

The collagen gels were freeze-dried using Delta 2-24 LSC (Martin Christ, Germany) and spongious matrices were obtained.

Methods

Flow Analysis

The rheological behaviour of the tested hydrogels was conducted with a rotational viscometer Multi-visc Rheometer-Fungilab equipped with standard spindle TR 9 and

ultrathermostat ThermoHaake P5. The rheological experiments were performed at 37°C±0.5°C.

FTIR-ATR Analysis

FT-IR spectral measurements were recorded by spectrophotometer Jasco FT/IR 4200. All the spectra were recorded at the following parameters: spectral range 4000-600 cm^{-1}, resolution 4 cm^{-1} with 30 acquisitions per each sample.

In vitro *Release of Sodium Diclofenac*

The *in vitro* kinetics release of DFNa from the designed spongious matrices was determined using a "sandwich" device adapted to a paddle dissolution equipment, as described in our previous studies (Ghica *et al*., 2017). The amount of released DFNa at different period of time was spectrophotometrically assessed at λ=276 nm.

RESULTS AND DISCUSSION

The samples from Table 1 were analyzed by flow analysis and after their freeze-drying were analyzed by FT-IR and *in vitro* release of sodium diclofenac.

The results of the rheological experiments carried at 37°C for the control gels (without DFNa) led to the cumulative rheograms plotted as viscosity versus shear rate and illustrated in Figure 1a.
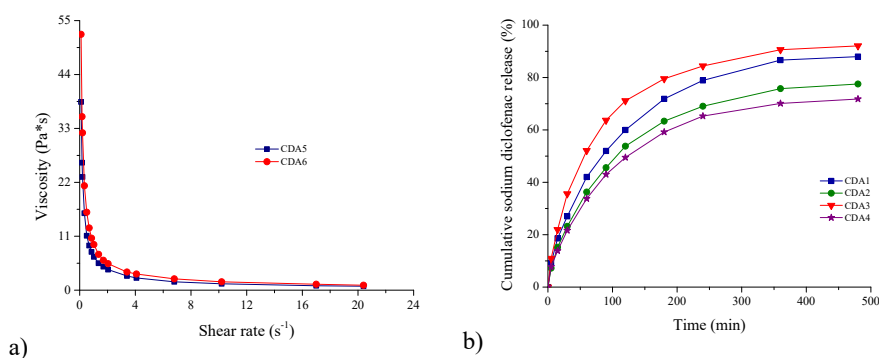
Figure 1. a) Plots of viscosity as a function of shear stress for the collagen hydrogels with sodium alginate evaluated at 37°C; b) Cumulative release profiles of sodium diclofenac from spongious collagen matrices as a function of time

Figure 1a shows the influence of the composition on the viscosity of the gels tested at 37°C. Thus, the viscosity increases when increasing sodium alginate concentration.

For the graphs shown in Figure 1a it results that the viscosity of the tested systems decreases with increasing shear rate, indicating a non-Newtonian pseudoplastic character. Pseudoplastic behaviour is a desirable requirement for topical systems both in terms of conditioning and of skin application, forming a continuous film at the application site. For the quantification of the pseudoplastic behaviour of the tested

control gels, the Power law model expressing the relationship between viscosity and shear rate is used (eq. 1).

$$\eta = m \cdot \dot{\gamma}^{-n} \tag{1}$$

where m and n are parameters correlated with the formulations of the hydrogels and are determined by linearization of eq. (1) by the double logarithm method. It can be appreciated that the value of m corresponds to the viscosity obtained for the shear rate value of $1 \cdot s^{-1}$ (Ghica *et al.*, 2016; Kaya *et al.*, 2014; Albu *et al.*, 2012). The values of the previously described parameters m and n as well as the R^2 - determination coefficient of the model are listed in Table 2 for the formulations tested at 37°C.

Table 2. The values of the m and n parameters and the determination coefficient specific to the Power law model applied to control gels evaluated at 37°C

Gel	m	n	R^2
Gel CDA5	6.953	0.742	0.9998
Gel CDA6	9.523	0.741	0.9997

The values obtained for the determination coefficient R^2 are higher than 0.99, indicating that the experimental data well fitted this model. From Table 2 it can be seen that the rheological parameter m obtained for the control gel with 0.20% sodium alginate recorded a higher value of about 1.37 times than the control gel with 0.15% sodium alginate.

The composite gels were freeze-dried and spongious matrices were obtained. Their results of the FT-IR spectrum are presented in Figure 2.
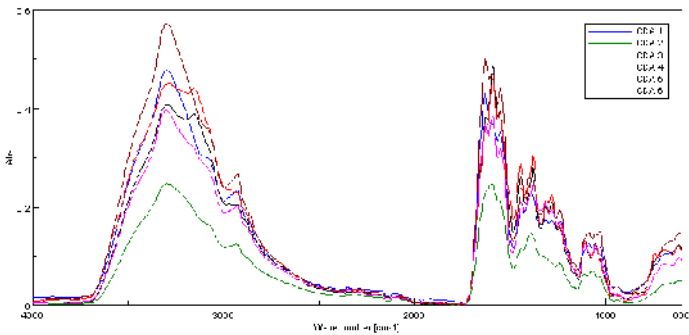
Figure 2. FT-IR spectra of spongious matrices

From the FT-IR spectrum the typical bands from collagen can be observed: amide A (3297 cm⁻¹), B (3097 cm⁻¹), I (1631 cm⁻¹), II (1550 cm⁻¹) and III (1442 cm⁻¹) (Albu, 2011). Corresponding to alginate, a peak can be observed toward 2931 cm^{-1}, assigned to the C–H antisymmetric stretching vibration and a peak at 1403 cm^{-1}, assigned to the C=O. The peak assigned to stretching vibration modes (3425 cm^{-1}), specific to alginate, doesn't exist, maybe because of the reaction between carboxyl group of alginate and NH of collagen (Fan et al., 2013). Being in a small amount, diclofenac doesn't influence the FT-IR spectrum of the spongious matrices.

The influence of the spongious matrices composition on sodium diclofenac release was analyzed by comparing the kinetic profiles. Thus, the cumulative percentages of the *in vitro* drug release recorded as a function of time, are shown in Figure 1b.

The cumulative diclofenac percentage varies between 71.78% (CDA4 sample with maximum DFNa and maximum sodium alginate) and 92.08% (CDA3 sample with maximum DFNa and minimal sodium alginate) (Table 3). In the first 60 minutes, the release of the sodium diclofenac was rapid (a "burst release" effect), followed by a step in which the anti-inflammatory drug is slowly delivered during the other 7 hours of the experiment. The kinetic profiles described above are pursued in the healing of skin lesions for which an important element is local inflammation. The "burst release" effect, after contacting the skin with the skin lesion and wetting it by wound exudation, provides a rapid reduction in inflammation associated with skin lesions. On the other hand, gradual release of the drug provides a local anti-inflammatory effect over a longer period of time necessary to cure a skin lesion (Ghica et al., 2017).

It is noticed that for the matrices formulated with the same amount of DFNa, the released drug percentage is dependent on the percentage of the biopolymer - sodium alginate. Thus, an amount of 0.2% sodium alginate present in the formulation results in a 13% decrease of released drug percentage for the sample with 0.1% DFNa, and 28% decrease for the sample with 0.2% DFNa. For matrices with a lower sodium alginate content (CDA1 and CDA3), a higher percentage of drug is released when DFNa is 0.2%, while for matrices with a content of 0.2% sodium alginate (CDA2 and CDA4), the sample with a lower drug content releases more compared to the similar sample with DFNa at maximum level.

The experimental kinetic data were analyzed with the Power law model (eq. 2) and its particular case, Higuchi model (n=0.5):

$$\frac{m_t}{m_\infty} = k \cdot t^n \tag{2}$$

where, m_t/m_∞ represents the fraction of drug released at time t, k - the kinetic constant, n - the release exponent characteristic for the drug release mechanism.

Correlation coefficient values as well as kinetic parameters specific to the Power law model are shown in Table 3.

Table 3. Drug released percentage; kinetic parameters and correlation coefficients for Power law model; correlation coefficient for Higuchi model

Spongious matrices with DFNa	DFNa Released percentage (%)	Kinetic constant (1/minn)	Release exponent	Correlation coefficient (Power law mode)	Correlation coefficient (Higuchi model)
CDA1	87.96	0.080	0.40	0.9862	0.9779
CDA2	77.51	0.068	0.41	0.9843	0.9768
CDA3	92.08	0.119	0.35	0.9782	0.9563
CDA4	71.78	0.064	0.40	0.9836	0.9755

The kinetic data best fitted the Power law model, with correlation coefficients ranging from 0.9782 to 0.9862, higher values than those recorded for the Higuchi model (between 0.9563 and 0.9779, Table 3). Thus, the release exponent between 0.35 and 0.41 indicates a non-Fickian drug transport mechanism.

CONCLUSIONS

The tested gels showed non-Newtonian pseudoplastic flow with shear thinning at a working temperature of 37°C, this being a mandatory requirement for topical systems in terms of conditioning as well as under the appearance of skin and the formation of a continuous film at the application site. Spongious matrices based on collagen, alginate and diclofenac with glutaraldehyde were prepared by lyophilization. The FT-IR analysis showed that collagen kept its structure in all the samples. The recorded kinetic profiles show that the designed spongious matrices could be promising supports for drug delivery systems with potential use in the treatment of injuries and relieving pain.

REFERENCES

Albu, M.G. (2011), *Collagen Gels and Matrices for Biomedical Applications*, Lambert Academic Publishing, Saarbrücken.

Albu, M.G. *et al*. (2012), "Rheological behavior of some collagen extracts", *Leather and Footwear Journal*, 12(3), 193-200.

Barbour, K.E. *et al*. (2017), "Vital Signs: Prevalence of Doctor Diagnosed Arthritis and Arthritis-Attributable Activity Limitation - United States, 2013-2015", *Morbidity and Mortality Weekly Report,* 66(9), 246–253, https://doi.org/10.15585/mmwr.mm6609e1.

Chiu, C.T. *et al*. (2008), "Development of two alginate-based wound dressings", *Journal of Materials Science: Materials in Medicine*, 19(6), 2503-2513, https://doi.org/10.1007/s10856-008-3389-2.

Fan, L. *et al*. (2013), "Preparation and characterization of sodium alginate modified with collagen peptides", *Carbohydrate Polymers*, 93, 380–385, https://doi.org/10.1016/j.carbpol.2013.01.029.

Ghica, M.V. *et al*. (2017), "Development, Optimization and In Vitro/In Vivo Characterization of Collagen-Dextran Spongious Wound Dressings Loaded with Flufenamic Acid", *Molecules*, 22(9), 1552, https://doi.org/10.3390/molecules22091552.

Ghica, M.V. *et al*. (2016), "Flow and thixotropic parameters for rheological characterization of hydrogels", *Molecules*, 21(6), E 786, https://doi.org/10.3390/molecules21060786.

Goh, C.F., and Lane, M.E. (2014), "Formulation of diclofenac for dermal delivery", *International Journal of Pharmaceutics*, 473(1-2), 607-616, https://doi.org/10.1016/j.ijpharm.2014.07.052.

Hsies, L.F. *et al*. (2010), "Efficacy and Side Effects of Diclofenac Patch in Treatment of Patients with Myofascial Pain Syndrome of the Upper Trapezius", *Journal of Pain and Symptom Management*, 39(1), 116-125, https://doi.org/10.1016/j.jpainsymman.2009.05.016.

Kaya, D.A. *et al*. (2014), "The influence of marine algae and natural plant oils on collagen-based cream properties", *Proceedings of the 5th International Conference on Advanced Materials and Systems (ICAMS),* 237-242.

Kok, A.G. *et al*. (2018), "Coprescribing proton-pump inhibitors with nonsteroidal anti-inflammatory drugs: risks versus benefits", *Journal of Pain Research*, 11, 361-374, https://doi.org/10.2147/JPR.S156938.

Mason, L. *et al*. (2004), "Topical NSAIDs for chronic musculoskeletal pain: systematic review and meta-analysis", *BMC Musculoskeletal Disorders*, 5, 28-35, https://doi.org/10.1186/1471-2474-5-28.

Ong, C.K.S., Tan, C.H. and Seymour R.A. (2007), "An evidence-based update on non-steroidal anti-inflammatory drugs", *Journal of Clinical Medicine and Research*, 5(1), 19-34, https://doi.org/10.3121/cmr.2007.698.

Ramshaw, J.A.M., Wekmeister, J.A. and Dumsday, G.J. (2014), "Bioengineered collagens:Emerging directions for biomedical materials", *Bioengineered*, 5(4), 227-233, https://doi.org/10.4161/bioe.28791.

ANTIFUNGAL ACTIVITY OF *Origanum syriacum* L. ESSENTIAL OILS AGAINST *Candida spp.*

NİZAMİ DURAN[1], DURMUŞ ALPASLAN KAYA[2]

[1]*Microbiology & Clinical Microbiology Department, Medical Faculty, Hatay Mustafa Kemal University, Turkey, nizamduran@hotmail.com*

[2]*Hatay Mustafa Kemal University, Faculty of Agriculture, Field Crops Department, Turkey, alpaslankaya@yahoo.com*

The infections caused by Candida species have been reported to cause serious life-threatening infections. Because the increased drug resistance among candida spp., new drug researches are intensively carried out. *Origanum syriacum* L. is a valuable medicinal plant in terms of its components. The aim of this study was to investigate components and the antifungal activity of *Origanum syriacum* L. essential oils on the growth of *Candida spp.* By GC-MS was highlighted that thymol (42,18 %), carvacrol (33,95 %), cymene (8,87 %) and γ-terpinene (8,21 %) are the main components. Antifungal activity of the essential oils of *Origanum syriacum* L. was evaluated by microdilution method. The most notable activity was obtained against *C. dubliniensis*, *C. albicans* and *C. parapsilosis*. MIC values were found to be 15.6 *C.* for *C. dubliniensis* and 31.2 µg/ml for *C. parapsilosis* and *C. albicans*. MIC values against *C. glabrata*, *C. kefyr*, *C. intermedia* were found to be 62.5, MIC values for *C. krusei* and *C. glabrata* were 125 µg/ml. The highest activity in terms of MBC values in the study was obtained against *C. intermedia* and *C. parapsilosis* (62.5 µg/ml). Our results are particularly promising to have significant activity against *C. dubliniensis*, *C. albicans* and *C. parapsilosis*. *Origanum syriacum* L. essential oils, which were also effective against non-albicans Candida species, may be a new hope for the treatment of candida infections.

Keywords: Candida, *Origanum syriacum* L., essential oils, antifungal, resistance

INTRODUCTION

Candida species are microorganisms found in the normal flora of many body parts such as human skin and mucosa. *Candida albicans* and Candida species other than *Candida albicans* have also been reported to cause serious life-threatening infections. Especially, in recent years, the increased drug resistance among candida spp. is striking. Therefore, new drug researches are intensively carried out (Spampinato and Leonardi, 2013).

Origanum syriacum L. is a valuable medicinal plant in terms of its components. It is possible to find many studies about Origanum genus. It has been reported to have major components of thymol and carvacrol in component analysis of *Origanum syriacum* L. It has been reported that these components have considerable pharmacological properties.

Candida species are the most common microorganisms found in the skin and mucous membranes of humans. It is found in the mouth and gastrointestinal tract of 30-50% of healthy people (Spampinato and Leonardi, 2013; Sanguinetti *et al.*, 2015). Due to some predispose causes; Candida spp. can cause superficial, deep, acute and/or chronic infections in humans. Most candida infections are endogenous infections. Candida albicans is most frequently isolated from Candida infections. In recent years, the incidence of candidiasis caused by Candida species other than *C. albicans* has increased. Mortality and mortality are high in infections caused by candidiasis. In recent years, the increase in candida species other than *Candida albicans* and the use of antifungal drugs for prophylactic purposes have led to an increase in drug resistance. The increase in the frequency of Candida species other than *Candida albicans* has led to

the development of resistance especially in azole derivative antifungals. It has also been shown that many Candida isolates develop amphotericin B resistance. Therefore, the search for new antifungal agents especially on natural products continues intensively (Sanguinetti *et al*., 2015; Golabek *et al*., 2015).

The aim of this study was to identify the components of *Origanum syriacum* L. essential oils and to investigate their antifungal activity against Candida spp.

MATERIALS AND METHODS

Clinical isolates and standard candida strains were used in the study. Eight strains were used from each of the clinical isolates used in the study. The strains used were:*C. albicans, C. tropicalis, C. kefyr, C. krusei, C. glabrata, C. dubliniensis, C. intermedia, C. parapsilosis*. Clinical isolates were Candida strains isolated from samples sent to routine mycology laboratory from various clinical specimens. Isolated strains were inoculated into Sabouraud-dextrose-agar media for identification and incubated at 37 °C for 48 hours. For typing, isolates were evaluated in terms of germ tube test, hif formation in corn flour aged with Tween 80, pseudo-hif formation, blastospor and chlamydospor formation properties. When needed, automated culture systems (Vitek-2, BioMerieux France) were utilized for typing.

Plant Materials

Origanum syriacum L. plants were harvested in Hatay province of Turkey during the full bloom period, when the amount of active substance was most intense and after being dried in the shade at room temperature.

Preparation of Plant Extracts

Plant material was weighted and placed in a round bottom flask with a volume of distilled water as extraction solvent; the herba-water mixture was refluxed about 2 h, during which the oil was collected in the side arm of the system. The installation was allowed to stand for about half hour to prevent the oil to reach room temperature. The oil was dried over anhydrous sodium sulphate and then stored in dark color glass bottles and keep to refrigerator (about 4 °C) until use for analysis.

GC/MS Analysis

Analysis of essential oil was performed using the Thermo Scientific Focus gas chromatograph equipped with a DSQ II single quadrupole mass spectrometer, Triplus autosampler and fused-silica capillary columnTR-5MS (5% phenyl-polysilphenylene-siloxane, 30 m×0.25 mm inner diameter, film thickness 0.25 μm). The injection volume was 2 μL. The samples were injected with a split ratio of 250:1 by using helium (99.99%) as carrier gas, at a flow rate of 1 mL/min; ionization energy was 70 eV. The transfer line temperature of the mass spectrometer was 220 °C, while the temperature of orifice injection was of 220 °C. The temperature of oven was programmed in the range 50–220 °C at a rate of 3 °C/min. Data acquisition was made in the scanning mode. Identification was done on full scan mode in the m/z range of 50–650 a.m.u.

Determination of Minimal Fungicidal Concentration (MFC)

Antifungal activity of the essential oils of *Origanum syriacum* L. was evaluated by microdilution method. Clinical and standard isolates were grown in SDA (Saboraud's Dextrose Broth) medium at 37 °C for 48 hours. Final candida concentrations were adjusted to 10^8 cfu/mL with reference to the McFarland turbid meter.

Determination of Minimum Inhibitory Concentrations (MIC)

MIC values of *Origanum syriacum* L. essential oils were determined by the broth microdilution test. Firstly, all isolates were subcultured in Saboraud Dextrox Broth and incubated for 24 h at 37 °C. Then, two-fold serial dilutions of essential oils were made in Saboraud Dextrox Broth to achieve a concentration range from 0 to 500 µg/ml. (500, 250, 125, 62.5, 31.2, 15.6, 7.8, 3.9, 1.8, 0.9) The broth microdilution tests were performed according to the NCCLS guidelines (CLSI, 2008).

RESULTS

Seventeen essential oil components, representing 98,76 %, were detected in the essential oil of *Origanum syriacum* L. (Figure 1, Table 1). The major essential oil constituents were thymol (42,18 %), carvacrol (33,95 %), cymene (8,87 %) and γ-terpinene (8,21 %).
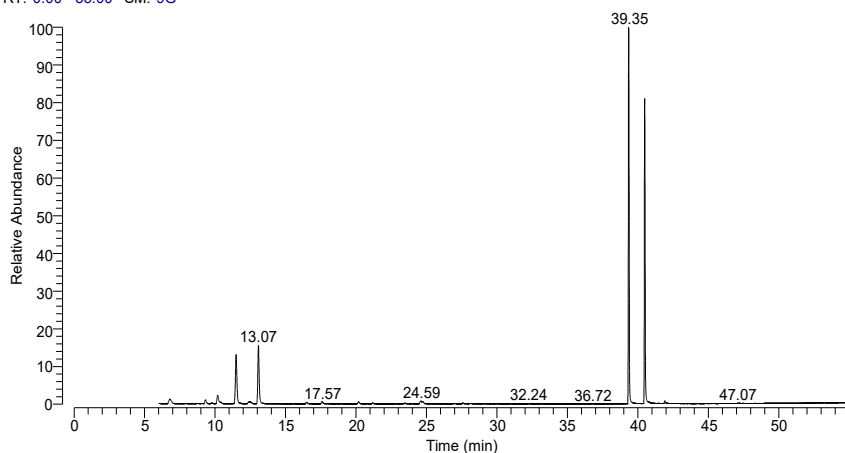
Figure 1. GC/MS chromatogram of *Origanum syriacum* L.

Table 1. Essential oil components of *Origanum syriacum* L.

RT	Compound Name	SI	RSI	Cas #	%
6,78	α-Pinene	942	969	80-56-8	1,02
9,31	β-Myrcene	956	985	123-35-3	0,64
9,76	α-Phellandrene	855	923	99-83-2	0,13
10,19	α-Terpinene	962	979	99-86-5	1,40
11,49	γ-Terpinene	988	992	99-85-4	8,21
12,45	Eucalyptol	876	889	470-82-6	0,61

RT	Compound Name	SI	RSI	Cas #	%
13,07	Cymene	984	995	25155-15-1	8,87
16,47	3-Octanol	925	947	589-98-0	0,23
17,57	1-Octen-3-ol	955	982	3391-86-4	0,31
20,16	4-Thujanol	934	962	546-79-2	0,31
21,15	Linalool	913	930	78-70-6	0,15
24,58	trans-Caryophyllene	958	969	87-44-5	0,35
24,75	Terpinen-4-ol	930	954	562-74-3	0,20
27,55	α-terpineol	859	900	2438-12-2	0,12
28,12	Borneol	813	867	10385-78-1	0,08
39,35	Thymol	970	982	89-83-8	42,18
40,48	Carvacrol	966	966	499-75-2	33,95

The MIC and MBC results of *Origanum syriacum* L. were given in Table 2. In the study, considerable activities of *Origanum syriacum* L. essential oils were determined against all candida strains. The most notable activity was obtained against *C. dubliniensis*, *C. albicans* and *C. parapsilosis*. MIC values were found to be 15.6 *C.* for *C. dubliniensis* and 31.2 µg/ml for *C. parapsilosis* and *C. albicans* (Figure 2). MIC values against *C. glabrata*, *C. kefyr*, *C. intermedia* were found to be 62.5, MIC values for *C. krusei* and *C. glabrata* were 125 µg/ml. Table 2 also shows MFC values. The highest activity in terms of MFC values in the study was obtained against *C. intermedia* and *C. parapsilosis* (62.5 µg/ml) (Table 2).
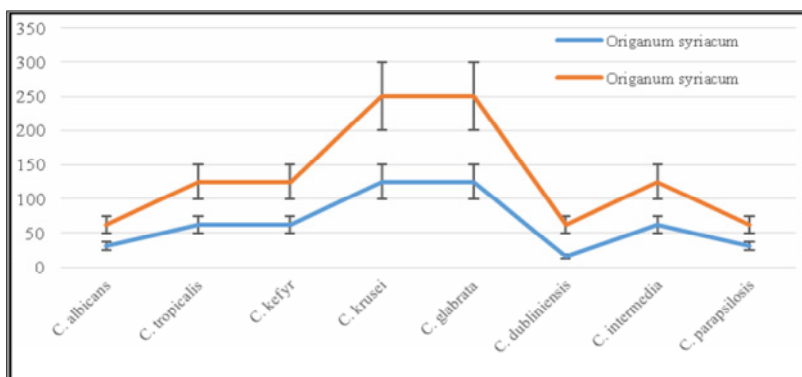
Figure 2. MIC and MFC values of *Origanum syriacum* L. essential oils against *Candida* species

Table 2. Comparison of MIC and MFC values of *Origanum syriacum* L. essential oils and fluconazole against *Candida* species

| *Candida* species | *Origanum syriacum* L. | | Fluconazole | |
	MIC values µg/ml	MFC values µg/ml	MIC values µg/ml	MFC values µg/ml
C. albicans	31.6	62.5	1.8	3.9
C. tropicalis	62.5	125	3.9	3.9
C. kefyr	62.5	125	1.8	1.8
C. krusei	125	250	1.8	3.9

C. glabrata	125	250	3.9	7.8
C. dubliniensis	15.6	125	3.9	3.9
C. intermedia	62.5	62.5	1.8	3.9
C. parapsilosis	31.2	62.5	1.8	3.9

DISCUSSION AND CONCLUSION

Recently, the prolongation of life span depending on the developments in medicine has led to an increase in the number of elderly and immunosuppressed patients (Spampinato and Leonardi, 2013; Sanguinetti *et al*., 2015; Sardi *et al*., 2013).

Candida infections have recently been isolated, especially in intensive care units and immunosuppressive patients. Due to its endogenous origin, *C. albicans* is the first line in nosocomial candida infections. But recently there has been a significant increase in the frequency of human infections caused by non-albicans candida species (Sardi *et al*., 2013).

It is known that antifungal treatment is more difficult to respond to non-albicans species such as *C. tropicalis*, *C. krusei*, *C. glabrata*, *C. parapsilosis* and *C. lusitaniae*. Drug resistance is known to show significant increases in all candida species (Sanguinetti *et al*., 2015). For this reason, our results have a great prospect of investigating new active drug in increasing drug resistance.

Our results are particularly promising having significant activity against *C. dubliniensis*, *C. albicans* and *C. parapsilosis*. *Origanum syriacum* L. essential oils, which were also effective against non-albicans Candida species, may be a new hope for the treatment of candida infections.

REFERENCES

Clinical and Laboratory Standards Institute (2008), "Reference Method for Broth Dilution Antifungal Susceptibility Testing of Yeast"; Approved Standard-Third Edition. CLSI document M27-A3. Wayne: Clinical and Laboratory Standards Institute.

Gołąbek, K. *et al*. (2015), "Selected mechanisms of molecular resistance of *Candida albicans* to azole drugs", *Acta Biochim*, Pol. 62(2), 247-51, https://doi.org/10.18388/abp.2014_940.

Sanguinetti, M. *et al*. (2015), "Antifungal drug resistance among Candida species: mechanisms and clinical impact", *Mycoses*, 58 Suppl 2, 2-13, https://doi.org/10.1111/myc.12330.

Sardi, J.C. *et al*. (2013), "Candida species: current epidemiology, pathogenicity, biofilm formation, natural antifungal products and new therapeutic options", *J Med Microbiol*, 62, 10-24, https://doi.org/10.1099/jmm.0.045054-0.

Spampinato, C. and Leonardi, D. (2013), "Candida infections, causes, targets, and resistance mechanisms: traditional and alternative antifungal agents", *Biomed Res Int*, 204237, https://doi.org/10.1155/2013/204237.

SYNERGISTIC ACTIVITIES OF *Hypericum perforatum L.* AND GLABRIDIN AGAINST DRUG RESISTANT *H. pylori* ISOLATES

NİZAMİ DURAN[1], DURMUŞ ALPASLAN KAYA[2]

[1]*Microbiology & Clinical Microbiology Department, Medical Faculty, Hatay Mustafa Kemal University, Turkey, nizamduran@hotmail.com*

[2]*Hatay Mustafa Kemal University, Faculty of Agriculture, Field Crops Department, Turkey, alpaslankaya@yahoo.com*

Glabridin and *Hypericum perforatum L.* have many pharmacological activities such as antimicrobial activity, antiproliferative, cytotoxic, anticancerogenic, antiproliferative and antioxidant effect. The aim of this study was to determine the components and to investigate the antimicrobial activity of *Hypericum perforatum L.* and glabridin against drug resistant *H. pylori* isolates. The main essential oil components of *Hypericum perforatum L. determined by GC-MS* were caryophyllene (19,13 %), germacrene-D (13,22 %), α-Pinene (12,59 %) and β-helmiscapene (8,99 %). We also aim to determine the synergistic activity of these two natural products against the drug-resistant *H. pylori* strains. MIC values of *Hypericum perforatum* L. essential oils and glabridin against drug resistant *H. pylori* isolates were carried out by modifying the method described previously. In the experiments in which 1:1 ratio of *Hypericum perforatum* L. essential oils and glabridin was used, the MIC values (µg/mL) were as follows: 8 For standard strain; 4 for drug sensitive strain; 8 for metronidazole resistant strain; and 16 for clarithromycin resistant strains. In conclusion, it was found that *Hypericum perforatum L.* essential oils and glabridin had significant antimicrobial activity against HP strains in our study.

Keywords: *Hypericum perforatum,* glabridin, *H. pylori,* drug, resistant, strain

INTRODUCTION

Today, it is thought that about half of the world's population is colonized with *H. pylori*. Nearly all infected persons with *H. pylori* can develop gastritis and mild functional changes, peptic ulcer, ulcer complications, stomach cancer and maltoma (Makola Di Peura and Crowe, 2007).

Antibiotics such as Clarithromycin, Metronidazole, Amoxicillin and tetracycline are used for the treatment of *H. pylori* infections. For treatment, some of these drugs are given in combination. However, increased resistance to antibiotics has resulted in treatment failures. Therefore, treatment of drug-resistant *H. pylori* infections can lead to serious morbidity and mortality (Tonkic *et al*., 2012; Silva *et al*., 2012; Choi *et al*., 2018; We *et al*., 2014).

Therefore, new drug researches are being carried out intensively. Natural products such as plant extracts and essential oils are very important sources for new drug research (Silva *et al*., 2012). Natural products are very popular due to low cytotoxic and side effects. Among these natural products, *Hypericum perforatum* L. In addition, liquorice are two important medicinal plants.

Glabridin is one of the most commonly studied liquorice root flavonoids. Glabridin is a prenylized isoflavonoid derived from the root of *G. glabra* L. It has many pharmacological properties such as antioxidant, anti-inflammatory, antiatherogenic, estrogenic, neuroprotective, anti-inflammatory, anti-osteoporotic, skin whitening and regulating energy metabolism (Simmler *et al*., 2013).

In addition, glabridin has been reported to have many pharmacological activities such as cytotoxic activity, antimicrobial activity, estrogenic and anti-proliferative activity against human breast cancer cells. It also affects melanogenesis, inflammation,

low-density lipoprotein oxidation and mitochondrial functions from oxidative stress (Choi, 2005).

Glabridin is known to have many pharmacological activities such as antimicrobial activity, antiproliferative effect and cytotoxic effect (Choi, 2005).

Hypericum perforatum L. has been widely used in folk medicine throughout history. Anticancerogenic, antimicrobial, antiproliferative and antioxidant efficacy of *Hypericum perforatum* L. has been reported in various studies (Kaçar and Özkan, 2004).

In this study, we aimed to investigate the antimicrobial activity of *Hypericum perforatum* L. and Glabridin against drug resistant *H. pylori* isolates. We also aim to determine the synergistic activity of these two natural products against the drug-resistant *H. pylori* strains.

MATERIALS AND METHODS

Experiments were performed by using drug sensitive and resistant bacteria. Also, HP NCTC (11637) strain was selected as the control strain. All clinical samples were isolated from the laboratory. Clarithromycin and metronidazole resistance of isolates were evaluated by E-test method (AB Biodisk, Sweden) (Fukazawa *et al*., 1999). In order to isolate, the samples were inoculated to Mueller Hinton agar with 5% sheep blood and HP agar. Then, the incubation of plates were performed at 37°C under microaerophilic conditions (Camy-Gen, Oxoid). The conventional techniques (gram staining, catalase, urease etc.) were used for the identification of *H. pylori* isolates (Owen, 1995). Standard HP NCTC (11637) strain was obtained from the Microbiology Department of Hacettepe University, Medical School.

GC/MS Analysis

Analysis of essential oil was performed using the Thermo Scientific Focusgas chromatograph equipped with a DSQ II single quadrupole mass spectrometer, Triplus autosampler and fused-silica capillary columnTR-5MS (5% phenyl-polysilphenylene-siloxane, 30 m×0.25 mm inner diameter, film thickness 0.25 µm). The injection volume was 2 µL. The samples were injected with a split ratio of 250:1 by using helium (99.99 %) as carrier gas, at a flow rate of 1 mL/min; ionization energy was 70 eV. The transfer line temperature of the mass spectrometer was 220°C, while the temperature of orifice injection was of 220°C. The temperature of oven was programmed in the range 50–220°C at a rate of 3°C/min. Data acquisition was made in the scanning mode. Identification was done on full scan mode in the m/z range of 50–650 a.m.u.

Preparation of Bacterial Suspension

Glabridin was purchased from Sigma (Sigma, USA). In order to solve glabridin, DMSO was selected as the solvent. MIC values of *Hypericum perforatum* L. essential oils and glabridin against drug resistant *H. pylori* isolates were carried out by modifying the method described by Imamura et al. For this purpose, the microdilution broth method was used. Clinical isolates and standard *H. pylori* strain were suspended in Brucella Broth (BBL 4311086) with 5% fetal calf serum (FCS). *Hypericum perforatum*, *Glabridin* and antibiotics were diluted from 0.5 to 256 µg/mL by 2-fold serial dilution. All bacterial strains were incubated in Brucella Broth agar containing 5% FCS at 37°C under microaerophilic conditions. The bacterial cell concentration in the experiments

was adjusted to 1×10^8 cells/mL. MIC assays were evaluated at the end of 5 days of incubation (Hirschl and Makristathis, 2007).

Determination of Minimum Bactericidal Concentration (MBC)

Bacterial strains were diluted from 1024 to 0.5 µg/mL (1024, 512, 256, 128, 64, 32, 16, 8, 4, 2, 1, 0.5 µg/mL). MBC assay was studied according to method described by O'Mahnoy et al 2005. Briefly, 900 µL of solution containing different concentrations of *Hypericum perforatum* L. essential oils and *Glabridin* was added to 100 µg/ml of bacterial suspension (1×10^8 cells/mL) and incubated at the 37°C under microaerophilic conditions for 72 hours. At the end of incubation, 100 µL of each dilution was inoculated to *H. pylori* agar for growth. As positive controls, metronidazole (100 µg/mL), clarithromycin (10 µg/mL), amoxicillin (10 µg/mL), levofloxacin (20 µg/mL) and tetracycline (40 µg/mL) were selected. DMSO (1%; w/v) was used as negative control. All experiments were performed in triplicate.

Antimicrobial Sensitivity Tests

Resistance against clarithromycin and metronidazole in clinical isolates were determined by the E test method as described by Farshad et al. In the present study, the following values were accepted as resistance threshold: ≥8 µg/mL for metronidazole and ≥1 µg/mL for clarithromycin. HP NCTC 11637 was used as control strain.

The resistance threshold in this study was as follows: 8 µg/ml for metronidazole and 1 µg/mL for clarithromycin. HP NCTC 11637 was used as standard strain.

Statistical Analysis

Chi-square and Student's t-test were used to analyze of data. $p \leq 0.05$ was considered as statistically significant. All statistical analyses were performed by using SPSS for Windows Version 17.0.

RESULTS

Forty-four essential oil components, representing 98,6 %, were detected in the essential oil of *Hypericum perforatum* L. (Figure 1, Table 1). The main essential oil components were caryophyllene (19,13 %), germacrene-D (13,22 %),α-Pinene (12,59 %) and β-helmiscapene (8,99 %).
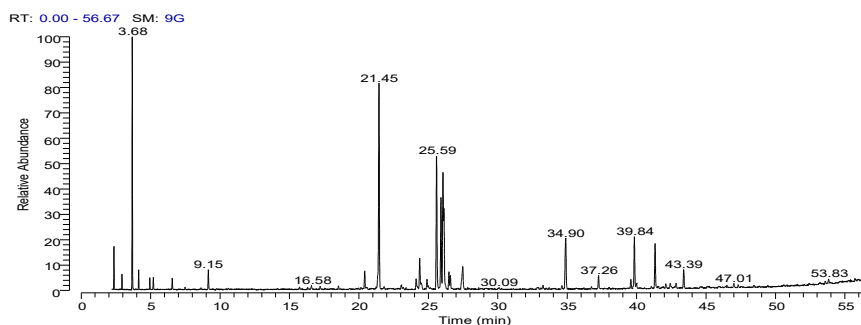
Figure 1. GC/MS chromatogram of *Hypericum perforatum* L.

Table 1. The main essential oil components of *Hypericum perforatum L.*

RT	Compound Name	SI	RSI	Cas #	Area %
3,68	α-Pinene	991	992	80-56-8	12,59
21,45	trans-Caryophyllene	979	984	87-44-5	19,13
25,59	Germacrene D	968	974	23986-74-5	13,22
25,91	β-helmiscapene	963	981	17066-67-0	8,99
26,12	α-helmiscapene	952	960	473-13-2	5,47
34,89	Caryophyllene oxide	950	960	1139-30-6	5,26

Figure 2 presents results for *Hypericum perforatum* L. essential oils in *H. pylori* NCTC 11637 strain and clinical *H. pylori* strains found to be sensitive to antimicrobial agents. It was found that the essential oils showed significant bactericidal activity at 8 µg/mL for *H. pylori* NCTC 11637 strain, while MIC value was 16 µg/mL for the drug-sensitive clinical isolates. It was found that MIC value for drug-sensitive clinical isolates was significantly higher when compared to standard *H. pylori* strain ($p<0.05$).

Similarly, as shown Figure 2, when the efficacy of Glabridin against *H. pylori* is evaluated; the MIC value for the standard *H. pylori* strains (16 µg/ml) was lower than for drug-sensitive strains (32 µg/ml). A statistically significant difference was found between the MIC values obtained against the standard strain and the drug-sensitive strains ($p<0.05$).

It was found that *Hypericum perforatum* L. essential oils and glabridin had higher MIC values when compared to standard antibiotics (metronidazole, clarithromycin, amoxicillin, levofloxacin and tetracycline) used in HP treatment (Figure 3).

In our study, MIC value was found to be 8 µg/mL for metronidazole, 4 µg/mL for clarithromycin, 2 µg/mL for amoxicillin, 1 µg/mL for levofloxacin and 8 µg/mL for tetracycline whereas MIC value of glabridin was 64 µg/mL in metronidazole-resistant HP isolates. MIC value was found to be 4 µg/mL for metronidazole, 4 µg/mL for clarithromycin, 2 µg/mL for amoxicillin, 2 µg/mL for levofloxacin and 4 µg/mL for tetracycline whereas 32 µg/mL for glabridin in clarithromycin-resistant *H. pylori* isolates (Figure 3). Also, MIC value of *Hypericum perforatum* L. essential oils against *H. pylori* was 32 µg/mL in both metronidazole-resistant and clarithromycin-resistant HP isolates.

In the experiments in which 1:1 ratio of *Hypericum perforatum* L. essential oils and Glabridin was used, the MIC values were as follows: 8 for standard strain; 4 for drug sensitive strain; 8 for metronidazole resistant strain; and 16 for clarithromycin resistant strains (Figure 4).
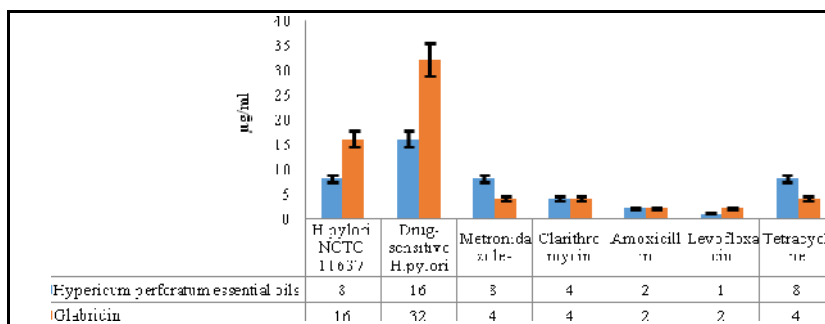
Figure 2. MIC values of standard drugs, *Hypericum perforatum* L. essential oils and Glabridin against the *H. pylori* isolates

	H.pylori NCTC 11637	Drug-sensitive H.pylori	Metronidazole	Clarithromycin	Metronidazole-resistant H.pylori	Resistant H.pylori
Hypericum perforatum essential oils	8	16	8	4	64	32
Glabridin	16	32	4	4	32	32
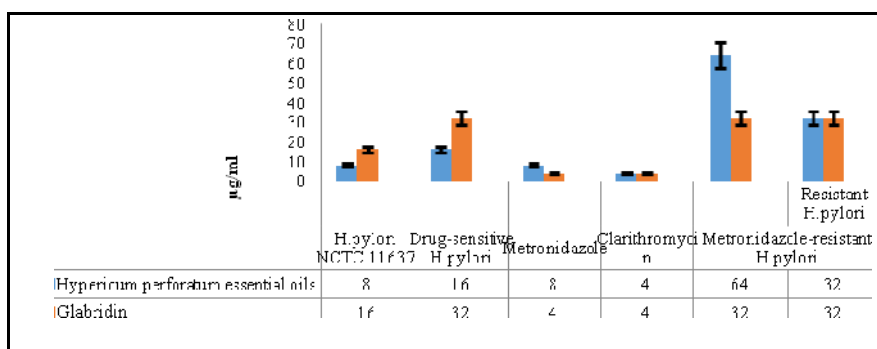
Figure 3. Comparison of MIC values of standard drugs with *Hypericum perforatum* L. essential oils and Glabridin against the drug sensitive and resistant *H. pylori* isolates

	H.pylori NCTC 11637	Drug-sensitive H.pylori	Metronidazole	Clarithromycin	Metronidazole-resistant H.pylori	Resistant H.pylori Clarithromycin
Hypericum perforatum essential oils + Glabridin	8	4	8	4	8	16
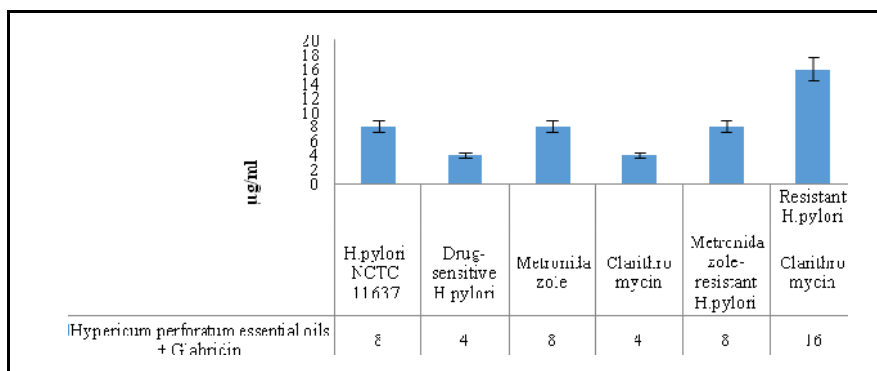
Figure 4. MIC values of the combined use of *Hypericum perforatum* L. essential oils and Glabridin against drug-resistant *H. pylori* isolates

DISCUSSION AND CONCLUSION

Today, treatment of individuals infected with drug-resistant *H. pylori* strains is extremely difficult. Our results show that both *Hypericum perforatum* L. essential oils and glabridin were quite effective against *H. pylori* colonizing nearly half of the world's population. In our study, MIC values of both *Hypericum perforatum* L. essential oils and glabridin against drug-sensitive *H. pylori* isolates of were found to be lower than drug-resistant strains.

Another important finding of our study was that the combined use of *Hypericum perforatum* L. essential oils and Glabridin was more potent against drug-resistant *H. pylori* strains. Further studies *in-vivo* are needed in this regard.

It should not be forgotten that the combined use of natural products which have antimicrobial effectiveness in combating drug-resistant strains may exhibit additive or synergistic effects.

In conclusion, it was found that *Hypericum perforatum* L. essential oils and Glabridin had significant antimicrobial activity against *H. pylori* strains in our study.

REFERENCES

Choi, J.H. *et al*. (2018), "Current Status of the third-line *Helicobacter pylori* eradication", *Gastroenterol Res Pract*, 6523653, https://doi.org/10.1155/2018/6523653.

Choi, E. (2005), "The licorice root derived isoflavan glabridin increases the function of osteoblastic MC3T3-E1 cells", *Biochem. Pharm*, 70, 363-368, https://doi.org/10.1016/j.bcp.2005.04.019.

Fukazawa, K. *et al*. (1999), "Antimicrobial resistance testing of *H. pylori* epsilometer test and disk diffusion test", *Nihon Rinsho*, 57(1), 76-80.

Hirschl, A.M. and Makristathis, A. (2007), "Methods to detect *Helicobacter pylori*: from culture to molecular biology", *Helicobacter*, Suppl 2, 6-11, https://doi.org/10.1111/j.1523-5378.2007.00560.x.

Kaçar, O. and Azkan, N. (2004), "Sarı Kantaron'da (*Hypericum perforatum* L.) Hiperisin ve Üst Drog Herba Verimi ile Bazı Morfolojik ve Agronomik Özellikler Arasındaki İlişkiler", *Uludag Üniv. Zir. Fak. Derg.*, 18(2), 109-122.

Makola Di Peura, D.A. and Crowe, S.E. (2007), "Helicobacter pylori infection and related gastrointestinal diseases", *J Clin Gastroenterol*, 41, 548-58, https://doi.org/10.1097/MCG.0b013e318030e3c3.

O'Mahony, R. *et al*. (2005), "Bactericidal and anti-adhesive properties of culinary and medicinal plants against *Helicobacter pylori*", *World Journal of Gastroenterology*, 11, 7499-507, https://doi.org/10.3748/wjg.v11.i47.7499.

Owen, R.J. (1995), "Bacteriology of *Helicobacter pylori*", *Baillieres Clin Gastroenterol*, 9(3), 415-46.

Silva, O. *et al*. (2012), "Anti-*Helicobacter pylori* activity of Terminalia macroptera root", *Fitoterapia*, 83(5), 872-6, https://doi.org/10.1016/j.fitote.2012.03.019.

Simmler, C., Pauli, G.F., Chen, S.N. (2013), "Phytochemistry and biological properties of glabridin", *Fitoterapia*, 90, 160-84, https://doi.org/10.1016/j.fitote.2013.07.003.

Tonkic, A. *et al*. (2012), "Epidemiology and diagnosis of *Helicobacter pylori* infection", *Helicobacter*, 17, 1-8, https://doi.org/10.1111/j.1523-5378.2012.00975.

Wu, T.S. *et al*. (2014), "Eradication of *Helicobacter pylori* infection", *Med Sci*, 30(4), 167-72, https://doi.org/10.1016/j.kjms.2013.11.003.

COMPOSITE SCAFFOLDS FOR BONE REGENERATION MADE OF COLLAGEN/HYDROXYAPATITE/EUCALYPTUS ESSENTIAL OIL

ANDREI DAN FLOREA[1], ELENA DĂNILĂ[2,3], RODICA ROXANA CONSTANTINESCU[3], MĂDĂLINA ALBU KAYA[3], ALPASLAN DURMUŞ KAYA[4], GHEORGHE COARĂ[3], LUMINIŢA ALBU[3], CIPRIAN CHELARU[3]

[1]*University Politehnica of Bucharest, Faculty of Medical Engineering, 1-7 Gheorghe Polizu Str., 011061, Bucharest, Romania*

[2]*University Politehnica of Bucharest, Faculty of Applied Chemistry and Materials Science, Bucharest,1-7 Gheorghe POLIZU Str., 011061, Bucharest, Romania*

[3]*INCDTP - Division: Leather and Footwear Research Institute, 93 Ion Minulescu Str., 031215, Bucharest, Romania*

[4]*Hatay Mustafa Kemal University, Faculty of Agriculture, Field Crops Department, 31034, Antakya-Hatay, Turkey*

Bone regeneration is a serious problem nowadays because of the increased number of people suffering from infections, arthritis and bond loss. The aim of the present study was to develop and characterize collagen – hydroxyapatite – essential oil matrices for bone regeneration. In our study we wish to develop biomaterials which mimic bone composition and prevent allergic or toxic effects. The matrices obtained by freeze-drying were characterized by FT-IR analysis, water uptake capacity and microbiological analysis. The results obtained from analyses confirmed that collagen–hydroxyapatite-essential oils matrices exhibit proper characteristics for bone regeneration.

Keywords: collagen hydroxyapatite, essential oils, bone regeneration.

INTRODUCTION

Bone grafting is ideal for bone defects reconstruction. Due to the fact that allografts can transmit certain diseases or may have problems related to sterilization, it has been chosen to be made by synthetic and natural materials. Increasing the osteointegration and antibacterial properties of these grafts and replacing them with the host bone is considerably important. Literature studies have also shown that various substituents, such as bone morphogenetic proteins, parathyroid hormones, or platelet-rich plasma, have been added to allografts or synthetic materials. Clinical applications of these substituents have shown good bone formation, but their subsequent application has been limited due to the high cost or potential adverse reactions (Habibovic, 2011). The alternative came from combining synthetic and natural materials like hydroxyapatite (HA) and collagen (COLL) with essential oils like eucalyptus essential oil (EEO). Hydroxyapatite, similar to chemical composition and morphology of bone apatite, can provide a good adhesion to the local tissue due to its surface and has been shown that it has the ability to enhance osteoblast proliferation and differentiation. Collagen is widely found in bone and skin (Type I), cartilage (Type II) and blood vessel (Type III), increasingly being used as a composition in artificial bone. As a natural polymer, it has excellent biocompatibility, which allow cell attachment and growth, and biodegradability in order to be easily absorbed by the body. Collagen-hydroxyapatite (COL-HA) composite imitates natural bone tissue (He *et al*., 2017).

Essential oils from plant extracts are natural antimicrobial agents; incorporation of essential oil into synthetic materials may not only enhance the materials antimicrobial properties but also reduce water- solubility, vapor-permeability and slow lipid oxidation

of the product (Hafsa *et al.*, 2016; Stegarus and Lengyel, 2017). One example is eucalyptus essential oils which present several properties such as antimicrobial, antihyperglycemic, antioxidant and anthelmintic properties (Herculano *et al.*, 2014).

The aim of this study was to prepare and characterize some collagen – hydroxyapatite-eucalyptus essential oil scaffolds in order to facilitate bone reconstitution.

MATERIALS AND METHODS

Materials

The type I fibrillar collagen gel having a concentration of 2.54% (w/v) and acid pH, was extracted from calf hide using the protocol that has been previously described (Albu, 2011). Hydroxyapatite was purchase from Sigma Aldrich (Germany). Eucalyptus (*Eucalyptus globulus*) essential oil was obtained in Department of Medicinal and Aromatic Plants, Faculty of Agriculture, Mustafa Kemal University, Hatay, Turkey from wild plants from the province of Hatay in the period of their blooming, by hydrodistilation using a Neo-Clevenger apparatus. Glutaraldehyde (GA) was purchase from Merck (Germany). All the chemicals were of analytical grade and the water was distilled.

Preparation of Collagen Hydrogels/Composite Scaffolds

The concentration of each collagen gel was adjusted at 1,2% (w/v) and 7.4 pH using a solution of sodium hydroxide with 1M concentration (the pH of the physiological medium in human body). Hydroxyapatite and eucalyptus essential oil were added to collagen gel (w/v), in different proportions, and then the composite gels were cross-linked with 0.025% glutaraldehyde (GA) solution (reported to collagen dry substance) as Table 1 presents.

Table 1. Composition of collagen hydrogels

	COLL%	HA%	EEO%	GA%
1.C		-	-	
2.CE	1.2	-	0.5	0.025
3.CH		50	-	
4. CHE		50	0.5	

The collagen gels, in order to be analysed, were freeze-dried using Delta 2-24 LSC (Martin Christ, Germany) lyophilizer, using a 48 hours lyophilization programme and composite scaffolds were obtained.

Water Up-take Capacity

Water Up-take

The obtained collagen samples were tested by water up-take. They were firstly immersed in water at 37°C then withdrawn and weighed at fixed time intervals. The equation used (eq. 1) for water absorption determination was:

%Water up-take = (Wt – Wd)/ Wd (g/g)   (1)

where Wt is the weight of the swollen samples at immersion time t, and Wd denotes the weight of the dry samples. All the samples were studied in triplicate.

FTIR-ATR Analysis

FT-IR spectral measurements were recorded by spectrophotometer Jasco FT/IR-4200. All the spectra were recorded at the following parameters: spectral range 4000-600 cm^{-1}, resolution 4 cm^{-1} with 30 acquisitions per each sample.

Microbiological Analysis

All the samples have been tested for antimicrobial activity against *Escherichia coli*, according to SR EN ISO 20645/2005 Control of antibacterial activity / Diffusion test on the gelled plate.

A volume of gelose (Tryptic Soya Broth) for the lower layer without bacteria was prepared. 10 ml of gelose was introduced into sterilized Petri dish and allowed the gelose to solidify. A volume of gelose for the upper layer was prepared and cooled to 45°C in a water bath. 150 ml of gelose was inoculated with 1 ml of bacterial solution of *Escherichia coli* (1-5 x 10 8 μg / ml). The container is vigorously stirred for the uniform distribution of the bacteria. 5 ml of solution was introduced in each Petri dish and allowed the gelose to solidify. The samples were placed on the surface of the nutrient medium and then incubated at 37°C between 18h and 24h.

RESULTS AND DISCUSSION

Figure 1 presents the water up-take during 24 hours for the studied samples:
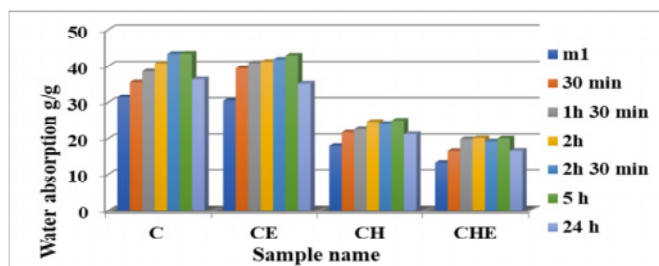
Figure 1. Water absorption during 24 hours for collagen sponges

The crosslinked collagen (C) absorbed the higher amount of water than the others. The samples with crosslinked collagen, hydroxyapatite and eucalyptus essential oil (CHE) absorbed lower amount of water due to their more compact structure.

In figure 2 are presented the FT-IR spectra for collagen samples:
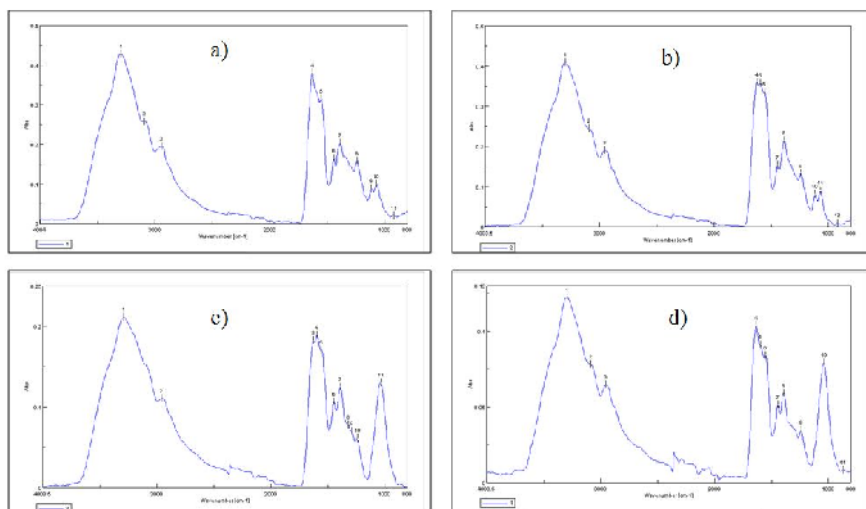
Figure 2. The FT-IR spectra of collagen samples: a-C sample; b-CE sample; c-CH
sample; d- CHE sample

The spectrum of collagen sample (C) (Fig. 2 a) exhibited typical amide bands specific for collagen: 3295 cm^{-1} and 2091 cm^{-1} for amide A (-NH- stretching) and B (-CH$_2$-) respectively, 1629 cm^{-1} was attributed to amide I (C=O stretching), 1552 cm^{-1} to amide II (N-H deformation) and 1444 cm^{-1} to amide III (N-H deformation) (Albu, 2011).

In the case of sample with essential oil (CE) (Fig.2 b), in the FT-IR spectra it can be observe a displacement of spectral bands characteristic of the amide groups (I, II and III) because of essential oil, also were observed the bands of 1,8-cineole (a major component in eucalyptus essential oil composition) attributed to C–O–C symmetrical (1116 cm^{-1}) and asymmetrical (1239 cm-1) stretching vibrations as well as to CH$_3$ symmetrical deformation at 1386 cm^{-1} (Sirvaityte et al., 2011).

In the FT-IR spectrum of the samples with hydroxyapatite (CH and CHE) (Fig. 2 c and d), it can be observed the spectral band characteristic for PO$_4$ groups of hydroxyapatite: 1035 cm^{-1} (CH sample) and 1039 cm^{-1} (CHE sample) (Chang, 2002).

The results of microbiological analysis are shown in Figure 3:

Figure 3. Microbiological results for collagen samples: 1-C sample; 2-CE sample; 3-CH sample; 4-CHE sample

The evaluation was based on the absence or presence of bacterial multiplication in the area of contact between the gelose and the sample and on the occurrence of a possible inhibition area around the samples, the results being shown in the Table 2:

Table 2. Effect of antibacterial treatment on collagen samples

Sample*	Inhibition area (mm)	Total number of aerobic germs (UFC/ cm^2)	Evaluation
1	0	7 UFC/ cm^2	Insufficient effect
2	0	Absent	Satisfactory effect
3	0	Absent	Satisfactory effect
4	0	Absent	Satisfactory effect

*1-C sample; 2-CE sample; 3-CH sample; 4-CHE sample

The result is considered to have a "satisfactory effect" if no bacterial growth is observed. The samples tested do not allow the development of aerobic germs for the tested bacteria, which prove the eucalyptus essential oil efficiency.

CONCLUSIONS

Type I collagen with hydroxyapatite and essential oil were used in order to obtain composite scaffolds for bone regeneration. The combination between components were highlighted by FT-IR spectra changes when hydroxyapatite and essential oil were added. The samples with crosslinked collagen, hydroxyapatite and eucalyptus essential oil absorbed lower amount of water due to their more compact structureand hydrophobic character of essential oil. The samples were tested against *E. coli* and the

results show that all the samples with eucalyptus essential oil present a satisfactory antibacterial activity.

The results showed that collagen-hydroxyapatite-essential oil matrices are potentially novel candidates as scaffolds for bone tissue engineering applications, but more tests will be performed on the samples.

REFERENCES

Albu, M.G. (2011), *Collagen Gels and Matrices for Biomedical Applications*, Lambert Academic Publishing, Saarbrücken, 23-24.

Chang, M.C. and Tanaka, J. (2002), "FT-IR study for hydroxyapatite/collagen nanocomposite cross-linked by glutaraldehyde", *Biomaterials*, 23(24), 4811-8.

Hafsa, J. *et al*. (2016), "Physical, antioxidant and antimicrobial properties of chitosan films containing Eucalyptus globulus essential oil", *LWT – Food Science and Tehnology*, 68, 356-364, https://doi.org/10.1016/ j.lwt.2015.12.050.

Habibovic, P. and Barralet, J.E. (2011), "Bioinorganics and biomaterials: bone repair", *Acta biomaterialia*, 7(8), 3013-3026, https://doi.org/10.1016/j.actbio.2011.03.027.

He, X. *et al*. (2017), "Incorporation of microfibrillated cellulose into collagen-hydroxyapatite scaffold for bone tissue engineering", *International Journal of Biological Macromolecules*, 115, 385-392, https://doi.org/10.1016/j.ijbiomac.2018.

Herculano, E.D. *et al*. (2014), "Physicochemical and antimicrobial properties of nanoencapsulated Eucalyptus staigeriana essential oil", *LWT-Food Science and Technology*, 61(2015), 484-491, https://doi.org/10.1016/j.lwt.2014.12.001.

Sirvaityte, J. *et al*. (2011), "Application of commercial essential oils of eucalyptus and lavender as natural preservative for leather tanning industry", *Revista de chimie*, 62(9), 884-893.

Stegarus, D.I. and Lengyel, E. (2017), "The antimicrobial effect of essential oils upon certain nosocomial bacteria", 17th International Multidisciplinary Scientific GeoConference (SGEM 2017), 17, 61, 1089-1096.

STUDY ON THE FUNCTIONALIZED GRAPHENE MODIFIED WATERBORNE POLYURETHANE MATERIALS

SONG GUO[1,2], ZHIWEN DING[1,2], XIAOYAN PANG[*1,3], WENQI WANG[2], YUETAO YIN[2], GUANQUN YOU[2]

[1]*China Leather and Footwear Research Institute Co. Ltd., Beijing 100015, China, pang_xiaoyan@126.com*

[2]*China Leather and Footwear Industry Research Institute (Jinjiang) Co., Ltd, Jinjiang 362200, China*

[3]*Sichuan University, National Engineering Laboratory for Clean Technology of Leather Manufacture, Chengdu 610065, China*

A new type of waterborne polyurethane (WPG) is fabricated using the functionalized graphene. The mechanical properties, wear resistance, and heat aging resistance of the modified polyurethane materials were tested. The results show that the initial thermal decomposition temperature (Td5) of polyurethane films increased from 217°C to 244°C, the mechanical property of modified polyurethane film firstly decreases and then increases with the increase of functionalized grapheme. In addition, the wear resistance of modified polyurethane film decreases following the increase of functionalized grapheme. Furthermore, the heat aging resistance is best when the content of functionalized grapheme is 0.02% (wt). The centrifugal stability test shows when the content is less than 0.04%, the products are stable.

Keywords: waterborne polyurethane; functionalized graphene; heat resistance

INTRODUCTION

Graphene oxide is a functionalized graphene attained through the oxidation of graphite. The functional group just replaces few carbon atoms, meanwhile not destroying the crystalline cells of the whole graphene. Accordingly, graphene oxide still retains the crystalline characteristics of graphene. In the meantime, graphene oxide sheets contain extensive amounts of oxygen (hydroxyl, epoxy, glycol, ketone and carboxyl functional groups), which are capable of changing the van der Waals forces of their interaction, bringing to them enhanced compatibility with the organic polymers. At the edge of the sheet, there are also some carbonyl and carboxyl groups, making the graphene oxide sheets more hydrophilic, which make them more convenient to disperse in some solvents (Hou *et al*., 2015; Yang *et al*., 2016).

In the current paper, functionalized graphene modified polyurethane is employed for the preparation of high physical materials, which are capable of enhancing not only the heat resistance, but also the water resistance and aging resistance of waterborne polyurethane, in addition to improving the overall performance of materials. It is considered as quite helpful for developing the environment-friendly and high-performance composite materials.

MATERIAL AND METHODS

Materials

Graphene oxide (GO), prepared in the laboratory with the use of the Hummers method; Isophorone diisocyanate (IPDI), industrial grade, Bayer China Ltd.; Stannous octoate catalyst (T-9), industrial grade, Jining Huakai Resin Co., Ltd.; Polypropylene

glycol (PPG-2000), industrial grade (110 °C vacuum dewatering 2h), Jiangsu Hai'an Petrochemical Plant; 2,2-Dimethylolpropionic acid (DMPA), industrial grade, Jiangxi Southwest City Hongdu Chemical Technology Development Co., Ltd.; 1,4-butanediol (BDO), analytically pure, Komio reagent; Triethylamine (TEA), analytical grade, Tianjin Hengxing Chemical Reagent Manufacturing Co., Ltd.; Acetone, analytical grade, Beijing Chemical Plant; Universal Rally Machine, GT-AI-7000S, High Speed Rail Testing Instrument Co., Ltd.; Thermogravimetric Analyzer, Mettler TGA1100SF, METTLER TOLEDO Instrument Co., Ltd., Switzerland; Taber wear testing machine, GT-7012-T, High Speed Rail Testing Instrument Co., Ltd..

Experimental Methods

Preparation of Polyurethane Emulsion

In a 500-ml flask equipped with a stirrer, a thermometer, together with a condenser, IPDI 27 g, PPG-2000 30 g, DMPA 3.3 g was added; the temperature was raised to 85°C, followed by reaction under a N2 atmosphere for a period of two 2 hours, and 8 g of GO/DMF solution was added. Subsequently, BDO 4.1g was added, followed by adding an appropriate amount of acetone in order to lower the viscosity, and the reaction was performed at a temperature of 75°C to react to a predetermined NCO value. Following cooling down to the room temperature, 2.5 g of neutralizer TEA was added. Subsequent to reacting for a period of 5 min, the reaction product was poured into an emulsified bucket, followed by addition of deionized water; moreover, the emulsion was attained with the help of high-speed stirring and shearing. The NCO value of the system during the reaction was determined by the di-n-butylamine titration. Eventually, acetone in the emulsion was distilled off subjected to the lowered pressure.

Configure GO/DMF solution: add a specific amount of dried graphene oxide to 8g DMF, together with dispersing it on a 600w power ultrasonic disperser for a period of 1h. The amount of GO is termed as the total weight of the material: 0% (G-0); 0.01% (G-1); 0.02% (G-2); 0.04% (G-3); 0.06% (G-4); and 0.08% (G-5).

Preparation of Cured Film

The prepared polyurethane emulsion was placed horizontally at the Teflon plate following 48h at the room temperature and placed in a vacuum drying oven. The sample was dried to a constant weight at a temperature of 60°C and, eventually, a film with the thickness of almost 100μm was obtained.

Characteristic Method

(1) The test of TGA
Mettler TGA1100SF thermogravimetric analyzer was employed for the purpose of testing TGA with a heating rate of 20°C /minute in nitrogen atmosphere. The sample weight is between 7~8mg and the temperature falls in the range between 25°C and 800°C.
(2) Tensile strength and elongation at break of the cured film
In accordance with GB/T 1040-2006 and GB/T 2918-1998, the tensile strength and elongation at break of the cured film were measured on the universal tensile machine.
(3) Determination of cured film hardness

In accordance with GB/T 6739-2006 paint and varnish pencil method, determine the hardness of the cured film.

(4) Cured film wear resistance test

Refer to GB/T 1768-2006 standard, use Taber instrument and rubber grinding wheel, load 500g, rotate 1000 rpm, measure sample quality prior to and subsequent to rotation, followed by calculating wear in accordance with the formula (1).

Wear▯ m=sample quality before test (m1)-sample quality after test (m^2) (formula 1)

(5) Heat aging resistance (Huang, 2010).

In accordance with GB/T9349-2002B method (oven method), the sample was placed in an oven for heat aging for a period of 48 hours, followed by measuring the mechanical strength of the test piece.

RESULTS AND DISCUSSION

Polyurethane Film Heat Resistance
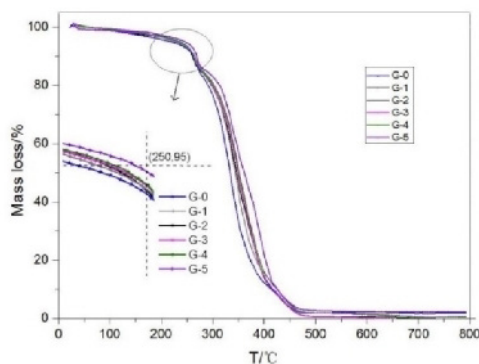
Figure 1. TGA curves of the polyurethane film

Fig. 1 is the TGA curve of the polyurethane film. Following the addition of GO, the thermal decomposition of the hard segment is delayed, and GO, as a modified material, is able to act as a partial hard segment.

As evident from Fig. 1, by increasing the amount of graphene oxide, the Td5 of the modified polyurethane manifests an increasing law; moreover, as the graphene oxide mass fraction is 0.08%, the initial decomposition temperature manifests an increase by 27°C. This is likely to be owing to the fact that graphene oxide is capable of providing additional heat capacity, requiring more heat in order to break the urethane bond (Khatua and Das, 2004).

Mechanical Properties

Tab. 1 presents the mechanical characteristics of the polyurethane film. The tensile strength and elongation at break of the polyurethane film increase first, followed by decreasing, which is due to the fact that by using graphene oxide for the modification of the polyurethane, the level of crosslinking of the polyurethane film is increased, and the tensile strength and elongation at break of the polyurethane film are increased as well.

Since the tensile characteristics of graphene are weak, accordingly, with the increase in the amount of graphene oxide, the tensile and tensile characteristics of the entire polyurethane chain decline.

Table 1. Mechanical characteristics of polyurethane film

NO.	G-0	G-1	G-2	G-3	G-4	G-5
Tensile strength /Mpa	20.1	23.9	19.6	16.5	16.5	14.4
Elongation at break /%	420	550	550	420	280	260
Hardness	2B	2B	B	B	B	HB

Polyurethane Film Wear Resistance
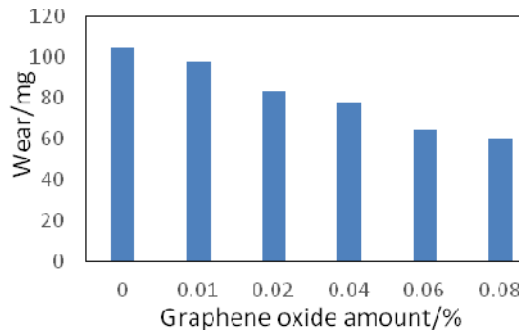
Figure 2. The test results of wear resistance of polyurethane film

Fig. 2 presents the test results of the wear resistance of polyurethane film. With the increase in the amount of graphene oxide, the wear of the polyurethane film manifests a gradual decline, which is owing to the robust interaction between graphene oxide and polyurethane molecular chains. In the meantime, the increase in the amount of graphene oxide gives rise to an increase in the hardness of the polyurethane film, lowering the deformation ability of the friction surface, and minimizing the area where the abrasion takes place. Besides, the bonding force between carbon atoms in layers is below the bonding force between adjacent carbon atoms in the same layer, making the graphene oxide layer have a lower coefficient of friction, accordingly enhancing the wear resistance of the modified polyurethane composite (Liu *et al*., 2015; Sun *et al*., 2016).

Polyurethane Film Heat Aging Resistance

Fig. 3 presents the tensile strength of polyurethane film both before and after the heat aging. As revealed by the experiments, when the amount of graphene oxide is 0.02%, the mechanical characteristics of the polyurethane film are less affected, and better heat aging resistance can be attained.
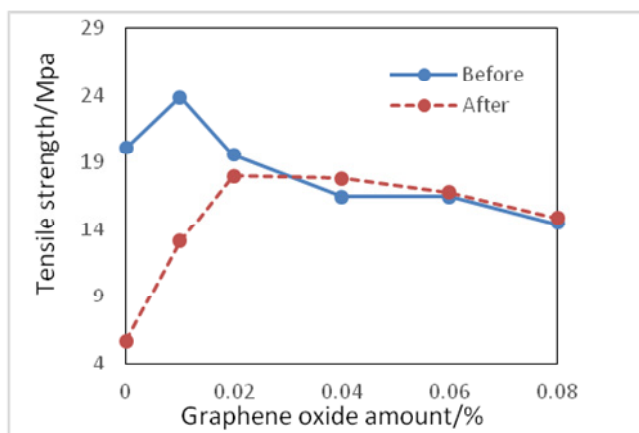
Figure 3 The tensile strength of polyurethane film before and after heat aging

CONCLUSIONS

In the current research work, graphene oxide was put to use for the modification of the polyurethane materials, together with investigating the effects of different amounts of graphene oxide on the mechanical characteristics, wear resistance and heat aging resistance of polyurethane.

As revealed by the results:

(1) The introduction of graphene oxide has the potential of improving the heat resistance, heat aging resistance and wear resistance of the polyurethane. Graphene oxide, being a hard segment in polyurethane, is able to enhance the hardness of the polyurethane film; moreover, when the amount of graphene oxide is small, the mechanical characteristics of the modified polyurethane film can be enhanced. However, with the increase in the amount, the mechanical characteristics of the polyurethane film are degraded.

(2) In this research work, the overall performance of polyurethane was optimized when the amount of graphene oxide was 0.02%.

REFERENCES

Hou, Y. *et al*. (2015), "Preparation and properties of functionalized graphene modified waterborne polyurethane", *Journal of Textile Research*, 36(10), 80-85.
Huang, W. (2010), "Study on improving the aging resistance of polyurethane materials", *Anhui Chemical Industry*, 36(03), 44-46.
Khatua, B.B. and Das, C.K. (2004), "Interchain crosslinkable polymer blends of polyurethane and polyacrylic elastomer (sulfur cure)", *Journal of Applied Polymer Science*, 93(2), 845-853, https://doi.org/10.1002/app.20542.
Liu, S. *et al*. (2015), "Corrosion Resistance and Wear Property of Graphene-Epoxy Coatings", *Tribology*, 35(05), 598-605.

Sun, Z. *et al*. (2016), "The Preparation and Properties of Graphene/Polyurethane Composites for Leather Finishing", *Leather Science and Engineering*, 26(05), 10-15.

Yang, H. *et al*. (2016), "Synthesis and Characterization of Graphene/Polyurethane Composites", *Polymer Materils Science and Engineering*, 32(5), 28-32.

THE STATUS OF LEATHER SUPPLY CHAIN IN EGYPT: AN EXPLORATORY STUDY FOR THE INNOLEA PROJECT

SANDRA SAMY GEORGE HADDAD

College of International Transport and Logistics, Arab Academy for Science, Technology and Maritime Transport, sandra_hdd@yahoo.com

Egypt has a traditional wealth in manufacture and use of leather and leather products as demonstrated on the walls of the tombs of pharaonic civilization. Nowadays the status of leather supply chain in Egypt has deteriorated and only account for a minor percentage of the Egyptian GDP. The INNOLEA (Erasmus+) project aims at developing and enhancing the leather supply chain through the establishment of leather innovation centers in Egypt and Jordan. The project also aims to create a link between university research activities and the leather sector which shall foster innovation and lead to manufacturing of high quality products. In this regard four focus group discussions have been organized with a total of nineteen participants (4-5 in each group) from different leather sector stakeholders (industry and academia). The outcomes of this research emphasized a number of steps to be undertaken to ensure a bright future the Egyptian leather supply chain with its main phases, tanning and leather products manufacturing. The industry has to undergo major technological advancements, produced leather products have to comply with the international norms and standards, government should increase its intervention and monitoring of this industry and support it stakeholders and labor professional skills and training have to be giving more emphasis and get developed.

Keywords: leather, leather products, quality, supply chain, Egypt, innovation center

INTRODUCTION

Egypt is sitting at its strategic location in the heart of the old world, at the North East of Africa with an area slightly over one million square kilometers (CIA World Factbook, 2018). Egypt emerged as one of the world's first nation states in the tenth millennium BC. and is considered a cradle of civilization. Ancient Egypt saw some of the earliest developments of writing, agriculture, urbanization, organized religion and central government (AFSTA Congress, 2018). Egyptian history has a traditional wealth in manufacture and use of leather and leather products as demonstrated on the walls of the tombs of pharaonic civilization. A statue displayed in the Egyptian Museum in Cairo of King Pepi II (2235-2141 B.C) shows the king holding his leather back bag. It is the earliest sign in the history of humanity of leather products (Elnaggar *et al*., 2017).

According to a 2017 study, the Egyptian economy sectoral analysis showed that 55.7% of the Egyptian GDP is generated by the service sector, followed by the industrial sector with a 33.1% of the GDP where the leather industry's contribution to the industrial sector added value is limited to the level of 0.4% (CAPMAS, 2017). This presents an opportunity for development of the leather sector.

This research is part of the "Innovation for the Leather Industry in Jordan and Egypt (INNOLEA)"; an Erasmus+ project which aims to fill the current gap in the area of specialized services for the leather sector with the establishment of four leather centers in local universities in Jordan and Egypt. This paper focuses on presenting the status of the Egyptian leather supply chain and exploring the current situation of the leather industry. The paper highlights the areas of developments and opportunities for the leather supply chain with a special focus on assessing the sector's capacities and identifying training needs. The results of this research shall be used as a corner stone for classifying the leather supply chain players status and needs and designing the prospective training and testing centers' action plan.

LITERATURE REVIEW

The Egyptian leather industry has witnessed instability in recent years. The total number of leather facilities in Egypt is more than 17,000 but about 5,000 factories have been closed and more than 150,000 workers have been laid off due to several reasons, foremost of which is the stream of imports (CAPMAS, 2016). The Ministry of Commerce and Industry issued a decree to protect the Egyptian leather industry, which included reviewing the Egyptian standards for imported leather products and introduced a customs tariff on imported leather products. The government is also in the process of reconsidering the rules governing the control of the production requirements for factories producing natural and industrial leathers (IMC, 2017).

In response to industrial and environmental needs, the Egyptian government made the decision to transfer the tanning industry, presently situated in Old Cairo, in the heart of the capital, to the industrial area near of Badr City (Al-Robikki area), which is situated approximately 45 kilometers from the capital (Egypt Today, 2016). This decision by the government is of particular importance, on the one hand it was a choice imposed by the limits of environmental acceptability of urban industrial development, and on the other, it expressed a desire to take the opportunity to support and strengthen the Egyptian tanning industry by helping it to become part of an industrial economy (Knecht and Zaki, 2017).

The Egyptian leather supply chain consist of the suppliers of animal hides and skins to the tanneries that convert them in into leather which is then exported or converted by leather products manufacturers into footwear, leather goods, garments, bags and sports goods. The manufactures either export or sell the products to retail shops to be in turn sold to final consumers. The substantial part of the industriy and business in Egypt remains with the tanneries and the manufacturing companies (FAO, 2016).

At present the Egyptian small and medium scale tanneries, that do not have the capital to move the Al-Robikki new industrial zone, are not in a bright situation. Moreover, only a few are industrially organized and able to offer a product suitable for the international market. This is particularly true for about 320 tanneries in Old Cairo, which are predominantly artisan workshops, with insufficient and often obsolete machinery. Their production appears to lack a rational organization, and the spaces they occupy are in buildings which are completely inadequate for running a modern production (Unido, 2016).

The tanneries in Egypt used a variety of animal skins and hides to extract leather such as bovine animals, sheep, lambs, and goats. Egyptian wealth of cow hides, sheep and goat skins are characterized by high quality fibrous structure as well as unique grain pattern-well known at the overseas markets. The animal wealth of the country is estimated at 8 M. bovines (cow/buffaloes), 6 M. sheep and 5 M. Goats; which follows in general a small-scale pattern of animal husbandry rather than large scale herds raising (FAO, 2016).

Slaughter and flaying are undertaken at authorized slaughter houses as well as informal village private slaughters. Thus, during the informal slaughter practices a part of country's wealth of hides and skins is jeopardized and subject to serious post- mortem defects. This leads to eventual marked reduction in the raw material value and sequent lower grade/value of manufactured leather whether semi- processed, crust or finished (FAO, 2016).

On the manufacturing side, the leather products in Egypt are classified into three main subsectors: footwear, leather goods and leather garments. The biggest sector is footwear representing 85 percent of the Egyptian industrial activities among the leather-based industries but still facing severe competition with imported products (CAPMAS, 2015; FAO, 2016).

Therefore, based on the secondary data collected the leather sector in Egypt carries a high potential but shows a gap with the international standards. That was the main driver of the INNOLEA project which is directed towards supporting the leather supply chain development through the establishment of leather centers providing totally new services such as; quality testing; certification of products; training; informative seminars on fashion trends, organization of production, funding opportunities etc. The centers shall be established at the Arab Academy for Science, Technology and Maritime Transport (AASTMT) and South Valley university (SVU). The project also aims to create a link between university research activities and the leather sector which shall enhance innovation and manufacturing.

RESEARCH METHODOLOGY

Insufficient reliable statistics, lack of extensive previous studies and records on the leather industry status, tannery, production, fabrication and exports in Egypt made it difficult to collect the necessary information. Thus, qualitative data gathering methods were vital in extracting in-depth information about the industry from the different leather supply chain stakeholder. In this regard four focus group discussions have been organized by the Egyptian partners in the INNOLEA project on the 28th of March in Cairo and the 24th of April 2018 in Alexandria. Total number of participants in the four focus groups is nineteen participants (4-5 in each group) from different leather sector stakeholders (industry and academia). Each focus group discussion took about 120 minutes. To ensure comparability between the focus groups, the same set of questions were asked to participants at each meeting. The questions were set to be compatible with the Egyptian market, reflecting an in-depth investigation of the current situation of the sector in Egypt.

It is worth mentioning that these national focus groups were the first of their kind relating academic staff to their counterparts' leather industrial experts in Egypt. The focus groups also included representatives from Egyptian Industrial Chamber as policymakers. The discussions were fruitful in identifying the problems and challenges facing this vital sector in Egypt, to determine its needs, and to recommend solutions to promote and enhance its performance to compete in the global market. They also focused on describing the status of the leather industry in Egypt, areas of collaboration between leather industry and academia, and recommendations to the government to help the leather industry sector in Egypt.

DATA ANALYSIS AND INTERPRETATION

After analyzing the outcomes of the focus groups' discussions, the status of the leather supply chain in the country was described, future of the industry was discussed, government policies were recommended and areas for collaboration with universities were explored.

The Status of the Leather Supply Chain

The Egyptian lather industry was characterized as random and governed by a weak legal framework. The supply chain of leather consists of small fragmented firms with limited ability to pump investment for growth. Meanwhile, the government plans to regulate and rationalize the industry through establishing a new leather industrial area called El Robbiki in Cairo. Nevertheless, huge infrastructure development is need in Alexandria too as tannery areas are older than Cairo.

Moreover, the Egyptian leather industry is facing a major threat as the Chinese products are invading the Egyptian market. The size of the Egyptian markets attracts low cost foreign leather products especially from China and the Egyptian leather products do not stand strong in the face of this severe competition. The Chinese synthetic leather products are well designed with acceptable quality for a considerable market segment of Egyptians and offered at cheap prices. This decreases the opportunities of Egyptian leather products to compete. Consumers are shifting to synthesized leather due to the soaring up prices of natural leather as well as increase in the price of materials associated with the production process. The annual Egyptian imported footwear and belts exceed 100 Million pieces.

In addition, some of the produced leather products are of poor quality which provides limited chances to compete with foreign products or to export. Majority of tanneries export raw leather (crust, dry crust, wet blue "recently illegal") to China, India, Spain and Italy. Few exporters/producers export high quality competitive finished leather products. These factories export Egyptian leather to Romania, Turkey and China.

The leather supply chain with its two main phases (tanning and manufacturing leather products) lack integration. Both areas are also in continuous disputes.

The status of leather tanning: The status of leather tanning was discussed and described by the participants. There are over 300 registered tanneries in Egypt. 80% of the high quality Egyptian semi-finished hides and skins (wet-blue and crust) are exported without added value, and the remaining low quality 20% are directed to the local market. Tanneries view exporting leather as being more profitable than selling locally. Leather finished products are not up to standards of European countries, however, raw leather quality is very good, demanded, conforms to specifications of the importing countries and can compete abroad. Reaching the stage of crust and dry crust need minor valued added activities (lining, decreasing, wet blue, spraying, dry crust) which is not costly, materials used are not expensive and widely available. Tannery owners prefer workers that inherited the craft to higher education graduates as they prefer traditional methods. Waste and scrap are considered a threat to the environment that needs to be addressed.

Most workers in the industry especially tanneries are uneducated and with minor skills. Tanneries' owners are seeking improvements through the help of foreign technicians from Bangladesh and India. There is a great need for more training involving employees throughout the production process. The government is also giving more care for leather tanning than leather manufacturing.

As for the status of leather manufacturing: only a few producers operate at a large scale and follow international standards. The industry in general is not strong as producers are not engaged in mass production due to limited capital resources of the majority of companies operating in the industry. Most producers are mainly small enterprises and family businesses that have inherited the craft years ago. According to participants' information, there are over 17,000 workshops for leather products manufacturing in Egypt. Supply of local materials and tools is very limited. Meanwhile, leather manufacturing requires high quality accessories, manufacturing components and auxiliaries. Many supporting industries are not available or available at low quality in Egypt. Some of the parts that are needed to manufacture leather products are prohibited to be imported by laws.

The Future of the Leather Industry in the Country

Leather industry has a great potential in case of solving its problems, which cannot be achieved with government intervention to further regulate the industry. The internal as

well as external markets are very promising. Europe is a wide market that proposes a large opportunity for Egyptian leather products because of the high-quality natural leather (but low processing quality). Processors believe that Europeans like to wear leather and value high quality leather. For the local market, it is easier to compete, as Egyptian consumer are not experienced with differences in quality of leather, thus, their expectations are not very high, and their perception of quality is lower than that of Europeans.

If slaughtering is regulated and done according to standards volumes of locally produced hides and skins can cover both the Egyptian market needs and the export activities of the finished leathers. Manufacturers see the potential to convert the exported "crust" leather, which presents 80% of the total produced skins, to fabricated items, and gain the added value by exporting these finished products in case production techniques get advanced and partly automated. Moreover, as leather represents 45-65% of the value of finished leather products, and the rest is in the form of accessories, auxiliaries and other components (fabric, zipper, etc.), this can be seen as an opportunity for supporting industries to be developed.

In addition to the technical improvements need, the logistics of the supply chain of leather have to be worked on in terms of the establishment of distribution centers for different types of leather to provide the manufacturers with their needs and to cover a wider geographical area. Also, other logistics activities such as professional purchasing, packaging an inventory management are vital for the future of the industry. Participants also emphasized their need for appropriate marketing strategies domestically and internationally to promote Egyptian leather products.

The Needed Steps and Regulations from the Government to Help the Leather Industry in the Country

The government should regulate the industry and put greater emphasis on the inspection of imported and exported leather and leather products. It should set higher penalties for those who violate laws and export raw leather. The formation of an official body, to set specifications of leather and regulate the exportation and importation of leather and related material, is needed. The government official body shall also oversee quality control to ensure all needed specs are being followed at all stages of production.

Moreover, accredited labs should made available to test the quality of the raw leather and apply the international certifications alongside professional training for labors, technicians, engineers and designers. Financial support shall also be regulated and subsidies, for small and medium factories working on finished leather products, are required. The government should also work of establishing a supporting industry such as local chemical factories, accessories and auxiliaries to manufacture raw materials needed for the leather production, instead of importing them. Exports shall be encouraged by the government to participate in international exhibition by facilitating the procedures for the companies to get involved. and subsidizing participation

Industry-Academia Collaboration

The role of the universities is appreciated as a neutral party, as companies may be reluctant to incorporate in the training with the concern of disclosing its industrial secrets. There is a need for academic institutions to provide the market with qualified staff, advanced testing equipment and well trained technicians. The government shall encourage more universities to develop an educational program to teach and train students and

workers. There are only a few educational institutions such as, he leather department in Helwan University which provide a high level of educational and vocational training.

Graduates from the academic institutes need to be trained on leather products fabrication and processing particularly in the stage of finished goods design, marketing and sales. The tannery owners highlighted a need for more trainings in the areas of deficiencies especially tanning which is the first stage in the leather supply chain. The current lack of knowledge at this stage affects the quality of the whole chain. Current standards and specifications can be developed by the academic institutions to match the fast progress in this industry. That may include specifications of both input materials and finished goods.

CONCLUSION

Analysis of the discussions indicated a level of deterioration in leather supply chain in Egypt and highlighted the root causes behind it. Areas of collaboration between the leather industry sector and the academia in Egypt have been identified and suggested to be partly fulfilled in the proposed leather innovation Centers that will be established through the INNOLEA project at AASTMT and SVU. In addition, suggestions and recommendations to the government have been identified in these focus group discussions.

To summarize the outcomes of this research and to ensure a bright future for this industry, the leather supply chain with its main phases, the tanning and leather finishing processes, have to undertake major technological advancements. Produced leather products have to comply with the international norms and standards. Government should increase its intervention and monitoring of this industry and support it stakeholders. Finally, labor professional skills and training have to be giving more emphasis and appropriately developed.

REFERENCES

AFSTA Congress (2018), African Seed Trade Association [online], available at: http://afsta.org/congress/blog/2017/09/28/afsta-congress-2018/
CAPMAS (2015), Egypt profile. Cairo: Central Agency for Public Mobilization and Statistics.
CAPMAS (2016), Egypt profile. Cairo: Central Agency for Public Mobilization and Statistics.
CAPMAS (2017), Egypt profile. Cairo: Central Agency for Public Mobilization and Statistics.
CIA (2015), The World Fact Book [online], available at: https://www.cia.gov/library/publications/the-world-factbook/geos/eg.html.
Egypt Today (2016), Inside Old Cairo's Leather Tanneries, Cairo [online], available at: http://www.egypttoday.com/Article/10/3107/Inside-Old-Cairo-s-Leather-Tanneries.
Elnaggar et al. (2017), "The characterization of vegetable Tanning and coloring agents in ancient Egyptian leather from the collection of the metropolitan museum of art", Archaeometry, 59(1), 133–147.
FAO (2016), FAO in Egypt: Food and Agriculture Organization of the United Nations [online], available at: http://www.fao.org/countryprofiles/index/en/?iso3=EGY.
IMC (2017), Industry Modernization Centre [online], available at: http://www.imc-egypt.org/
Knecht and Zaki (2017), "Egypt pins export hopes on new leather production city", Reuters Egypt [online], available at: https://www.reuters.com/article/us-egypt-industry-leather-int/egypt-pins-export-hopes-on-new-leather-production-city-idUSKCN1B31P7.
UNIDO (2016), UNIDO activities in Egypt 2015–2016, United Nations Industrial Development Organization [online], available at: https://www.unido.org/sites/default/files/2016-04/UNIDO_Egy_2015-2016__web__0.pdf.

NOVEL MYCO-COMPOSITE MATERIAL OBTAINED WITH *FUSARIUM OXYSPORUM*

OVIDIU IORDACHE[2], ELENA PERDUM[2], ELENA CORNELIA MITRAN[1,2], ANDREEA CHIVU[2], IULIANA DUMITRESCU[2], MARIANA FERDEŞ[1], IRINA-MARIANA SĂNDULACHE[2]

[1]*Politehnica University of Bucharest, 1-7 Polizu Street, Bucharest, Romania*

[2]*The National Research Development Institute for Textiles and Leather, 16 Lucretiu Patrascanu Street, 030508, Bucharest, Romania*

Modern world environmental challenges dictate the need for obtaining of alternative materials in various industrial sectors. Filamentous fungi strains are complex microorganisms that are able to produce rich enzymes batteries that are able of breaking down a wide variety of organic substrates. Present work explored the potential of *Fusarium oxysporum* strain for creating a novel biocomposite structure, based on an alternative substrate, composed of recycled shredded paper and worn coffee. Strain was successfully grown on an alternative nutritive substrate, which allowed formation of a 64.23μm biofilm on the surface of the substrate, and development of a homogenous hyphal matrix inside the aerial structure of the substrate, yielding a high rigidity material. Both optical and SEM analyses revealed even distribution of the hyphae and partial enzymatic hydrolysis of the recycled paper, which acted as a carbon source for cell development. Flammability analysis conducted on the biofilm surface of the material revealed very good fire retardant properties, withstanding close flame contact up to 80 seconds, after which smoldering fire occurred. Preliminary results are promising in exploiting the potential of an important plant pathogen in obtaining high added value materials, based on use of organic wastes which serve a double functionality, with nutritive role and mechanical substrate.

Keywords: biocomposite, fungi, *Fusarium oxysporum*

INTRODUCTION

Microorganisms derived biomaterials have lately enjoyed great attention, as self-growing natural composites, based on fungal mycelium, represent the latest trend in the biocomposites market. Creation of sustainable packaging materials is dictated by two major factors, regarding conventional materials: high consumption of nonrenewable resources and disposal of petrochemical based materials into the environment (Maachia *et al*., 2005), which need a very long biodegradation process. The production of 1m^3 of polystyrene consumes 4,667 Megajoules (MJ) of energy and release into the atmosphere a quantity of 462 kg of CO_2 while the production of 1m^3 of fungal obtained material uses 652 MJ and releases 31kg of CO_2 (Holt *et al*., 2012). Robust, low-cost, non-toxic manufacturing processes for the packaging industry represent major factors driving future markets and demands for bio-based materials in the European Union. Biomaterials obtained using fungal mycelium are safe and inert, lightweight, strong and durable, flame resistant and insulating, comparable with plastic packaging materials (polystyrene) and they can be used for large area of applications including decorative products, electronics packaging materials, building blocks, acoustic tiles etc. (Haneef *et al*., 2017). No studies were conducted on *Fusarium oxysporum* (of Ascomycota Division) strain for obtaining of biocomposites, so far. This particular strain, which is a known plant pathogen agent, was selected because of the rich battery of enzymes it possesses (can produce cellulase, pectinase, protease, xylanase etc.) (Kashiwa *et al*., 2016), fast growing rate and colonization capability of the substrate. Filamentous fungi strains are the most efficient and competitive microorganism used for the production of

mycelium derived materials due to their physiological, enzymological and biochemical properties.

MATERIALS AND METHODS

Microbial Strain and Substrate

The microbial strain used in obtaining of the myco-composite was *Fusarium oxysporum* obtained from Politehnica University of Bucharest strains collection. Fresh culture of the strain was obtained in Potato-Dextrose nutrient broth (Scharlau), in final volume of 100mL broth, previously sterilized at 121°C for 15'. Furthermore, the strain was incubated at 28°C for 10 days, until it reached metabolic maturity, and the appearance of the dark-purple aerial mycelium at the broth-air interface inside the flask.

Inoculation substrate was designed to act as both mechanical support substrate and nutritive substrate. Substrate was composed of shredded used paper and worn coffee, mixed in a ratio of 10:1 grams, and 0.5g of anhydrous D(+)-Glucose (Scharlau). All the substrate ingredients were thoroughly mixed, hydrated with sterile water, left at rest for 3 hours, at room temperature (28°C) for the water to drain, and then sterilized at 121°C for 15 minutes. After sterilization, the substrate was inoculated with the microbial strain by mixing the substrate volume with only the microbial biomass (approximately 4 grams of biomass) and thoroughly mixed in order to obtain a highly homogenized mix, and to allow the mechanical break of the biomass, for a better distribution in the substrate. The inoculated substrate was then incubated at 28°C, in a sterile Petri dish, in the dark, for 14 days. After the incubation period, the microbial growth was stopped by inactivating the biocomposite at 130°C for 3 hours, which also led to loss of constituent water.

SEM and Optical Microscopy Analysis

Microscopic analysis and morphological characterization on both obtained structure and constituent parts (paper and grounded coffee) was performed by scanning electron microscopy (SEM) using a Quanta 200, Fei (Netherlands) electron microscope. Morphological analyses were performed on the GSED detector, ESEM mode, spot beam size of 4.0, 10kV filament voltage, with image acquisition at 27.2 seconds.

Optical microscopy analysis was carried out on an Olympus SZX7 stereomicroscope, with 7:1 zoom ratio, built-in electrostatic discharge protection, and advanced Galilean optical system for highly resolved images. For assessment of surface biofilm morphological structure and specific filamentous growth on the back of the material, analyses were carried out at magnification levels of 0.67x and 2x.

Flammability Analysis

Flammability analysis on the developed composite was carried out on Flexiburn equipment, from James H. Heal & Co. Ltd. (England), according to SR EN ISO 6941:2004 international standard. Flame height was set to approximately 4.5cm, and the material (9x9cm dimension) was held above the peak of the flame in two time intervals, namely for 10 seconds and for 80 seconds.

RESULTS AND DISCUSSIONS

Following start of biomass development, microbial development on the surface of the substrate was possible starting with the 2nd day, where white mycelia net could be visible colonizing the surface. Growth during the incubation period allowed *Fusarium oxypsorum* biofilm formation on the entire surface of the substrate, obtaining a highly homogenized surface, with dark-brown pigmentation and increased rigidity (Figure 1).

Figure 1. *Fusarium oxysporum* substrate surface biofilm development

However, due to possible high humidity content in the substrate formulation, combined with substrate thickness (~1.5cm), biofilm formation only occurred on the surface of the substrate, but microbial development can also be detected in the obtained biocomposite section (Figure 2), which presents both hyphal development, and hydrolyzed substrate.

Figure 2. Biocomposite section highlighting microbial development

The microbial developed matrix that occurred at the surface of the substrate allows for increased cells cohesion within the structure (Flemming *et al*., 2010), consisting of various constitutional matrix components such as proteins and glycoproteins, neutral polysaccharides, carbohydrates (such as glucose, mannose), nucleic acids etc. This complex composition is in high dependency with a multitude of factors, starting from the strain used, substrate composition, ratio between the constituent components of the substrate, humidity, pH value, incubation temperature and period, affecting the balance between structural components, the most important being in protein composition variation (Zarnowski *et al*., 2014).

Furthermore, for morphological characterization, substrate was visualized under a stereomicroscope, for both microbial biofilm specific morphology and in-section hyphal development (Figure 3).

Biofilm surface

| 0.67x | 3x |

Back of the material

| 0.67x | 3x |
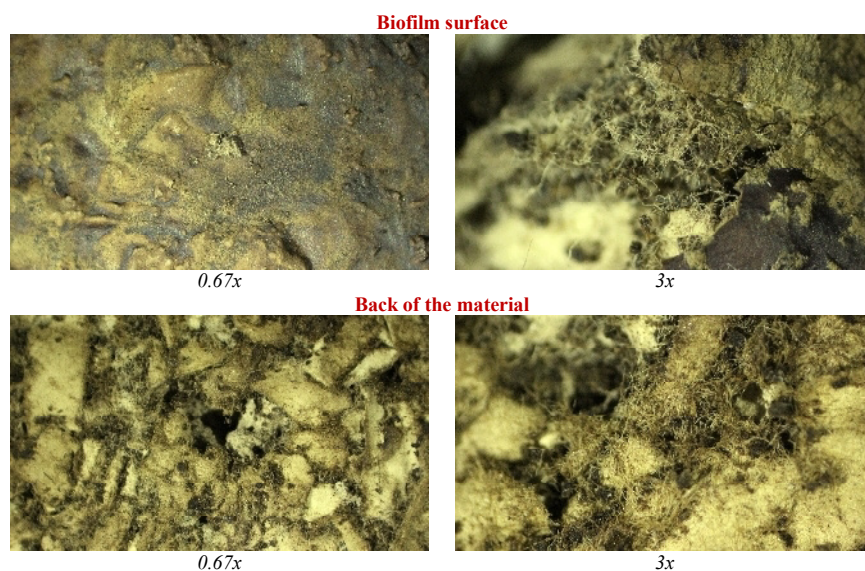
Figure 3. Biocomposite stereomicroscopy analysis

Visual inspection shows clear separation between biofilm structure and hyphal development structure, with homogenous matrix development that occurred on the surface of the material. Section analysis shows short hyphal segments that developed within the aerial structure of the biocomposite. Even though the substrate was formulated having high thickness, combined with high humidity content, the strain development was able to penetrate even the inferior layers of the substrate, where hydrolysis occurred, and the whole process was driven as a self-sustaining one, with both substrate hydrolysis and cell growth occurring concomitantly.

In order to investigate the microscopic structure even more, SEM analysis was conducted on both biocomposite surfaces (biofilm surface and back of the biofilm) (Figure 4 & 5).

| 500x | 1000x | 4000x |
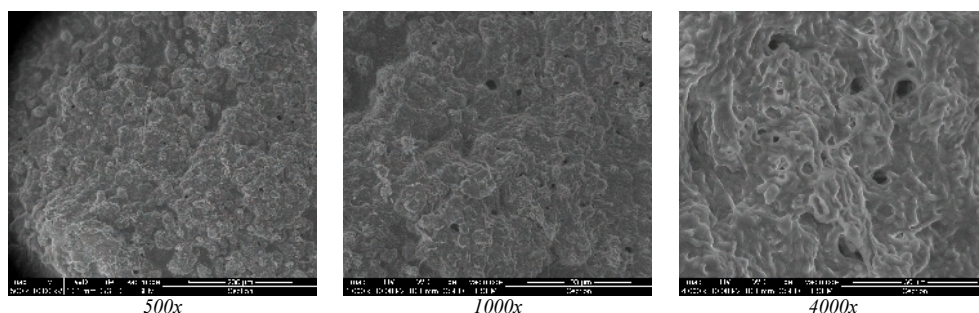
Figure 4. Surface of the biofilm structure SEM analysis

| 500x | 1000x | 4000x |
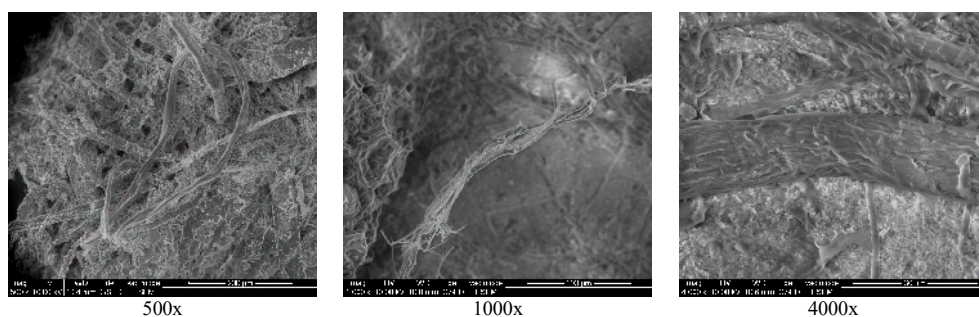
Figure 5. Back of the biofilm structure SEM analysis

Biofilm analysis revealed a smooth and homogenous structure, with no visible hyphal development on the surface, compared to the back of the biofilm, where hyphal structures can be visible, colonizing cellulose fibers. Furthermore, section analysis was carried out which revealed close interconnection of the biofilm development stage of the strain with the hyphal development, including measurement of the biofilm thickness, reported as 64.23µm (Figure 6).
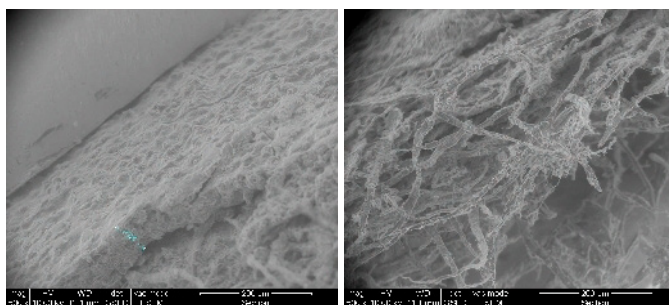
Figure 6. Biocomposite section SEM analysis

Even though the highest microbial activity takes place at the surface of the substrate, hyphal development inside the substrate structure, due to its aerial structure, allowed production of exo-enzymes, which were responsible with substrate hydrolysis. Thus allowing for a double effect, on one side, this allowed breaking down of constituents which were used as nutrients, mainly carbon source, for synthesis of cell wall, and on the other side, mechanical cohesion of the substrate.

Flammability assays are very important in characterization of fire retardant properties of packaging materials. Polystyrene materials can release a complex mixture of toxic chemicals (including styrene gas), and even fire retardant compounds that are currently used in inducing fire retardant properties can cause significant environmental disruptions. Flammability analysis revealed fire retardant properties of the biocomposite, when flame was applied on the biofilm surface, both after 10 seconds and after extended to 80 seconds, the material did not maintain combustion (Figure 7). However, after maintaining the flame above 80 seconds threshold, the material was consumed by smoldering fire, during a time span of approximately 30 minutes.
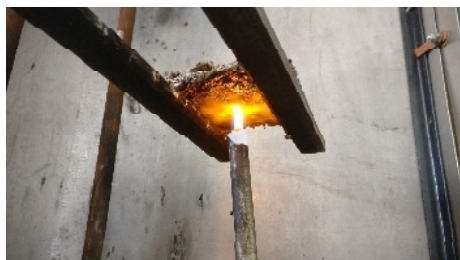
Figure 7. Biocomposite flammability test

CONCLUSIONS

Fusarium oxysporum is a soil-borne plant pathogen in agricultural environment. Present work has successfully explored the ability of the strain to be used for obtaining a biocomposite structure, on recycled shredded paper and worn coffee. Flammability test showed promising results, with the material being able to withstand flame contact for as long as 80 seconds, without catching fire. In the near future, this kind of biotechnologies can completely replace obtaining of petrochemical-based packaging materials, with sound innovation in sustainable packaging design. This kind of materials propose novel structures, that are environmentally safe, fire resistant, VOC free, and 100% sustainable, with compostable mycelium materials that have a wide range of applicability: the packaging industry will be more competitive by replacing petroleum-derived polymers with sustainable and fully biodegradable compostable materials.

REFERENCES

Flemming, H.C. and Wingender J. (2010), "The biofilm matrix", *Nature Reviews Microbiology*, 8(9), 623–33. pmid:20676145.

Haneef, M. *et al*. (2017), "Advanced Materials From Fungal Mycelium: Fabrication and Tuning of Physical Properties", *Scientific Reports*, 7, 41292, https://doi.org/10.1038/srep41292.

Holt, G.A. *et al*. (2012), "Fungal Mycelium and Cotton Plant Materials in the Manufacture of Biodegradable Molded Packaging Material", *Biobased Materials and Bioenergy*, 6, 431-439, https://doi.org/10.1166/jbmb.2012.1241.

Kashiwa, T. *et al*. (2016), "Sequencing of individual chromosomes of plant pathogenic Fusarium oxysporum", *Fungal Genetics and Biology*, vol. 98, January 2017, 46-51.

Maachia, L. *et al*. (2005), "Assessment of the petrochemical industry pollution on the Skikda bay, Algeria", *International Journal of Environmental Research and Public Health*, Dec, 2(3-4), 463-8.

Zarnowski, R. *et al*. (2014), "Novel entries in a fungal biofilm matrix encyclopedia", *MBio*, 5(4), p. e01333–14, pmid:25096878.

GRAPHENE OXIDE AND METAL PARTICLES NANOCOMPOSITES FOR INHIBITION OF PATHOGENIC BACTERIA STRAINS

VIRGINIJA JANKAUSKAITĖ[1], POVILAS LOZOVSKIS[2], VIRGILIJUS VALEIKA[3], ASTRA VITKAUSKIENĖ[2]

[1]*Kaunas University of Technology, Faculty of Chemical Technologies, Kaunas, Lithuania, Studentų St. 56, LT-51423 Kaunas, Lithuania, virginija.jankauskaite@ktu.lt*

[2]*Lithuanian University of Health Science, Faculty of Medicine, Mickevičiaus St. 9, LT-44307 Kaunas, Lithuania, lozovskis@gmail.com, astravitka@hotmail.com*

[3]*Kaunas University of Technology, Faculty of Chemical Technologies, Kaunas, Lithuania, Radvilėnų Av. 19, LT-51423 Kaunas, Lithuania, virgiijus.valeika@ktu.lt*

The most effective means to protect against bacterial invasion and to reduce the risk of dangerous infections are antibacterial components synthesis. Preliminary investigations show that hybrid coatings of graphene oxide doped with silver and copper nanoparticles have long-term bactericidal effect on a wide spectrum of standard bacterial strains. In this study the possibilities to use hybrid graphene oxide and metal nanoparticles composites for the inhibition not only standard bacteria, but also clinically important bacteria strains, which have developed multiple resistances to antibiotics, have been investigated. Resistant to antibiotics bacteria often cause dangerous infections in medical institutions of many countries due to the acquired resistance to many classes of antibiotics and the ability to obtain resistance to all antibiotics through mutations. Nanocomposite samples were characterized by TEM and SEM microscopy. The antibacterial activity was evaluated against gram-negative, gram-positive and clinical antibiotics resistant A. baumannii bacteria strains by solutions dilution method. The investigations demonstrated that hybrid nanocomposite shows synergistic mechanism of action and characterizes high efficiency against multidrug-resistant bacteria, such as A. baumannii bacteria strains decrease of viability.

Keywords: Graphene oxide and metal nanoparticle composites, multi-drug resistant bacteria, antibacterial activity

INTRODUCTION

The continuous increasing demand and use of antibiotics by population, in hospitals, and for veterinary purposes has led to accumulation of antibiotics in the environment. Continuous exposure of the bacterial fauna to even small concentrations of antibiotics or active metabolites could lead to the development of antibiotic resistant bacteria strains. The infections by these bacteria are causing health care systems tremendous amount of expenses. Therefore, the development of novel antibacterial agents looks promising in this context. For instance, silver (Ag) nanoparticles are known to exhibit combinations of mechanisms (Singh *et al*., 2015), e.g. disruption of bacteria cell morphology, DNA condensation, inhibition of ribosome interaction, accumulation at lethal concentration in cell, protein denaturation, inhibition of DNA replication, depletion of adenosine triphosphate, modulation of cellular signaling, generation of reactive oxygen species, oxidative stress, etc. Copper (Cu) nanoparticles are also proved to have bactericidal effect, the mechanisms of which may involve disruption of DNA helical structure through Cu ion cross-linking within and between nucleic acid strands and related mechanisms, which intervene cell biochemical processes (Kruk *et al*., 2015). Graphene and graphene oxide (GO) were also reported to exhibit bacterial toxicity effect, including cutting of intracellular metabolic routes, oxidative stress and rupture of cell membrane (Akhavan and Ghaderi, 2010). Therefore, the assembly of the mentioned

nanoderivatives into nanocomposite materials was supposed to show enhanced bactericidal effect.

In this paper, ability of nanocomposite obtained by silver and copper nanoparticles precipitation on graphene oxide sheets to inhibit not only gram-negative and gram-positive bacteria, but also antibiotic resistant bacteria strains, was investigated. The morphology and antibacterial activity of the hybrid nanocomposite was evaluated.

EXPERIMENTAL

Materials

Highly concentrated GO dispersion in water (concentration – 5 g/L; flake size – 0.5-5 μm) was obtained from Graphene Laboratories Inc. and used as received. Chemicals for nanoparticles synthesis were purchased from Sigma-Aldrich. The metal nanoparticles were synthesized by simple and cost-effective chemical reduction methods. The Cu nanoparticles colloidal solution (~2.5 mg/L) was prepared using appropriate amount of copper(II) chloride dehydrate as precursor and L-ascorbic acid as reductor. High concentrated Ag NPs colloidal solution (~12 mg/L) was prepared by new silver nitrate reduction with polyvinylpyrrolidone (Mn=10 000) method. The graphene oxide doped with Ag and Cu nanoparticles (GO–Ag–Cu) nanocomposite solutions were prepared by mixing highly concentrated GO dispersion with Cu and Ag nanoparticles colloidal solutions with 1:1:1 ratio, respectively. The corresponding thin nanocomposite films were assembled on the glass cover slips using same technique and technological parameters as described in (Lazauskas *et al.*, 2014).

Characterization

TEM images were acquired on Tecnai G2 F20 X-TWIN (FEI) equipped with field emission electron gun with accelerating voltage of 200 kV. Elemental analysis was performed using an energy dispersive X-ray (EDX) spectrometer. Samples were prepared for TEM by diluting colloidal solutions of nanocomposites in ethanol and placing a drop of solution on a Lacey carbon grid and left overnight at 21 °C.

SEM micrographs were acquired using field emission scanning electron microscope Quanta 200 FEG (FEI) and e-line plus multi-application nanoengineering workstation (Raith).

Antibacterial Activity Measurement

The antibacterial activity of hybrid GO–Cu–Ag nanocomposite was evaluated against gram-negative *Escherichia coli (E. coli)* (ATCC 25922), *Pseudomonas aeruginosa (P. aeruginosa)* (ATCC 27853), *Klebsiella pneumoniae (K. pneumoniae)* (ATCC 700603), which developed resistance to β-lactams, fluoroquinolones and aminoglycosides, and gram-positive *Staphylococcus aureus (S. aureus)* (ATCC 25923) and methicillin-resistant *Staphylococcus aureus (MRSA),* which are resistant to β-lactams, fluoroquinolones and macrolides, bacteria strains. Additionally, for investigations 79 clinical *Acinetobacter baumannii (A. baumannii)* strains have been separated from the various clinical materials in microbiology laboratory using standard procedures. Standard bacteria were cultured in *Tryptone Soya Broth (TSB)* solution (30 g/L). Bacteria were first cultured in a tube with 30 mL of TSB. The incubation was

performed at 37 °C and oscillated at a frequency of 150 rpm for 24 h to obtain the overnight phase of the bacteria. Following that, about 1 mL amount of the bacteria were pipetted from the overnight phase into another tube with freshly prepared 30 mL of TSB, respectively. Bacteria were grown at 37 °C in the incubator shaker for another 5 h to obtain the bacteria with higher activity. The stationary phase bacteria were diluted to concentration ca. 103 CFU/mL with NaCl solution (0.85%) and mixed with GO and nanoparticles colloidal solution with 1:1 ratio. Afterwards, the samples were taken and placed on Petri dishes surface, and incubated at 37 °C for 24 h. Bacteria survival was recorded over a 6h period.

Antibiotic resistant *A. baumannii* strains were cultivated overnight on 5% blood agar (BD, USA) at temperature of 37°C. Saline was used to make *A. baumannii* inoculate of concentration of 0.5 MF. One part of inoculate was mixed with 9 parts of GO–Cu–Ag nanocomposite colloidal solution. The sample was mixed by pipetting and placed at 37°C for incubation of 1 h and 2 h. Incubated mix was spread on 5% blood agar plate with 1µl loop and then cultivated 24 h at 37°C. The bacterial growth was evaluated next day using mass spectroscopy method for determination of bacteria species.

RESULTS AND DISCUSSIONS

Morphology of GO–Ag–Cu Nanocomposite

At first, the morphology of hybrid nanocomposite was evaluated. TEM image of GO-Cu-Ag nanocomposite is shown in Figure 1a and 1b. It clearly illustrates that Ag and Cu nanoparticles are precipitated on GO sheets. The nanoparticles are well dispersed across the GO surface with relatively low density of assembled aggregates. In order to quantify the nanoparticle presence, EDX point analysis on the GO wrinkle with high concentration of nanoparticles was performed (Figure 1b). The EDX spectrum confirms the presence of Ag and Cu nanoparticles on GO nanosheet surface. Fig. 1c shows SEM image of GO multilayer film assembled on glass coverslip surface using vertical dip-coating technique. The GO multilayer film was found to be uniform with a dense distribution of microscopic wrinkles on its surface. It is known that GO nanosheets may tend to yield wrinkled assemblies due to the solution phase properties, such as pH, and, thus, are solution phase property dependent. Addition of Ag and Cu nanoparticles colloid solutions disrupt GO sheets and sharp edges of GO are formed (Fig. 1d). It is reported that sharp edges of sheets could cut through the bacterium's cell membrane causing intracellular matrix to leak, eventually leading to the GO toxicity mechanism. As can be seen from Figure 1d, the nanocomposite exhibits Ag and Cu nanoparticles decorated GO sheets. Figure 1e shows killed *E. coli* bacteria strains after contact with GO-Cu-Ag nanocomposite as a bactericidal agent. In some cases were found that bacteria are microencapsulated with GO sheets (Figure 1f).

Antibacterial Activity of Hybrid Nanocomposite

Figure 2 shows survival curves of gram-negative and gram-positive bacteria strains during 6 h period after contact with GO-Cu-Ag nanocomposite as a bactericidal agent. GO–Cu–Ag nanocomposite markedly affected *S. aureus, E. coli, K. pneumoniae* and *P. aeruginosa* cellular viability during 3 h period of incubation. Though MRSA showed higher resistance, but this bacterium did not survive 6 h period. It is a good indication that synergistic effect of applied nanoderivatives with multiple toxicity mechanisms

(due to the morphological diversity) has stronger bactericidal effect. Based on obtained results, the predicted bacterium inactivation mechanism via interaction with GO–Cu–Ag nanocomposite was devised (Jankauskaitė *et al*., 2016).
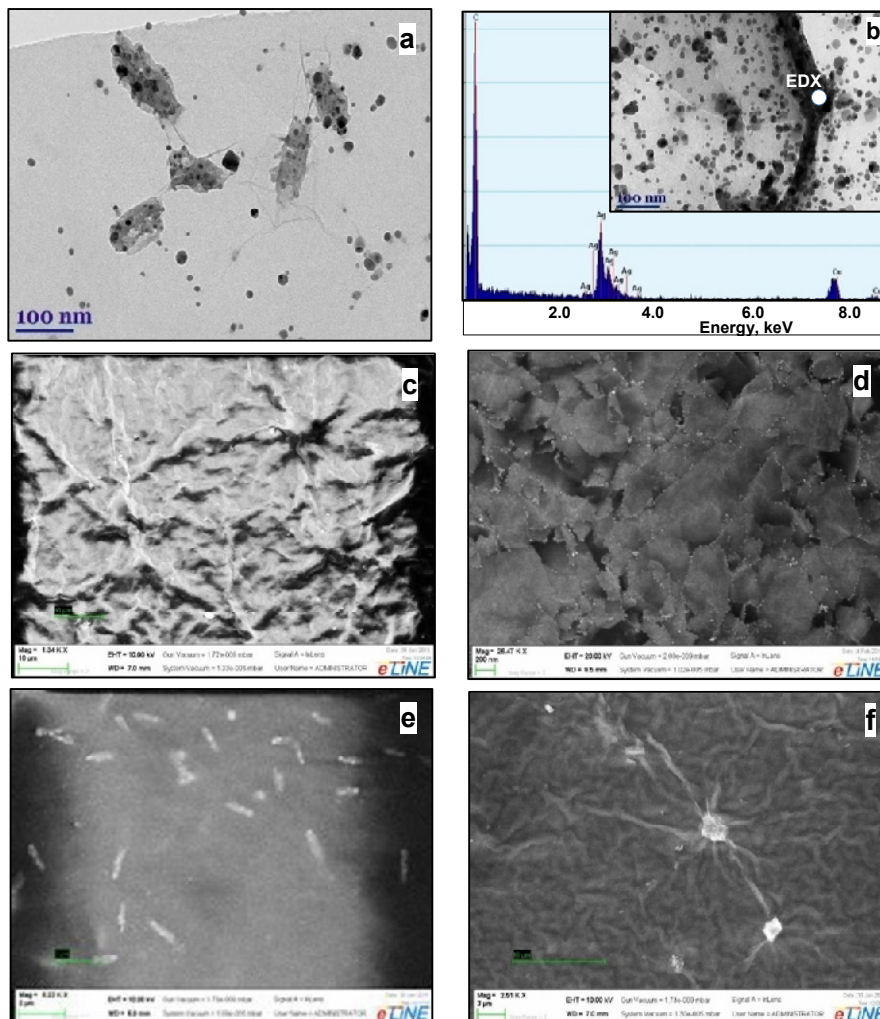
Figure 1. Hybrid GO–Cu–Ag nanocomposite TEM image (a) and EDX spectrum (b); SEM images of GO nanosheet (c) and GO–Cu–Ag nanocomposite (d), *E. coli* bacteria killed after interaction with nanocomposite (e), bacteria microencapsulated with GO sheets (f)

The positively charged Cu and Ag nanoparticles mainly adsorb on the negatively charged GO nanosheet surface (Figure 1a). Thus, it is expected that Cu and Ag nanoparticles are able to interact with entire bacterium's surface. This is specifically

relevant in regard to the effect that nanoparticles had on gram-negative bacteria (*E. coli, P. aeruginosa, and K. pneumonia*), which have a larger surface area compared to gram-positive bacteria represented by *S. aureus* and MRSA, which are more spherical and have less surface area. Furthermore, MRSA resistance to Cu and Ag nanoparticles could be the product of a decreased cross-linking of peptidoglycan strands which leads to the exposure of more D-Ala-D-Ala residues resulting in areas of bind and trap for nanoparticles. It is predicted that the nanoparticle interactions with bacterial cell membrane are mainly caused by to electrostatic attraction, which increases the membrane permeability eventually leading to rupture and leakage of intracellular component, resulting in cell's death. It is also possible that nanoparticles interaction with cell membrane could also cause the deterioration of the energy metabolism by interfering with the electron transport (respiratory) chains. The gram-negative bacteria were more susceptible to nanoparticles which can be explained in part by the difference in the presence of peptidoglycans present in *S. aureus*. Relative resistance of MRSA is also possibly explained by the fact that this bacterium has a much thicker cell wall which is partially responsible for their resistance to vancomycin. Finally, another potential mechanism of the GO sheets on gram-negative bacteria such as *E. coli* and *P. aeruginosa* is damage of the flagellum, a vital organelle that confers virulence to these bacteria. This can result in bactericidal properties and immobilization of bacteria. Furthermore, the enfolded GO sheet fragments with sharp edges could instantly cut through the bacterium's cell membrane upon contact. This ability increases with addition of nanoparticles colloidal solutions that influences on the fragmentation of GO nanosheets.
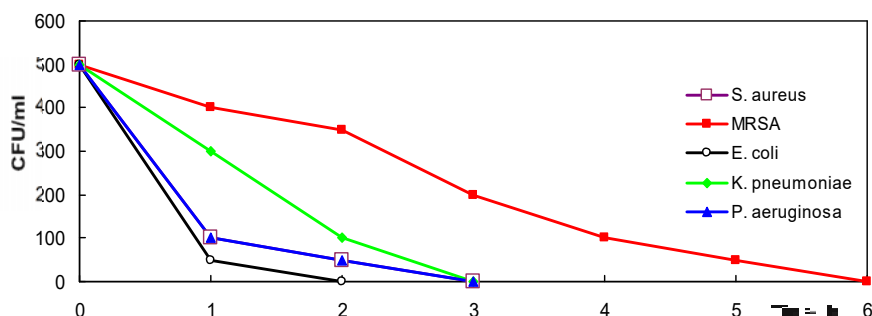
Figure 2. Survival curves of different bacteria strains during 6 h period with GO–Cu–Ag nanocomposite

Thus, the morphological diversity of nanoparticles and GO construct the synergistic bactericidal effect (Figure 2), which is found to be more effective than individual nanoderivatives.

Thus, it is important to consider the use of GO–Ag–Cu nanocomposite in the applications that require materials with high antibacterial effectiveness. Therefore, the influence of GO–Ag–Cu nanocomposites on the antibiotic resistant bacterium strains was evaluated. Generally, *A. baumannii* strains have acquired resistance mechanisms for the most of tested antibiotics (Afzal-Shah et al., 2001). It was found that 22.8% of strains were resistant to all tested antibiotics. As can be seen from Table 1, after 1 h of incubation GO–Ag–Cu nanocomposite showed better performance on strains that were

susceptible, than resistant to ceftazidime, and ciprofloxacine, doxycycline, carbapenems (imipenem and meropenem), gentamicin, tigecycline.

Table 1. Effect of hybrid GO–Cu–Ag nanocomposite on multi-drug resistant
A. baumannii strains

	Susceptible to antibiotics		Resistant to antibiotics	
	1 h	2 h	1 h	2 h
Ceftazidime	100.0	66.7	37.0	76.7
Ciprofloxacin	100.0	83.3	37.0	75.3
Carbapenem	77.8	77.8	37.1	75.7
Doxycycline	57.6	51.5	30.4	93.5
Gentamicin	69.2	92.3	36.4	72.7
Amikacin	56.2	93.8	61.9	71.4
Tigecycline	63.3	80.0	34.7	73.5

After 2 h of incubation GO–Ag–Cu nanocomposites effect on strains that were resistant and susceptible to antibiotics became similar. On the other hand, some of effected *A. baumannii* strains showed recovery after 2 h of incubation.

CONCLUSIONS

Cu and Ag nanoparticles precipitated on GO sheets is markedly effective bactericidal agent against wide range of gram-negative and gram-positive bacteria strains due to the possible synergy of the multiple toxicity mechanisms. A systematic morphology analysis of the corresponding nanoderivatives was performed employing SEM and TEM and provided guideline information for addressing toxicity mechanisms.

GO–Cu–Ag nanocomposite also show significant effect on antibiotic resistant *A. baumannii* strains that are susceptible to β-lactams (ceftazidime, carbapenems) and ciprofloxacin after a short exposition, but it is needed longer incubation time to effect resistant *A. baumannii* strains. GO–Cu–Ag nanocomposite inhibits growth of aminoglycoside (gentamicin, amikacin) and tygecycline susceptible strains as well as resistant after 2 h of exposition.

REFERENCES

Afzal-Shah, M., Woodford, N. and Livermore, D.M. (2001), "Characterization of OXA-25, OXA-26, and OXA-27, molecular class D beta-lactamases associated with carbapenem resistance in clinical isolates of Acinetobacter baumannii", *Antimicrobial Agents and Chemotherapy*, 45(2), 583-588, https://doi.org/10.1128/AAC.45.2.583-588.2001.

Akhavan, O. and Ghaderi, E. (2010), "Toxicity of graphene and graphene oxide nanowalls against bacteria", *ACS Nano*, 4(10), 5731-5736, https://doi.org/10.1021/nn101390x.

Jankauskaitė, V. *et al.* (2016), "Bactericidal effect of graphene oxide/Cu/Ag nanoderivatives against *Escherichia coli*, *Pseudomonas aeruginosa*, *Klebsiella pneumoniae*, *Staphylococcus aureus* and Methicillin-resistant *Staphylococcus aureus*", *International Journal of Pharmaceutics*, 511(1), 90-97, https://doi.org/10.1016/j.ijpharm.2016.06.121.

Kruk, T. *et al.* (2015), "Synthesis and antimicrobial activity of monodisperse copper nanoparticles", *Colloids Surface B*, 128, 17-22, https://doi.org/10.1016/j.colsurfb.2015.02.009.

Lazauskas, A. *et al.* (2014), "Thermally-driven structural changes of graphene oxide multilayer films deposited on glass substrate", Superlattices and Microstructures, 75, 461-467, https://doi.org/10.1016/j.spmi.2014.08.006.

Singh, R. *et al.* (2015), "Bacteriagenic silver nanoparticles: synthesis, mechanism, and applications", *Applied Microbiology and Biotechnology*, 99(11), 4579-4593, https://doi.org/10.1007/s00253-015-6622-1.

STUDY OF WOUND-DRESSING MATERIALS BASED ON COLLAGEN, SODIUM CARBOXYMETHYLCELLULOSE AND SILVER NANOPARTICLES USED FOR THEIR ANTIBACTERIAL ACTIVITY IN BURN INJURIES

SORINA-ALEXANDRA LEAU[1], ŞTEFANIA MARIN[2,3], GHEORGHE COARĂ[3], LUMINIŢA ALBU[3], RODICA ROXANA CONSTANTINESCU[3], MĂDĂLINA ALBU KAYA[3], IONELA-ANDREEA NEACŞU[4]

[1]University Politehnica of Bucharest, Faculty of Medical Engineering, 1-7 Gheorghe Polizu Str., 011061, Bucharest, Romania

[2]University Politehnica of Bucharest, Center of Surface Science and Nanotechnology, Splaiul Independentei 313, Romania

[3]INCDTP - Division: Leather and Footwear Research Institute, 93 Ion Minulescu Str., 011061, Bucharest, Romania

[4]University Politehnica of Bucharest, Science and Engineering of Oxide Materials and Nanomaterials Department, Splaiul Independentei nr.313, 060042, Bucharest, Romania

There are 2 types of bacteria that can produce serious infections and in many cases they lead to intestinal infections, meningitis or even toxic shock syndrome: *Escherichia coli* (*E.coli*) and *Staphyloccocus aureus* (S.*aureus*) . They are the most common source of infection worldwide and it's really necessary to understand their mecanism of action. The objective of this study was to develop and characterize wound-dressing materials based on collagen (COLL), sodium carboxymethylcellulose (CMC-Na) and silver nanoparticles (AgNPs) designed to be used for burn injuries. We chose to use a composite material because it has multiple desirable effects, both on the wound and against the bacteria. Type I fibrillar collagen gel was extracted from calf hide. Sodium carboxymethylcellulose was used because it's biocompatible and non-toxic. Silver nanoparticles were used for their antimicrobial activity. Obtained wound-dressing material was characterized by FT-IR spectroscopy, scanning electronic microscopy, water up-take and degradation in collagenase solution. The results showed that this combination of materials is ideal for a faster healing of the wound and it considerably reduces the risk of infection.

Keywords: collagen, carboxymethylcellulose, silver nanoparticles (AgNPs).

INTRODUCTION

Burns are tissue lesions produced by radiation exposure, thermal, chemical or electric agents (Herndon, 2012). Destruction of the skin protective barrier can lead to infections because the surface of the wound contains necrotic tissue and it's a suitable area for the adherence of bacteria (Deirdre, 2006). There are 2 types of bacteria classified according to Gram's method: Gram-negative bacteria and Gram-positive bacteria. For example, *Escherichia coli (E.coli)* is a Gram-negative bacteria (it has a thin membrane which is difficult to penetrate and because of this it's often resistant to antibiotics). Some types of *E. coli* can produce a toxin named Shiga which is one of the most powerfull toxins that can cause intestinal infection. *Stapyloccocus aureus (S.aureus)* is a Gram-positive bacteria and it has a thick membrane. It may cause sepsis, toxic shock syndrome or meningitis (Schaalje, 2018; Stegarus and Lengyel, 2017).

According to a study conducted by World Health Organization, an estimated 180.000 deaths occur every year as a direct result of burn injuries, especially in low- and middle-income countries (Anenden, 2018). The purpose of researchers is to treat bacterial infections through the most innovative methods and a good solution is represented by biocompatible wound-dressing materials.

Study of Wound-Dressing Materials Based on Collagen, Sodium
Carboxymethylcellulose and Silver Nanoparticles Used for Their Antibacterial
Activity in Burn Injuries

Collagen (COLL) is the main protein in different tissues with many uses in medicine: wound care, tissue regeneration, bone grafts, cosmetic surgery and cardiac applications (Burdusel, 2016). Carboxymethylcellulose (CMC-Na) is derived from cellulose and it has unique properties such as biodegradability, non-toxicity and biocompatibility (Hollabaugh, 1945). Silver nanoparticles (AgNPs) provide a high level of biocompatibility, non-toxicity and biodegradability and can be considered as an effective antibacterial based wound dressing material for different kinds of wounds (Sathish, 2018).

Depending on the severity of the burns the material can be cross-linked with glutaraldehyde (GA) to incorporate a large amount of exudate in order to release nanoparticles faster. The aim of this study was to prepare and characterize wound-dressing materials based on collagen, carboxymethylcellulose and silver nanoparticles for more fast and safe healing, considerably improving the quality of life.

The aim of this study was to develop and characterize collagen – carboxymethylcellulose matrices with silver nanoparticles in order to be used in wound healing taking in consideration the collagen biocompatibility and the antimicrobial activity of silver nanoparticles.

MATERIALS AND METHODS

Materials

The type I fibrillar collagen gel having a concentration of 1% (w/v) was extracted from calf hide using technology currently available at the Research-Development Textile Leather National Institute Division Leather and Footwear Research Institute-Collagen Department (Albu, 2011). CMC-Na having a concentration of 1% was purchased from Fluka. Silver nanoparticles were obtained in the National Centre for Micro and Nanomaterials (CNMN) from University Politehnica of Bucharest. Glutaraldehide was purchased from Merck (Germany) and collagenase was purchased from Sigma-Aldrich (China).

Preparation of Wound-Dressing Materials

The concentration of each collagen gel was adjusted from 2,26% to 1% and 7,4 pH (the pH of the physiological medium in human body) using 1M sodium hydroxide. Silver nanoparticles (AgNPs) were in the form of colloidal solution because they offer better homogeneity and ensure their distribution inside the material for long-term antibacterial action. Silver nanoparticles (AgNPs) and carboxymethylcellulose (CMC-Na) were added to collagen gel (w/v) and then the samples were cross-linked with 0,025% glutaraldehyde (GA). All this informations are specified in Table 1.

Table 1. Names and composition of wound-dressing gels

Samples	Collagen, %	CMC-Na, %	AgNPs (mL)	GA, %
1	1	1	10	0,025
2	1	1	20	0,025
3	1	1	10	0
4	1	1	20	0
5	1	1	0	0,025
6	1	1	0	0

The gels for wound-dressing materials based on collagen, in order to be analyzed, were freeze-dried with Delta 2-24 LSC lyophilizer (Martin Christ, Germany) using a 48-hour lyophilization program and composites in spongious form were obtained.
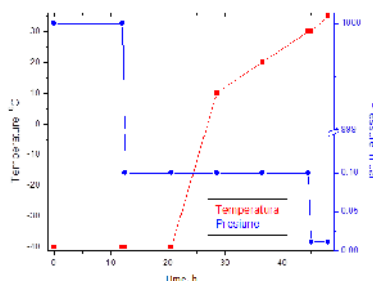
Figure 1. 24 hours lyophilization program used to obtain the matrices

Methods

FTIR-ATR Analysis

FT-IR spectral measurements were recorded using a Nicolet iN10 MX FT-IR spectrometer with MCT liquid nitrogen cooled detector in the measurement range 4000-400 cm^{-1}. Spectral collection was made in reflection mode at 4 cm^{-1} resolution. For each spectrum, 32 scans were co-added and converted to absorbance using Ominc Picta software (Thermo Scientific).

Enzymatic Degradation

Enzymatic degradation was accomplished by immersing pieces of the lyophilized samples in a collagenase solution and monitoring the degradation over time. To monitor mass loss, samples were weighed at different time intervals, and calculated using the following equation:

$$\%Weight\ loss = Wi - Wt\ /\ Wt \times 100 \tag{1}$$

where W1 represents the initial mass and Wt represents the weight of the sample after the time interval t.

Scanning Electron Microscopy (SEM)

The investigation of the samples was carried out with the aid of the Scanning Electron Microscope INSPECT F50 provided with a Field Emission Gun (FEG) with a resolution of 1, 2 nm and a dispersive X-ray energy spectrometer with a resolution at MnK of 133 eV. For the proper conductivity of the samples, they were covered with gold for 60 seconds.

Study of Wound-Dressing Materials Based on Collagen, Sodium
Carboxymethylcellulose and Silver Nanoparticles Used for Their Antibacterial
Activity in Burn Injuries

Antimicrobial Activity

The control of antimicrobial activity was tested against *E. coli* (gram negative), *S. aureus* (gram positive) strains. Firstly, the gel for the lower layer without bacteria was prepared. 10 ml of gel was put into each sterilized Petri dish and allow it to solidify. Secondly, gel for the upper layer was prepared and cooled down to 45°C in a water bath. Inoculation 150 ml of gelose with 1 ml of bacterial working solution (1-5 x 10 8 μg / ml) was performed. The samples were placed on the surface of the nutrient medium and then incubated at 37^0C between 18h and 24h.

RESULTS AND DISCUSSION

After the lyophilization process, wound-dressing materials based on collagen (COL), carboxymethylcellulose (CMC-Na) and silver nanoparticles, cross-linked were obtained, having the structure presented in Figure 2.
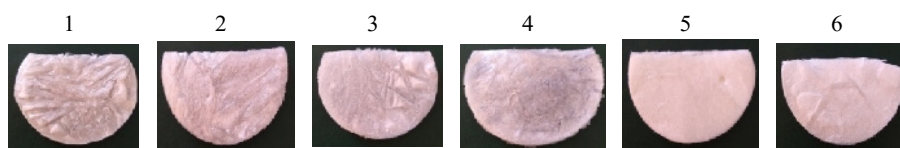
Figure 2. The aspect of the wound-dressing materials

All the samples from Table 1 were analyzed by FT-IR spectroscopy and the spectra are presented in Figure 3.
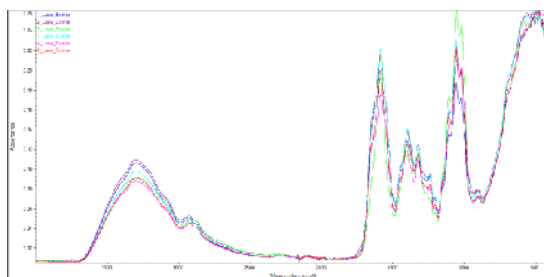
Figure 3. FT-IR spectra of all the samples

From Figure 3 it can be observed the typical amide bands of collagen i.e. 3303 cm-1 and 2924 cm^{-1} for amide A and B respectively, 1630 cm^{-1} was ascribed to amide I (C=O stretching), 1544 cm^{-1} to amide II (N-H deformation) and 1238 cm^{-1} to amide III (N-H deformation) (Albu, 2011). The spectra, also showed, the characteristics peak of silver nanoparticles at 1625 and 1516, 1384 and 1047 cm^{-1}. Figure 4 presents SEM images of all the samples.
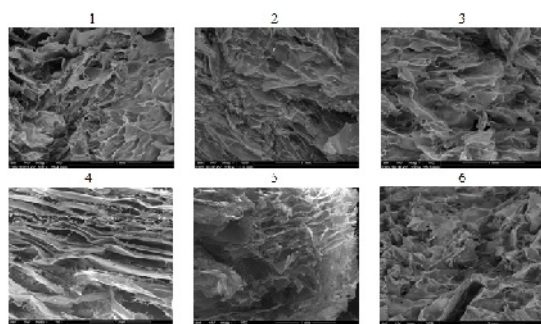
Figure 4. SEM images

In all the samples, the collagen structure is highly present. Samples 1 and 2 have a more disorganized structure and the sample 3 and 4 are cross-linked with glutaraldehyde (GA) and they have a more compact structure. Sample 5 and 6 presented the specific structure of collagen, fibrils with interconnected pores.

For enzymatic degradation tests, the samples were introduced into a collagenase solution (collagenase is an enzyme that breaks collagen structures) for 24 hours. The test results are presented in Figure 5.
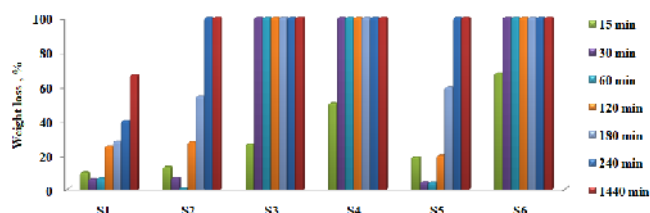
Figure 5. Weight loss of samples in collagenase solution over 24 hours

As it can be seen, the cross-linked samples 1, 2 and 5 showed a slower degradation compared to the rest of samples. The most stabile sample seems to be sample 1, with 10 ml AgNPs solution and glutaraldehyde, which 24 hours lost around 70% from its weight.

In Figure 6 is presented the antimicrobial activity of all the sample, tested against *Escherichia coli* (gram negative), *Staphyloccus aureus* (gram positive).

Study of Wound-Dressing Materials Based on Collagen, Sodium
Carboxymethylcellulose and Silver Nanoparticles Used for Their Antibacterial
Activity in Burn Injuries
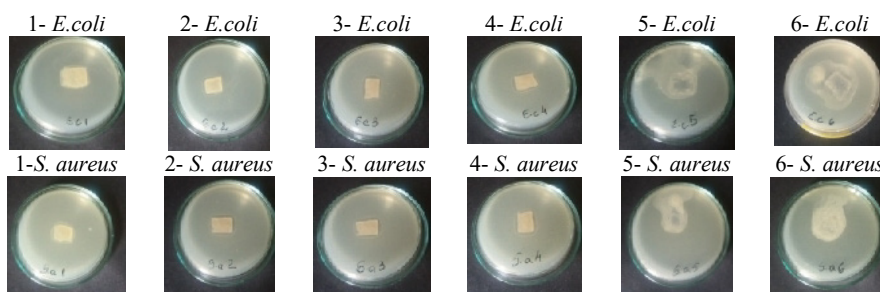
Figure 6. Zones of inhibiton, against E. coli and S. aureus strains, of all the samples

From Figure 6 can be observed that all the samples 1-4, containing silver nanopaticles, and developed zone of inhibition against both *S. aureus* and *E. coli* strains. The result is considered to have a "satisfied effect" if no bacterial propagation is observed. Those probes do not allow the development of aerobic germs for the bacteria tested.

CONCLUSIONS

Type I collagen with carboxymethylcellulose and silver nanoparticles and their combinations were used in order to obtain matrices for tissue regeneration and antimicrobial activity. The combinations between components were highlighted by FT-IR spectra where the specific peaks of both polymers were found. The most compact samples were the one cross-linked and the most stabile was sample 1. The antimicrobial activity was proved by the zones of inhibition developed against *S. aureus* and *E. coli* strains. Thus, the samples are potentially novel candidates as scaffolds for tissue engineering applications.

Acknowledgement

REFERENCES

Albu, M.G. (2011), *Collagen Gels and Matrices for Biomedical Applications*, Lambert Academic Publishing, Saarbrücken, 23-24.

Anenden, H. (2018), "Burns", World Health Organization, http://www.who.int/news-room/fact-sheets/detail/burns.

Burdusel, A.C. *et al*. (2016), "Development and Characterization of Collagen - Carboxymethylcellulose Materials for Lenses", Proceedings of The 6th International Conference on Advanced Materials and Systems, ICAMS 2016, https://doi.org/10.24264/icams-2016.II.4.

Church, D. *et al*. (2006), "Burn Wound Infections", *Clinical Microbiology Reviews*, 19(2), 403-434, https://doi.org/10.1128/CMR.19.2.403-434.2006.

Herndon, D. (2012), "Chapter 4: Prevention of Burn Injuries", *Total burn care*, Edinburgh: Saunders, p.46, ISBN 978-1-4377-2786-9.

Hollabaugh, C.B., Burt, H.L. and Walsh, A.P. (1945), "Carboxymethylcellulose. Uses and applications", *Industrial and Engineering Chemistry*, 37(10), 943-947, https://doi.org/10.1021/ie50430a015.

Kumar, S.S.D. *et al*. (2018), "Recent advances on silver nanoparticle and biopolymer-based biomaterials for wound healing applications", *International Journal of Biological Macromolecules*, 115, 165-175, https://doi.org/10.1016/j.ijbiomac.2018.04.003.

Schaalje, J. (2018), "Medical Terminology: Gram-Positive vs. Gram-Negative Bacteria", American College of Healthcare Sciences (http://info.achs.edu/blog/bid/282924/medical-terminology-gram-positive-vs-gram-negative-bacteria).

Stegarus, D.I. and Lengyel, E. (2017), "The antimicrobial effect of essential oils upon certain nosocomial bacteria", *17th International Multidisciplinary Scientific GeoConference (SGEM 2017)*, 17, 61, 1089-1096.

INFLUENCE OF THE FORMULATION AND PREPARATION TECHNIQUE ON THE FLUFENAMIC ACID RELEASE FROM DIFFERENT COLLAGENIC SUPPORTS DESIGNED FOR WOUND HEALING

MARIA MINODORA MARIN[1,3], ŞTEFANIA MARIN[2,3], ELENA DĂNILĂ[1,3], MĂDĂLINA GEORGIANA ALBU KAYA[3], MIHAELA VIOLETA GHICA[4], LĂCRĂMIOARA POPA[4], RĂZVAN MIHAI PRISADA[4], GHEORGHE COARĂ[3], CIPRIAN CHELARU[3]

[1]University Politehnica of Bucharest, Faculty of Applied Chemistry and Materials Science, Bucharest,1-7 Gheorghe POLIZU Str., 011061, Bucharest, Romania

[2]University Politehnica of Bucharest, Center of Surface Science and Nanotechnology, Splaiul Independentei 313, Romania

[3]INCDTP - Division: Leather and Footwear Research Institute; 93 Ion Minulescu Str., 031215, Bucharest, Romania, icpi@icpi.ro

[4]"Carol Davila" University of Medicine and Pharmacy, Faculty of Pharmacy, Physical and Colloidal Chemistry Department, 6 TraianVuia Str., 020956, Bucharest, Romania, mihaelaghica@yahoo.com

Drug delivery systems with controlled release are one of the top applications for human health, a new domain in material science with biomedical application. The aim of this study was to obtain and characterize some drug delivery systems based on collagen, dextran and flufenamic acid (matrices, membranes and fibers) for wound healing. The samples were analyzed by FT-IR and *in vitro* release of flufenamic acid. From the FT-IR spectra it can be seen that collagen macromolecule keeps its triple helix structure. The percentage of drug delivered is influenced by the degree of cross linking, the presence of dextran in the designed formulations and the collagen support preparation technique.

Keywords: collagen, dextran, flufenamic acid

INTRODUCTION

Drug delivery systems with controlled release are one of the top applications for human health, a new domain in material science with biomedical application (Vallet-Regi *et al*., 2007). Natural polymers have been increasingly studied for applications in health care due to their biocompatibility, biodegradability and non-toxicity. Collagen is a potentially useful biomaterial, since it is the major constituent of the connective tissue and allows the controlled drug release within targeted tissues (Helary *et al*., 2006). Dextran is a non-toxic, hydrophilic homopolysaccharide which can be synthesized from sucrose with dextransucrase or from maltodextrins with dextrinase (Bachelder *et al*., 2018). Dextran is commonly used to decrease vascular thrombosis (Booi *et al*., 2011), to reduce inflammatory response (Gombocz *et al*., 2017) and to prevent ischemia – reperfusion injury in organ transplantation (Banz *et al*., 2019), in which dextran acts as a mild reactive oxygen species scavenger and reduces excess platelet activation. Due to its properties dextran has been extensively explored in biomedical and pharmaceutical applications (Robless *et al*., 2014). Flufenamic acid is a non-steroidal anti-inflammatory drug (NSAID) and a member of the anthranilic acid derivatives (fenamates) (Psomas *et al*., 2013).

The aim of this study was to obtain and characterize drug delivery systems based on collagen, dextran and flufenamic acid (matrices, membranes and fibers) for wound healing.

MATERIALS AND METHODS

Materials

The type I fibrillar collagen gel having a concentration of 2.54% (w/v) was extracted from calf hide using a technology developed in our institute, Collagen Department (Albu, 2011). Dextran from Leuconostoc spp. (Mw 15,000–25,000) was purchased from Fluka (USA), flufenamic acid was purchased from ICN Biochemicals (USA), and Glutaraldehyde (GA) from Merck (Germany). Sodium hydroxide was of analytical grade.

Preparation of the Collagen Composites

Control gels with a 1.2% collagen concentration and a pH value of 7.4 were obtained from the original collagen gel under continuous stirring with distilled water and 1M NaOH solution. 0.5% flufenamic acid (FA) previously dissolved in 1 M NaOH solution along with the dextran in the amounts indicated in Table 1 was added over the 1.2% collagen gel. Some of the hydrogels were cross-linked with glutaraldehyde and left for 24 hours at 4°C for maturation / cross-linking. The amounts of dextran, flufenamic acid and glutaraldehyde were reported to collagen dry substance. Collagen gels with flufenamic acid were obtained with various amounts of dextran, un- and cross-linked, and coded G1-G4.

Table 1. Composition of collagen gels

Sample	Collagen (g%)	Dextran* (g%)	Glutaraldehyde* GA (g%)
G1	1.2	0	0
G2	1.2	0	0.006
G3	1.2	0.6	0.006
G4	1.2	1.2	0.006

*The amounts of dextran and GA were reported to collagen dry substance

The spongious matrices corresponding to previously obtained collagen gels were obtained by lyophilization using the Delta LSC 2-24 Martin Christ, Germany. The collagen matrices were coded according to the composition of the gels from which they were obtained, as follows: M1, M2, M3, respectively M4.

Collagen fibers were prepared from the same composition of flufenamic acid gels (Table 1) but, unlike matrices, they were lyophilized at the pH corresponding to the isoelectric point. They were coded as follows: F1, F2, F3 and F4, respectively.

Membranes were obtained by free drying at 25°C of the gels shown in Table 1 and coded Mb1, Mb2, Mb3, Mb4.

The following coding is also used: Series I consisting of: M1, F1, Mb1; Series II: M2, F2, Mb2; Series III: M3, F3, Mb3; Series IV: M4, F4, Mb4.

FT-IR Analysis

FT-IR spectral measurements were performed with a spectrophotometer Jasco FT/IR 4200. All the spectra were recorded at the following parameters: spectral range 4000-600 cm^{-1}, resolution 4 cm^{-1} with 30 acquisitions per each sample.

In vitro *Release of Flufenamic Acid from Collagen Composites*

The release studies were conducted using a "sandwich" device adapted to a paddle dissolution equipment, as detailed in our previous work (Ghica *et al*., 2017). The amount of flufenamic acid released at different time intervals was evaluated by UV spectroscopy at $\lambda=288$ nm.

RESULTS AND DISCUSSION

The samples were analyzed by FT-IR and *in vitro* release of flufenamic acid.

Figures 1-3 show the overlapped spectra for M1-M4 matrices, Mb1-Mb4 membranes, respectively for the matrix, fiber and collagen membrane derived from gel G1, corresponding to Series I.
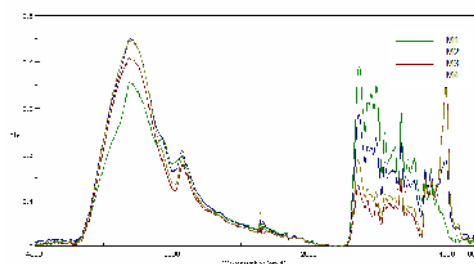
Figure 1. FT-IR spectra for M1, M2, M3 and M4 matrices
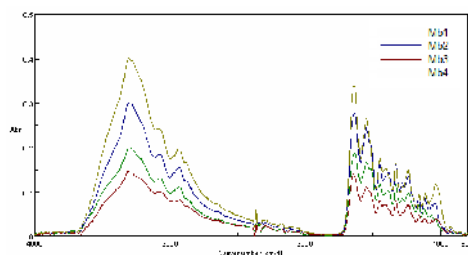
Figure 2. FT-IR spectra for membranes Mb1, Mb2, Mb3 and Mb4
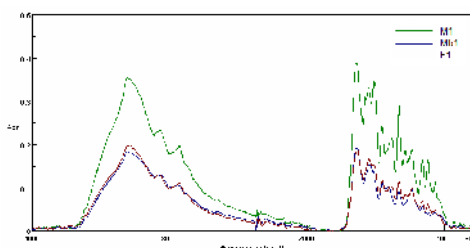
Figure 3. FT-IR spectra for matrix, membrane and collagen fiber Series I - M1, Mb1 and F1

From the spectra shown in Figures 1-3 it can be seen that the collagen macromolecule keeps its triple helix structure. Band changes are due to the addition of dextran, which also influences additional cross linking. The composition of the matrices, membranes and fibers being the same, Figure 3 shows that the drying or lyophilization conditioning process does not influence the movement of the bands, and differences can only be observed at their intensities.

The cumulative kinetic profiles corresponding to the flufenamic acid percentage released from the supports corresponding to each series are represented in Figures 4-7.
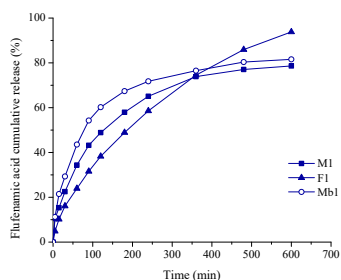
Figure 4. The cumulative kinetic profiles corresponding to the release of flufenamic acid from the Series I collagen supports (M1, F1, Mb1)
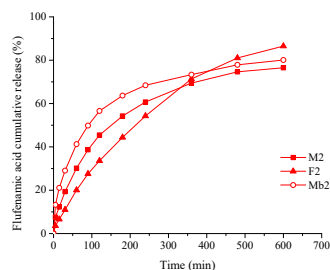
Figure 5. The cumulative kinetic profiles corresponding to the release of flufenamic acid from the Series II collagen supports (M2, F2, Mb2)
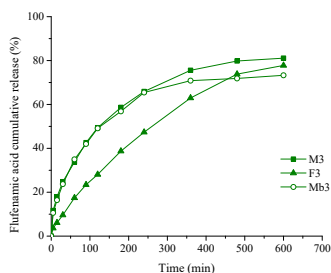
Figure 6. The cumulative kinetic profiles corresponding to the release of flufenamic acid from the Series III collagen supports (M3, F3, Mb3)
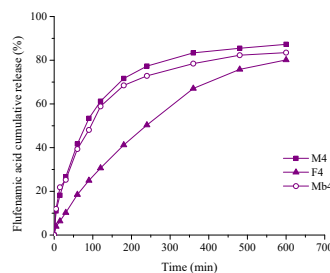
Figure 7. The cumulative kinetic profiles corresponding to the release of flufenamic acid from the Series IV collagen supports (M4, F4, Mb4)

Figures 4-7 and Table 2 show the influence of the collagen supports preparation process on the percentage of flufenamic acid released during 10 hours of kinetic experiment. Thus for Series I, the percentage of FA released varies as follows: F1> Mb1> M1, an increase of 11.85% for F1 compared to Mb1, respectively an increase of 16.04% compared to M1 being recorded. For Series II, the order of variation is the same as for Series I, the percentage of AF released being 11.35% lower for M2 in comparison with F2, and 4.22% in comparison with Mb2, respectively. For Series III, the highest % of AF released was obtained for M3, followed by F3 and Mb3. There is an increase of 4.07 % for M3 compared to F3 and 10.63% compared to Mb3, respectively. For IV series, the lowest % of AF was released from F4 support, 8.28% lower than from M4 and 4.00% respectively compared to Mb4 (Table 2). It is also noted the influence of GA

cross linking on the percentage of AF released (Series I and II). Obviously, for Series I and II, cross linking with GA results in a decrease in the percentage of drug released after 10 hours from experiment beginning of 2.44% for M2, 5.16% for F2 and 1.81 % for Mb2, compared to M1, F1 and Mb1 respectively (Table 2). The amount of dextran present in the series II ÷ IV has a different influence on the % of AF released. Thus, for matrices, the highest % of AF is obtained for M4, about 1.08 times higher than M3, and 1.14 times than M2. For fibers, the slowest release is recorded for F3, 10.12% less compared to F2 and 2.97% less compared to F4. For membranes, the highest percentage of AF is released by Mb4, about 1.04 times more than Mb2 and 1.14 times more than Mb3 respectively (Table 2). It is noted that in the first hour flufenamic acid release was quite rapid, the percentage of drug released varying between 17.45% (F3 sample) and 43.53% (Mb1 sample). After this rapid release period, the so-called "burst release" stage, it is noted that the non-steroidal anti-inflammatory agent is slowly released during the next 9 hours of the experiment.

The kinetic profiles described above are pursued in the healing of skin lesions for which an important element is the local inflammation. The "burst release" effect, after support contact with the skin lesion and its wetting by the wound exudates, provides a rapid reduction in inflammation and pain associated with lesions of various etiologies. On the other hand, the gradual drug release provides a local anti-inflammatory and analgesic effect over a longer period of time necessary for the wound healing.

In order to establish the drug release mechanism from the collagen supports, the Power law model (eq.1) and its particular case Higuchi (n = 0.5) were applied:

$$\frac{m_t}{m_\infty} = k \cdot t^n \tag{1}$$

where, m_t/m_∞ represents the fraction of drug released at time t, k - the kinetic constant, n - the release exponent characteristic for the drug release mechanism.

The highest values of the determination coefficients are obtained for the Power law model (between 0.9577 and 0.9941), showing that this model best describes the mechanism of the drug release from the designed collagen supports. The values of the release exponent ranged from 0.31 to 0.41 for matrices and membranes, and between 0.58 and 0.64 for fibers, indicating a non-Fickian drug transport mechanism from the designed formulations. The values of the parameters specific to Power law model, as well as the determination coefficients specific to this model and for the Higuchi model, are shown in Table 2.

Table 2. Parameter values specific to the Power law model; the determination coefficients specific to the Power law model and the Higuchi model; percentage of drug released

Flufenamic acid support	Higuchi model	Power law model	Release exponent	Kinetic constant (1/minn)	Released percentage (%)
M1	0.9585	0.9788	0.38	0.072	78.63
F1	0.9910	0.9937	0.58	0.023	93.80
Mb1	0.9036	0.9610	0.31	0.116	81.57
M2	0.9698	0.9803	0.41	0.056	76.51
F2	0.9886	0.9924	0.62	0.017	86.53
Mb2	0.9244	0.9757	0.32	0.110	80.09
M3	0.9674	0.9856	0.38	0.074	81.09

Flufenamic acid support	Higuchi model	Power law model	Release exponent	Kinetic constant (1/minn)	Released percentage (%)
F3	0.9857	0.9933	0.64	0.013	77.77
Mb3	0.9367	0.9698	0.35	0.082	73.30
M4	0.9206	0.9577	0.36	0.099	87.28
F4	0.9866	0.9913	0.62	0.015	80.15
Mb4	0.9286	0.9659	0.34	0.099	83.49

CONCLUSIONS

The percentage of drug released is influenced by the degree of cross-linking, the presence of dextran in the designed formulations and the preparation technique of the collagen supports. Thus, the percentage of flufenamic acid released from collagen drug delivery systems varies in the order: for Series I and Series II - fiber, membrane and matrix, for Series III - matrix, fiber and membrane and for Series IV - matrix, membrane and fiber. For collagen drug delivery systems obtained by the same preparation technique, the percentage of flufenamic acid released varies in the order: (i) for matrices: M4, M3, M1, M2; (ii) for fibers: F1, F2, F4, F3; (iii) for membranes: Mb4, Mb1, Mb2, Mb3.

The flufenamic acid release characteristics show the potential application of the designed collagen supports in wound lesions with different etiologies.

REEFRENCES

Albu, M.G. (2011), *Collagen Gels and Matrices for Biomedical Applications*, Lambert Academic Publishing, Saarbrücken.

Bachelder, E.M. *et al*. (2008), "Acetal-derivatized dextran: an acid-responsive biodegradable material for therapeutic applications", *Journal of the American Chemical Society*, 130(32), 10494–10495, https://doi.org/10.1021/ja803947s.

Banz, Y. *et al*. (2009), "Dextran sulfate modulates MAP kinase signaling and reduces endothelial injury in a rat aortic clamping model", *Journal of Vascular Surgery*, 50(1), 161–170, https://doi.org/10.1016/j.jvs.2009.01.067.

Booi, D.I. (2011), "Perioperative fluid overload increases anastomosis thrombosis in the free TRAM flap used for breast reconstruction", *European Journal of Plastic Surgery*, 34(2), 81–86, https://doi.org/10.1007/s00238-010-0466-9.

Ghica, M.V. *et al*. (2017), "Development, optimization and *in vitro/in vivo* characterization of collagen-dextran spongious wound dressings loaded with flufenamic acid", *Molecules*, 22(9), 1552, https://doi.org/10.3390/molecules22091552.

Gombocz, K. *et al*. (2007), "Influence of dextran-70 on systemic inflammatory response and myocardial ischaemia-reperfusion following cardiac operations", *Journal of Critical Care*, 11(4), R87, https://doi.org/10.1186/cc6095.

Helary, C. *et al*. (2006), "Dense fibrillar collagen matrices: a model to study myofibroblast behaviour during wound healing", *Biomaterials*, 27(25), 4443–4452, https://doi.org/10.1016/j.biomaterials.2006.04.005.

Psomas, G. and Kessissoglou, D.P. (2013), "Quinolones and non-steroidal anti-inflammatory drugs interacting with copper (II), nickel (II), cobalt (II) and zinc (II): structural features, biological evaluation and perspectives", *Dalton Transaction*, 42, 6252–6276, https://doi.org/10.1039/c3dt50268.

Robless, P. *et al*. (2004), "Dextran 40 reduces *in vitro* platelet aggregation in peripheral arterial disease", *Platelets,* 15(4), 215–222, https://doi.org/10.1080/09537100410001682814.

Vallet-Regi, M. *et al*. (2007), "Mesoporous materials for drug delivery", *Angewandte Chemie International Edition in English*, 46(40), 7548-7558, https://doi.org/10.1002/anie.200604488.

NEW COMPOSITIONS WITH CROSSLINKED AND UNCROSSLINKED COLLAGEN POLYDISPERSIONS FOR SYSTEMIC TREATMENTS IN AGRICULTURE

MIHAELA-DOINA NICULESCU[1], EDYTA GRZESIAK[2], CARMEN GAIDĂU[1], DORU GABRIEL EPURE[3], CLAUDIU ŞENDREA[1], MIHAI GÎDEA[4]

[1]*INCDTP - Division: Leather and Footwear Research Institute, 93 Ion Minulescu St, district 3, Bucharest, Romania, icpi@icpi.ro, mihaelaniculescu59@yahoo.com*

[2]*Leather Industry Institute, 73, Zgierska St, Lodz, Poland*

[3]*SC Probstdorfer Saatzucht Romania SRL, 20 Siriului St, sector 1, Bucharest, Romania*

[4]*University of Agronomic Science and Veterinary Medicine, 59, Marasti St, district 1, Bucharest, Romania*

The main property of collagen polydispersions is their molecular profile, dependent on both raw materials origin and the extraction process. The paper presents collagen extracts from leather by-products, by thermal and enzymatic hydrolysis at alkaline pH with improved properties by additivation with glycerol and crosslinking with Tara tannin extract. Structural analysis by Dynamic Nuclear Magnetic Resonance Spectroscopy showed manifestations which may be attributed to the interaction of glycerol and Tara tanning extract with polypeptide chains and to the role of glycerol as plasticizer, partially compensated by the addition of Tara crosslinking. New combinations of crosslinked and uncrosslinked collagen polydispersions were applied in cereals and legume seed treatment, so as to provide free amino acid content immediately available for stimulation of germination and a layer of polypeptides that would slowly release amino acids for growth stimulation. The results were quantified by an increase in cereal seed germination of over 15% and a much more pronounced development of plants, which have reached lengths over 10% higher compared to untreated seeds. For the most of legumes, the new treatment led to development of total biomass (root and cotyledons) and to a higher permeability for the water imbibition of the seeds.

Keywords: collagen polydispersions, crosslink, structural analysis.

INTRODUCTION

Most collagen-based materials, in the form of gelatin, collagen hydrolysate, or complex 2D / 3D structures, such as membranes, hydrogels, aerogels, have been created for medical applications. However, due to the intrinsic or acquired functionalities, collagen materials have applications in many niche areas: in cosmetics, for the preparation of various make-up, cleaning and maintenance products, such as shampoo, creams, hair curling products (Langmaier *et al*., 2002); obtaining surfactants (Langmaier *et al*., 2002; Stepan *et al*., 2008); precipitation of polyphenols in the winemaking process (Ortiz-Barrera *et al*., 2015); obtaining food cling films (Wang *et al*., 2015); additivation of aminoplast adhesives to limit formaldehyde emissions from thermally treated adhesive films (Sedliacik *et al*., 2011; Niculescu *et al*., 2012).

Based on the results of studies that showed that protein extracts do not have toxic or genotoxic effects and do not adversely affect eukaryotic cells and the soil ecosystem (Corte *et al*., 2014), their applications were extended to the field of agriculture, particularly soil remediation (Zainescu *et al*., 2010) and fertilization of crops (Sirbu *et al*., 2009). The most recent studies have been focused on obtaining collagen hydrolysates from tanned leather by-products for the fertilization of horticultural crops (Gaidau *et al*., 2009, Pati *et al*., 2015), grain seed treatment to stimulate germination and reduce amounts of insecticide-fungicide (Gaidau *et al*., 2013), the fertilization of

wheat and rice crops (Coelho *et al*., 2015), the use of fish skin collagen extracts to increase the yield of rape by stimulating growth and reducing silique dehiscence (Gidea *et al*., 2017), the use of bovine hide collagen hydrolysate in the foliar treatment of vines to alleviate the effects of iron deficiency due in particular to calcareous soils (Tudor *et al*., 2017).

In this research, collagen was recovered from secondary sources, namely bovine hide by-products from semiprocessed leather, by thermo-enzymatic processes. Compared to collagen functionalization models by cross-linking with glutaraldehyde, chitosan, cellulose, gluten, etc., proposed by other research (Oechsle *et al*., 2016; Tian *et al*., 2016), collagen extracts obtained in the form of gelatin and hydrolysates were combined with glycerol and Tara vegetable extract and new collagen-based compositions were created with favorable properties of increasing the germination rate of the seeds and plant growth.

EXPERIMENTAL PART

Materials

The bovine leather by-products was obtained from SC Pielorex SA, Romania with the following characteristics: 50-70% volatile matter, 0.5-12.5% total ash, 14-17% total nitrogen, aqueous extract pH value of 3.5-8.0, were obtained in Leather and Footwear Research Institute, Bucharest, Romania. Calcium oxide, acetic acid, glycerol were products of SC Chimopar SA Romania. Alcalase 2.4L was obtained from Novozymes Denmark.

Procedures

Bovine gelatin was obtained from half-processed bovine hide byproducts by thermal hydrolysis at 70-90°C, pH=5.5-6.0, duration 3-5 hours and concentration under vacuum at a ratio of 4:1. The collagen hydrolysate was obtained from wet blue shavings in a vessel equipped with thermal isolation, refrigerator, automated stirring, in water a solid to liquid ratio of 1:5 at 80°C, with 10% $Ca(OH)_2$ during 5 hours. The solution was filtered, heated to 65-68°C, pH adjustment at 8.5-9.0 when 1% Alcalase 2.4L was added and hydrolysis was continued for 3 hours. The enzyme deactivation was done at 90°C by stirring for 10 min. (Niculescu *et al*., 2014).

The Tara vegetable extract was obtained by hydrolyzing Tara powder (Gaidau *et al*., 2014) in water a solid/liquid ratio of 1/4 at 60-80°C for 1-2 hours, centrifugation and vacuum filtration on cellulosic membranes.

The new compositions were made by continuously stirring the collagen polydispersions additivated/crosslinked with glycerol, tannin extract at 50-60°C for 40-90 minutes. The additive/crosslinker content is related to the moisture-free dermal substance content. For analytical reason cast films from the formulated compositions were dried in the forced convection oven.

Analytical Methods

The collagen polydispersions were analysed in terms of dry substance (SR EN ISO 4684:2006) and total ash (SR EN ISO 4047:2002) by gravimetric methods, total nitrogen and protein substance (SR ISO 5397:1996), aminic nitrogen (ICPI protocol) by

volumetric methods, pH (SR EN ISO 4045:2008) by potentiometric method. The collagen additives interaction and its secondary structure were non-invasively investigated by NMR-MOUSE (Magritek Ltd). The tensile strength and elongation of films were investigated by Testing Machine H5KT.

RESULTS AND DISCUSSIONS

In this research, the following collagen extracts were developed: GB gelatin; H1 diluted hydrolysate, H2 diluted hydrolysate, with the chemical characteristics presented in Table 1.

Table 1. Characteristics of collagen extracts

Characteristics	MU	Gelatin GB	Collagen hydrolysates H1	H2
Dry substance	%	6.70	9.49	29.07
Total ash	%	1.04	4.02	6.05
Total nitrogen	%	17.73	16.30	16.31
Protein substance	%	99.64	91.61	91.66
Amino nitrogen	%	0.40	2.03	1.33
pH	-	5.81	8.19	8.07

For the additivation of collagen extracts, a Tara vegetable extract was made with 5% dry substance and 4 tanning substances which were combined in various formulations with collagen extracts to achieve polydispersions with film-forming properties in order to treat cereal and legume seeds.

Compositions of collagen-based polydispersions, in which the components are related to the collagen extract content, are shown in Table 2.

Table 2. Compositions of collagen-based polydispersions

Protein polydispersions	Collagen extract, %	Additive / crosslinker, % Glycerol	Tara extract
P1	GB, 80	20	-
P2	GB, 85	10	5
P3	H2, 75	10	15

Some of the compositions were cast into films and the structural and mechanical properties were studied, in order to extend the applications of these compositions and to create functional supports for very small seeds (to facilitate planting) or for different types of biodegradable packaging (e.g. for seedlings).

Currently, the richest and most complete structural information on organic compounds is provided by dynamic NMR spectroscopy (Badea *et al*., 2016). The NMR measurements of the additivated/crosslinked collagen films used basic gelatin (GB) as control. The relaxation times determined by NMR measurements are shown in Table 3 and exemplified in Figure 1.

Table 3. Relaxation times for films

Sample	T1 (ms)	Exponential T2	
		T2long (ms)	T2long (ms)
GB	77.09	1.29	0.18
P1	40.14	8.71	2.04
P2	51.39	3.45	1.26

Decreasing the longitudinal relaxation time T1 can indicate a swelling of the films by mobilizing interstitial water and can be attributed to the interaction between the additive and the Tara tanning extract with the polypeptide chains. The transverse relaxation time T2 is a measure of the degree of mobility of the polypeptide chains: T2long - the amorphic area and the T2short - the rigid area. The growth tendency of T2 for P1, P2 films compared to raw gelatin (GB) indicates a peptide chain mobilization due to the plasticizing role of glycerol, partly compensated by the addition of Tara crosslinker.
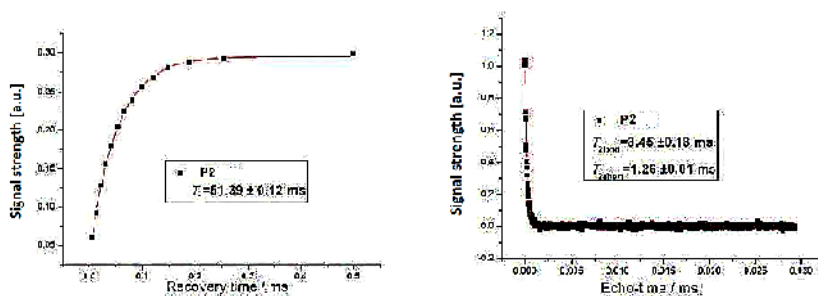
Figure 1. Curves of relaxing times T1; T2

This conclusion is supported by the results of physical-mechanical analyses of the two types of additivated/crosslinked collagen films, presented in Figure 2.

(a)   (b)
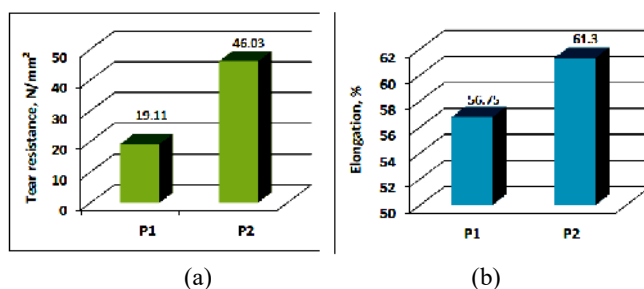
Figure 2. Mechanical properties of collagen films: (a) resistance; (b) elongation

Elongation and tensile strength tests highlight the improvement of the film's mechanical properties by cross-linking with Tara extract, tensile strength being about 2.5 times higher for the crosslinked film compared to the additivated film.

Testing collagen-based compositions in cereal grain (wheat) treatment demonstrated an increase in germinative energy from 72% of the control treated with water (A) to 93% of the sample treated with P3 polydispersions. It was found that after 10 days from the onset of the experiment, all the plants remained viable, and those treated with P3 collagen polydispersions were more developed compared to the control, Figure 3.

Treatment of legume seeds (e.g. chickpeas, beans, soy, peas) with collagen polydispersions (P3, H1, H2) resulted in 7-10% increase in germination rate, early plant growth and a more pronounced increase in total biomass (root and cotyledons) compared to untreated seeds, Figure 4.
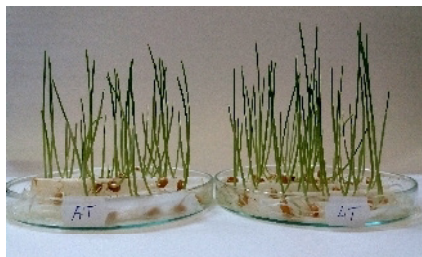
Figure 3. Development of wheat plants
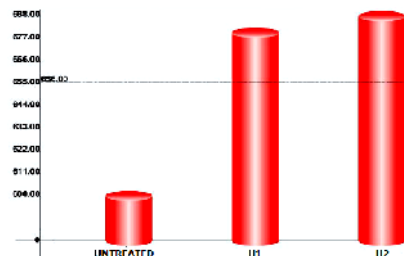
Figure 4. Biomass increase of peas

Early plant growth indicates greater permeability to water absorption. It was been noted that the stimulation of leguminous plant growth as a result of seed treatment with collagen polydispersions is influenced by the pH of the products used, the increase being higher in the case of treatment with H2 which has a slightly lower pH than H1.

CONCLUSIONS

• Collagen extracts have the ability to form films, whose flexibility, elasticity and strength characteristics can be modified depending on the degree of additivation with flexibility improvers and crosslinkers that enhance the resistance of films in order to adapt to application requirements.

• Treating cereal grains with collagen polydispersions leads to an increase in germination of approx. 25% and stimulation of plant growth.

• Treating legume seeds with collagen polydispersions results in early plant growth, due to faster water imbibition and a total biomass increase of approximately 15%.

• Crosslinked and uncrosslinked collagen polydispersions presents properties that can be exploited to increase agricultural output.

REFERENCES

Badea, E., Sendrea, C., Carsote, C., Adams, A., Bluemich, B., Iovu, H. (2016), "Unilateral NMR and thermal microscopy studies of vegetable tanned leather exposed to dehydrothermal treatment and light irradiation", *Microchemical Journal*, 129, 158-164, https://doi.org/10.1016/j.microc.2016.06.013.

Coelho, L., Ferreira, M.M., Bastos, A.R.R. *et al.* (2015), "Leather Industry Waste as a Nitrogen Source for Wheat and Rice in Succession", *Revista Brasileira de Ciencia do Solo*, 39(5), 1445-1455, https://doi.org/10.1590/01000683rbcs20140608.

Corte, L., Dell'Abate, M.T., Magini, A. *et al.* (2014), "Assessment of safety and efficiency of nitrogen organic fertilizers from animal-based protein hydrolysates - a laboratory multidisciplinary approach", *Journal of the Science of Food and Agriculture*, 94(2), 235–245, https://doi.org/10.1002/jsfa.6239.

Gaidau, C., Niculescu, M., Stepan, E., Taloi, D., Filipescu, L. (2009), "Additives and Advanced Biomaterials Obtained from Leather Industry By-products", *Revista de Chimie*, 60(5), 501-508.

Gaidau, C., Niculescu, M., Stepan, E., Epure, D.-G., Gidea, M. (2013), "New Mixes Based on Collagen Extracts with Bioactive Properties, for Treatment of Seeds in Sustainable Agriculture", *Current Pharmaceutical Biotechnology*, 14(9), 792-801, https://doi.org/10.2174/13892010146661312277112020.

Gaidau, C., Simion, D., Niculescu, M.D., Paun, G., Popescu, M., Bacardit, A., Casas, C. (2014), "Tara Tannin Extract Improvement. Part I: Extraction and Concentration Through Membranary Filtration Techniques", *Revista de Chimie*, 65(8), 929-933.

Gidea, M., Stepan, E., Enascuta, E.C., Gaidau, C., Niculescu, M.D., Epure, D.G., Cioineag, C., Sandulescu, E.B., Epure, L.I. (2017), "Researches on the biostimulating and antidehiscent effect of products based on fish collagen crosslinked to rape crop", *Journal of Biotechnology*, 256, Supplement, S100.

Langmaier, F., Mladek, M., Kolomaznik, K., Sukop S. (2001), "Collagenous Hydrolysates from Untraditional Sources of Proteins", *International Journal of Cosmetic Science*, 23(4), 193-199, https://doi.org/10.1046/j.0412-5463.2001.00081.x.

Langmaier, F., Mladek, M., Kolomaznik, K., Maly, A. (2002), "Degradation of Chromed Leather Waste Hydrolysates for the Production of Surfactants", *Tenside Surfactants Detergents*, 39(2), 31-34.

Niculescu, M.D., Sedliacik, J., Gaidau, C., Jurkovic, P., Matyasovsky, J. (2012), "Complementary methods for recovery and valorisation of proteins from chrome leather wastes", *Leather and Footwear Journal*, 12(2), 85-100.

Niculescu, M.D., Gaidau, C. (2014), New Collagen Extracts Conditioning for Applications in Crop Protection Against Pests", *Revista de Chimie*, 65(12), 1457-1461.

Oechsle, A.M., Häupler, M., Weigel, F., Gibis, M., Kohlus, R, Jochen, W. (2016), "Modulation of extruded collagen films by the addition of cogelling proteins", *Journal of Food Engineering*, 171, 164–173, https://doi.org/10.1016/j.jfoodeng.2015.10.004.

Ortiz-Barrera, E., Macias-Carranza, V., Cabello-Pasini, A. (2015), "Precipitation of wine polyphenols using collagen from fish skin and fish swim bladder", *CyTA-Journal of Food*, 13(4), 597-602.

Pati, A., Chaudhary, R. (2015), "Soybean plant growth study conducted using purified protein hydrolysate-based fertilizer made from chrome-tanned leather waste", *Environmental Science and Pollution Research*, 22(24), 20316-20321, https://doi.org/10.1007/s11356-015-5549-5.

Sedliacik, J., Matyasovsky, J., Smidriakova, M. *et al.* (2011), "Application of collagen colloid from chrome shavings for innovative polycondensation adhesives", *Journal of The American Leather Chemists Association*, 106(11), 332-340.

Sirbu, C. *et al.* (2009), "Fertilizers with Protein Chelated Structures with Biostimulator Role", *Revista de Chimie*, 60(11), 1135-1138.

Stepan, E., Velea, S., Gaidau, C., Filipescu, L., Ghiga, M.D., Radu, A.C. (2008), "Surfactants obtained from unconventional resources", 7th World Surfactants Congress, Paris, France, CESIO 2008.

Tian, Z., Duan, L., Wu, L., Shen, L., Li, G. (2016), "Rheological properties of glutaraldehyde-crosslinked collagen solutions analyzed quantitatively using mechanical models", Materials Science and Engineering, 63, 10–17, https://doi.org/10.1016/j.msec.2016.02.047.

Tudor, E., Cioroianu, T., Sirbu, C., Dumitru, M., Grigore, A., Parvan, L., (2017), "Fertilizer for the Treatment of Iron Chlorosis. Physico-chemical and agro-chemical properties", *Revista de Chimie*, 68(1), 65-68.

Wang, L.F., Rhim, J.W. (2015), "Preparation and application of agar/alginate/collagen ternary blend functional food packaging films", *International Journal of Biological Macromolecules*, 80, 460-468, https://doi.org/10.1016/j.ijbiomac.2015.07.007.

Zainescu, G., Voicu, P., Gherghina, A., Sandru, L. (2010), "Application of tannery organic wastes in degraded soils remediation", *Journal of Biotechnology*, 150, 290-290, https://doi.org/10.1016/j.jbiotec.2010.09.233.

STUDY REGARDING THE DEVELOPMENT OF THE FUNCTIONAL TEXTILES WITH ANTIMICROBIAL PROPERTIES

FLOAREA PRICOP, LAURA CHIRILĂ, ALINA POPESCU, MARIAN RAŞCOV, RĂZVAN SCARLAT

The National Research & Development Institute for Textile and Leather, 030508, Bucharest, Romania, E-mail: certex@ns.certex.ro

The antimicrobial fibres, with encapsulated antimicrobial agents, prevent the bacteria developing and maintain the body under hygienic conditions a longer time, refreshing and facilitating the skin respiration, eliminating the possibility of giving out the unpleasant odour. The capsules continuously migrate towards the fibre surface, until exhaustion, achieving a protection zone on the surface. The clothing products and socks made of antimicrobial fibres preserve their antimicrobial effect after numerous washings, unlike the textiles covered with polymers that contain antimicrobial agents that retain their antimicrobial effect only several washings. The main objective of the research was the development of advanced technologies and functional textiles with ecological impact on the environment and human body, the promotion of raw materials using superior hygienic-functional characteristics as well as antibacterial and anti-allergic properties. Finally, both the performances of the hygienic and functional characteristics of the developed textile products and the positive impact over the environment were accomplished due to the antimicrobial fibres and by using the ecological finishing technologies and treatment with plant extracts with antimicrobial and anti-allergic properties. Microencapsulation can prolong the shelf life of various volatile and non-volatile cosmetic ingredients by delaying oxidation and evaporation. The suitability of microcapsules for cosmetic textiles applications depend on the range of diameter, mechanical robustness and content release profile of microcapsule to offer appropriate potential for specific functionality.

Keywords: antimicrobial fibres, bioactive textiles, extracts from plants.

INTRODUCTION

With the development of the textile and technology industry, the demand for value-added functional materials is growing. The trend in the worldwide is focused on: the use of a material for various applications - multifunctional textiles, and on the other hand on their functionalization that falls within the group of cosmetic textiles, only for a certain purpose in a narrow field.
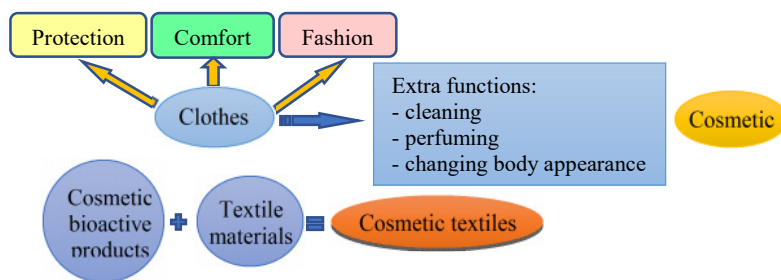
Figure 1. Functions of cosmetic textiles

The European Cosmetic directive has define cosmetic product as "any textile article containing a substance or preparation that is released over time on different superficial

parts of the human body, notably on human skin, and containing special functionalities such as cleansing, perfuming changing appearance, protection, keeping in good condition or the correction of the body odours is called a cosmetic textiles" (Almeida, 2005). Figure 1 shows functions of cosmetic textiles. Cosmetic textiles induce a state of well-being in the human body, causing a healthy balance between the human body and the mind. The properties of functional textiles have to correspond to high quality standards, respecting the increased efficiency conditions with minimal impact on the environment.

METHODS OF ACCOMPLISHING

The "cosmetic textiles" functional textiles are created by micro-encapsulation, grafting, nanotechnology and coating techniques by incorporating various body care and health products that are gradually transferred to the skin through movement, pressure, or the effect of natural skin heat (Figure 2).
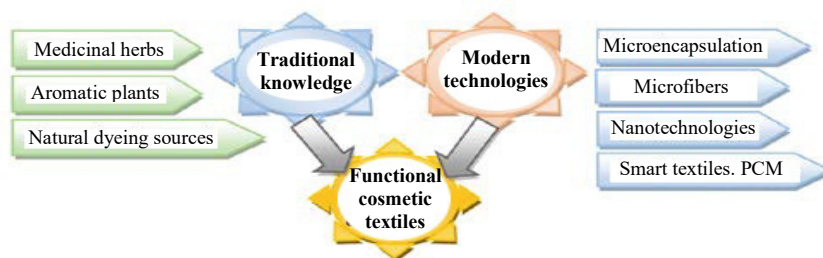
Figure 2. Accomplishing ways for cosmetic functional textiles

APPLICATION IN TEXTILES AND ISSUES RELATED TO THEM

Application in textiles and issues related to them microcapsules can be applied to textiles by padding, coating, spraying, immersion or exhaustion. A binder is required for all these methods. The binder may be acrylic, polyurethane, silicone, starch, etc. Its role is to fix the capsules onto the fabric and to hold them in place during wear and washing. Microcapsules can be applied to various fibres both natural and synthetic (Ocepek and Forte-Tavčer, 2008). Release mechanisms of the core for cosmetic textiles are friction, pressure, biodegradation and for aromatherapy and fragrance textiles these methods are friction and diffusion through polymer wall (Nelson, 2002).

The smaller the microcapsules, the greater the covering of the product and the longer the fragrance will last, as it takes longer for the capsules to be ruptured by physical pressure (Roshan, 2015). In practice the aim is to produce textiles with microcapsules which would last for as many wash cycles as possible. A method of fixing fabric aromatic microcapsules has been developed. The fabric is first treated with a nitrogenous cationic compound and the microcapsule wall is manufactured to adhere to this layer. The produced capsules are 0.1 to 100 μm in size and are made using interfacial or in situ polymerization methods. Typical encapsulated compounds include perfumes (Nelson, 2002). Scientists investigated that using this resin with an initiator allows the fragrant to remain on the fabric for more than 50 wash cycles (Li, 2005).

Researchers have reported that there are also some issues related to the durability of microcapsules during washing, drying, maintenance and resistance to the functionalized textiles in many washing cycles. Increasing durability implies the correct choice of the textile support, the method of preparation of the microcapsules and their application on the support.

TECHNOLOGICAL FLOW OF COSMETIC TEXTILES

- Selection of the extraction systems for natural and essential products to be applied to textile materials;
- Testing them;
- Selection of essential oils and microcapsules taking into account the desired functionalities, treatment methods and the type of textile material;
- Preliminary preparation of the textile support in order to increase the affinity → changing the surface of the textile materials by different chemical methods → treatment of the textile material with the dispersions/emulsions of the microcapsules with essential oils → condensation of the impregnated textile material → drying;
- Investigation the influence of functionalization processes on the technical and qualitative characteristics of textile materials by physical-mechanical, physical-chemical, biological and toxicological analyses.

Generally, major cosmetic ingredients from inorganic and synthetic chemicals, and plant derivatives are original. Various scientific and medical researchers have proved that plant derivatives are safer than chemicals and animal derivatives as cosmetics. The efficacy of cosmetic textiles should be tested using the same testing tool & testing conditions as for cosmetics. The ISO/DIS 11930 test may be successful in testing the efficacy of cosmetic textiles, although this test is designed for cosmetics. Figure 3 shows functional effects of cosmetic textiles:
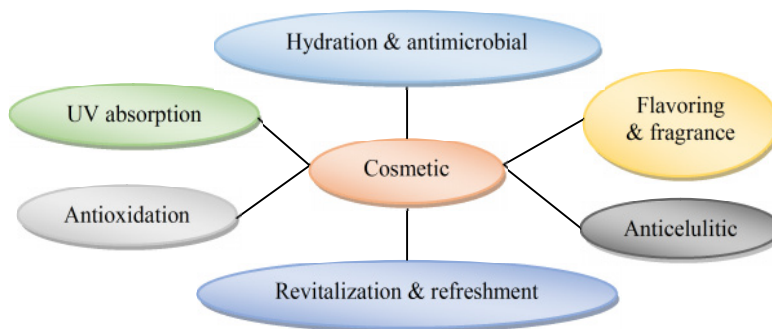
Figure 3. Functional effects of cosmetic textiles

FUNCTIONAL EFFECTS OF COSMETIC TEXTILES

The moisturizing effect of cosmetic textiles on the skin consists in wrinkle reduction, maintaining a soft and supple appearance of the skin.

Nanotechnology can lead to the development of hydrophilic textile surfaces. The integration of TiO_2 increases the possibility of moisture absorbance on textile surfaces through the photocatalytic process (Mahltig *et al.*, 2005). This approach can be used to develop quick-dry textiles for sports or outdoor clothing.

The antimicrobial effect prevents the growth of bacteria and maintains the body in hygienic conditions with essential oils (lavender, fennel, Aloe Vera, rosemary) (Mathis and Mehling, 2010). The fabric has features, such as: calming, antioxidation and anti-aging. The use of antimicrobial fibres that have encapsulated antimicrobial agents prevents the development of bacteria and keeps the body in hygienic conditions for a long time, eliminating the possibility of creating unpleasant odors, refreshing and facilitating the breathing of the skin (Drambei and Pricop, 2011). Antibacterial microcapsules migrate continuously to the outside of the fibres, until exhausted, creating a surface protection area. The clothing products made of this type of yarns maintain their antimicrobial effect after many washings (50-200).

The fragrance effect consists in eliminating the possibility of creating unpleasant odours, refreshing a special fragrance with essential oils (rose, lavender, basil, rosemary, etc.) and facilitating skin breathing. The incorporation of deodorant into a textile substrate is conducted during polymerisation at the finishing stage.

The refreshing and relaxing effect is achieved either by using phase change materials in the form of microcapsules (menthol encapsulation, Aloe Vera together with emulsifiers and very durable synthetic cooling), or by increasing the area of contact between the surfaces with high transmission of moisture and human body. Scientific researches on Aloe Vera have proved that textiles treated with it are very pleasant to wear, having a significant effect on energy levels, which offers a feeling of well-being. Aloe Vera is used to obtain antibacterial, antiviral, antimycotic effects (Eshun and He, 2004).

A textile structure that is able to release **revitalising** aromas synthesised by plants and fruit based ingredients like ginger, menthol, orange or rosemary at a slow rate comes under the category of vitalising textiles. These ingredients are added to textiles using the microencapsulation technique. The durability of this function remains even after a number of washings. Cosmetic textiles vitamins are suitable for bathrobes and other similar purposes (Welch, 2013).

The UV protection effect is conferred by the type of fabric, the number of wash cycles of the material, the UV protection factor that can be improved, and the use of Zn nanoparticles, iron oxide, zinc oxide, titanium oxide, oxalic bi-reactive and various other chemicals. To improve the UV protection factor of textiles, are used Zn nanoparticles, iron oxide, zinc oxide, titanium oxide, bi-reactive oxalic acid and various other chemicals (Singh, 2005).

The textile structures that work to offer a **slimming effect** by means of yarn properties, fabric structure and finishes are called cosmetic textiles for slimming. The use of compressional garments has offered a third option for slimming, as well as a reduction in muscle damage and a maintaining muscle function. Functional muscles give a better appearance and a good-looking effect by accelerating blood flow in veins. Cosmetic textiles for slimming provide rehabilitation to the wearers. Anti-cellulite fabric contains a combination of agents, such as caffeine, retinol, vitamin E which may

reduce the outer appearance of cellulite. In addition, it was claimed that slimming effect persists, even after the garment has been washed several times.

EFFICACY OF COSMETOTEXTILES

The efficacy of cosmetic textiles should be tested using the same testing tool & testing conditions as for cosmetics. The Group WG-25 agreed to set some guidelines to solve the complexity of this problem. The ISO/DIS 11930 test may be successful in testing the efficacy of cosmetic textiles, although this test is designed for cosmetic.

Perfume Performance Analysis

This analysis is required to test the performance of various perfumed textiles. Headspace gas chromatography/mass spectrometry (Headspace GC/MS) is a specific technique used to analyze volatile compounds. A specimen is placed in an airtight closed sampling vessel and then subjected to a temperature with a known temperature profile. The vapors in the vessels are sampled to analyze the odor issues, for identification of polymer additives and for residual solvent analysis according to various ASTM standards like ASTM - D3362, D3452, D4128 (Salaün *et al*., 2009).

Durability

The Group WG25 formed a separate subgroup to emphasize the durability aspect of cosmetic textiles. For wash fastness, a lot of testing methodologies are recommended by this subgroup. The efficiency of a binder to bind microcapsules on a textile surface depends on the compatibility of the different interfaces of the products involved in the finishing process. The choice of binder adapted to fix the microcapsules can be finalized by making a comparison of the surface energy components induced by various components in terms of the contact angle. Generally, the adhesion of microcapsules is closely dependent on the chemical nature and structure of the textile substrates (Zhu and Chai, 2005).

CONCLUSION

The complex documentary study presented in this article for this new field of cosmetic textiles regarding how to make functional textiles, the effects of textiles on their various technologies for accomplishing them, will be used in research projects. The correlation of the bioactive extracts properties with the raw material type, textile fabrics and application technologies will contribute to the accomplishing of a large variety of functionalised textiles.

Antimicrobial fibres and yarns that have encapsulated antimicrobial agents that prevent bacterial growth and keep the body in hygienic conditions for longer time, eliminating the possibility of creating unpleasant odours, refreshing and facilitating breathing (Drambei and Pricop, 2011). Antibacterial microcapsules migrate continuously to the outside of the fibres until exhausted, creating a surface protection area. The clothing products made of this type of yarns maintain its antimicrobial effect after numerous washings (50-200).

The optimization of the quantity of cosmetic ingredients and enhancing the durability of cosmetic effect are the two real challenges in this field. Cosmetic textiles

have to be designed so as the blend of the fabric, cosmetic finishes technologies and fashion to work together, in order to obtain an optimum cosmetic effect.

REFERENCES

Almeida, L. on centrum.tul.cz/centrum/itsapt/portugal2005/Almeida_ITSAPT.ppt.

Almeida, L. (2005), "Functional finishes", *Proceedings of 5th World Textile Conference "AUTEX",* Portorož, 77-82.

Drambei, P. and Pricop, F. (2011), "Aspects regarding antimicrobial behavior of the textile products containing amicor fibers", *Proceedings of 3rd Scientific-Professional Conference "Textile Science and Economy"*, Zrenjanin, 74-80.

Eshun, K. and He, Q. (2004), "Aloe Vera: A valuable ingredient for food, pharmaceutical and cosmetic industries-a review", *Critical Review in Food Sci. & Nutrition*, 44(2), 91-96, https://doi.org/10.1080/10408690490424694.

Gupta, D., Chattopadhayay, R. and Bera, M. (2011), "Compression stockings structure property analysis", *Asian Text. J.,* 20(1), 39-45.

Li, S., Boyter, H. and Qian, L. (2005), "UV curing for encapsulated aroma finish on cotton", *Journal of the Textile Institute*, Vol. 96 (6), 407-411, https://doi.org/10.1533/joti.2005.0116.

Mahltig, B., Haufe, H., Bottcher, H. (2005), "Functionalization of textiles by inorganic sol-gel coatings", *J. Mat. Chem.*, 15(41), 4385-4398, https://doi.org/10.1039/b505177k.

Mathis, R. and Mehling, A. (2010), *Cognis GmbH*, 46(12).

Nelson, G. (2002), "Application of microencapsulation in textiles", *International Journal of Pharmaceutics*, 242(1-2), 55-62, https://doi.org/10.1016/S0378-5173(02)00141-2.

Ocepek, B. and Forte-Tavčer, P. (2008), "Microencapsulation in textiles", *XVIth International Conference on Bioencapsulation*, Ireland, 1-4.

Roshan, P. (2015), "Functional finishes for textiles: Improving Comfort, Performance and Protection", *Woodhead Publishing Series in Textiles*, Elsevier, 1-14.

Salaün, F. *et al*. (2009), "Application of contact angle measurement to the manufacture of textiles containing microcapsules", *Text. Res. J.,* 79(13), 1202-1212, https://doi.org/10.1177/0040517508100724.

Singh, M.K. (2005), "Sun protective clothing", *Asian Textile Journal*, 14(1-2), 91-97.

Trenell, M.I. *et al*. (2006), "Compression garments and recovery from eccentric exercise: A (31) P-MRS study", *J. of Sport Sci. and Med.*, 5(1), 106-114.

Welch, P.B. (2013), "Chinese art: a guide to motifs and visual imagery", 237.

Zhu, J.Y. and Chai, X.S. (2005), "Some recent developments in headspace gas chromatography", *Current Analytical Chem.*, 1, 79-83, https://doi.org/10.2174/1573411052948488.

STUDY ON THE AROMA-THERAPEUTIC EFFECTS OF TEXTILES FUNCTIONALIZED BY HERBAL EXTRACTS

FLOAREA PRICOP[1], ALINA POPESCU[1], MARIAN RAŞCOV[1], LAURA CHIRILĂ[1], RĂZVAN SCARLAT[1], MARIA BUZDUGAN[2], ANGELA CEREMPEI[3], EMIL MUREŞAN[3]

[1]*The National Research & Development Institute for Textile and Leather, 16 L. Patrascanu Str., 030508, Bucharest, Romania, e-mail: certex@ns.certex.ro*

[2] *Magnum SX SRL, 61 FERDINAND I Blvd., Sector 2, 02138, Bucharest, Romania*

[3] *"Gheorghe Asachi" Technical University of Iasi, Faculty of Textiles, Leather and Industrial Management, 28 Prof. Dr. Docent D. Mangeron Blvd, 700050, Iasi, Romania*

This study, referring to the biologically active compounds compatible with textile materials, reveals its influence on human psychophysiological activity. In the COFUND-MANUNET III-AromaTex project, essential oils extracted from lavender, rosemary, mint, thyme were studied and selected to be used for obtaining of aroma-therapeutic effects on textiles, as well as other various effects, such as: skin hydration and anti-acne, revitalizing and reducing stress, improving of microcirculatory blood flow and cellular metabolism. In recent years, electrophysiological studies have been reported worldwide that have shown that different flavors affect spontaneous brain activities and cognitive functions that can be measured by the EEG encephalogram. The presented study contributes to the optimization of formulations which contain essential oils adapted to the conditions of technologies application for deposition and immobilization on textiles, with a particular emphasis on the desired therapeutic effect and the controlled release of essential oils. Aromatherapy application in textile industry led to a series of value-added products that give besides comfort a number of other properties (anti-acne, antimicrobial, fragrance, anti-inflammatory sedation, or soothing properties). In recent years, aromatherapeutic textiles were applied in many fields such as food, cosmetics, medicine, tobacco, textiles, leather, papermaking and pharmaceutical industries. The purpose of this chapter was to present the essential oils used in textile finishing, textile supports used for aroma finishing, embedding methods and the controlled release of essential oils.

Keywords: aromatherapy, essential oils, textile materials.

INTRODUCTION

Aromatherapy is one of the complementary therapies which use essential oils as the major therapeutic agents to treat several diseases. The essential or volatile oils are extracted from the flowers, barks, stem, leaves, roots, fruits and other parts of the plant by various methods. It came into existence after the scientists deciphered the antiseptic and skin permeability properties of essential oils. Inhalation, local application and baths are the major methods used in aromatherapy that utilize these oils to penetrate the human skin surface.

Although medicinal plants have been used for centuries as remedies for human diseases, in Romania in recent years, they have reached a great interest due to their low toxicity, pharmacological activities and economic viability. It shows a more pronounced shift from chemical and nonsustainable products to natural products that are not harmful, biodegradable and with health and wellness benefits (West and Annett-Hitchcock, 2014; Boulekbache-Makhlouf *et al.*, 2016).

Natural additives from plants can be compounds, groups of compounds, or essential oils (Boulekbache-Makhlouf *et al.*, 2016). Among natural additives, essential oils present a particular interest due to multiple benefits it shows such as antiviral, antifungal, antibacterial, antioxidant, antiparasitic, insecticidal, radical-scavenging properties, anti-inflammatory, antiseptic, germicide, healing and emollient effects.

Essential oils are made up of complex mixtures of several hydrocarbons (alcohols, terpenes, aldehydes, esters, phenols, oxides and ketones) and are obtained by conventional or advanced methods (Figure 1) (Ghosha and Chipot, 2015; El Asbahani *et al*., 2015).

Essential oils are fat soluble and thus they have the ability to permeate the skin membranes and drained into the systemic circulation, which reaches all targets organs (Radulovic *et al*., 2011; Kandori, 2002). Essential oils are considered "vital force" of the plants.
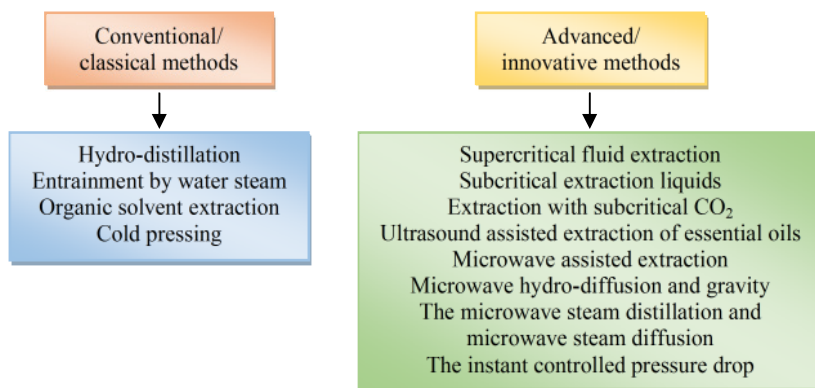
Figure 1. Extraction methods of essential oils (Cerempei 2017)
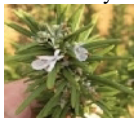
The role of these oils in plants is similar to that of the blood in the body. Fat-soluble structure of essential oils is similar to that of cells and tissues in the human body. This makes them compatible with human proteins and allows them to be easily identified and accepted by the body. Due to the fat-soluble structure and very small-size molecules, essential oils serve as transport agents that easily penetrates the cell membrane. Only one application of essential oils is sufficient to stimulate and revitalize the entire body. Recent research has shown that essential oils are able to penetrate the barrier blood/brain due to their small size (≤500 amu) (Balabai, 1988).

CHEMICAL COMPOSITION OF THE MAIN ESSENTIAL OILS USED IN RESEARCH

Essential oils represent less than 5% from vegetal dry matter and are complex mixtures of volatile compounds extracted from plants (Abraham *et al*., 2013; Rachwalik *et al*., 2012).

Chemical composition of the main essential oils used in textile industry, identified by gas chromatography (GC) and GC-mass spectrometry (GC-MS), is presented in Table 1 (Duhamela *et al*., 2016; Skalicka-Woz´niak and Walasek, 2014; Timung *et al*., 2016; Jamali *et al*., 2013; González-Rivera, 2016; Kumar *et al*., 2010).

Table 1. The chemical composition of the main essential oils to be used in the project

Essential oil	Chemical type	Main compounds Composition	Composition (%)	References
Peppermint	Oxygenated compounds	Menthol	36	10,11,12
		Menthone	21,24	
		Menthyl acetate	6.92	
		Eucalyptol	6.58	
		Isomenthone	4.71	
		Neomenthol	4.06	
Lavender	Monoterpenes Oxygenated monoterpenes	α-Pinene	3.4%	15
		1,8-cineole	33.0%	
		Camphor	23.1%	
		α-Bisabolool	14.1%	
Rosemary	Monoterpene Bicyclic Monoterpenes	β-Pinene	4.1%	15
		α-Pinene	28.2%	
Thyme	Oxygenated compounds	Oxygenated compounds	14.1–77.6	13,14
			0.5–27.8	
		Thymol	0.2–16.3	
	Monoterpenes	Borneol 0.2–16.3	3.8–6.6	
		γ-Terpinene	3.5–7.9	
		p-Cymene	1.2–7.8	
		α-pinene		

INFLUENCE OF THE PHYSICO-CHEMICAL AND MICROBIOLOGICAL PROPERTIES OF ESSENTIAL OILS ON TREATED TEXTILES

Antiseptic of the respiratory, analgesic, sedative and balancing of the central and vegetative nervous system (Bouchekrit *et al*., 2016; Leimann *et al*., 2009).

Indications: insomnia, neurasthenia, and in cases of palpitations of nervous origin of the heart, in general, in all cases of psychosomatic diseases. Due to its sedative effect it is recommended in migraines and other headaches.

Applied externally it is very effective to calm rheumatic pains, whether of joint or muscular origin. Useful in dislocations, sprains, contusions and muscular strains. As an antiseptic and healing agent it is used to wash ulcers and infected wounds, as well as in minor burns. Physicochemical properties and microbiological properties are presented in tables 2 and 3 (Cerempei, 2017; Zarrad *et al*., 2015; Al-Jabri and Hossain, 2016).

Table 2. Physicochemical properties

Relative density	0.9400 – 1.0950
Density of alcohol	0 – 10 G.L.
Relative ph	4.50 – 8.00

Table 3. Microbiological properties

Determination	Limit (UFC / mL)	Method used
Aerobic mesophilics	105	NOM-092-SSA1-1994
Mushrooms and yeast	103	NOM-111-SSA1-1994
Escherichia coli	10	NOM-113-SSA1-1994

FUNCTIONALIZATION OF TEXTILES WITH PLANT EXTRACTS AND APPLICATIONS IN MEDICINE

Due to essential oils that can act both at local level and through odor, they have great important applications in many fields such as food, cosmetics, medicine, tobacco, textile, leather, papermaking, pharmaceutical and perfume industries (Hu *et al*., 2001).

Essential oils add much value to the textile materials. The most commonly used essential oil in aroma finishing is lavender essential oil due to its properties: anti-acne, antibacterial, calming, anti-inflammatory, treatment of eczema and dermatitis. The introduction of the concept of aromatherapy for textiles has brought increasing demands for consumers in terms of quality, comfort and functionality of textile products. There was a shift in their values.

Aroma finish is a process by which the textile materials are treated with bioactive systems (e.g., chitosan/essential oil, alginate/essential oil systems) and finally get the multifunctional properties such as therapeutic effects and a feeling of well-being and freshness in the wearer.

Aromatherapy textiles are used in medicine and alternative healing, home textiles, body-care textiles, household cleaning and cosmetic products.

The aromatherapy materials that first appeared on the market were socks for women who like fragrances. Hosiery and intimate apparel have been the more widely explored product categories to apply aroma finishing. In recent years, a number of companies around the world turned their attention to aromatherapy textiles. Woolmark™ is applying aroma technology to hosiery, lingerie, socks, outdoor clothing, underwear, carpeting and other interior textiles.

The Benefits of Aromatherapy

- It's fast;
- It's efficient;
- It's discreet;
- Makes long-term transformations;
- It's nice;
- It's the fastest way to raise your personal vibration;
- Helps a lot of healing processes;
- Increases the power of medication assimilation;
- Maintains a reference standard in thinking, feelings and human experiences;
- It gives great chances to special cases, prevents various aspects of bacterial and fungal diseases;
- It's a system for treating the environment in which people work;
- Creates a pathogen-damaging environment (viruses, bacteria etc.).

CONCLUSIONS

The complex studies carried out in this new field have revealed that bioactive compounds (essential oils) have more than a therapeutic but also ecological, social effect, contributing to the increase in the value of the products and their quality.

The techniques proposed in the project are ecological, with no environmental consequences. Ecological, biodegradable and biocompatible products will be used in the project to obtain aroma therapeutic and skin/body care textile products. The environmental impact is as low as possible, contributing to life and health quality.

REFERENCES

Abraham, M.H. *et al*. (2013), "Determination of solvation descriptors for terpene hydrocarbons from chromatographic measurements", *Journal of Chromatography A.*, 1293, 133-141, https://doi.org/10.1016/j.chroma.2013.03.068.

Cerempei, A. (2017), "Aromatherapeutic Textiles", *Active Ingredients from Aromatic and Medicinal Plants*, Hany El-Shemy, IntechOpen, https://doi.org/10.5772/66510.

AL-Jabri, N.N. and Hossain, M.A. (2018), "Chemical composition and antimicrobial potency of locally grown lemon essential oil against selected bacterial strains", *Journal of King Saud University – Science*, 30(1), 14-20, https://doi.org/10.1016/j.jksus.2016.08.008.

Balabai, I.V. (1988), *Rasteniea, coterie nas leceat*, I.V. Balabai, A.C. Nistrean, Chisinau, 351.

Bouchekrit, M. *et al*. (2016), "Essential oils from Elaeoselinum asclepium: chemical composition, antimicrobial and antioxidant properties", *Asian Pacific Journal of Tropical Biomedicine*, 6(10), 851-857, https://doi.org/10.1016/j.apjtb.2016. 07.014.

Boulekbache-Makhlouf, L. *et al*. (2016), "Essential oils composition, antibacterial and antioxidant activities of hydrodistillated extract of Eucalyptus globulus fruits Z. Bey - Ould Si Saida, H. Haddadi – Guemghar", *Industrial Crops and Products,* 89, 167-175.

Duhamel, N. *et al*. (2016), "Convenient synthesis of deuterium labelled sesquiterpenes", *Tetrahedron Letters*, 57(40), 4496-4499.

El Asbahani, A. *et al*. (2015), "Essential oils: from extraction to encapsulation", *International Journal of Pharmaceutics,* 483, 220-243, https://doi.org/10.1016/j.ijpharm.2014.12.069.

Ghosha, S. and Chipot, N. (2015), "Embedding aromatherapy essential oils into textile fabric using β-cyclodextrin inclusion compound", *Indian Journal of Fibre & Textile Research*, 40, 140-143.

González-Rivera, J. *et al*. (2016), "Coaxial microwave assisted hydro-distillation of essential oils from five different herbs (lavender, rosemary, sage, fennel seeds and clove buds): chemical composition and thermal analysis", *Innovative Food Science & Emerging Technologies*, 33, 308-318.

Hu, J. *et al*. (2001), "Properties of aroma sustained-release cotton fabric with rose fragrance nanocapsule", *Chinese Journal of Chemical Engineering*, 19(3), 523-528.

Jamali, C.A. *et al*. (2013), "Phenological changes to the chemical composition and biological activity of the essential oil from Moroccan endemic thyme (Thymus maroccanus Ball)", *Industrial Crops and Products*, 49, 366-372, https://doi.org/10.1016/j.indcrop.2013.05.016.

Kandori, I. (2002), "Diverse visitors with various pollinator importance and temporal change in important pollinators of Geranium thunbergii (Geraniaceae)", *Ecological Research*., 17, 283-294, https://doi.org/10.1046/j.1440-1703.2002.00488.x.

Kumar, A. *et al*. (2010), "Chemical composition, antifungal and antiaflatoxigenic activities of Ocimum sanctum L. essential oil and its safety assessment as plant based antimicrobial", *Food and Chemical Toxicology*, 48(2), 539-543.

Leimann, F.V. *et al*. (2009), "Antimicrobial activity of microencapsulated lemongrass essential oil and the effect of experimental parameters on microcapsules size and morphology", *Materials Science and Engineering: C*., 29(2), 430-436.

Radulovic, N. *et al*. (2011), "Chemical composition and antimicrobial activity of the essential oils of Geranium columbinum L. and G. lucidum L. (Geraniaceae)", *Turkish Journal of Chemistry*, 35, 499-512.

Rachwalik, R. *et al*. (2012), "Transformations of monoterpene hydrocarbons on ferrierite type zeolites", *Applied Catalysis A: General,* 427–428, 98-105, https://doi.org/10.1016/j.apcata.2012.03.037.

Skalicka-Woz´niak, K. and Walasek, M. (2014), "Preparative separation of menthol and pulegone from peppermint oil (Mentha piperita L.) by high-performance counter-current chromatography", *Phytochemistry Letters*, 10, XCIV-XCVIII.

Timung, R. *et al*. (2016), "Composition and anti-bacterial activity analysis of citronella oil obtained by hydro-distillation: process optimization study", *Industrial Crops and Products*, 94, 178-188.

West, A.J. and Annett-Hitchcock, K.E. (2014), "A critical review of aroma therapeutic application for textiles", *Journal of Textile and Apparel, Technology and Management,* 9(1), 1-13.

Zarrad, K. *et al*. (2015), "Chemical composition, fumigant and anti-acetylcholinesterase activity of the Tunisian Citrus aurantium L. essential oils", *Industrial Crops and Products*, 76, 121-127, https://doi.org/10.1016/j.indcrop.2015.06.039.

IDENTIFYING THE OPTIMUM METHOD FOR MODIFYING THE ZINC OXIDE SURFACE IN ORDER TO OBTAIN A HIGH DEPOSIT DEGREE OF THE FUNCTIONING AGENT

MARIA SÖNMEZ[1], DENISA FICAI[2], ANTON FICAI[2], OVIDIU OPREA[2], IOANA LAVINIA ARDELEAN[2], ROXANA TRUŞCĂ[2], LAURENŢIA ALEXANDRESCU[1], MIHAELA NIŢUICĂ[1], MARIA DANIELA STELESCU[1], MIHAI GEORGESCU[1], DANA GURĂU[1]

[1]INCDTP–Division: Leather and Footwear Research Institute, 93 Ion Minulescu St., Bucharest, Romania, maria.sonmez@icpi.ro

[2]Politehnica University of Bucharest, Faculty of Applied Chemistry and Material Science, 1-7 Polizu St., Bucharest, Romania

The aim of this study is to identify the optimal method of surface modification of ZnO nanoparticles in order to obtain a high deposition rate of the polydimethylsiloxane (PDMS) functionalizing agent. Thus, in order to identify the optimal route, the surface of ZnO nanoparticles were functionalized by 3 methods, ultrasonic, magnetic stirring and vacuum adsorption, followed by advanced powder characterization, FTIR, SEM, EDS, DSC-TG. The FTIR analysis recorded on the surface modified ZnO powder highlights the functional groups in the PDMS, regardless of the synthesis method, which confirms that the functionalization took place. However, based on the intensity of PDMS functional groups, it can be concluded that the highest deposition rate is obtained in the case of ultrasonography, followed by the magnetic stirring and vacuum adsorption method. This different deposition rate can be attributed to the fact that ultrasonication leads to ZnO particles being broken down into smaller particles, resulting in a higher contact surface with PDMS. The SEM image obtained on the commercial ZnO powder and the ZnO / PDMS powder, highlights their extremely varied morphology and demonstrates that the modification does not influence either the shape or size of the ZnO. EDS analysis confirms that functionalization took place due to the presence of the Si element alongside the other Zn and O major elements. The DSC-TG analysis obtained on the ZnO / PDMS powder indicated an organic mass loss, from the organosilane structure, of 5.51% in the range of 365-530°C. The results obtained provide the premise that these functionalized ZnO nanoparticles in addition to antibacterial properties will improve compatibility / dispersibility in various polymeric matrices.

Keywords: functionalization methods, zinc oxide, polydimethylsiloxane.

INTRODUCTION

Infectious diseases caused by a high number of bacteria pose a serious threat to human health. One of the major bacteria that causes 1.5 million deaths annually due to food and beverage contamination is *Sigella flexneri* (Kotloff *et al*., 1999). Other bacterial strains, which frequently infest food and slop a high number of illnesses, has *Escherichia coli*, *Campylobacter jejuni*, *Staphylococcus aureus*, *Pseudomonas aeruginosa*, *Enterococcus faecalis*, *Salmonella types*, and *Clostridium perfringens*, (Sirelkhatim *et al*., 2015; Stegarus *et al*., 2017). To deactivate or kill these bacterium, numerous metallic salts, nanoscale metals and metallic oxides have been tested as promising inorganic antimicrobials. Metal oxides are used in many applications, Catalysis, sensors, medicine, varistors, rubber and plastics, cosmetics, personal care products, etc. (Oprea *et al*., 2014). The most frequent metal oxides, use as anti-bacterial agents, in various products, are TiO_2, CuO, ZnO, MgO, etc. (Mahmoodi *et al*., 2018). Of these, ZnO is considered the most promising safe and anti bacterial agent (Zhao *et al*., 2018). In addition to the bacterial properties, ZnO is frequently used as an agent of inorganic reinforcement in various polymers, with a view to improving the thermal properties, mechanical and chemical (Simões *et al*., 2017; Cetin *et al*., 2018). ZnO is

often used in various polymeric films, for the manufacture of the active antimicrobial packaging (Naveed ul Haq *et al*., 2017). The most common polymers / mixtures of polymers in which ZnO is used, in order to obtain thin films are, PET- poly(ethylene terephthalate) / PBS-poly(butylene succinate), co-polymer (Threepopnatkul *et al*., 2014), - PET/PEG - poly(ethylene glycol) (Ji *et al*., 2015), polyurethane - PU (Chen *et al*., 2013), cases - PP (Hadi *et al*., 2016), etc. The main problem in obtaining homogeneous composite materials is very difficult because ZnO possesses a large surface area and a surface energy increases, leading to an agglomeration in the matrix of copolymers / polymers, altering the physico-mechanical properties. In order to reduce the agglomeration of ZnO in the polymeric matrix, it is necessary to modify its surface. The most used coupling agents are: oleic acid (Aysa *et al*., 2017), stearic acid (Ji *et al*., 2015), 3-aminopropyltrimethoxysilane - APTS, 3 - thiolpropyltrimethoxysilane - TPTS, (El-Nahhal *et a*l., 2016; Lu *et al*., 2018), etc.

MATERIALS AND METODS

Materials

The materials used in this study were the following: zinc oxide nanopowder, <100nm particle size, molecular weight - 81.39, assay ~ 80% Zn basis, surface area - 15-25 m^2/g; 2-propanol (isopropanol), grade - anhydrous, assay - 99.5%, molecular weight - 60.10, vapor density – 2.1 (vs air), vapor pressure – 33 mmHg (20°C) and 44 mmHg (25°C); poly (dimethylsiloxane) (PDMS), grade - analytical standard, vapor pressure - 153 mmHg (20°C), density - 0.82 g/mL, molecular weight - 236.53 wt.%.

Method

Surface modification of ZnO particles with PDMS was performed by three methods:

Method a - consists in the modification of the ZnO surface with PDMS by ultrasonography, using 1 g of the commercial ZnO powder, over which has been added, 10 ml of isopropanol (with the role of reaction /scattering medium). Mixture containing ZnO and isopropanol has been inserted into the plastic tubes with a volume of 50 mL and immersed in the ultrasonic bath, previously heated to 40°C. After 5 minutes of mixing ZnO with isopropanol, using an automatic syringe, 1 mL of PDMS were added, and allowed to mix/react for 2h. After 2 h, the centrifuge tubes were removed from the ultrasonic bath, left at room temperature, approximately 10-15 minutes, filtered and washed with isopropanol in abundance to remove unreacted PDMS followed by drying in a hot air oven at 80°C for 4-6 hours followed by milling and morpho-structural characterization (SEM, EDAX, DSC-TG, FTIR).

Method b - is similar to that described above, with the mention that in this case the surface modification of ZnO with PDMS has been achieved by the magnetic stirring, with the possibility of adjusting the temperature (40°C) and the rotational speed (300 rpm).

Method c - in this case the nanoparticles surface modification has been achieved by the adsorption method under vacuum, using a special container glass, equipped with a special connection for the vacuum pump and a glass funnel with plastic lid, where the isopropyl alcohol and PDMS solution is injected. In this container, over 1 gram of ZnO powder, a solution consisting of 5 mL of isopropyl alcohol and 1 mL PDMS introduced under vacuum, using a syringe was added. After adsorption, container has been placed

in a thermostated bath at 40°C for 2 h. The following stages are identical to those described above.

RESULTS AND DISCUSSION

FTIR Spectrometry

FTIR spectrometry was used for the purpose of investigating the bonds which are formed between the molecules of PDMS and the ZnO powder surface. In theFigure 1 are shown the spectra recorded on the commercial ZnO powder and those of ZnO powder functionalized with PDMS, by the 3 methods described. The IR spectra obtained on the ZnO powder modified with PDMS, through all 3 methods, they highlight the bands characteristic to functional groups of organosilane, namely the bandwith from the 2904 cm^{-1} is assigned to groups CH3, band from 1089-1015 cm^{-1} are assigned to stretching groups of Si-O-Si and those of approx. 1259 cm^{-1} are characteristic to - CH3 deformation groups, from Si-CH3 bond. The band at 796 cm^{-1} is characteristic to stretching bond Si-C- originating from Si-CH3. The ZnO band can be observed at approx. 436 cm^{-1}. As it can be seen, the method of using ultrasonic bath, seems to be optimum, because a higher deposition rate of PDMS on the surface of ZnO is obtained compared to the use of the magnetic stirring method and the one under vacuum adsorption. This can be confirmed by the much higher bandwidth intensities of the bending CH3 groups originating from Si-CH3 bond, Si-O-Si groups (1089-1015 cm^{-1}) and the stretch Si-C bonds from CH3 (791cm^{-1}) in the case of ZnO/PDMS powders modified by ultrasonography compared with the use of other methods. A possible explanation for depositing a more thick layer of PDMS could be attributed to the fact that ultrasonography would facilitate the breakage of ZnO particles into smaller particles, which would lead to an increase in the specific surface area, and implicitly to a higher net deposition rate PDMS.
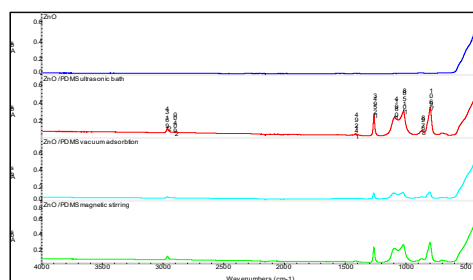
Figure 1. The FTIR spectra of ZnO powders functionalized with PDMS, by the 3 methods

Scanning Electron Microscopy (SEM)

The Scan electronic microscopy (SEM) images have been recorded both on the simple powder of ZnO and modified with PDMS. As you can see inFigure 2 image A, recorded on the un treated powder of ZnO, to a 50000x magnification, particle size varies in the range 63.81 - 279 nm, with particles shapes extremely varied: acicular, in the form of canes, rectangular, etc, and very well defined (monodisperse without

agglomeration). In the case of ZnO / PDMS powder (image B), it is noted that the presence of organo-silane do not affect significantly, the shape and size of the particles. More than that, sharp contours between the particles of ZnO are observed.
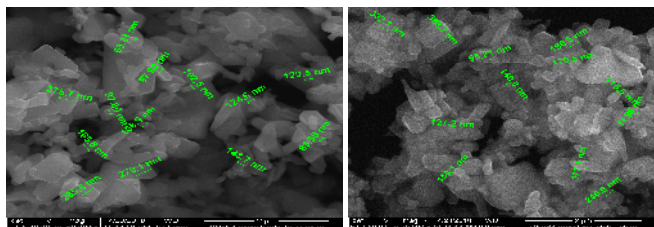
Figure 2. SEM image of commercial ZnO (left) and ZnO /PDMS powder obtained by ultrasonography (right)

Energy Dispersive Spectroscopy (EDS) Analysis

EDS analysis is an effective method of identifying the constituent elements and their relative proportions (atomic, weight), present in a sample. As shown inFigure 3, in the case of the spectrum recorded on the pure ZnO powder, the following elements could be identified, Zn and O. Peak corresponding to the Zn, appears in the spectrum at different intensities, which shows that he represents the main component which can be found in the sample. Other items in addition to Zn and O could not have been identified, which show that the ZnO powder used, is of high purity. Quantitative analysis of ZnO powder is shown inTable 1, and shows as the percentage, the weight and nuclear content of the 2 types of components.
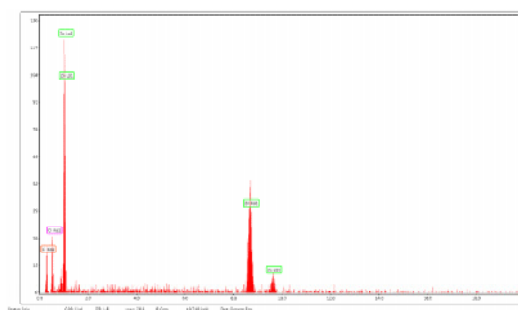
Figure 3. The EDS spectrum of the commercial ZnO powder

Table 1. Quantitative analysis of commercial ZnO powder

Element	Weight, %	Atomic, %
O K	28.23	61.65
Zn K	71.77	38.35

The spectrum shown inFigure 4, obtained on the ZnO/PDMS powder by ultrasonography, indicates the presence of the following components, Zn, Si, and O. It should be noted that the relative strength between peaks varies significantly, and is the

most intense for Zn. The presence of an extra peak namely Si, confirm once again the results obtained by FTIR, DSC-TG and demonstrates that ZnO surface functionalization was conducted successfully. The percentage and atomic weight between the three elements (O: Si: Zn) is shown inTable 2.
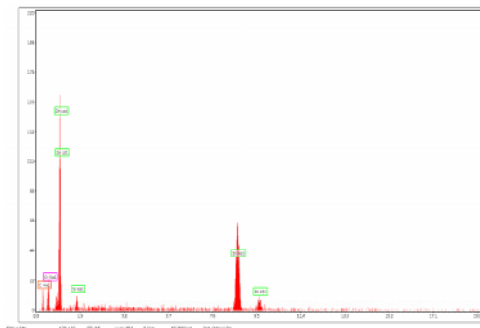
Figure 4. The EDS spectrum of the ZnO/PDMS powder, ultrasonic

Table 2. Quantitative analysis of ZnO/PDMS powder, ultrasonic

Element	Weight, %	Atomic, %
O K	22.82	52.64
Si K	5.04	6.62
Zn K	72.15	40.74

Complex Thermal Analyses

Thermal analysis recorded on the ZnO/PDMS powder,Figure 5, shows a good stability up to 365°C (losing only 0.35 percent of the mass). There is a single-stage of decomposition, in accordance with the TG curve in the range 365-530°C, with the onset to 395.7°C, when there is a loss of mass of 5.51% accompanied by a slightly exothermic effect, with maximum at 411°C. The residual mass is 93.96%.
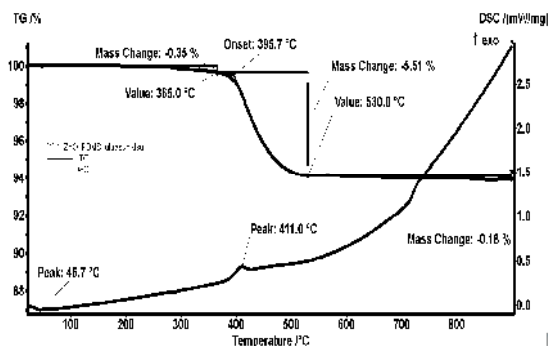
Figure 5. Thermal analysis of ZnO/PDMS powder

CONCLUSIONS

The morpho-structural and thermal analyzes obtained on the ZnO powder modified with PDMS, demonstrates that depending on your chosen route may get different deposition degrees of organo-silane. The results obtained provide the premise that these nanoparticles of functionalized ZnO, in addition to the bacterial properties will improve the compatibility / dispersability in various polymeric matrix (PET, PVC etc.).

REFERENCES

Aysa, N.H. *et al*. (2017), "Preparation and surface modification of zinc oxide nanoparticles", *Journal of Babylon University/Pure and Applied Sciences*, 25, 497-503.

Cetin, G. *et al*. (2018), "A novel antibacterial nanofibers mat made of co-axial electrospun polycaprolactone/silver nitrate/ zinc oxide composites", *Advanced Nano-Bio-Materials and Devices*, 2, 275-86.

Chen, H. *et al*. (2013), "Dispersivity of modified ZnO and characterization of polyurethane/ZnO composites", *Polymer Composites*, 35, 237-44, https://doi.org/10.1002/pc.22655.

El-Nahhal, I.M. *et al*. (2016), "Synthesis & characterization of silica coated and functionalized silica coated zinc oxide nanomaterials", *Powder Technology*, 287, 439-46, https://doi.org/10.1016/j.powtec.2015.09.042.

Hadi, N.J. *et al*. (2016), "Rheological behavior of waste polypropylene reinforced with zinc oxide nanoparticles", *WIT Transactions on Engineering Sciences*, 105, 201-11, https://doi.org/10.2495/AFM160171.

Ji, P. *et al*. (2015), "Influence of surface modification of zinc oxide nanoparticles on thermal behavior and hydrophilic property of PET–PEG composites", *Polymer Composites*, 37, 1-9.

Kotloff, K. *et al*. (1999), "Global burden of Shigella infections: implications for vaccine development and implementation of control strategies", *Bull World Health Organ*, 77, 651-66.

Lu, P.J. *et al*. (2018), "Methodology for sample preparation and size measurement of commercial ZnO nanoparticles", *Journal of Food and Drug Analysis*, 26, 1-9, https://doi.org/10.1016/j.jfda.2017.07.004.

Mahmoodi, S. *et al*. (2018), "Copper nanoparticles as antibacterial agents", *J Mol Pharm Org Process Res*, 6, 1-7.

Naveed Ul Haq, A. *et al*. (2017), "Synthesis approaches of zinc oxide nanoparticles: the dilemma of ecotoxicity", *Journal of Nanomaterials*, 1-14, https://doi.org/10.1155/2017/8510342.

Oprea, O. *et al*. (2014), "ZnO Applications and Challenges", *Current Organic Chemistry*, 18, 1-12, https://doi.org/10.2174/13852728113176660143.

Simões, D.N. *et al*. (2017), "Thermoplastic elastomers containing zinc oxide as antimicrobial additive under thermal accelerated ageing", *Materials Research*, 20, 325-30, https://doi.org/10.1590/1980-5373-mr-2016-0790.

Sirelkhatim, A. *et al*. (2015), "Review on zinc oxide nanoparticles: Antibacterial activity and toxicity mechanism", *Nano-Micro Lett*, 7, 219-42, https://doi.org/10.1007/s40820-015-0040-x.

Stegarus, D.I. and Lengyel, E. (2017), "The antimicrobial effect of essential oil upon certain nosocomial bacteria", *International Multidisciplinary Scientific GeoConference Surveying Geology and Mining Ecology Management, SGEM*, 17(61), 1089-1096, https://doi.org/10.5593/sgem2017/61/S25.142.

Threepopnatkul, P. *et al*. (2014), "Effect of TiO2 and ZnO on thin film properties of PET/PBS blend for food packaging applications", *Energy Procedia*, 56, 102-11, https://doi.org/10.1016/j.egypro.2014.07.137.

Zhao, S.W. *et al*. (2018), "The preparation and antibacterial activity of cellulose/ZnO composite: a review", *Open Chem*, 16, 9-20, https://doi.org/10.1515/chem-2018-0006.

POLYMERIC COMPOSITES BASED ON PLASTIFIED PVC AND ZINC OXIDE NANOPARTICLES

MARIA DANIELA STELESCU, LAURENŢIA ALEXANDRESCU, MARIA SÖNMEZ, MIHAI GEORGESCU, MIHAELA NIŢUICĂ, DANA GURĂU

INCDTP - Division: Leather and Footwear Research Institute, 93, Ion Minulescu St., 031215, Bucharest, Romania

The paper presents the obtaining method and characterization of polymeric composites based on polyvinyl chloride plasticized with 60% dipropylheptylphthalate for medical and food applications. In order to obtain materials with antibacterial and antifungal properties, specific to the mentioned domain, zinc oxide nanoparticles, functionalized with polydimethylsiloxane by ultrasonography, were used. The influence of 1, 3, and 7 parts of functionalized zinc oxide nanoparticles added to 100 parts of polymer, on the physical-mechanical properties, the melt flow index, the abrasion resistance and the structure, was investigated. The polymeric composites were processed on a Plasti-Corder Brabender 350 E mixer at 165-180°C and 150-180 revolutions per minute. The obtained show that adding zinc oxide nanoparticles into the composition led to an increase of hardness, max. 4°ShA, an improvement in tear resistance, elongation at break and resistance to tearing. Abrasion resistance has good values below 300 mm3. The melt flow index is over 62 g/10 min at 165°C with a 5 Kg pressure, showing very good processing by the injection method of the new polymeric composites. The FTIR spectra of the samples indicate that the new composites have a stable structure, due to a very good compatibility / interaction with the polymer matrix, the plasticizer does not tend to migrate to the surface although a large amount of plasticizer (60%) is used.

Keywords: polyvinyl chloride, nanofiller, zinc oxide.

INTRODUCTION

Poly (vinyl chloride) (PVC) is a versatile polymer, used in flexible, semirigid, and rigid forms. In worldwide plastic production, it is second only to polyolefin. The rapid expansion and consumption of PVC is due to lower cost, greater availability, good mechanical properties, and diversity of its properties (Titow, 1984; Braun and Bezdadea, 1986; Stelescu, 2013). It is the most used polymer in the manufacture of medical devices such as: blood bags and tubes, containers and intravenous components, dialysis equipment, inhalation masks and examination gloves, etc (Chiellini *et al*., 2013).

The paper present the obtaining process and characterization of polymeric composites based on plasticized PVC for medical and food applications. In order to obtain composites with antibacterial and antifungal properties, specific for the medical/food domain, zinc oxide nanoparticles (ZnO) (Bazant *et al*., 2014; Alexandrescu *et al*., 2017) were used. The antibacterial activity of ZnO nanoparticles has been proven on various bacterial strains (Stegarus *et al.,* 2017). They even have antibacterial activity against spores resistant to high temperatures and high pressure (Elashmawi *et al*., 2010; Arya *et al*., 2016; Mallakpour and Darvishzadeh, 2018). To improve dispersion in the polymeric matrix of ZnO nanoparticles, they were functionalized (Mallakpour and Darvishzadeh, 2018; Chung *et al*., 2016; Mallakpour and Darvishzadeh, 2018).

EXPERIMENTAL

Materials

Materials used to obtain the polymer composites based on plasticized polyvinyl chloride and ZnO nanoparticles are as follows: (1) PVC with a 70K-wert value, (2) Dipropylheptylphthalate (DPHF) (density 0.984 g/cm3, pH 7, 99.5% purity), non-toxic plasticizer, mainly used by the pharmaceutical, food and cosmetics industries, (3) PVC stabilizer - Calcium stearate (Ca content 11%, melting point 127°C), (4) Antioxidant Irganox 1010 (pentaerythritol tetrakis (3-(3,5 di-tert-butyl-4-hydroxyphenyl)propionate) was produced by BASF Schweiz AG (active ingredient 98%, melting point of 40°C). (5) Functionalizing agent – polydimethylsiloxane -PDMS. (6) ZnO nanoparticles.

Polymer Composites Preparation

The obtaining of polymeric nanocomposites based on PVC matrix with ZnO functionalized nanoparticles was accomplished in several stages, as follow: functioning of nanoparticles, PVC plasticizing, obtaining, and test polymeric composites.

Functioning of ZnO nanoparticles was performed by ultrasonography with the functionalizing agent - polydimethylsiloxane (PDMS).

PVC plasticizing was achieved by absorption of plasticizer (DPHF) into PVC by mixing them in a plasticorder PLV 330 Brabender at 70 rpm, temperature 40°C for 10min. For a good thermal stability, temperature stabilizer and antioxidants were added.

Preparing the polymer composites based on plasticized PVC and functionalized ZnO nanoparticles on a Plasti-Corder Brabender Mixer 350 E, with the following features: 3 heating/cooling zones, range temperature 0-300°C, capacity 350 cm³, mixing speed 300 RPM max. Table 1 presents the formulations of plasticized PVC/ZnO composites. Processing technology: the temperature is set to 178°C, plasticized PVC containing stabilizer and antioxidant is added; after soaking and plasticizing (3 min.) the functionalized nanoparticles are added for 2 minutes. Continue mixing at a 150-180 revolutions per minute and temperature of 165°C for 3 minutes until the ingredients is embedded, and the mixture is homogeneous. This operation was registered by the Plasti-Corder Brabender Mixer 350E recording system. The Brabender mixing charts (Figure 1) show that the maximum momentum occurs at 120-180s and the maximum mixing forces are small (18-20N/mm). Temperatures at the maximum momentum did not exceed the temperature of 178°C. This is due to the fact that a large amount of plasticizer (60%) has been used and mixing is slow (150-180 revolutions / minute).

Table 1. Formulations of the polymer composites

Ingredients	Samples Codes			
	C0	C1	C3	C7
PVC – K 70 (g)	100	100	100	100
ZnO/PDMS (g)	-	1	3	7
Dipropylheptylphthalate (g)	150	150	150	150
Calcium stearate (g)	2.5	2.5	2.5	2.5
Irganox 1010 (g)	2.5	2.5	2.5	2.5

The plates for physico-mechanical and structural characterization were obtained in an electrical laboratory press, by means of compression method, at a temperature of

175°C, preheating for 2 min (without pressing), 5 min modeling and 5 min cooling, both at a force of pressing of 300 kN. Specimens of l50mm x 150mm x 2mm and 70mm x 70mm x 6mm were obtained, and were conditioned for 24 hours at room temperature before being characterized.
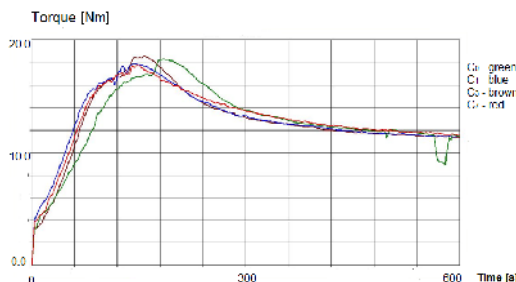
Figure 1. Overlapped Brabender mixing charts: the control sample and polymer composites

Specimen Characterization

Physical-Mechanical Characteristics. Tensile strength and tearing strength tests were carried out with a Schopper strength tester with testing speed 460 mm/min, using dumb-bell shaped specimens according to ISO 37/2012, and angular test pieces (Type II) according to EN 12771/2003, respectively. Hardness was measured by using a hardness tester according to ISO 7619-1/2011 using 6-mm thick samples. Elasticity (rebound resilience) was evaluated with a Schob test machine using 6-mm thick samples, according to ISO 4662/2009.

The densities of elastomer samples were measured according to ISO 2781/2010.

Abrasion resistance was carried out according to ISO 4649/2010, the cylinder method, using a pressure of 10N. Abrasion resistance was expressed by relative volume loss in relation to calibrated abrasive paper. A wearing tester with abrasive cloth having granulation of 212–80 mm (PE 80). The samples used were obtained from rolled blends and pressed into sheets, then cutting with a rotating die and have cylindrical shape, with a diameter of 16mm and height of min. 6 mm.

Melt flow index was determinate at 180°C and a pressure force of 5 kg, with Melt Flow Index – Haake equipment.

Fourier transformed infrared spectroscopy (FT-IR). The structural determinations were carried out on an IR molecular absorption spectrometer with double beam, in the range of 4000-530 cm^{-1}, using a 4200 FT-IR equipped with ATR crystal diamond and sapphire head.

RESULTS AND DISCUSSIONS

Physico-Mechanical and Rheological Characteristics

Table 2 shows the physico-mechanical and rheological characteristics of the polymeric composites obtained. The analysis of the results shows the following:
- The *hardness* of the control sample is 47°Sh A, and increases with a few units up to 51°Sh A with the addition of nanoparticles, due to the nanofiller reinforcement effect;

- High elasticity values are observed for this degree of plasticization, (8-10%) a performant feature of these materials;
- *The tensile strength* is in the range of 3.7-5.8 N/mm^2 and increases with the amount of nanofiller introduced into the compound;
- *Tear resistance* shows high values (24-26.5 N/mm), which indicate a performant material;
- *The elongation at break* shows high values, increasing from 300% up to 500% when adding 7% ZnO, this property increase proportionally to the amount of nanoparticles introduced into the composite.
- *Density* is low, of 1.1 g/cm^3 and the values for a*brasion resistance* are very good, under 300 mm^3.
- The values for *melt flow* are higher due to the degree of plasticizer (60%) are between: 91 (control sample) and 62.3g/10 min. (165°C, 5 Kg force), indicating a very good processing by the injection method of the new polymeric composites. Values decrease when adding ZnO nanofiller as a result of reinforcement of the mixture.

Table 2. Physical and mechanical characteristics for polymeric composites

Phyisico-mechanical characteristics	Samples Codes			
	C0	C1	C3	C7
Hardness, °Sh A	47	51	51	51
Elasticity, %	8	10	10	10
Tensile strength, N /mm^2	3.7	5.0	5.3	5.8
Elongation at break, %	300	460	460	500
Tear resistance, N /mm	24	26.5	24	26.5
Density, g/cm^3	1.1	1.1	1.1	1.1
Abrasion resistance, mm^3	195	197	297	231
Melt flow index(165°C and 5 Kg force) g/10min	91.0	88.7	87.4	62.3

Fourier Transform Infrared Spectroscopy (FT-IR)

The FTIR spectrum recorded on the clean PVC powder (Figure 2) shows numerous characteristic bands associated with this type of polymer.

Figure 3 show FTIR spectra of polymeric composites based on PVC plasticized with DPHF containing ZnO nanoparticles functionalized with PDMS. For all composites, the presence of PVC characteristic groups can be observed. The appearance of additional bands (relative to the pure PVC spectrum) at approximately 1724 and 1121 cm^{-1} is attributed to carbonyl (C = O) stretching vibration from the plasticizer structure - DPHF and confirms that plasticization of PVC has been successfully completed. The presence of the benzene ring in the DPHF at approximately 1429 cm^{-1} could not be detected, in the obtained composites, since it overlaps the characteristic groups of PVC. However, at 739 cm^{-1} (associated with the bending vibration, outside the plane), the presence of a benzene nucleus in the plasticizer can be emphasized, but at a much lower intensity. The presence of ZnO / PDMS nanoparticles could not be identified in the spectrum, because characteristic bands occur at approx. 526 cm^{-1} which overlap also over the functional groups from the plasticizer structure. However, there is a significant increase in the intensity of the methylene groups at approximately 2923 and 2857 cm^{-1} in the case of composites containing varying percentages of ZnO / PDMS (1, 3, and 7% respectively) relative to the control mixture, containing only plasticizer, due to the introduction of additional methylene groups derived from PDMS. The intensity of these

bands is the higher when increasing the amount of ZnO / PDMS introduced into the blend.
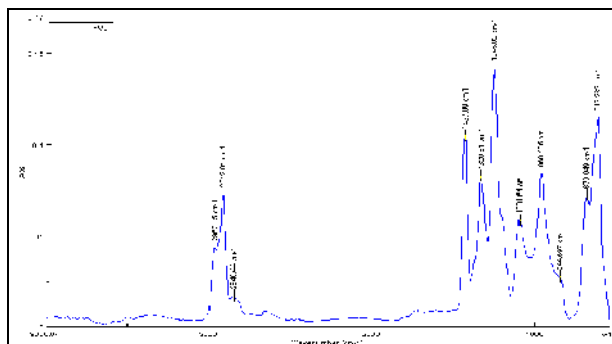
Figure 2. FTIR spectrum of PVC powder
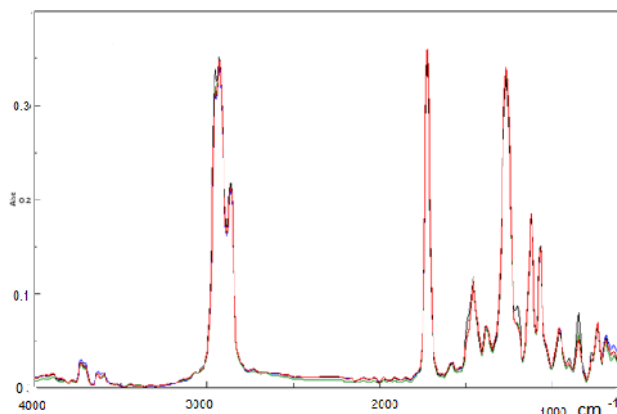
Figure 3. FTIR spectra of composites based on plasticized PVC and ZnO nanoparticles: C0 - green line, C1 - brown line, C3 - red line, C7 - blue line

There is a significant increase in the intensity of carbonyl groups at approximately 1724 cm-1 (Figure 3), which can be attributed to the fact that even at very high concentrations of plasticizer, it remains stable in the PVC structure (does not tend to migrate to the surface) due to a very good compatibility / interaction with the polymer matrix.

CONCLUSIONS

New types of polymeric composites based on polyvinyl chloride plasticized with 60% dipropylheptyl phthalate containing zinc oxide nanoparticles functionalized with polydimethylsiloxane were obtained by ultrasonography. These were obtained on a Plasti-Corder Brabender Mixer 350 E at 178°C, 150-180 revolutions per minute and 165°C for 3 minutes, and a total mixing time of 10 minutes. The temperatures at

maximum momentum did not exceed the scheduled temperature of 178°C due to the fact that a large amount of plasticizer (60%) was used and the mixing was slow. With the increase of the functionalized zinc oxide quantity, there was an increase in hardness, tear strength, elongation at break and tear resistance, and a decrease in the melt flow index. The new polymeric composites have a stable structure. The plasticizer does not tend to migrate to the surface, thus they can be easily processed by the injection method. New polymeric composites can be used in biomedical and food applications such as: blood bags and tubes, intravenous components, and containers, dialysis equipment, inhalation masks, examination gloves, packaging, footwear, etc.

REFERENCES

Alexandrescu, L. *et al*. (2017), "Polymer nanocomposites PE/PE-g-MA/EPDM/nanoZnO and TiO2 dynamically crosslinked with sulfur and accelerators", *Proceeding 2nd International Conference on Structural Integrity*, https://doi.org/10.1016/j.prostr.2017.07.040.

Arya, P.K. *et al*. (2017), "Thermo-mechanical performance of PVC/ZnO nanocomposites", *Phase Transitions*, 90, 7, 695-702, https://doi.org/10.1080/01411594.2016. 1263991.

Bazant, P. *et al*. (2014), "Microwawe-Assisted synthesis of Ag/ZnO Hybrid Filler, Preparation, and Characterization of Antibacterial Poly(vinyl chloride) Composires Made from the Same", *Polymer Composites*, 35, 19-26, https://doi.org/10.1002/pc.22629.

Braun, D. and Bezdadea, E. (1986), "Encyclopedia of PVC", L.I. Nass and C.A. Heiberger, Eds., Ch 1, ISBN 9780824774271.

Chiellini, F. *et al*. (2013), "Perspectives On Alternatives To Phthalate Plasticized Poly(Vinyl Chloride) In Medical Devices Applications", *Prog Polym Sci*, 38, 1067-1088, https://doi.org/10.1016/j.progpolymsci.2013.03.001.

Chung, Y.T. *et al*. (2016), "Functionalization of zinc oxide (ZnO) nanoparticles and its effects on polysulfone-ZnO membranes, *Desalination and Water Treatment*, 57, 17, 7801-7811, https://doi.org/10.1080/19443994.2015.1067168.

Elashmawi, I.S. *et al*. (2010), "Structure and performance of ZnO/PVC nanocomposites", *Physica B: Condensed Matter*, 405(19), 4163-4169, https://doi.org/10.1016/j.physb.2010.07.006.

Mallakpour, S. and Darvishzadeh, M. (2018), "Ultrasonic treatment as recent and environmentally friendly route for the synthesis and characterization of polymer nanocomposite having PVA and biosafe BSA modified ZnO nanoparticles", *Polymers for Advanced Technologies*, 29(8), 2174-2183, https://doi.org/10.1002/pat.4325.

Mallakpour, S. and Darvishzadeh, M. (2018), "Nanocomposite materials based on poly(vinyl chloride) and bovine serum albumin modified ZnO through ultrasonic irradiation as a green technique: Optical, thermal, mechanical and morphological properties", *Ultrasonics Sonochemistry*, 41(85-99), https://doi.org/10.1016/j.ultsonch.2017.09.022.

Stegarus, D.I and Lengyel, E. (2017), "The antimicrobial effect of essential oil upon certain nosocomial bacteria", *International Multidisciplinary Scientific GeoConference Surveying Geology and Mining Ecology Management, SGEM,* 17(61), 1089-1096, https://doi.org/10.5593/sgem2017/61/S25.142.

Stelescu, M.D. (2013), "Polymer Composites Based on Plasticized PVC and Vulcanized Nitrile Rubber Waste Powder for Irrigation Pipes", *ISRN Materials Science*, Volume 2013, Article ID 726121, 5 pages, https://doi.org/10.1155/2013/726121.

Titow, W.V. (1984), *PVC Technology*, ch 2, Elsevier Applied Science Publishers, 4th edition, https://doi.org/10.1007/978-94-009-5614-8.

DYNAMIC VULCANIZED THERMOPLASTIC ELASTOMERS BASED ON ETHYLENE-PROPYLENE TERPOLYMER AND POLYETHYLENE

MARIA DANIELA STELESCU[1], LAURENŢIA ALEXANDRESCU[1], MIHAI GEORGESCU [1], NICULINA ZUGA[2], MIHAELA NIŢUICĂ[1]

[1]*INCDTP - Division: Leather and Footwear Research Institute, 93, Ion Minulescu St., 031215, Bucharest, Romania*

[2]*Constantin Cantacuzino National College, Targoviste, Romania*

The paper presents the studies on the obtaining and characterization of new types of dynamically vulcanized thermoplastic elastomers based on ethylene-propylene terpolymer rubber and polyethylene. As a vulcanizing agent, a phenolic resin (0-15 parts per 100 parts rubber) was used in the presence of dehydrated stannous chloride. Mixtures were obtained by the dynamic vulcanization technique in a Plasti-Corder Brabender mixer at 80 rpm and a temperature of 170°C. Analyzing variations of physical-mechanical characteristics depending on the amount of resin introduced into the blends, it was observed that 100% modulus, tensile strength, and tear strength increased to an optimal point after which they tended to decrease. By dynamically crosslinking the elastomer in the thermoplastic polymer melt there was a significant improvement in the resistance to repeated flexures, behavior to permanent deformation at compression, and resistance to the action of toluene. New materials can be used in various fields such as: the footwear industry (soles, heels and plates), protection equipment, obtaining gaskets, hoses, technical rubber products for cars, etc.

Keywords: dynamic vulcanized thermoplastic elastomers, EPDM, physical-mechanical characteristics

INTRODUCTION

The thermoplastic elastomers (TPE) is a rubbery material with properties and functional performance similar to those of conventional vulcanized rubber at room temperature, yet it can be processed in a molten state as a thermoplastic polymer at elevated temperature (Walker and Rader, 1988; Legge *et al*., 1987; Naskar, 2004). The unique characteristics of TPEs make them very useful and attractive alternatives to conventional elastomers in a variety of applications and markets, such as the automotive industry. Depending on the chemical composition, the main types of thermoplastic elastomers are: styrene butadiene elastomers (SBS), thermoplastic elastomers olefin (TPO), thermoplastic polyurethanes (TPU), thermoplastic vulcanizers (TPV), thermoplastic copolyesters (CPE), ionic thermoplastic elastomers ETI) etc (Mirci, 2005; Stelescu, 2011). The TPVs represent the second largest group of soft thermoplastic elastomers, after styrenic-based block copolymers.The TPVs represent the second largest group of soft thermoplastic elastomers, after styrenic-based block copolymers. Commercial types of dynamic vulcanizates are commonly based on blends of unsaturated ethylene-propylene terpolymer elastomer (EPDM) and polypropylene (Stelescu, 2011; Puydac, 1991). A wide range of TPVs can be obtain, which differ from each other by the types of thermoplastic elastomers and polymers used, the blended elastomer ratio, the vulcanization system used, etc. The vulcanization systems used are selected depending on the type of elastomer used or the desired characteristics of the finished products. Thus, it is possible to use: (1) vulcanization with sulfur and vulcanization accelerators, crosslinking with peroxides in the presence of vulcanizing coagents, crosslinking with phenolic resins, etc. The amount and type of vulcanization agents used significantly influence the physico-mechanical, chemical and rheological properties of the obtained products - TPVs granules or finished products.

In this paper were analyzed new types of dynamic vulcanized thermoplastic elastomers based on ethylene-propylene terpolymer rubber and high density polyethylene in which a phenolic resin in the presence of dehydrated stannous chloride was used as a vulcanizing agent. The influence of the phenolic resin quantity on the physico-mechanical and chemical characteristics of the obtained thermoplastic vulcanizates was analyzed.

MATERIALS AND METHODS

Materials

The following raw materials were used: (1) EPDM Nordel NDR 47130 (ethylene content 67%, 5-ethylidene-2-norbornene (ENB) content 4.9%, crystallinity degree 9%, density 0.97 g/cm^3, Mooney viscosity at 125°C: 130); (2) HDPE Hostalen GC 7260 (density 0.962 g /cm^3, softening temperature Vicat B/50 of 72°C) (3) zinc oxide (97.1 % active ingredient) Werco Metal, Zlatna Romania, (4) phenolic resin Ribetak 75-30 (8,8% methyl and melting point of 85°C) and stannous chloride dehydrate (molecular weight 225.65, 98.6% purity) were used as a crosslinking agent, (5) antioxidant pentaerythritol tetrakis(3-(3,5-di-tert-butyl-4-hydroxyphenyl)propionate Irganox 1010 (melting point of 40°C, 98 % active ingredient).

Method

Thermoplastic vulcanized are obtained by dynamically crosslinking an elastomer into a molten thermoplastic polymer under strong shear forces, when forming micron-sized cross-linked rubber particles finely dispersed in a thermoplastic matrix (Stelescu, 2011). Therefore, in order to obtain the blends is important to use internal mixer that allows efficient mixing of ingredients, due to the shear forces occurring during the rotation of the screws. At the same time, it is necessary to provide a suitable temperature for melting the thermoplastic polymer – the polyethylene.

Blends were obtained by mixing in a 70 cm^3 Plasti-Corder PLV 330, Brabender equipment at 80 rpm, and temperature of 175°C. The mixing sequence involved, first adding the thermoplastic polymer into the mixer. After melting HDPE (3-4 min), EPDM rubber was embedded (3-4 min). When a homogeneous melt was achieved, the antioxidant and zinc oxide were added (1-2 min). Finally, phenolic resin and stannous chloride were added and the mixing process was continued for about 2 min. Blends were homogenized on a laboratory roller mill heated at 155-165°C. Plates required for physical-mechanical tests were obtained by pressing in an electrical press at 170°C, for 5 min and pressure of 150 MPa. After molding, the mix was cooled at room temperature under pressure. The blend formulations containing EPDM and HDPE are presented in Table 1.

Table 1. Formulations of the thermoplastic elastomers

Ingredients	Samples Codes						
	R0	R1	R2	R3	R4	R5	R6
EPDM (g)	60	60	60	60	60	60	60
HDPE (g)	40	40	40	40	40	40	40
ZnO	2	2	2	2	2	2	2
Phenolic resin (g)	0	4	8	12	16	20	24
SnCl2 x 2H2O (g)	0	0.8	1.6	2.4	3.2	4	4.8
Antioxidant (g)	1	1	1	1	1	1	1

Specimen Characterization

Tensile properties were measured by means of a Schopller tester. *Tensile strength* was determined using dumb-bell shaped specimens according to ISO 37/2012. Residual elongation is the elongation of a specimen measured 1 min after rupture in a tensile test. It was calculated using the formula:

$$\text{Residual elongation (\%)} = \frac{L - L_0}{L_0} \times 100$$

(1)

where: L_0 is the initial length between two marks and L is the length between the marks 1 min after the sample broke in a tensile test.

Tear strength was measured according to EN 12771/2003 using angular test pieces (type II).

Hardness, in Shore A, was measured by means of a hardness tester according to ISO 7619-1/2011.

Elasticity was determined with a Schob type test machine (according to ISO 4662/2009).

Test specimens were cut off from plates of 150 x 150 x 2 mm^3 or 50 x 50 x 6 mm^3 by means of an automatic punching die.

Accelerated ageing tests were carried out according to ISO 188/2001 using the hot air circulation oven method. Similar samples to those used for tensile testing and for hardness determination were used. Test duration was of 7 days and temperature of 70±1ºC. The results were compared with those from samples not subjected to ageing.

The densities of samples were measured according to ISO 2781/2010.

Abrasion resistance test was carried out according to ISO 4649/2010, the cylinder method using a pressure of 10 N. Abrasion resistance was expressed by relative volume loss in relation to calibrated abrasive paper. A wearing tester with abrasive cloth and abrasive based on normal electro-corundum on dressed cloth substrate with granulation of 212–80 µm (PE 80), whose abrasiveness must be of 180–220 mg control rubber. The samples used were obtained from rolled blends and pressed by cutting with a rotating die and have cylindrical shape, with a diameter of 16 mm and height of min. 6 mm.

Flexion resistance (Ross Flex) was determined according to SR 7645/1994. Samples were obtained by punching rubber plates and have rectangular shape. The test was performed using a Ross Flex equipment, monitoring crack marks on each sample at intervals of 1h, 2h, 4h, 8h, 24h, 48h, 72h, 96h.

The *permanent deformation in compression test* was carried out according to SR 8664:1970. Samples were obtained by punching rubber plates and have the shape of 6 mm thick discs. Determinations were performed for a compression of 25% at the temperature of 23ºC for 22 h.

Determination of *toluene action* was performed according to ISO 1817/2015. The test pieces of known weight, m_0, were immersed in toluene in diffusion test bottles and kept at room temperature for 22 hours. After immersion the samples were removed from the solvent and the wet surfaces were quickly dried using a tissue paper and re-weighted, m_i.

To calculate the percentage change in mass Δm_{100} the following formula was used (2):

$$\Delta m_{100} = \frac{m_i - m_0}{m_0} x 100$$

(2)

where m_0 is the initial mass of the test piece and m_i is the mass of the test piece after immersion.

To calculate the percentage change in volume ΔV_{100} the following formula was used (3):

$$\Delta V_{100} = \left(\frac{m_i - m_{i,w} + m_{s,w}}{m_0 - m_{0,w} + m_{s,w}} - 1 \right) x100 \qquad (3)$$

where

$m_{0,w}$ is the initial mass of the test piece (plus sinker if used) in water;

$m_{i,w}$ is the mass of the test piece (plus sinker if used) after immersion in water;

$m_{s,w}$ is the mass of the sinker, if used, in water.

RESULTS AND DISCUSSION

Analyzing variations of physical-mechanical characteristics depending on the amount of resin introduced into the blends, the following are noticed: (1) the hardness varies with 2°Sh A and the elasticity with max 28.6% when increasing the amount of resin; (2) the tensile strength and tear strength increase to an optimum point that corresponds to an amount of about 8 parts per 100 parts of rubber (phr) resin incorporated into the blend, after which they tend to drop, (3) values of elongation at break and residual elongation, are lower than those control sample (without resin) due to elastomer cross-linking (Elias, 2008).

Table 2. Characteristics of blends

Characteristics	Samples Codes						
	R_0	R_1	R_2	R_3	R_4	R_5	R_6
Hardness, ºSh A	94	96	95	95	95	95	96
Elasticity, %	28	24	22	22	22	22	20
100 % modulus, N/mm^2	7	10.4	10.2	10.5	11.2	12.3	-
Tensile strength, N/mm^2	7.3	15.7	17.2	16.7	14.8	15.7	14.9
Elongation at break, %	607	273	240	207	200	173	100
Residual elongation, %	303	79	52	46	37	36	33
Tear strength, N/mm	71	107	108	106.5	101	99	100

Blends R_0 and R_2 have been selected. For these, other characteristics were determined in order to define field of application, these were: resistance to accelerated aging, abrasion resistance, permanent compression deformation, behavior at Ross Flex repeated flexing, toluene action testing (see Figure 1 and Table 3).

Figure 1 show both mixtures exhibited very good behavior after accelerated aging. The non-resin (R_0) control mixture showed a decrease in tensile and tears strength. Instead, R_2 showed an increase in tensile and tears strength, probably continuing the cross-linking due to maintaining of high temperature.

Analyzing the characteristics presented in Table 3, we can see the following: (a) the specific weight increases by dynamic crosslinking of the elastomer with phenolic resin, leading to more compact blends with a better macromolecule packaging; (b) abrasion resistance values are very good, which recommends the use of these polymer alloys in a large number of industrial applications; (c) R_2 sample shows a very good resistance to repeated flexions, much better than R0, the control sample (same composition with R_2 but not dynamically crosslinked); (d) the best behavior at permanent deformation at 25% compression was obtained for sample R_2 - 2.2 times better than the control sample R_0; this indicates that the dynamic crosslinking of the elastomer has led to a significant improvement in this feature; (e) the same behavior was observed for toluene resistance,

namely the mass and volume variation after 72 h immersion in toluene was about 2 times lower for the sample R_2 than for the R_0 sample, indicating that the sample in which elastomer has been dynamically crosslinked has a higher resistance to the action of toluene than that in which the elastomer is not reticulated (Stelescu *et al*., 2017).

Based on the results previously presented, determining fields of application was done by including characteristics of obtained thermoplastic elastomers EPDM/HDPE in product standards. Depending on these, the following areas of application were selected: in the footwear industry (soles, heels and plates), protection equipment (boots, etc), obtaining gaskets, hoses, technical rubber products for cars etc.

(a)   Hardness, ºShA   (b) Elasticity, %,   (c) 100 % Modulus, N/mm^2

(d) Tensile strength, /mm^2 (d) Tear strength, N/mm
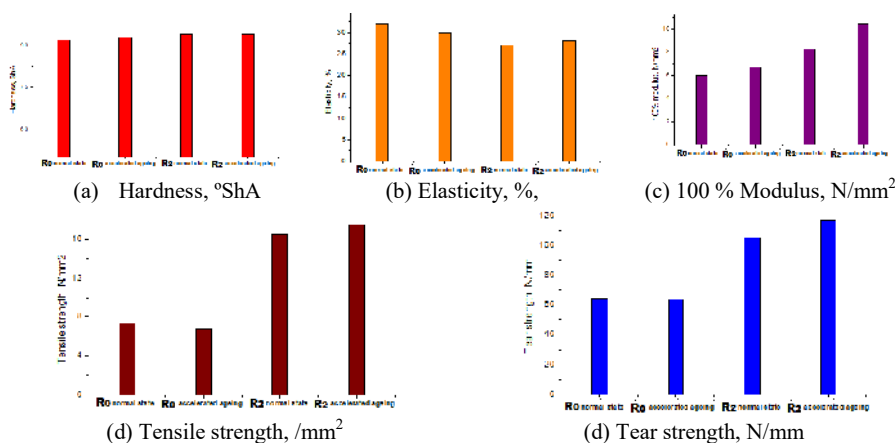
Figure 1. Properties in normal state and properties after accelerated ageing for R_0 and R_2 blends

Table 3. Chemical and physico-mechanical characteristics of the composites

Characteristics	Samples Codes	
	R_0	R_2
Specific weight, g/cm^3	0.97	0.98
Abrasion Resistance, mm^3	80	91
Permanent deformation in compression, 25 %, at 23ºC x 22h, %	24.7%	11.8%
Ross Flex flexions at 23ºC (no. of cycles)	46000	Over 150000
Determination of the toluene action after 72h:		
-mass variation, %	115	57
-volume variation, %	178	86.3

CONCLUSIONS

By dynamic vulcanization of the elastomer, blends of ethylene-propylene terpolymer elastomer and thermoplastic polymers – polyethylene, new elasto-plastic materials with improved properties have been obtained.

The blends had a good behaviour to accelerated ageing, indicating a good lifespan of products made of these materials. This contributes to a large extent to environmental

protection, as it leads to a reduced amount of wastes. Values of resistance to abrasion are very good and allow obtaining products which can be used in extraordinary friction conditions. The specific weight of samples is low, which allows obtaining light products with low material consumption etc.

Due to their performing characteristics, the new materials can be used for the manufacturing of products like as hoses, gaskets, rubber shoes, protective equipment etc.

The potential users of the new elasto-plastic materials will be economic operators processing rubber and plastics, footwear and car component manufactures etc.

REFERENCES

Collection of commented standards - RUBBER, 1994, Romanian Institute for Standardization, Bucharest.

Collection of commented standards - PLASTICS, 1998, Romanian Institute for Standardization, Bucharest.

Elias, H.G. (2008), *Macromolecules*, Vol. 3, Physical Structures and Properties, Publisher: Wiley - VCH Verlay GmbH & Co KGaA, Weinheim, ISBN 9783527311743.

Legge, N.R. *et al*. (Eds.) (1987), *Thermoplastic Elastomers: A Comprehensive Review*, Hanser, Munich, https://doi.org/10.1002/pol.1989.140270710.

Mirci, L.E. (2005), *Thermoplastic Elastomers*, Publisher Ed. Art Press and Ed. Augusta, Timişoara.

Naskar, K. (2004), "Dynamically vulcanized PP/EPDM thermoplastic elastomers Exploring novel routes for crosslinking with peroxides", Ph.D. Thesis, University of Twente, Enschede, The Netherlands, ISBN 90 365 2045 2, Printed by Print Partners Ipskamp, Post Box 33, 7500 AH Enschede, The Netherlands.

Puydak, R.C. *et al*. (1991), "Dynamically vulcanized alloys having two copolymers in the crosslinked phase and a crystalline matrix", U.S. 5,073,597, Original Assignee Advanced Elastomer Systems LP.

Stelescu, M.D. (2011), *High-performance thermoplastic elastomers based on ethylene-propylene terpolymer rubber (EPDM) which can be used in the footwear industry*, Publisher Ed. Performantica, Iasi, ISBN 9789737308092.

Stelescu, M.D. et al. (2017), "Development and Characterization of Polymer Ecocomposites based on Natural Rubber Reinforced with Natural Fibres", *Materials* (Basel), 10(7), 787, https://doi.org/10.3390/ma10070787.

Walker, B.M. and Rader, C.P. (Eds.) (1988), *Handbook of Thermoplastic Elastomers*, Van Nostrand Reinhold Co., New York, Chapter 16, ISBN 978-0-442-29184-6.

THE WASTES OF VINE STEM AND TURKISH RED PINE AS AN ALTERNATIVE BIOSORBENT FOR THE REMOVAL OF LEATHER DYES

GOKHAN ZENGIN[1*], EBRU MAVIOGLU AYAN[2], YUNUS EMRE TEKIN[1], ARIFE CANDAS ADIGUZEL ZENGIN[1], BEHZAT ORAL BITLISLI[1]

[1]*Ege University, Engineering Faculty, Leather Engineering Department, 35100, Bornova Izmir, Turkey, email: candas.adiguzel@ege.edu.tr, 1yunusemretekin@gmail.com, oral.bitlisli@ege.edu.tr, *Corresponding author e-mail: gokhan.zengin@ege.edu.tr*

[2]*Ege University, Science Faculty, Chemistry Department, 35100, Bornova Izmir, Turkey, email: ebru.mavioglu@ege.edu.tr*

The use of high amount water in the industries such as leather, textile and paper causes hazardous wastewater for the environment due to the contents of organic compounds and heavy metals. Discharging high amount of leather dyes such as acid and metal complex to ecosystem pose a problem due to their resistance to biological treatments. Vine stem and Turkish red pine sawdust are agricultural wastes and could be an alternative bio-sorbents for the leather industry due to their cost effectiveness. For this purpose, it was aimed to determine the removal efficiencies of the dyestuff Acid Brown 282 SGR by the use of vine stem and Turkish red pine sawdust. The batch adsorption technique was used for the study and the effect of the pH, biosorbent amount and contact time was investigated. The functional groups of the bio-sorbents were determined by attenuated total reflectance spectra (ATR-IR). The biosorption data showed that Langmuir model was the best fitted model for the sorption of Acid Brown 282 SGR. The maximum adsorption capacities were found as 25.91and 26.67 for vine stem and Turkish pine sawdust respectively. The results revealed that vine stem and Turkish red pine sawdust could be used as low-cost biosorbents for the removal of dyestuff remaining after the dyeing process of leathers.

Keywords: biosorption, vine stem, red pine sawdust.

INTRODUCTION

Synthetic dyes used in various industries such as textile, chemistry and leather industries, pose an important risk for the environment if they are discharged to groundwater, surface water or rivers without any removal process. Due to the harmfulness of many synthetic dyes to human beings and environment, the removal of dyes becomes a very important topic for the researchers (Chiou and Li, 2002). Various types of dyestuffs are used in leather industry and their removal from the dyeing baths constitutes a major problem due to the treatment methods difficulty.. Adsorption, chemical reduction and oxidation, ion exchange, reverse osmosis, chemical precipitation and filtration techniques etc. are well known for the use of dye removal (Allen *et al.,*2005). Active carbon is an effective adsorbent, but it is quite expensive (Sanghi *et al.*, 2002). The adsorption process is more economical and effective (Ferrero, 2007). So, up to now different adsorbents such as clay (Kashif Uddin, 2017), peat (Allen *et al*., 2004), fly ash, walnut shell (Nazari Moghaddam *et al.,* 2010), chitin (Wawrzkiewicz *et al.*, 2017) and leather shaving waste (Zengin *et al.*, 2010) have been investigated due to their low-cost. Turkish red pine sawdust and vine stem are lignocellulosic biomasses. They have negative surface charge of the outer surfaces (Nethaji *et al*., 2010) and they are endemic to Turkey.

In Turkey, approximately 300.000 tons of vine stem wastes are emerging annually in pruning. In 2011, 17.5 million m^3 industrial woods were consumed and lumber production was one of the biggest subdivision of industrial wood production which was produced 2.3 million m^3 annually (Annon, 2010). After the production of lumber, high

amount of sawdust were generated as a waste. Although there were a couple of study on
red pine sawdust such as additional substance for pyrolysis of wood-plastic composite
(Vaisanen *et al*., 2016), sintering performance (Findorak *et al*., 2014), and usage for
biocomposite derived substance (Das *et al*., 2016), these waste are widely used for solid
fuel, animal bedding material. Although various adsorbents were used for removal of
the dyestuffs, there has not been any study about the use of the non-modified vine-stem
and Turkish red pine sawdust on the remaining dyestuff after the dyeing process of
leather industry.

For this purpose, the aim of this study was to investigate the adsorption properties of
vine stem and Turkish red pine sawdust as cheap adsorbents. The adsorption properties
of the vine stem and Turkish red pine sawdust on the removal of anionic dyestuff (Acid
brown 282 SGR) were investigated with the use of batch adsorption technique.

MATERIALS AND METHODS

Materials

The vine stem was collected from the vineyards of Manisa, Izmir and Turkish red pine
sawdust was obtained from a timber company in Torbalı, Izmir. These biosorbents were
milled and washed with pure water until the color of the washing water became clear.
Then, the biosorbents were dried at room temperature and re-milled until having a particle
size of less than 0.2 mm. Later, they were dried in the oven at 110°C and stored in a sealed
box. Acid Brown 282 SGR (CAS 12219-65-7) anionic dyestuff that has been widely used
in dyeing process of leather manufacturing was used for the absorption experiments.

Methods

The batch adsorption technique was used in the experiments. A certain amount of
the biosorbent and known concentration of dye solution (100 mL) were shaken with an
orbital shaker at room temperature at certain time intervals. The rate of the shaker was
150 rpm. The pH of the solution was adjusted using pH-meter with glass electrode
before mixing. The biosorbents were removed by Whatman filter paper at the end of
each experiment. Then the absorbance of dye in the filtrate was measured by UV
spectrophotometer. Triplicate experiments were performed and the mean values were
given as a result.

Characterization of adsorbents was determined by attenuated total reflectance
Fourier transform infrared (ATR/FTIR) spectra (Spectrum 100, Perkin-Elmer).

RESULTS AND DISCUSSION

Characterization of Biosorbents

The FT-IR analysis of vine stem and Turkish red pine sawdust used as biosorbents
are shown in Figure 1 and 2. The figures are representing the most important bands that
are observed in an infrared spectrum of vegetable sources such as woods, barks and
their assignment to functionality.
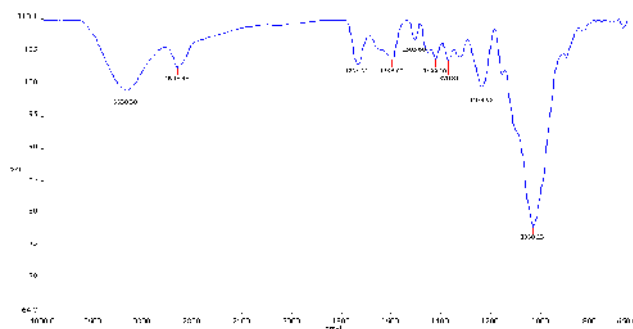
Figure 1. FT-IR spectra of vine stem waste
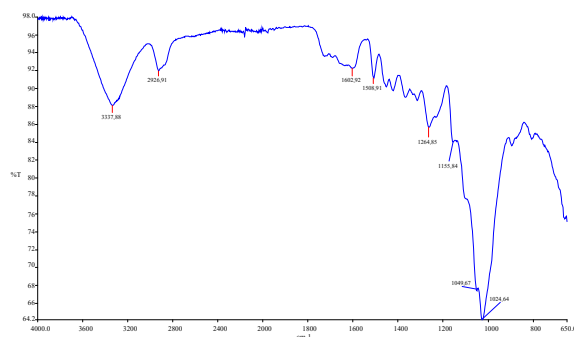
Figure 2. FT-IR spectra of Turkish red pine sawdust

The bands of C—O deformation vibrations are the region of 1023–1030 cm^{-1} (1024 cm^{-1} for TPS and 1030cm^{-1} for VS). 3000 and 3600 cm-1 bands attributed to the associated OH- functional group of phenols, alcohols, and carboxylic acids for each biosorbent. For vine stem, the bands at 2923 cm^{-1} and 1734 cm^{-1} can be assigned to the C—H bonds of aliphatic acids and C—O stretching bonds of aromatic ethers, esters respectively. The bands 2926 cm^{-1} and 1602 cm^{-1} can be assigned to C-H bond of aliphatic acids, and aromatic C=C sym stretching bands for TPS, respectively. The band 1509 cm^{-1} can be assigned to the ring in-plane bending. Phenol bands appear at 1232 and 1234 cm^{-1}. The C—O stretching of ketones and esters give band at 1705 and 1575 cm^{-1}, respectively. The ether groups are in the 1500-900 cm^{-1} region. The bands at 878 and 753 cm^{-1} show the aromaticity (Mavioglu Ayan *et al*., 2011).

The Adsorption of Vine Stem

The Effect of Contact Time

80 ppm of Acid brown SGR 282 (pH 2) and 0.1 g biosorbent were mixed and shaken at an orbital shaker for 2, 4, 8 and 24 hours. The contact time was chosen as 4 hours because no significant effect on the adsorption capacity was found for the contact time after 4 hours (Figure 3).
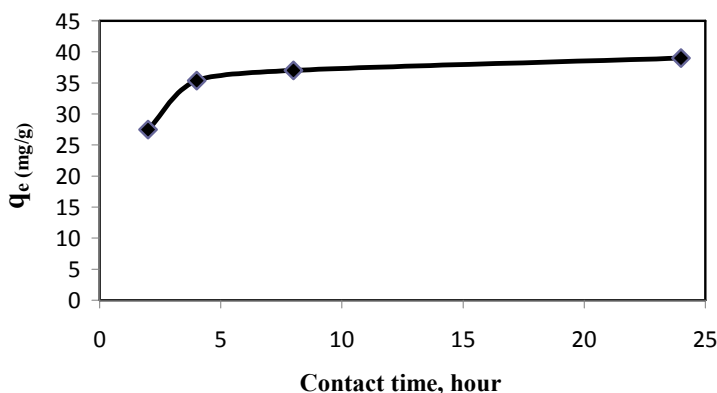
Figure 3. The effect of contact time on the biosorption of Acid brown SGR 282 with vine stem

The Effect of pH

80 ppm of dyestuff solution was prepared at different pH values (2, 4, 7, and 10). Then the dye solutions were mixed with 0.1 gram of biosorbent for 4 hours at the orbital shaker. The best removal was determined at pH 2. The biosorption of each sorbent was decreased with the increased pH value as expected from the anionic dyes. There is not any study about the adsorption of Acid brown SGR 282 which is in the group of anionic dyestuffs. This is compatible with the adsorption studies with anionic dyestuff (Mavioglu Ayan *et al*., 2011; Balarak *et al.,* 2015). The vine stem is lignocellulosic material and has negative groups on its surface. Since the dye has a negative charge, there is repulsion between the dye and vine stem at higher pH due to the increased OH⁻ groups (Nethaji *et al*., 2012).

The Effect of Biosorbent Amount

80 ppm of dyestuff solutions (pH 2) and different amounts of vine stem and Turkish red pine sawdust (0.05, 0.1, 0.2, 0.5, 1.0g) were mixed for 4 hours at a shaker, separately. The highest removal was obtained for 0.1 g for each sorbent.

The Adsorption Isotherm

100 mL of dyestuff solutions (pH 2) at different initial concentration ranging from 20-100 ppm were shaken with 0.1 g vine stem and Turkish red pine sawdust for 4 hour. Langmuir and Freundlich isotherms were tested and found that the biosorption is belonging to the Langmuir isotherm. A Langmuir isotherm suggests that adsorption is a single layer. The maximum adsorption capacity was found to be 25.91 mg/g and the Langmuir constant (K_L) was calculated as 0.003721 L / g. Potential binding sites in the biosorbent are phenols, alcohols, and carboxylic acids.

The Adsorption of Turkish Red Pine Sawdust

The Effect of Contact Time

100 ppm of dyestuff solutions (pH 2) and 0.1 g biosorbent were mixed with orbital shaker for different contact time (2, 4, 8 and 24 hours). As seen in Figure 4, after 4 hours there is not significant effect of the contact time on biosorption of anionic Acid brown SGR 282. Therefore, the optimum contact time was 4 hour.
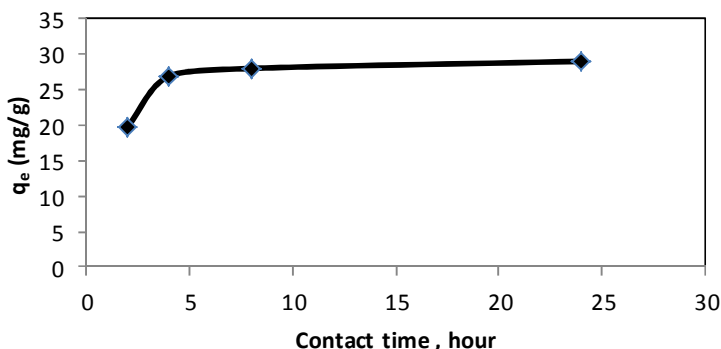
Figure 4. The effect of contact time on the biosorption of Acid brown 282 SGR with Turkish pine saw dust

The Effect of pH

100 ppm of dyestuff solutions were mixed with 0.1 gram of biosorbent at the shaker for 4 hours. The biosorption of Turkish red pine sawdust was decreased with the increased pH value of the solution as expected from the acidic dyes and the best removal was observed at pH 2. There is not any study about the adsorption of acid brown 282 SGR with any other adsorbent.

The result was found compatible with the biosorption studies of acidic dyes (Mavioglu Ayan *et al*., 2011; Balarak *et al.,* 2015). Turkish red pine is lignocellulosic material. As seen in the results of vine stem, biosorption was decreased with pH increase.

The Effect of Biosorbent Amount

100 ppm of dyestuff (pH 2) and different amounts of Turkish red pine sawdust (0.05, 0.1, 0.2, 0.5, 1.0) were mixed for 4 hours at a shaker. The highest removal was obtained for 0.1 g biosorbent.

The Adsorption Isotherm

100 mL of dyestuff solutions (pH 2) at different initial concentration (20-100 ppm) were shaken with 0.1 g Turkish red pine for 4 hour. Langmuir and Freundlich isotherms were tested to obtain the adsorption capacity. The results showed that the biosorption belongs to the Langmuir isotherm. The maximum adsorption capacity is found to be 26.67 mg /g and the Langmuir constant (K_L) was calculated as 0.017618 L/g. Potential binding sites in the biosorbents are phenols, alcohols, and carboxylic acids.

CONCLUSIONS

In this study, the adsorption properties of vine stem and Turkish red pine sawdust were investigated as cheap adsorbents and following conclusions have been drawn;

    a. The results are important because no any other study on the removal of Acid brown 282 SGR dye was found in literatures.

    b. The adsorption capacity of the biosorbents was found good.

    c. The results indicated that the biosorbents had significant effect on the adsorption of the Acid Dyestuff.

    d. After the adsorption, dyestuff enriched biosorbent could be a composite substance for the clay bricks.

    e. Moreover they can also be used as a solid fuel due to their high calorie.

REFERENCES

Allen, S.J. *et al*. (2004), "Adsorption isotherm models for basic dye adsorption by peat in single and binary component systems", *Journal of Colloid and Interface Science*, 280, 322-333.

Allen, S.J. *et al*. (2005), "Kinetic modeling of the adsorption of basic dyes by kudzu", *J Colloids Surf*, 286, 101–109, https://doi.org/10.1016/j.jcis.2004.08.078.

Balarak, D. *et al*. (2015), "Biosorption of Acid Red 88 dyes using dried Lemna minor biomass", *J. Sci. Technol. Environ. Inform*, 01, 81-90, https://doi.org/10.18801/jstei.010215.10.

Chiou, M.S. and Li, H.Y. (2002), "Equilibrium and kinetic modeling of adsorption of reactive dye on cross-linked chitosan beads", *Journal of Hazardous Materials*, B93, 233–248.

Das, O. *et al*. (2016), "Biocomposites from waste derived biochars: Mechanical, thermal, chemical, and morphological properties", *Waste Management*, 43, 560-570, https://doi.org/10.1016/j.wasman.2015.12.007.

Ferrero, F. (2007), "Dye removal by low cost adsorbent: Hazelnut Shells in comparison with wood sawdust", *Journal of Hazardous Materials*, 142, 144-152, https://doi.org/10.1016/j.jhazmat.2006.07.072.

Findorak, R. *et al*. (2014), "The effect of saw-dust addition from pine and oak wood on iron-ore sintering performance", *14th International Multidisciplinary Scientific Geoconference (SGEM)*, Vol III, 973-980.

Global Agricultural Information Network (2010), *Forest Products Report for Turkey*, 05.05.2010.

Kashif Uddin, M. (2017), "A review on the adsorption of heavy metals by clay minerals, with special focus on the past decade", *Chemical Engineering Journal*, 308, 438-462, https://doi.org/10.1016/j.cej.2016.09.029.

Mavioglu Ayan, E. *et al*. (2011), "Biosorption of Dyes by Natural and Activated Vine Stem. Interaction between Biosorbent and Dye", *Clean – Soil Air, Water*, 39(4), 406–412, https://doi.org/10.1002/clen.201000369.

Nazari Moghaddam, A.A. *et al*. (2010), "Adsorption of Methylene Blue in Aqueous Phase by Fly Ash, Clay and Walnut Shell as Adsorbents", *Journal of World Applied Sciences*, 8, 229-234.

Nethaji, S. and Sivasamy, A. (2012), "Adsorptive removal of an acid dye by lignocellulosic waste biomass activated carbon: Equilibrium and kinetic studies", *Chemosphere*, 82, 1367-1372, https://doi.org/10.1016/j.chemosphere.2010.11.080.

Sanghi, R. and Bhattacharya, B. (2002), "Review on decolorisation of aqueous dye solutions by low cost adsorbents", *Color Technol*, 118, 256-269, https://doi.org/10.1111/j.1478-4408.2002.tb00109.x.

Vaisanen, T. *et al*. (2016), "Improving the properties of wood-plastic composite through addition of hardwood pyrolysis liquid", *Journal of Thermoplastic Composite Materials*, 29(11), 1587-1598, https://doi.org/10.1177/0892705716632862.

Wawrzkiewicz, M. *et al*. (2017), "Enhanced removal of hazardous dye form aqueous solutions and real textile wastewater using bifunctional chitin/lignin biosorbent", *International Journal of Biological Macromolecules*, 99, 754-764, https://doi.org/10.1016/j.ijbiomac.2017.03.023.

Zengin, G. *et al*. (2012), "Determination of dyestuffs remaining in Dyeing Processes of vegetable-tanned leathers and their removal using shavings", *Pol. J. Environ. Stud*., 21(2), 479-506.

TANNIN-INSPIRED HYDROGELS WITH CONSIDERABLE SELF-HEALING AND ADHESIVE PROPERTIES

QIUXIA ZHAO[1,2], SHENGDONG MU[1,2], YANRU LONG[1], XIONG LIU[1,2], XIAOWEI GU[1], JIN ZHOU[1], WUYONG CHEN[1,2], CARMEN GAIDĂU[3], HAIBIN GU[1,2]

[1]*Sichuan University, Key Laboratory of Leather Chemistry and Engineering of Ministry of Education, Chengdu 610065, China, guhaibinkong@126.com*
[2]*National Engineering Laboratory for Clean Technology of Leather Manufacture, Sichuan University, Chengdu 610065, China*
[3]*INCDTP - Division: Leather and Footwear Research Institute, 93 Ion Minulescu st., Bucharest, 031215, Romania*

Hydrogel materials are attracting considerable attention owing to their wide applications such as wound closure, drug delivery, tissue engineering, cell therapy, wrinkle fillers, etc. Considering the unique tannin chemistry including excellent chelating properties to metals, easily oxidability and superior ability to bind proteins, herein, the natural gallol-containing tannic acid (TA), an extract of plant materials such as Chinese gallnuts, cacao, green tea leaves and fruit peels, was used as a natural phenolic crosslinker to fabricate the self-healing and adhesive hydrogels based on the oxidation of polyphenol groups with the aid of NaIO4 under alkaline condition. The properties of the obtained hydrogels were well characterized by rheometer, universal testing machine, thermogravimetry (TG), dynamic mechanical analysis (DMA) and scanning electron microscope (SEM). The feed molar ratio of $NaIO_4$ to TA was found to play an essential role in gelation time (3-15 min), physical properties (MPa range of tensile strength and 50-220% of elongation at break), adhesive strength (up to 36KPa) as well as self-healing efficiency (up to 73%) of the fabricated hydrogels. By using TA and gelatin with complete natural origin, this study opens a new path toward the preparation of biocompatible self-healing and adhesive hydrogel materials with improved properties.

Keywords: gelatin; tannin acid; hydrogel; self-healing; adhesives

INTRODUCTION

Recently, inspired by the catecholic chemistry of dopamine (DOPA), mussel-inspired hydrogels for self-healing and tissue adhesive have drawn increasingly attention owing to their biomedical applications such as wound dressing, tissue sealants, scaffolds for tissue engineering and encapsulation of drug (Mehdizadeh *et al*., 2012). However, the costly price and potential neurotransmission effect of DOPA limit its application in commercial filed, and thus the seeking of alternatives to DOPA is extraordinary necessary (Guo *et al*., 2018).

Hence, tannic acid (TA), a natural plant-derived polyphenolic compound with extensive sources, is employed as a desired alternativefor mussel-inspired self-healing materials. TA is capable to precipitate proteins (collagen and gelatin) by multi-point hydrogen-bond and hydrophobic actions. The two adjacent phenolic hydroxyls of gallolsin TA can also chelate metal ions (e.g. Fe^{3+}, Al^{3+}, Cr^{3+}) in the form of oxygen anion (O-) to form a stable pentacyclic complex, and although the third phenol hydroxylis not involved in the formation of pentacyclic complex, it can promote the dissociation of the other two adjacent OH groups, and thus accelerating the formation of pentacyclic complex and promoting its stability (Fan *et al*., 2017). In addition, TA has good antioxidant capacity. Its gallols can also be oxidized to form quinones that further take placenucleophilic addition reactions. Thus, like the versatile DOPA containing

catechol, TA could also be used to fabricate functional materials including self-healing and adhesive hydrogels.

Herein, a one-pot method is described to fabricate TA-modified gelatin hydrogels through supramolecular interactions as well as covalent bonds under oxidizing conditions. The strong multi-point hydrogen-bond and hydrophobic interactions between TA and gelatin are first inhibited to a large extent in alkaline conditions to obtain their homogeneous mixture, and sodium periodate ($NaIO_4$) was then added as oxidant to prepare oxidation-crosslinked gelatin hydrogels with considerable self-healing and adhesive properties. The effect of $NaIO_4$ dosage was systematically investigated on the gelling time, self-healing adhesive, viscoelastic and thermal properties and morphology of the obtained hydrogels.

MATERIALS AND METHODS

Gelatin (10 g) and TA (0.5 g) was blended in 100 ml deionized water and heated at 70 °C for 1 h to get a mixed solution with an ultimate gelatin concentration of 10% (w/v), then the pH value was adjusted to 11 using 2 M NaOH. The obtained solution was further stirred for 24 hours at 70°C to yield the wine-red transparent precursor solution of hydrogel. Various amounts of NaIO4 solutions (10 %, w/v) were added to the precursor solution under vigorous stirring at 50°C. The reaction mixture was further stirred at 50°C until the sol-gel transformation. The feed molar ratios of $NaIO_4$ to TA are 5:1, 10:1, 15:1, 20:1 and 25:1, respectively, and the obtained hydrogels are named as **NA-5, NA-10, NA-15, NA-20** and **NA-25,** respectively.

RESULTS AND DISCUSSIONS

Gelling Time

Gelling time of the hydrogels was measured by inverting test tube method (Fig 1 A) at 50°C, and it was determined at the time when there was no visual flow observed by inverting the vial. As shown in Fig 1B, the feed molar ratio of NaIO4to TA played an essential role in the process of gelling. Along with the increase of NaIO4 dosage, the gelling time is decreased from 15 min for **NA-5** to the shortest 2.35 min for **NA-15,** and then slighted improved to 3 min for **NA-20**, which is probably due to the improved density of crosslinking of the hydrogel.
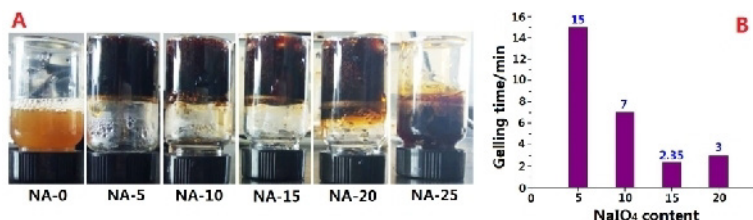
Figure 1. Photographs of gelation (A) and gelling time (B) at different amount of $NaIO_4$

Self-healing and Adhesive Properties

Cylindrical hydrogels with a diameter of 10mm and height of 100mm were prepared and immersed into 30% (w/w) $(NH_4)2SO_4$ for one day before performing the tensile test. The aim of immersion operation is to improve the mechanical strength of hydrogels so that the gels could be strong enough to withstand the clamp of tensile test machine. A cylindrical piece of hydrogel was cut in half, and the two halves were then reattached to one another. After 2 h under wet conditions, the separated hydrogel pieces had adhered again to form one hydrogel, indicating its preliminary self-healing ability. The stress-strain curves (Fig.2A) were then recorded for the original and self-healed hydrogels, and the self-healing rate was calculated by the following equation:

Self-healing rate (%) = S_{after}/S_{before} × 100%   (1)

Where Sbefore is the tensile stress of original hydrogel at break, and Safter is tensile stress of self-healed hydrogel at break. The self-healed hydrogel **NA-15** recovers 72.84% tensile strength compared with the original hydrogel (Fig.2B).

A lap shear test was also performed to evaluate the adhesive strength of the hydrogel. A piece of cow-skin with the shape of 1.5 cm × 10 cm rectangle was smeared with 1ml of the gelatin/TA/NaIO4 mixture. Then another piece of cow-skin was placed on the treated one, and the contacted area was kept as 1.5 cm × 8 cm. 24 h later, the samples were measured by the lap shear test, and the results were shown in Fig. 2C. Along with the increase of $NaIO_4$ used, the average adhesive strength of hydrogel shows similar change tendency to the self-healing rate (Fig.2B). Specially, it firstly increases from 8.52 KPa of **NA-5** to 36.31 KPa of **NA-15** and then decreases to 9.79 KPa of **NA-20**, which suggested an optimal amount of $NaIO_4$ for leather adhesive.
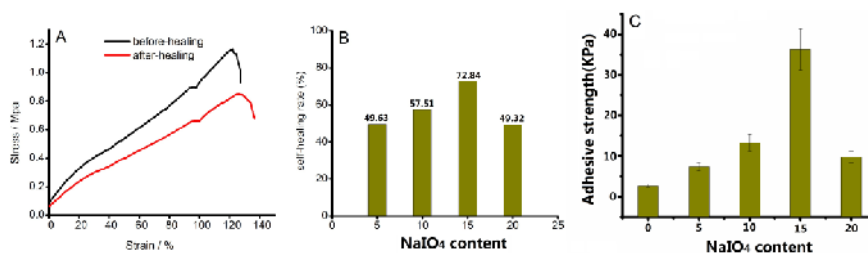
Figure 2. Stress-strain curves of NA-15(A), self-healing rates (B) adhesive strength (C) of hydrogels

Rheological Analysis and DMA

Rheological analysis was also performed for the **NA-10** hydrogel to qualitatively monitor its viscoelasticity. A strain amplitude sweep was firstly measured to investigate the linear viscoelastic region and the crossover point where storage modulus (G') is equaled to loss modulus (G''). As shown in Fig.3A, both G' and G'' remain constant at a low strain amplitude (0.1%-25%), and after that, when the strain further increases, the G'' value firstly starts to improve, and G' value subsequently shows a dramatic decrease, indicating a shear-thinning behavior of hydrogel. As a result, a cross over point is observed at the strain of approximately 700%, implying the destruction of the hydrogel network. Besides, the value of G' is consistently much higher than that of G''

in the frequency sweep test range (Fig.3B), showing a Hooke an-like frequency-independent behavior and further indicating a stable formation of hydrogel (Fan, 2017).
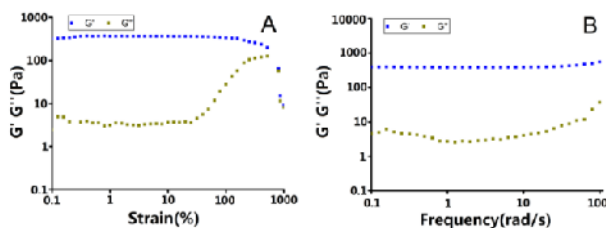
Figure 3. Strain amplitude sweep test (0.1-1000%) of **NA-10** hydrogel at a fixed frequency of 1 rad s-1 (A) and its frequency sweep test (0.1-100rad s-1) at a fixed strain of 1% (B)

In the DMA curves (Fig.4A) both G' and G'' values of **NA-10** hydrogel precipitously decrease with the growth of temperature, indicating the hydrogel gradually became soft. The crossing point of G' and G'' is observed at 54 °C, corresponding to the transformation of gel to sol.

TG Analysis

Fig. 4B provides the TG curves of hydrogels at various amount of $NaIO_4$. In general, all the hydrogels decompose in a two-step mode. The first weight loss occurs below 100°C, which is probably due to the volatilization of water and other small molecules in hydrogels. The second stage of weight loss is observed at 250 °C or so, which is associated with the degradation and carbonization of hydrogel network. Notably, at the same testing temperature, the higher the dosage of $NaIO_4$ is, the smaller the weight loss of the obtained hydrogel is, namely, the more stable the hydrogel is.
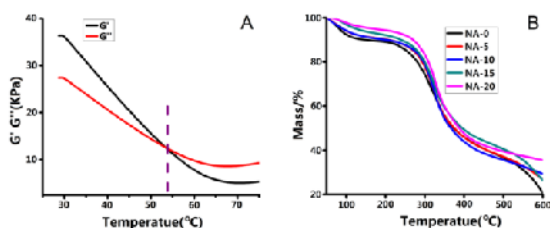
Figure 4. Dynamic thermo mechanical properties (A) of NA-10 and TG curves (B) of various hydrogels

SEM Analysis
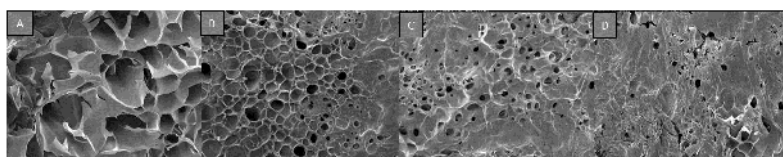
Figure 5. SEM images of **NA-5** (A), **NA-10** (B), **NA-15** (C), **NA-20** (D) hydrogels

The interior structure of the obtained hydrogels was investigated by SEM analysis. As shown in Fig.5, all the lyophilized hydrogels exhibited a porous three-dimension structure with different shape and porosity. The pore size progressively decreases with the increase of NaIO$_4$ used. For **NA-5** hydrogel, the SEM image (Fig.5A) provides a petal-shaped porous structure with a pore diameter of 213 ± 58 μm. In the SEM of **NA-10** hydrogel (Fig. 5B), there are clear thick boundary between the pores, and the pore diameter is decreased to 73 ± 21 μm. For **NA-15** and **NA-20** hydrogels, the pore diameter is further declined to 35 ± 10μm, and the number of pores is greatly reduced, too. Furthermore, thick cracks are found for **NA-20**, which is attributed to its high crosslinking density.

CONCLUSIONS

In conclusion, we successfully fabricated tannin-inspired self-healing hydrogels through a facile one-pot method in which TA was introduced to gelatin via both supramolecular interaction and covalent bonds in alkaline condition. The crosslinking of these hydrogels was easily accomplished by oxidizing the homogeneous gelatin-TA solution in the presence of NaIO$_4$. Similar to mussel-inspired hydrogels, the resulting product exhibited sticky and self-healing nature. The amount of NaIO$_4$ added can be used to modulate the gelling time, self-healing, mechanical property, adhesive strength as well as the interior pore size of gelatin hydrogels. Besides, owing to the remarkable thermal properties, viscoelasticity and porosity the present hydrogels will be an excellent candidate for wound closure, tissue adhesive and cell delivery. Additionally, considering the accessibility and low price of TA as well as the biocompatibility of gelatin, the simple and feasible method developed in this work offers a practical strategy for the preparation of self-healing and adhesive materials in biomedical field.

REFERENCES

Fan, H. *et al.* (2017), "Tannic Acid-Based Multifunctional Hydrogels with Facile Adjustable Adhesion and Cohesion Contributed by Polyphenol Supramolecular Chemistry", *ACS Omega*, 2(10), 6668-6676, https://doi.org/10.1021/acsomega.7b01067.

Guo, J. *et al.* (2018), "Development of tannin-inspired antimicrobial bioadhesives", *Acta Biomater*, 72, 35-44, https://doi.org/10.1016/j.actbio.2018.03.008.

Mehdizadeh, M. *et al.* (2012), "Injectable citrate-based mussel-inspired tissue bioadhesives with high wet strength for sutureless wound closure", *Biomaterials*, 33(32), 7972-83, https://doi.org/10.1016/j.biomaterials.2012.07.055.

Zhao, X. *et al.* (2017), "Antibacterial anti-oxidant electroactive injectable hydrogel as self-healing wound dressing with hemostasis and adhesiveness for cutaneous wound healing", *Biomaterials*, 122, 34-47, https://doi.org/10.1016/j.biomaterials.2017.01.011.

II.

NANOTECHNOLOGY
AND
NANOMATERIALS

EXPERIMENTAL AND FIRST PRINCIPLES STUDY OF STRUCTURAL, ELECTRONIC AND OPTICAL PROPERTIES OF $ZN_{0.875}MN_{0.125}O$ THIN FILM

BAHRI DEGHFEL[1], ABDELHAFID MAHROUG[2], RABIE AMARI[2], AMMAR BOUKHARI[2], ABDELOUHAB BENTABET[3]

[1]*University of Mohamed BOUDIAF, Laboratory of Materials Physics and its Applications, Faculty of Sciences, Physics Department, 28000 M'sila, Algeria, badeghfel@gmail.com*

[2]*University of Mohamed Boudiaf, Faculty of Technology, Mechanical Engineering Department, 28000, Algeria, hafidmahroug@yahoo.fr, a.lamari28@gmail.com, ammar.boukhari@gmail.com*

[3]*University of Mohamed El Bachir El Ibrahimi, Laboratory of characterization and valuation of natural resources, Bordj-Bou-Arreridj 34030, Algeria, a.bentabet@gmail.com*

$Zn_{0.875}Mn_{0.125}O$ thin films are fabricated by a simple sol-gel spin-coating technique on glass substrates using zinc acetate dehydrate [Zn(CH3COO)2·2H2O] and manganese acetate tetrahydrate [$Mn(CH_3COO)_2 4H_2O$]as a starting material and doping source. Isopropanol and monoethanolamine (MEA) were used as solvent and stabilizer, respectively. X-ray diffraction, ultraviolet-visible spectroscopy and photoluminescence spectroscopy are employed to investigate the effect of Mn doping on the structural, electronic and optical properties of ZnO thin films. The obtained results are compared with those using first-principles calculation based on density functional theory (DFT) with local density approximation (LDA) plus Hubbard U (DFT–LDA+U) method. This latter represents the theoretical framework to deal with strongly correlated materials to predicted successfully the electronic properties of such materials.

Keywords: Sol-gel spin-coating technique, Mn-doped ZnO thin film, DFT.

INTRODUCTION

ZnO is a wide band-gap (3.37eV) compound semiconductor that have received considerable attention (Yaakob *et al*., 2014; Ozgur *et al*., 2005). The Mn ferromagnetic element is widely used in doping II–IV-based hosts, like Mn–ZnO (Luo *et al*., 2005; Zhao *et al*., 2010). Previous studies (Luo *et al*., 2005; Zhao *et al*., 2010; Zhao *et al*., 2012) have found that the Mn–Mn interaction is dominated by antiferromagnetic (AFM) coupling. The doping of ZnO thin films by Mn element presents a feasible means to adjust the band gap. The tuning of the band gap allows DMS to be used as UV detectors and light emitters.

The first-principles and pseudopotentials method based on conventional density functional theory (DFT) cannot efficiently describe the localization of strongly correlated *d* and *f* electrons of transition material (Anisimov *et al*., 1997; Dudarev *et al*., 1998). The DFT–LDA+U approach (Yaakob *et al*., 2014; Anisimov *et al*., 1997) can significantly improve the calculation including transition metal localization.

Variety of techniques have been used to prepare ZnO thin films. Because of its simplicity, low cost, safety, large area deposition, controllability of compositions and uniformity of thickness, the sol–gel method has attracted much attention (Amari *et al*., 2018; Mahroug *et al*., 2017).

The aim of this study is to investigate experimentally and theoretically by using first-principles calculations, the structural, electronic and optical properties of $Zn_{0.875}Mn_{0.125}O$ Thin film.

EXPERIMENTAL AND THEORETICAL DETAILS

Sol–gel spin coating method was used to prepare Mn-doped ZnO thin films on glass substrate. Zinc acetate dihydrate [Zn (CH$_3$COO)$_2$. 2H$_2$O] and manganese acetate tetrahydrate [Mn(CH$_3$COO)$_2$. 4H$_2$O] were used as a starting material and dopant source, respectively, and the isopropanol was added as stabilizer. The molar ratio of the solvent (monoethanolamine; MEA) to metal ions was fixed at 1.0 and the concentration of metal ions was 0.7 M. The Mn dopant concentration was chosen as 12.5 mol%. The subsequent steps were discussed in our previous works (Amari *et al*., 2018; Mahroug *et al*., 2017).

An X-ray diffractometer (XRD) (Bruker 8 Advance; λ=1.5406 A°), UV-vis spectrophotometer (UV-3101 PC-Shimadzu) and spectrofluorimeter (Perkin Elmer LS 50B; excitation source at 325 nm), was used to characterize the structural properties, the optical transmission spectra and the photoluminescence (PL) of the ZnO thin films, respectively.

First-principles calculations of structural, electronic and optical properties of Mn-doped ZnO material (Zn$_{1-x}$Mn$_x$O x=12.5%) with wurtzite structure were performed using DFT as implemented in CASTEP code (Clark *et al*., 2005). The 2.2.2 ZnO supercell containing 32 atoms is used and the substitutional method is adopted (Zhao et al., 2012) to achieve this concentration in which two Zn atoms are substituted by Mn and different geometry configurations for Mn atoms were taken. The exchange-correlation function is treated by the generalized gradient approximation (GGA) in the scheme of Perdew–Burke–Ernzerhof (PBE) (Perdew *et al*., 1996). Also, the valence-electron configurations for the oxygen, zinc and manganese atoms are employed as 2s^2 2p^4, 3d^{10} 4s^2 and 3d^5 4s^2, respectively. The cut-off kinetic-energy of 450 eV was used. The 7.7.4 k-point grid was adopted over the first Brillouin zone sampling mesh. The optimization convergence for energy change, maximum force, maximum stress, and maximum displacement were set at 5×10^{-6} eV/atom, 0.01 eV/Å, 0.02 GPa, and 5.0 × 10^{-4} Å, respectively. Furthermore, the SCF convergence threshold is fixed at 5.0 10^{-7} eV per atom. The semiempirical LDA+U approach (Anisimov *et al*., 1997) with effective Hubbard U values of 7 eV to treat the transition metal of Zn *3d* and *Mn 3d* electrons was employed.

RESULTS

The total energies of the five different geometry configurations for substitution of Zn by Mn, marked as A: Pm (C_s^1), B: Cm (C_s^3), C: P3m1 (C_{3v}^1) , D: P3m1 (C_{3v}^1) and E: Cm (C_s^3), are presented in Table 1.

Table 1. Total energy for different geometry configurations. Energy corresponds to configuration A is chosen as an energy reference

Configuration	E (eV)
A	0
B	-0,978
C	-0,0249
D	-0,0433
E	0,0085

Total energy in configuration A was chosen as an energy reference. It is clear from the figure that the ground state is found to be the configuration B corresponding to symmetry group Cm (C_s^3). So, this configuration will be considered for Mn-doped ZnO material with x=12,5%.

The optimized lattice constant along c-axis is found to be around 5.34A° which is slightly underestimated by around 2% by our experimental result (5.23A°) extracted from XRD pattern (figure 2). The (002) diffraction peak is stronger than the other peaks, indicating a preferential growth direction along the c-axis due to its lowest surface free energy among (002) planes.
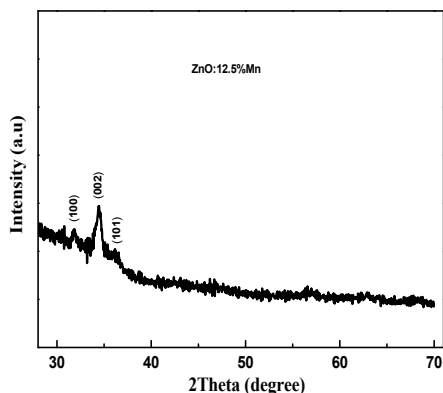
Figure 2. XRD pattern of $Zn_{1-x}Mn_xO$ (x=12.5%) thin film

The optical transmission spectra at room temperature of $Zn_{1-x}Mn_xO$ (x=12.5%) thin films is shown in figure 3. It revealed that the sample is transparent in the visible optical region with an average transmittance about of 62%.
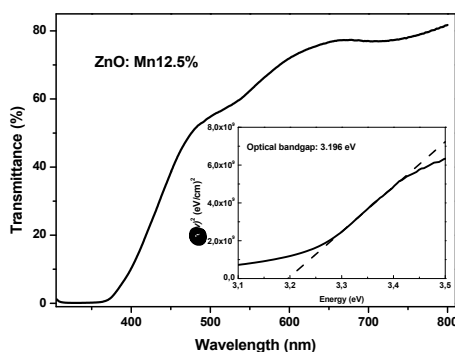
Figure 3. Optical transmission spectra of $Zn_{1-x}Mn_xO$ (x=12.5%) thin film. Inset presents a plot of $(\alpha h\upsilon)^2$ vs. photon energy (hυ)

The absorption coefficient α is related to the optical band gap energy Eg as:

$$\alpha h \nu = constant\,(h\nu \quad Eg)$$ (1)

The absorption coefficient α can be calculated by the equation

$$\alpha = \frac{1}{t}\ln\left(\frac{1}{T}\right)$$ (2)

where T is the transmittance index and t is the film thickness. The Eg value is therefore determined by extrapolating the linear portion of the plot relating $(\alpha h\nu)^2$ versus $h\nu$ (inset in figure 3).

The obtained value of Eg is 3.196 eV. which is highly underestimated by the theoretical value obtained here (0.91 eV). It is well known that the conventional DFT can underestimate the experimental band gap and despite the incorporation of the semi-empirical LDA+U approach, there is still a significant gap between experience and theory.

CONCLUSION

Structural, electronic and optical properties of $Zn_{0.875}Mn_{0.125}O$ thin films are investigated experimentally and theoretically, within the framework of DFT. The optimized lattice constant is found in a good agreement with the experimental one extracted from XRD pattern. This latter revealed that the preferential growth direction was along the c-axis. The fabricated thin film was transparent in the visible optical region with an average transmittance about of 62%. The deduced experimental band gap was found underestimated by the theoretical one.

REFERENCES

Amari, R. *et al*. (2018), "Structural, Optical and Luminescence Properties of ZnO Thin Films Prepared by Sol-Gel Spin-Coating Method: Effect of Precursor Concentration", *Chinese Physics* Letter, 35, 016801, https://doi.org/10.1088/0256-307X/35/1/016801.

Anisimov, V.I., Aryasetiawan, F. and Lichtenstein, A.I. (1997), "First-principles calculations of the electronic structure and spectra of strongly correlated systems: the LDA+U method", *Journal of Physics: Condensed Matter*, 9, 767–808, https://doi.org/10.1088/0953-8984/9/4/002.

Clark, S.J. *et al*. (2005), "First principles methods using CASTEP", *Zeitschrift für Kristallographie*, 220, 567–70, https://doi.org/10.1524/zkri.220.5.567.65075.

Dudarev, S.L. *et al*. (1998), "Electron-energyloss spectra and the structural stability of nickel oxide: An LSDA+U study", *Physical Review B*, 57, 1505, https://doi.org/10.1103/PhysRevB.57.1505.

Luo, J. *et al*. (2005), "Structure and magnetic properties of Mn-doped ZnO nanoparticles", *Journal of Applied Physics*, 97, 086106, https://doi.org/10.1063/1.1873058.

Mahroug, A. *et al*. (2017), "Synthesis, Structural, Morphological, Electronic, Optical and Luminescence Properties of Pure and Manganese-Doped Zinc Oxide Nanostructured Thin Films: Effect of Doping", *Journal of Nanoelectronics and Optoelectronics*, 12, 1–10, https://doi.org/10.1166/jno.2018.2271.

Ozgur, U. *et al*. (2005), "A comprehensive review of ZnO materials and devices", *Journal of Applied Physics*, 98, 041301, https://doi.org/10.1063/1.1992666.

Perdew, J.P., Burke, K. and Ernzerhof, M. (1996), "Generalized Gradient Approximation Made Simple", *Physical Review Letters*, 77, 3865, https://doi.org/10.1103/PhysRevLett.77.3865.

Yaakob, M.K. *et al*. (2014), "First Principles LDA+U Calculations for ZnO Materials", *Integrated Ferroelectrics*, 155, 15–22, https://doi.org/10.1080/10584587.2014.905086.

Zhao, L. *et al*. (2010), "The electronic and magnetic properties of (Mn, N)-codoped ZnO from first principles", *Journal of Applied Physics*, 108, 113924, https://doi.org/10.1063/1.3511365.

Zhao, L. *et al*. (2012), "The electronic and magnetic properties of (Mn,C)-codoped ZnO diluted magnetic semiconductor", *Chinese Physics B*, 21, 097103, https://doi.org/10.1088/1674-1056/21/9/097103.

HALLOYSITE NANOTUBES AS INNOVATIVE CONSOLIDANTS FOR HISTORICAL LEATHER

EMANUEL HADÎMBU[1,2], ELENA BADEA[1,3], CRISTINA CARŞOTE[4],
CLAUDIU ŞENDREA[1], LUCREŢIA MIU[1]

[1]*INCDTP - Division: Leather and Footwear Research Institute, Advanced Research for Cultural Heritage (ARCH Lab) Group, Ion Minulescu 93, 031215 Bucharest, Romania*

[2]*Faculty of Applied Chemistry and Material Science, University Politehnica of Bucharest, Gheorghe Polizu 1-7, 011061, Bucharest, Romania*

[3]*Department of Chemistry, Faculty of Sciences, University of Craiova, Calea Bucureşti 107 I, 200585, Craiova, Romania*

[4]*National Museum of Romanian History, Calea Victoriei 12, 030026 Bucharest, Romania*

Historical leathers, in a huge variety of items as footwear and garments, bookbinding, wall tapestry, upholstery, harnesses, armours, storage vessels, household tools, cases, musical instruments, toys, ritual objects are regarded as important testimonials of our cultural heritage. It is vital therefore that these objects remain well preserved along with all the knowledge involved, from their material aspects and value use to historical, cultural and artistic values. One of the most difficult challenges in leather conservation concerns with consolidation and pH control. To set up a novel green protocol for the long-term protection of historical and archaeological leather we have investigated the filling and stabilization process of vegetable-tanned leathers treated with various mixtures based on halloysite nanotubes (HNTs).

Keywords: vegetable leather, halloysite nanotubes, stabilization

INTRODUCTION

For millennia man has used animal hides in their day by day life for producing footwear, garments, for building their shelters (e.g. tents, yurts), household objects and tools, military accessories (armors, shields, helmets, etc.), boats, musical instruments and even toys. Later, in Middle Ages, the production of artistic objects or components has developed, e.g. travel chests, jewelry boxes, upholstery, wall tapestries, bookbindings, furniture accessories, etc. Nowadays, such artistic, historical and archaeological objects are preserved in museums, libraries or archives, places where history is kept alive and tell us about our ancestors.

Most of the historical leathers are vegetable tanned, alum-tawed or tanned with smoke or fats. Along with the industrial revolution, through the 1850s, the first investigations performed on early and current (industrial) leather showed that the presence of sulphur dioxide in the urban atmosphere strongly affects the performance of the leather: the so-called red rot phenomenon (Haines, 1977) promoted by the atmospheric pollution has proved to be detrimental to collagen structure. Even today museums, libraries, private collections and historical places owing leather artworks are facing this unresolved problem.

The current treatment options, however, are very few, and all commercial products such as Klucel-G and silicone oil showed critical drawbacks (Ludwick, 2012). Recently the use of nanoparticles in conservation has started to be explored, halloysite nanotubes being used as consolidating materials for archeological wood and paper (Cavallaro *et al*., 2015; Cavallaro *et al*., 2014).

EXPERIMENTAL DETAILS

Chemicals

Halloysite nanotubes (HNTs) from Sigma Aldrich, polyethylene glycol 400 and 1-chlorobutane from Alfa Aesar, glacial acetic acid 99.84% from Chimreactiv, ethanol 96% from Chemical Company, sodium chloride from Salrom, urea from Sigma Life Science, beeswax from EcoNatura and concentrated wool keratin hydrolysate obtained in our laboratory, were used.

Preparation of Nanoparticle Dispersions Applied on Leather Samples

HNTs dispersions were prepared using four different dispersion media: polyethylene glycol 400 (PEG); concentrated keratin hydrolysate (Ke) with neutral pH; sodium chloride (2%) and urea (2%) in ethyl alcohol solution (48%) (Ur) (Badea et al., 2014); 2% beeswax in 1-chlorbutan (Bw). The concentration of HNTs was 0,1% for PEG, Ke and Ur dispersions, while 0,5% HNTs was added to the Bw alcoholic dispersion. All dispersions were ultrasonicated 10 minutes before applying on leather.

Mimosa tanned calf leather obtained in our micro pilot unit was used to test the effect of the various HNTs dispersions.

The samples were immersed for 10 minutes in the HNTs dispersion using a Petri dish placed on a shaker plate (Compact Digital Rocker from Thermos Scientific) at 100 rpm; every two minutes the sample was turned around. Treated samples were hanged and dried at room temperature.

The hydrothermal stability analysis was carried out at both macroscopic and microscopic levels, using the standard method SR EN ISO 3380-2003 and Micro Hot Table (MHT) method, respectively. The MHT system is made of a Linkam-LTS 120 heating plate, a Nikon SMZ745T stereomicroscope equipped with a MDH5 video camera and a computer for the temperature increase control and image acquisition. The shrinkage activity measurements were performed up to 90°C as described earlier (Sendrea et al., 2017).

FTIR-ATR analysis was carried out using an Alpha portable spectrometer from Bruker Optics equipped with Platinum diamond ATR at a resolution of 4 cm^{-1} and 32 scans. The spectral rage was 4000-650 cm^{-1}. FTIR-ATR spectra were acquired on both sides of leather samples, corium and grain (Carşote et al., 2014).

SEM high magnification images were achieved with a FEI Quanta 200 microscope at an acceleration potential of 10 kV.

Wettability was determined by dynamic contact angle measurements carried out with a Drop Shape Analyzer DSA100 from KRÜSS, the sample being placed horizontally.

Non-Invasive Single-Sided ^{1}H NMR measurements were performed at room temperature using a Magritek GmbH NMR MOUSE PM2 controlled by a Kea 2 spectrometer operating at 27 MHz ^{1}H resonance frequency as described earlier (Badea et al., 2016). The Carr-Purcell-Meiboom-Gill (CPMG) pulse sequence was used to measure the spin-spin relaxation time $T_{2\text{eff}}$. The CPMG curves were best analyzed by a combination of two exponential functions. The spin-lattice relaxation times, T_1, were measured with a saturation-recovery pulse sequence.

RESULTS AND DISCUSSION

Hydrothermal Stability Measurement

The values of shrinkage temperature reported in Table 1 indicate a stabilizing effect for all treated samples, Bw_HNT treatment being the most effective treatment. It should however be mentioned that, even though T_s increases, there is a net decrease of the first shrinkage temperature (Figure 1) which could be attributed to the destabilization of collagen populations with lowest thermal stability due to the solutions used to disperse the HNTs.

Table 1. Thermal stability measured by both the standard method SR EN ISO 3380-2003 and MHT method

Sample/ Treatment	Shrinkage temperature (standard method), °C	Shrinkage activity determined by MHT method		
		T_f, °C	T_s, °C	T_l, °C
CM_Ref	66	41.6	58.2	79
CM_Ke	67	24.2	60.6	83.4
CM_Ke_HNT	68	24.7	61.1	80.1
CM_Ur	70	33	61.1	79.3
CM_Ur_HNT	70	34.4	59.7	85
CM_PEG	68	34.3	64.4	80.2
CM_PEG_HNT	70	35	63.1	81.6
CM_Bw	69	24.4	63.1	81.6
CM_Bw_HNT	71	26.2	65.3	79.3

T_f-first shrinkage temperature, T_s-shrinkage temperature and T_l-last shrinkage temperature [6]
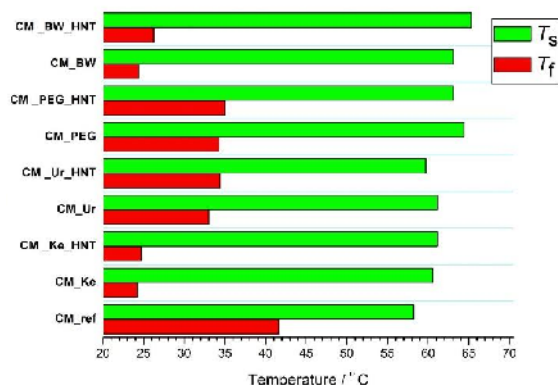
Figure 1. Values of main shrinkage temperature T_s and first shrinkage temperature T_f before and after the consolidation treatment

ATR-FTIR Measurements

The ATR-FTIR spectra of the treated and untreated samples are shown in Figures 2 and 3, for corium side and gran side, respectively. The HNTs characteristic bands at 3695 cm^{-1}, 3624 cm^{-1}, 1027 cm^{-1}, 908 cm^{-1}, 529 cm^{-1} and 463 cm^{-1} are evident for the CM_Bw_HNT_c and CM_Ur_HNT_f spectra suggesting the presence of the nanotubes on the corium and grain surface of these samples, as demonstrated by SEM observations (Figure 5). On the other part the Ur_HNT dispersion shown a much better penetrability

on the leather corium side. The much lower intensity or the absence of these bands for the samples treated with Ke_HNT and PEG_HNT dispersions indicate a more effective penetration of the nanotubes into the structure of the leather.
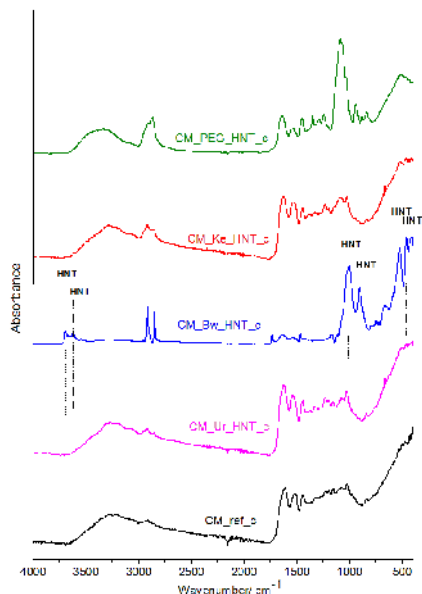
Figure 2. ATR-FTIR spectra of untreated and treated leather samples - corium side
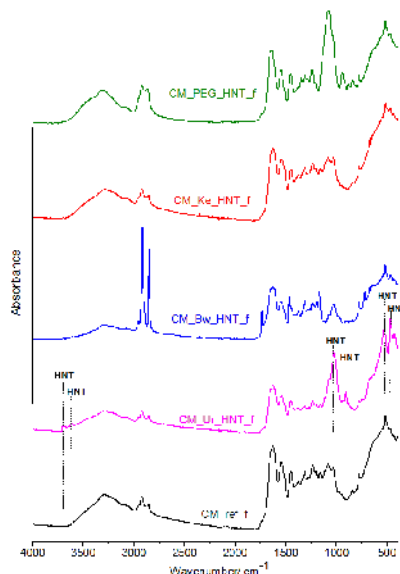
Figure 3. ATR-FTIR spectra of untreated and treated leather samples - grain side

SEM Observations

SEM high-resolution images of the network of collagen fibres on the surface of parchment were used to assess their state and follow their deterioration (Della Gatta *et al*., 2005). SEM furnished a collection of local images that show a network of integral collagen fibres with clear contours and sharp edges (Figure 4). No shape changes resulted after the treatments using various HNTs dispersions, only a slight coating effect was observed in the case of leather treated with the Bw_HNT dispersion (Figure 5).

Wettability Measurements

The hydrophobic effect is generated only by the BW treatment, the presence of HNT causing an increase in the contact angle by up to 10-15° (Figure 6). For all other treatments the presence of HNT caused a slight hydrophilic effect.

NMR MOUSE Measurements

The overall model of water hydration in collagenous tissues/materials involves the monomolecular layer in which the water molecules are H-bonded to the helical structures and several outer polymolecular layers which are considerably more mobile (Bella *et al*., 1995). The specific interaction between water and such structures has an important

contribution to the stabilization of the investigated materials. The values of spin-spin (T2eff) and spin-lattice (T1) relaxation times obtained for the investigated leathers and listed in Table 2 show a significant difference between untreated and treated samples.
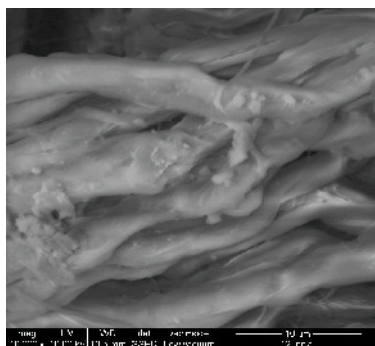
Figure 4. High magnification SEM showing the typical morphology of intact fibre network - untreated leather sample
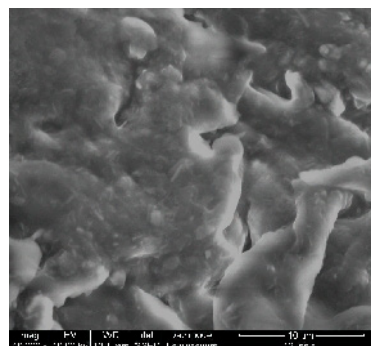
Figure 5. High magnification SEM showing the presence of HNTs on the grain surface of CM_Bw_HNT sample

T_1 values increase suggesting that the degree of ordering of water in all treated samples decreases. On the other part, $T_{2eff-long}$ clearly differentiates between the samples treated with urea (CM_Ur_HNT) and keratin hydrolysate (CM_Ke_HNT) and that treated with PEG (CM_PEG_HNT), suggesting a destabilising effect of the latter.
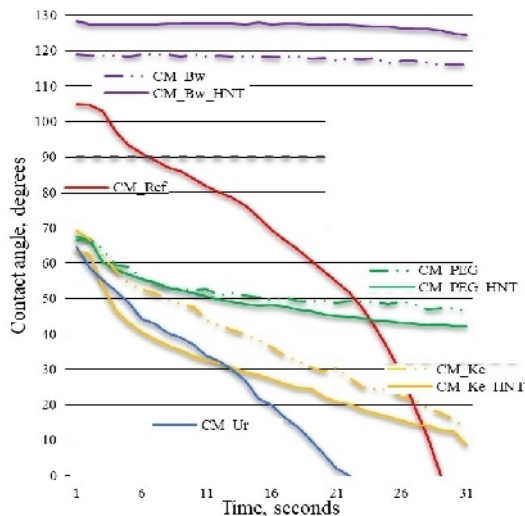
Figure 6. The variation of contact angle value on time depending for all types of treatments

193

Table 2. Values of spin-lattice relaxation time T_1, and spin-spin relaxation times $T_{2\text{eff\_long}}$ and $T_{2\text{eff\_short}}$ in untreated and treated leathers

Sample/ Treatment	Spin-lattice relaxation time, T_1	Spin-spin relaxation time, $T_{2\text{eff}}$	
	T_1 (ms)	$T_{2\text{long}}$ (ms)	$T_{2\text{short}}$ (ms)
CM_Ref	34.5	2.71	0.01
CM_Ur_HNT	37.9	2.27	0.01
CM_PEG_HNT	37.2	4.56	0.01
CM_Ke_HNT	37.3	2.45	0.01

CONCLUSIONS

The main conclusions can be summarized as follows:

- All treatments result in an increase in thermal stability at the macroscopic level, while at the microscopic level there is an increase in the degree of heterogeneity.
- The rehydrating effect increases in the order of PEG_HNT <Ke_HNT <Ur_HNT
- The hydrophobic effect is generated only by BW_HNT treatment.

Acknowledgments

REFERENCES

Badea, E. *et al*. (2014), "Validazione di interventi di recupero conservativo di manufatti in pergamena", in *Lo Stato dell'Arte 12*, Nardini Editore, Florence, 463-470.

Badea, E. *et al*. (2016), "Unilateral NMR and thermal microscopy studies of vegetable tanned leather exposed to dehydrothermal treatment and light irradiation", *Microchem J*, 129, 158-165, https://doi.org/10.1016/j.microc.2016.06.013.

Bella, J., Brodsky, B. and Berman, H. (1995), "Hydration structure of a collagen peptide", *Structure*, 3(9), 893-906, https://doi.org/10.1016/S0969-2126(01)00224-6.

Carşote, C. *et al*. (2014), "Characterization of a byzantine manuscript by infrared spectroscopy and thermal analysis", *Rev Rou Chim*, 59(6-7), 429-436.

Cavallaro, G. *et al*. (2014), "Halloysite nanotubes as sustainable nanofiller for paper consolidation and protection", *J Therm Anal Calorim*, 117, 1293–1298, https://doi.org/10.1007/s10973-014-3865-5.

Cavallaro, G. *et al*. (2015), "Thermal and dynamic mechanical properties of beeswax-halloysite nanocomposites for consolidating waterlogged archaeological woods", *Polym Degrad Stab*, 120, 220-225, https://doi.org/10.1016/j.polymdegradstab.2015.07.007.

Della Gatta, G. *et al*. (2005), "Assessment of damage in old parchment by DSC and SEM", *J Therm Anal Cal*, 82, 637-649, https://doi.org/10.1007/s10973-005-0944-7.

Haines, B.M. (1977), "Deterioration in leather bookbindings - our present state of knowledge", *The British Library Journal*, 3(1), 59-70.

Ludwick, L. (2012), "A comparative study on surface treatments in conservation of dry leather", PhD Thesis, Göteborgs Universitet.

Sendrea, C. *et al*. (2017), "The effect of gamma irradiation on shrinkage activity of collagen in vegetable tanned leather", *Revista de Chimie*, 68(7), 1535-1538.

PEPTIDE NANOPHOTONICS – FROM BIO-WAVEGUIDES TO INTEGRATED PHOTONIC DEVICES

AMIR HANDELMAN[1], BORIS APTER[1], GIL ROSENMAN[2]

[1]*Faculty of Engineering, Holon Institute of Technology, Holon, Israel, handelmana@hit.ac.il*

[2]*Tel Aviv University, Faculty of Engineering, Physical-Electronics Department, Tel Aviv, Israel*

Optical waveguiding phenomena in bioinspired chemically synthesized peptide nanostructures can be used to revolutionize emerging fields of precision medical trials and health monitoring. New biomedical light therapy tools and implantable optical biochips can be produced using bioinspired peptide nanostructures due to a unique combination of their intrinsic biocompatibility and remarkable multifunctional optical properties. This essay highlights a new field of peptide nanophotonics. It covers peptide nanotechnology and fabrication processes of peptide integrated optical circuits, basic studies of linear and nonlinear optical phenomena in biological and bioinspired nanostructures, and passive and active optical waveguiding in peptide nanostructures. We show that optical properties of this new generation of biooptical materials are governed by fundamental biological processes. Refolding of the peptide secondary structure is followed by wideband optical absorption and visible tunable fluorescence. In peptide optical waveguides, such a new biooptical effect leads to switching from a passive waveguiding mode in native α-helical phase to an active one in β-sheet phase. Discovery of an active waveguiding effect in β-sheet fiber structures below the optical diffraction limit opens an avenue for future development of new bionanophotonics devices using ultrathin peptide/protein fibrillar structures for advanced biomedical and nanotechnology applications.

Keywords: bioinspired peptide nanostructures, optical waveguides, photonic integrated devices.

INTRODUCTION

The field of nanophotonics combines fundamental physics, advanced optical materials, and nanotechnology. Optical waveguides (Hunsperger, 2009), which confine and guide light within their structures, are the basic components of integrated chips that can be used in various applications. Such integrated devices that include optical waveguides and combine linear and nonlinear optical and electronic circuits can be used as building blocks of optical communication devices (Prasad, 2004). Medical analysis techniques and disease monitoring are other examples of applications that can benefit from integrated chips that include optical waveguides and photonic devices (Yun and Kwok, 2017).

Nowadays, both biomedical research and clinical research are focused on development of nano- and micro-tools and advanced methods of diagnosis, therapy, and surgery (Vanneman *et al.,* 2012). Photonic technologies are crucial in such new developments for rapid application of the emerging precise light theranostics in medical trials (Humar *et al*., 2016). Light strongly influences basic biological processes that stimulate application of new biomedical photonic techniques that exploit diverse photochemical, photobiological, and photothermal (Mohammad-Hadi *et al*., 2018) effects and methods of light-induced therapies, such as photodynamic and optogenetic therapies in addition to traditional optical bioimaging and diagnostics (Paragios *et al.*, 2014).

Here we present a new paradigm of emerging biooptical physics and nanotechnology based on multifunctional bioinspired peptide nanomaterials toward new biomedical nanotherapy tools and implantable integrated optical biochips. Recent research revealed that peptide nanostructures poses unique set of optical properties

such as nonlinear optical, electrooptical (Gilboa *et al.*, 2017), and optical waveguiding effects (Handelman *et al.*, 2016; Handelman *et al.*, 2018). These newly discovered properties of peptide nanostructures paved the way toward new physics of light propagation in biological and bioinspired nanostructures followed by nanofabrication of optical peptide waveguides. Such nanoscale light waveguides of biological origin can be applied in biomedical theranostics and optical implantable biochips where they are integrated with operating electronics. This new field of peptide nanophotonics (Handelman *et al.*, 2018) is the main subject of my talk.

EXPERIMENTAL

Light waveguiding is observed in two different regimes passive and active[10]. The passive mode guides the injected light through its optical transmission window and is described by the classical optics of reflection, refraction and diffraction. The key problem in passive optical waveguiding circuits is effective coupling of a light beam to POW. To provide light coupling in our peptide rectangular structures, we designed and fabricated a planar FFF-POW-based Y-splitter for the blue spectral range by incorporating of diffractive grating coupling elements at all of its three ports using FIB-tool (Figure 1a,b). The FDTD simulations were performed by the use of the grating coupler realistic 3D model imported to the FDTD simulation software from AFM image data (Figure 1a). Figure 1 demonstrates the experimental results of effective light coupling, waveguiding, splitting and outcoupling under broadband white LED illumination of the input grating.
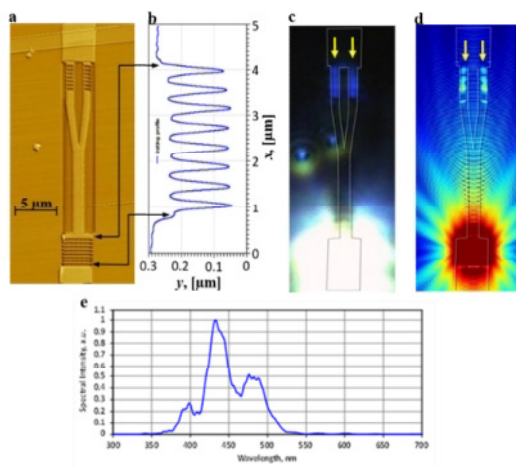
Figure 1. Experimental and simulation observation of the efficient optical coupling, waveguiding and outcoupling in the 1x2 optical-power Y-splitter under white LED illumination of the input grating.

RESULTS AND DISCUSSION

Two elongated, blue light spots observed at the output gratings (Figure 1c) indicate selective wave coupling through grating elements, acting also as an optical filter. The FDTD simulations setup with reproduced experimental conditions shows a good agreement with our experimental data (Figure 1c,d).

CONCLUSIONS

We introduced all-peptide photonic integrated splitter, composed of bioinspired planar peptide wafers of a large area treated by high resolution patterning. This development opens the avenue for a new field of peptide integrated biooptics where multifunctional peptide optical materials can be fabricated as optical integrated circuits combined with electronic components and interconnections towards lab-on-biochips. Further feature of these peptide structure is their ability to transform from passive to active waveguiding regime in peptide materials by reconfirmation of their secondary structure.

Acknowledgement

REFERENCES

Gilboa, B. *et al*. (2017), "Strong Electro-Optic Effect and Spontaneous Domain Formation in Self-Assembled Peptide Structures", *Adv Sci*, 4, 1700052, https://doi.org/10.1002/advs.201700052.

Handelman, A. *et al*. (2016), "Linear and nonlinear optical waveguiding in bio-inspired peptide nanotubes", *Acta Biomater*, 30, 72, https://doi.org/10.1016/j.actbio.2015.11.004.

Handelman, A. *et al*. (2018), "Peptide integrated optics", *Adv Mater*, 30, 1705776. https://doi.org/10.1002/adma.201705776.

Humar, M. *et al*. (2016), "Toward biomaterial-based implantable photonic devices", *Nanophotonics*, 5, 60-80, https://doi.org/10.1515/nanoph-2016-0003.

Hunsperger, R. (2009), *Integrated Optics: Theory and Technology*, Springer, Berlin, 2009.

Mohammad-Hadi, L. *et al*. (2018), "Photodynamic therapy in 3D cancer models and the utilisation of nanodelivery systems", *Nanoscale*, 10, 1570, https://doi.org/10.1039/C7NR07739D.

Paragios, N. *et al*. (2014), *Handbook of Biomedical Imaging: Methodologies and Clinical Research*, Springer, USA.

Prasad, P.N. (2004), *Nanophotonics*, John Willey & Sons, Inc.

Vanneman, M. and Dranoff, G. (2012), "Combining immunotherapy and targeted therapies in cancer treatment", *Nat Rev Cancer*, 12, 237, https://doi.org/10.1038/nrc3237.

Yun, S.H. and Kwok, S.J.J. (2017), "Light in diagnosis, therapy and surgery", *Nat Biomed Eng*, 1, https://doi.org/10.1038/s41551-016-0008.

STUDIES ON STRUCTURAL, SURFACE MORPHOLOGICAL, OPTICAL, LUMINESCENCE AND UV PHOTODETECTION PROPERTIES OF SOL GEL OXIDES THIN FILMS

ABDELHAFID MAHROUG, RABIE AMARI, AMMAR BOUKHARI, BAHRI DEGHFEL, E. BEN REZGUA

University of Mohamed BOUDIAF, Laboratory of Materials Physics and its Applications,28000 M'sila, Algeria, hafidmahroug938@gmail.com

ZnO and ZnCoO thin films have been deposited onto glass substrates by sol–gel spin coating method. Zinc acetate dihydrate, cobalt acetate tetrahydrate, Isopropanol and monoethanolamine (MEA) were used as a precursor, doping source, solvent and stabilizer respectively. The molar ratio of MEA to ions metal was maintained at 1.0 and a concentration of metal ions is 0.6 mol.L^{-1}. The XRD results showed that both films crystallized under hexagonal wurtzite structure and presented a preferential orientation along the c-axis with the maximum crystallite size was found is 25nm. Atomic force microscope (AFM) images revealed the good uniformity for both films, an increase of surface roughness is observed with doping. The average transmittance in the visible region was higher than 85% for both films and the optical band gap of Zinc oxide films decreased with Co doping. Photoluminescence of the films showed a ultraviolet (UV) and defect related visible emissions like violet, blue and green, and indicated that cobalt doping resulted in red shifting of UV emission and the reduction in the UV and visible emissions intensity. Ours thin films shows the best photocurrent properties.

Keywords: Sol–gel technique; TM-doped Zinc Oxide thin film; Structural properties; Optical properties; Luminescence; Defects

INTRODUCTION

In recent years, Zinc oxide has attracted great interests because of their potential applications in optics and optoelectronic devices such as ultraviolet (UV) photodetectors, light-emitting diodes (LEDs), laser diodes (LDs), catalysts, gas sensors and transparent conducting electrodes (Hou *et al*., 2014; Mahroug *et al*., 2014; Abeda *et al*., 2015; Vijayalakshmi *et al*., 2014) due to its wide band-gap (3.37eV) and large exciton binding energy (60 meV) (Özgür *et al*., 2005). Additionally, the excellent optical properties of ZnO and the possibility of band gap engineering through transition metal ions (TM = Co; Mn; Ni …) doping strongly encourages the exploration of the magneto-optical properties of the TM-doped ZnO system. Various deposition techniques have been used to prepare ZnO thin films. Among these techniques, sol-gel method has a distinct advantage: simple, economic and easy to perform doping incorporation (Mahroug *et al*., 2014). In this study, ZnO and ZnCoO thin films have been deposited on glass substrates by sol– gel spin coating process and the effects of the Co doping on the structural morphological, and optical properties of the films have been investigated.

EXPERIMENTAL DETAILS

ZnO and ZnCoO (3%mol Co) thin films were prepared on glass substrates, using sol-gel spin coating technique, Zinc acetate dihydrate ($Zn(CH_3COO)_2.2H_2O$) with 0.6mol/L, cobalt acetate tetrahydrate [$Co(CH3COO)_2.4H_2O$] (3%mol) isopropanol and monoethanolamine (MEA) were used as a precursors, solvent and stabilizer, respectively. The solutions underwent a stirring at 55°C for 2 hours to be homogenous

and clear, followed by aging at room temperature during 24h. The resulting solutions were deposited at 2500 rpm for 30 s. After each coating, the films were preheated at 250°C for 10 min. Finally, these films were annealed at 500°C for 1h.

Structural and morphological properties of the films were analysed using XRD with Cu Kα line (λ= 0.154 nm) and atomic force microscopy AFM with tapping mode. The optical properties were obtained by transmission spectra (UV-Vis in 300- 800 nm region), photoluminescence spectroscopy (using a 325 nm xenon lamp as excitation source). The photocurrent measurements were performed in an electrochemical cell using a UV light of 365nm.

RESULTS AND DISCUSSION

Structure and Surface Morphology of ZnO Thin Films

Figure 1a shows the XRD patterns of ZnO and ZnCoO thin films. The results indicate that both samples are polycrystalline hexagonal wurtzite structure and no other crystalline phase was found. The intensity of the diffraction peaks is decreased with Co content, indicating that the film crystallinity is deteriorated. The preferential orientation was determined using a texture coefficient TC(hkl) (Caglar, 2013). A sample with randomly oriented crystallite presents TC(hkl) = 1, while values higher than 1 indicate the abundance of crystallites in a given (hkl) direction. After the calculation of texture coefficients, It is seen that the highest TC values (TC = 1.5) are in (002) plane for both films. which indicates that the films grew preferential c-axis orientation. The crystallite size of the films was estimated by the Scherrer formula (Mahroug et al., 2014): $D = K\lambda / \beta\cos\theta$, where D is crystallite size, K is constant of 0.9, λ is X-ray wavelength, β is full width at half maximum, θ is diffraction angle, respectively. The (002) peaks were used to estimate the crystallite size. The calculated average crystallite sizes of ZnO and ZnCoO thin films are 25, 24nm, respectively. Compared with undoped ZnO, cobalt doping in ZnO thin films resulted with a slightly decrease in crystallite size. The surface morphology of the films is studied by atomic force microscopy in tapping mode and it gives information about surface roughness and average grain size of the films. 2D and 3D surface images over a 1×1 μm^2 area and histogram of films are shown in Figure 1b. Good uniformity is observed for both films. The root-mean square (RMS) surface roughness strongly increased with Cobalt dopant. The roughness values of ZnO and ZnCoO thin films are 9 nm and 23 nm respectively. As remarked in the histograms, significant shift of the particle height distributions to high values with Co doping. Indeed a rough surface of the film shows an interest for certain applications such as solar cells.

a

b   *ZnO*
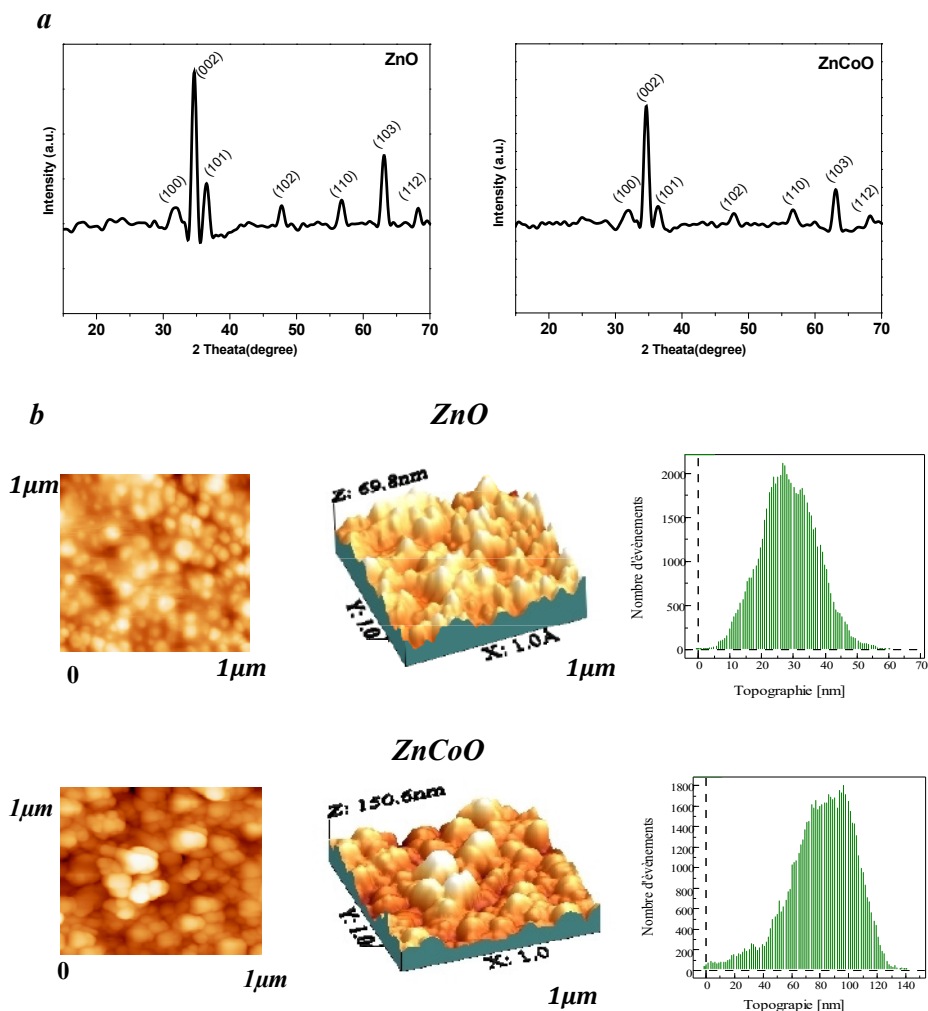
ZnCoO

Figure 1. XRD patterns (a) and tapping mode AFM images (2D and 3D) of surface morphologies (b) of ZnO and ZnCoO thin films

Optical Properties

Transmittance

The optical transmittance spectra of thin films in the wavelength range 300- 800 nm at room temperature are shown in Figure 2a. The average transmittance in the visible region was higher than 85% for both films. Further, an red shift of the absorption edges can be observed in the doped thin film. Compared with pure ZnO film, three absorption

bands in visible region appear in the spectra of the ZnCoO thin films. These three absorption bands are attributed to the transitions of Co^{+2} ions substitute for Zn^{+2} ions in the hexagonal ZnO wurtzite structure (Weakliem, 1962). To evaluate the bandgap energy (E_g) from the optical absorption spectra, $(\alpha h\nu) = A(h\nu-E_g)^{1/2}$ (Mahroug et al., 2014) relationship is employed, where α is the absorption coefficient (α = -1/D lnT, where T is the transmittance and D is the film thickness), A is a constant, hν is the photo energy, E_g is the optical bandgap. The bandgap is then evaluated by extrapolating the linear region of $(\alpha h\nu)^2$ vs. the photon energy. The optical band gap energy decreases from 3.28 to 3.25eV with Co dopant. This decrease can be attributed to the sp–d spin–exchange interaction between the band electrons and the localized d electrons of the Co^{2+} ions substituting Zn^{+2} ions (Belghazi et al., 2009).

Luminescence Properties

Photoluminescence (PL) spectroscopy was used to study the luminescence properties of ZnO thin films. Figure 2b shows the room temperature photoluminescence emission spectra of ZnO and ZnCoO thin films. Both films exhibit an UV emission at 380nm, is originated from the exciton recombination corresponding to the near-band edge transition (NBE) of ZnO (Li et al., 2012), and more visible emissions peaks are observed at 409nm, 442nm, 472 nm and 520 nm, which may be attributed to the energy of transition of electron from conduction band to the V_{Zn}, the energy of transition of electron from Zn_i to valence band, the electron transition from the level of the ionized oxygen vacancies to the valence band and the transition from Zn_i to O_i levels, respectively (Xu et al., 2001; Elilarassi and Chandrasekaran, 2013; Sabri et al., 2012). The UV emission is seen to display red shift and the emission peaks intensity decreased with Co dopant.
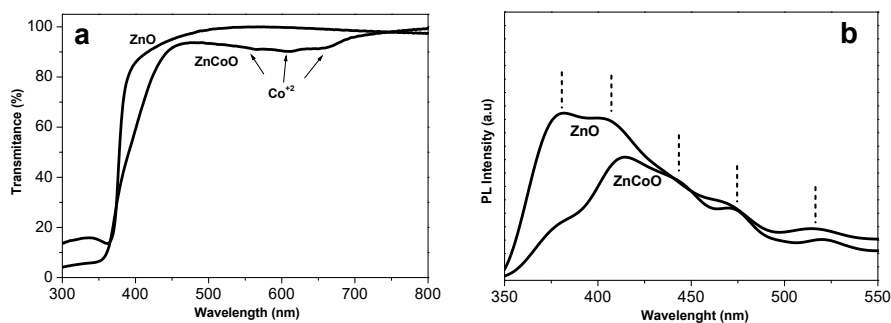
Figure 2. Transmittance spectra of ZnO and ZnCoO thin films (a), Photoluminescence (PL) spectra of ZnO and ZnCoO thin films (b)

UV Photodetection and Photocurrent Studies

Fig.3 shows the photo-response of the ZnCoO thin films obtained by a chronoamperometric method under intermittent illumination with a 365 nm wavelength light. The photocurrent curve has an almost rectangular response under light illumination with a significant increase of current. This is due to the increase of electrical conductivity of semiconductor material, by generating of electron-hole pair,

when light with energy greater than the band gap energy is absorbed (Mahroug *et al.*, 2014).
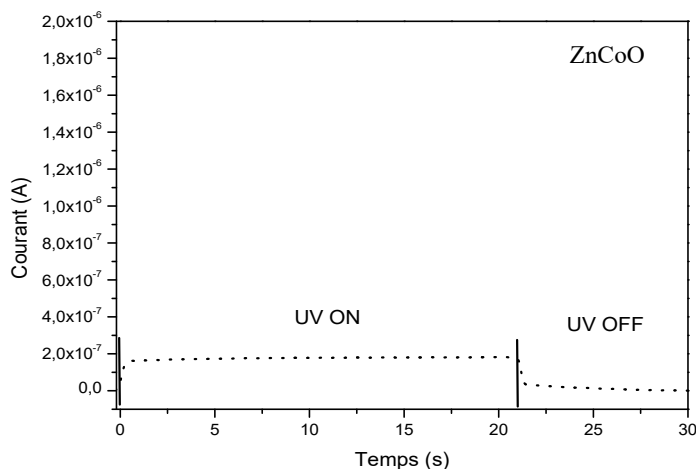
Figure 3. Photocurrent response of ZnCoO thin film

CONCLUSIONS

ZnO and ZnCoO thin films were prepared using a sol–gel spin coating method.

The X-ray diffraction spectra indicated that the films are polycrystalline with a hexagonal wurtzite structure, high *c*-axis orientation, along the (002) plane and the maximum crystallite size of about 25 nm. AFM studies revealed the good uniformity for both films, an increase of surface roughness is observed with Co. The average transmittance in the visible region was higher than 85% for both films and the optical band gap of Zinc oxide films decreased with Co doping. PL analysis of films shows an UV emission at 380nm, and violet, blue and green emission. Co doping causes a red shift of UV emission, a reduction in the intensity of UV and visible emissions. Our films presented photo-responses and a significant photocurrent was observed.

REFERENCES

Abeda, C. *et al.* (2015), "Mg doping induced high structural quality of sol–gel ZnO nanocrystals: Application in photocatalysis", *Appl. Surf. Sci.*, 349, 855, https://doi.org/10.1016/j.apsusc.2015.05.078.

Belghazi, Y. *et al.* (2009), "Elaboration and characterization of Co-doped ZnO thin films deposited by spray pyrolysis technique", *J. Microelectronics*, 40, 265, https://doi.org/10.1016/j.mejo.2008.07.051.

Caglar, Y. (2013), "Sol–gel derived nanostructure undoped and cobalt doped ZnO: Structural, optical and electrical studies", *J. Alloys Compd*, 560, 181, https://doi.org/10.1016/j.jallcom.2013.01.080.

Elilarassi, R. and Chandrasekaran, G. (2013), "Influence of Co-doping on the structural, optical and magnetic properties of ZnO nanoparticles synthesized using auto-combustion method", *Mater. Sci: Mater Electron*, 24(1), 96-105, https://doi.org/10.1007/s10854-012-0893-4.

Hou, Y., Mei, Z. and Du, X. (2014), "Semiconductor ultraviolet photodetectors based on ZnO and Mg$_x$Zn$_{1-x}$O", *J. Phys. D: Appl. Phys.*, 47, 283001, https://doi.org/10.1088/0022-3727/47/28/283001.

Li, P. *et al.* (2012), "Structural and optical properties of Co-doped ZnO nanocrystallites prepared by a one-step solution route", *J. Luminescence*, 132, 220-225, https://doi.org/10.1016/j.jlumin.2011.08.019.

Mahroug, A. *et al*. (2014), "Structural, optical and photocurrent properties of undoped and Al-doped ZnO thin films deposited by sol–gel spin coating technique", *Mater. Lett.*, 134, 248, https://doi.org/10.1016/j.matlet.2014.07.099.

Özgür, Ü. *et al*. (2005), "A comprehensive review of ZnO materials and devices", *J. Appl. Phys.*, 98, 041301, https://doi.org/10.1063/1.1992666.

Sabri, N.S. *et al*. (2012), "Emission properties of Mn doped ZnO nanoparticles prepared by mechanochemical processing", *J. Lumin.*, 132, 1735, https://doi.org/10.1016/j.jlumin.2012.02.020.

Vijayalakshmi, K. *et al*. (2014), "Growth of high quality ZnO:Mg films on ITO coated glass substrates for enhanced H2 sensing", *Ceram. Int.*, 40, 6171, https://doi.org/10.1016/j.ceramint.2013.11.070.

Weakliem, H.A. (1962), "Optical Spectra of Ni2+, Co2+, and Cu2+ in Tetrahedral Sites in Crystals", *J. Chem. Phys.*, 36, 2117, https://doi.org/10.1063/1.1732840.

Xu, P.S. *et al*. (2001), "Electronic structure of ZnO and its defects", *Sci. China Ser.*, A44, 1174, https://doi.org/10.1007/BF02877436.

NEW STRUCTURED EMULSIONS BASED ON RENEWABLE RESOURCES GENERATED BY LEATHER AND FUR INDUSTRY, WITH APPLICATION IN AGRICULTURE

DEMETRA SIMION[1], CARMEN GAIDĂU[1], CORINA CHIRILĂ[1], MARIANA DANIELA BERECHET[1], MIHAELA NICULESCU[1], DORU GABRIEL EPURE[2]

[1]*INCDTP - Division: Leather and Footwear Research Institute, 93 Ion Minulescu St., 031215, Bucharest, Romania, icpi@icpi.ro*

[2]*SC Probstdorfer Saatzucht Romania SRL, 20 Siriului St., 1, Bucharest, Romania*

The paper is focused to development of new structured emulsions, based on bolaform and gemini surfactants and collagen, keratin additives, with applications in agriculture as foliar fertilizers. Collagen and keratin are renewable resources generated by leather and fur industry. The preparation of new emulsions was based on optimisation of main parameters system: composition, emulsifiers, shearing speed and temperature in a two-stage process. The used lipophilic nonionic emulsifier is a long chain fatty acid ester-isopropyl oleate, the hydrophilic emulsifier is a diester of sucrose and a vegetable oil in order to obtain a multiple water-oil-water emulsion due to the ability of surfactants to orient and make honeycomb formations. The saturation of an aqueous solution of collagen and keratin hydrolysates with microelements was done up to 40% by using 2% of diester of sucrose. Due to biodegradability, nontoxicity, adherence to surfaces, surfactants based on sugar may used as fertilizers in agriculture. We have elaborated a new method for including microelements and collagen or keratin hydrolysates in emulsions, with application as a new class of foliar fertilizer. Experiments regarding the nutritional and biostimulation capacity on plant growth, were performed with dilutions of these new structured emulsions on wheat seeds (Tamino and Mirastar type) and plants. The germination of wheat seeds was monitored and a stimulation effect was recorded against the control samples. The use of new emulsions in foliar fertilization of wheat plants indicated an increase in plant length as compared to the water-treated control samples, which demonstrates a stimulating growth effect.

Key words: bolaform and gemini surfactants, new structured emulsions, foliar fertilizers for agriculture

INTRODUCTION

The aim is to create new structured emulsions based on surfactants (bolaform and gemini) and collagen, keratin additives with potential applications in agriculture as foliar fertilizers.

Collagen and keratin additives are renewable resources generated by leather and fur industry. Bolaamphiphiles and Gemini are new classes of amphiphilic surfactants with large potential of applications due to the high ability to deliver active substances (Niculescu and Gaidau, 2014). In this study the nonionic lipophilic emulsifier is a long-chain fatty acid ester-isopropyl oleate, the hydrophilic emulsifier - sucrose diester, and thyme oil.

The aim is saturation of an aqueous solution of microelements or collagen/keratin hydrolysate (<40%) in an aqueous solution of sucrose diester (2%). The hydrophilic properties of non-ionic surfactants are provided by hydroxyl groups (OH), ether linkages (-O-), amide groups (-CONH-), etc. Such groups are found in sugar, polyethers and similar combinations. Sugar esters and ethers with tenside properties are known as surfactants based on carbohydrates.

Surfactants used in this study, figure 1, are sucrose esters - *R alkyl radicals C_8-C_{18}.*
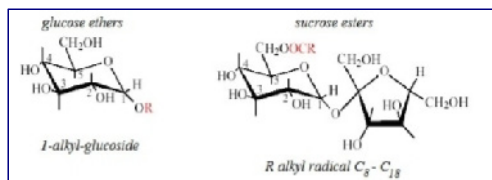
Figure 1. Representation of sucrose ethers and esters (Gaidau *et al*., 2013)

Experiments regarding the nutritional and biostimulation capacity on plant growth were performed with dilutions of new structurated emulsions obtained on wheat seeds (Tamino and Mirastar type) and plants (Gaidau *et al*., 2009). The germination and growth of the plants were monitored and a stimulation was recorded against the control samples. Other formulations aimed at obtaining foliar blends containing microelements, collagen and keratin hydrolysates that have been applied to wheat plants. The results indicated an increase in plant length by 20% as compared to the water-treated control samples, which demonstrates a stimulating growth effect. The good results obtained in applications of keratin and collagen hydrolysates introduced in the new structured emulsions dilutions, in the agriculture show that can be used as foliar fertilizers with ecological effects.

RESULTS AND DISCUSSION

Technological Process of Obtaining New Structured Emulsions

The two-step emulsification process is used in this paper, where the result is a multiple nanostructured emulsion due to the properties of surfactants used to orient and form honeycomb formations at the nano and micro levels. The main types of multiple emulsions are water-oil-water and oil-water-oil. Two types of emulsifiers are used: a hydrophobic I one, isopropyl oleate (for W/O emulsion) and a hydrophilic II one-diester of sucrose based on sugar (for O/W emulsion). In the first step, water, vegetable oil (3%), lipophilic-isopropyl oleate surfactant (2%) are added and homogenized by stirring at 60°C to obtain a water-oil emulsion. In step II a solution of microelements saturated up to 40% (or collagen/keratin hydrolysate) and a sugar-based surfactant-hydrophilic-diester (2%) are added to the water-oil emulsion, and homogenized by stirring at 60°C, obtaining a multiple water-oil-water emulsion (W/O/W).
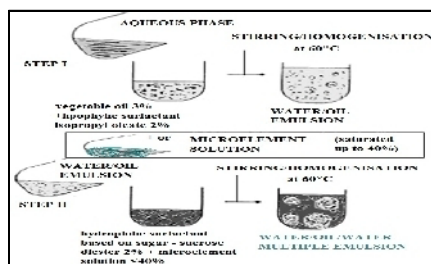
Figure 2. Representation of the two-step technological process of obtaining nano- and micro- structured emulsions (Gaidau *et al*., 2013)

Finally, a multiple W/O/W nano and microstructured emulsion is obtained by mixing/stirring at 60°C. The thermal introduction of phase inversion for oil-water concentrated emulsions is preceded by obtaining a W/O/W emulsion. The technological process is analogous to obtaining emulsions by replacing microelements with collagen hydrolysate or a 1:1 hydrolysed collagen-keratin blend. In order to obtain new structured nano and microemulsions an important part is to select the characteristics of the working parameters: system composition, emulsifiers, shear rate, tension, stirring speed, temperature. Long-chain fatty acid esters, including isopropyl oleate, vegetable oils, have been used to vary the physico-chemical properties of multiple emulsions as well as to attempt to control the transfer rate of the solute through the oil phase. Structured and stable micro and nanoemulsions are formed, able to incorporate microelements or collagen/keratin hydrolysates with a 40% saturation, and the properties derive from the surfactants used, as well as the conditions and working parameters. In our research we have elaborated a new method for including micoelements and collagen or keratin hydrolysates in stable emulsions with the final purpose of application as a new class of foliar fertilizer.

Characterisation of New Structured Emulsions

The three types of emulsions with: microelements (MC), collagen hydrolysates (HC) and collagen/keratin hydrolysate (HK) mixture were characterized by dynamic light diffusion and optical microscopy. Dynamic light diffusion test showed that all three types of emulsions are nano and microstructured. The size, percentage of the particles and Zeta potential were determined (indicating their stability). MC emulsions have sizes ranging between: 42 nm, 225 nm, 5269 nm and Zeta potential was: -20.7 mV. HK emulsions have particle sizes ranging between: 109.7 nm, 621.8 nm, 3371 nm with value of -13.5 mV for Zeta potential. For the third sample, HC, with collagen hydrolysate, experimental results are given emulsion particles of 44.8 nm and 776.3 nm and Zeta potential was -2.74 mV. The influence of high molecular weights of collagen and keratin were revealed through higher particle size of emulsions and lower value for Zeta potential. Optical microscopy images (Figure 3) show that emulsions with collagen/keratin hydrolysate (HK) and emulsions with microelements (MC) are structured in honeycomb formations and only the collagen hydrolysate (HC) emulsions are oriented and agglomerated in a chain. The results are in agreement with literature data (Nuraje et al., 2013) related to the formation of honeycomb and chain structures in multiple water-oil-water emulsions.

Figure 3. Optical microscopy images (1000x) of emulsions structures: a) honeycomb of HK emulsion; b) honeycomb of MC of; c) chain structure of HC emulsion

Dilutions of the four samples made using the presented technology, as follows: 1) emulsion with microelements only (MC), 2) emulsion with collagen hydrolysates (HC) and 3) emulsion with collagen/keratin hydrolysate (HK) in 1:1 ratio and 4) emulsion with keratin hydrolysate (HK). Dilutions of these four samples are presented in Table 1.

Table 1. Dilutions of obtained and tested samples

Sample	Dilution 1
1	10 ml of sample 2) + 990 ml distilled water (solution I)
2	14 ml of sample 4) + 986 ml distilled water (solution II)
3	10 g of sample 1) + 990 ml distilled water (solution III)
4	6 g of sample 3) + 994 ml distilled water (solution IV)
	Dilution 2
5	42 ml of solution I + 956 ml distilled water
6	255 ml of solution II + 745 ml distilled water
7	231 g of solution III + 769 ml distilled water
8	442 ml of solution IV + 558 ml distilled water
	Dilution 3
9	2,3 ml of sample 3) + 997,7 ml distilled water
10	Control

The four solutions, I-IV, from Table 1 were also microbiologically tested, to determine behaviour to fungal attack of *Fusarium* spp, carrying out analysis seven days from inoculations, with images presented in figure 4.
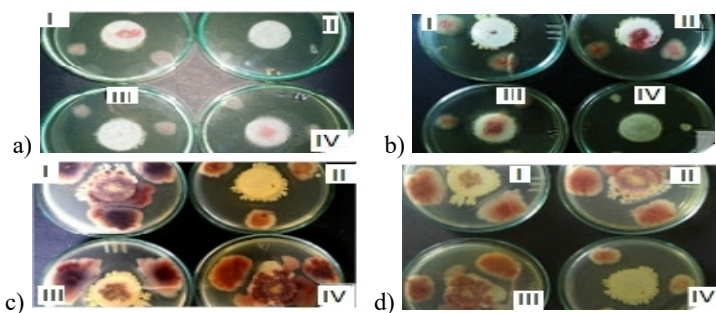
Figure 4. Images of the 4 solutions I-IV (from Table 1) with fungal attack of *Fusarium spp* for 7 days: a) after 2 days; b) after 3 days; c) after 6 days; d) after 7 days

After 7 days the appearance of the 4 solutions attacked by Fusarium spp is shown in figure 5.

| solution I | solution II | solution III | solution IV |

Figure 5. Images of the 4 solutions I-IV (from Table 1) with fungal attack of *Fusarium spp* for 7 days

The best results were registered for solution II which contains only keratin hydrolysate. The evolution of solution II upon Fusarium spp attack for 7 days was presented in figure 6.

a)	b)	c)	d)
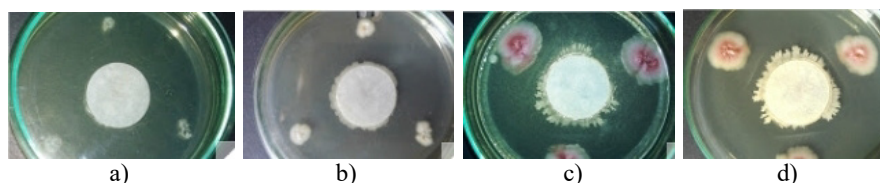
Figure 6. Images of solution II (from table 1) with fungal attack of *Fusarium spp* for 7 days: a) after 2 days; b) after 3 days; c) after 6 days; d) after 7 days

Experiments regarding the nutritional and plant growth biostimulation capacity, were performed with dilutions 1-10 (table 1) of these new structured emulsions on wheat seeds (Tamino and Mirastar type) and plants. The germination of wheat seeds was monitored and a stimulation effect was recorded against the control samples. Experiments on wheat seeds indicated a biostimulatory effect in the first 5 days of germination in the presence of samples 1-10 from table 1. For Mirastar wheat type sample 6 from table 1, containing keratin hydrolysate, showed the highest germination rate and the shortest germination time, figure 7.

Figure 7. Germination rate evolution of sample 6 Mirastar wheat

Samples 2 and 3 from table 1 had a strong phytotoxic effect on both types of wheat. Samples 6 and 7 from table 1 stimulated germination in both Tamino and Mirastar types. Germination rate for the two types, Tamino and Mirastar, ar comparatively presented for the 10 sampes from table 1, in figure 8.
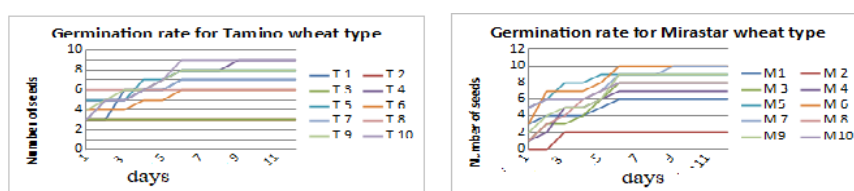
Figure 8. Germination rates for the two types of wheat, Tamino and Mirastar for the 10 samples from table 1

The experimental on obtaining foliar blends containing microelements, collagen and keratin hydrolysates that have been applied to wheat plants showed an increase in plant length by 20% as compared to the water-treated control samples, which demonstrates a stimulating growth effect. The good results obtained in applications of keratin and collagen hydrolysates in agriculture show that they can be the basis for obtaining new biomaterials with various ecological applications.

Plants were sprayed with the 10 samples from table 1, and shown in figure 9.

Figure 9. a) Method of spraying plants with the 10 samples from table 1; b) Growth of
plant stimulated with the 10 samples, after 10 days

The use of new emulsions in foliar fertilization of wheat plants indicated an increase in plant length as compared to the water-treated control samples, which demonstrates a stimulating growth effect.

CONCLUSIONS

Studies from this research report led to the following conclusions:

- The most effective method of obtaining multiple emulsions (e.g. phase inversion, single step emulsification, etc.) is the two-step emulsification process
- Inversion of multiple emulsion phases occurs when the dispersed droplets are packed tightly into the fluid in which they are suspended
- The thermal induction of phase inversion for O/W concentrated emulsions is preceded by obtaining an W/O/W emulsion. When an aqueous solution of a hydrophilic emulsifier is introduced into an oil containing a lipophilic surfactant, the W/O/W emulsion is obtained due to the inversion of the phases by modifying the HLB of the surfactant mixture.

REFERENCES

Gaidau, C. *et al*. (2009), "Additives and advanced biomaterials obtained from leather industry by-products", *Revista de Chimie*, 60, 5, 501-507.
Gaidau, C. *et al*. (2013), "New Mixes Based on Collagen Extracts with Bioactive Properties, for Treatment of Seeds in Sustainable Agriculture", *Current Pharmaceutical Biotechnology Journal*, 14, 9, 792-801, https://doi.org/10.2174/1389201014666131227112020.
Niculescu, M.D. and Gaidau, C. (2014), "New collagen extracts conditioned for applications in crop protection against pests", *Revista de Chimie*, 65, 12, 1457-1461.
Nuraje, N. *et al*. (2013), "Bolaamphiphilic molecules: Assembly and applications, Progress", *Polymer Science*, 38, 302– 343.
Tran, H.D. *et al*. (2011), "The oxidation of aniline to produce "polyaniline": a process yielding many different nanoscale structures", *J Mater Chem*, 21, 3534-3550, https://doi.org/10.1039/C0JM02699A.
Varasteanu, D.S. (2014), "Surfactants based on proteins - Obtaining and applications" (in Romanian), PhD thesis, "Politehnica" University of Bucharest.

III.

EMERGING TECHNIQUES

DUE DILIGENCE FOR HEALTHY WORKPLACES IN THE EUROPEAN TANNING INDUSTRY

LUMINIȚA ALBU[1], GHEORGHE BOSTACA[1], DOREL ACSINTE[2]

[1]*INCDTP-Division Leather and Footwear Research Institute, 93 Ion Minulescu str., sector 3, 031215, Bucharest, Romania, email: icpi@icpi.ro*

[2]*Romanian Leather & Fur Producers Association (APPBR), 93 Ion Minulescu str., sector 3, 031215, Bucharest, Romania, email: appb.ro@gmail.com*

Corporate Social Responsibility is vital to pursue the systemic changes needed within business and value chains to achieve the Sustainable Development Goals (https://www.un.org/sustainabledevelopment/sustainable-developmentgoals/). The fashion industry is no exception. Much needs to be done in Global Value Chains of the fashion industry to redress reputation, regain its appeal and respect its ambitions. COTANCE and industriAll-Europe, the leather sector's European Social Partners, want to spearhead this process in their Industry. The health & safety in tannery workplaces represents a key priority for leather value chains and the Social Dialogue at sector level is the right instrument for setting Due Diligence standards which are technically feasible, appropriate and effective, and can lead businesses to exploit new opportunities and gain enhanced competitiveness. In the frame of an EU sponsored Social Dialogue project, with the support of the University of Northampton (UK), was launched a survey to find out more about the levels of maturity and integration of health and safety practices in tannery workplaces and its communication along the leather value chain. This paper presents the main outcomes from this survey (http://www.euroleather.com/index.php/ documents/245-due-diligence-survey-report).

Keywords: tanning industry, safety & healthy workplaces.

INTRODUCTION

Leather is a fabulous product. It is the result of the recycling of hides and skins of animals slaughtered for the production of meat for human consumption. Without tanneries, these organic residues, if not properly disposed of, would constitute a major health hazard. Thanks to its beauty and usefulness, leather has become a globally traded commodity generating a global value of trade of over 82 billion US dollars (FAO stat) annually. Nearly every country in the World has a tanning sector, but not all work to meet correct social or environmental standards.

A survey was set up to explore current practices in reporting and communicating health and safety risks along the leather supply chain and how they are managed in tanneries. The aim was to provide a snapshot of the current situation within the value chain in relation to the perceived importance, reporting models, motivations and certification/auditing practices on health and safety in company-owned or outsourced tannery operations.

The COTANCE and industriAll-Europe survey ran from October 2017 to February 2018 in the context of their EU-funded Social Dialogue project. They were assisted by the University of Northampton (UoN) for collating the survey results.

The survey's target audience consisted of all the leather value chain stakeholders, from those directly involved in the production of leather, to those producing and selling leather articles to the final consumers and including suppliers of machinery and

chemicals as well as miscellaneous organisations following the leather sector such as NGO's, associations, hide traders, consumers, consultants and designers, etc.

This paper presents the main conclusions of the Social Partners of the European Leather Industry. With leather being a 'Global Value Chain', the research reflects practices that span beyond European borders and the implications from the findings have global resonance for the leather value chain.

Due Diligence Leather project was carried out within the framework of the European Social Dialogue and was funded by the European Commission. The project was leaded by COTANCE (Confederation of National Associations of Tanners and Dressers of the European Community) & industriAll Europe (European Trade Union), and the partners were the following leather national owners' associations: UNIC (Italy), VDL (Germany), ACEXPIEL (Spain), FFTM (France), UKLF (UK), APPBR (Romania), SG (Sweden).

METHODOLOGY

The research adopted a quantitative methodological approach to the data collection process, which involved the design and build of an online survey. The online survey was launched between October 2017 and February 2018 and responses were sought via email sent to pre-identified stakeholders. The survey's target audience consisted of:

- Tanneries and Trade Unions
- Brands and Leather Buyers
- Tannery Suppliers
- Other Stakeholders
- (NGOs, research centres, regulators, consultants and federations).

The survey sought to provide quantitative data that would answer the overall research aim and three specific research questions:

- *How European tanneries are regulated and controlled with regard to key health and safety requirements, and whether or how their own leather supply chain can be monitored?*
- *How leather products manufacturers and importers set tannery workplace standards and monitor tannery workplace conditions in their supply chain?*
- *How observers and other stakeholders observe and interact with the leather value chain?*

The survey was designed specifically for each of the four stakeholder groups so as to ensure that the questions were context specific. However, there were a high number of questions that were the same across the surveys, so as to ensure that the research could also engage in comparative analysis between groups. The survey was designed in English, before being translated by the project partners into six other language versions (German, Spanish, French, Italian, Portuguese and Romanian). Each of the survey language versions contained all four of the stakeholder group sub-surveys.

In total, 238 participants responded to the survey, giving an estimated response rate (based upon the primary database engaged) of 34.1%. The respondents were engaged from 27 different countries globally, although 92.9% (n=221) of the respondents were from Europe. However, participants did engage from across the globe including: North America (n=5); South America (n=1); Asia (n=6); Middle East (n=1); Oceania (n=2); and Africa (n=2). The data can therefore be viewed as global in scope, albeit with a strong focus towards the European leather market. This European bias to the sample

should not be viewed negatively, but rather as a representative factor of the global leather value chain and the role that Europe can play in improving H&S standards in other regions. All data was analysed in SPSS version 22.0 or Stata. Both are statistical analysis software packages that allow detailed examinations of datasets, over and above mere comparisons of averages. The analysis included descriptive tests (means and median average values), and comparative analysis using cross-tabulation Pearson Chi-squared tests.

The latter Chi-squared tests allows for a comparison of two or more categorical datasets to see if the observed differences between them arose by chance or not (e.g. differences in yes/no responses amongst the different stakeholder groups). This allows the research to state whether there are indeed significant differences between different stakeholder responses or not.

Figure 1. Due diligence survey questionnaires structure
(http://www.euroleather.com/index.php/documents/245-due-diligence-survey-report)

RESULTS AND DISCUSSIONS

There is no hesitation among European leather value chain partners in clearly ranking workplace health and safety as a key priority (Figure 2).
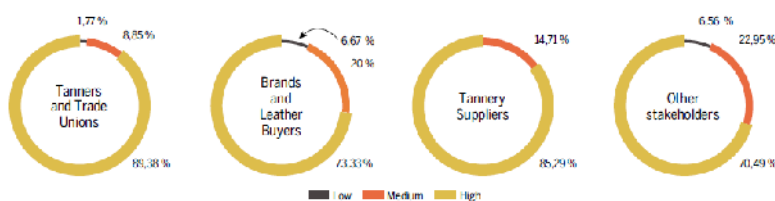
Figure 2. Ranking of Health & Safety as a priority

Internal transparency, however, seems to be a common feature in the majority of businesses in the leather supply chain. Leather buyers and sellers make their Health & Safety Risk Assessment Reports (H&S RAR) available to personnel, with 70% of tanneries and trade unions and 77% of brands and leather buyers doing so (Figure 3). The EU-OSHA Directive 89/391/EEC "Framework Directive" indicating that it is the responsibility of employers to inform employees regarding the risks associated with the work they conduct, seems to be widely acknowledged in the sector.
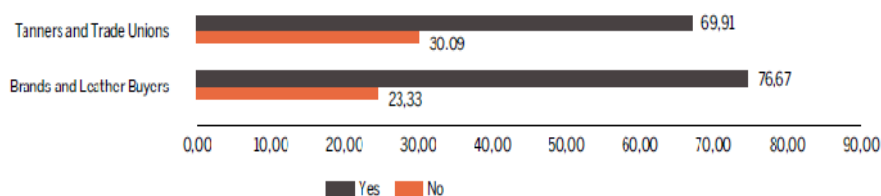
Figure 3. Availability of the H&S RAR for all the personnel (%)

All stakeholder groups concur in general that a H&S RAR is a useful tool for testifying how workplace safety is managed in a tannery (Figure 4). However, there are some differences between groups, that are most likely related to their position in the leather value chain. Interestingly, the number of respondents in the 'other stakeholder' group, without an opinion, is relatively large (39%). The 'other stakeholder' group is composed of NGOs, research centres, and consultants, of which a certain number may not necessarily be acquainted with H&S RARs. However, 56% agree about the usefulness of the instrument. All other groups show a much higher trust rate, with four-fifths of tanners and trade unions and tannery suppliers, and nearly 97% of brands and leather buyers, answering in the affirmative.
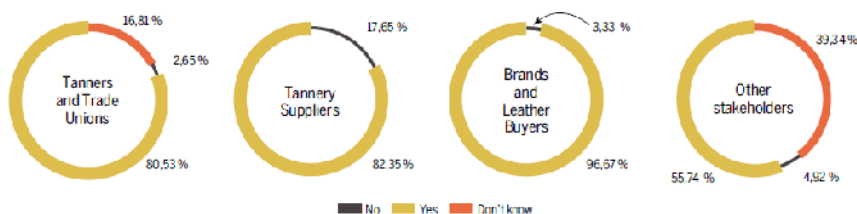
Figure 4. Usefulness of the H&S RAR, for each stakeholder group (%)

The survey investigated which tannery specific references for workplace safety the stakeholders were aware of, proposing a number of answers, including both tannery specific (OiRA Tannery Tool) and non-tannery specific (SA 8000, ISO, CEN), as well as an environmental auditing protocol with a certain reputation in the leather sector, but that does not have a H&S section (LWG).

The results demonstrate that, to a large extent, all four stakeholder groups ignore the only tannery-specific tool for tannery workplace risk assessment (Figure 5). ISO, a system of standards that provides only a framework that needs to be adapted to the specific needs of the sector, is the leading reference point, followed by the LWG which does not address H&S in its auditing protocol. SA 8000, a generic tool, occupies the third rank.

The least recognized reference is OiRA, only known/used by 6% of respondents overall, albeit nearly 10% of tanneries and trade unions were aware of it. OiRA was developed in 2012 and after 5 years of existence has already reached a certain sector audience. There is, however, a high potential for the OiRA tannery tool.
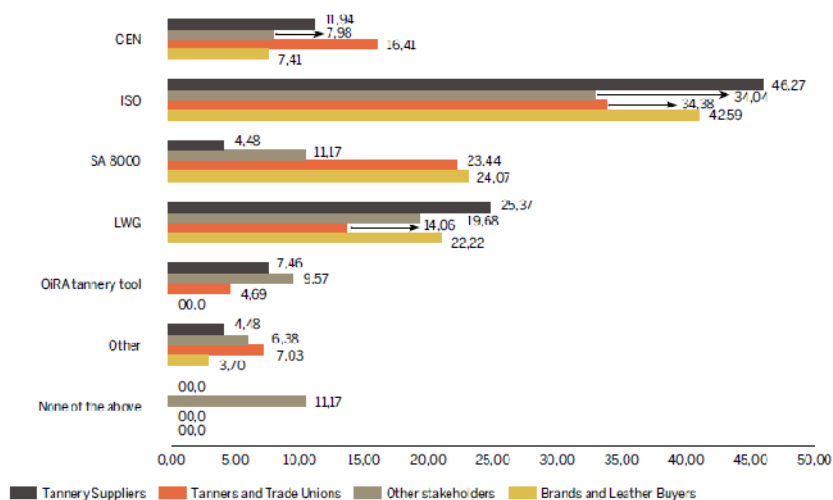
Figure 5. References for workplace safety acknowledged by the stakeholder groups (%)

The majority of stakeholders have not considered the free OiRA tool for the identification of tannery workplace risks, and tanners and their customers do not use this instrument for setting up their company RAR (for the former) or the H&S requirements to suppliers (for the latter) (Figure 6).

This result evidences the low awareness of the OiRA tool in the leather value chain. However, with respect to the dimension of the organization, the results show that 'large' and 'medium' enterprises are less likely to use the OiRA tool. Therefore, OiRA use and awareness is more prevalent in smaller organisations.
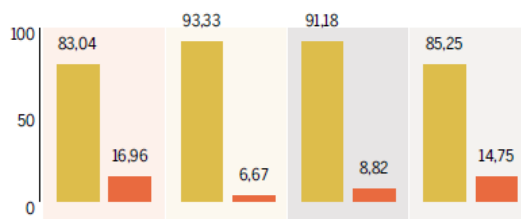
Figure 6. The use of the Online Interactive Risk-Assessment for Tanneries (%)

All the results and main conclusions of the Social Partners of the European Leather Industry are presented in *Due Diligence for Healthy Workplaces in the Tanning Industry – Final Report* (http://www.euroleather.com/index.php/documents/245-due-diligence-survey-report).

With leather being a 'Global Value Chain', the research reflects practices that span beyond European borders and the implications from the findings have global resonance for the leather value chain.
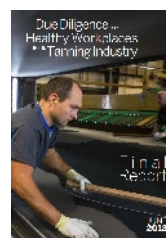
CONCLUSIONS

▪ Tannery workplace safety is a key priority across leather value chain partners, but maturity levels vary in understanding how to implement due diligence;

▪ There is a wide confusion across stakeholders about sector specific instruments used to assess tannery workplace safety, while the OiRA tannery tool deserves to be more widely known;

▪ The customers of leather down the value chain (brands and retail groups) have a key role to play in furthering health & safety in tannery workplaces;

▪ Implementing due diligence for health and safety at tannery workplaces bears great business opportunities, while failure to enforce good practice involves high risks and loss of competitiveness.

Acknowledgments

REFERENCES

*** https://www.un.org/sustainabledevelopment/sustainable-developmentgoals/
*** http://www.euroleather.com/index.php/documents/245-due-diligence-survey-report

INNOLEA - INNOVATION FOR THE LEATHER INDUSTRY IN JORDAN AND EGYPT

LUMINIŢA ALBU[1], VIORICA DESELNICU[1], PANAIYOTA VASSILEIOU[2], DANA CORINA DESELNICU[3], MAHMOUD SAYED ABDELSADEK[4], SAHAR EL BARKY[5], FAHMI ABU AL RUB[6], FADEL ALLABADI[7], EHAB AL-GHABEISH[8], DESIREE SCALIA[9], LINA TSAKALOU[10], ALCINO MARTINHO[11], VIRGINIJA JANKAUSKAITE[12]

[1]INCDTP-Division Leather and Footwear Research Institute, Bucharest, RO

[2]National Technical University of Athens, GR

[3]University POLITEHNICA Bucharest, Bucharest, RO

[4]South Valley University, EG

[5]Arab Academy for Science Technology & Maritime Transport, EG

[6]Jordan University of Science and Technology, JO

[7]Amman Chamber of Industry, JO

[8]Al-Balqa Applied University, JO

[9]Centro Italiano Per L'Apprendimento Permanente, IT

[10]Creative Thinking Development, GR

[11]Centro Tecnológico das Indústrias do Couro, PT

[12]Kaunas Technologijos Universitetas, LT

The paper presents the project INNOLEA, which is a three-year capacity building project co-funded by European Commission through Erasmus+ Program. The project aims to fill an apparent gap in the area of specialized services for the leather sector in Jordan and Egypt and to utilize the experience and expertise of EU partners to establish four-leather-research centers within the universities of both countries.

Keywords: leather center, leather quality, innovation, competitiveness

INTRODUCTION

INNOLEA is a three-year Erasmus+ project co-funded by European commission which aims o fill an apparent gap in the area of specialized services for the leather sector in Jordan and Egypt and to utilize the experience and expertise of EU partners to establish four-leather-research centers within the universities of both countries.

These centers will help the project partners in both countries to implement the various tasks of the project and to provide access to the stakeholders in the leather sector to business development services, such as quality testing, product certification, training, fashion trends, production organization, funding opportunities in order to develop this sector and improve its competitiveness.

The project also aims to create and maintain cooperation among Universities and businesses in EU, Jordan, and Egypt and to foster the innovation and manufacturing of high value and quality products of leather.

Project duration: 15.10.2017-14.10.2020.

AIMS & OBJECTIVES

● INNOLEA project aims to fill an apparent gap in the area of specialized services for the leather sector with the establishment of four leather centres in local Universities,

two in Jordan and two in Egypt, utilizing the experience and expertise of EU partners in the area of services for the leather sector.

• Through the creation of these centres and the further tasks that will be implemented in this project, the leather sectors in Jordan and Egypt will be offered access to business development services, such as quality testing, product certification, training, fashion trends, production organization, BtoB and funding opportunities, and subsequently the Jordanian and Egyptian leathers sector will have a valuable ally for its further development;

• The project also aims to create and maintain a link between Universities and businesses of the leather sector that will foster innovation and the manufacturing of high value quality products, as well as further cooperation between EU and Jordan and Egypt Universities and leather businesses;

• The project also aims to help encourage the Egyptian and Jordanian governments to favour the establishment of leather centres within universities and to promote research and projects between EU and Egypt and Jordan universities in the leather sector, by creating a research innovation and training network, which will continue to operate and after the end of the current project.

CONSORTIUM

The consortium was established on the basis of combining the different backgrounds, experience and expertise of the partners. it includes all the skills, recognised expertise and competences required to carry out all aspects of the work programme. The consortium comprises 12 institutions from 7 countries representing different parts of Europe and the Mediterranean.

There is a mixture of institutions with different profiles, capacities and complementary competences that are appropriate for the development of the work programme (higher education institutions, companies and non profit institutions, research and training centres and business associations).

Most of the partners are experienced in implementing transnational projects, required to carry out all aspects of the project work programme and complement one another regarding their role in the project. in this manner, the project provides for a stable partnership.

PROJECT PARTNERS

- ✓ NTUA National Technical University of Athens (Greece) - *Coordinator*
- ✓ AAST Arab Academy for Science Technology & Maritime Transport (Egypt);
- ✓ ACI Amman Chamber of Industry (Jordan);
- ✓ BAU Al-Balqa Applied University (Jordan);
- ✓ CIAPE Centro Italiano Per L'Apprendimento Permanente (Italy);
- ✓ CRETHIDEV Creative Thinking Development (Greece);
- ✓ CTIC Centro Tecnológico das Indústrias do Couro (Portugal);
- ✓ INCDTP- Division ICPI Institutul de Cercetare Pielarie Incaltaminte (Romania);
- ✓ JUST Jordan University of Science and Technology (Jordan);
- ✓ KTU Kauno Technologijos Universitetas (Lithuania);
- ✓ SVU South Valley University (Egypt);
- ✓ UPB Universitatea Politehnica din Bucuresti (Romania).

WORK PACKAGES

The project comprises a set of implementation activities that will materialize the project objectives, supported by preparation, management, quality and dissemination activities that will ensure the propagation of its results even after the project has ended.

WP1 Research and state of the art - LEAD: JUST

Preparation activities the result of which is the creation of a cross-country research report which will contain an analysis of the importance of the leather sector for the economies of Egypt and Jordan, the training needs for staff in leather centres, and the most favourite pedagogical approach for trainers of staff in the leather centres.

In order for the report to be produced, complementing desk and field research shall be performed in both direct beneficiaries countries (Egypt and Jordan), based on a methodology created specifically for the research, with an aim to obtain a realistic view of the national leather sectors regarding its needs, prospects, and anticipated services. The other local partners could provide these two organisations with information and contacts.

WP2 Capacity building and setting up of leather centres - LEAD: UPB

A capacity building programme will be prepared and implemented to enhance the skills of Jordanian and Egyptian experts in running and managing leather centres, followed by the actual setup and operational organization of the Leather Centres. The activities carried out in this stage are the core part of the project.

At this stage, the centres will be equipped with basic leather testing equipment and the relative books and standard protocols, after their staffs has undergone an advanced Capacity Building training in the EU leather centres' premises, based on appropriately developed training material.

EU partners as well as Chambers of Commerce of the two countries will help in the setting up of the centres and in testing their operation. A business model will also be developed for the leather centres, to support their sustainability as well as a collaboration platform that will be used as a shared workspace and the ground of new projects and joint activities. The main outcome from this activity is the Leather Centres pilot operation, which will provide validation of the successful operation of the centres and their readiness to enter into a sustainable cooperation with businesses from the leather sector.

WP3 Quality Evaluation - LEAD: CRETHIDEV

Quality evaluation will be present throughout the duration of the project, making use of milestones and indicators in order to accurately determine whether the project is on schedule and the objectives are continually met. The outcomes of each activity shall be evaluated before the finalisation of the deliverables of the activity, in the context of the validation step of each activity.

WP4 Dissemination and Exploitation - LEAD: CIAPE

Dissemination will be thoroughly described and guided through a dissemination and exploitation plan. Dissemination tools include the development of a database of contacts, printing of brochures, a website for the project, social media presence, the organization of two roundtables, organization of a final conference in Egypt for the propagation of results etc.

EXPECTED RESULTS

◊ The Universities where the leather centers will be established will have the opportunity to expand the fields of their applied research to topics regarding leather.

◊ The staff of the leather centers will be trained by European partners, experts in offering services to the leather sector, gaining, thus, from their experience in setting up and managing this kind of centers.

◊ The collaboration website platform that will be set up will be a virtual space aiming at favouring collaboration, where the leather centers and other stakeholders interested in the leather sector will be able to communicate with each other, to be informed about activities, developments and trends, events, projects, funding opportunities, other players, similar institutes or have access to useful links (associations of the leather sector, other Institutes, standardization bodies etc) in the region and worldwide.

◊ Through the dissemination activities and tools (roundtables, database of contacts, project website and online collaterals, brochures, newsletters and recommendations on "How leather centres are useful for the economic development of the region") that will be developed and implemented in the two countries during the project's lifespan, the following target groups will be reached and informed about the project and its outcomes as well as its potential results: Relevant stakeholders such as companies, BIOs, policy-makers, training centers, investment promotion agencies, corporate executives and investors, International Finance Institutions providing funds for development, researchers and academics and representatives of civil society.

◊ The sustainable business model for leather centers that will be created will be the basis for the creation of more leather centers in the two countries or in the whole region.

◊ With the creation of the centers, the leather sector will have a valuable interlocutor when discussing with Policy makers. The latter, on the other hand, will be able to consult experts in the field of leather, in their decision making.

CONCLUSION

After project finalization will be obtained: a) - Establishing and equipping of **4 leather centres,** in **2** Jordanian and **2** Egyptian universities; b) **- Fostering academia-industry collaboration in the leather industry**; c) **- Capacity building of staff**, working in leather manufacturing and tannery: Promoting their potentials for better safety and quality.

REFERENCES

*** http://innolea.just.edu.jo

LEAMAN - MANAGER IN AN EFFICIENT AND INNOVATIVE LEATHER COMPANY

LUMINIȚA ALBU[1], ALCINO MARTINHO[2], DIMOS PAPAKONSTANTINOU[3], ROSA ANA PÉREZ FRANCÉS[4], MALGORZATA SIKORSKA[5], DESIREE SCALIA[6], CARLOS VAZ DE CARVALHO[7], VIORICA DESELNICU[1]

[1]*INCDTP-Division Leather and Footwear Research Institute, Bucharest, Romania*

[2]*Centro Tecnológico das Indústrias do Couro, Portugal*

[3]*Creative Thinking Development, Greece*

[4]*INESCOP - Instituto Tecnologico Del Calzado Y Conexas, Spain*

[5]*FRP - Fundacja Rozwoju Przedsiebiorczosci, Poland*

[6]*Centro Italiano Per L'Apprendimento Permanente, Italy*

[7]*Virtual Campus, Portugal*

The leather industry, as a global industry, being highly dependent on access to raw materials and to export markets, is in a quickly changing business environment, which is particularly challenging for SME-dominated sectors, as are the leather and leather related ones. In order to remain competitive, businesses must be able to adapt to changes. Shortage of raw materials, the globalisation of production, environmental reasons, and the change of the profile of the leather industry outside EU, have caused a consequent change in the model for the leather production in Europe. However, Europe remains the leader in fashion, design and quality, as well as in leather science and technological innovation. There are opportunities in new technologies and new, innovative materials as well as in exports also as the demand in emerging markets is growing. Within that context, the necessary qualification requirements for working in the European leather industry must be redefined in order for the labour market to be reinvigorated with skilled professionals that will offer their full potential to the industry. Consequently, there is a need to restructure the leather production model across Europe towards an innovation and export oriented mentality. This change would require the leather manger to possess more and transverse skills, both technological and non-technological. Subsequently, the industry must better anticipate and manage change, and adapt to the future skills requirements. The paper presents the LEAMAN project aims and main outcomes that will result in better qualified professionals in the European leather and leather associated industries and promote both lifelong learning and equal opportunities in the knowledge-based society.

Keywords: managerial skills, innovative leather company

INTRODUCTION

The leather industry, as a global industry, being highly dependent on access to raw materials and to export markets, is in a quickly changing business environment, which is particularly challenging for SME-dominated sectors, as are the leather and leather related ones. In order to remain competitive, businesses must be able to adapt to changes. Shortage of raw materials, the globalisation of production, environmental reasons, and the change of the profile of the leather industry outside EU, have caused a consequent change in the model for the leather production in Europe.

However, Europe remains the leader in fashion, design and quality, as well as in leather science and technological innovation. There are opportunities in new technologies and new, innovative materials as well as in exports also as the demand in emerging markets is growing.

Within that context, the necessary qualification requirements for working in the European leather industry must be redefined in order for the labour market to be reinvigorated with skilled professionals that will offer their full potential to the industry. Consequently, there is a need to restructure the leather production model across Europe towards an innovation and export oriented mentality. This change would require the leather manger to possess more and transverse skills, both technological and non-technological. Subsequently, the industry must better anticipate and manage change, and adapt to the future skills requirements.

LEAMAN aims to create a framework that will result in better qualified professionals in the European leather and leather associated industries. Through the creation of a European Qualification Framework (EQF), with the use of ECVET scores, the project aims to promote both lifelong learning and equal opportunities in the knowledge-based society, as well as the further integration of the European labour market for all relevant professionals, such as existing and potential managers in the leather industry. LEAMAN addresses both technological and non-technological issues, from leather science to the application of new technologies, and from fundamental managerial skills, financial or project management skills, to issues regarding health and safety at the workplace, social responsibility or traceability in the leather value chain.

The partnership enroled in this project was established on the basis of combining the different backgrounds, experience & expertise and comprises the following partners:

- ✓ CTIC - Centro Tecnológico das Indústrias do Couro (Portugal) - *Coordinator*
- ✓ CIAPE - Centro Italiano Per L'apprendimento Permanente (Italy)
- ✓ CRE.THI.DEV (Greece)
- ✓ FRP - Fundacja Rozwoju Przedsiebiorczosci (Poland)
- ✓ INCDTP - Division Leather & Footwear Research Institute (Romania)
- ✓ INESCOP - Instituto Tecnologico Del Calzado Y Conexas (Spain)
- ✓ VC - Virtual Campus (Portugal)

The main objective of LEAMAN project is to provide a set of instruments to re-engineer the leather industry and to offer to the existing and aspiring managers the most up-to-date information and knowledge tools.

This will be reached through the following **specific objectives**:

- A research report, based on desk and field research, depicting the state of the art for the leather and connected industries;
- A European Qualification Framework (EQF) of the New Manager for Efficient and Innovative Leather SMEs;
- The MOOC Being a manager in an Efficient and Innovative Leather Company: freely accessible and open licensed training platform dedicated to the improvement of knowledge and skills of managers and potential managers;
- A Virtual Challenge Community, a community made of relevant stakeholders active in the sector of leather and connected ones;
- A Decalogue of benefits deriving from the collaboration between companies, research and training centers.

LEAMAN project aims to reach a large number of persons inside and outside the partnership, by maximizing the visibility of the project, promoting the projects' objectives and results, by creating a level of involvement of relevant stakeholders and ensuring that the project potential audience will be as large and relevant as possible. This was done by using different communications activities and channels (the training MOOC platform, social networks, newsletters, meetings, multiplier events, and the innovative leather product competition and crowd-funding campaign), by promoting the project and its results among European involved and/or interested organizations, and, at a national and regional/local level, by promoting the project results among target organisations and end-users.

The **target groups** of the project are:

➢ VETs, policy-makers, associations and organisations dealing with leathers, universities, research centres dealing with the project topics, companies (both the leather and the connected ones) and trainers;

➢ Managers of the leather industry and potential ones, managers of the leather connected industries and potential ones will be offered an up-to-date open access training course appropriate to their actual needs with technological and non-technological contents;

➢ 1500 persons in total are expected to be impacted, by one way or another, by the project results, either by their participation in multiplier events (6 Multiplier Events are envisaged – one in each participating country), learning labs and validation workshops or by registering to the Virtual Challenge Community, by using the EQF, by visiting and testing the MOOC and the platform, by getting informed by the newsletter and by participating in the innovative leather products competition.

ACTIVITIES AND RESULTS

A comprehensive **Analysis of State of the art and the Training Needs of the sector**, identified by the managers and VET providers from participating countries.

✓ The first part - **State of the art**, based on a desk research;

✓ The second part - **The field Survey Analysis** - implemented using 2 different questionnaires that were defined based on the desk research results and designed according to standard research methodology:

Need Analysis & State of the Art - Research Report

• *Questionnaire* for Managers and Potential Managers - 31 questions - 123 respondents

• *Questionnaire* for Experts&VET professionals - 22 questions - 70 respondents

Based on the research report, an **European Qualification Framework (EQF)** of the New Manager for Efficient and Innovative leather SMEs, was produced in order to serve as a reference tool to compare the qualification levels of the different qualifications systems and will be constructed around existing EQF at national levels, inputs, addressing knowledge, skills and competences, organised in learning outcomes.

EQF Definition of the new manager for efficient and innovative leather SME's

The methodology for development of the Training Programme:
- Definition of the units of learning outcomes;
- Establishing of ECVET points;
- Assessment of learning outcomes.

The steps of the developing process are presented in the following chart:
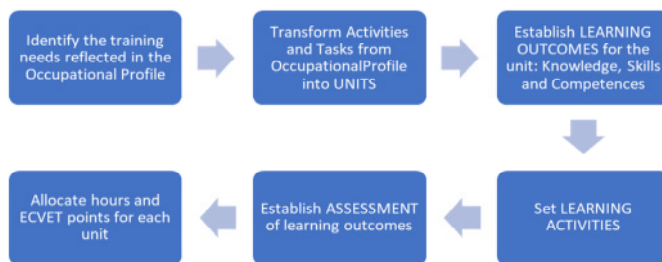
The Activities and Tasks from the occupational profile have been transformed into the following Units of the Training Programme:

Unit 1. Human resources and innovation management
Unit 2. Business management and internationalization
Unit 3. Tanning processes development
Unit 4. Standardization and Quality Control
Unit 5. Environmental impact of the tanning industry
Unit 6. Health and Safety at Work (HSW) at tanning company

Each Unit has a main Objective and the EQF definition has been established by transforming the Knowledge, Skills, autonomy and responsibility from the previous Occupational Profile.

Training units, hours, ECVET points		
	EQF 5	
UNIT	Hours	ECVET points
Unit 1. Human resources and innovation management	140	8
Unit 2. Business management and internationalization	280	16
Unit 3. Tanning processes development	240	16
Unit 4. Standardization and Quality Control	140	8
Unit 5. Environmental impact of the tanning industry	140	8
Unit 6. Health and Safety at Work (HSW) at tanning company	60	4
TOTAL	1000	60

According to the results of the field survey, the content of the training material and the **MOOC** (Massive Open Online Courses) *"Being a manager in an Efficient and Innovative leather company"* was produced, being focused on specific knowledge and skills for actual managers and potential ones of leather industries and connected fields. The MOOC will be freely accessible and open licensed.

The MOOC has the following structure (7 Units x 4 Lessons):
1: Business Management
2: Innovation management
3: Leather processes development
4: Standardization and Quality Control
5: Environmental impact of the tanning industries
6: Health and Safety at Work
7: Personal and transversal skills

The Virtual Challenge Community - another result **-** is integrated by relevant stakeholders active in the sector of leather and connected ones and aims to facilitate the exchange of information, knowledge and experience. It also served as a platform for **the innovative leather products competition** that will, till the end of the project, lead to the launch of a crowd funding campaign for the winners of the competition for the most innovative leather products.

Leaman Competition

The purpose of the Competition was to promote innovative leather products, services, solutions or technologies and inspire interested stakeholders' creativity.

Participants to the competition were asked to share ideas and brainstorm for creating innovative leather products. The ideas of innovative leather products were voted online. The Competition was opened for all interested stakeholders from partners countries: Greece, Italy, Poland, Portugal, Romania and Spain. Participants were required to submit their submissions based on the application forms (stage 1) via the Virtual Challenge Community platform and prepare business plans (stage 2) and presentations on VCC platform and on partners websites (stage 3) before the date of 15.06.2018 for submission online. Stage 4 included online voting for the best ideas and took place between 16-30.06.2018. Three projects with the highest score were awarded.
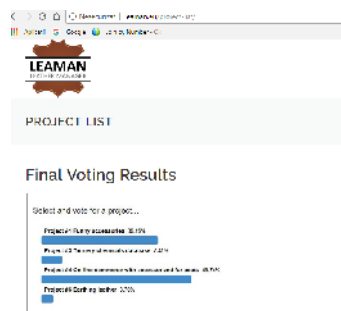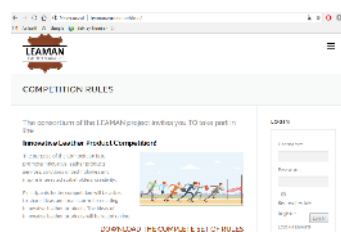
Stage 5 concerned announcement of the results at the meeting in Poland on 5.07.2018 and on partners websites and VCC platform. In stage 6 three of the best projects will be submitted to Indiegogo.com platform for crowdfunding – this stage is in developing now.

Furthermore, the virtual community will host the **Decalogue** of benefits deriving from the collaboration between companies, research and training centres in developing innovative leather products.

CONCLUSIONS

Results of desk and field research conducted in the first stage of LEAMAN project have shown that co-operation between SMEs and knowledge institutions (R&Ds, HEIs) has been generally established on the basis of joint research and the provision of support services. Joint research is sought as an essential part of research institutions activities, SMEs are interested in co-operation to develop new materials and products. There is a variety of support services provided by HEIs, technology/research centres, training and consultancy institutions, VETs that leather companies are using or could use.

Co-operation among leather companies, R&Ds, HEIs and training/consultancy centres offers a lot of benefits.

The list below highlights the top 10 motivations (*Decalogue of benefits*):
1. Approach to updated knowledge and innovative technologies
2. Optimise resources
3. Have access to funding opportunities
4. Know and develop new business management ideas for leather companies
5. Implement sustainability and environmental approach
6. Protect your IP and IPR
7. Ensure more safety and health at workplaces
8. Develop new markets and internationalization
9. Provide education and lifelong learning
10. Have multidisciplinary approach to complex problems

REFERENCES

www.leaman.eu

Co-funded by the
Erasmus+ Programme
of the European Union

CULTURAL IDENTITY IN PRODUCT DESIGN OF FASHION TECHNOLOGY – TOOLS AND METHOD

MARLENA POP[1], IVONA MANEA[2], BIANCA ANDRONACHE[2]

[1]*INCDTP - Division: Leather and Footwear Research Institute, Bucharest, Romania, pop_marlen@yahoo.ca*

[2]*Pestos Production SRL, Il Passo brand, Romania, ivonamanea@yahoo.com, biancandronache@yahoo.com*

In the 21st century, in a context of globalization of economies and technologies, cultural technologies strike a discordant note because they work on the basis of cultural icons, and specific societal imaginary. In this field, Technical engineering, informatic (logic-mathematical) and cultural (cognitive-emotional) languages need to find a common denominator in order to respond to the complexity of consumers' demands for modern products. Interdisciplinary approaches should not remain only at academic or technological level, transdisciplinarity may be a holistic key to the success of some disciplines, in the context in which co-creation and collaborative design are nowadays common in leadership and user-oriented creation. The article presents the laboratory verification, together with young designers, of a method of generating the identity, practical design of product creation by using a mix of cultural instruments, a method substantiated by the main author of this article. The purpose of this practical method is to make creative individuals aware of the importance of cultural work instruments in fashion technologies.

Keywords: cultural work instrument, artistic imaginary, identity design, fashion technology

INTRODUCTION

The development of design theories and scientific research in the last 10-15 years, and the design thinking and the typologies of this field, have also led to the humanistic approach of practice in fashion design and research of fashion. New research directions have emerged in product design that contribute to a better understanding of both product and design, not only by the consumer, but also by the professional practice and research in design. Design research is innovation-oriented, by finding elements of attractiveness of the existing product, or by invention, by designing a product with new, original attributes. In both types of design research, specific work instruments are used that belong to classical, IT, or cultural technologies. The last years have been dominated by the interest of both designers and marketers, both in terms of revenue growth through design, but especially in terms of knowledge of the consumer's needs in relation to the product, to its personalization techniques, and the awareness of creativity. Interactive design, UX design, Emotional design, Co-design, or Sustainable Cultural Identity of design are as many research directions in innovation design that led to the formation of research and training companies. Humanities for fashion is based on a specific aesthetic research. As Kawamura (2005) says, "fashion is the immaterial dimension of modern culture". It is used in marketing as a working tool for understanding people's relationship with creative and cultural objects. The relationship between product experience and values aesthetic is important in the context of cultural studies, "because implicit and explicit values are often seen as key determinants of culture" (Desmet and Hekkert, 2007). In this context, of articulating the human experience with the practical, more technical environment of design, if we want to understand emotional design as consumer-centered practice, it is necessary to understand the content and the imaginative meaning of the design concept. Practically, by reading the aesthetics of design, by understanding the metaphor or visual metonymy, the aesthetic emotion is

achieved, which gives the feeling of aesthetic pleasure. Paul Hekkert (2006) "proposes to restrict the term aesthetic to the pleasure attained from sensory perception, as opposed to anesthetic. An experience of any kind, e.g. of an artwork, a product, a landscape, or an event, thus comprises an aesthetic part, but the experience as a whole is not aesthetic". The purpose of this practical method is to make creative individuals aware of the importance of cultural work instruments in fashion technologies, which they use intuitively or as initial informational baggage (Nahin *et al.*, 2014). The approach of this experience with the students, which outlines a method of analyzing the content of the design project, is one required in current practice, because fashion humanist research must also be in the designer's creative studio, not just in cultural studies.

In fact, both the artist and the art consumer, both the designer and the design consumer, must belong to the same symbolic universe in order for the work or product to be correctly received, assessed and considered valuable in itself, both for the soul and the mind of each individual. In a more technical way, emotional design is necessary in the conceptualization of any type of product, for the simple reason that each of us, consumers of globalized civilization products, such as minimalist design, based only on functionality, feel it is not enough. Design based on a marketing story begins to stop working because the human being of today, living in an information society, wants more out of a product. In this context, the identity design becomes not only a research object but also a work instrument in any kind of conceptualization of a modern product. The epistemological landmarks of this research call into question both theories of philosophical or artistic approach to the imaginary, as well as its "monads" - the myth and archetype, which in turn express themselves through story, symbol or visual sign in the research of emotional design fashion. The theories on the philosophy of the imaginary show that the real-symbolic-imaginary triad is used as a starting point in any humanistic, analysis, because these three elements represent the levels of the individual's relation to the world. That is why through this fashion design project we assert that emotional design that uses theme-specific cultural instruments based on research of the imaginary can provide the consumer with a smart and sensitive product at the same time. Basically, this research project seeks, on the one hand, to identify the typology of the archetypal imaginary in fashion, and on the other hand, through laboratory experiments, intends to verify the integration mechanisms of the archetypal elements expressed by icono-plastic sign, identity sign and sign-symbol in the sketches of ideas for future products. All these are generated by the cultural instruments used: international trends in fashion, philosophical, mythological or archetypal thematizations, and the awareness of personal ideation as a psycho-cultural work instrument. Cultural technologies in fashion design use content instruments as work instruments: philosophical imaging, visual archetypes and visual cultural items, also using cultural expression instruments that are defined by artistic language, with its own syntax and stylistics (Figure 1).

Figure 1. Cultural work instruments (author)

The transversal actions of creation offered by visual language use both content codes and the aesthetic material basis, by means specific to visual language, as an instrument of cultural expression. Thus, ideation processes are obtained which bring new aesthetic elements both through innovation and through the creative diversity of aesthetic concepts. Transforming such an idea into a product concept involves transversal actions, stylistic declination and commercial (assortment) declination. Thus, through this design thought process, with the help of cultural instruments, a greater variety of cultural objects and creative products are developed, transforming the specific matter into an emotional and cultural product. In fashion design, cultural content instruments are:

Generic cultural instruments:
- Global, industrial trends,
- Identity imaging (figure 2),
- Market and consumption study.

Specific cultural instruments:
- Cultural artistic trends in fashion,
- Media and reference events,
- Styling.
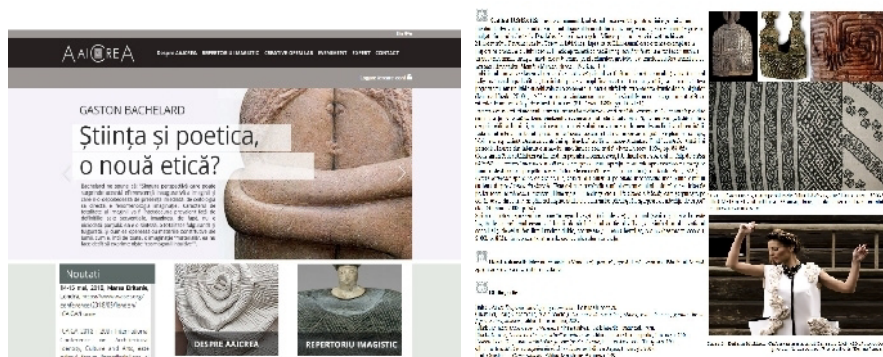
Figure 2. Identity imaging: The Romanian Repertory of Images, www.aaicrea.ro

METHODOLOGY

From the humanist practices in industry, such as semiotics, history, philosophy, psychology and the theory of different design practices and specific visual languages, the closest form of communication to any type of consumer, cultural identity design is centered on visual stylistics and semiotics. Among the general theoretical frameworks used so far in the development of identity and emotional design, the most often used are those of Norman and Verganti (2004) who proposed three levels of pleasant experiences based on neurobiological emotion theory, and Hassenzahl (2010) who proposed six positive experiences of clients in relation to the product. The cultural content instruments are defined by the thematic elements, and those of artistic expression in product design, by the semiotic ones, the metaphor and the visual metonymy. In order to develop a visual metaphor, or metonymy, the designer needs a general cultural instrument of synthesis to help him express and conceive the configuration of a new product. In order to implement the method of generating creation through the mix of

cultural instruments, the method substantiated by the main author of this article, a training was carried out with all the young designers of Pestos Production SRL Bucharest, in the 2017-2018. Explaining the role and importance of research in design, the structure of the method of generating creation through the mix of cultural instruments, and the methodology used to carry out the experiments generated many additional questions and explanations, which demonstrated young people's need for knowledge. In general, the following aspects of the method were explained:

- Definitions, types and cognitive schemes of research in the practice of art and design for the fashion, clothing and textiles industry;

- Structure of research in design and the process of its development in the stages of ideation and creation of the new product concepts - "Design Thinking" instrument;

- The definition and types of cultural instruments used in product creation and design: international fashion trends, inclusive and identity thematizations, such as the Romanian Repertory of Images and awareness of personal creativity;

- Definition, typology and examples of identity design;

- What is and which is the importance of the Romanian Repertory of Images as a cultural instrument for developing the cultural sustainability of modern Romanian products;

- Experiment methodology that primarily seeks to use cultural content tools and perform transversal visual conceptual hybridization actions.

By explaining the stages of ideation and of conceptualization of the teams' and individual project, it was easier to follow the steps of the method and work was more relaxed and continuous (fig. 3).

* Activating the team and choosing the Romanian term from the Romanian Repertory of Images;

* Brainstorming session with the team to identify the ideological field of the chosen term;

* Analytical session for reading the definition of the term and identifying its cultural items;

* Individual proposals for the atmosphere page of the term (individual moodboard);

* Making the moodboard of the term by the entire team, specifying materials and the chromatic palette;

* Associating a clothing architecture from the streetwear study and from next season trends, with the atmosphere page and the choice of a certain typology of clothing;

* Outlining a new idea by associating the details of the atmosphere page with the chosen clothing architecture, integrating the Romanian element chosen from the Repertory and visually defined by the whole team;

* Analysis-synthesis of creative activity and making a decision on the concept idea;

* Developing the concept idea by individual stylistic declinations;

* Developing the new concept and presenting it in several variants of the sketch of idea through commercial declinations;

* Choice, by the team, of sketches of ideas that can be presented in a common moodboard;

* Elaboration of team moodboard;

* Elaboration of individual sketchboard with details of materials and palette, set by the team;

* Choosing the best sketches for the team sketchboard;

* Choosing the best three sketches, one for each team, for transposition into the material as laboratory research stage.

Figure 3. The steps of the method

RESULTS

The design team came up with a complex imaginative mood-board, which can be transposed visually by the values identity of the brand, values identity of the trends and Romanian values identity. The team came up with a complex imaginative mood-board, which can be transposed visually by the product collection for a/w 2018-2019.

Figure 4. The cultural identity of the brand design: Ivona Manea and Bianca Andronache

CONCLUSIONS

The mix of cultural tools method allows the designer to become aware of his own creativity and the context of the collaborative imaginative environment.

The knowledge base of young designers at any creative individual can be developed on the recommendation of the study or work environment of each person who implements the identity design method and development identity design. It was also noted that collaborative design is more semantically, cognitively and emotionally charged than average individual design.

In addition, experiments have shown that the cultural sustainability of creative industries products will exist as long as the appropriate cultural instruments are used, both in terms of semiotic and semantic code, and aesthetic material resource.

This synthetic method of the mix of cultural instruments suggests the need for a deeper approach to typology of the synthesis elements required to develop an effective practice in identity design, specific to fashion design.

The elements of visual semiotics, like metaphor and visual metonymy, require a thorough study conjugating the expression with the ideation of the content of a fashion project.

REFERENCES

Desmet, P. and Hekkert, P. (2007), "Framework of Product Experience", *International Journal of Design*, 1(1), ISSN 1991-3761.

Hassenzahl, M. (2010), "Experience design: Technology for all the right reasons", *Synthesis Lectures on Human-Centered Informatics*, https://doi.org/10.2200/S00261ED1V01Y201003HCI008.

Hekkert, P. (2006), "Design aesthetics: principles of pleasure in design", *Psychology Science*, 48(2), 157-172.

Kawamura, Y. (2005), *Fashion-ology: An introduction to fashion studies*, New York, NY: Berg.

Nahin, A.F.M.N.H. *et al*. (2014), "Identifying emotion by keystroke dynamics and text pattern analysis", *Behaviour & Information Technology*, 33(9), 987-996, https://doi.org/10.1080/0144929X.2014.907343.

Norman, D.A. and Verganti, R. (2014), "Incremental and radical innovation: Design research versus technology and meaning change", *Design Issues*, 30(1), 78-96, MIT Press.

EQUIPMENTS AND SUPPORT SYSTEMS FOR INTERVENTION IN EMERGENCY SITUATIONS - THE CONCEPTUAL SCHEME

ADRIAN SĂLIŞTEAN, DOINA TOMA, CLAUDIA NICULESCU, SABINA OLARU

The National Research Development Institute for Textiles and Leather, 16, Lucretiu Patrascanu, 030508 Bucharest, Romania; e-mail: certex@certex.ro, webpage: http://www.certex.ro

The aim of the project is strengthening the operational response capacity of the National Emergency Situation Management System structures. The objective is to develop and implement the integrated support equipment and systems in an architecture that meets the technical and especially operational requirements specific to emergency response actions. The concept is an integrated system with two components: protective equipment and support system for intervention actions. The originality is the support system as a complex UAS that consists of one or more ultralight multifunctional sail air vectors with a configuration that can be adapted to the nature of the intervention: monitoring, observation and logistics, air transport, detection of intervention staff using the PPE that is equipped with a special radio ID transponder. PPE must respond to increasingly evolved and varied threats that act on users. PPE are designed to remain effective and functional across a wide range of tactical and operating environments: from arctic temperatures in the desert, high and low humidity, in urban and rural environments, forested, marine, underground and almost in all imaginable locations. The novelty of PPE is the modular multilayer structure made of yarns / fibers with integrated protection properties (flame resistance and / or cutting resistance/ water, chemical and body fluid rejection/ antimicrobial protection etc.).

Keywords: Unmanned Aerial System (UAS), Personal protective equipment (PPE), Emergency response

INTRODUCTION

Emergency response is a series of organized and coordinated precaution and actions during the time between the detection of possible event and stabilizing the situation. An emergency response decision support system needs to assist decision makers to evaluate emergency plans and select an appropriate plan of action during an emergency by supporting heterogeneous emergency response data sources and providing decision makers with access to appropriate emergency rescue knowledge. It also needs to provide differentiated services to meet particular requirements.

Decision making in emergency response is an extremely time-sensitive and challenging task that requires immediate and effective response from decision makers who are surrounded by a variety of uncertain information and are under huge pressure from the need to coordinate action. An emergency response decision support system needs to assist decision makers to evaluate emergency plans and select an appropriate plan of action during an emergency by supporting heterogeneous emergency response data sources and providing decision makers with access to appropriate emergency rescue knowledge. It also needs to provide differentiated services to meet particular requirements.

There are four main emergency response functions - emergency assessment, risk operations, population protection and incident management. The four functions provide a framework for organizing response activities to a wide variety of emergencies, natural hazards, technological accidents, terrorist attacks, and sabotage.

- Emergency assessment: The emergency response activities in the response phase relate to the understanding of the behavior of the hazard-generating factors but also of the risk to human life and material damage.

- Risk operations: Risk operations aim at mitigating emergency situations but are only implemented when needed. Their applicability varies greatly from one hazard to another.

- Protection of the population: The information collected during the emergency assessment is the basis for the choice of population protection actions.

- Incident management: Incident management involves the development of an incident management policy, a set of consistent, repeatable, measurable processes and procedures and the use of appropriate administrative, managerial, technical or legal means to detect analyze and respond to incidents serious.

Regardless of the emergency structure that acts against the timer, time is the greatest enemy, and the scoring scale is the response time, which must be very low. With the latest Unmanned Aerial Vehicles (UAV) technology, the risks that influence response time can be reduced.

Also unmanned aerial devices allow rapid surveillance of dangerous situations, risk analysis and assessment can provide information to control centers, being an eye in the sky.

Starting from the premise that the way of manifestation of the emergency situations and their management system in the future will be very different from the past context, we have proposed to develop an integrated support equipment and systems that respond to the challenges and needs of these field that need to be addressed in an organized and integrated manner.

EXPERIMENTAL PART

Operational and Performance Requirements for an Integrated System

The Emergency Assessment is the first phase with the following operating requirements:

- A1: Collecting information from where events occurred: fires, explosions, industrial accidents, floods, etc.;

- A2: Detection of the NBC contamination level of an area;

- A3: Patrolling of some areas (border, communication routes, infrastructure - electrical networks, transport pipelines etc.) for the purpose of preventive detection of emergency situations.

On the basis of the collected data, it is possible to move to the second phase of efficient incidents management through:

- B1: Persistent surveillance of the area where events occur that have a continuous spatial and temporal evolution (fires, floods, natural disasters, industrial accidents, etc.);

- B2: Appropriate equipment for intervention staff with PPE tailored specifically to the event produced;

- B3: Locating and tracking in real time intervention teams;

- B4: Search for missing persons in natural environments covered with dense vegetation;

- B5: Temporary provision of radio communication coverage of mobile radio communications networks in isolated / hard-to-reach areas or where terrestrial networks are unavailable / degraded;

- B6: Small-scale logistics transport in remote areas.

Component and Capabilities of the Integrated System Support

The conceptual block scheme of the integrated support system for emergency interventions is presented in Figure 1.
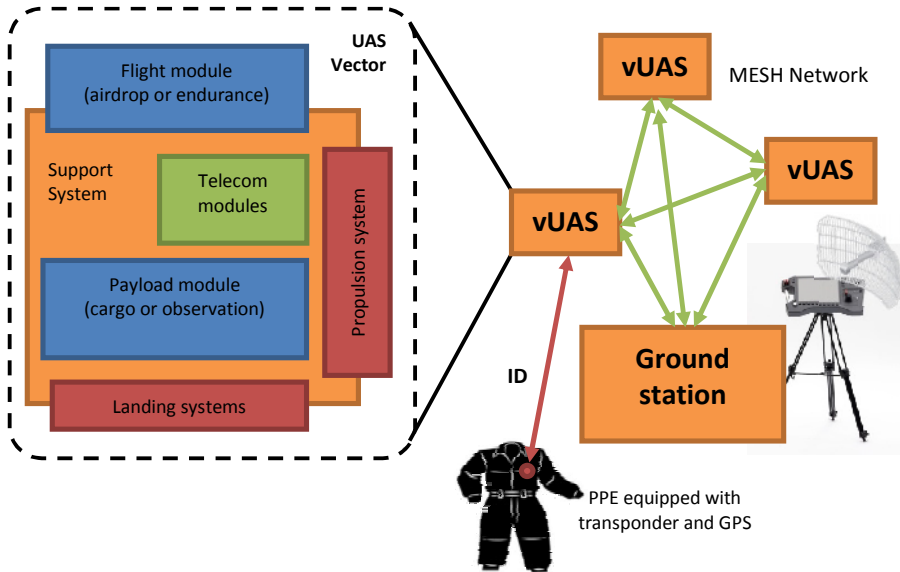
Figure 1. The conceptual block scheme of the integrated support system for emergency interventions

Personal Protective Equipment

Protective equipment must remain effective and functional in a wide range of tactical and operating environments: from arctic to desert temperatures, high and low humidity, in urban and rural environments, forested, marine, underground and almost all locations imaginable.

In the development of protective equipment for intervention, innovative solutions have been applied, resulting in a modular protective clothing system, customized for various emergency response environments.

The modular system consists of:

- The service uniform (base layer) that provides risk protection with the highest probability of occurrence in case of an intervention action;

- Modular outer layers specific to the type of intervention mission that is physically modular but performs unitarily and fully functional within an IPE system, depending on the specificity of the intervention mission.

Support System in Intervention Actions

The innovative solution applied to the development of support systems for emergency intervention consists of a UAS support system with adaptable configuration depending on the nature of the intervention:

- An endurance flight module made of high glide paraglider wing;

- A para-drop unit, in particular a ram-air parachute attached to the automated control unit.

- Upgrading the detection capability as required: dedicated sensors for NBC; attaching a transponder to detect and locate intervention staff using protective clothing.

Component Elements of the Support System

1) UAS vectors (vUAS)

UAV, flexible wing type paraglider, with dual-electrically / thermally propelled and interchangeable load:

- C1: Video stabilized support: HD day-night and / or FLIR (Forward looking infrared) camera and / or LiDAR (Light Detection and Ranging) sensor;

- C2: NBC sensor suite including: gas detector and volatile organic compounds; ionizing radiation detector and aerosol sample collector;

- C3: Detection and location unit for multiband and telecommunication relay in GSM band;

- C4: Cargo unit.

2) The PPE transponder

The transponder is a miniature device within the PPE, with the role of receiving the GPS signal and then retransmits it with a unique identification number.

3) Command and Control Station (SCC)

This station is used for controlling and monitoring the air vectors and transmitting the data in real time to the command point of the intervention and consists of: antennas (a fixed antenna and a tracking antenna); data transceiver; microcomputer; HID (Human Interface Devices); rechargeable battery and generator. Transmission of these data is encrypted by high-speed terrestrial data transmissions in the 5GHz or 4G band if there is no access to a terrestrial telecommunication hub.

RESULTS AND DISCUSSION

From the analysis of the situations faced by the Flexible Wing (Knache, 1992), it has emerged that this must be a hybrid ram-air paraglider. This type of wing harmoniously combines the performance of a classic dual skin wings with that of a single skin wings, figure 2. The paraglider wing profile is the main determinant of flight performance (Poynter, 1984).

Figure 2. Types of flexible wing profiles

A flat wing was designed with the attack board cut off to create the air circulation inside the canopy volume. We made the following estimates:

- the load factor has been preserved the same as for the flat wing;
- the drag coefficient CD0 changes substantially, it can vary between (0,5 ÷ 1,0) CD0 for the flat wing.

Projected span of flexible wing: 6.5m

CONCLUSION

1. The modular configuration of UAS support system and load variants of the UAS support system are:
- C1: video suite: permanently mounted (for observation, monitoring);
- C2: NBC sensor set: if necessary (for investigation area, NBC hazard detection);
- C3: sensor detection and localization sensor set: if necessary (for locating missing persons, fire detection and wind direction detection);
- C4: cargo unit: if necessary (or emergency transport, medicines and supplies in remote areas, small cargo, up to 10kg).

2. The flexible ram-air wing will be a hybrid ram-air glider with 6.5 meter span.

REFERENCES

Green, L.V. and Kolesar, P.J. (2004), "Improving emergency responsiveness with management science", *Manage Sci*, 50(8), 1001–1014, https://doi.org/10.1287/mnsc.1040.0253.
Knache, T.W. (1992), *Parachute Recovery Systems – Design Manual*, Para Publishing, Santa Barbara, California.
Poynter, D. (1984), *The Parachute Manual - A Technical Treatise on Aerodynamic Decelerators*, Vol.2, Santa Barbara, California.

IV.

SMART MATERIALS

CHEMICAL COMPOSITION OF ESSENTIAL OILS FROM *Origanum onites* L. AND *Cymbopogon citratus*, AND THEIR SYNERGISTIC EFFECTS WITH ACYCLOVIR AGAINST HSV-1

NİZAMİ DURAN[1], DURMUŞ ALPASLAN KAYA[2]

[1]*Microbiology & Clinical Microbiology Department, Medical Faculty, Hatay Mustafa Kemal University, Turkey, nizamduran@hotmail.com*

[2]*Hatay Mustafa Kemal University, Faculty of Agriculture, Field Crops Department, Turkey, alpaslankaya@yahoo.com*

Origanum onites L. and *Cymbopogon citratus* have a number of pharmacological activities such as antimicrobial, anti-inflammatory and antioxidant. In this study, we aimed to investigate the components and the synergistic effect of *Origanum onites* L. and *Cymbopogon citratus* and their combinations with acyclovir against HSV-1 on HEp-2 cell line. The main essential oil components of Origanum onites L. were Thymol (68,28%), γ-Terpinene (5,50%), p-Cymene (5,47%) and Linalool (4,40%) and for Cymbopogon citratus the main components were E-Citral (47,53%), Z-Citral (36,29%), β-Myrcene (9,31%). Initially, 100 $TCID_{50}$ (Tissue Culture Infective Dose) of HSV-1 on HEp-2 was calculated in the study. Antiviral activity studies were carried out at the concentration of 1, 10 and 100 $TCID_{50}$ of HSV-1. The antimicrobial efficacy of the *Origanum onites* L. and *Cymbopogon citratus* essential oils were assessed alone and in combination with acyclovir. In addition, the efficacy of acyclovir was determined on 100 $TCID_{50}$ of HSV-1. In conclusion, the essential oils of *Origanum onites* L. and *Cymbopogon citratus* against HVS-1 were found to have a significant inhibitory effect on viral replication. We think that the essential oils of *Origanum onites* L. and *Cymbopogon citratus* may be a very important agent against herpesviruses. In particular, the essential oils of *Cymbopogon citratus* can be a very promising plant.

Keywords: Acyclovir, HSV-1, Linalool, rosmarinic acid, HEp-2 cell line, antiviral

INTRODUCTION

Origanum species are plants that are commonly used as spices and marketed under the name of thyme. The genus Origanum is take place in the family Labiatae. Origanum genus has a large variation between species. This species is composed of many species and subspecies (Ozkan *et al*., 2010).

Cymbopogon citratus is a widely used in folk medicine. The essential oils of *Cymbopogon citratus* have various pharmacological activities. Terpenes, alcohols, ketones, aldehyde and esters are the important compounds. It has also been reported that Citral α, Citral β, Nerol Geraniol, Citronellal, are among the important phytoconstituents (Akhila, 2010; Oloyede, 2009).

Herpes viruses are broad-spectrum infectious agents that can range from superficial infections to deep tissue infections. It has been reported to cause serious morbidity and mortality, especially in immunosuppressed individuals. Medication is insufficient due to increased drug resistance in cases such as meningitis. For this reason, new active substance investigations continue against herpes viruses (Roizman, 1996).

In this study, we aimed to investigate the synergistic effect of *Origanum onites* L. and *Cymbopogon citratus* and their combinations with acyclovir against HSV-1 on HEp-2 cell line.

MATERIALS AND METHODS

Plant Materials

Origanum onites L. and *Cymbopogon citratus* essential oils were supplied from market.

GC/MS Analysis

Analysis of essential oil was performed using the Thermo Scientific Focus gas chromatograph equipped with a DSQ II single quadrupole mass spectrometer, Triplus autosampler and fused-silica capillary column TR-5MS (5% phenyl-polysilphenylene-siloxane, 30 m×0.25 mm inner diameter, film thickness 0.25 μm). The injection volume was 2 μL. The samples were injected with a split ratio of 250:1 by using helium (99.99 %) as carrier gas, at a flow rate of 1 mL/min; ionization energy was 70 eV. The transfer line temperature of the mass spectrometer was 220 °C, while the temperature of orifice injection was of 220 °C. The temperature of oven was programmed in the range 50–220 °C at a rate of 3 °C/min. Data acquisition was made in the scanning mode. Identification was done on full scan mode in the m/z range of 50–650 a.m.u.

Determination of Minimum Bactericidal Concentration (MBC)

To dissolve the essential oils dimethyl sulfoxide [(DMSO); Sigma, USA] was used. In order to find the non-toxic concentration of DMSO, 1x 10^6 Hep-2 cells were inoculated into each well of micro plates containing RPMI medium (Gibco-BRL)], and cells were allowed to incubate for 48 hours in the presence of decreasing amounts of DMSO (25, 12.5, 6.25, 3.12, 1.56, 0.78, 0.39%). The non-toxic concentration was determined up to 3.12%. DMSO concentrations lower than 3.12%did not inhibit the growth of the HEp-2 cells. In the experiments, *Origanum onites* L. and *Cymbopogon citratus* essential oils were dissolved in 1 % DMSO.

Cytotoxicity Tests

To evaluate cytotoxicity of the essential oils, the HEp-2 cell line (human larynx epidermoid carcinoma cell line) was selected. The cells were cultured in RPMI medium with 10% (w/v) fetal bovine serum (FBS). The cells were incubated for 48 h at 37°C in an atmosphere with 5% CO_2.

To determine the effects of propolis samples on HEp-2 cells, they were infected with propolis. Then the infected and non-infected Hep-2 (uninfected with propolis) cells were observed under inverted microscopy. To evaluate the effects of the essential oils on HEp-2 cells, 1×10^5 cells were inoculated into flat bottomed microplates. Then, the cells were allowed to adhere for 6 h at 28 °C. And the cells were allowed to grow for an additional 72 hours. And then, the essential oils of *Origanum onites* L. and *Cymbopogon citratus* were diluted and decreasing amounts (2560, 1280, 640, 320, 160, 80, 40, 20, 10 and 5 μg/ml) were inoculated per well, and incubated for 96 hours. All experiments were performed in triplicate. The Cytotoxic concentrations of essential oils were determined by both cell morphological evaluation with invert microscopy and cell viability by trypan blue method. The highest non-cytototoxic (on HEp-2 cells) concentrations of the essential oils of *Origanum onites* L. and *Cymbopogon citratus*

were determined to be 1280 and 640 µg/mL, respectively. Therefore, the essential oils concentrations were selected lower than 640µg/mL.

Virus Titrations

Firstly, 100 $TCID_{50}$ (Tissue Culture Infective Dose) of HSV-1 on HEp-2 was calculated in the study. Antiviral activity studies were carried out at the concentration of 1, 10 and 100 $TCID_{50}$ of HSV-1. The antimicrobial efficacy of the *Origanum* Onites L. and *Origanum* Onites L. essential oils were assessed alone and in combination with acyclovir. In addition, the efficacy of acyclovir was determined on 100 $TCID_{50}$ of HSV-1. In the study, *Origanum onites* and *Cymbopogon citratus* were studied at concentrations of 320, 160, 80, 40, 20, 10 and 5 µg/ml.

RESULTS

Origanum onites L. and *Cymbopogon citratus* essential oil components results were given Table 1, 2 and Figure 1, 2.
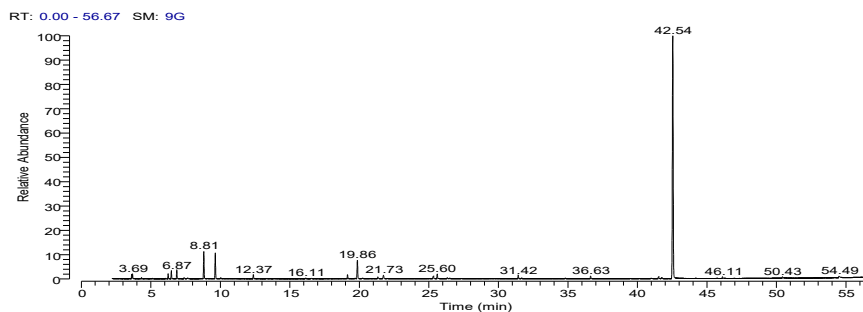
Figure 1. GC/MS chromatogram of *Origanum onites* L.

Table 1. The main essential oil components of *Origanum onites* L.

RT	Compound Name	SI	RSI	Cas #	%
6,48	β-Myrcene	969	974	123-35-3	1,47
6,87	α-Terpinene	974	983	99-86-5	1,64
8,81	γ-Terpinene	989	993	99-85-4	5,50
9,64	p-Cymene	975	975	99-87-6	5,47
19,86	Linalool	994	995	78-70-6	4,40
42,54	Thymol	969	969	89-83-8	68,28
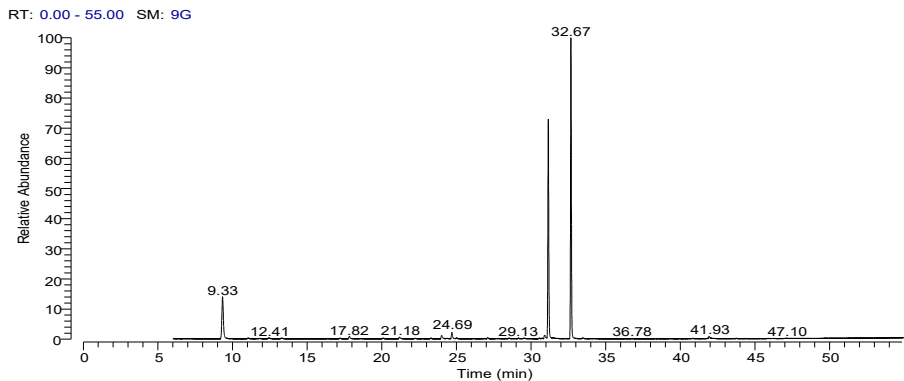
Figure 2. GC/MS chromatogram of *Cymbopogon citratus*

Table 2. The main essential oil components of *Cymbopogon citratus*

RT	Compound Name	SI	RSI	Cas #	%
32,67	E-Citral	977	977	141-27-5	47,53
31,15	Z-Citral	988	989	106-26-3	36,29
9,33	β-Myrcene	979	985	123-35-3	9,31
24,69	Verbenol	881	885	18881-04-4	1,19

The main essential oil components of *Origanum onites* L. were Thymol (68,28 %), γ-Terpinene (5,50 %), p-Cymene (5,47 %) and Linalool (4,40 %) and for Cymbopogon citratus the main components were E-Citral (47,53 %), Z-Citral (36,29 %), β-Myrcene (9,31 %).

In the experiments, it was determined that the concentration of 2.5 µg/ml of acyclovir completely inhibited viral replication at 100 $TCID_{50}$ of virus (Figure 3).

In the experiment, the essential oils of *Origanum onites* L. inhibited virus replication at the concentrations of 20, 40, and 80 µg/ml for 1, 10, 100 $TCID_{50}$ values, respectively, whereas *Cymbopogon citratus* inhibited these three different viral titers at concentrations of 10, 20, and 40 µg/ml (Figure 4). In addition, the *Origanum onites* L. and acyclovir combination inhibited virus replication at the concentrations of 1.5, 2.5, and 5.0 µg/ml for 1, 10, 100 $TCID_{50}$ of values, respectively. In addition, the *Cymbopogon citratus* and acyclovir combination inhibited virus replication at the concentrations of 1.0, 1.5 and 1.5 µg/ml for 1, 10, 100 $TCID_{50}$ of values, respectively (Figure 5).
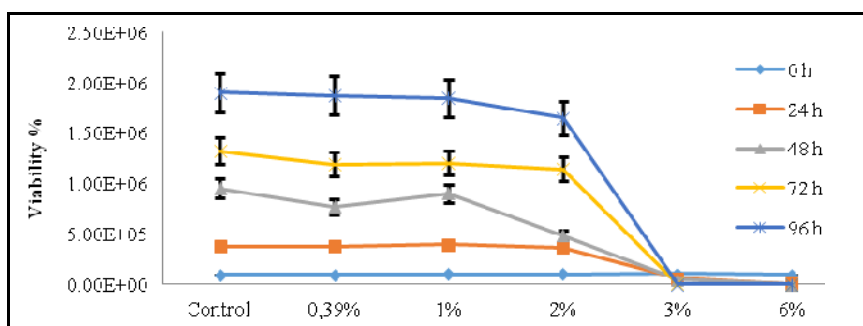
Figure 3. Effect of DMSO on cell viability in HEp-2 Cell Culture
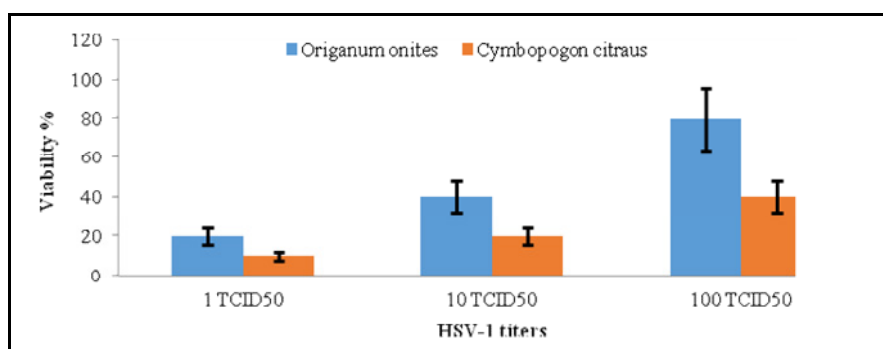
Figure 4. Antiviral activities of *Origanum onites* and *Cymbopogon citratus* essential oils against HSV-1
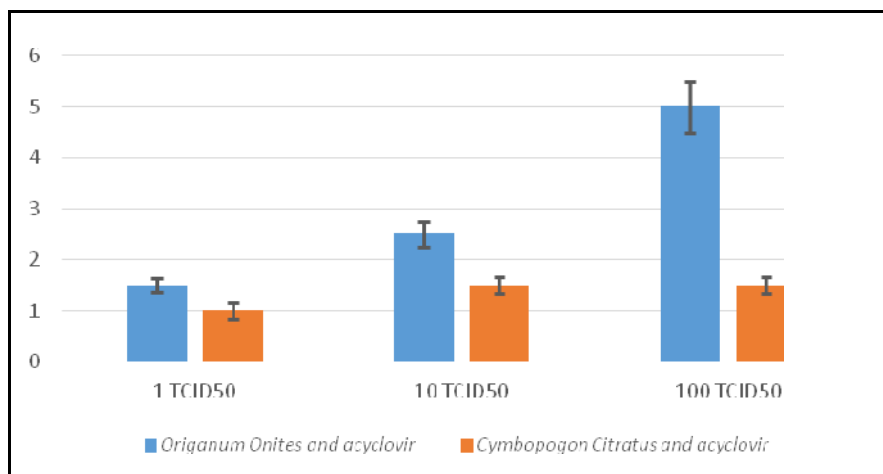
Figure 5. Antiviral activities of Acyclovir plus *Origanum onites* and *Cymbopogon citratus essential* oils against HSV-1

DISCUSSION AND CONCLUSION

In conclusion, the essential oils of *Origanum onites* L. and *Cymbopogon citratus* against HVS-1 were found to have a significant inhibitory effect on viral replication. The essential oils of *Cymbopogon citratus* and acyclovir showed very strong synergism against HSV-1. The essential oils of *Origanum onites* L. acid with acyclovir significantly reduced viral replication at low concentrations of HSV-1 (1 and 10 $TCID_{50}$), but did not show a significant decreasing in viral replication against 100 $TCID_{50}$titres of virus. It is thought that these two substances may be useful for decreasing viral replication in HSV-1 infections.

Considering the increased resistance to antiviral drugs in recent years, we think that the essential oils of *Origanum onites* L. and *Cymbopogon citratus* may be a very important agent against herpesviruses. In particular, the essential oils of *Cymbopogon citratus* can be a very promising plant.

REFERENCES

Akhila, A. (2010), *Essential oil-bearing grasses: the genus Cymbopogon*. CRC Press, Taylor and Francis Group, p. 108.

Oloyede, O.I. (2009), "Chemical profile and antimicrobial activity of *Cymbopogon citratus* leaves", *J. Nat. Prod.*, 2, 98-103.

Ozkan, G., Baydar, H. and Erbas, S. (2010), "The influence of harvest time on essential oil composition, phenolic constituents and antioxidant properties of Turkish oregano (*Origanum onites* L.)", *J Sci Food Agric*, 90(2), 205-9, https://doi.org/10.1002/jsfa.3788.

Roizman, B. (1996), "Herpesviridae", in: Fields, B.N., Knipe, D.M., Howley, P.M., eds., *Fields virology*, Philadelphia, Lippincott-Raven, 2221-30.

THE ANTIMICROBIAL ACTIVITIES OF *Myrtus communis* AND *Micromeria fruticosa* ESSENTIAL OILS

DURMUŞ ALPASLAN KAYA[1], NİZAMİ DURAN[2]

[1]*Department of Field Crops, Agriculture Faculty, Hatay Mustafa Kemal University, Turkey,*
alpaslankaya@yahoo.com

[2]*Hatay Mustafa Kemal University, Faculty of Agriculture, Field Crops Department, Turkey,*
nizamduran@hotmail.com

This study was aimed to investigate the antimicrobial activity of *Myrtus communis* and *Micromeria fruticosa* against four Gram-positive (Methicillin resistant *Staphylococcus aureus*, Methicillin sensitive *Staphylococcus aureus*, *Staphylococcus epidermidis*, *Enterococcus faecalis*) and four Gram-negative [(*Escherichia coli, Pseudomonas aeruginosa, Klebsiella pneumonia, Enterobacter aerogenes*) bacteria by employing broth microdilution methods. The main components determined by GC-MS for *Myrtus communis* essential oil were Eucalyptol (45,41%), α-Pinene (20,86%), Linalool (9,71%), α-Terpineol (6,11%) and Limonene (5,88%) and for *Micromeria fruticosa* L. essential oil were Pulegone (58,32%), p-Menthan-3-one (12,99%) and Levomenthol (9,85%). Antibacterial activities of *Myrtus communis* and *Micromeria fruticosa* essential oils were searched against Methicillin resistant *Staphylococcus aureus*, Methicillin sensitive *Staphylococcus aureus*, *Staphylococcus epidermidis*, *Enterococcus faecalis*, *Escherichia coli, Pseudomonas aeruginosa, Klebsiella pneumonia and Enterobacter aerogenes*. In order to evaluate the MIC values of the bacterial strains, Minimal inhibition concentrations (MICs) determined by the National Committee for Clinical Laboratory standards. Amikacin was selected as standard drug for bacterial strains. As a result, it has been found that *Myrtus communis* and *Micromeria fruticosa* essential oils are very promising against these bacteria, which are among the major infectious agents in the world as well as in our country. Essential oils of these plants have been found very promising in the production of new antimicrobials. Further in vivo studies are needed in this regard.

Keywords: *Myrtus communis, Micromeria fruticosa,* essential oils, Gram positive, Gram negative, bacteria

INTRODUCTION

Increasing antibiotic resistance in bacteria all over the world has become a big problem. The unauthorized use of antibiotics increases resistance to antibiotics day by day. Gram-positive (methicillin resistant Staphylococcus aureus, methicillin sensitive Staphylococcus aureus, Staphylococcus epidermidis, Enterococcus faecalis) and Gram-negative bacteria (*Escherichia coli, Pseudomonas aeruginosa, Klebsiella pneumonia, Enterobacter aerogenes*) are among the causes of serious morbidity and mortality. New drug studies against these kinds of infection agents have great prospects. The presence of methicillin-resistant strains, especially in staphylococci, can lead to serious consequences for both hospital infections and community-acquired infections (Utta and Wells, 2016; Wenzel, 2007; Burke, 2003; Doshi *et al*., 2009; Vasoo *et al*., 2005; Nam *et al*., 2011).

In this study, it was aimed to investigate the antimicrobial activity of *Myrtus communis* and *Micromeria fruticosa* against four Gram-positive (methicillin resistant *Staphylococcus aureus (ATCC 33591)*, methicillin sensitive *Staphylococcus aureus* [*(ATCC 25923)*, *Staphylococcus epidermidis (12228)*, *Enterococcus faecalis (ATCC 29212)*], and four Gram-negative [(*Escherichia coli (ATCC 25922), Pseudomonas aeruginosa (ATCC 27853), Klebsiella pneumonia* (ATCC 13883)*, Enterobacter aerogenes* (ATCC 13048)] bacteria by employing broth microdilution methods.

MATERIALS AND METHODS

Plant Materials

Myrtus communis and Micromeria fruticosa plants were harvested during the full bloom period, which the amount of active substance was most intense and after being dried in the shade at room temperature.

Preparation of Plant Extracts

Plant material was weighted and placed in a round bottom flask with a volume of distilled water as extraction solvent; the herba-water mixture was refluxed about 2 h, during which the oil was collected in the side arm of the system. The installation was allowed to stand for about half an hour to prevent the oil to reach room temperature. The oil was dried over anhydrous sodium sulphate and then stored in dark color glass bottles and keep to refrigerator (about 4 °C) until use for analysis.

GC/MS Analysis

Analysis of essential oil was performed using the Thermo Scientific Focus gas chromatograph equipped with a DSQ II single quadrupole mass spectrometer, Triplus autosampler and fused-silica capillary column TR-5MS (5% phenyl-polysilphenylene-siloxane, 30 m×0.25 mm inner diameter, film thickness 0.25 μm). The injection volume was 2 μL. The samples were injected with a split ratio of 250:1 by using helium (99.99 %) as carrier gas, at a flow rate of 1 mL/min; ionization energy was 70 eV. The transfer line temperature of the mass spectrometer was 220 °C, while the temperature of orifice injection was of 220 °C. The temperature of oven was programmed in the range 50–220 °C at a rate of 3 °C/min. Data acquisition was made in the scanning mode. Identification was done on full scan mode in the m/z range of 50–650 a.m.u.

RESULTS

GS/MS analysis results of essential oils and their main components were given in Table 1, 2 and Figure 1, 2.
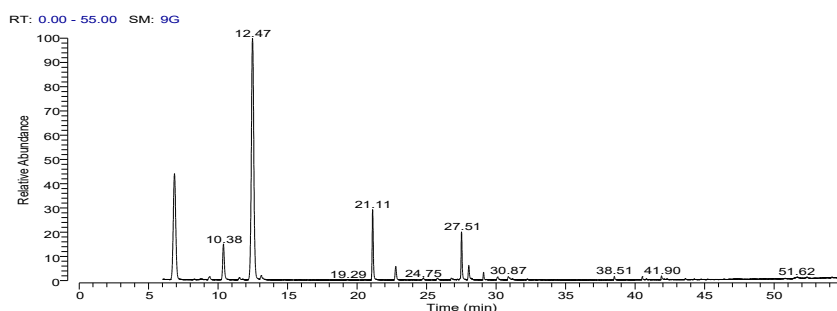
Figure 1. MIC and MFC values of *Myrtus communis* L.

Table 1. The main essential oil components of *Myrtus communis* L.

RT	Compound Name	SI	RSI	Cas #	%
6,86	α-Pinene	987	990	80-56-8	20,86
10,38	Limonene	984	990	138-86-3	5,88
12,47	Eucalyptol	988	988	470-82-6	45,41
21,12	Linalool	994	994	78-70-6	9,71
27,51	α-Terpineol	983	984	98-55-5	6,11

RT: 0.00 - 55.00 SM: 9G
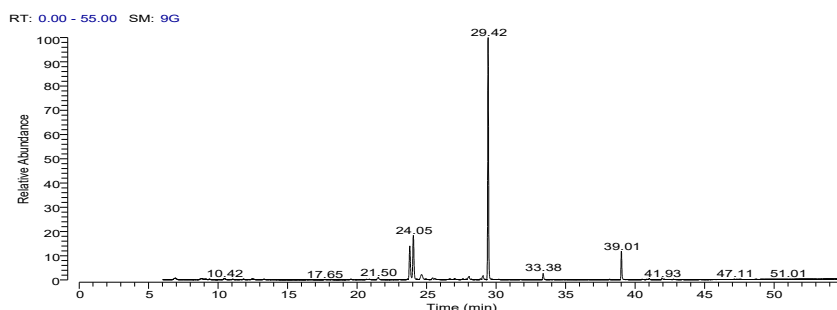
Figure 2. MIC and MFC values of *Micromeria fruticosa* L.

Table 2. The main essential oil components of *Micromeria fruticosa* L.

RT	Compound Name	SI	RSI	Cas #	%
23,79	Levomenthol	987	992	2216-51-5	9,85
24,05	p-Menthan-3-one	988	992	491-07-6	12,99
24,63	trans-Caryophyllene	956	966	87-44-5	1,96
29,04	bicyclogermacrene	944	964	100762-46-7	1,17
29,42	Pulegone	987	987	89-82-7	58,32
33,38	p-Menth-1-en-3-one	968	981	89-81-6	1,61

The main components of *Myrtus communis* essential oil were Eucalyptol (45,41%), α-Pinene (20,86%), Linalool (9,71%), α-Terpineol (6,11%) and Limonene (5,88%) and for *Micromeria fruticosa* L. essential oil were Pulegone (58,32%), p-Menthan-3-one (12,99%) and Levomenthol (9,85%).

In the study, it was found that *Myrtus communis* essential oils showed the highest antibacterial activity of methicillin sensitive *Staphylococcus aureus* (ATCC 25923) and *Staphylococcus epidermidis* (ATCC 12228) at the 50 μg/ml concentration among the Gram-positive bacteria. Besides this, *Micromeria fruticosa* essential oils showed the highest antibacterial activity against *S. epidermidis* at the 25 μg/ml concentrations (Figure 3).

In the combined use of Myrtus communis and Micromeria fruticosa essential oils, a statistically significant decrease in the MIC values of all tested Gram-positive bacteria was found (p <0.01).

In study, it was found that *Myrtus communis* essential oils showed the highest antibacterial activity against *Klebsiella pneumonia* (ATCC 13883) at the 75 μg/ml concentration among Gram-negative bacteria. *Micromeria fruticosa* essential oils showed the highest antibacterial activity against *Klebsiella pneumonia* (ATCC 13883) and *Enterobacter aerogenes* (ATCC 13048) at the 50 μg/ml concentrations (Figure 4).

In the combined use of *Myrtus communis* and *Micromeria fruticosa* essential oils, a statistically significant decrease in the MIC values of all tested Gram-negative bacteria was found ($p<0.01$). MIC values of standard drugs and essential oils are given in figures 5 and 6 in the study.
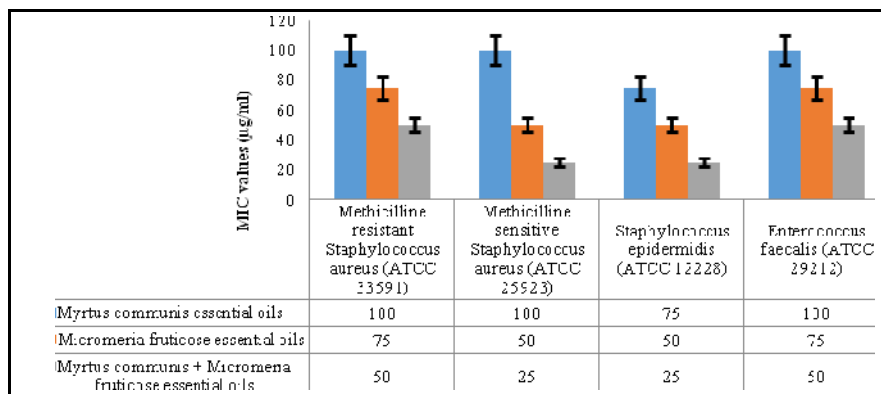
Figure 3. MIC values of *Myrtus communis* and *Micromeria fruticosa* essential oils against Gram-positive bacteria

Figure 4. MIC values of *Myrtus communis* and *Micromeria fruticosa* essential oils against Gram-negative bacteria

	Methicilline resistant Staphylococcu s aureus (ATCC 33591)	Methicilline sensitive Staphylococcu s aureus (ATCC 25923)	Staphylococcu s epidermidis (12228)	Enterococcus faecalis (ATCC 29212)
Myrtus communis essential oils	100	100	75	100
Micromeria fruticose essential oils	75	50	50	75
Myrtus communis + Micromeria fruticose essential oils	50	25	25	50
amikacin	4	2	2	16
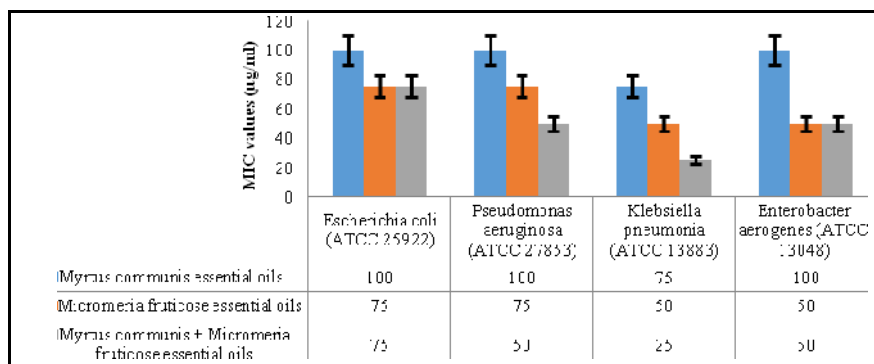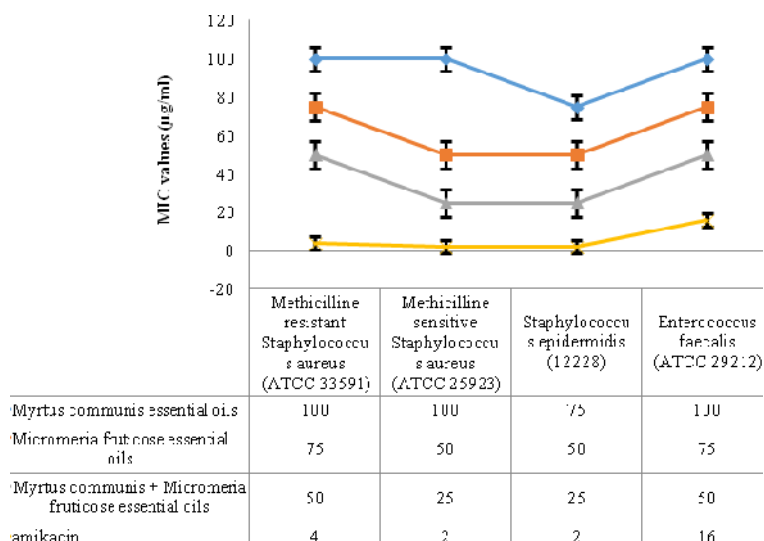
Figure 5. Compare the MIC values of standard drugs with *Myrtus communis* and
Micromeria fruticosa essential oils against Gram-positive bacteria

	Escherichia coli (ATCC 25922)	Pseudomonas aeruginosa (ATCC 27853)	Klebsiella pneumonia (ATCC 13883)	Enterobacter aerogenes (ATCC 13048)
Myrtus communis essential oils	100	100	75	100
Micromeria fruticose essential oils	75	75	50	50
Myrtus communis + Micromeria fruticose essential oils	75	50	25	50
amikacin	4	6	8	2
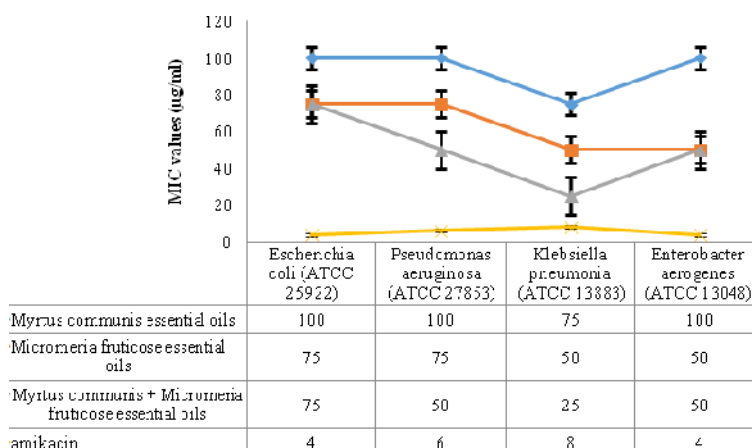
Figure 6. Compare the MIC values of standard drugs with *Myrtus communis* and
Micromeria fruticosa essential oils against Gram-negative bacteria

DISCUSSION AND CONCLUSION

In our study, it was determined that essential oils of *Myrtus communis* and *Micromeria fruticosa* essential oils have considerable antibacterial activity against both Gram-positive and Gram-negative bacterial agents. *Micromeria fruticosa* essential oils

have been found to be more effective than *Myrtus communis* essential oils against both Gram-positive and Gram-negative infection agents. More importantly in our study, the combined use of *Myrtus communis* and *Micromeria fruticosa* essential oils was found to be significantly more effective against both Gram-positive and Gram-negative bacteria.

As a result, it has been found that *Myrtus communis* and *Micromeria fruticosa* essential oils are very promising against these bacteria, which are among the major infectious agents in the world as well as in our country. Essential oils of these plants have been found very promising in the production of new antimicrobials. Further *in vivo* studies are needed in this regard.

REFERENCES

Burke, J.P. (2003), "Infection control - a problem for patient safety", *N Engl J Med*, 348(7), 651-656, https://doi.org/10.1056/NEJMhpr020557.

Doshi, R.K. *et al*. (2009), "Healthcare-associated infections: epidemiology, prevention, and therapy", *Mt Sinai J Med*, 76(1), 84-94, https://doi.org/10.1002/msj.20070.

Nam, H.M. *et al*. (2011), "Antimicrobial susceptibility of Staphylococcus aureus and characterization of methicillin-resistant Staphylococcus aureus isolated from bovine mastitis in Korea", *Foodborne Pathog Dis*, 8(2), 231-8, https://doi.org/10.1089/fpd.2010.0661.

Utta, E. and Wells, C. (2016), "The global response to the threat of antimicrobial resistance and the important role of vaccines", 179-197, https://doi.org/10.3233/PPL-160442.

Vasoo, S., Barreto, J.N. and Tosh, P.K. (2005), "Emerging issues in gram-negative bacterial resistance: an update for the practicing clinician", *Mayo Clin Proc*, 90(3), 395-403, https://doi.org/10.1016/j.mayocp.2014.12.002.

Wenzel, R.P. (2007), "Health care-associated infections: major issues in the early years of the 21st century", *Clin Infect Dis*, 45 (Suppl 1), S85-S88, https://doi.org/10.1086/518136.

ANTIPROLIFERATIVE EFFECTS OF *Origanum syriacum* L. AND *Myrtus communis* L. ON HUMAN COLON CANCER CELL LINE

ŞEVKET ÖZTÜRK[1], NİZAMİ DURAN[2]

[1]*Hatay Mustafa Kemal University, Faculty of Agriculture, Field Crops Department, osevket@hotmail.com*

[2]*Microbiology & Clinical Microbiology Department, Medical Faculty, Hatay Mustafa Kemal University, Turkey, nizamduran@hotmail.com*

In this study, we aimed to investigate the composition and antiproliferative efficacy of *Origanum syriacum* L. and *Myrtus communis* L. essential oils on the HCT cell line. Also, it was aimed to search the synergistic activities of *Origanum syriacum* L. and *Myrtus communis* essential oils with MTX (Methotrexate) on HCT 116 cells. The main essential oil components of *Origanum syriacum* L. were Thymol (42,18%), Carvacrol (33,95%), Cymene (8,87%), γ-Terpinene (8,21%) and for *Myrtus communis* L. the main essential oil components were Eucalyptol (45,41%), α-Pinene (20,86%), Linalool (9,71%). In this study, HCT 116 human colon cancer cell line and Vero cell line were used. To determine the non-cytotoxic concentration of *Origanum syriacum* L. and *Myrtus communis* L. essential oils Vero cell line was selected. The cytotoxic activity of the essential oils was measured using the MTT method and the results were evaluated as IC50. The Inhibition concentrations of the essential oils of *Origanum syriacum* L. and *Myrtus communis* L. essential oils against cancer HCT 116 and Vero cells were evaluated. It has been found that the essential oils of the *Origanum syriacum* L. and Myrtus communis have an important antiproliferative effect on human colon cancer cells. In our study findings, we think that these two plant essential oils may be a potent drug active compound for cancer treatment.

Keywords: Candida, *Origanum syriacum* L., essential oils, antifungal, resistance

INTRODUCTION

Colorectal cancers are the third leading cause of death among all cancer types. Colorectal cancers have only been reported to cause about 600 deaths per year in the Americas. It is known that the incidence of colorectal cancers is increasing every year. Today, the drugs used for the treatment of cancer are limited. Because of the large number of side effects of cancer drugs and the lack of high efficacy of drugs, more effective cancer drug researches continue rapidly (Garcia *et al*., 2007; Yabroff *et al*., 2008; Vogelaar *et al*., 2006).

Today, it is known that the most important active ingredient researches concentrate on natural products. Among these natural products, *Origanum syriacum* L. and *Myrtus communis* L., which have very rich bioactive components, are important plants. These two plants contain significant terpenoid flavonoids in their essential oil contents (Al-Kalaldeh *et al*., 2010; Aidi *et al*., 2009; Aidi *et al*., 2010).

In this study, we aimed to investigate the antiproliferative efficacy of *Origanum syriacum* L. and *Myrtus communis* L. essential oils on the HCT cell line. In addition, it was aimed to search the synergistic activities of *Origanum syriacum* L. and *Myrtus communis* L. essential oils with MTX (Methotrexate) on HCT 116 cells.

MATERIALS AND METHODS

Plant Materials

Origanum syriacum L. and *Myrtus communis* L. plants were harvested during the full bloom period, which the amount of active substance was most intense and after being dried in the shade at room temperature.

Preparation of Plant Extracts

Plant material was weighted and placed in a round bottom flask with a volume of distilled water as extraction solvent; the herba-water mixture was refluxed about 2 h, during which the oil was collected in the side arm of the system. The installation was allowed to stand for about half an hour to prevent the oil to reach room temperature. The oil was dried over anhydrous sodium sulphate and then stored in dark color glass bottles and keep to refrigerator (about 4 °C) until use for analysis.

GC/MS Analysis

Analysis of essential oil was performed using the Thermo Scientific Focus gas chromatograph equipped with a DSQ II single quadrupole mass spectrometer, Triplus autosampler and fused-silica capillary column TR-5MS (5% phenyl-polysilphenylene-siloxane, 30 m×0.25 mm inner diameter, film thickness 0.25 μm). The injection volume was 2 μL. The samples were injected with a split ratio of 250:1 by using helium (99.99 %) as carrier gas, at a flow rate of 1 mL/min; ionization energy was 70 eV. The transfer line temperature of the mass spectrometer was 220 °C, while the temperature of orifice injection was of 220 °C. The temperature of oven was programmed in the range 50–220 °C at a rate of 3 °C/min. Data acquisition was made in the scanning mode. Identification was done on full scan mode in the m/z range of 50–650 a.m.u.

Determination of Non-Toxic DMSO Concentration

In order to dissolve the essential oils of *Origanum syriacum* L. and *Myrtus communis* L., DMSO (dimethyl sulfoxide) was used. To determine the non-toxic concentration of DMSO on Vero cell line, $1×10^6$ cells were inoculated into each well of flat bottomed plates. RPMI-1640 was selected as a growth medium. Plates were incubated 96 hours in the presence of decreasing amounts of DMSO (8%, 4%, 2%, 1%, 0.5%).

To determine the non-cytotoxic concentration of *Origanum syriacum* L. and *Myrtus communis* L. essential oils Vero cell line was selected. The cells were cultured in RPMI 1640 supplemented with 10% fetal calf serum 1% (w/v). Cells were incubated in a humidified atmosphere at 37 ºC in 5% CO_2.

Cytotoxicity Tests

In this study, HCT 116 human colon cancer cell line was used. Vero cell line were used as healthy cell line. Then, non-toxic concentrations of *Origanum syriacum* L. and *Myrtus communis* L. essential oils were determined on Vero cells. Cytotoxicity of these two essential oils on the cells was determined by MTT (3- (4,5-Dimethylthiazol-2-yl)-2,5-diphenyltetrazolium bromide) method. The effects of different concentrations (1.25,

2.5 5, 10, 15, 20, 25, 30, 40, 50, 60, 70, 80, 90 and 100 µg/ml) of *Origanum syriacum* L. and *Myrtus communis* L. essential oils on human colon cancer cells were investigated. After incubation of the cells treated with *Origanum syriacum* L. and *Myrtus communis* L. essential oils, firstly, morphological evaluation was made by inverted microscope. And, the cells were collected and cell viability was determined by trypan blue exclusion method.

Statistical Analysis

Statistical analyses were performed using Student t-test. The *p* value <0.05 was considered significant. All statistics in the present study were done using SPSS program.

RESULTS

GS/MS analysis results of *Origanum syriacum* L. and *Myrtus communis* L. essential oils and their main components were given in Table 1,2 and Figure 1,2.

Figure 1. GC/MS chromatogram of *Origanum syriacum* L.

Table 1. The main essential oil components of *Origanum syriacum* L.

RT	Compound Name	SI	RSI	Cas #	%
6,78	α-Pinene	942	969	80-56-8	1,02
10,19	α-Terpinene	962	979	99-86-5	1,40
11,49	γ-Terpinene	988	992	99-85-4	8,21
13,07	Cymene	984	995	25155-15-1	8,87
39,35	Thymol	970	982	89-83-8	42,18
40,48	Carvacrol	966	966	499-75-2	33,95

Figure 2. GC/MS chromatogram of *Myrtus communis* L.

Table 2. The main essential oil components of *Myrtus communis* L.

RT	Compound Name	SI	RSI	Cas #	%
6,86	α-Pinene	987	990	80-56-8	20,86
10,38	Limonene	984	990	138-86-3	5,88
12,47	Eucalyptol	988	988	470-82-6	45,41
21,12	Linalool	994	994	78-70-6	9,71
27,51	α-Terpineol	983	984	98-55-5	6,11

The main essential oil components of *Origanum syriacum* L. were Thymol (42,18 %), Carvacrol (33,95 %), Cymene (8,87 %), γ-Terpinene (8,21 %) and for *Myrtus communis* L. the main essential oil components were Eucalyptol (45,41 %), α-Pinene (20,86 %), Linalool (9,71 %).

The inhibition concentrations of the essential oils of *Origanum syriacum* L. and *Myrtus communis* L. essential oils against cancer HCT 116 and Vero cells were evaluated. The IC_{50} values of *Myrtus communis* L. were determined as 25 µg/ml and 15 µg/ml for HCT 116 and Vero cells, respectively (figure 3). The IC_{50} values of *Origanum syriacum* L. were determined as 15 µg/ml and 10 µg/ml for HCT 116 and Vero cells, respectively (Figure 3).

The IC_{50} value for MTX against MCF-7 cells was determined to be 5 µg/ml. This value was calculated for the essential oils of *Origanum syriacum* L. plus MTX as 2.5 µg/ml. The IC_{50} value for MTX against MCF-7 cells was determined to be 2.5 µg/ml. This value was calculated for the essential oils of *Myrtus communis* L. plus MTX as 1.25 µg/ml. It had been found that the essential oils of *Origanum syriacum* L. and *Myrtus communis* L. essential oils enhanced synergistically the effect of MTX against HCT 116 cells (Figure 4, 5).
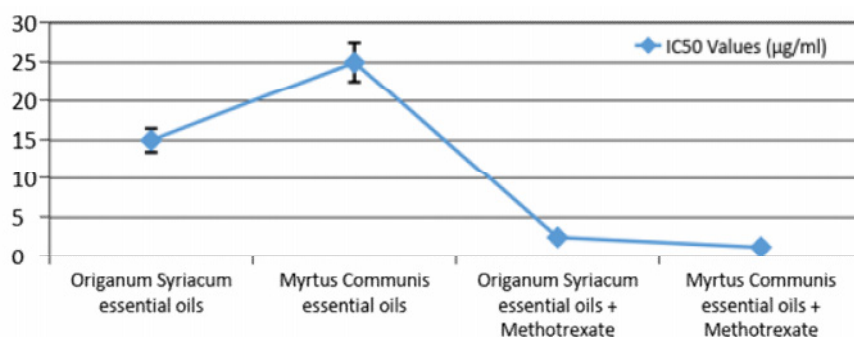
Figure 3. Effects of the essential oils of *Origanum syriacum* L. *and Myrtus communis* L. on the proliferation of HCT 116 cell line
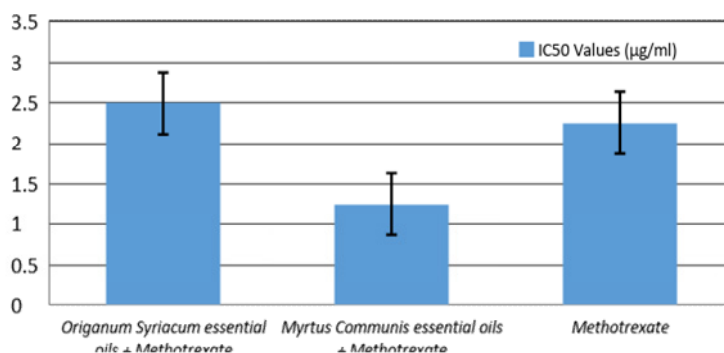
Figure 4. Comparison of MIC values of Methotrexate with the essential oils of *Origanum syriacum* L. *and Myrtus communis* L. on the proliferation of HCT 116 cell line
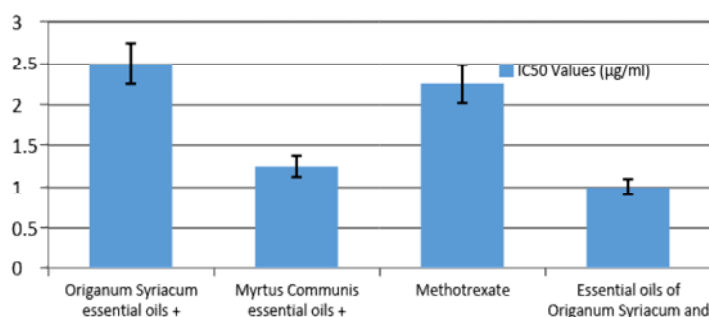
Figure 5. Comparison of the combined use of *Origanum syriacum* L. and *Myrtus communis* L. essential oils with the combined use of these essential oils with Methotrexate on HCT 116 cells

DISCUSSION AND CONCLUSION

This work is a preliminary work on the essential oils of *Origanum Syriacum* and *Myrtus Communis*. In this study, it has been found that the essential oils of the *Origanum syriacum* and *Myrtus communis* have an important antiproliferative effect on human colon cancer cells. As in our country, cancer is the second most important cause of death worldwide. The availability of a new effective and potent anti-cancer drug will be crucial for humanity. In our study findings, we think that these two plant essential oils may be a potent drug active compound for cancer treatment. In addition, further *in-vivo* studies are needed.

REFERENCES

Aidi Wannes, W., Mhamdi, B., Marzouk, B. (2009), "Variations in essential oil and fatty acid composition during *Myrtus communis* var. *italica* fruit maturation", *Food Chem*, 112, 621–626, https://doi.org/10.1016/j.foodchem.2008.06.018.

Aidi Wannes, W., Mhamdi, B., Sriti, J. (2010), "Antioxidant activities of the essential oils and methanol extracts from myrtle (*Myrtus communis* var. *italica* L.) leaf, stem and flower, *Food Chem Toxicol*, 48, 1362-1370, https://doi.org/10.1016/j.fct.2010.03.002.

Al-Kalaldeh, J.Z., Abu Dahab, R., Afifi, F.U. (2010), "Volatile oil composition and antiproliferative activity of *Laurus nobilis, Origanum syriacum, Origanum vulgare,* and *Salvia triloba* against human breast adenocarcinoma cells", *Nutr* Res, 30, 271-278, https://doi.org/10.1016/j.nutres.2010.04.001.

Garcia, M. *et al*. (2007), *Global Cancer Facts and Figures*. Atlanta, GA: American Cancer Society, 200.

Vogelaar, I., van Ballegooijen, M. and Schrag, D. (2006), "How much can current interventions reduce colorectal cancer mortality in the U.S.? Mortality projections for scenarios of risk-factor modification, screening, and treatment", *Cancer*, 107(7), 1624-1633, https://doi.org/10.1002/cncr.22115.

Yabroff, K.R., Bradley, C.J., Mariotto, A.B. (2008), "Estimates and projections of value of life lost from cancer deaths in the United States", *J Natl Cancer Inst*, 100(24), 1755-1762, https://doi.org/10.1093/jnci/djn383.

V.

MATERIALS ENGINEERING AND PERFORMANCE

EXTENSIONS OF FOOTWEAR AND LEATHER GOODS DESIGN IN DAY-TO-DAY LIFE

TRAIAN FOIAŞI

INCDTP - Division: Leather and Footwear Research Institute, 93 Ion Minulescu, Bucharest, Romania, email: icpi@icpi.ro

The fashion market world is a broad field of design experiments, a field where fashion professionals can extract, from specific situations, conditions that reveal a cultural phenomenon of social communication in the declared and outlined trend or cultural trend phase. An outfit is complete when accompanied by accessories, shoes, handbags, matching jewelry, and elements that complement fashion trends. In the game of fashion, accessories that accompany the outfit not only make the difference, but they always bring their essential contribution to perfecting the outfit. The role of the designer is to discover the rules for a cultural phenomenon expressed through high-class fashion, to break it into communication codes through aesthetic expressions, to discover the innovative direction by knowing the central and marginal elements of the aesthetic current, so as to spot the energies of the fashion market, to adhere to the rules of design and to the science of making a product in this area of day-to-day life.

Keywords: fashion, design, accessories, day-to-day life.

INTRODUCTION

A simple walk in the city becomes an immense challenge for the fashion designer. The pulse of the street, the fluster of shops, work places, lunch breaks, relaxation, and last but not least, having fun with your friends, inspire you to a joyful, colorful, optimistic collection. Day-to-day life offers the most varied forms of expression and manifestation of fashion, from minimalism to exoticism, from theater, film, to sports and beauty techniques. The choice of shapes, volumes, materials and accessories that will constitute components of the concept collection will be part of the data obtained from the artistic approach of the fashion designer. Today's fashion depends very much on ideas, individuality and authenticity of engaging in everyday life more than ever, designers look at their origins, where they started, to see where they are at the moment, why they do what they do, what their signatures mean to the public and where their values are. Fashion, by definition, talks about change and is relevant not only to the clothes and accessories (footwear, leather goods) that we wear. The quality of life contributes to our well-being, provides the safety we need. Style is a reflection of personal choice and today's fashion is a reflection of personal style. A fashion trend is born, it develops, expands and dies away under the influence of everyday life.

IDEA SKETCHES, GENERATORS OF MODERN AESTHETIC CONCEPTS IN DAY-TO-DAY FASHION
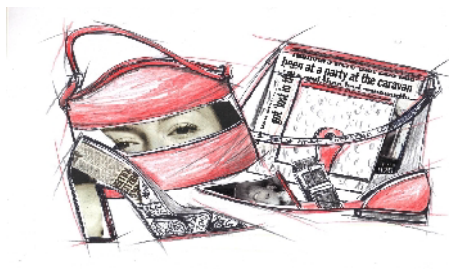
Figure 1. Artistic theater-film prints combined with bright red take you to the show world

Figure 2. Graphics, lines with optical effects and colors convey lightness and are part of daily chic
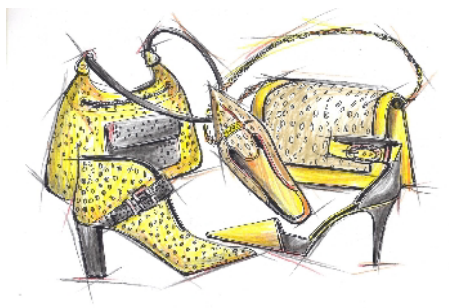
Figure 3. Polka-dot pressings and reptile effects convey comfort and relaxation
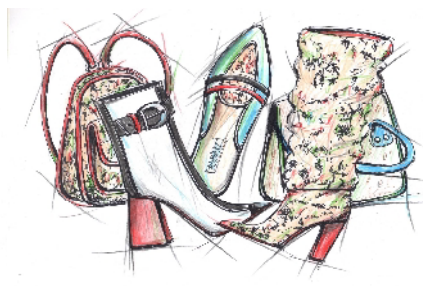
Figure 4. Vegetable designs combined with strong colors, black and white contrasts emphasize a day-to-day elegance note

COLLECTION - CONCEPT - TRANSFER FROM IDEA TO CONCRETE

The transfer of identification of shapes, volumes, materials, accessories, sketches of ideas and, last but not least, the fashion creator's restlessness in developing a concept collection with extensions in everyday life involves a multiple collaboration between creative technology and fashion design. Fashion design does not just express a new idea, but also a cultural communication through the product (the message of the product idea), a technical communication through the technical sketch of the product, a commercial communication through a collection portfolio and an advertising communication through the fashion illustration. Thus, the sketch, as a graphic form of expression of the product idea, is a working tool, mandatory in all stages of design, in all forms of fashion manifestation. Synthetic leather, laser engraved, printed, with external effects used in 3D technology, plus high-tech textiles, will satisfy the wearer's comfort. Unlike stylism, footwear design does not only deal with the image of the product and the image elements of the elaborate stylistic concept, but also with the

transposition into components and patterns of an idea sketch. In design, ideational logic is organized on the principles of classical logic, and from an economic point of view, the organization of the product concept is based on the principles of efficiency. Footwear design involves a complex process of ideation, conceptualization, design, graphic design, advertising, illustration. Trend samples are designed to provide industry customers with clear and practical solutions to fashion trends in a particular fashion sector.
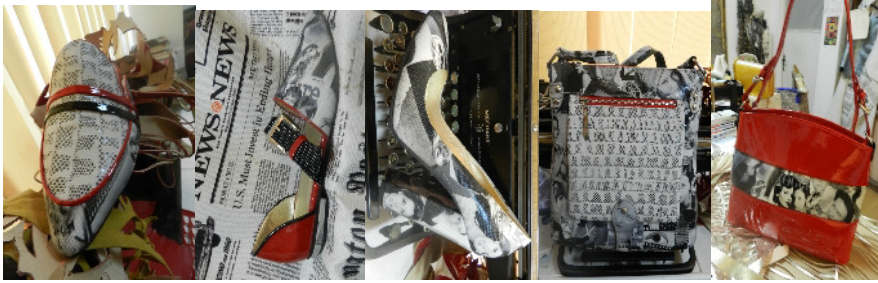
Figure 5. Theater-film prints are supported by the nickel accessories and patent leather accents
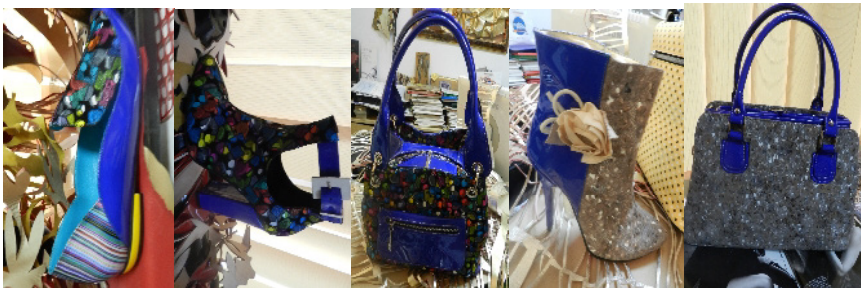
Figure 6. The play of colors is a reminder of relaxation, clubbing, joy

Figure 7. Harmonizing colors and decorative elements transform the classic into challenge

Figure 8. Everyday life can become a memory. COURREGES, the avantgardist of the 60s, leaves room for interpretation

Figure 9. 2018-2019 concept collection with extensions in day-to-day life

CONCLUSIONS

The melange of images becomes a challenge for specialists in the field and receptors alike. Accessory designers create concept pieces, making a prototype first. The received images become defining elements of the creative artistic concept, and they are transposed into artistic and aesthetic proposals as applied research. The way to get the first elements that prefigure the object imagined by the designer of the high-end product is filtered by successive stages, that can be cultural, emotional and less pragmatic as an initial approach. In footwear design, the designer takes into account both stylistic, technological, marketing and financial elements, demonstrating once again that fashion design is an industry that belongs to a separate economy with its cultural and artistic components but which remains an industry. Trend samples are designed to provide industry customers with clear and practical solutions to fashion trends in a particular fashion sector of the industry. It provides a database of creative ideas that will

contribute to the competitiveness of industrial products in a unitary conceptual direction, allowing specialists to have a new inspiration for their own projects, to better understand the fashion market, to identify new models. These will be the starting point for their implementation in the industry. The sketches of ideas elaborated and presented in the paper address different themes in terms of artistic form and facilitate the quick understanding of the sketch-object approach for specialists in the field.

Acknowledgement

REFERENCES

Ars Sutoria, no. 420, Milano 2017.
Ars Sutoria, no. 421, Milano 2017.

COMPARATIVE STUDY ON THE LIGHT FASTNESS PROPERTIES OF DIFFERENT WHITE TANNING AGENTS

HUSEYIN ATA KARAVANA, ERSIN ONEM, ALI YORGANCIOGLU, NILAY ORK EFENDIOGLU, ARIFE CANDAS ADIGUZEL ZENGIN, BEHZAT ORAL BITLISLI

Ege University, Engineering Faculty, Leather Engineering Department, 35100, Izmir, Turkey, huseyin.ata.karavana@ege.edu.tr, ersin.onem@ege.edu.tr, ali.yorgancıoglu@ege.edu.tr, nilay.ork@ege.edu.tr, candas.adiguzel@ege.edu.tr, oral.bitlisli@ege.edu.tr

The main causes of leather goods damage is fading as well as the damages caused by sweat and body grease, mechanical deformation and ageing. Tanning agents have varied efficiency on the UV durability and stabilization of collagen. It is because they have different bond strengths and binding mechanisms with leather. In this study, light fastness properties of the leathers tanned with the most commonly used white tanning agents were aimed to evaluate by using ATLAS XENOTEST ALPHA+ test instrument according to ISO 105-B02 standard test method and the leathers tanned with chromium tanning agent were used as a comparison. Blue wool test references were evaluated according to grey scale, and the evaluation of the color change for the tanned and dyed leathers against UV application of an artificial light source representative of natural daylight was carried out. In addition to light fastness test, colorimetric measurements of the treated samples and color changes before and after the UV application were also spectrophotometrically determined by Konica Minolta CM-3600d test device. The results showed that chromium tanned leathers provided the best light fastness results compared to other leathers tanned with white tanning materials. Zirconium and phosphonium tanned leathers had the same values and better than aluminum and vegetable tanned leathers.

Keywords: Leather, light fastness, tanning agents.

INTRODUCTION

Fading is one of the main causes of damage to leather goods, apart from damages caused by sweat and body grease, mechanical deformation and ageing. The light fastness of a material describes its resistance to fading by light, in particular by the constant radiation of UV light (Gülümser *et al.*, 2008). Sunlight is reaching to earth as electromagnetic radiation. The spectral form and intensity of light exposed on a dyed material have great effect on fading degree. The radiation between 290-400 nm is named as Ultra violet or UV. This radiation up to 400 nm have more energy and can break ionic, hydrogen and even covalent bonds in the material (Omur and Mutlu, 2016; Demir *et al.*, 2008). Materials that resist this effect are referred to be lightfast.

Leather products such as garment, upholstery and the leathers used for upper and automotive purposes are required a considerable fading characteristic during the daily use. Tanning operation plays a key role in improving the durability and stability of leather by strong crosslinks in the triple helical collagen matrix. It is the main process of leather manufacturing, which makes the hide and skin durable and less susceptible to decomposition (Heidemann, 1993).

In the leather industry, different tanning agents can be used to produce different types of leather products with different bonding mechanism. Nowadays mineral tanning is of technical importance for leather manufacturing considering the properties and performance (Covington, 1997). Mineral tannage is the preference in many leather types so that leathers become softer, lighter and more flexible as well as having higher hydrothermal stability as compared to vegetable tannage. The mineral tanned leathers are proper to dyeing process and can be finished in different methods. Among the

mineral tanning agents, chromium salts have known as ideal tanning agent considering the characteristics that provides to final leather (Covington, 2009).

Although chromium salts are the mostly used tanning agent due to their high hydrothermal stability and good organoleptic properties, their usage has been limited because of adverse effects on environment and human health. Therefore, recently alternative tannages have been replaced with chromium in order to make use of the mineral tanning advantages lacking with other organic tanning procedures (Ogata *et al*., 2018; Moretto, 2015).

In today's trends toward chrome-free tanning technology (Madhan *et al*., 2007); zirconium, aluminum, organic phosphonium salts and vegetable tannins are the alternative options to chromium tannage. Although mineral tanned leathers have advantages such as better durability, high performance and good dyeability, however they are not chemically stable and satisfactorily soft and flexible as well as having appropriate hydrothermal stability compared to chromium salts (Li *et al*., 2006; Fathima *et al*., 2006, 2005, 2003).

To reveal the tanning material effect on the light fastness properties of leathers, in this study, the light fastness properties of various white tanning agents such as aluminum, zirconium, phosphonium and tara were investigated in order to compare with the commonly used chromium salt.

MATERIALS AND METHODS

Materials

Commercially pickled Spanish sheepskins were used for tanning operations. Tanning agents used in the study were industrially produced, commercially available products: chromium salt from ''Sisecam Chemicals,'' aluminum salt from ''Zschimmer and Schwarz GmbH & Co. KG,'' phosphonium and zirconium salts from ''Clariant'' and tara tannin from ''Silvachimica S.r.l'' Other chemicals used in the production were provided from various suppliers.

Depickling, Tanning and Post-tanning Processes

Depickling process was applied for all leathers before tanning operations. Following the depickling process, the skins were tanned with chromium and different type of white tanning agents by conventional methods. Post-tanning processes were performed as shown in Table 1. Two independent processes were applied for each tanning agent.

Table 1. Post-tanning processes for differentiated tanning operations

Process	%	Chemicals	Temp (^{o}C)	Time (min)	Remarks
Neutralization	100	Water	40		
	1	HCOONa		2x20	7 ^{o}Bé
	0.8	NaHCOO$_3$		3x20	pH 5.5
Washing x 3	200	Water	30	20	Drain
Retanning	100	Water	40		
	3	Syntan		20	
	4	Dicyandiamide resin		20	
	3	Acrylic syntan		20	
Fatliquoring	+50	Water	60		

Process	%	Chemicals	Temp (°C)	Time (min)	Remarks
	3	Synthetic fatliquoring agent			
	2	Phosphoester fatliquoring agent			
	2	Lanoline based fatliquoring agent			
	3	Sulphited natural fatliquor		60	
Dyeing	1	Dye auxiliary	40	20	
	4	Dyestuff		45	
	2.5	HCOOH		30	pH 4.0
Washing x 3	200	Water	30	20	Drain
		Horsing-Drying-Dry drumming-Toggling			

Light Fastness Test of the Leathers

Light fastness tests of the leathers were performed by using ATLASXENOTEST ALPHA+ test instrument in accordance with the standard ISO 105-B02 in triplicates. A specimen of the leather to be tested is exposed to artificial light under controlled conditions, together with a set of reference materials. The colour fastness is assessed by comparing the change in colour of the test specimen with that of the reference materials used. Blue wool test references (1 to 8) were evaluated to the scale (according to grade 4 – contrast between the exposed and the unexposed portions of the specimen), then the grey scale was used for evaluation of the leathers colour change against UV application of an artificial light source representative of natural daylight (Xenon arc fading lamp) with ISO 105-A02.

Colorimetric Measurements

Konica Minolta CM-3600d brand spectrophotometer was used for measuring the colours of the leathers which were processed with different tanning agents. The effect of each tanning material on the leather colour has been examined before and after the UV application of an artificial light source representative of natural daylight. Then they were compared with the original samples. The colour differences between the control sample and the leathers processed with tanning agents were calculated according to CIE Lab-76 colour difference formula (CIE, 1976). Colorimetric measurements were carried out on both tanned and dyed leathers in triplicates.

RESULTS AND DISCUSSIONS

Colorimetric measurements and grey scale evaluations of the tanned leather samples before and after light fastness tests were given in Table 2. The tests were also performed after the post-tanning operations for the dyed leathers as provided in Table 3.

Table 2. Colorimetric measurements and grey scale evaluations of the tanned leathers

Leather samples	Before analysis			After analysis			Color difference (ΔE)	Grey scale evaluation
	L	a	b	L	a	b		
Chromium tanned	79.13	-6.35	0.89	78.77	-7.74	1.47	1.55	4/5
Aluminum tanned	90.32	0.34	7.96	93.08	0.42	5.23	3.89	3
Zirconium tanned	92.03	0.23	7.55	94.11	0.29	4.95	3.32	3/4
Phosphonium tanned	91.35	0.12	7.95	93.38	0.11	5.84	2.94	3/4
Tara tanned	91.36	0.23	8.28	85.65	1.74	21.06	14.09	2

Table 3. Colorimetric measurements and grey scale evaluations of the dyed leathers

Leather samples	Before analysis			After analysis			ΔE	Grey scale evaluation
	L	a	b	L	a	b		
Chromium tanned	60.28	5.14	27.52	67.08	1.31	19.98	10.85	2/3
Aluminum tanned	56.87	10.16	32.33	65.81	6.63	25.97	11.52	2/3
Zirconium tanned	60.11	10.95	34.44	68.18	7.66	27.69	11.02	2/3
Phosphonium tanned	63.34	8.71	32.13	71.55	5.57	24.62	11.57	2/3
Tara tanned	54.44	10.55	29.41	61.06	8.30	26.51	9.57	2/3

The tanned leathers exhibited very slight differences in lightness values (L) except vegetable tanned leathers after the light fastness tests as indicated in Table 2. For yellowness (b) wet blue samples showed a slight increase, whereas aluminum, zirconium and phosphonium tanned leathers showed lower values than the original samples after the UV application. Tara tanned leathers gave the highest b value and exposed to high changes by increasing the yellowness value of the leathers. The colour differences (ΔE) showed that vegetable (tara) tanned leathers have the maximum ΔE values of 14.09. Besides, chromium tanned leathers yielded the minimum ΔE value of 1.55 which was the sign of minimum colour (ΔE) differences for the wet blue leathers as compared to control sample.

These differences were also observed and confirmed by the grey scale evaluations. Chromium tanning material provided the best light fastness value (4/5) compared to other white tanning materials. Zirconium and phosphonium tanned leathers had the same values (3/4) and better than aluminum (3) and vegetable tanned leathers (2).

After the post-tanning operations, no significant color differences between the leathers differentiated in tanning operations were observed. Minimum ΔE value was determined from vegetable tanned leathers while the highest value was seen from phosphonium tanned leathers. According to the grey scale evaluation, same light fastness values (2/3) were obtained for each dyed sample because of the dyeing process as seen in Table 3.

Most coloured materials can fade or change in color when they are exposed to light for prolonged periods of time. In a photochemical reaction it is necessary that at least one of the reacting molecules has absorbed light. This compound is then in an excited state. In systems in which the stability of a dyestuff is of interest, three basic types of photochemical reactions are possible. Firstly, the dye can absorb light and then decompose, because the dye molecules are not chemically stable in their excited form. Reactions with other substances present in the system are in this case not necessary for

the photodecomposition of the dye. A second possibility is that the photo-excited dye molecules are unstable only if certain other substances are also present in the system. These substances concerned are absent; the activated dye molecules are reconverted into their stable ground states by physical deactivation processes. Under these conditions no fading occurs. A third possibility is that substances, other than dyestuff, absorb the light and then react in their photo-excited state with the dyestuff (Ozgunay, 2008; Crews, 1987; Padfield and Landi, 1966).

The highest light fastness value was obtained with chrome tanned leathers as expected due to the strong covalent bonding between chromium and collagen. On the other hand, aluminum tanned leathers showed the poor fastness values among the white mineral and organic tanning agents since it forms only electrostatic interactions with collagen.

Aromatic organic structures tend to absorb high energy ultraviolet radiation and for this reason they are less radiation stable than aliphatic organic compounds. Tannins based on aromatic organic compounds cannot be high lightfast because of their nature. In our study it is also revealed that the lowest light fastness values were obtained from vegetable tanned leathers and their dyed forms.

CONCLUSION

In the study, the light fastness properties of sheep leathers tanned with different white tanning materials were aimed to determine to compare the results with the chromium tanned leathers and following conclusions have been drawn;
   a. The highest color difference was observed from the leathers tanned with tara vegetable tannin after the light fastness test.
   b. The leathers tanned with chromium salts gave the best light fastness value compared to white mineral tanning agents.
   c. Slight differences were determined after the light fastness test for the white mineral tanning agents.
   d. After the post tanning operations, high ΔE values were obtained compared to tanned leathers. But they showed only slight differences in terms of color change after the light fastness tests.

REFERENCES

CIE (Comission Interantionalle DeL'Eclairage) (1976), *Official recommendations on uniform colour spaces colour difference equations metric colour terms*.
Covington, A.D. (1997), "Modern Tanning Chemistry", *Chemical Society Reviews* 26, 111, https://doi.org/10.1039/cs9972600111.
Covington, A.D. (2009), *Tanning Chemistry – The Science of Leather*, Cambridge, Royal Society of Chemistry Publishing, 592.

Crews, P.C. (1987), "The fading rates of some natural dyes", *Studies in Conservation*, 32, 65-72, https://doi.org/10.1179/sic.1987.32.2.65.

Demir, A., Öktem, T. and Seventekin, N. (2008), "Reaktif boyalı pamuklu materyallerin ışık haslığına UV absorplayıcıların etkisi", *Tekstil ve Konfeksiyon*, 2, 211-220.

Fathima, N.N. *et al*. (2003), "Effect of zirconium(IV) complexes on the thermal and enzymatic stability of type I collagen", *Journal of Inorganic Biochemistry*, 95, 47–54, https://doi.org/10.1016/S0162-0134(03)00071-0.

Fathima, N.N. *et al*. (2005), "Iron-phosphonium combination tanning: Towards a win-win approach", *Journal of the American Leather Chemists Association*, 100, 273-281.

Fathima, N.N. *et al*. (2006), "Wet white leather processing: A new combination tanning system", *Journal of the American Leather Chemists Association*, 101, 58-65.

Giles, C.H. (1965), "The fading of coloring matters", *Journal of Applied Chemistry*, 15, 541-550, https://doi.org/10.1002/jctb.5010151201.

Gülümser, T., Karagöz, E., Akçakoca, P. (2008), "Pamuk liflerinin fluoresan boyar maddeler ile boyanması ve ışık haslığının geliştirilmesi üzerine bir araştırma", *Tekstil ve Konfeksiyon*, 4, 284-288.

Heidemann, E. (1993), *Fundamentals of Leather Manufacture*, Roetherdruck, Darmstad, 647.

ISO 105-B02:2000/Amd.2.2000(E), Colour fastness to artificial light: Xenon arc fading lamp test.

ISO 105-A02, Textiles – Tests for colour fastness – Part A02: Grey scales for assessing change in colour.

Li, Y. *et al*. (2006), "Reaction mechanism of tereakis hydroxymethyl phosphonium with collagen protein", *Journal of the Society of Leather Technologist and Chemists*, 90, 214-216.

Madhan, B. *et al*. (2007), "Combination tanning based on tara: An attempt to make chrome-free garment leather", *Journal of the American Leather Chemists Association*, 102, 198-204.

Moretto, A. (2015), "Hexavalent and trivalent chromium in leather: What should be done?", *Regulatory Toxicology and Pharmacology*, 73, 681-686, https://doi.org/10.1016/j.yrtph.2015.09.007.

Ogata, K. *et al*. (2018), "Self-conversion of hexavalent chromium formed in chrome-tanned leather during long-term storage and perfect inhibition with a combination of inhibitors", *Journal of the Society of Leather Technologists and Chemists*, 102, 53-58.

Omur, S. and Mutlu, M.M. (2016), "Modification of mimosa and quebracho tannins and the lightfastness properties of the proccesed leathers", *Tekstil ve Konfeksiyon*, 26, 230-235.

Ozgunay, H. (2008), "Lightfastness properties of leathers tanned with various vegetable tannins", *Journal of the American Leather Chemists Association*, 103, 345-351.

Padfield, T. and Landi, S. (1966), "The light-fastness of the natural dyes", *Studies in Conservation*, 11, 181-195, https://doi.org/10.1179/sic.1966.022.

NEW PRODUCTS BASED ON ESSENTIAL OILS FOR FINISHING NATURAL LEATHERS WITH ANTIFUNGAL PERFORMANCES – PART 1

OLGA NICULESCU, GHEORGHE COARĂ, CIPRIAN CHELARU, DANA GURĂU

INCDTP – Division: Leather and Footwear Research Institute, 93 Ion Minulescu, Bucharest, Romania, email: icpi@icpi.ro

Research aims the replacement of potentially toxic biocides with ecologic materials – essential oils extracted from plants. Some biocides used in the leather industry have a certain toxicity, and are prohibited by the directives in force. Products with antifungal and antibacterial properties were obtained, containing cedar essential oil, emulsion of beeswax and lanolin mixture in a 1/3 ratio, stabilized with ethoxylated lauryl alcohol and ethyl alcohol. This paper presents the process of obtaining and characterization, by physico-chemical and spectral analyses, of new product based on cedar essential oil, ethyl alcohol, non-ionogenic surfactants from the category of polyethoxylated fatty alcohols and wax emulsions containing beeswax, lanolin and non-ionogenic emulsifier. Cedar essential oil contains: thujopsene – 37.25% and cuparene – 9.47% with antibacterial and antifungal properties, cedrenol – 20.79% and cedrene – 20.03% with antimicrobial properties as main components. The spectrum of the product based on cedar essential oil, contains all the bands of components: an intense band at about 2925 cm^{-1} and weaker one at about 2874 cm^{-1} assigned to asymmetrical and symmetrical stretching vibrations of methyl and methylene groups of cedar oil, beeswax and lanolin; a weak band around 1643 cm^{-1} due to the stretching of the C = O bond of ester groups, two more intense bands at 1455 and 1374 cm^{-1} specific to compounds containing long aliphatic chains, and bands at about 1087 and 1045 cm^{-1} assigned to C-O-C bonds of ether. The prepared product are yellowish white fluids, homogenous, with 11-18% dry substance, pH – 3.8-4.5, density – 0.805-0.820 g/cm^3.

Keywords: essential oils, FT-IR spectrometry, Gas Chromatography Mass Spectrometry (CG/MS)

INTRODUCTION

In order to prevent the emergence and growth of microorganisms, biocides are used in various stages of leather processing, improving resistance to biological attack and preventing deterioration of mechanical and chemical properties of leather (Heidemann, 1994; Chirita *et al*., 1999; Niculescu *et al*., 2013; Niculescu *et al*., 2015).

Biocides (based on beta-naphthol, benzothiazole and sulfone derivatives, organic sulfur compounds, etc.) used in the leather industry have a certain toxicity to humans and the environment, some of which are prohibited by the directives in force (pentachlorophenol, polyhalogenated phenolic compounds) (Directive 2010/75/EU).

Recent research aims to fully or partially replace potentially toxic biocides with environmentally friendly materials.

The literature indicates the use of oregano, aloe vera, eucalyptus, lavender, or coriander essential oils to treat tanned leather in wet finishing operations, in the composition of the fatliquoring mixture or for surface treatment (Bayramoglu, 2007; Cadirci *et al*., 2010; Sirvaityte *et al*., 2011; Niculescu *et al*., 2017).

Essential oils are highly concentrated in biologically active compounds with different properties: antiseptic, antibacterial, immunostimulatory etc. (Romanian Pharmacopoeia, 1998; European Pharmacopeia, 2005). These can be used to protect against damage caused by fungi and bacteria. Cedar essential oil contains: thujopsene – 37.25% and cuparene – 9% with antibacterial and antifungal properties, cedrenol – 21% and cedrene – 20% with antimicrobial properties as main components (Moldovan, 2001; David *et al*., 2008).

The effectiveness of biocides is established using biological methods of assessing mold and bacteria attack on leather. Assessment is performed using standardized, leather-specific methods (ST 12697/A 91/2008).

EXPERIMENTAL

Materials

Cedar essential oil (Solaris Plant, Bucharest), containing 37.25% thujopsene, 20.03% cedrene, 20.79% cedrenol, cuparene etc.

Beeswax (Happynatura, Bucharest), solid with specific odour, yellow colour, melting point 62-65°C.

Lanolin (Medchim, Bucharest), solid greasy compound with specific odour, light yellow colour, melting point 38-42°C.

Nonionic emulsifier – lauryl alcohol ethoxylated with 7 moles of ethylene oxide (Elton, Bucharest), melting point -15^{0}C, ignition point over 170^{0}C, density – 0.97 g/cm^3 at 40^{0}C, pH – 5-7, viscosity – 25 mPa x s.

Ethanol (Chemical Company, Germany), density – 0.789 g/cm^3 at 20^{0}C, boiling point – 78^{0}C, melting point –114^{0}C, water solubility – in any proportion.

Methods

The product with antifungal properties was prepared in an equipment consisting of a reaction vessel with 3L capacity and a heating system (electric bath with temperature control). The 3-necked reaction vessel, made of high-temperature resistant glass, is equipped with a propeller stirrer to homogenize the reaction mass, a thermometer for temperature control and condenser connected to the water source to maintain the temperature constant during the preparation process.

Gas Chromatography Mass Spectrometry (GC/MS) Analysis: Analysis of the essential oils carried out by using Agilent 7890 A GC System equipped with Agilent 5795 C MS, and HP-5 MS (0.25 mm x 30 m i.d., film thickness 0.25). The carried gas helium (99.9%) at a flow rate of 1 mL/ min; ionization energy was 70 eV. Mass range m/z 50-650 amu. Data acquisition was scan mode. MS transfer line temperature was 250 ^{0}C, MS Ionization source temperature was 230 ^{0}C, the injection port temperature was 250 ^{0}C. The samples were injected with 250 split ratio. The injection volume was 1 μL. Oven temperature was programmed in the range of 50 to 250 ^{0}C at 3^{0}C/ min. The structure of each compound was identified by comparison with their mass spectrum (Nist 05 and Wiley 7 library).

Attenuated Total Reflectance Fourier transform infrared spectroscopy (ATR-FTIR) measurements were run with a Jasco instrument (model 4200), in the following conditions: wavenumber range – 4000-600 cm^{-1}; data pitch – 0.964233 cm^{-1}; data points – 3610: aperture setting – 7.1 mm; scanning speed – 2 mm/s; number of scans – 30; resolution – 4 cm^{-1}; filter – 30 kHz; angle of incident radiation – 45°.

Components Used to Obtain Antifungal and Antibacterial Products

The chromatogram of cedar oil is shown in figure 1, and identification of compounds in their composition is presented in table 1.
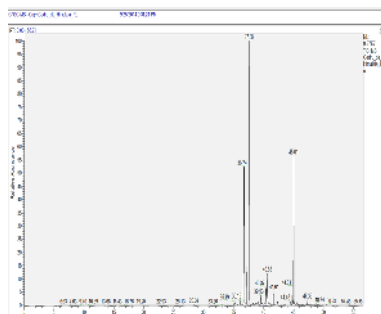
Figure 1. Chromatogram of cedar oil

Table 1. Identification of organic compounds in the cedar essential oil by GC-MS

RT	Amount, %	Compounds
35.19	0.87	α-Humulen
36.13	0.57	trans-Cariofilen
36.74	20.03	Cedrene
37.11	4.58	α-Funebren
37.56	37.25	Tuiopsen
38.62	0.50	Aromadendrene
39.08	1.08	ar-Cucumen
40.65	9.47	Cuparen
40.92	1.10	Z,Eα-Farnesen
41.61	1.63	α-Longipinen
44.46	0.51	Epiglobulol
45.01	20.79	Cedrenol
45.69	0.87	cis-Farnesol
47.38	0.74	α-Bisabolol

Cedar essential oil contains: thujopsene – 37.25% and cuparene – 9.47% with antibacterial and antifungal properties, cedrenol – 20.79% and cedrene – 20.03% with antimicrobial properties as main components.

Obtaining Antifungal and Antibacterial Products

The antifungal product based on cedar essential oil (marked AF-C-2) was obtained from 80 % cedar essential oil, 10 % wax emulsion, 5-10 % ethanol and 5-10% ethoxylated lauryl alcohol.

The wax emulsion was obtained from: 15-20% wax mixture 1/3, 10% ethoxylated lauryl alcohol reported to the amount of wax emulsified and water under stirring (300-500 rot/min), at 60-80^{0}C.

The wax mixture was obtained by beeswax and lanolin (1:3) liquefied by heating at 80-90^{0}C and stirring for 40-60 min (60-80 rot/min).

RESULTS AND DISCUSSION

Physical-Chemical Characteristics of Antifungal Product Based on Natural Oils and Waxes

The prepared product AF-C-2, are yellowish white fluids, homogenous, with 11-18% dry substance, pH – 3.8-4.5, density – 0.805-0.820 g/cm^3.

FT-IR Characterization of Components Used and Produced with Antifungal Properties Obtained

FT-IR spectra of the components of the antifungal products AF-C-2, containing cedar oil, beeswax and lanolin and of the films obtained thereof by evaporation are presented in figure 2.
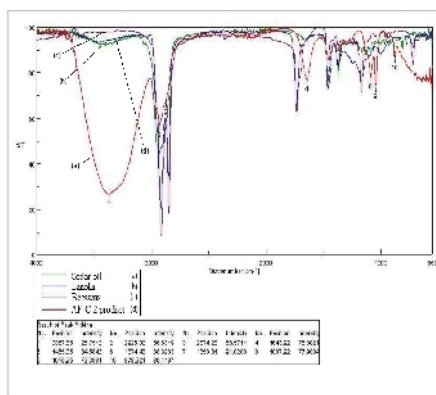
Figure 2. Overlapping FT-IR spectra of cedar oil, waxes and film obtained from the antifungal and antibacterial product AF-C-2

The spectrum of the AF-C-2 contains all the bands of components: an intense band at about 2925 cm^{-1} and weaker one at about 2874 cm^{-1} assigned to asymmetrical and symmetrical stretching vibrations of methyl and methylene groups of cedar oil, beeswax and lanolin; a weak band around 1643 cm^{-1} due to the stretching of the C = O bond of ester groups, two more intense bands at 1455 and 1374 cm^{-1} specific to compounds containing long aliphatic chains, and bands at about 1087 and 1045 cm^{-1} assigned to C-O-C bonds of ether.

CONCLUSIONS

▪ Cedar essential oil contains: thujopsene – 37.25% and cuparene – 9.47% with antibacterial and antifungal properties, cedrenol – 20.79% and cedrene – 20.03% with antimicrobial properties as main components.
▪ The spectrum of the AF-C-2 contains all the bands of components.
▪ The prepared product AF-C-2, are yellowish white fluids, homogenous, with 11-18% dry substance, pH – 3.8-4.5, density – 0.805-0.820 g/cm^3.

▪ The prepared antifungal and antibacterial product made of natural components (beeswax, lanolin, cedar essential oil) will be tested to determine the resistance to fungi of the natural leathers treated with this product.

Acknowledgements

REFERENCES

Bayramoglu, E.E. (2007), "Unique biocide for the leather industry: essential oil of oregano, *JALCA*, 102(11), 347.

Cadirci, B. *et al*. (2010), "Physical and antimicrobial characteristics of aloe vera treated split suede leather", *JALCA*, 105(2), 34.

Chirita, Gh. and Chirita, M. (1999), *Tratat de chimia şi tehnologia pieilor şi blănurilor*, vol. I, Ed. Gh. Asachi, Iaşi.

Council of Europe (2005), *European Pharmacopeia*, vol. II, ESCOP Strasbourg.

David, V. and Medvedovici, A. (2008), *Methods of separation and chromatographic analysis*, University of Bucharest Press.

Heidemann, E. (1994), *Fundamentals of Leather Manufacturing*, Eduard Roether KG Druckerei und Verlag, Darmstadt.

Moldovan, Z. (2001), *Instrumental Analysis Methods*, University of Bucharest Press.

Niculescu, O. and Manta, A. (2013), "Products with antifungal properties for finishing natural leather and leather items", Patent Application OSIM A/00538.

Niculescu, O. *et al*. (2015), "Obtaining and characterizing a product with antifungal properties based on essential oils and natural waxes for finishing natural leathers", *Rev. Chim. (Bucharest)*, 66(11), 1733-1736.

Niculescu, O. *et al*. (2017), "Finishing product for improving antifungal properties of leather", *Leather and Footwear Journal*, 1, 31-38, https://doi.org/10.24264/lfj.17.1.4.

Sirvaityte, J., Siugzdaite, J. and Valeika, V. (2011), "Application of commercial essential oils of Eucalyptus and Lavender as natural preservative for leather tanning industry", *Rev. Chim. (Bucharest)*, 62(9), 884.

*** (1998), *Romanian Pharmacopoeia*, 10th edition, Medical Ed., Bucharest.

***, Directive 2010/75/EU of the European Parliament and of the Council of 24 November 2010 on industrial emissions (integrated pollution prevention and control).

***, ST 12697/A 91/2008, Standard for Determination of Leather Resistance to Fungi.

NEW PRODUCTS BASED ON ESSENTIAL OILS FOR FINISHING NATURAL LEATHERS WITH ANTIFUNGAL PERFORMANCES – PART 2

OLGA NICULESCU, GHEORGHE COARĂ, CIPRIAN CHELARU, DANA GURĂU

INCDTP – Division: Leather and Footwear Research Institute, 93 Ion Minulescu, Bucharest, Romania, email: icpi@icpi.ro

Research aims the replacement of potentially toxic biocides with ecologic materials – essential oils extracted from plants. Some biocides used in the leather industry have a certain toxicity, and are prohibited by the directives in force. This paper presents the resistance to mold of leather treated with the developed essential oil-based products, development of the *Aspergillus niger* strain on leather samples over time, i.e. macroscopic images of the samples treated with antifungal products based on cedar and coriander oils. Because the product made of cedar essential oil is less efficient, mixtures of the two antifungal products (based on cedar and coriander oils) were used on the surface leather in the final dressing composition. Testing of antifungal products based on cedar and coriander oils was carried out monitoring the manner in which mold growth is influenced by the treatment applied to the sample through the resistance to mold in simulated contamination conditions. These products improve leather and leather product resistance to fungi, while ensuring a higher quality of leather objects.

Keywords: natural leathers, essential oils, *Aspergillus niger*

INTRODUCTION

In order to prevent the emergence and growth of microorganisms, biocides are used in various stages of leather processing, improving resistance to biological attack and preventing deterioration of mechanical and chemical properties of leather (Heidemann, 1994; Chirita *et al*., 1999; Niculescu *et al*., 2013; Niculescu *et al*., 2015).

Biocides (based on beta-naphthol, benzothiazole and sulfone derivatives, organic sulfur compounds, etc.) used in the leather industry have a certain toxicity to humans and the environment, some of which are prohibited by the directives in force (pentachlorophenol, polyhalogenated phenolic compounds) (Directive 2010/75/EU). Recent research aims to fully or partially replace potentially toxic biocides with environmentally friendly materials. The literature indicates the use of oregano, aloe vera, eucalyptus, lavender, or coriander essential oils to treat tanned leather in wet finishing operations, in the composition of the fatliquoring mixture or for surface treatment (Bayramoglu, 2007; Cadirci *et al*., 2010; Sirvaityte *et al*., 2011; Niculescu *et al*., 2017).

Essential oils are highly concentrated in biologically active compounds with different properties: antiseptic, antibacterial, immunostimulatory etc. (Romanian Pharmacopoeia, 1998; European Pharmacopeia, 2005). These can be used to protect against damage caused by fungi and bacteria. Cedar essential oil contains: thujopsene – 37.25% and cuparene – 9% with antibacterial and antifungal properties, cedrenol – 21% and cedrene – 20% with antimicrobial properties as main components (Moldovan, 2001; David *et al*., 2008).

The effectiveness of biocides is established using biological methods of assessing mold and bacteria attack on leather. Assessment is performed using standardized, leather-specific methods (ST 12697/A 91/2008).

EXPERIMENTAL

Materials

Roda Wax MONO (Triderma, Germany), wax emulsion for ground coat: dry substance – 36.87%, pH (10% solution) – 4.2, Ford cup viscosity $\Phi4$ – 12, kinematic viscosity, cSt – 8.97, density – 0.957 g/cm^3;

Roda-Cryl 87 (Triderma, Germany), acrylic binder for ground coat, dry substance – 34.50%, pH (10% solution) – 6.0, Ford cup viscosity Φ4 – 14, density – 1.025 g/cm^3;

Roda-Pur Wx 1418 (Triderma, Germany) polyurethane binder for ground coat: dry substance – 19-21%, pH (10% solution) – 7.5-9.5.

Roda-Pur 5011 (Triderma, Germany), polyurethane binder used as a fixing agent (final dressing) for finishes applied to natural leather: dry substance – 40%, pH (10% solution) – 5.5, Ford cup viscosity Φ4 – 7, density – 1.053 g/cm^3.

Product (marked AF-C-2) with antifungal properties (made from cedar essential oil, beeswax, lanolin, ethanol and lauryl alcohol ethoxylated with 7 moles of ethylene oxide: dry substance – 11%, pH (10% solution) – 3.8, density –0.810 g/cm^3 (INCDTP–Division Leather and Footwear Research Institute Bucharest, Romania).

Product (marked AF-C-1) with antifungal properties (made from coriander essential oil, beeswax, lanolin, ethanol and lauryl alcohol ethoxylated with 7 moles of ethylene oxide: dry substance – 12%, pH (10% solution) – 4.5, density –0.820 g/cm^3 (INCDTP–Division Leather and Footwear Research Institute Bucharest, Romania).

The crust bovine leathers natural grain assortments, mineral tanned and wet finished by retanning, fatliquoring and dyeing (1.2-1.4 mm thick, dyed black and brown) (INCDTP – Division Leather and Footwear Research Institute Bucharest, Romania).

Methods

Bioassay was used to determine the resistance to bacteria and fungi of leather. Method for resistance to fungi is provided in STAS 12697 / A 91: 2008 "Leather. Mold attack test." It examines how the growth of mold is influenced by existing treatment on the leather sample treated with biocides through mold resistance under simulated contamination. Aspergillus niger was inoculated in 3 points (right, center and left of the sample) according to the procedure of ASTM D 4576-86, "Standard test method for mold growth resistance of blue stock (leather)". The duration of incubation is 28 days, fungal observations being made at intervals of 7, 14, 21 and 28 days. The development of Aspergillus niger strain on leather samples analyzed was expressed according to standard notation by ranking from 0 to 5.

Testing of Antifungal Products Based on Cedar and Coriander Oils

The framework technology for dry finishing of bovine leather into natural grain box assortments, is presented in table 1.

Table 1. Framework technology for dry finishing of bovine hides into natural grain box

Operation	Dispersion composition/application method
Application of dispersion I (basecoat)	30 g/L aqueous wax emulsion (Roda wax MONO) 150 g/L aqueous acrylic dispersion (Roda-cryl 87) 150 g/L aqueous polyurethane dispersion (Roda-Pur Wx 1418) 670 g/L water Application by spraying (2 passes dispersion I)
Intermediate pressing	In hydraulic press with the mirror or fog plate, parameters: - temperature – 50-60°C; pressure – 50-100 atm
Application of dispersion I	By spraying (2-3 passes dispersion I)

Operation	Dispersion composition/application method
Application of final dressing (fixing)	Emulsion/dispersion with the following composition: 700 g/L aqueous polyurethane emulsion (Roda pur 5011) 20 g/L aqueous wax emulsion for handle 280 g/L water Application by spraying (2 passes final dressing)
Final pressing	In hydraulic press with the mirror plate, parameters: - temperature – 70-80°C; pressure – 50-100 atm.

Because the product made of cedar essential oil is less efficient, mixtures of the two antifungal products (AF-C-1, AF-C-2) were used on the surface leather in the final dressing composition.

Antifungal product based on coriander essential oil (AF-C-1) was obtained by the same method, using essential oil, wax emulsion, ethanol and ethoxylated lauryl alcohol.

Testing of antifungal products based on cedar (AF-C-2) and coriander oil (AF-C-1) was carried out monitoring the manner in which mold growth is influenced by the treatment applied to the sample through the resistance to mold in simulated contamination conditions.

Finished leathers were further treated with final dressing whose composition includes AF-C-2 and AF-C-1 products in various proportions (samples AF 1-AF 9) and leathers untreated with the products AF-C-2 and AF-C-1 (samples M1 and M2) (Table 2).

Table 2. Technological variants for treating bovine hides into natural grain box assortments

Sample	Final dressing composition	Treated leather assortments
AF 1	1000 g/L product AF-C-2	Film-coated brown box leather
AF 2	1000 g/L product AF-C-2	Uncoated brown box leather
AF 3	1000 g/L product AF-C-2	Film-coated black box leather
AF 4	1000 g/L product AF-C-2	Uncoated black box leather
AF 5	750 g/L product AF-C-2 250 g/L Roda pur 5011	Film-coated brown box leather
AF 6	750 g/L product AF-C-2 250 g/L Roda pur 5011	Uncoated brown box leather
AF 7	400 g/L product AF-C-1 400 g/L product AF-C-2 200 g/L Roda pur 5011	Film-coated brown box leather
AF 8	400 g/L product AF-C-1 400 g/L product AF-C-2 200 g/L Roda pur 5011	Film-coated black box leather
AF 9	400 g/L product AF-C-1 400 g/L product AF-C-2 200 g/L Roda pur 5011	Uncoated black box leather
M1	0	Film-coated brown box leather
M2	0	Uncoated brown box leather

RESULTS AND DISCUSSION

Biological Characterisation of the Obtained Leather Assortments
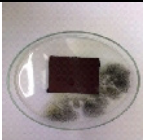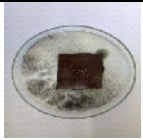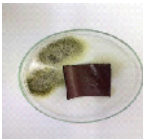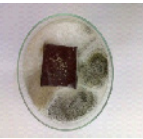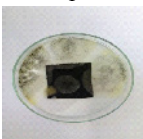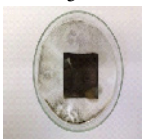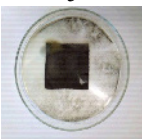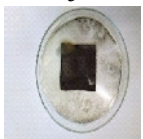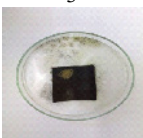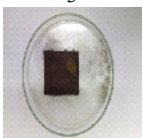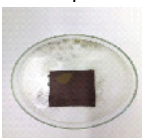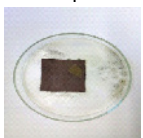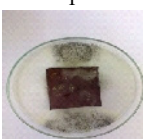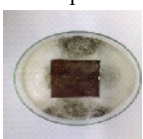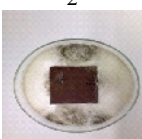
The samples treated with different amounts of antifungal product based on cedar oil, AF-C-2, and mixture of the two antifungal products (AF-C-1, AF-C-2), on the surface
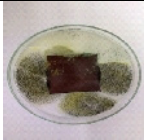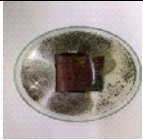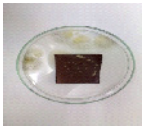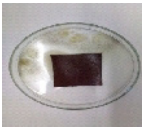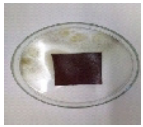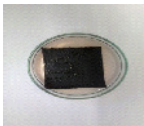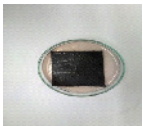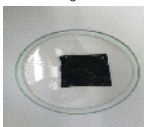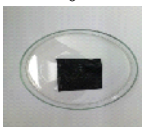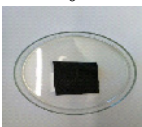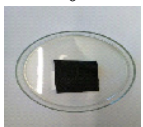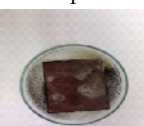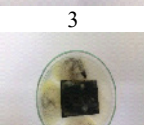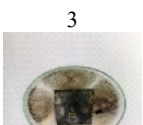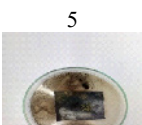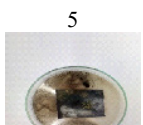
of unfinished and finished leather in the final dressing composition, were inoculated with biological material – *Aspergillus niger* spores.

The goal was to monitor the influence of the treatment applied to the sample on mold growth through the mold resistance under simulated contamination, according to STAS 12697/A 9:2008 „Finished leathers. Mold resistance testing".

Aspergillus niger spores were inoculated in three areas: right side, center and left side of the sample, according to the procedure specified in ASTM D 4576-86 „Standard test method for mold growth resistance of blue stock (leather)". Incubation was 28 days, but observations were also performed at 7, 14 and 21 days. *Aspergillus niger* strain development was assessed by ranking: 0 – absence of stems and a strong fungitoxic effect, 5 – an almost non-existent effect (the mold covers the entire surface of the specimen).

Table 3. Macroscopic images of samples treated with AF-C-2 and AF-C-1 products after 7, 14, 21 and 28 days

Sample/day	7	14	21	28
AF 1	0	2	2	3
AF 2	1	3	5	5
AF 3	3	3	4	4
AF 4	1	1	2	3
AF 5	2	4	5	5

Sample/day	7	14	21	28
AF 6				
	2	5	5	5
AF 7				
	0	1	1	2
AF 8				
	0	0	0	0
AF 9				
	1	1	1	2
M1				
	3	3	5	5
M2				
	3	4	5	5

Mold development on leather specimens, and macroscopic images of samples treated with AF-C-1 and AF-C-2 after 7, 14, 21 and 28 days from treatment, are presented in table 3. The numbers under the images are the marks given according to the standard.

The most resistant to mold are leather samples (film-coated and uncoated brown Box leathers) treated with 80% mixture of the two antifungal products (AF-C-1, AF-C-2) in equal proportions; the samples do not develop fungi for 28 days (mark 0 for sample AF 8 and mark 2 for samples AF 7 and AF 9).

The leather samples AF 5- AF 6 (film-coated and uncoated brown and black Box leathers) treated with AF-C-2 with Roda pur 5011 containing 75% AF-C-2, as such received marks ranging between 2 and 4 after 7 days and marks 5 after 7 days.

Product AF-C-2 is less efficient, and leather samples (film-coated and uncoated brown and black Box leathers) treated with the product AF-C-2 as such received marks ranging between 3 (AF 1, AF 4) and 5 (AF 2, AF 3) after 28 days.

Using the product as such, mattifies the film and reduces resistance to abrasion.

CONCLUSIONS

▪ The prepared antifungal and antibacterial products made of natural components (beeswax, lanolin, cedar and coriander essential oil) improve resistance of finished leather to biological factors (fungi) and can complement the treatment with biocides used for natural leather, which are toxic for humans and the environment), within the wet processing operations.

▪ Product made of cedar essential oil is less efficient, and leather samples treated with the product AF-C-2 as such received marks ranging between 3 and 5 after 28 days.

▪ The most resistant to mold are leather samples treated with 80% mixture of the two antifungal products in equal proportions; the samples do not develop fungi for 28 days (mark 0) and mark 2.

▪ Products, compatible with the materials used in the final dressing, can be used in surface treatment of finished leather and leather products in the final dressing composition.

▪ This products can be used as such in surface finishing of buffed bovine hides such as suede, buffo or nubuck to obtain a fatty/waxy feel and a better resistance to fungi of the dermal substrate.

REFERENCES

Bayramoglu, E.E. (2007), "Unique biocide for the leather industry: essential oil of oregano, *JALCA*, 102(11), 347.
Cadirci, B. *et al*. (2010), "Physical and antimicrobial characteristics of aloe vera treated split suede leather", *JALCA*, 105(2), 34.
Chirita, Gh. and Chirita, M. (1999), *Tratat de chimia şi tehnologia pieilor şi blănurilor*, vol. I, Ed. Gh. Asachi, Iaşi.
Council of Europe (2005), *European Pharmacopeia*, vol. II, ESCOP Strasbourg.
David, V. and Medvedovici, A. (2008), *Methods of separation and chromatographic analysis*, University of Bucharest Press.
Heidemann, E. (1994), *Fundamentals of Leather Manufacturing*, Eduard Roether KG Druckerei und Verlag, Darmstadt.
Moldovan, Z. (2001), *Instrumental Analysis Methods*, University of Bucharest Press.
Niculescu, O. and Manta, A. (2013), "Products with antifungal properties for finishing natural leather and leather items", Patent Application OSIM A/00538.
Niculescu, O. *et al*. (2015), "Obtaining and characterizing a product with antifungal properties based on essential oils and natural waxes for finishing natural leathers", *Rev. Chim. (Bucharest)*, 66(11), 1733-1736.
Niculescu, O. *et al*. (2017), "Finishing product for improving antifungal properties of leather", *Leather and Footwear Journal*, 1, 31-38, https://doi.org/10.24264/lfj.17.1.4.
Sirvaityte, J., Siugzdaite, J. and Valeika, V. (2011), "Application of commercial essential oils of Eucalyptus and Lavender as natural preservative for leather tanning industry", *Rev. Chim. (Bucharest)*, 62(9), 884.
*** (1998), *Romanian Pharmacopoeia*, 10th edition, Medical Ed., Bucharest.
***, Directive 2010/75/EU of the European Parliament and of the Council of 24 November 2010 on industrial emissions (integrated pollution prevention and control).
***, ST 12697/A 91/2008, Standard for Determination of Leather Resistance to Fungi.

VI.

MATERIALS PROCESSING AND PRODUCT MANUFACTURING

EFFECTS OF PLANTING DENSITY AND HARVESTING TIME ON LEAF AND ESSENTIAL OIL YIELD OF BAY LAUREL (*Laurus nobilis* L.) CULTURED IN SHRUB FORM

FİLİZ AYANOĞLU, DURMUŞ ALPASLAN KAYA, NADIRE PELIN BAHADIRLI

Hatay Mustafa Kemal University, Faculty of Agriculture, Field Crops Department, Turkey,
filizayanoglu@gmail.com, alpaslankaya@yahoo.com, pelinbahadirli@gmail.com

Bay laurel leaves and fruits are usually obtained from naturally grown plants. Therefore, it is not always possible to obtain the product at the same quality. For this reason, plantation for leaf production should be established separately from fruit production to obtain quality products. The aim of the study was to investigate the feasibility of the production of the bay laurel plant such as field crops in a shrub form. It is also important to know the ontogenetic variability on the amount of active substance and determine suitable plant density and appropriate harvesting time in order to increase leaf yield and essential oil with desired quality characteristics. Three different planting frequencies (1x1.5m; 1x3 m; 1x1x3 m) and three different harvesting times (one form per year, two forms per year and two years per form) were applied to the experiment. The experiment was established with a total of 1080 seedlings. In the experiment, the shoot length (16,84 - 31,50 cm), number of shoots (4,77 - 16,00 plants/plant), fresh weight (6,88 - 27,80 kg/da), dry weight (4,15 - 26,63 kg/da), dry leaf yield (2,57 - 17,29 kg/da), leaf area (20,41 - 24,56 cm2), chlorophyll SPAD value (32,36 - 39,5 kg/da), total ash content (7,96 - 11,46 %), essential oil content (2,06 - 3,12%) and essential oil yields were determined.

Keywords: Bay laurel, essential oil, plant density, harvesting time

INTRODUCTION

Bay laurel is an evergreen and dioic forest tree or shrub with a yellow flower and small and oval-black fruit. Bay laurel, which is originated from Asia, is grown naturally in Turkey, Greece, Italy, Spain, Portugal, France, Yugoslavia, Syria, Morocco, Algeria, Mediterranean Islands, California, Mexico and the Canary Islands (Ercan, 1983; Baytop, 1999). It is especially grown in the Mediterranean coasts and in the Aegean, Marmara and Black Sea borders and in the inner parts of these coasts in Turkey (Baytop, 1991). Leaves are used as spices, 2-5 cm wide and 5-10 cm in length, hard, dull, short stem, hairless, bright, wavy sides, dark green, yellowish gray green, elliptical, aromatic, spicy and bitter taste (Akgül, 1993). Flowering period varies depending on the region and species between February and May. The ripening time of the fruits is mid of October to November. After ripening the fruits spontaneously pour out. The shooting ability is excessive (Cengiz, 1979).

Laurel tree is spread over 131 862 hectares of land in Turkey. Turkey is one of the few countries that export the highest quality bay leaf and meets about 90% of the world's bay laurel leaf requirement. Among the medical and aromatic plants exported, bay laurel leaf is the most exported products with cumin, thyme, carob and capari (Şafak and Okan, 2004). Bay leaves and fruits used in processing in our country are generally obtained from naturally grown plants. The lack of cultivation of bay laurel prevents production with standard raw materials and excessive cuttings cause genetic resources to be destroyed.

It is stated that bay leaf has antioxidant, analgesic, anti-inflammatory, anticonvulsant (antiepileptic) and antifungal benefits (Simic *et al*., 2004; Sayyah *et al*., 2002; Sayyah *et al*., 2003; Rodilla *et al*., 2008). The bay leaves contain essential oil. The amount of essential oil and the physicochemical structure of oil varies depending on the production

area, production time, and the age of the shoots. The amount of essential oil is higher in young shoots than in older shoots. In addition, the rate of volatile oil is higher in low-lying coastal regions (Acar, 1987, Acar, 1988, Ceylan and Özay, 1990, Gültekin, 1997). The main components of bay leaf essential oil are 1,8-cineole, trans-sabinene hydrate, α-terpinyl acetate, methyl eugenol, sabinene, eugenol and α-pinene (Tanker and Tanker, 1976, Acar, 1987, Kekelidze *et al*., 1987, Ceylan and Özay 1990, Baytop, 1991, Akgul, 1993, Gültekin, 1997, Kilic *et al*., 2004, Mohammadreza, 2008, Ayanoglu *et al*., 2010).

The aim of the study was to investigate the feasibility of the production of the laurel plant such as field crops. Thus, without waiting for many years for leaf production, it will be possible to increase the productivity of leaf and essential oil to be taken from the unit area and to obtain the product with desired quality characteristics. It is also important to know the ontogenetic variability of the amount of active substance during the growth period of a plant in order to determine the appropriate harvesting time of the medical plants. Therefore, determining the most suitable harvesting period in terms of leaf and volatile oil yield in bay laurel cultivation in bush form is another aim of the study.

MATERIALS AND METHODS

Plant Materials

The plants used in the experiment were obtained by sowing bay laurel seeds in pots. Seedlings were planted to the trial area when they were one year old.

Methods

The bay laurel plants were planted in the trial area in March. Three different planting density (1x1.5m; 1x3m; 1x1x3m) and three different harvesting times (twice a year, once a year and every two years) were applied in the experiment. One harvest per year (November), two harvests per year (July and November), and harvest (November) every two years. July is entering the summer dormant period and November is the period that trees entered to rest in the region.

The experiment was established with 4 replications and consisted of 36 plots in total. The size of each plot is 72 m^2 and the number of plants in the plots are 20, 30 and 40 plant/plot depending on the planting density. 1080 plants were used in the experiment. The plants were irrigated by drip irrigation method. Trial pattern was split plot on randomized blocs. The plants were harvested at 25-30 cm height on the first harvesting period (Sarı *et al*., 2010). Dry weight (kg/da), dry leaf yield (kg/da), leaf area (cm^2), chlorophyll SPAD value, essential oil content (%), essential oil yield (l/da) and total amount of ash (%) were determined. Dry leaf samples of bay laurel hydro distilled for three hours and the essential oil ratio were determined volumetrically by using Neo-Clevenger apparatus.

RESULTS AND DISCUSSION

The results of analysis of the essential oils obtained by water distillation a re shown in Table 2.

Two years results about shoot length, number of shoots, leaf area, chlorophyll content and total ash content are given in Table 1. Shoot lengths of plants were ranged

between 16,84-31,50 cm. Number of shoots were ranged between 4,77 to 16,00 piece/plant.

Contrast to shoot number, shoot lengths were found lower in twice a year harvest. There was no significant difference between once a year harvest and twice a year harvest. Leaf area of the plants were found between 20,41-24,56 cm2 . The lowest leaf area value found in once a year harvest while the highest results were obtained from twice a year harvest in the first year. Chlorophyll content of the samples were measure with SPAD chlorophyll meter. SPAD values were ranged between 32,26-39,21. The highest value were obtained in the first year twice a year harvest with 40 plants/plot application. Total ash content were ranged between 7,96-11,46%. The highest value were obtained once a year harvest in the first year of the study.

Table 1. Results of shoot length, number of shoots, leaf area (cm^2), chlorophyll content (SPAD value) and total ash content due to harvesting period and planting densities

Year	Plant density	Harvest	Shoot length	Number of shoots	Leaf area	Chlorophyll Content	Total Ash Content
2015	1 m x 1 m (40 plant/72 m^2)	2 times/year	17,11	13,83	21,13	39,21	11,35
		1 time/year	31,42	10,18	21,45	36,15	9,76
		1 time/2 years	–	–	–	–	–
	1 m x 1 m x 3 m (30 plant/72 m^2)	2 times/year	17,13	12,52	21,02	32,80	10,85
		1 time/year	31,50	7,96	21,45	35,83	11,46
		1 time/2 years	–	–	–	–	–
	1 m x 3 m (20 plant/72 m^2)	2 times/year	16,84	16,00	24,56	33,41	9,05
		1 time/year	27,60	7,50	21,21	32,36	10,98
		1 time/2 years	–	–	–	–	–
2016	1 m x 1 m (40 plant/72 m^2)	2 times/year	14,40	11,55	21,65	35,76	10,46
		1 time/year	30,16	10,17	21,39	36,18	8,68
		1 time/2 years	21,01	5,95	21,08	32,26	10,05
	1 m x 1 m x 3 m (30 plant/72 m^2)	2 times/year	16,59	12,05	21,54	33,49	8,85
		1 time/year	27,89	6,96	21,13	36,04	8,13
		1 time/2 years	26,69	4,96	21,77	34,12	9,79
	1 m x 3 m (20 plant/72 m^2)	2 times/year	19,45	10,78	23,81	33,72	9,82
		1 time/year	31,44	6,04	20,41	32,40	7,96
		1 time/2 years	17,10	4,77	21,12	33,51	10,02

The results of the fresh weight, dry weight, dry leaf yield, essential oil content and essential oil yields were given in Table 2. Fresh weight results were found as lowest in

6,88 kg/da in once in two year harvest (20 plant/plot) while highest value found as 27.80 kg/da in once a 2 years harvest (40 plant/plot). The lowest values for the dry weight in the experiment were obtained from the applications which were formed every two years with 4,15 kg/da and 20 plants on the plots, and the highest dry weight values were obtained from applications with an average of 26.63 kg/da once a year harvest and 40 plants on the plots .

The lowest values for dry leaf yield in the experiment were obtained from applications with 2.57 kg/da every 2 years and 20 plants in the plot. The highest dry leaf yield values were obtained with an average of 17,29 kg/plant once a year harvest and 40 plants in the plot applications.

Although the values are generally close to the other applications in twice a year harvest, it is determined that is not suitable when considering the labor costs. On the other hand, when the plants harvested in July, they are unable to produce enough shoots for harvest until November. Lower yield values were obtained in the plots with 20 plants/plot.

Table 2. Results of fresh weight, dry weight, dry leaf yield and essential oil content due to the different harvesting period and planting densities

Year	Plant density	Harvest	Fresh Weight	Dry Weight	Dry Leaf Yield	Essential Oil Content
2015	1 m x 1 m (40 plant/72 m^2)	2 times/year	27,55	13,26	11,95	3,12
		1 time/year	25,80	26,63	13,66	2,10
		1 time/2 years	_	_	_	_
	1 m x 1 m x 3 m (30 plant/72 m^2)	2 times/year	20,28	9,74	8,84	2,62
		1 time/year	18,32	17,61	11,12	2,09
		1 time/2 years	_	_	_	_
	1 m x 3 m (20 plant/72 m^2)	2 times/year	12,51	6,16	5,91	2,80
		1 time/year	17,34	11,46	7,14	2,06
		1 time/2 years	_	_	_	_
2016	1 m x 1 m (40 plant/72 m^2)	2 times/year	18,45	8,20	9,01	2,36
		1 time/year	25,05	23,36	17,29	2,80
		1 time/2 years	27,80	16,01	9,37	2,15
	1 m x 1 m x 3 m (30 plant/72 m^2)	2 times/year	17,82	8,87	7,55	2,96
		1 time/year	17,96	17,19	10,12	2,11
		1 time/2 years	20,64	12,68	7,75	2,90
	1 m x 3 m (20 plant/72 m^2)	2 times/year	11,99	5,86	4,51	2,67
		1 time/year	17,26	11,21	6,99	2,99
		1 time/2 years	6,88	4,15	2,57	2,88

There was no significant difference among the applications as regard to essential oil contents. Özcan and Chalchat (2005), reported that bay laurel essential oil contents vary between 1.4-2.6 % in their studies. Ayanoğlu *et al*. (2010), found that the leaf area

ranged from 5.78 cm^2 to 49.00 cm^2, chlorophyll content 35.70-66.90, and the essential oil content from 0.45 to 6.00 % in their study conducted in native flora of Hatay province in Turkey.

CONCLUSION

According to the two years harvest values obtained in the study, it is obvious that the plantation density with 1 x 1.5 m had greater values for yield and yield components. These are preliminary results. However, bay laurel is a long-lived perennial plants, the studies and investigations will be continued on the densities. The planting pattern of 1m x (1m x 3m) may be preferred as it is a suitable model for machine cultivation.

Twice a year harvests are definitely not recommended. The plants are unable to produce enough shoots for second harvest until November. For this reason, the harvests carried out every two years become more efficient and after the harvest in two years. The most important result of the study was to reveal that the bay laurel plant is possible to produce such as field crops. Thus, it was determined that the bay laurel plant could easily be produced for leaf and the essential oil rather than destruction of the natural vegetation.

REFERENCES

Acar, İ. (1987), Defne (Laurus nobilis L.) Yaprağı Ve Yaprak Eterik Yağının Üretilmesi Ve Değerlendirilmesi, Orm. Araş. Ens. Yayınları, Teknik Bülten Seri No. 186, Ankara.

Acar, İ. (1988), Türkiye'deki Yayılışı İçerisinde Akdeniz Defnesi (Laurus nobilis L.)'nin Yaprak Kalitesi Üzerine Araştırmalar, Ormancılık Araştırma Enstitüsü Yayınları Teknik Bülten Serisi No: 202.

Akgül, A. (1993), Baharat Bilimi ve Teknolojisi. Gıda Teknolojisi Dergisi Yayınları, No: 15., S: 75-76. Ankara. Anonim, 1995. Orman tali ürünlerinin üretim ve satış esasları. Orman Bakanlığı, Ormana Genel Müdürlüğü, İşletme ve Pazarlama Dairesi Başkanlığı Tebliğ No: 283, Tasnif No: IV- 1434. S: 36-38.

Ayanoğlu, F. *et al*. (2010), Hatay Yöresinde Doğal Olarak Yetişen Defne (Laurus nobilis L.) Bitkisinin Kalite Özelliklerinin Belirlenmesi ve Seleksiyonu. Tubitak Projesi Sonuç Raporu (108O878), 296s.

Baytop, A. (1991), Farmasötik Botanik. İstanbul Üniversitesi Eczacılık Fakültesi Ders Kitabı. İstanbul. Baytop, T., 1999. Türkiye'de Bitkiler ile Tedavi (Geçmişte ve Bugün). İstanbul Üniversitesi Eczacılık Fakültesi Yayınları (İlaveli İkinci Baskı). İstanbul, No.3255, Nobel Tıp Kitapevleri, s. 3-4, 226.

Cengiz, Y. (1979), Ormancılık Araştırma Enstitüsü Yayınları Teknik Raporlar Serisi No: 5.

Ceylan, A. and Özay, N. (1990), Defne Yaprakların (Folia lauri)'da Ontogenetiksel Kalite Araştırması, E.Ü.Z.F. Dergisi, Cilt: 27, s. 1 s. 71-77.

Ercan, A.S. (1983), Defne Yaprağı ve Yağının İhracatı Geliştirmesi. İhracatı Geliştirme Etüd Merkezi Yayınları No: 74 s.2-9.

Göker, Y. and Acar, M.İ. (1983), Orman Yan Ürünlerinden Akdeniz Defnesi. İstanbul Üniversitesi Orman Fakültesi Dergisi, Seri: B, Cilt:33, Sayı:1, İstanbul.

Gültekin, İ. (1997), Defne Yapraklarının (Folia Lauri)'da Ontogenetik ve Morfogenetik Varyabilite. Ege Üniversitesi Fen Bilimleri Enstitüsü Tarla Bitkileri Anabilim Dalı, Yüksek Lisans Tezi, İzmir.

Kekelidze, N.A., Dzhanikashvıli, M.I., Kutateladze, V.V. (1987), Defne Yapraklarının Ontogenez Sırasında Eterik Yağ Bileşenlerinin Yığıntı ve Düzenleme Dinamiği, Fiziologiya-İ Biokhimiya-Kul'turnykh-Restenii, 19:6, S. 607- 614.

Kılıç, A. *et al*. (2004), "Volatile Constituents and Key Odorants In Leaves, Buds, Flowers, And Fruits of Laurus nobilis L.", *J Agric Food Chem*, 52, 1601-6, https://doi.org/10.1021/jf0306237.

Mohammadreza, V. (2008), Phenological Variation of Laurus nobilis L. Essentıal Oil From Iran Verdian-rizi et al. EJEAFChe, 7 (11), 3321-3325.

Muller-Riebau, F.J. *et al*. (1997), "Seasonal variations in the chemical compositions of essential oils of selected aromatic plants growing wild in Turkey", *Journal of Agricultural and Food Chemistry*, v.45 (12), 4821-4825, https://doi.org/10.1021/jf970110y.

Özcan, M. and Chalchat, J.C. (2005), "Effect of different locations on the Chemical composition of essential oils of laurel (Laurus nobilis L.) leaves growing wild in Turkey", *Journal of Medicinal Food*, 8(3), 408-411, https://doi.org/10.1089/jmf.2005.8.408.

Rodilla, J.M. *et al*. (2008), "Laurus novocanariensis essential oil: Seasonal variation and valorization", *Biochemical Systematics and Ecology*, 36, 167-176, https://doi.org/10.1016/j.bse.2007.09.001.

Sayyah, M. *et al*. (2003), "Analgesic and antiinflammatory activity of the leaf essential oil of Laurus nobilis Linn.", *Phytotherapy Research*, 17, 733-736, https://doi.org/10.1002/ptr.1197.

Sayyah, M., Valizadeh, J. and Kamalinejad, M. (2002), "Anticonvulsant activity of the leaf essential oil of Laurus nobilis against pentylenetetrazole- and maximal electroshock-induced seizures", *Phytomedicine*, 9, 212-216, https://doi.org/10.1078/0944-7113-00113.

Simic, M., Kundakovic, T. and Kovacevic, N. (2004), "Preliminary assay on the antioxidative activity of Laurus nobilis extracts", *Fitoterapia*, 74(6), 613-616, https://doi.org/10.1016/S0367-326X(03)00143-6.

Şafak, İ. and Okan, T. (2004), Kekik, Defne Ve Çam Fıstığının Üretimi Ve Pazarlaması Doğu Akdeniz Ormancılık Araştırma Müdürlüğü Doa Dergisi (Journal of Doa) Sayı: 10 Sayfa: 101-129.

Şahin, S. *et al*. (2008), Yeni Teknolojilerle Baharatlardan Esansiyel yağ Ekstraksiyonu ve Bu Yağların Fiziksel, Antioksidan ve Antimikrobiyal Özellikleri. Tubitak Proje Sonuç Raporu, Proje No: 104O265. 76s.

Tanker, M. and Tanker, N. (1976), Farmakognozi Cilt 2, Reman Basımevi, İstanbul. URL, 1. http://www2.ogm.gov.tr/istatistikler/istatistik.aspx. (son güncellenme tarihi: 26.08.2010)

Wagner, H.W. and Sefc, K.M. (1999), Identity 1.0. Centre for Applied Genetics, University of Agricultural Science, Vienna.

Yalçın, H. *et al*. (2007), "Gas Chromotography/Mass Spectrometry Analysis of Laurus nobilis Essential oil composition of Northern Cyprus", *Journal of Medicinal Food*, December 1, 10(4), 715-719.

ASPECTS REGARDING ACCOMPLISHING MULTILAYERED FILTRATION MEDIA, USING ELECROSPUN WEBS

ADELA BARA[1], CRISTINA BANCIU[1], ELENA CHIȚANU[1], VIRGIL MARINESCU[1];
MAGDALENA-VALENTINA LUPU[1], ANGELA DOROGAN[2], EFTALEA CĂRPUȘ[2],
CARMEN GHIȚULEASA[2]

[1]*The National Institute for Research and Development in Electrical Engineering, 313 Splaiul Unirii, Bucharest, Romania, email: office@icpe-ca.ro;*

[2]*The National Research and Development Institute for Textile and Leather, 16 Lucretiu Patrascanu Street, 030508, Bucharest, Romania, e-mail: certex@ns.certex.ro*

Filtration media are widely used in industry in various forms for the filtration and removal of particles from fluids. Filtration media represented by the non-woven fibrous materials with the fibers disposed close enough to each other so the inter-fiber spacing or effective pore size to be small enough but in a sufficiently thick layer, able to trap the particles in a desired size range. The present work presents an improved multilayered filtration media that includes a self - supporting highly permeable substrate layer, *textile type,* which provides support structure for the media and has a low relative efficiency and low relative flow restriction, a thin, non-self - supporting, efficiency layer of fine fibers - *electrospun polymer layer* and a smooth, non-self - supporting protective cover layer of fibers which is self-adhering to the efficiency layer and adds negligible efficiency and flow restriction to the overall media.

Keywords: agrotextiles, property, application.

INTRODUCTION

Filtration media are widely used in industry in various forms for the filtration and removal of particles from fluids. Increasing demands from industrial and environment protection reasons for higher degrees of filtration, led to the need for filtration media with smaller fibers and pores size for trapping a smaller class of particles from the fluids to be developed. According, filtration media represented by the non-woven fibrous materials (generally consists of a matrix or mass of fine diameter fibers) with the fibers disposed close enough to each other so the inter-fiber spacing or effective pore size to be small enough but in a sufficiently thick layer, able to trap the particles in a desired size range.

The filter media are then fabricated into the desired form for the particular application (panels, pleated cartridges, flat disks and canisters, etc.), as is generally known in the state of the art. A diversity of materials has been used, including fiberglass, metals, ceramics, and a wide range of polymer materials were used in making non-woven fine fiber filter media.

The present work presents an improved multilayered filtration media that includes a self supporting highly permeable substrate layer, *textile type,* which provides support structure for the media and has a low relative efficiency and low relative flow restriction, a thin, non-self supporting, efficiency layer of fine fibers - *electrospun polymer layer* and a smooth, non-self supporting protective cover layer of fibers which is self-adhering to the efficiency layer and adds negligible efficiency and flow restriction to the overall media.

The three-layer microfiltration media is characterized by high particle capture efficiency and minimal flow restriction.

The present work provides an improved multilayered filtration media that includes a selfsupporting mono or multilayer *textile structure,* a thin fibrous *polymer electrospun layer* and a protective cover layer of fibers.

EXPERIMENTS

Research objective of the work is to develop and validate at the laboratory scale, a demonstration model of textile type filters containing micro/nanofibrous layers produced by electrospinning, with the aim to separate the suspended particles from aqueous solutions.

The textile filter is a multilayer composite (figure 1), which includes:
- Superior hydrophilic electrospun web layer (1);
- Inner polimeric porous electrospun web layer, with micro/nano filtering features (2);
- Inferior woven fabric layer, with support and supplementary filtering features (3).
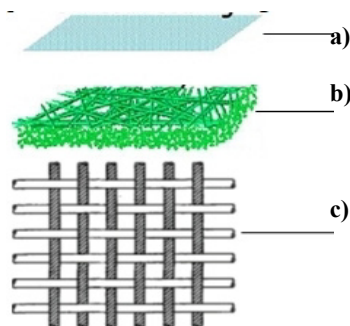
Figure 1. Multilayer flexible composite filter structure concept

Experiments suppose two stages, namely:
- filter component accomplishing,
- filter system accomplishing.

Raw Materials and Methods

Electrospun polimeric layers are engineered to have filtering behaviors, by using cellulose acetate polimeric solutions, together with some solvents, as follow:
− cellulose acetate (AC), from Aldrich;
− acetone (A), from Aldrich;
− *N,N*-dimethylformamide (D), from Alfa Aesar,
− chloroform (C), from Chimreactiv.

Woven fabrics are made of man-made-fibers, namely: PVC, PES, PA. These are conventional fibers in textile domain, but with a technical end-use indication.

For the weaving stages, there have been used 100% fibers in yarns, and in woven fabrics.

Electrospinning device is laboratory type, and the process of electrospinning was o conventional process. Waving process was realized on a automatized Picanol weaving machine, rapier type.

All the processing stages are conventional, with no additional devices, settings.

RESULTS

Component Parts of Filtering System, Textile Type

There were realized three types of electrospinning solutions. In figure 2 there details with the three electrospinning solutions.

Variant binary solvent system DMF/ chloroform (code DC11) was selected to be the superior web electrospun layer with hydrophilic behavior.

But ternary system DMF/acetone/chloroform (code DAC121) was selected to be the inner layer, an electrospun web, with filtering behavior.
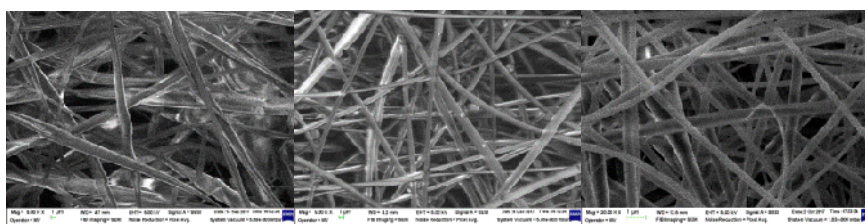
Figure 2. SEM images of cellulose acetate electrospun from several solutions: (a) binary system DMF/ acetone; (b) binary solvent system DMF/ chloroform (DC11); (c) ternary system DMF/acetone/chloroform (DAC121)

Table 1. Specific characteristic for woven fabrics, selected to be part of the two demonstrators

Characteristics of selected woven fabrics	V04	V05
Nature of yarn raw materials	PES	PA
Composition, %	100	100
Specific mass, g/m2	297.5	82
Thickness, mm	0.504	0.160
Warp no/cm	14.00	42.0
Weft no/ cm	12.00	39.8
Air permeability, 100Pa, l/m2/s	435.00	1281.65
Mass specific density, g/cm3	1.38	1.13
Theoretically cover degree, %	0.6570	0.6790
Cover degree, flatting considering	0,7320	0,7408

Selected woven fabrics for electrospinning 2 layer depositions have fabric report no more than 4 and are balanced to yarn density, yarn length density, on warp and weft.

Demonstrative Model Accomplishing

For demonstrative models validation, were realized 2 (two) variants of models, differentiated by woven fabric support.

In figure 3 are presented the electrospinning devices (3 a) and detail of filtering system, textile type, realized with the woven fabric variants V04, V05.
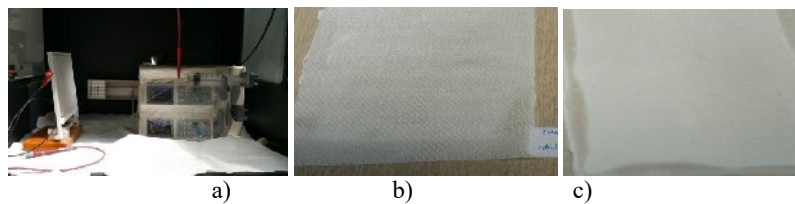
Figure 3. Demonstrative model a) flash of the electrospinning process; b) DAC121/ DC 11 web fibers electrospun deposition on fabric support, variant V04 (demonstrative model MD1) and V05 (demonstrative model MD2).

In figure 4 there are details of the 2 (two) web electrospun layers, namely superior (a) and inner (b).
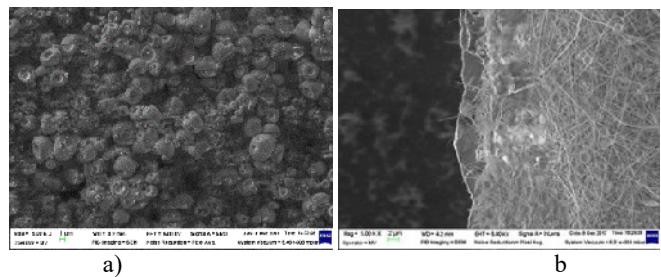
Figure 4. SEM image of demonstrative model DAC/DC: a) surface detail of superior covering web layer b) surface detail of inner filtering web layer

After the filtering system realization, in the two variants, MD1 and MD2, the stability, the uniformity between system layers were investigated using Carl Zeiss FESEM/FIB/EDS Auriga. Contact angle also was tested on MD1 and MD2. In image from figure 5 it is a detail in this respect.
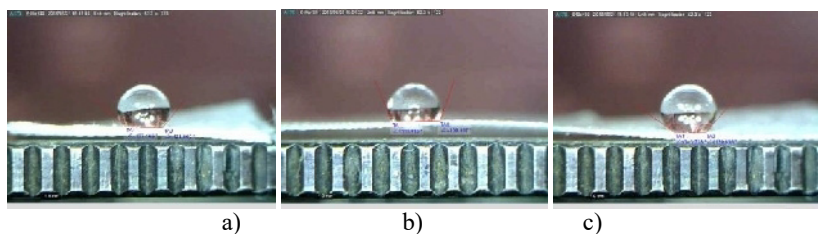
Figure 5. Contact angle a) DAC121/DC11 web electrospun layers; b) V04 woven fabric filtering support; c) filtering system, MD1

Evaluation of the Filtered Particle Retained Capacity

For filtering capacity evaluation, in order to validate on laboratory scale, of demonstrative model, MD1 and MD2, were used colloidal solution of Ag (SCAg), of 50 ppm, respective NpZnO suspensions, of same concentration. MD1 (DAC121/DC11-V04) and MD 2 (DAC121/DC11-V05).

The samples of demonstrators are fixed between the 2 rings so that to be exposed to the referential solution to be filtered, in respect of micro and nano particles (figure 6).

In figure 6a it is a detail on validation, filtering installation type.

In 6b and 6c images there are details before and after filtration on the superior layer of the filtering systems for the demonstrator.

a)   b)   c)
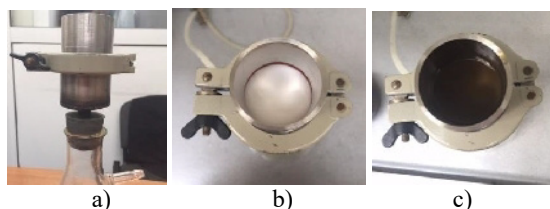
Figure 6. Evaluation of filtering capacity

Before and after filtering process the efficiency validation was done through spectrophotometric method, of light absorption in UV-Vis.

Absorption spectra (figure 7) were obtained on UV-Vis-NIR, V-570 type (Jasco, Japan), for the colloidal suspensions of Ag, in reference solution and in the solutions resulted after filtering process, for MD1 and MD2.
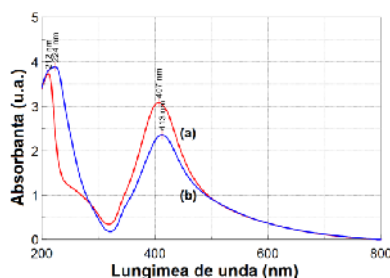
Figure 7. Absorbency spectra in UV-Vis for SCAg: a) reference, b) MD1

Also the filtered particle dimensions were evaluated, using DLS method. In figure 8 micro and nano particles of AG are visible on the surface of filtering system, MD1.
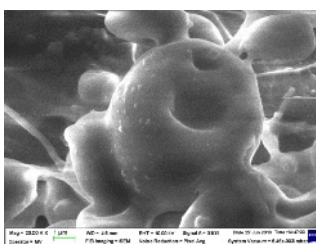
Figure 8. NpAg filtered on filter surface, for MD1 – particle dimensions 154,4 – 303 nm from reference solution SAg

CONCLUSION

Research objective of the work is to develop and validate at the laboratory scale, a demonstration model of textile type filters containing micro/nanofibrous layers produced by electrospinning, with the aim to separate the suspended particles from aqueous solutions.

The textile filter is a multilayer composite, which includes:

- Superior hydrophilic electrospun web layer;
- Inner polimeric porous electrospun web layer, with micro/nano filtering features;
- Inferior woven fabric layer, with support and supplementary filtering features.

Variant binary solvent system DMF/ chloroform (code DC11) was selected to be the superior web electrospun layer with hydrophilic behavior and ternary system DMF/acetone/chloroform (code DAC121) was selected to be the inner layer, an electrospun web, with filtering behavior.

Selected woven fabrics for electrospinning 2 layer depositions have fabric report no more than 4 and are balanced to yarn density, yarn length density, on warp and weft. Two woven fabrics, one PES type and one PA type were selected for realization of 2 demonstrators (MD1 and MD2).

After the filtering efficiency evaluation, MD1 demonstrator was validated as final solution at this stage of the research.

This is a partial solution, having in view that from now the working hypothesis could be enlarged, by developing the filtering process and media features, especially from static to dynamic status.

Acknowledgment

REFERENCES

Chitanu, E. *et al*. (2017), "Study of electrospun cellulose acetate fibers", *8th TEXTEH International Conference*, 19 – 20 October, Bucharest.

Chitanu, E. *et al*. (2017), "PAN/ZnO composite electrospun fibers for UV shielding applications",*10th International Symposium on Advanced Topics in Electrical Engineering (ATEE)*, March 23-25, Bucharest, Romania, IEEE, pp. 227-230, https://doi.org/10.1109/ATEE.2017.7905098.

Cioara, L. and Cioara, I. (2001), "Optimization of the technological parameters in processes of filter weaving", *Proceedings of TECHNITEX*, Portugal, vol.1, 467-470.

Dikenson, C. (1994), *Filters and Filtration Handbook*.

Dorogan, A. and Cramariuc, B., "Aspects about processing of polymeric solutions on electrospinning equipment - deposition stage", *Asian Academic Research Journal of Social Science & Humanities*, ISSN: 2278-859X.

A REVIEW ON CATABOLIC ACTIVITY OF MICROORGANISMS IN LEATHER INDUSTRY

MERAL BIRBIR, PINAR CAGLAYAN

Marmara University, Faculty of Arts and Sciences, Biology Department, Istanbul,Turkey,
Corresponding Author: mbirbir@marmara.edu.tr

A tremendously diverse group of microorganisms originated from animal skins/hides, animals' feces, preservation salt, dust, barn, water, air, soil, feed have been found on salted hides/skins. Growth and catabolic activities of these microorganisms have been supported by high organic and inorganic contents of salted hides/skins. As known, detail examination of catabolic activities of microorganisms offers an important information about their critical roles on hide/skin biodegradation. The goal of this review is to summarize experimental results of the previous studies to understand biodegradation capabilities of the microorganisms isolated from leather industry. Catabolic activities of microorganisms belonging to non-halophilic bacteria, moderately halophilic bacteria, extremely halophilic archaea and the members of family *Enterobacteriaceae* were summarized in the present study. The characterization of these microorganisms was performed according to molecular methods, conventional biochemical tests in the previous studies. Examination of research articles showed that aerobic microorganisms isolated from salted hides/skins produced protease, caseinase, lipase, β-galactosidase, amylase, cellulase, DNase, lecithinase and urease. Moreover, the isolates produced acid from different carbon sources, reduced nitrate to nitrite, produced NH_3 from peptone, decarboxylated different amino acids found in hides/skins. These studies demonstrated that salted hides/skins had a wide diversity of microorganisms which have different catabolic activities to breakdown carbon and energy sources for their growth.

Keywords: Bacteria, Archaea, Leather industry

INTRODUCTION

Skin is composed of water (64%), fats (2%), structural proteins (29% collagen, 2% keratin, 0.3% elastin), non-structural proteins (1% albumins and globulins, 0.7% mucins and mucoids), mineral salts (0.5%), other substances (0.5%) (Highberger, 1956; Hien, 2006). Freshly slaughtered skins are an ideal growth supporting organic medium for microbial cells which made up water, nucleic acids, proteins, polysaccharides, and fats. Presence of different of microorganisms on cattle hides, sheep and goat skins was detected by researchers and their high prevalence on hides and skins were related to high nutritional content of hides and skins. While some of these microorganisms are related to normal microbial flora of the animal hides and skins, the others may be contaminant microorganisms found in the air, water, soil, pasture, animal feeds, animal feces, barn, slaughterhouse, and tanneries (Sverre, 1956; Birbir and Ilgaz, 1996; Ulusoy and Birbir, 2015). When the animal is alive, growth of these contaminant microorganisms have been prevented by acidic pH of the hides/skins as well as normal microbial flora of the animals. After flaying process, these microorganisms release different enzymes to break down proteins, fats and carbohydrates into their building blocks for their carbon, nitrogen, hidrogen, and the other needs to grow. Hence, hides and skins are salted to prevent the growth and damage of these non-halophilic microorganisms but preservation salt contaminates hides and skins with extremely halophilic archaea, halotolerant, slightly halophilic and moderately halophilic bacteria.

NON-HALOPHILIC BACTERIA ON HIDES AND SKINS

In the study of Venkatesan and colleagues (1970), non-halophilic protease positive *Achromobacter liquefaciens, Alcaligenes marshalli*, *Bacillus cereus*, *Bacillus circulans, Bacillus megatherium, Bacillus pantothenticus, Bacillus subtilis, Brevibacterium insectiphilum*, *Micrococcus roseus* and *Staphylococcus aureus* were isolated from three fresh goat skins obtained from India. After 24 hours curing process of the goat skins, non-halophilic protease positive *Alcaligenes marshalli*, *Bacillus cereus*, *Bacillus megaterium, Bacillus subtilis, Kurthia variabilis*, *Micrococcus rubens, Staphylococcus aureus* were isolated.

Twenty-one isolates of *Bacillus cereus* (4)*, Bacillus megaterium* (2)*, Bacillus sphaericus* (3)*, Bacillus subtilis* (7), *Kurthia variabilis* (1), *Micrococcus roseus* (2), *Staphylococcus aureus* (2) were isolated from newly slaughtered 10 fresh cattle hides collected from slaughterhouse in Istanbul, Turkey. All *Bacillus* species, two *Staphylococcus aureus* species (86% of the isolates) were able to digest gelatin. We detected that 81%, 62%, 81%, 10%, 52% of the isolates respectively produced urease, amylase, reduced nitrate to nitrite, produced indol from tryptophan, produced *acetoin* from glucose (Birbir and Ilgaz, 1996).

Sixty-six bacterial isolates of *Bacillus brevis* (2), *Bacillus cereus* (8)*, Bacillus licheniformis* (3), *Bacillus megaterium* (2)*, Bacillus pumilus* (3), *Bacillus sphaericus* (5), *Bacillus subtilis* (10), *Kurthia variabilis* (3), *Micrococcus candidus* (1), *Micrococcus luteus* (10), *Micrococcus roseus* (*3*)*, Micrococcus rubens* (6), *Staphylococcus aureus* (7) and *Staphylococcus epidermidis* (3) were obtained from one week old 15 salted cattle hides collected from tanneries of Turkey. High catabolic activities and different bacterial species were detected at salted hides compare to the fresh cattle hides. Proteolytic activities were observed in all *Bacillus* species, all isolates of *Micrococcus* roseus, *Staphylococcus aureus* and *Staphylococcus epidermidis*. While 56% of the isolates reduced nitrate to nitrite and produced urease enzyme, 46%, 32% and 5% of the isolates produced amylase, the neutral product acetoin from glucose, and indol from tryptophan, respectively (Birbir and Ilgaz, 1996).

Furthermore, 71 isolates of *Bacillus cereus* (3), *Bacillus firmus* (1), *Bacillus licheniformis* (4)*, Bacillus megaterium* (7)*, Bacillus pumilus* (4), *Bacillus sphaericus* (8), *Bacillus subtilis* (24)*, Kurthia variabilis* (1), *Micrococcus candidus* (1), *Micrococcus luteus* (5), *Micrococcus roseus* (6), *Micrococcus rubens* (3), *Staphylococcus aureus* (3) and *Staphylococcus epidermidis* (1) were isolated from two months old 25 salted cattle hides. Proteolytic activities (96 % of the isolates) were observed in all *Bacillus* species, all isolates of *Micrococcus luteus, Micrococcus roseus* and *Staphylococcus aureus* and all isolates of *Staphylococcus epidermidis, Kurthia variabilis,Micrococcus candidus.* While 79% and 90 of the isolates respectively reduced nitrate to nitrite and produced urease enzyme, 65%, 49%, 8% of the isolates produced amylase, acetoin from glucose, and indol from tryptophan, respectively. Epidermis, dermis and hipodermis layers and collagen fibers of the hides were damaged by bacterial attack (Birbir and Ilgaz, 1996).

In another study, 256 non-halophilic Gram-negative bacterial isolates of *Acinetobacter baumannii* (3), *Acinetobacter calcoaceticus* (2), *Acinetobacter haemolyticus* (1), *Acinetobacter junii ssp. johnsonii* (5), *Acinetobacter lwoffii* (5), *Aeromonas caviae* (1), *Aeromonas hydrophila* (1), *Alcaligenes faecalis* (3), *Burkholderia gladioli* (7), *Citrobacter amalonaticus* (1), *Citrobacter ferundii* (3), *Comamonas testesteroni* (2), *Edwardsiella tarda* (1), *Enterobacter aerogenes* (4), *Enterobacter agglomerans* (4),*Enterobacter amnigenus* (12), *Enterobacter cloacae* (22), *Enterobacter gergoviae* (9), *Enterobacter intermedius* (4),

Enterobacter liquefaciens(3), *Enterobacter sakazakii* (8), *Escherichia coli*(9), *Hafnia alvei*(14), *Klebsiella oxytoca* (1), *Klebsiella pneumoniae ssp. ozanae* (1), *Mannheimia haemolytica* (3), *Pasteurella multocida* (4), *Pasteurella pneumotropica* (5)*, Proteus mirabilis* (1), *Pseudomonas aeruginosa* (1), *Pseudomonas fluorescens* (9), *Pseudomonas luteola* (29), *Pseudomonas maltophila* (2), *Pseudomonas paucimobilis* (1), *Pseudomonas pseudoalcaligenes* (1), *Pseudomonas putida* (16), *Salmonella choleraesuis ssp. arizonae* (1), *Salmonella paratyphi A* (1), *Salmonella typhimurium* (1), *Serratia marcescens* (1), *Sphingomonas paucimobilis* (5), *Stenotrophomonas maltophila* (12), *Vibrio fluvialis* (27), *Vibrio vulnificus* (5), *Yersinia pseudotuberculosis* (1), *Yersinia ruckeri* (4) were isolated from ten salted hides cured in England, Australia and Turkey (Aslan and Birbir, 2012).

Moreover, 396 Gram-positive bacteria such as *Aerococcus urinae* (5), *Aerococcus viridans* (24), *Aneurinibacillus aneurinilyticus* (4), *Bacillus amyloliquefaciens* (3), *Bacillus cereus* (3), *Bacillus firmus* (8), *Bacillus laterosporus* (1), *Bacillus lentus* (15), *Bacillus licheniformis* (16), *Bacillus megaterium* (10), *Bacillus mycoides* (4), *Bacillus pumilus* (20), *Bacillus subtilis* (14), *Bacillus thuringiensis* (17)*, Brevibacillus laterosporus* (2), *Enterococcus avium* (17), *Enterococcus casseliflavus* (3), *Enterococcus durans* (6), *Enterococcus faecalis* (12), *Enterococcus faecium* (14), *Enterococcus gallinarum* (23)*, Geobacillus stearothermophilus* (3), *Geobacillus thermoglucosidiasius* (3)*, Kocuira kristanea* (4), *Kocuira varians* (4), *Lactococcus lactis* (13), *Paenibacillus pabuli* (3), *Streptococcus acidominimus* (13), *Streptococcus bovis* (2), *Streptococcus pluranimalium* (4), *Streptococcus thermophilus* (1), *Streptococcus uberis* (7)*, Staphylococcus aureus* (7), *Staphylococcus capitis* (15), *Staphylococcus caprae*(2), *Staphylococcus chromogenes*(2),*Staphylococcus cohnii* (17), *Staphylococcus epidermidis* (1), *Staphylococcus hominis* (9), *Staphylococcus hyicus* (7), *Staphylococcus intermedius* (32), *Staphylococcus lentus* (1), *Staphylococcus lugdunensis* (3), *Staphylococcus sciuri* (3), *Staphylococcus xylosus* (15), *Staphylococcus warneri* (1)*, Virgibacillus panthothenticus* (3) were isolated (Aslan and Birbir, 2011). While 68%, 52%, 43% of Gram-negative bacterial isolates and 70%, 69% and 57% of the Gram-positive bacterial isolates demonstrated respectively proteolytic, lipolytic and both proteolytic and lipolytic activities (Aslan and Birbir, 2012;Aslan and Birbir, 2011).

Extremely Halophilic Archaea and Moderately Halophilic Bacteria on Salted Hides and Skins

Kallenberger (1985) stated that halophilic microorganisms found in curing salt contaminate hides and skins. Examination of 131 brine-cured cattle hides collected from USA showed that 94% of salted hide samples were contaminated with extremely halophilic archaea (Bailey and Birbir, 1993). Fifty three percent of these extremely halophilic archaea showed protease activities. When 35 salted hides cured in France and Russia were examined, it was observed that 29%, 37%, 86%, 91% of the samples respectively contained halotolerant, slightly halophilic, moderately halophilic bacteria, and extremely halophilic archaea (Birbir, 1997).

In the study of Akpolat *et al*. (2015), 101 extremely halophilic archaea such as *Halorubrum tebenquichense* (54), *Halorubrum saccharovorum* (24), *Halorubrum lipolyticum* (1), *Halorubrum kocurii* (1), *Halorubrum terrestre* (1), *Halococcus morrhuae* (2), *Halococcus dombrowskii* (9), *Halococcus qingdaonensis* (3), *Natrinema versiforme* (1), *Natrinema pellirubrum* (3), *Halostagnicola larsenii* (1), *Haloterrigena saccharevitans* (1) were isolated from salted sheep skins collected from Spain. Proteolytic and lipolytic activities of these isolates were detected as 15% and 5%.

In a study carried out with salted cattle hides imported from Australia and England, 13 moderately halophilic bacteria such as *Alkalibacillus salilacus, Salimicrobium album*, *Salimicrobium halophilum*, *Salimicrobium luteum*, *Marinococcus halophilus*, *Halomonas koreensis*, *Halomonas alimentaria*, *Halomonas elongata*, *Halomonas halmophila*, *Halomonas eurihalina*, *Thalassobacillus devorans*, *Chromohalobacter salexigens*, *Oceanobacillus picturae* and five extremely halophilic archaeal species such as *Halorubrum saccharovorum*, *Halorubrum tebenquichense*, *Halorubrum lacusprofundi*, *Natrinema pallidum* and *Natrinema gari* were isolated from these hides. Amylase, protease, lipase, caseinase, urease, pullulanase and DNase activities of the moderately halophilic isolates were respectively detected as 15%, 31%, 15%, 15%, 31%, 8%, 38%. Amylase, protease, urease, DNase activities of the extremely halophilic isolates were detected as 20%. In addition, 54%, 77%, 54, 38, 15 of the moderately halophilic isolates and 40%, 60%, 40%, 20%, 20% of the extremely halophilic archaeal isolates respectively used citrate as a sole carbon source, reduced nitrate to nitrite, produced acid from glucose, sucrose and lactose (Caglayan *et al*., 2015).

In a study of Bilgi *et al*. (2015), 186 extremely halophilic archaea were isolated from eight salted hides and skins cured in Turkey, Iraq, Turkmenistan, Kazakhstan and Armenia. Isolation of extremely halophilic archaeal isolates of *Natronococcus* sp., *Natronococcus jeotgali*, *Natrialba aegyptia*, *Halovivax* sp. E107, *Halovivax asiaticus*, *Halococcus morrhuae*, *Halococcus thailandensis*, *Halococcus dombrowskii*, *Halorubrum* sp. CH3, *Natrinema pallidum*, *Natrinema versiforme*, *Haloterrigena thermotolerans*, *Halobacterium noricense* was stated by researchers. While all isolates had DNase activities, 12%, 57%, 11%, 35%, 18% of the isolates showed positive reactions for caseinase, protease, amylase, esterase, lipase activities. Moreover, it was detected that 8% and 62% of the isolates produced indole from tryptophan and reduced nitrate to nitrite.

In addition, 39 bacterial isolates of moderately halophilic bacteria such as *Staphylococcus saprophyticus* subsp. *saprophyticus* (7), *Staphylococcus xylosus* (2), *Staphylococcus equorum* subsp. *equorum* (1), *Staphylococcus arlettae* (6), *Bacillus pumilus* (6), *Bacillus licheniformis* (2), *Salinicoccus roseus* (3), *Gracilibacillus dipsosauri* (5), *Chromohalobacter beijerinckii* (2), *Chromohalobacter canadensis* (1), *Halomonas eurihalina* (2), *Halomonas zhanjiangensis* (1), *Halomonas venusta* (1) were isolated from 25 goat skins cured in Bulgaria, Israel, China, Australia, South Africa, Russia, France and Turkey. Protease, lipase, β-galactosidase, urease, caseinase, amylase, lecithinase, cellulase activities of the isolates were detected as 87%, 64%, 59%, 46%, 28%, 26%, 8% and 5% (Birbir *et al*., 2015; Caglayan *et al*., 2017). Indole production from tryptophan, citrate utilization, hydrogen sulfide (H$_2$S), reduction of nitrate to nitrite, ammonia production from peptone by the isolates were respectively detected as 3%, 31%, 5%, 51%, 85%. Moreover, acid production from glucose, sucrose, galactose, mannose by the isolates were found as 92%, 85%, 56%, 74%, respectively.

In a study of Caglayan *et al.* (2017), 77 bacterial isolates of moderately halophilic bacteria such as *Staphylococcus equorum* subsp. *equorum* (4), *Staphylococcus cohnii* subsp. *cohnii* (3), *Staphylococcus xylosus* (2), *Staphylococcus lentus* (2), *Staphylococcus saprophyticus* subsp. *saprophyticus* (1), *Salimicrobium salexigens* (4), *Bacillus pumilus* (2), *Bacillus licheniformis* (7), *Bacillus safensis* (2), *Bacillus siamensis* (1), *Bacillus tequilensis* (2), *Salinicoccus roseus* (2), *Planococcus rifietoensis* (1), *Alkalibacillus halophilus* (1), *Gracilibacillus dipsosauri* (4), *Marinococcus luteus* (1), *Marinococcus tarijensis* (1), *Oceanobacillus picturae* (1), *Halomonas halmophila* (5), *Halomonas eurihalina* (1), *Halomonas zhanjiangensis* (4), *Halomonas venusta* (2), *Halomonas alkaliphila* (3),

Salinivibrio costicola subsp. *alkaliphilus* (4), *Chromohalobacter canadensis* (6), *Chromohalobacter beijerinckii* (6), *Chromohalobacter japonicus* (3), *Chromohalobacter israelensis* (1), *Idiomarina loihiensis* (1) were isolated from 23 salted sheep skins cured in Australia, Bulgaria, Dubai, Greece, Israel, Kuwait, South Africa, Turkey and U.S.A. Protease, lipase, β-galactosidase, amylase, caseinase, DNase, urease, cellulase, lecithinase activities of these isolates were respectively found as 60%, 43%, 39%, 26%, 23%, 17%, 12%, 12%, 10%. Indole production from tryptophan, citrate utilization, production of H_2S, reduction of nitrate to nitrite, production of ammonia from peptone by the isolates were detected as 12%, 47%, 8%, 78%, 87%, respectively. Acid production from glucose, sucrose, galactose, mannose by the isolates were found as 95%, 71%, 78%, 90%.

Utilization of different amino acids found in the skin by 137 moderately halophilic bacterial species belonging to genera *Halomonas*, *Planococcus*, *Salimicrobium*, *Alkalibacillus*,*Salinicoccus*,*Staphylococcus*,*Bacillus*,*Chromohalobacter*,*Gracilibacillus*, *Idiomarina*,*Marinococcus*, *Oceanobacillus, Salinivibrio* was investigated. Arginine was used by all moderately halophilic isolates obtained from the salted goat and sheep skins. L-hydroxyproline, L-proline, L-tyrosine, L-alanine, L-glycine amino acids were respectively utilized by 66%, 64%, 85%, 66%, 86% of the isolates but L-cysteine was used only 4% of the isolates. These results showed that salted sheep and goat skin isolates were able to utilize L-hydroxyproline, L-proline, L-tyrosine, L-alanine, L-glycine and L-cysteine amino acids found in the skin structure Caglayan *et al*. (2018).

Bacterial Species of the Family *Enterobacteriaceae* on the Salted Hides and Skins

In the other study, Ulusoy and Birbir (2015) examined members of the family *Enterobacteriaceae* on the salted hides and skins. While 27 isolates of *Enterobacter cloacae* (2), *Enterobacter sakazakii* (1), *Raoultella planticola* (1), *Raoultella ornithinolytica* (1), *Serratia odorifera* (1), *Serratia liquefacicens* (1), *Serratia plymuthica* (1), *Serratia rubidaea* (3), *Escherichia coli* (2), *Escherichia vulneris* (1), *Cedecea lapagei* (3), *Ewingella americana* (2), *Klebsiella pneumoniaea ssp. ozaenae (1), Klebsiella oxytoca* (2), *Proteus vulgaris* (2), *Yersinia enterocolitica* (3) were obtained from the hides salt cured in Dubai, Turkey and Israel and 28 isolates of *Citrobacter koseri* (1), *Enterobacter cloacae* (2), *Escherichia coli* (4), *Escherichia vulneris* (1), *Klebsiella pneumoniaea ssp. ozaenae* (1), *Klebsiella oxytoca* (1), *Proteus vulgaris* (2), *Proteus penneri* (1), *Raoultella planticola* (1), *Serratia odorifera* (1), *Serratia liquefacicens* (1), *Serratia plymuthica* (3), *Serratia ficaria* (1), *Serratia marcescens* (2), *Serratia rubidaea* (4), *Yersinia enterocolitica* (2) were obtained from the skin samples salt cured in Australia, Lebanon, U.S.A., South Africa. Protease, urease, β-galactosidase, lipase activities of the isolates were respectively found as 45%, 35%, 90%, 30%. Moreover, 25%, 35%, 35%, 45%, 35%, 70% of the isolates respectively were found to be positive for tryptophan deaminase, arginine dihydrolase, ornithine decarboxylase, lysine decarboxylase, indol production, utilization of citrate. While all isolates produced acid from glucose, 75%, 70%, 90% of the enteric isolates produced acid from sucrose, arabinose, mannitol, respectively.

CONCLUSIONS

All of these studies carried out fresh, salted hides and skins clearly showed that non-halophilic bacteria, moderately halophilic bacteria, extremely halophilic archaea and bacterial species of the family *Enterobacteriaceae* were metabolically active to degrade

proteins, fats, carbohydrates and use their building blocks for their nutritional and structural needs, growth and energy. While most of the examined hides and skin samples had bad odor and red, yellow, cream discolorations, some of them had hair slip which were related to microbial activities. These experimental study results clearly demonstrated that most of the organisms found on the skins and hides were belong to contaminant microorganisms found in the air, water, soil, curing salt, pasture, animal feeds, animal feces, barn, slaughterhouse, and tanneries. These studies also showed that traditional salt curing process does not prevent the growth of these different species of microorganisms causing huge economic losses in leather industry. Hence, we suggest using effective antimicrobial applications to exterminate these hide and skin degrading microorganisms in the leather industry.

REFERENCES

Akpolat, C. *et al*. (2015), "Molecular Identification of Moderately Halophilic Bacteria and Extremely Halophilic Archaea Isolated from Salted Sheep Skins Containing Red and Yellow Discoloratios", *The Journal of the American Leather Chemists Association*, 110, 211-220.

Aslan, E. and Birbir, M. (2011), "Examination of Gram-Positive Bacteria on Salt-Pack Cured Hides", *The Journal of the American Leather Chemists Association*, 12(106), 372-380.

Aslan, E. and Birbir, M. (2012), "Examination of Gram-Negative Bacteria on Salt-Pack Cured Hides", *The Journal of the American Leather Chemists Association*, 4(107), 106-115.

Bailey, D.G. and Birbir, M. (1993), "A Study of the Extremely Halophilic Microorganisms Found on Commercially Brine-Cured Cattle Hides", *The Journal of the American Leather Chemists Association*, 88, 285-293.

Bilgi, S.T., Yapici, B.M. and Karaboz, I. (2015), "Determination of Hydrolytic Enzyme Capabilities of Halophilic Archaea Isolated from Hides and Skins and Their Phenotypic and Phylogenetic Identification", *The Journal of the American Leather Chemists Association*, 110, 33-42.

Birbir, M. and Ilgaz, A. (1996), "Isolation and Identification of Bacteria Adversely Affecting Hide and Leather Quality", *Journal of the Society of Leather Technologists and Chemists*, 80, 147-153.

Birbir, M. (1997), "Investigation of Salt-cured France and Russian Hides for Halophilic Bacteria", *Journal of Turkish Microbiology Society*, 27, 68-73.

Birbir, M., Ventosa, A. and Caglayan, P. (2015), "Characterization of Moderately Halophilic Bacteria Found on the Sheep and Goat Skins", The Scientific Research Project Commission of Marmara University, Project Number FEN-C-DRP-040712-0281.

Caglayan, P. *et al*. (2015), "Characterization of Moderately Halophilic Bacteria from the Salt-pack Cured Hides", *Journal of the Society of Leather Technologists and Chemists*, 5, 250-254.

Caglayan, P. *et al*. (2017), "Screening of Industrially Important Enzymes Produced by Moderately Halophilic Bacteria Isolated from Salted Sheep Skins of Diverse Origin", *The Journal of the American Leather Chemists Association*, 112(6), 207-216.

Caglayan, P. *et al*. (2018), "Investigation of Moderately Halophilic Bacteria Causing Deterioration of The Salted Sheep and Goat Skins and Their Extermination via Electric Current Applications", *The Journal of the American Leather Chemists Association*, 113(2), 41-52.

Hien, N.T.P. (2006), "A Rapid Quantitative Assay for Bacterial Protease Activity", *Master Thesis*, The Graduate Faculty of Texas Tech University.

Highberger, H.J. (1956), "The Chemical Structure and Macromolecular Organization of the Skin Proteins", in: O'Flaherty, F., Roddy, W.T., Lollar, R.M. (eds.), *The Chemistry and Technology of Leather*, Reinhold Publishing Corporation, New York, 1, 65-193.

Kallenberger, W.E. (1985), "Halophilic Bacteria in Hide Curing", *PhD Thesis*, Division of Graduate Studies and Research of the University of Cincinati, Department of Basic Science Tanning Research of the Collage of Arts and Science.

Sverre, D. (1956), "Prevention of Microbial Deterioration of Leather", *The Journal of the American Leather Chemists Association*, 51,113-117.

Ulusoy, K. and Birbir, M. (2015), "Identification and Metabolic Activities of Bacterial Species Belonging to the *Enterobacteriaceae* on Salted Cattle Hides and Sheep Skins", *The Journal of the American Leather Chemists Association*, 110, 86-199.

Venkatesan, R.A., Nandy, S.C. and Sen, S.N. (1970), "Effect of Storage and Pretanning Operations on the Bacterial Flora and Its Population on Goat Skin", *Leather Science*, 17, 395-404.

AGROTEXTILE SYSTEMS - STRATEGIC ELEMENTS FOR SUSTAINABLE DEVELOPMENT OF THE AGRICULTURE

EFTALEA CĂRPUŞ[1], ANGELA DOROGAN[1], FLOAREA BURNICHI[2]

[1]*The National Research and Development Institute for Textile and Leather, 16 Lucretiu Patrascanu Street, 030508, Bucharest, Romania, e-mail: certex@ns.certex.ro*

[2]*R&D Resort for Vegetables, Buzău (Romania), SCDL Buzău*

"Agriculture is the backbone of our country; Textile can be the backbone of Agriculture?" Today, agriculture and horticulture has realized the need of tomorrow and opting for various technologies to get higher overall yield, quality and tasty agro-products. This review works as an introduction about the *agro-textile* products available currently to bang the agriculture. This gives the idea about the properties and classification of the agrotextile products.

Keywords: agrotextiles, property, application.

INTRODUCTION

Textiles and clothing is a diverse sector that plays an important role in the European manufacturing industry. In 2017, the overall size of the Textile & Clothing industry in the EU-28 represents a turnover of €181 billion and investments of €4.9 billion. Thanks to a revival of the EU activity, the 176,400 T&C companies still employ over 1.7 million workers. EU external trade was more dynamic than the previous year with almost €48 billion of T&C products exported and €112 billion imported from third markets (Euratex, 2016).

The sector, playing a crucial role in the economy and social well-being, has undergone radical change recently to maintain its competitiveness by moving towards high value-added products (EC, Textiles and clothing in the EU).

Innovation is the key of success for textiles' companies, just as in other economic field (McAdam and McClelland, 2002). One of the segments of this industry that has received significant attention across the world is technical textiles. Technical or engineered textiles are defined as products that are used for functional purposes. These textiles have applications in multiple areas of economic activity, such as aerospace, shipping, sports, agriculture, defense and health care (Wazir Advisors Pvt. Ltd. and FICCI, 2016). Messe Frankfurt divides technical textiles into following twelve categories (fig. 1).

Figure 1. Twelve main categories of technical textiles [Source: www.messefrankfurt.com]

Agro-textile is a crucial and emerging sector among all the twelve sectors of technical textiles, which are also known as Agrotech or Agro textiles. In more detailed definition *textiles for agriculture are used for crop protection, fertilization, aquaculture, horticulture and forestry*.

Agro Textile market is expected to reach over US$ 14,363.2 Mn by 2025 at a CAGR of 5.5% from 2017 to 2025. The worldwide agro textile market was evaluated at US$ 8,921.9 Mn for the year 2016 (Credence Research, 2016).

Figure 2. Different agro-textile products; source: http://agrotextile.com/agro-textile-products.html

REVIEW ON AGRO TEXTILE PRODUCTS

Sustainable development is a response to the current global challenges of climate change, atmospheric pollution, the risk of resource depletion and threats to biodiversity, but also to the economic growth problem, which is in contrast to the idea of protecting the environment and resources. In this context, the circular economy is considered a practical solution to the global trend of exhaustion natural resources. Circular economy as a concept based, for industrial ecology, cradle to cradle philosophy, biomimicry, and natural capitalism (Fontel, 2017).

"Agrotextiles" gives multidimensional views and solutions to the problems being faced by agro industry.

Today agro textile plays a significant role to control environment for crop production, eliminate variations in climate, weather change and generate optimum condition for plant growth. Adopting the high-tech farming technique, where textile structures are used, could enhance quality and overall yield of agro-products.

Agriculture is also an important user of products from end-use sectors such as geotextiles for drainage and land reclamation, protective clothing for employers who have ta handle sprays and hazardous equipment, transport textiles for tractors and lorries, conveyor, belts, hoses, filters and construction of silos, tank and piping (Horrocks and Anand, 2016).

The main process used for technical textiles are: knitting, weaving, braiding, nonwoven etc. (Palamutcu and Devrent, 2017; Bharamkar, 2013) (figure 3).

| nonwoven | woven | knitted |
| knotted | braided | twine |
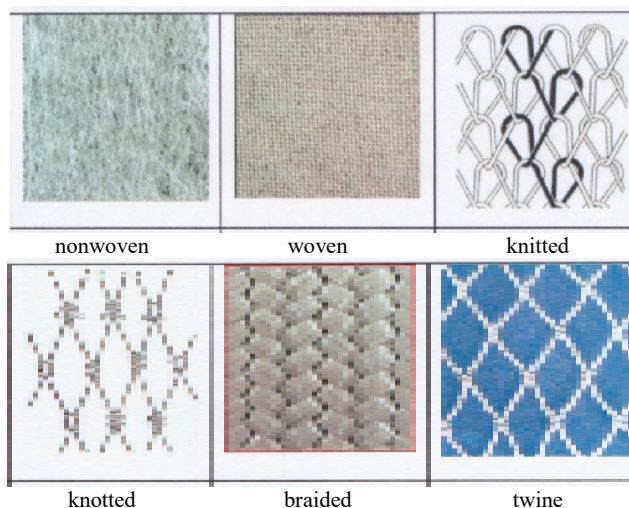
Figure 3. Textile surface types, used in agro textiles

There are many techniques to produce nonwoven fabrics: needle-punched nonwovens, stitch-bonded nonwovens, thermally bonded nonwovens, hydro entangled nonwovens, spun bonded nonwovens, Wet nonwovens (https://fashionarun.page.tl/AGRICULTURAL-TEXTILES.htm; Desai).

There are many ways and techniques to produce technical textile, specialty literature has provided the following methods to manufacture technical textile: thermo-forming, three dimensional weaving, three dimensional knitting, fabrics produced using nanotechnology, heat-set synthetics, finishing treatments

Various innovations in industry, such as induction of advanced materials have opened up potentials for innovation in shading and crop protection, including capillary nonwovens, floating covers, and textiles incorporating pesticides, fertilizers, superabsorbent polymers and seeds which are expected to drive market growth over the next eight years (Agro Textiles Market Analysis, 2018 - 2025).

The usages of fibres in the technical textile area are not only the high functional fibres alone, but also the natural (due to bio-degradability and compatibility), table 1 (Sadik, 2017).

Table 1. Fibers for technical textile

Fibre used in technical textiles	% of usage
Regular fibres	69
High tenacity fibres	28
High performance fibres	2
Special performance fibres	1
TOTAL	100

Classification of Agrotextile Products

Agrotextile products can be classified based on three categories (Kruthika, 2017; Sarwar, 2016; Global Agro Textiles Market 2018; Agrawal, 2013):

- Based on fabric production: woven, knitted, non woven;
- Based on the area of application:
    - Agriculture: sunlight/wind/weed/protection; water retention, physical damage protection
    - Horticulture: ultraviolet radiation/wind/bird/insect protection;
    - Forestry: soil protection, weed protection for tree plantation;
    - Aquaculture: fishnets, antifouling nets, ultraviolet radiation protection;
    - Animal husbandry: belts for animal identification, filtering milk.
- Based on the products: shade nets, windshield nets, bird protection nets, crop covers, plant nets, root ball nets, anti-insect nets, harvesting nets, mulch mats/ground covers, anti-hail nets, finishing nets, turf reinforcement/protection nets, pallet net covers, woven sacks/bags, leno bags.

The global Agro Textiles market has been classified on the basis of product type into:
- Shade net,
- Mulch mat,
- Ground cover,
- Crop cover,
- Insect net,
- Pond liners.

Properties Required for Agro Products

- Resistance to solar-radiation: the product should withstand solar radiation according to the external environment without creating harm to crops;
- Resistance to weather: with respect to the climatic changes product must work in effect for production;
- Resistance to ultraviolet radiation: product should avoid the degradation of molecular chains due to ultraviolet rays and keep them away;
- Retention of water: the water poured is to be segregated and let the crop to absorb whenever it is essential;
- Biodegradability: as the products are placed over and under the crops it is important to have biodegradable property;
- Weight of the product: in order to let the crops grow without disturbance less weight materials to be selected;
- Resistance to microorganisms: to protect the living being around the crop field it should resist microorganisms;
- Construction of material: stable constructions is essential for long life of product.

Advantage of Textile Used in Agriculture

- Increase crop production;
- Avoid the soil from drying out;
- Decrease the requirement of fertilizers, pesticides and water;
- They make product quality better;
- Increase the early maturing of crops and non-seasonal plants;
- Protects from climatic changes and its effect.

CONCLUSION

The study shows the basic introduction regarding agro textile products and their role in the sustainable development of agriculture, environmental protection and human health.

REFERENCES

Agrawal, S.K. (2013), Application of Textile in Agriculture, *International Journal of Advance Research In Science And Engineering*, 2(7), 9-18.

Bharamkar, V. (2013), "Manufacturing process of agrotextile", *Technical textiles*, July 20, http://textilecentre.blogspot.com/2013/07/manufacturing-process-of-agro-textiles.html.

Credence Research (2016), "Agro Textile Market is Expected to Reach over US$ 14,363.2 Mn by 2025 at a CAGR of 5.5% from 2017 to 2025", https://www.credenceresearch.com/press/global-agro-textile-market.

Desai, A., "Textiles used in modern agriculture to smart farming", http://www.academia.edu/35687669/Textiles_used_in_modern_agriculture_to_smart_farming.

Euratex (2016), The EU-28 "Textile and Clothing Industry in the Year 2016", Key Figures 2016, http://euratex.eu/fileadmin/user_upload/images/key_data/Euratex_Keyfigures_-_2016-HR.pdf.

European Commission, Textiles and clothing in the EU, https://ec.europa.eu/growth/sectors/fashion/textiles-clothing/eu_en.

Fontel, P. (2017), "Model of circular business ecosystem for textiles", ISBN 978-951-38-8587-8, https://www.vtt.fi/inf/pdf/technology/2017/T313.pdf.

Horrocks, A.R. and Anand, S.C. (Eds.) (2016), *Handbook of Technical Textiles*, 2nd edition, Woodhead Publishing.

Kruthika, V. (2017), "Review on Agro Textile Products and Their Properties", http://textilelearner.blogspot.com/2017/03/agro-textile-products-properties.html.

McAdam, R. and McClelland, J. (2002), "Sources of new product ideas and creativity practices in the UK textile industry", *Technovation*, 22, 113–121.

Palamutcu, S. and Devrent, N. (2017), "Technical Textiles for Agricultural Applications", *International Interdisciplinary Journal of Scientific Research*, 3(1), https://www.iijsr.org/data/frontImages/gallery/Vol._3_No._1/1._1-8.pdf

Sadik, S. (2017), "Fibers for Technical Textile", https://textilestudycenter.com/fibers-technical-textile.

Sarwar, M.G. (2016), "Agrotech-Agro textiles", https://www.slideshare.net/sawpnobazz/agrotechagro-textiles.

Wazir Advisors Pvt. Ltd. and FICCI (2016), "Knowledge Paper on Technical Textiles: Towards a Smart Future Technotex 2016", Fifth International Exhibition & Conference on Technical Textiles, April 21 – 23, 2016, Mumbai, India, http://ficci.in/spdocument/20811/1-Technotex- 2016-Knowledge- Paper.pdf

West Bengal Agro Textile Corporation, Technotex, W.L. Gore & Associates, Texel Industries Limited and Lohia Corp Limited (2018), "Global Agro Textiles Market 2018", http://ereports.market/global-agro-textiles-market-2018.

***, "Agro Textiles Market Analysis by Product (Shade-nets, Mulch-mats, Bird Protection Nets, Fishing Nets), by Application (Agriculture, Aquaculture, Horticulture & Floriculture) & Segment Forecasts, 2018 - 2025", https://www.grandviewresearch.com/industry-analysis/agro-textiles-market.

***, Agricultural textiles, https://fashionarun.page.tl/AGRICULTURAL-TEXTILES.htm.

WATERPROOF PROCESS IN FOOTWEAR INDUSTRY

ADRIANA CHIRILĂ, ALINA IOVAN-DRAGOMIR

"Gheorghe Asachi" Technical University of Iasi, Faculty of Textiles, Leather and Industrial Management, 28 D. Mangeron, Iasi, Romania, Adriana8chirila@gmail.com, adragomir@tex.tuiasi.ro (corresponding author)

Waterproofing is the ability to prevent water from entering and has been a concern for people long before the invention of modern substances, chemicals or technologies. This paper presents water proof process in footwear industry. The paper has three parts: introduction, case study and conclusion. In the first part, are presented two popular methods to provide protection against water for shoes. In the footwear industry the usual methods of waterproofing are by adding a waterproof bootie inside the shoes or by attaching a protective membrane on the semi-finished uppers. Both methods have gathered quite a following among users and both promise to protect the user in harsh conditions, but also offer breathability and comfort. These waterproofing methods are the OutDry® and Gore-Tex® technologies. In the second part, it is presented a case study; it is analyse waterproof for defected pair a hiking boots constructed using OutDry Technology. In order, it was use 2 testing methods: centrifuge test and dynamic footwear water penetration test. In conclusion, waterproofing footwear using innovative methods and processes can be challenging and manufacturers need to adapt and evolve in order to comply with the standards. But difficulties are not a deterrent; they represent opportunities to become better professionals, more knowledgeable users of technology and a more conscious industry on the environmental impact of footwear manufacturing processes.

Keywords: footwear, waterproof, technology.

INTRODUCTION

Ages before the use of special processes and technology, humans used substances found in nature to gift everyday objects with waterproof qualities. On naval ships, tar and pitch were the main methods for sealing the hulls of boats. These materials were sealing all the wooden connections of the vessel together, keeping the water out. Oil was another trick sailors had in the sixteenth century; back then sails were greased with oil to ensure that the fabric could withstand the difficult sea environment and intense storms. The use of common bees wax began to rise in popularity as a waterproofing method around the end of the nineteenth century. In the clothing industry wax-covered threads could be weaved into somewhat waterproof garments and leather footwear was rubbed and coated with bees wax or animal fat to make it impermeable to water. All of these past forms of waterproofing, by tar, oil, wax, or animal fat aimed at a common goal, of keeping water out and the people using those objects dry and comfortable.

Coming into more modern times, waterproofing has been adapted and new technologies have emerged and evolved. In the footwear industry the usual methods of waterproofing are by adding a waterproof bootie inside the shoes or by attaching a protective membrane on the semi-finished uppers. Both methods have gathered quite a following among users and both promise to protect the user in harsh conditions, but also offer breathability and comfort. Two main representatives of these waterproofing methods are the OutDry® and Gore-Tex® technologies.

OutDry® Technology

OutDry® is an innovative construction process that can be used to make gloves, backpacks and footwear completely waterproof yet breathable. The patented method

does not leave seams or gaps because the fabric layers are heat-bonded together. In this case the binding process becomes more important that the material itself because it helps fabrics achieve optimum water-resistance. Without space between the impenetrable waterproof complex and the fabrics that make the uppers, water is not able to permeate the layers and get trapped in the footwear. This construction assures that there is no chance for the water to leak through the fabric after long exposures to wet environments. This method of applying the membrane does not affect the breathability of materials (Figure 1).

Figure 1. Applying OutDry® membrane to footwear uppers

Figure 2. Gore-Tex® Technical details

OutDry® fabrics have an advantage point in the fact that they do not require the use of durable water repellent or DWR coatings, which most of times are not environmentally friendly and need many years to breakdown, while causing a lot of harm to the environment in the process.

Gore-Tex® Technology

Gore-Tex® is a special material made of PTFE (Polytetrafluoroethylene) a hydrophobic compound, is a microporous material with a very low water-adsorption rate and also extremely durable. It is commonly known as Gore-Tex® fabric and it was developed and patented by the brand with the same name (Figure 2).

The Gore-Tex® fabric can be analyzed from three main perspectives as a membrane, a laminate and a fabric technology.

- Gore-Tex® is considered a membrane because it contains over 9 billion breathable pores per square inch, which is why it allows for moisture transfer from the interior of the shoes towards the exterior and away from the body.
- The material is also viewed a laminate because it is bonded between the outer and inner linings and creates a single layer with all three elements working as one.
- And finally, it is considered a fabric technology because it comes in roles and can be tailored for different products with diverse construction requirements and maintains its waterproof and highly breathable qualities.

OutDry® versus Gore-Tex®

Looking at the qualities of these fabrics a comparison can be made on a technical level. Considering the waterproof rating both technologies claim to be fully waterproof. Fabrics with a water column of 10.000 mm and higher are considered to be fully waterproof. Diverse waterproof fabrics behave differently and not all withstand water pressure at the same level.

In this matter OutDry® has a rating of around 20.000 mm, passing the water column test, making it fully waterproof.
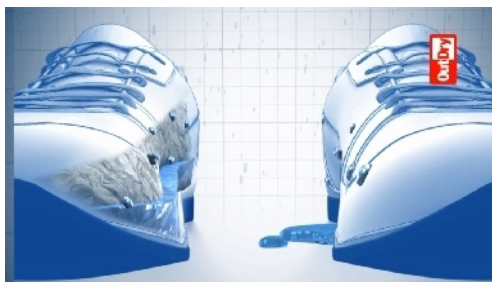
Figure 3. Footwear construction: a). Waterproof Gore-Tex® type construction with bootie; b). OutDry® membrane lamination

Gore-Tex®, by comparison, starts at 28.000 mm and can go above that value for certain products, making it considerably more adapted than OutDry® to withstand heavy water conditions. However, there is another element to be taken into consideration with the Gore-Tex® technology, the use of DWR (durable water repellant) coatings.

OutDry® is a two-layer fabric, bound together by a heat source. There is no need for DWR treatments to protect the shoes in harsh water conditions because it leaves no gaps in between the layers and the uppers are fully waterproof. Gore-Tex®, on the other hand, utilizes DWR treatments to minimize water contact and this helps further waterproof the fabric.

If only the water columns levels are analyzed then Gore-Tex® is in advantage, but considering the water resistance capabilities in time then OutDry® comes as the superior choice because DWR coatings tend to degrade overtime. This degradation makes the shoes more vulnerable to bad weather conditions and also gives them a tendency to overheat, due to the pores clogging from the water. Usually the DWR coatings and treatments require regular maintenance so that the footwear keeps up its protective qualities against the weather. DWR treatments are also concerning for their environmental impact and health issues they might produce because of PFCs (Perfluorinated compounds). Member compounds of this large chemical family are linked to several types of tumors and neonatal deaths and toxicity in the liver and endocrine system, as stated by EU research and the United States Environmental Protection Agency. This is why major sports brands are beginning to use PFC-free materials when waterproofing their products.

When comparing these two materials one of the most important qualities, breathability, must be taken into account in order to avoid overheating and excessive sweating during footwear usage. On this point, OutDry® provides an adequate level of

breathability, keeping moisture away from the body. However it has been showed that it has a tendency to overheat, more than the Gore-Tex® option.

QUALITY EVALUATION FOR A DEFECTIVE PAIR OF HIKING BOOTS CONSTRUCTED WITH OUTDRY WATERPROOF TECHNOLOGY (CASE STUDY)

Before proceeding to the quality evaluation of a defective pair of hiking boots constructed with the OutDry® waterproof technology, must be stated the fact that these shoes are not branded by the company in question.

Figure 4. Footwear sample with waterproof issues (personal archive)

Figure 5. Water level in the tank (personal archive)

In fact several shoe manufacturers have acquired the legal rights to use this technology and produce waterproof footwear under the directions and process standards patented by OutDry®. The quality and performance of the footwear often depends on the manufacturers capacities of implementing and following the process standard.

The article (Figure 4) under consideration is a pair of woman hiking boots that was returned by the user for waterproof issues. The general state of the shoe showed clear signs of use with water stains and mud debris reaching the collar. There were no evident puncture marks, torn or unstitched material on the exterior of the shoe.

The first test to be performed was the centrifuge test. The test was performed following the OutDry® standard OUTDRY OS – 05, version 1. Similar to a static footwear water penetration test, the shoes were placed and secured in a water tank where the water level was set for 2 cm above the flexion point of the sole (Figure 5). Tray centrifugation was set for 250 rotation per miute for the duration of 10 minutes. The insock of the shoes was wrapped in paper with high water absorption qualities and inserted back in the tested footwear.

After analyzing the output for the centrifuge machine, no water penetration marks were observed inside the footwear concluding that the tested pair passed the centrifuge test.

The second test to be performed was a dynamic footwear water penetration test, using a machine mimicking the foot movement and flexion of the metatarsophalangeal joint. The pneumatic machine used for testing was a SATRA STM 505 model, a

Dynamic Footwear resistance Tester, commonly found in testing laboratories for water resistance tests.

The internal manufacturer requirements set for waterproof footwear in the dynamic water penetration test is a value of 50000 flexion correlated to moderate use of the hiking footwear in the terrain it was designed for. The tested pair of hiking boots failed this requirement because water marks could be observed on the insock paper after 4000 flexion.
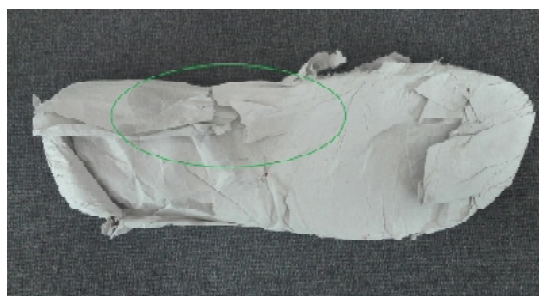
Figure 6. Water stains in the paper insock after 4000 flexion on the Dynamic Footwear Resistance Machine (personal archive)

The following step was to cut open the failed sample and analyze the internal components affecting the waterproof parameters: the OutDry® membrane, the gasket and the aquablock tape. The shoe was cut in half from toe to heel displaying a transversal image of its construction.

Figure 7. The aquablock overlap and stitching forming a hard point (personal archive)

Figure 8. Two overlapped OutDry® membranes identified in the tested pair of hiking boots (personal archive)

The water penetration point was identified on the medial lateral inside if the shoe, where the ends of the aquablock tape overlap (Figure 7). It was noted that the finishing overlap of the tape was of 6 mm when the requirements are set for 7 – 15 mm. Also the reinforcement stitching formed a hard point in the area. Other remarks referred to the gasket that was correctly placed, covering the stitching completely and the aquablock tape, which was straight without wrinkles.

Further research was necessary in order to identify the direct cause of the failed waterproof issue. Under the effect of a heat gun, the layers of the uppers were separated.

In doing so two layers of OutDry® membrane could be observed indicating that the shoe was previously repaired (Figure 8).

Going deeper into the issue it was revealed that the first membrane split in the counter area during the laminating process. Because removing the membrane could potentially cause damage to the uppers, the preferred solution was to add a second membrane to the shoe, leaving the first one in place. The overlapping thickness of the two membranes and the added material plus the inadequate stitching of the aquablock tape have combined and created a waterproof problem. At the same time the work process and the temperature parameters for OutDry® and gasket were not adapted to this situation that deviates from the standards.

What this case comes to prove is that the manufacturer using the waterproof technology must thoroughly assimilate the process knowledge before venturing into production. Constant evaluations of the work techniques must be made and direct supervision should be the norm for key working stations in the production line.

CONCLUSION

Traditional manufacturing methods have helped the footwear industry develop and are a great source of knowledge and experience. From household items have spurred innovative ideas that have thrusted the footwear production methods further into the future.

If only the water columns levels are analyzed then Gore-Tex® is in advantage, but considering the water resistance capabilities in time then OutDry® comes as the superior choice.

Waterproofing footwear using innovative methods and processes can be challenging and manufacturers need to adapt and evolve in order to comply with the standards. But difficulties are not a deterrent; they represent opportunities to become better professionals, more knowledgeable users of technology and a more conscious industry on the environmental impact of footwear manufacturing processes.

REFERENCES

Dragomir, A. (2009), "Materii prime pentru încălțăminte", Editura Performantica, ISBN 978-973-730-476-6, Iași.

Marlocchi, A. (1998), U.S.Patent No.6855171B2, OutDry Technologies Corp.

Majbaur, R.K. (2015), "Study about polymer applications in footwear", Plastic Technology Arcada University of Applied Science, Finland.

***, Life cycle assessment of a pair of GORE-TEX® branded waterproof and breathable hiking boots.

***, https://www.scarpa.co.uk/technical/

***, https://www.gore-tex.com/technology/what-is-gore-tex.

***, https://patents.justia.com/patent/9315002

***, https://www.satra.com/test_equipment/machine.php?id=78

MECHANICAL PROPERTIES OF ARC WELDED IN VACUUM Ti-6Al-4V ALLOY

NIKOLAY VASILEV FERDINANDOV, DANAIL DIMITROV GOSPODINOV,
MARIANA DIMITROVA ILIEVA, ROSSEN HRISTOV RADEV

University of Ruse, 8 Studentska str., Ruse, Bulgaria, nferdinandov@uni-ruse.bg

Titanium alloys are known for their good mechanical properties, low density, excellent corrosion resistance and low thermal conductivity. These properties define titanium and its alloys as highly suitable for medicine, automotive and aerospace industries. Unfortunately, the thermal cycle during welding of alpha-beta alloys (Ti-6Al-4V) can significantly change their strength, toughness and plasticity. The scope of present work is to investigate the possibility for producing Ti-6Al-4V welds by arc discharge in vacuum and to establish the influence of the welding parameters on dimensions and mechanical properties of the welds. The experiments presented here were carried out in an installation for hollow cathode arc treatment in vacuum. Cylindrical and elliptical tantalum cathodes were used. The welding was carried out without filler material and groove. Tensile test and hardness test of specific welds zones were used for mechanical properties determination. The results, presented in this work, describe the dimensions of the fusion zone and heat affected zone of welds, produced by hollow cathode arc welding using different welding parameters. The mechanical properties of the welds were determined.

Keywords: Titanium Alloy, Welded Joints, Mechanical Properties.

INTRODUCTION

Titanium based alloys are known as a material suitable for aerospace and automobile industries and are widely used in medicine. This is due to their better performance as a construction material over other materials because of their good mechanical properties, low density, excellent corrosion resistance in most aggressive media, low thermal conductivity etc.

After heat treatment $\alpha+\beta$ alloys possess increased toughness and high strength. These alloys represent about 70% of the USA market of titanium alloys and Ti-6Al-4V (Gr-5, Gr-5ELI) composes 56% from the whole USA market of titanium and titanium alloys (Lütjering and Williams, 2007).

The presence of β-phase at room temperature has as a result grain size refinement and increase in strength, ductility, toughness and weldability; the existence of β-phase along with α introduces the possibility for heat treatment (Zubarev and Kolomenskij, 2010; Zubarev and Kolomenskij, 2011; Leyens and Peters, 2003).

Ti-6Al-4V can be subjected to different heat treatment depending on the desired combination of mechanical properties; most used heat treatment of this alloy includes: annealing and quenching with subsequent ageing. The lowest strength and the highest ductility are observed after annealing; and the highest strength together with reasonably good ductility the alloy demonstrates after quenching and ageing.

The heat affected zone is what defines the weldability of titanium alloys (Nerovnyj and Jampolskij, 2002; Muraviev and Kleshnina, 2010). The most important structural changes and connected to them changes in properties occur, except at the fusion zone, at the areas next to the weld metal, where the metal is being heated up to temperatures of $(0{,}9 \div 1{,}0)T_m$ (T_m – melting point). The next areas are subjected to phase transformations resulting in metastable phases formation.

The main difficulties connected to welding of titanium and its alloys are provoked by their high chemical activity, formation of pores and cold cracks, propensity for grain size enlargement near the weld. Welding of α+β alloys (including Ti-6Al-4V) can significantly change their strength, toughness and ductility. The low toughness is result of the phase transformations occurring at the weld metal and at the heat affected zone.

Titanium alloys are most often welded by TIG welding or welding in vacuum (Lisiecki, 2012; Niagaj, 2012; Ranatowski, 2008; Yassin *et al.*, 2012).

The aim of the present work is to investigate the possibility for welding titanium alloy Ti-6Al-4V by vacuum arc welding with hollow cathode and to determine the influence of welding parameters on geometric dimensions and mechanical properties of the produced welds.

METHOD AND MATERIALS

The presented here experiments were carried out in a device for vacuum arc welding with hollow cathode. Figure 1 represents the used device.
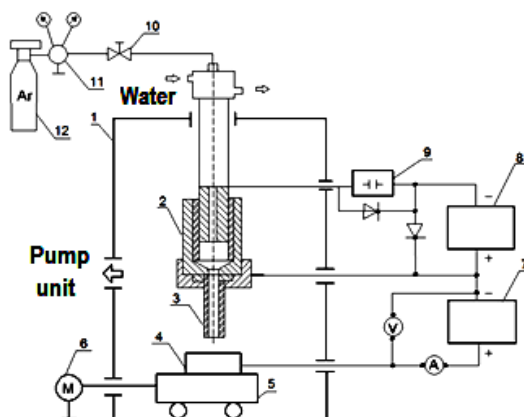
Figure 1. Scheme of the device for vacuum arc treatment: 1 – vacuum chamber; 2 – burner; 3 – hollow cathode; 4 – welded parts; 5- manipulator; 6 – electric motor; 7 – main power supply; 8 - auxiliary power supply; 9 - capacitor battery; 10 – gas supply; 11 - pressure reducing valve; 12 – container for plasma forming gas.

The device consisted of a 0.5 m^3 vacuum chamber, pump set, appliances for gas supply, flow-meters and welding power source. The welding burner (2) and the ancillary welding equipment (5), providing the reciprocating move, were mounted in the chamber (1). The required chamber pressure was achieved and maintained by the vacuum set, comprising three vacuum pumps - rotary vacuum pump, roots vacuum pump and diffusion vacuum pump. All experiments were carried out at pressure of 3 Pa. The plasma forming gas was Ar, purity 99.999%.

The working mode parameters are shown in Table 1. They were picked out according to recommendation for titanium alloys welding, taking into account the need for full penetration. The used cathodes were cylindrical and elliptical (Fig. 1, position 3). The cathodes were of tantalum foil; cathodes length was 30 mm and wall thickness –

0.2 mm. Dimensions and shapes of cathodes are shown in Table 1. The welding process was carried out without filler material and without groove.

Table 1. Welding modes

No	Current I, A	Welding speed V, mm/s	Cathode dimensions mm	Gas quantity Q, l/h
1	100	4,2	∅4	2,3-2,4
2	115	4,2	∅4	2,3-2,4
3	130	5,5	∅4	2,3-2,4
4	115	5,5	elliptical 5,6 x 2	2,3-2,4
5	130	6,5	elliptical 5,6 x 2	2,3-2,4

The welded parts were made from titanium alloy Ti-6Al-4V (Gr-5) with dimensions 100x50x2 mm (LxWxH). The chemical composition of the welded parts was determined by XRF and is given in Table 2.

Table 2. Ti-6Al-4V Chemical composition

V, %	Al, %	Ti, %
4,27	6,1	89,57

Figure 2 shows the produced weldments. The mechanical properties of the weldments were determined using tensile testing and hardness testing at some characteristic areas of weldments. Weldments were cut into specimens for tensile testing, as shown in Figure 2b.
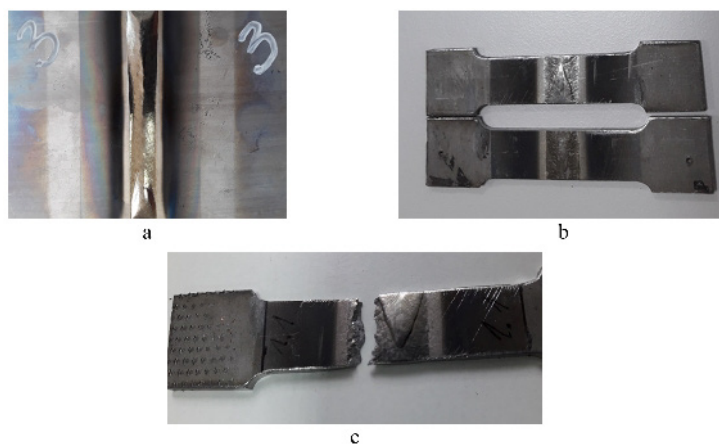
Figure 2. General appearance of produced welds (a); specimens for tensile testing (b); fractured after tensile testing specimen (c)

RESULTS

Table 3 summarises the dimensions of the fusion zones and heat affected zones of the produced weldments. The analysis of these dimensions indicated that during

welding with cylindrical hollow cathode (modes 1, 2, 3) the size of the fusion zone and heat affected zone increased with increasing current value (modes 1 and 2). Simultaneous increase in current value and welding rate (mode 3) led to formation of fusion zone and heat affected zone with same dimensions as the obtained at lower current (mode 3 vs. mode 1).

The change in the cathode cross section shape from cylindrical to elliptical, with the ellipse wide side along the welding axis, led to decrease in the dimensions of both the fusion zone and the heat affected zone (Table 3, modes 4 and 5).

Table 3. Dimensions of the obtained zones

Welding mode No	Fusion zone width, mm (see Fig. 3)	Dimension of heat affected zone, mm (see Fig. 3)
1	9	2,3
2	10,5	2,5
3	9	2,5
4	7	1,65
5	8	2,05

Table 4 and Figure 3 represent the measured values of mechanical properties of the as-delivered Ti-6Al-4V and of the produced by us weldments. The results in Table 4 indicated that welding worsened the behaviour of Ti-6Al-4V in tensile test, and that was demonstrated by lower yield strength, ultimate tensile strength and elongation. That was caused by structural changes that took place at the areas heated to temperatures above β-transus temperature (above 995 ±15 °C for Ti-6Al-4V). It should be noted that for all weldments the fracture occurred at the boundary between fusion zone and heat affected zone (Fig. 2 c). Similar behaviour was observed by other authors too (Denney and Metzbower, 1989; Kramár, Michalec and Kovačócy, 2012).

Hardness measurements were carried out at different, randomly chosen volumes of the characteristic zones of weldments; it was found out that all measured values were close (almost equal). That fact led to the conclusion that the hardness was uniformly distributed within each individual zone. Differences in hardness values were observed only in transition from one zone to another.

Base material demonstrated higher hardness as it is seen in Table 4. That fact is meaningful, considering the as-delivery state of the base metal: quenching and ageing, at which Ti-6Al-4V is characterized with hardness values of 360 up to 400 HV. The hardness values decreased at the transition from the base metal to the heat affected zone; the hardness showed its lowest values at heat affected zones. Measured hardness values at weld metal were higher than those at heat affected zone but still lower than those of base material (Table 4). Considering that: 1) the measured hardness values are typical for both annealed and quenched structures and 2) the cooling rates in our experiments were not determined, a definite statement about the state (annealed or quenched) of fusion zone and heat affected zone cannot be made.

In order to establish the structure of weld metal and heat affected zone, the produced weldments were aged at different temperatures. The ageing was carried out in a vacuum furnace for heat treatment, at pressure of 100 Pa and temperatures range from 350 to 550°C with step of 50°C, soaking time of 2 h.

Table 4. Mechanical properties of the base metal and weldments

Welding mode No	Yield strength $R_{p0,2}$, MPa	Tensile strength R_m, MPa	Elongation A, %	Hardness	
				Fusion zone	Heat affected zone
				HV5 (HRc)	
As delivered	1002	1089	10	390 (39,8)	
1	940	1010	5	363 (37,0)	359 (36,4)
2	780	975	5	369 (37,8)	356 (36,1)
3	840	930	4,5	364 (37,1)	353 (35,9)
4	843	957	5	366 (37,6)	355 (36,0)
5	850	955	6	365 (37,2)	350 (35,5)
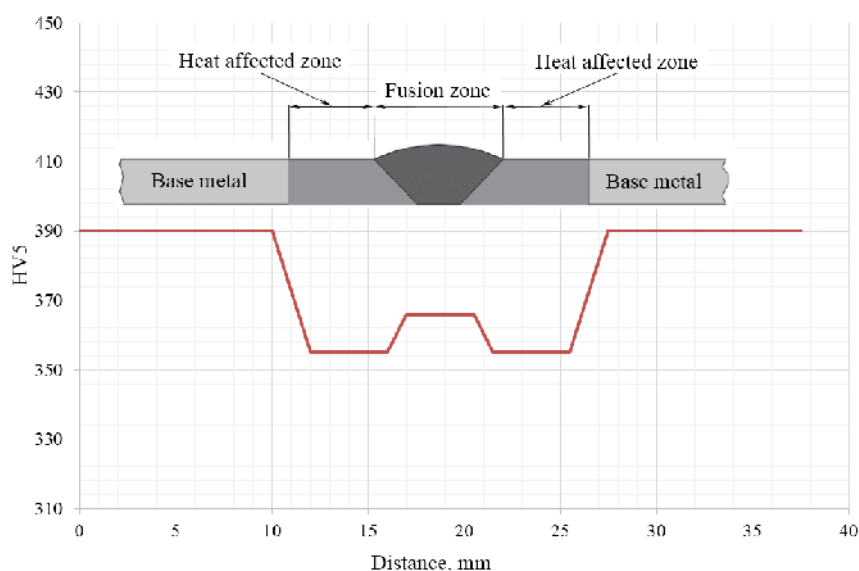
Figure 3. Hardness distribution at the different zones of weldments

Hardness testing after ageing showed increase in hardness values all over the specimens; that increase was up to 20-25 HV5. The measured hardness values after ageing at 500°C were highest in our experiments. The observed increase in hardness values could be attributed to incomplete ageing in as-delivery state of Ti-6Al-4V (inadequate ageing time or temperature). Heating at 500°C for 2 h caused ageing processes to become more completed, thus the hardness values increased. As for the hardness increase at heat affected zone and weld metal, it can be assumed that in some restricted volumes cooling rate after welding was sufficiently high for quenching; as a result quenching occurred at these restricted volumes. Ageing took place only at these volumes and led to hardness increase.

CONCLUSIONS

1- Altering the main welding parameters makes it possible to produce heat affected zones and fusion zones of different dimensions.
2- Using an elliptical cathode instead of a cylindrical one allows to reduce the geometric dimensions of fusion zone and heating affected zone
3- Produced weldments have lower mechanical properties viz. strength and ductility. Enhancement of these properties could be expected after welding modes that provide greater cooling rates.
4- Ageing after vacuum arc welding with hollow cathode leads to hardness increase.

REFERENCES

Denney, P.E. and Metzbower, E.A. (1989), "Laser Beam Welding of Titanium", Welding Research Supplement.

Kramár, T., Michalec, I. and Kovačócy P. (2012), "The laser beam welding of titanium grade 2 alloy", *GRANT journal*, ISSN 1805-062X, 1805-0638 (online), ETTN 072-11-00002-09-4.

Leyens, C. and Peters, M. (2003), *Titanium and Titanium Alloys*, WILEY-VCH Verlag GmbH & Co. KGaA, Weinheim.

Lisiecki, A. (2012), "Welding of titanium alloy by different types of lasers", *Archives of Materials Science and Engineering*, 58(2), 209-218.

Lütjering, G. and Williams, J.C. (2007), *Titanium*, Springer Verlag, Germany.

Muraviev, I., Kleshnina, O. and Kuznecov, A. (2010), Vlijanie rezhimov termicheskogo cikla svarki na strukturu i svojstva metalla shva titanovyh splavov, Svarochnoe proizvodstvo, #8. s. 3-9. ISSN 0491-6441.

Nerovnyj, V. and Jampolskij, V. (2002), Svarochnye dugovye processy v vakuume, Mashinostroenie, Moskva.

Niagaj, J. (2012), "Peculiarities of a-Tig Welding of Titanium and its Alloys", *Metallurgy and materials*, 57(1), https://doi.org/10.2478/v10172-010-0001-9.

Ranatowski, E. (2008), "Weldability of Titanium and its Alloys – Progress in Joining", *Advances in Materials Science*, Vol. 8, No. 2(16).

Yassin, A. *et al*. (2012), "Welding of Titanium (Ti-6Al-4V) Alloys: A Review", *Proceedings National Graduate Conference*.

Zubarev, Ju. and Kolomenskij, B. (2010), Vlijanie rezhimov svarki na udarnuju vjazkost' svarnyh soedinenij iz titanovyh splavov, Svarochnoe proizvodstvo, #4, s. 9-11. ISSN 0491-6441.

Zubarev, Ju., Kolomenskij, B., Tkachev, A., Klopov, K. (2011), Vlijanie termicheskih ciklov svarki i otzhiga na tehnologicheskuju plastichnost' listovyh titanovyh splavov, Metallovedenie i termicheskaja obrabotka metallov, #5, s. 29-31. ISSN 0026-0819.

STRUCTURE AND PITTING CORROSION OF Ti-6Al-4V ALLOY AND Ti-6Al-4V WELDS

NIKOLAY VASILEV FERDINANDOV, DANAIL DIMITROV GOSPODINOV,
MARIANA DIMITROVA ILIEVA, ROSSEN HRISTOV RADEV

University of Ruse, 8 Studentska str., Ruse, Bulgaria, mdilieva@uni-ruse.bg

The structure of Ti-6Al-4V alloy and Ti-6Al-4V weldments was examined. The welds were produced by hollow cathode arc discharge in vacuum using tantalum cathodes and different welding parameters. The corrosion behaviour of Ti-6Al-4V alloy and Ti-6Al-4V welds in solution containing Br⁻ was evaluated quantitatively using potentiodynamic polarization tests. The corrosion behaviour of the base metal and welds was compared. Open circuit potential, pitting potential, corrosion current densities and corrosion rates were determined. The influence of the structure and its change during welding on corrosion behaviour is discussed in the present paper.

Keywords: Titanium Alloy, Pitting Corrosion, Welded Joints.

INTRODUCTION

Titanium and titanium alloys are recognized as one of materials with extremely high corrosion resistance but in some specific conditions pitting corrosion of titanium can occur (Petit *et al.*, 1980; Heakal and Awad, 2011; Huo and Meng, 1990). In most environments the welds of titanium and titanium alloys possess the same corrosion resistance as the base metal. Nevertheless, when titanium welds are exposed to marginal or active conditions they can be subjected to accelerated corrosion attacks compared to base metal (Davis, 2006).

Welding of Ti and titanium alloys changes their structure. It is well known that titanium is a highly reactive metal with a standard electrode potential of -1,63 V, and its corrosion resistance is only due to the formation of TiO_2 passive film. The integrity of this passive film is governed by its structure that depends on the underlying metal structure. For instance, coarse metal structure is a condition for formation of less dense oxide layer and thus for facilitation of corrosion processes (Song *et al.*, 2009). The passive film can be destroyed by halide ions as they cause its electrochemical dissolution and open path for aggressive environments through it towards the bare metal surface. Electrochemical dissolution of the oxide layer is not observed only in presence of F⁻. Br⁻, Cl⁻ and I⁻ lead to breakdown of the passive film and Br⁻ are the most effective in this action (Basame and White, 2000). A number of researchers have reported that Ti and its alloys undergo pitting corrosion after polarization in environments containing bromine ions (Garfias-Mesias, 1998; Basame and White, 2000; Dugdale and Cotton, 1964; Beck, 1967; Beck, 1973; Shibata and Zhu, 1995).

The aim of the present work is to examine the corrosion behaviour of Ti-6Al-4V and its welds in an aggressive medium containing bromine ions and to find out relationship between the provoked by welding structural changes and corrosion resistance of the welds.

EXPERIMENTAL PROCEDURE

The material used in this study was 2 mm thick sheet of Ti6Al4V alloy. The specimens were prepared of as-delivered Ti-6Al-4V and of Ti-6Al-4V welded by vacuum arc welding with hollow cathode without filler material and without groove.

The chemical composition of the alloy was obtained by XRF and was as follows: 4.27% V, 6.1% Al, 89.57% Ti. Table 1 shows the welding parameters. The welding was carried out in a device for vacuum arc welding (Gospodinov *et al.*, 2018). After welding, specimens were cut from weldments (Figure 1a) in order to establish their mechanical properties at tensile test.

Table 1. Welding modes

No	Specimen	Current I, A	Welding speed V, m/s	Tantalum foil cathode shape and dimensions, mm	Gas quantity Q, l/h
1	W1	100	4.2	cylindrical ⌀4	2.3-2.4
2	W2	115	4.2	cylindrical ⌀4	2.3-2.4
3	W3	130	5.5	cylindrical ⌀4	2.3-2.4
4	W4	115	5.5	elliptical 5.6 x 2	2.3-2.4
5	W5	130	6.5	elliptical 5.6 x 2	2.3-2.4

After tensile testing (results not presented here) specimens from near the fractured surfaces were cut parallel to welding direction (along the line 1 - Figure 1b) in order to examine welds microstructure and corrosion behaviour. A cross sections normal to welding direction were cut for macrostructure and microstructure examination of weldments. For macrostructural and microstructural analyses specimens were cold-mounted in epoxy resin and prepared by grinding and mechanical polishing, followed by final polishing with Al_2O_3 suspension. Then specimens were etched with a mixture of 15 ml HNO_3, 15 ml HF and 75 ml H_2O for observation of macrostructure and with a mixture of 30 ml $C_3H_6O_3$, 10 ml HF and 10 ml HNO_3 for microstructural analysis.

Figure 1: a) specimens for tensile testing; b) fractured specimen

The samples for corrosion testing were cold-mounted in epoxy resin, grinded and mechanically polished, cleaned with deionized water and acetone. The analysed surface areas varied between 0.18 cm^2 and 0.21 cm^2 as the thicknesses of different welds were different. Potentiodynamic polarisation tests were carried out at room temperature in 1 M KBr aqueous solution open to air. A standard three-electrode cell was used with a saturated calomel electrode (SCE), a Pt counter electrode and the studied sample as a working electrode. All potentials were calculated versus standard hydrogen electrode (SHE). Before polarisation, all specimens were allowed to stabilise for a period of 120 minutes. The scan rate was 1 mV/s. The polarisation potentials changed from -450 mV/SHE to +2200 mV/SHE. Potentiostat RADELKIS OH-405 was used. Using Tafel extrapolation corrosion current densities i_{cor} and corrosion potentials E_{cor} were determined. Pitting potentials E_{pit} were determined from polarisation curves as the points at which a sharp increase in anodic current density was observed. Corrosion rates CR were calculated according to ASTM G102 – 89 (2015). As the fracture of all

specimens was brittle (Figure 1b) it was assumed the tensile testing did not influence the structure and corrosion behaviour of tested specimens.

RESULTS AND DISCUSSION

Structure of Tested Specimens

Figure 2 represents a cross section of one of the Ti–6Al–4V weldments. The remaining specimens had the same macrostructure and are not shown here. The fusion zone (FZ) was composed of coarse (2÷3 mm) grains, elongated towards fusion line. The transition from FZ to heat-affected zone (HAZ) was characterised by inhomogeneous in shape and dimensions grains. Within HAZ grain size decreased towards base metal (BM). The boundary between HAZ and BM was abruptly outlined.

Figure 2. Macrosection of a weldment: 1 – Base metal (BM); 2 – Boundary "Base metal/Heat-affected zone" (BM/HAZ); 3 – Heat-affected zone (HAZ); 4 – Boundary "Heat-affected zone/Fusion zone" (HAZ/FZ); 5 – Fusion zone (FZ)

Figure 3a shows the microstructure of the base metal. The structure of as-received Ti-6Al-4V consisted of two phases: α phase appeared white and intergranular β phase - black. The α-grains were elongated along the rolling direction of the metal sheet that was normal to welding direction. The same microstructure was reported by (Romero *et al.*, 2015). At lower magnification this fine two-phase structure appeared dark – Figure 3b. Figure 3b represents the microstructure at the boundary between the BM and the HAZ. The transition from BM to HAZ showed abrupt changes in microstructural features: grain shape changed from elongated to equiaxed and grain size increased. This fact indicated occurrence of recrystallization and phase transformations in the heat-affected zone implying that the temperature at HAZ was above β transus temperature of the alloy. Within HAZ a gradual increase in grain size was observed: larger grains were formed towards FZ. Near the boundary BM/HAZ the structure of HAZ consisted of comparatively fine, equiaxed recrystallized primary α grains (white) and acicular α+ β colonies (dark). In the direction of FZ the temperature of HAZ increased gradually during welding and thus phase transformation processes coarsened the microstructure in the same manner - Figure 3c. Meanwhile, the increased temperatures in HAZ towards FZ changed the phase composition: the amount of primary α grains decreased but that of acicular α+β colonies increased and colonies of acicular α'+β were formed (Figure 3c). A similar microstructure was observed by (Akman *et al*., 2009; Romero *et al.*, 2015) and it is characteristic for quenching form temperatures below the β transus temperature.

Figure 3d represents the microstructure at the HAZ/FZ boundary and Figure 3e – at the FZ normal to welding direction. The transition from HAZ to FZ was characterised by a mixture of equiaxed and elongated colonies of acicular α'+β; this microstructure was caused by partial melting. At the FZ acicular α'+ β colonies of different shape and dimensions were observed together with allotriomorphic α at prior β-grains boundaries. This microstructure implied that the cooling rate at the fusion zone was insufficient for

quenching. The same microstructure at FZ was observed at the tested for corrosion resistance surfaces - Figure 3f, i.e. grain size and shape along the weld and normal to it were identical.
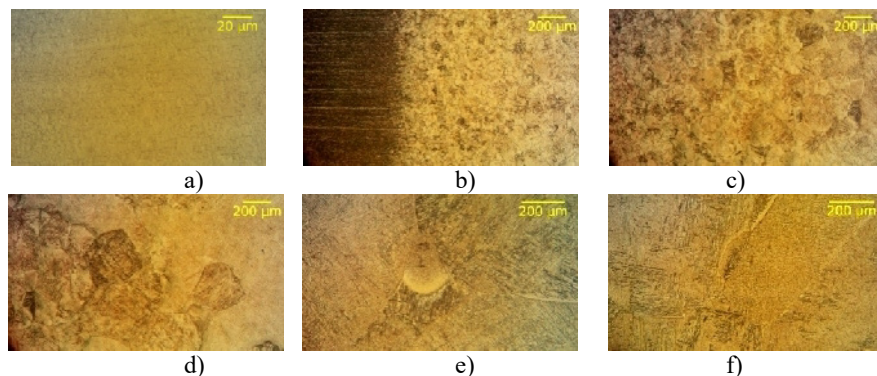
Figure 3. Microstructures of a weldment: a) as-delivered Ti-6Al-4V (position 1 in Figure 2); b) boundary BM/HAZ (position 2 in Figure 2); c) HAZ (position 3 in Figure 2); d) boundary HAZ/FZ (position 4 in Figure 2); e) FZ (position 5 in Figure 2); f) FZ along the weld

Polarisation Behaviour of Ti-6Al-4V and Welds in 1M KBr Aqueous Solution

The voltammetric behaviour of as-delivered Ti-6Al-4V and tested welds is presented in Figure 4. Before anodic polarization all specimens were held in the solution for 120 min. in order to stabilise to OCP. Table 2 summarises the OCPs and the corrosion parameters obtained from polarization curves. OCPs of the welds were lower than that of the BM and this suggested the welds were more prone to corrosion than the BM.

Potentiodynamic polarization curves of Ti-6Al-4V and all welds were similar in shape. The similarity between curves at their cathodic parts indicated that the cathodic reactions on all tested surfaces were alike. As the used medium was neutral, the cathodic reaction was oxygen reduction leading to OH^- formation.

A cathodic current can result in a reduction of the protective oxide layer, thus activating the metal surface (Riskin, 2008). As the corrosion stability of titanium and its alloys is totally dictated by the protective properties of the passive layer, highly reducing potentials can have deteriorating influence on layer's integrity and corrosion resistance. This phenomenon was observed in our experiments and was demonstrated by the differences in OCPs and E_{cor} (Table 2); similar results were reported by (Heakal and Awad, 2011). Moreover, the deteriorating influence of initial cathodic potential in combination with that of Br^- on protective properties of the passive layer led to absence of passive regions at the anodic parts of polarization curves; at anodic parts of all polarization curves, at potentials below 700-800 mV, slow anodic dissolution was observed. The measured anodic current densities of welds were higher than that of the BM and this fact indicated that less stable passive film was formed on welds' surfaces.
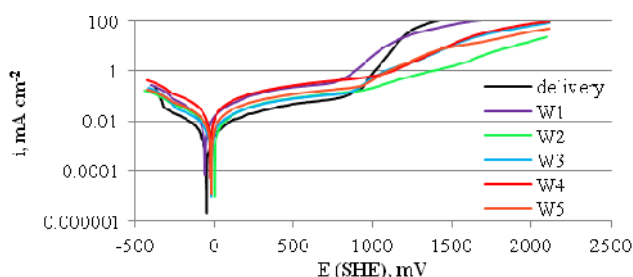
Figure 4. Potentiodynamic polarization curves of Ti-6Al-4V and welds in 1M KBr

Table 2. Electrochemical corrosion parameters of Ti-6Al-4V and weldments

Specimen	OCP, mV	E_{cor}, mV	E_{pit}, mV	i_{cor}, µA cm^{-2}	CR, mm/y
As-deliverd	115	-44	800	3.6	0.031
W1	25	-58	730	12.6	0.110
W2	75	3	900	9.6	0.083
W3	65	-19	800	4.5	0.039
W4	55	-22	930	23.4	0.203
W5	55	-18	900	9.8	0.085

As the potential increased in positive direction, current densities increased sharply at E_{pit}. Deep wide pits were observed on tested surfaces after polarization - Figure 5. During polarization above E_{pit} a yellow-orange solution was observed directly above the tested surfaces. That colour is characteristic for $TiBr_4$ and $TiOBr_2$. After polarization white precipitates, consistent with TiO_2 and TiO^{2+}, were observed in solution. A similarly coloured solutions and precipitates were observed by (Beck, 1973). These corrosion products and the pitted surfaces of specimens clearly indicated that the sharp rise in current densities was due to pitting corrosion and not only to oxygen evolution. They also indicated that the pitting corrosion mechanism of Ti-6Al-4V and its welds was the proposed by Beck model (Beck, 1973) of salt film formation and its hydrolysis near the metal surface.

Figure 5. Tested in 1M KBr surface of specimen W2 after polarization

The lowest i_{cor} and CR were calculated for as-delivered Ti-6Al-4V (Table 2). This information combined with the highest OCP and lowest anodic current densities bellow E_{pit} of BM led to conclusion that the welds were with lower corrosion resistance than the BM. The worsen corrosion behaviour of welds was attributed to their coarsened and transformed structure. The oxide film on self-passivating metals generates at grain boundaries. The BM was with finer structure than welded metal thus allowing a denser passive layer to be formed on its surface and to be kept relatively stable.

CONCLUSIONS

The presented experimental results allow the following conclusions to be made:

1) Vacuum arc welding with hollow cathode without filler material and without groove leads to formation of classical welded structures of Ti-6Al-4V.

2) The coarsened structure at the fusion zone of Ti-6Al-4V welds after vacuum arc welding with hollow cathode without filler material and without groove can increase the corrosion rate up to one order.

3) Titanium alloy Ti-6Al-4V and its welds undergo severe pitting corrosion in 1M KBr aqueous solution. The pitting corrosion mechanism is that, described by Beck.

REFERENCES

Akman, E. *et al*. (2009), "Laser welding of Ti6Al4V titanium alloys", *Journal of Materials Processing Technology*, 209(8), 3705-3713, https://doi.org/10.1016/j.jmatprotec.2008.08.026.

Basame, S.B. and White, H.S. (2000), "Pitting Corrosion of Titanium - The Relationship Between Pitting Potential and Competitive Anion Adsorption at the Oxide Film/Electrolyte Interface", *Journal of The Electrochemical Society*, 147(4), 1376-1381, https://doi.org/10.1149/1.1393364.

Beck, T.R. (1967), "Stress corrosion cracking of titanium Alloys: I . Ti:8-1-1 alloy in aqueous solutions", *J. Electrochem. Soc.*, 114(6), 551-556, https://doi.org/10.1149/1.2426647.

Beck, T.R. (1973), "Pitting of Titanium: I. Titanium-Foil Experiments", *J. Electrochem. Soc.*, 120(10), 1310-1316, https://doi.org/10.1149/1.2403253.

Beck, T.R. (1973), "Pitting of Titanium: II. One-Dimensional Pit Experiments", *J. Electrochem. Soc.*, 120(10), 1317-1324, https://doi.org/10.1149/1.2403254.

Davis, J.R. (2006), *Corrosion of Weldments*, ASM International.

Dugdale, I. and Cotton, J.B. (1964), "The anodic polarization of titanium in halide solutions", *Corrosion Science*, 4 (1–4), 397-411, https://doi.org/10.1016/0010-938X(64)90041-1.

Garfias-Mesias, L. *et al*. (1998), "Determination of precursor sites for pitting corrosion of polycrystalline titanium by using different techniques", *J. Electrochem. Soc.*, 145(6), 2005-2010, https://doi.org/10.1149/1.1838590.

Gospodinov, D.D. *et al*. (2018), "Welding of Grade 1 titanium by hollow arc discharge in vacuum", *International Scientific Conference Industry 4.0*, Varna, Bulgaria, 39-41.

Heakal, F. and Awad, Kh.A. (2011), "Electrochemical Corrosion and Passivation Behavior of Titanium and Its Ti-6Al-4V Alloy in Low and Highly Concentrated HBr Solutions", *Int. J. Electrochem. Sci.*, 6, 6483 – 6502.

Huo, Sh. and Meng, X. (1990), "The states of bromide on titanium surface prior to pit initiation", *Corrosion Science*, 31, 281-286, https://doi.org/10.1016/0010-938X(90)90120-T.

Petit, J.A., Kondro, B. and Dabosi, F. (1980), "Ion Beam Analysis Investigation of Pit Nucleation on Titanium in Bromide Media", *Corrosion*, 36(3), 145-151, https://doi.org/10.5006/0010-9312-36.3.145.

Riskin, J. (2008), *Electrocorrosion and protection of metals*, Elsevier, Oxford.

Romero, A. *et al*. (2015), "Ti6Al4V titanium alloy welded using concentrated solar energy", *Journal of Materials Processing Technology*, 223, 284-291, https://doi.org/10.1016/j.jmatprotec.2015.04.015.

Shibata T. and Zhu, Y.-C. (1995), "The effect of film formation conditions on the structure and composition of anodic oxide films on titanium", *Corrosion Science*, 37(2), 253-270, https://doi.org/10.1016/0010-938X(94)00133-Q.

Song, D. *et al*. (2009), "Corrosion behavior of ultra-fine grained industrial pure Al fabricated by ECAP", *Transactions of Nonferrous Metals Society of China*, 19(5), 1065-1070, https://doi.org/10.1016/S1003-6326(08)60407-0.

POLYMERIC COMPOSITES BASED ON RIGID PVC AND ZINC OXIDE NANOPARTICLES

MIHAI GEORGESCU, LAURENŢIA ALEXANDRESCU, MARIA SÖNMEZ,
MIHAELA NIŢUICĂ, DANIELA STELESCU, DANA GURĂU

National Research and Development Institute for Textile and Leather, Division Leather and Footwear Research Institute, 93, Ion Minulescu St., 031215, Bucharest, Romania

The paper presents the processing and characterization of polymeric nanocomposites based on polyvinyl chloride plasticized with only 20% diisononyl phthalate for rigid and medical applications. In order to obtain materials with antibacterial and antifungal properties, functionalized zinc oxide nanoparticles were used. The functionalization was achieved with polydimethylsiloxane by ultrasonographic method in a control temperature environment. The influence of 1, 3, and 7 percent of functionalized zinc oxide nanoparticles were tested on the physical-mechanical properties, and the structure. The polymeric composites were processed on a Plasti-Corder Brabender 350 E mixer at 165-180°C and 150-180 revolutions per minute. The results show that adding zinc oxide nanoparticles into the composition led to an improvement in tear resistance, and tensile strength. Abrasion resistance present extremely good values. The FTIR spectra of the samples indicate that the new composites have a stable structure, due to a very good compatibility / interaction with the polymer matrix, the plasticizer does not tend to migrate to the surface.

Keywords: polyvinyl chloride, plasticizer, zinc oxide nanoparticles.

INTRODUCTION

The development of polymeric nanocomposites, structures with geometric dimensions below 100 nm, has a great influence on materials science due to their special properties (e.g. excellent mechanical properties, antimicrobial resistance, high temperature resistance and aggressive work environments). Therefore, new materials can be found in a wide variety of different applications, such as biomedical applications, consumer goods, health, medical or food technology, automobiles and transport (Vindizheva *et al*., 2011; Vindizheva *et al*., 2012).

Being one of the largest polymers, polyvinyl chloride (PVC) is widely used and essential in almost all fields. The optimal ratio of properties and costs makes PVC a material capable of competing with both natural materials and other polymers in many areas of science and engineering. The range of traditional materials for PVC compositions is wide. Polyvinyl polyvinyl chloride (PVC) is one of the most commonly used types of polymers (40% of dedicated polymeric materials) for biomedical and food applications. Medical grade and food grade PVC has been selected as a representative polymer for the matrix of antimicrobial composite systems.

There are different types of nanoparticles which can be incorporated in the polymeric matrix, selected according to their properties and their application. ZnO found various applications in plastic industry, medical packaging, cosmetics, medical devices (Saehana *et al*., 2013), dentistry, and orthopedics, antibacterial coating (Arenas *et al*., 2013), the textile industry (Bazant *et al*., 2014; Alexandrescu *et al*., 2017), etc. Antibacterial activity has been proven on various bacterial strains (Stegarus and Lengyel, 2017).

The paper present the obtaining process and characterization of polymeric composites based on rigid PVC. In order to obtain composites with antibacterial and antifungal properties, zinc oxide nanoparticles (ZnO) (Bazant *et al*., 2014; Alexandrescu

et al., 2017) were used. To improve dispersion in the polymeric matrix of ZnO nanoparticles, they were functionalized (Mallakpour and Darvishzadeh, 2018a; Chung *et al*., 2016; Mallakpour and Darvishzadeh, 2018b).

EXPERIMENTAL

Materials

Materials used to obtain the polymer composites based on plasticized polyvinyl chloride and ZnO nanoparticles are as follows: (1) PVC with a 70K-wert value, (2) Diisononyl phthalate (DINP) (density 0.98 g/cm^3, boiling point 244 to 252°C, 99.5% purity, Mw= 418.618 g/mol), plasticizer, mainly used by the pharmaceutical, food and cosmetics industries, (3) PVC stabilizer - Calcium stearate (Ca content 11%,melting point 127°C), (4) Antioxidant Irganox 1010 (pentaerythritol tetrakis (3-(3,5 di-tert-butyl-4-hydroxyphenyl)propionate) from BASF Schweiz AG (active ingredient 98%, melting point of 40°C). (5) Functionalizing agent – polydimethylsiloxane –PDMS. (6) ZnO nanoparticles, white powder, with particle size of 21 nm from Sigma-Aldrich.

Method

The polymeric nanocomposites based on PVC matrix with ZnO functionalized nanoparticles was obtaining in several stages, as follow: functioning of nanoparticles, PVC plasticizing, obtaining, and test polymeric composites.

The functionalization stage of nanoparticles was achieved in an ultrasonic bath at 40°C with the functionalizing agent - polydimethylsiloxane (PDMS) added in drops over ZnO nanoparticles.

PVC plasticizing was achieved by absorption of plasticizer (DINP) into PVC by mixing them in a Plasticorder PLV 330 Brabender at 70 rpm, temperature 40°C for 10min. For a good thermal stability, temperature stabilizer and antioxidants were added.

Obtaining the polymer composites based on rigid PVC and functionalized ZnO nanoparticles on a Plasti-Corder Brabender Mixer 350 E, having the following features: 3 heating/cooling zones, range temperature 0-300°C, capacity 350 cm^3, mixing speed 300 RPM max. Table 1 presents the formulations of rigid PVC/ZnO composites. *Processing technology*: the temperature is set to 178°C, PVC containing stabilizer and antioxidant is added; after soaking and plasticizing (3 min.) the functionalized nanoparticles are added for 2 minutes. Continue mixing at a 150-180 revolutions per minute and temperature of 165°C for 3 minutes until the ingredients are embedded, and the mixture is homogeneous.

Table 1. Formulations of the polymer composites

Ingredients	Samples Codes			
	B1	B11	B12	B13
PVC – K 70 (g)	240	240	240	240
ZnO/PDMS (g)	-	2,4	7,2	12
Diisononyl phthalate (g)	60	60	60	60
Calcium stearate (g)	3	3	3	3
Irganox 1010 (g)	3	3	3	3

The specimen for physico-mechanical and structural characterization were obtained in an electrical laboratory press, by means of compression method, at a temperature of 175°C, preheating for 2 min, 5 min forming, and 5 min cooling both with a pressing force of 300 kN. Specimens of l50mm x l50mm x 2mm and 70mm x 70mm x 6mm, in a shape of a dumbbell, were obtained. Conditioned for 24 hours at room temperature, before being used for testing.
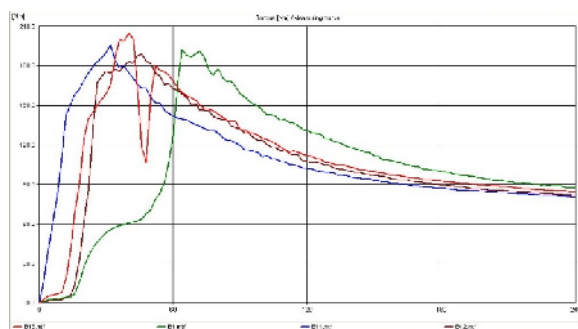
Figure 1. The overlapping Brabender mixing charts of control sample B1 and polymer composites based on 20% plasticized PVC with diisononylphthalate –DINP, and 1, 3, and 7% ZnO nanoparticles

The Brabender mixing charts (Figure 1) show that for samples with 20% diisononylphthalate plasticized PVC matrix, and embedding of 1, 3, and 7% ZnO nanoparticles, the maximum momentum times occurs at the same times, less than a minute, for the sample B11-B13. The forces increase to 200N/mm, as well as the temperatures, 265°C at the maximum torque and 165°C at the end of the process. This is due to the fact that the plasticizer used (diisononylphthalate) is more viscous, which implies higher forces, mixing times and temperatures.

Specimen Characterization

Physical-Mechanical Characteristics. Tensile strength and tearing strength tests were carried out with a Schopper strength tester with testing speed 460 mm/min, using dumb-bell shaped specimens according to ISO 37/2012, and angular test pieces (Type II) according to EN 12771/2003, respectively. Hardness was measured by using a hardness tester according to ISO 7619-1/2011 using 6-mm thick samples. Elasticity (rebound resilience) was evaluated with a Schob test machine using 6-mm thick samples, according to ISO 4662/2009.

The densities of elastomer samples were measured according to ISO 2781/2010.

Abrasion resistance was carried out according to ISO 4649/2010, the cylinder method, using a pressure of 10N. Abrasion resistance was expressed by relative volume loss in relation to calibrated abrasive paper. A wearing tester with abrasive cloth having granulation of 212–80 mm (PE 80). The samples used were obtained from rolled blends and pressed into sheets, then cutting with a rotating die and have cylindrical shape, with a diameter of 16mm and height of min. 6 mm.

Melt flow index was determinate at 180°C and a pressure force of 5 kg, with Melt Flow Index – Haake equipment.

Fourier transformed infrared spectroscopy (FT-IR). The structural determinations were carried out on an IR molecular absorption spectrometer with double beam, in the range of 4000-530 cm^{-1}, using a 4200 FT-IR equipped with ATR crystal diamond and sapphire head.

RESULTS AND DISCUSSIONS

Physico-Mechanical and Rheological Characteristics

Table 2 shows the physico-mechanical and rheological characteristics of the polymeric composites obtained. The analysis of the results shows the following:
- The *hardness* of the control sample is 61°Sh A, and increases, with 2 units, up to 63°Sh A with the addition of nanoparticles, due to the nanofiller reinforcement effect;
- Constant elasticity, rigid values, are observed for this degree of plasticization, (20%) a performant feature of these materials;
- *The tensile strength* has a high value of 23 N/mm^2 and increases with the amount of nanofiller added into the compound;
- *Tear resistance* shows high values from160 up to 177 N/mm, which present a rigid and performant material;
- *The elongation at break* shows small values, increasing from 240% up to 260% when adding 7% ZnO, this property increase proportionally to the amount of nanoparticles introduced into the composite. The values are small to the fact that this is a rigid PVC having only 20% plasticizer
- *Density* is 1.3 g/cm^3
- *Abrasion resistance* are extremely good, under 100 mm^3, due to the small of amount of plasticizer and the effect of the nanoparticles, which made it more durable.

Table 2. Physical and mechanical characteristics for polymeric composites

Physico-mechanical tests	Samples Codes			
	B1	B11	B12	B13
Hardness, °Sh A	61	62	62	63
Elasticity, %	16	16	16	16
Tensile strength, N /mm^2	23,0	23,1	24,3	25,0
Elongation at break, %	260	240	260	260
Tear resistance, N /mm	160	167	172	177
Density, g/cm^3	1,3	1,3	1,3	1,3
Abrasion resistance, mm^3	97	97	102	108

Fourier Transform Infrared Spectroscopy (FT-IR)

The FTIR spectrum recorded on the simple PVC powder (Figure 2) shows numerous characteristic bands associated with this type of polymer.

Figure 3 show FTIR spectra of polymeric composites based on PVC plasticized with DINP containing ZnO nanoparticles functionalized with PDMS. Taking as a comparison the spectrum recorded on the simple PVC powder, it can be observed, for all spectra, the presence of functional groups derived from the plasticizer structure, namely the band characteristic of the carbonyl group (from about 1720 to 1121 cm^{-1} in the case of the mixture - B1) and those of 1724 and 1126 cm^{-1} for blends containing

ZnO / PDMS nanoparticles. The presence of carbonyl functional groups shows clearly that PVC plastification has been optimally achieved.
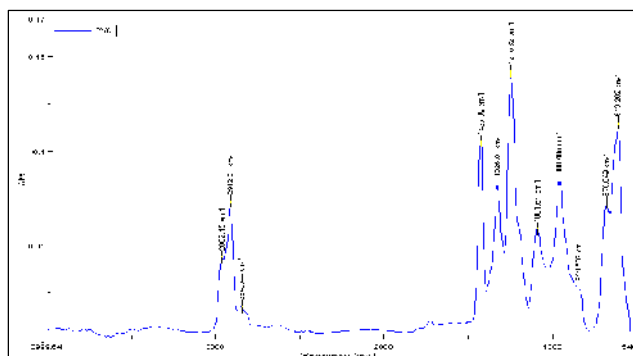
Figure 2. FTIR spectrum of PVC powder
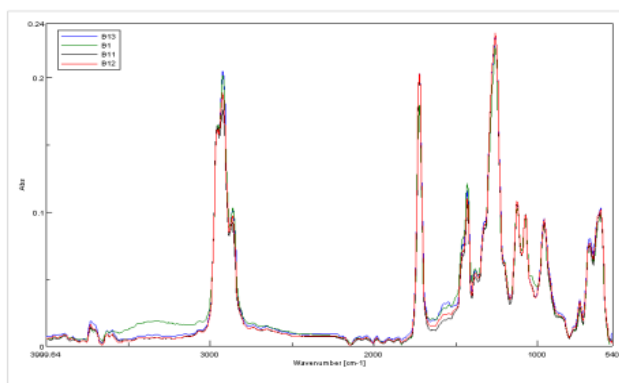
Figure 3. FTIR spectra of composites based on plasticized PVC and ZnO nanoparticles:
B1 - green, B11 - black, B12 - red, B13 - blue

There is a significant increase in the intensity of carbonyl groups at approximately 1724 cm^{-1} (Figure 3), which can be attributed to the fact that the plasticizer remains stable in the PVC structure (does not tend to migrate to the surface) due to a very good compatibility / interaction with the polymer matrix.

CONCLUSIONS

New types of polymeric composites based on polyvinyl chloride plasticized with 20% diisononyl phthalate containing zinc oxide nanoparticles were obtained. The functionalization of ZnO nanoparticles with polydimethylsiloxane was achieved by ultrasonic and constant temperature method. The PVC/ZnO nanocomposites were obtained on a Plasti-Corder Brabender Mixer 350 E at 178°C, 150-180 revolutions per minute and 165°C for 3 minutes, and a total processing time of 10 minutes. The temperatures at maximum momentum did exceed the scheduled temperature of 178°C

going up to 260°C due to the fact that amount of plasticizer was only 20%. With the increase of the functionalized zinc oxide quantity, there was an increase in hardness, tear strength, and tear resistance, but low values for elongation at break. This properties were obtained due to the synergy of the functionalized ZnO nanoparticles and low plasticizer amount in the PVC matrix. The plasticizer does not tend to migrate to the surface, thus they can be easily processed by the injection method. New polymeric composites can be used in biomedical and food applications such as: blood bags and tubes, intravenous components, and containers, dialysis equipment, inhalation masks, examination gloves, packaging, footwear, etc.

REFERENCES

Alexandrescu, L. *et al*. (2017), "Polymer nanocomposites PE/PE-g-MA/EPDM/nanoZnO and TiO2 dynamically crosslinked with sulfur and accelerators", *Proceeding 2nd International Conference on Structural Integrity*, https://doi.org/10.1016/j.prostr.2017.07.040.

Bazant, P. *et al*. (2014), "Microwawe-Assisted synthesis of Ag/ZnO Hybrid Filler, Preparation, and Characterization of Antibacterial Poly(vinyl chloride) Composires Made from the Same", *Polymer Composites*, 35, 19-26, https://doi.org/10.1002/pc.22629.

Chung, Y.T. *et al*. (2016), "Functionalization of zinc oxide (ZnO) nanoparticles and its effects on polysulfone-ZnO membranes, *Desalination and Water Treatment*, 57, 17, 7801-7811, https://doi.org/10.1080/19443994.2015.1067168.

Mallakpour, S. and Darvishzadeh, M. (2018a), "Nanocomposite materials based on poly(vinyl chloride) and bovine serum albumin modified ZnO through ultrasonic irradiation as a green technique: Optical, thermal, mechanical and morphological properties", *Ultrasonics Sonochemistry*, 41(85-99), https://doi.org/10.1016/j.ultsonch.2017.09.022.

Mallakpour, S. and Darvishzadeh, M. (2018b), "Ultrasonic treatment as recent and environmentally friendly route for the synthesis and characterization of polymer nanocomposite having PVA and biosafe BSA modified ZnO nanoparticles", *Polymers for Advanced Technologies*, 29(8), 2174-2183, https://doi.org/10.1002/pat.4325.

Stegarus, D.I and Lengyel, E. (2017), "The antimicrobial effect of essential oil upon certain nosocomial bacteria", *International Multidisciplinary Scientific GeoConference Surveying Geology and Mining Ecology Management, SGEM,* 17(61), 1089-1096, http://doi: 10.5593/sgem2017/61/S25.142.

Vindizheva, S. *et al*. (2012), *Naukoemk. Tekhnol.*, No. 1, 27.

Vindizheva, S. *et al*. (2011), *Plast. Massy*, No. 10, 34.

APPLICATION OF THIOL AMINO ACIDS IN A REDUCTIVE LIMING PROCESS

ENNO KLÜVER, MICHAEL MEYER

FILK gGmbH, Meissner Ring 1-5, D-09599 Freiberg, enno.kluever@filkfreiberg.de,
michael.meyer@filkfreiberg.de

Thiol containing amino acids cysteine and homocysteine were used as dehairing agents in an alkaline reductive liming process. It is shown that complete dehairing is achieved with amounts of 8 % w/w of the thiol amino acids, rendering them as effective as sodium sulfide on a molar basis. Cysteine and homocysteine can be used to establish a completely sulfide free liming process without fundamental changes of the remaining process parameters. Furthermore a method is presented for the preparation of homocysteine from lower-cost methionine. This method comprises a two step process including the demethylation of methionine in sulfuric acid, resulting in the formation of dimeric homocystine, and the subsequent reduction of homocystine to homocysteine with tin in acidic solution. Identity and purity of the reaction products were proved by HPLC analysis. The effectivity of freshly prepared homocysteine as a dehairing agent is comparable with commercial homocysteine thiolactone.

Keywords: Liming process, thiol, dehairing

INTRODUCTION

Traditional reductive liming processes employ sodium sulfide in alkaline medium. Sodium sulfide is an effective and low-cost dehairing agent. On the other hand, sodium sulfide is a highly toxic compound, requiring safety precautions and extensive waste water treatment. The formation of lethal hydrogen sulfide from sodium sulfide in tanneries is still not completely prevented. Thus the substitution of sodium sulfide by a non-hazardous alternative is a long held concern. Many variants have been investigated and reported in the literature in the last decades, including reductive liming with dimethylamine (Somerville *et al.*,1963), oxidative liming with hydrogen peroxide or other peroxo-compounds (Bronco *et al.*, 2005; Gehring *et al.*, 2003; Marmer *et al.*, 2003; Marmer and Dudley, 2005), oxidative liming with sodium chlorite (Covington, 2009), and enzymatic liming (Dettmer *et al.*, 2013; Paul *et al.*, 2001; Kanagaraj, 2009), Sivasubramanian *et al.*, 2008). None of these technologies became established except for niche applications. This is due to a multitude of disadvantages, including toxicity, high costs, corrosive reaction conditions, incomplete dehairing or insufficient grain quality.

The approach of the present work is the use of thiol containing amino acids as dehairing agent in a reductive liming process. Cysteine and homocysteine, which are the most prominent representatives of this chemical family, show no toxic properties. As thiol compounds they are able to act as reducing agents, resulting in the formation of dimers (cystine, homocystine). The redox potential of the cysteine/cystine pair ($E^0 = 0.40$ V) is in a similar range with sodium sulfide ($E^0 = 0.48$ V) (Covington, 2009). Homocysteine with a side chain, extended by one methylene group in regard to cysteine, is stable only as the thiolactone form (see Figure 1). The commercial price of the thiolactone is approximately 25 times the price of sodium sulfide, making it an unpromising competitor. The amino acid methionine is the methylated form of homocysteine and costs only twice as much as sodium sulfide. Thus the second approach in this work is the development of a method for the transformation of

methionine into homocysteine. A variety of chemical conversion reactions is reported in the system methionine-homocysteine-homocystine (Butz and du Vigneaud, 1932; Lavine and Floyd, 1954; Baernstein, 1932; Wagner, 1957; Nekrassova *et al.,* 2003). Many of them require expensive reagents or hazardous reaction conditions or are developed for analytical purposes on a small scale. With regard to a possible application on industrial scale we focused on a two step process, in which methionine is transformed into homocystine, which subsequently is reduced to homocysteine thiolactone. The reaction principles were taken from the literature (Butz and du Vigneaud, 1932; Lavine and Floyd, 1954; Schöberl and Wagner, 1958; Skakun-Todorović and Albahari, 1979) and adapted with regard to a potential future upscaling.

The present work demonstrates the suitability of cysteine and homocysteine as reductive dehairing agents in a liming process and presents a laboratory method for the production of homocysteine thiolactone from methionine.
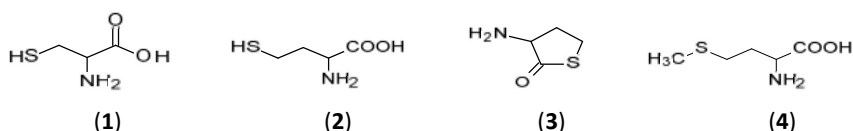
Figure 1. Structural formulae of (**1**) cysteine, (**2**) homocysteine, (**3**) homocysteine thiolactone, (**4**) methionine

MATERIALS AND METHODS

Materials

For liming experiments, L-cysteine (98 %) was purchased from abcr, DL-homocysteine thiolactone hydrochloride (99 %) was from Alfa Aesar. For the two step conversion process, DL-methionine (99 %) was purchased from abcr, tin powder (100 mesh, 99.5 %) was from Alfa Aesar. For analytical purposes in HPLC, DL-homocysteine (95 %, Sigma), DL-methionine (99 %, abcr), DL-homocystine (≥98 %, Sigma), DL-homocysteine thiolactone hydrochloride (99 %, Alfa Aesar) and DL-methionine methylsulfonium chloride (99 %, Sigma) were used as standards.

Liming and Tanning

Liming experiments with cysteine and homocysteine thiolactone were performed on a laboratory scale each with ca. 200 g bovine hide. Commercial cysteine and homocysteine thiolactone as well as homocysteine thiolactone solution, prepared from methionine, were used as reductive agents. The process steps were: washing (200 % water); liming (100 % water, cysteine or homocysteine, lime) at pH 12.5 over night with perpetual motion and occasional pH control; reliming (100 % water, 1.5 % lime) over night; washing (200 % water). Experiments were repeated with sodium hydroxide instead of lime at pH 13.5 under otherwise identical conditions. The amount of amino acid in the liming step varied and was 6, 8, and 10 %, regarding the hide weight.

The resulting pelts were delimed and pickled and subsequently tanned in a standard chrome tanning process using 8 % chromium sulfate at pH 2.7 for 16 h. The resulting wet blues were neutralized, washed and air dried.

Conversion of Methionine to Homocystine

Methionine (120 g) was boiled under reflux at 135 °C in 800 ml of sulfuric acid (64 %) for 3 h. After cooling down the solution was poured on 2400 g ice. Ammonia (13.5 %, ca. 2000 ml) was added until pH of 7.5 was reached. The precipitate was filtered, washed with water and dried. The reaction yielded 44 g homocystine.

Conversion of Homocystine to Homocysteine Thiolactone

Homocystine (44 g) was suspended in 100 ml water and dissolved by addition of 100 ml concentrated hydrochloric acid. 26 g tin powder were added, and the mixture was heated on a water quench (60 °C, 5 h). After cooling down the mixture was diluted with water and then ammonia was added until pH of 7.5 was reached. The precipitate (tin hydroxide) was filtered. 900 ml of the filtrate were concentrated in a rotary evaporator to 100 ml. This solution, containing 8 g homocysteine, was used in a liming experiment on 100 g bovine hide under conditions described above.

Identity and purity of homocystine and homocysteine thiolactone were verified by HPLC using an amino acid analyzer "Biochrom 30 plus" (Onken, Gründau, Germany), where the amino acids were separated chromatographically, derivatized with ninhydrin, and adsorption measured at wave length 570 nm. Homocysteine, methionine, homocystine, homocysteine thiolactone, and methyl methionine were used as standards.

RESULTS AND DISCUSSION

Liming with Cysteine and Homocysteine

Liming of bovine hides with cysteine or homocysteine under alkaline conditions yielded good results with all tested amino acid concentrations. While with 6 % amino acid some residual hair was visible in particular samples, dehairing was complete for the higher amounts (8 and 10 % amino acid). Figure 2 shows exemplarily pelts and wet blues, obtained by liming at pH 12.5 with 8 % cysteine and homocysteine, respectively (upper row). Pelts, which were treated in a sodium hydroxide liming process at pH 13.5, were likewise dehaired, but severely swollen (Figure 2, lower row).

The amount of amino acid needed for complete dehairing was higher than the usual amount of sodium sulfide, if calculated on a weight basis in regard to the hide weight (2.5 % sodium sulfate vs. 8 % amino acid). This was expected, since molar mass and reaction mechanism of these two different reagents differ. The dehairing effect is mainly based on the reductive opening of stabilizing disulfide bonds in the hair keratin. This is achieved by the action of one mole sulfide per mole disulfide bond, while in the case of amino acids two moles are needed. Taking into account the different molar masses of sodium sulfide (78.05 g/mol) and cysteine (121.16 g/mol) or homocysteine (135.18 g/mol), it can be deduced, that 8 % w/w of amino acid correspond to 2.3 - 2.6 % w/w of sodium sulfide on a molar basis. Thus the effectivity of cysteine and homocysteine as dehairing agents is considered comparable to that of sodium sulfide.

In contrast to sodium sulfide, liming with cysteine or homocysteine is a hair saving process.
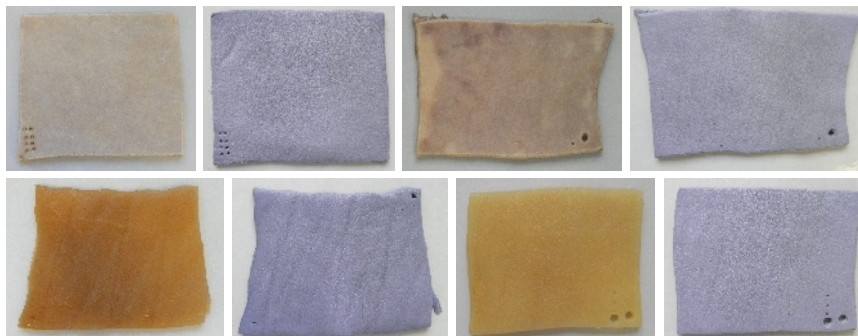
Figure 2. Pelts and wet blues from bovine hides after liming at pH 12.5 (upper row) and pH 13.5 (lower row) with 8 % cysteine (left) or 8 % homocysteine thiolactone (right)

Preparation of Homocysteine from Methionine

Based on literature data a two step process was chosen to convert methionine into homocysteine. This method uses common chemicals, like sulfuric acid, ammonia, hydrochloric acid and tin, which will be advantageous for future upscaling in terms of costs and availability. Figure 3 shows the chemical reactions proceeding in the two process steps.
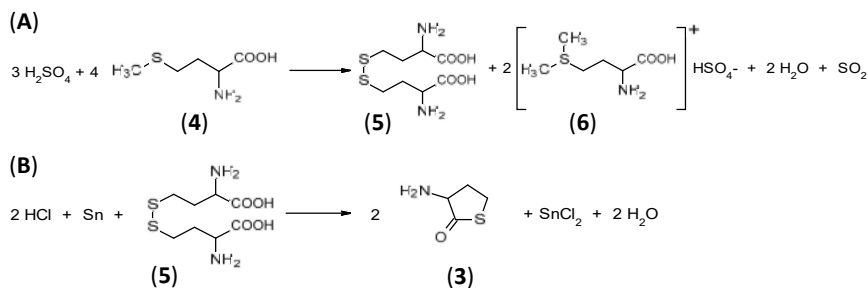
Figure 3. Reaction scheme for (A) the conversion of methionine (**4**) into homocystine (**5**) with methyl methionine (**6**) and sulfur dioxide as byproducts, and (B) the reduction of homocystine (**5**) to homocysteine thiolactone (**3**)

In the first step (A) methionine was demethylated in sulfuric acid, resulting in the formation of the dimer homocystine. Sulfur dioxide and the sulfonium salt of methyl methionine were detected as byproducts. After neutralization homocystine precipitated and was obtained in pure form by filtration and drying. In the second step (B) homocystine was reduced to homocysteine thiolactone by tin powder in acidic solution. In the original literature excess tin is precipitated with hydrogen sulfide (Schöberl and Wagner, 1958; Skakun-Todorović 1979). Since the aim in this study was the application of homocysteine in a sulfide free liming process, the use of hydrogen sulfide was

avoided. Ammonia was used instead in order to neutralize the solution and precipitate tin hydroxide, which was then filtrated. The remaining solution contained pure homocysteine. It was concentrated by means of a rotary evaporator until a volume was reached which complied with the conditions of the liming experiment. The neutralized and concentrated homocysteine solution was directly added in the liming step. The results were consistent with the results, presented above with commercial homocysteine thiolactone.

Purity and identity of the reaction products after the two process steps were confirmed by HPLC analysis, using commercial compounds as internal standards. Figure 4 shows the HPLC profiles of the precipitate after step (A), and the neutralized solution after step (B).
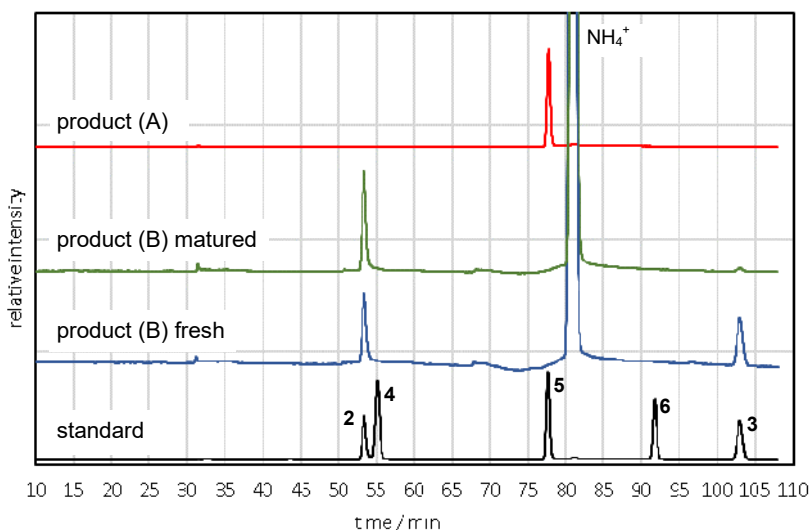
Figure 4. HPLC chromatograms of reaction products after step (A) and step (B); product after step (B) was measured freshly prepared ("fresh") and after 3 months storage ("matured"); the standard contains homocysteine (2), homocysteine thiolactone (3), methionine (4), homocystine (5), and methyl methionine (6)

The products of the two reaction steps proved to be pure homocystine (product (A)) and homocysteine (product (B)), respectively. The freshly prepared homocysteine solution contained homocysteine besides a considerable amount of homocysteine thiolactone. When the HPLC analysis was repeated after 3 months of storage, the thiolactone nearly completely disappeared and converted into the open-chain form.

CONCLUSION

Cysteine and homocysteine were successfully used as dehairing agents in a reductive liming process. The process parameters are identical to the parameters of conventional sulfide based liming processes. Thus it is possible to establish a completely sulfide free liming technology by replacing sodium sulfide with cysteine or

homocysteine while retaining all remaining process parameters. This is an important step towards sustainable sulfide free liming and a promising alternative to the recent developments in enzymatic unhairing.

Since commercially available homocysteine is a relatively expensive reagent compared with cysteine, a method was established for the preparation of homocysteine from the lower-cost methionine. The proposed two step process uses common and nonhazardous chemicals, which favors future upscaling and implementation in established process chains. On a laboratory scale the method converted methionine into homocysteine with a 36 % yield.

REFERENCES

Baernstein, H.D. (1932), "The determination of methionine in proteins", *J. Biol. Chem.*, 97, 663-668.

Bronco, S. *et al.* (2005), "Oxidative unhairing with hydrogen peroxide: development of an industrial scale process for high-quality upper leather", *J. Am. Leather Chem. Assoc.*, 100(2), 45-53.

Butz, L.W. and du Vigneaud, V. (1932), "The formation of a homologue of cystine by the decomposition of methionine with sulfuric acid", *J. Biol. Chem.*, 99, 135-142.

Covington, A.D. (2009), *Tanning Chemistry: The Science of Leather*, RSC Publishing, Cambridge.

Dettmer, A. *et al*. (2013), "Environmentally friendly hide unhairing: enzymatic hide processing for the replacement of sodium sulfide and deliming", *J. Cleaner Prod.*, 47, 11-18, https://doi.org/10.1016/j.jclepro.2012.04.024.

Gehring, A.G. *et al*. (2003), "Rapid oxidative unhairing with alkaline calcium peroxide", *J. Am. Leather Chem. Assoc.*, 98(6), 216-223.

Kanagaraj, J. (2009), "Cleaner leather processing by using enzymes: a review", *Adv. Biotech.*, 4, 13-18.

Lavine, T.F. and Floyd, N.F. (1954), "The decomposition of methionine in sulfuric acid", *J. Biol. Chem.*, 207, 97-106.

Marmer, W.N. *et al.* (2003), "Rapid oxidative unhairing with alkaline hydrogen peroxide", *J. Am. Leather Chem. Assoc.*, 98(9), 351-358.

Marmer, W.N. and Dudley, R.L. (2005), "Oxidative dehairing by sodium percarbonate", *J. Am. Leather Chem. Assoc.*, 100(11), 427-431.

Nekrassova, O. *et al.* (2003), "Analytical determination of homocysteine: a review", *Talanta*, 60(6), 1085-1095, https://doi.org/10.1016/S0039-9140(03)00173-5.

Paul, R.G. *et al.* (2001), "The use of neutral protease in enzymatic unhairing", *J. Am. Leather Chem. Assoc.*, 96, 180-185.

Schöberl, A. and Wagner, A. (1958), "Schwefelhaltige Aminosäuren", in Müller, E. *et al.* (ed.), "Houben-Weyl Methods of Organic Chemistry Vol. XI/2, 4th Edition: Amines II", Georg Thieme Verlag, Stuttgart.

Sivasubramanian, S. *et al.* (2008), "Ecofriendly lime and sulfide free enzymatic dehairing of skins and hides using a bacterial alkaline protease", *Chemosphere*, 70, 1015-1024, https://doi.org/10.1016/j.chemosphere.2007.09.036.

Skakun-Todorović, M.B. and Albahari, S.R. (1979), "Preparation of L-Cysteine-^{35}S hydrochloride by reduction of L-Cystine-[35]S", *J. Labelled Comp. Radiopharm.*, 16(6), 711-716, https://doi.org/10.1002/jlcr.2580160508.

Somerville, I.C. *et al.* (1963), "Rapid unhairing with dimethylamine", *J. Am. Leather Chem. Assoc.*, 58, 254-268.

Wagner, H. (1957), "Process for the production of homocysteine compounds", US Patent 2,935,529.

MANUFACTURING AND PROPERTIES OF NONWOVENS BASED ON WASTE FROM ELASTIC FIBERS

YELYZAVETA KUCHERENKO, YURIY BUDASH, VIKTORIIA PLAVAN, DARYA SHEVTSOVA, MARYNA HORBATENKO

Kiev National University of Technology & Design, 2, Nemirovich-Danchenko str., Kiev, Ukraine, 01011, Ku4erenko_Elizaveta@i.ua

The article proposes and implements the use of highly flexible combined filament yarns (Nylon 6.6/Lycra) as the main raw material for the production of needle-punched nonwoven materials for technical purposes. It has been found that the addition of PET fibers to the feedstock makes it possible to regulate the mechanical properties of the resulting nonwoven materials over a wide range. It is shown that an increase in the content of PET fibers from 20 to 50 wt. % increases the relative strength of non-woven fabric samples by a factor of 1.5÷3. In this case, the anisotropy of this index along and across the direction of carding decreases substantially, which indicates an increase in the homogeneity of the material. The addition of other fibrous components to the initial mixture makes it possible to adjust the amount of water absorption of the nonwovens. The greatest positive effect on the value of this indicator is the addition of hemp fibers (increases ~ 1.7 times), and the largest negative – PET fibers (reduces ~ 2 times). The introduction of a 50 wt. % flax fibers into the starting mixture by 20% reduces the overall heterogeneity of the distribution of fibers in the nonwoven material. The obtained results can be used to produce elastic nonwoven materials intended for insulating surfaces of complex shape under dynamic loading conditions.

Keywords: chemical fibers, nonwoven materials, fibrous waste.

INTRODUCTION

Daily in the world 3.5 million tons of garbage is thrown out. This number continues to grow and along with it the quantity of the discarded textiles continues to expand. For the biodegradation of natural fibers in a landfill it may take hundreds of years. At the same time, methane and CO_2 are released into the atmosphere during decomposition. The decomposition of synthetic fibers in the landfill lasts an order of magnitude longer, and poisonous substances can be released into the soil and groundwater (Wang, 2010). A rational option for the recycling of secondary raw materials is suggested by using of crushed fabrics as fillers of polymer composite materials, which are widely used in various industries (Briga-Sá *et al.*, 2013).

Ensuring the most efficient processing of textile waste products consumption and the further production of useful products and materials for society is a priority task of scientific and technical progress in the sphere of application of recyclable materials. This will help not only to avoid the negative impact of waste on the environment and consequently on human health, but also provide significant savings in natural resources, as well as funds for their development (Sparks, 2012).

The recovered fiber is a valuable raw material for the chemical and light industry (production of high-quality yarn (Chen *et al.,* 2016), fillers of polymer composite materials (Chen *et al*., 2012), heat-insulating materials and others) (Bartl, 2011). In addition to fibrous waste, the composites include a binding reagent (polyethylene, polypropylene, polyamide, etc.). In this way, the strength and density of the fibrous materials and other properties can be controlled. Most types of textile waste, and in

particular those made from chemical fibers, do not concede to primary raw materials in terms of their characteristics, but sometimes even exceed them.

The aim of the work was to develop a method for fibrous waste processing to produce nonwoven materials intended for insulating surfaces of complex shapes under dynamic loading conditions.

MATERIAL AND METHODS

Fibrous waste polyurethane/polyamide-6.6 (PU/PA-6.6) was preliminarily chopped on a staple machine with rotary knives. The cutting length was 30 mm. Then, the staple fibers were mixed with additional fibrous components in certain ratios. For the formation of a fibrous tissue, the carding machine (ChBV brand) was used. Working gaps between the parts of the carding machine were 0.3-0.4 mm. After preliminary carding, the canvas was removed from the take-up drum (diameter 200 mm). Depending on the composition and quality of the material obtained, the carding operation was repeated 2-3 times. The direction of the following carding operations coincided with the direction of the preliminary carding. Staple fibers of polyethylenetherephthalate (PET), polyacrylonitrile (PAN), linen (L), hemp (H) were introduced as an additional fibrous component in an amount of up to 50 wt, %.

Nonwoven materials were evaluated by such indicators as: surface density (ρ, g/m^2), water absorption (W_f,%), breaking load (P, H/5cm). The method of optical polarization microscopy was used to study the structure of fibers. To determine the heterogeneity of nonwovens, an image analysis method was used, followed by statistical processing of the obtained data.

Different ways for calculation of indicators for nonwoven materials heterogeneity were used (Ajmeri *et al.*, 2016; Ghassemieh *et al.*, 2002):

- standard error of the concentration of structural elements in the samples:

$$S = \sqrt{\frac{1}{n-1} \cdot \sum_{i=1}^{n} (P_i - P_{cp})^2} \tag{1}$$

- the relative mean error of the structural elements concentration in the samples (confidence level 0.95, Student's value 2.06), %:

$$\Delta P = \frac{t_{\gamma,f} \cdot S}{\sqrt{n} \cdot P_{cp}} \cdot 100\% \tag{2}$$

- coefficient heterogeneity, (K_n, %), which is the standard error, given the average concentration of structural elements in the sample:

$$K_H = \left(\frac{S}{P_{cp}}\right) \cdot 100\% \tag{3}$$

The fibrous PU/PA wastes before and after stapling operation is shown on the fig 1.
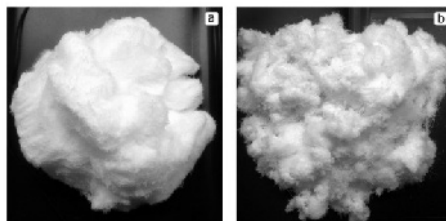
Figure 1. The fibrous PU/PA wastes before (a) and after (b) stapling operation

The slight cutting length (30 mm), which was used for stapling, is explained by the specific ability of PU fibers in the raw material to have large reversible deformations (~500%). Previous studies have shown that with a longer cutting length, a stable carding process is impossible because of the winding of separate, highly stretched filaments of PU fibers to the main shaft of the carding machine (Kucherenko, 2016).

The obtained tissue was stitched by a needle-punched operation on the OP-1 machine. For the finished nonwoven materials, the surface density, breaking load and water absorption were determined according to the procedure (Russell, 2006).

RESULTS AND DISCUSSION

Fig. 2a presents a microphotograph in polarized light of a combined PU/PA fiber structure.
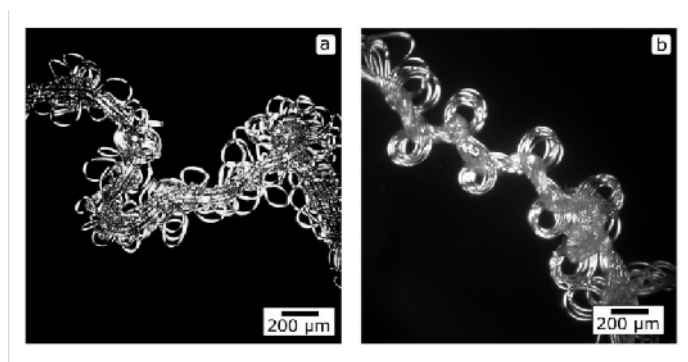
Figure 2. Microphotographs in polarized light: a) the structure of the original combined PU/PA fiber; b) PU/PA fibers after treatment with a selective solvent

It can be seen from the figure that the fiber consists of several central polyurethane filaments twisted with polyamide fibers having a loop structure. It is found that in fiber processing with PU selective solvent, there is the possibility of complete removal of the PU component (Fig. 2b). Further, a PU solution in an organic solvent can be used to produce paint and varnish compositions. The results of the study of the nonwoven materials properties in various compositions are presented in Table 1.

Table 1. Properties of non-woven samples

Fibrous composition of the material, wt. %	S, cm^2	ρ, g/m^2	W_{f}, %	W_f (relative)
PU/PA	25	128	415.6	1.00
(PU/PA)/L, 50/50	25	192	452.1	1.09
(PU/PA)/H, 50/50	25	128	684.4	1.65
(PU/PA)/PET, 50/50	25	320	203.8	0.49
(PU/PA)/PAN, 50/50	25	140	391.4	0.94

The obtained data indicates that the addition to the initial PU/PA mixture of other fibrous components changes the water absorption of the nonwoven fabric thus allowing to regulate this index in a sufficiently wide range. In this case the greatest positive effect on the value of water absorption is caused by the addition of hemp fibers, and the most

negative - PET fibers. In the first case, the water absorption increases by 1,7 times, while in the second case it decreases 2 times. The results obtained can be explained by the significant influence of other fibrous components on the structure and sorption capacity of nonwoven materials.

It was of some interest to evaluate the effect of additional fibrous components on the uniformity of fiber distribution in nonwoven materials. For comparison were used sample No. 1 (PU/PA) and sample No. 2 (PU/PA)/L, 50/50 wt. % (fig.3).
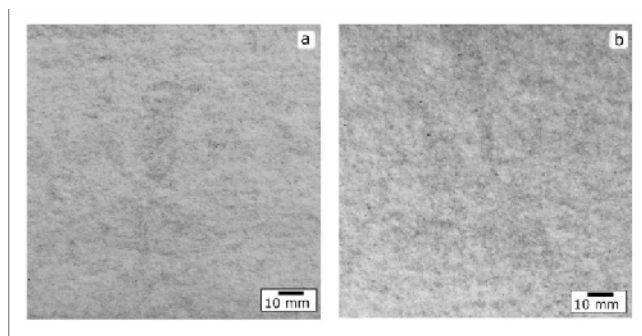
Figure 3. Image of the surface of samples of nonwoven materials: No. 1 (PU/PA) (a) and No. 2 (PU/PA)/L, 50/50 wt. %. (b)

The uniformity of the distribution in the sample as a whole and along and across the needle-punching direction determined by method of analysis of surface images. The results of the determination are given in Table 2 and in Fig. 4.

Table 2. Indicators of heterogeneity of non-woven samples

Sample material	Mixture composition	$S, \cdot 10^2$	ΔP, %	K_H, %
1	PU/PA	3.23	5.07	12.29
1H	PU/PA(horizontal direction)	3.03	4.76	11.56
1V	PU/PA(vertical direction)	1.74	2.72	6.60
2	(PU/PA)/L	2.13	3.72	9.03
2H	(PU/PA)/L(horizontal direction)	2.10	3.68	8.94
2V	(PU/PA)/L(vertical direction)	0.99	1.73	4.21

From the results presented, it can be seen that the addition of flax fibers to the original mixture reduces the coefficient of heterogeneity in the material as a whole12.3 to 9%. This indicates an improvement in the overall homogeneity of fiber distribution in nonwoven materials.

As for the first and second samples, the heterogeneity coefficients in both directions are significantly different (approximately 2-fold). In this case, the heterogeneity of the material in the transverse direction is much less than in the direction of material movement in the case of needle-punched.
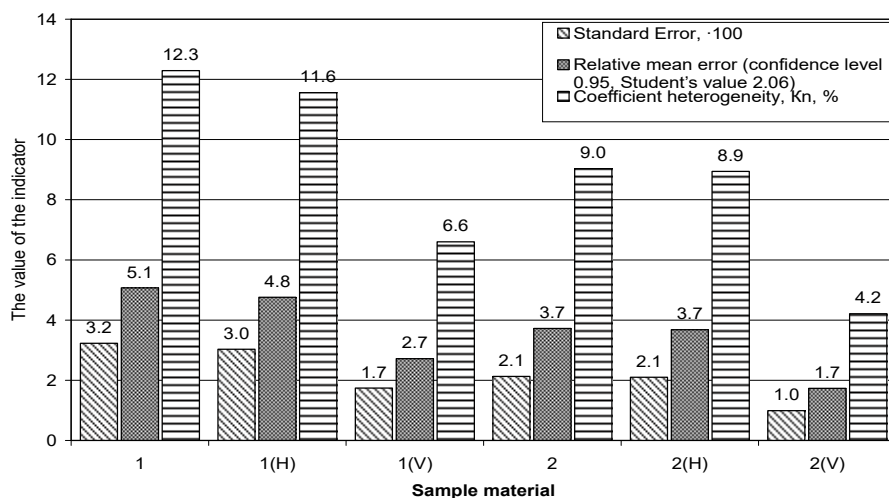
Figure 4. Comparison of the values of the uniformity for the
distribution of fibers, in samples of non-woven materials:1 - (PU / PA);
2 - (PU / PA) / L, 50/50 wt.% along (horizontally) and transverse.

The dependence of the tensile load of non-woven materials from the content of PET in the feedstock is shown on the Fig. 5.
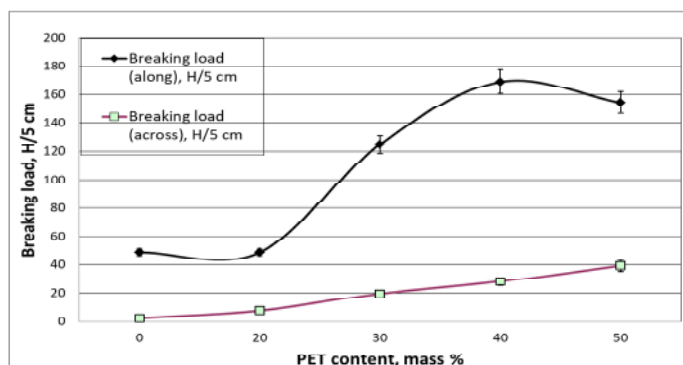
Figure 5. Dependence of the breaking load of nonwoven materials along
and across the direction of carding from the PET content

It can be seen that with the addition of 20% PET, the strength along the direction of carding is almost unchanged, while in the transverse direction it increases ~ 3-fold. As a result, the anisotropy index decreases substantially, which indicates an increase in the homogeneity of the nonwoven material.

With an increase in the PET content to 30%, there is a significant increase in strength both along and across the direction of carding (2.5 times). As a consequence, the anisotropy for this indicator is almost unchanged in comparison with the previous sample. The increase in PET in the non-woven fabric to 40-50% leads to a further

347

increase in its strength. But this growth is not as significant as in the previous sample. At the same time, the breaking load in the transverse direction continues to increase by 1.5-2 times compared to sample (PU/PA-6.6)/PET, 70/30).

For samples containing 40-50% PET, the strength growth rate in the direction perpendicular to carding (~ 1.9-2 times) begins to exceed the strength in the longitudinal direction (~ 1.2-1.3 times). This leads to a decrease in the anisotropy of this index, which reaches its minimum value for sample (PU/PA-6.6)/PET, 50/50).

CONCLUSION

It has been found that the addition of PET fibers to the feedstock makes it possible to regulate the physic-mechanical properties of the resulting nonwoven materials over a wide range. It is shown that an increase in the content of PET fibers from 20 to 50% increases the relative strength of nonwoven fabric samples by 1,5-3 times. In this case, the anisotropy of this index along and across the direction of carding decreases substantially, which indicates an increase in the homogeneity of the material. The addition of other fibrous components to the initial mixture makes it possible to adjust the amount of water absorption of the nonwoven fabric. The greatest positive effect on the value of this indicator is the addition of hemp fibers (increases ~ 1.7 times), and the largest negative - PET fibers (reduces ~ 2 times). The introduction of a 50% linen into the starting mixture reduces the overall heterogeneity of the fibers distribution by 20% in the nonwoven material. The obtained results can be used in the development of technology for elastic nonwoven materials intended for insulating surfaces of complex shape under dynamic loading conditions.

REFERENCES

Ajmeri, J.R. and Ajmeri, C.J. (2016), *Advances in Technical Nonwovens*, Elsevier Inc., https://doi.org/10.1016/B978-0-08-100575-0.00012-7.

Bartl, A. (2011), *Textile Waste, in: Waste*, Elsevier Inc., pp. 167–179, https://doi.org/10.1016/B978-0-12-381475-3.10012-9.

Briga-Sá, A. *et al.* (2013), "Textile waste as an alternative thermal insulation building material solution", *Construction and Building Materials*, 38, 155–160, https://doi.org/10.1016/j.conbuildmat.2012.08.037.

Chen, W. *et al.* (2016), "Selection and fabrication of a non-woven polycarbonate urethane cover for a tissue engineered airway stent", *International Journal of Pharmaceutics*, 514, 255–262. https://doi.org/10.1016/j.ijpharm.2016.06.047.

Ghassemieh, E., Acar, M. and Versteeg, H. (2002), "Microstructural analysis of non-woven fabrics using scanning electron microscopy and image processing. Part 1: Development and verification of the methods", *Proceedings of the Institution of Mechanical Engineers Part L: Journal of Materials: Design and Applications,* pp. 199–207, https://doi.org/10.1243/146442002760186720.

Kucherenko, Y.V. *et al*. (2016), "Obtaining and properties of nonwoven materials from fibrous waste", *Bulletin of the Kiev National University of Technology and Design. Technical sciences*, 4(100), 99-106.

Russell, S.J. (2006), *Handbook of Nonwovens*. Elsevier Inc., https://doi.org/10.1533/9781845691998.

Sparks, E. (2012), *Advances in Military Textiles and Personal Equipment*, Elsevier Inc., https://doi.org/10.1533/9780857095572.

Wang, Y. (2010), "Fiber and textile waste Utilization", *Waste and Biomass Valorization*, 1, 135–143, https://doi.org/10.1007/s12649-009-9005-y.

Yang, Y. *et al*. (2012), "Recycling of composite materials", *Chemical Engineering and Processing: Process Intensification*, 51, 53–68, https://doi.org/10.1016/j.cep.2011.09.007.

THE INFLUENCE OF EVA AND PE-g-AM COMPATIBILIZERS ON THE PROCESSABILITY, MECHANICAL AND STRUCTURAL PROPERTIES OF RECYCLED PET / HDPE MIX

MARIA SÖNMEZ[1], DENISA FICAI[2], ANTON FICAI[2], OVIDIU OPREA[2], IOANA LAVINIA ARDELEAN[2], ROXANA TRUŞCĂ[2], ZENO GHIZDAVET[2], LAURENŢIA ALEXANDRESCU[1], MIHAELA NIŢUICĂ[1], MARIA DANIELA STELESCU[1], MIHAI GEORGESCU[1], DANA GURĂU[1], DOINA CONSTANTINESCU[3]

[1]INCDTP – Division: Leather and Footwear Research Institute, 93 Ion Minulescu st., Bucharest, Romania, maria.sonmez@icpi.ro

[2]Politehnica University of Bucharest, Faculty of Applied Chemistry and Material Science, 1-7 Polizu St., Bucharest, Romania

[3]SC MONOFIL SRL, 1 Uzinei St., Savinesti, Romania

Protecting the environment by reducing PET waste has become a global priority. Recycling is considered one of the simplest and most environmentally friendly ways to reduce PET waste. However, during recycling, PET undergoes thermal / hydrolytic degradation, which leads to reduced molecular weights and low physical, mechanical, chemical, etc. properties. Thus, in order to prevent the degradation processes and to improve the mechanical and processing properties, various blends based on PETr / HDPE (60: 40 mass ratio) will be processed on a Brabender mixer in the presence / absence of the compatibilizers, EVA and PE-g-AM. The diagrams of torque versus time, recorded during processing demonstrate that PETr suffers degradation processes, which leads to a decrease in torque due to reduced viscosity /molecular weight and reduced physical-mechanical and processing properties. Instead, with the addition of EVA or PE-g-AM, in varying amounts, degradation processes are largely avoided. These observations are also supported by the values obtained from the Izod impact resistance tests, namely the higher the amount of compatibilizer, the higher the shock resistance due to the higher phase adhesion. The hardness of the blends progressively decreases, relative to the PETr control sample value, from 83 to at least 61°Sh D for the compatibilized blends. FTIR microscopy, performed on the obtained samples, shows higher homogeneity between PETr / HDPE if the addition of EVA or PE-g-AM is higher (20%). Melt flow index is improved for compatibilized blends compared to PETr and PETr / HDPE.

Keywords: polymer blends, compatibilisers, characterization.

INTRODUCTION

Polyethylene terephthalate (PET) is one of the most common thermoplastic polyesters used in various products such as carbonated beverage bottles, packaging foils, synthetic fibers used in the textile industry, electronics, and other applications due to its superior chemical, physical, mechanical and barrier (oxygen, carbon dioxide) properties. Due to the high consumption of PET products and its non-biodegradable nature, it raises many environmental problems, with a high interest in recycling and re-use. However, during recycling, PET suffers thermal and hydrolytic degradation, which leads to a lower molecular weight and, implicitly, to poor mechanical, thermal properties (Guessoum *et al.*, 2013). In this regard, to improve these properties, many research studies have focused either on mixing with one or more polymers or on the addition of reinforcing agents. The most common polymers used in PET blends are polypropylene-PP (Chen *et al.*, 2018), high density polyethylene - HDPE (Krehula *et al.*, 2015), and low density polyethylene-LDPE, etc.

A problem in the processing of these two classes of polymers (polyesters and polyolefins) is related to the thermodynamic incompatibility between the phases

(separation, lack of adhesion, weak dispersion) leading to poor mechanical and barrier properties. Thus, compatibility is fundamental to obtaining optimal properties for both PET and recycled / virgin polyolefin. Because of its structure, PET has the ability to chemically react with polar polymers and form polar-specific interactions such as hydrogen bonding (Dobrovszky and Ronkay, 2016). Improving the compatibility of these heterogeneous systems can be achieved by various methods including reactive mixing and injection molding processes. Thus, the improvement of phase compatibility is favored by the presence of block copolymers or graft copolymers because they have the ability to reduce interfacial tension, improve dispersion and adhesion between phases through interpenetration and entanglements at the polymer / polymer interface (Pracella *et al*., 2004). The most common block or grafted copolymers used to improve the compatibility between PET and polyolefin are maleic anhydride polyethylene (PE-g-MA), maleic anhydride-grafted styrene–ethylene/butylene–styrene (SEBS-g-MA), maleic anhydride-grafted EVA copolymer (EVA-g-MA), amino-telechelic polyethylene (ATPE), and ethylene vinyl acetate copolymer resins etc. (Todd *et al*., 2016; Taghavi *et al*., 2017).

MATERIALS AND METODS

Materials

Polyethylene terephthalate in the form of flakes was obtained by the industrial partner SC MONOFIL SRL by recycling of municipal waste bottles using a knife mill; ethylene vinyl acetate copolymer resins (EVA), Elvax, vinyl acetate content: 9wt%, anti-oxidant - butylated hydroxytoluene, DuPont; maleic anhydride modified mLLDPE (PE-g-AM) - Bondyram TL4109E, MFI 190ºC/2.16 Kg: 2, density g/cm^3: 0.905, melting point ºC/ºF: 117/243, VICAT softening point ºC/ºF: 85/185, maleic anhydride %: high, from Polyram, Israel; high density polyethylene, SIDPEC EGYPTENE® HD 6070 UA HDPE Injection Molding, Sidi Kerir Petrochemicals Co, Egypt.

Method

Before pelleting, PETr flakes were subjected to an advanced pre-drying process at 150°C in a hot air oven for a minimum of 24 hours to remove the adsorbed physical water. After flakes drying, binary (PETr / HDPE in 60:40 wt) or ternary (PETr / HDPE / PE-g-AM or EVA) mixtures formulations were processed in a Brabender mixer at 240°C with screws speed ranging from 30 rpm for about 2 minutes to 110 rpm for 5 minutes. The total mixing time in the Brabender mixer, from loading with the raw materials until all components were homogenized, was 7 minutes for all the processed blends. As Table 1 shows, the PETr / HDPE ratio was 60: 40 wt% for all samples and the amount of compatibilizers used (PE-g-AM or EVA) was 10 or 20 wt% relative to the total amount of PETr and HDPE present in the blend. Figure 1 shows a sudden drop in torque (from 220 to 145 Nm and subsequently to 30 Nm) for PETr melt mixing - sample 0, depending on time and screws speed (30 or 110 rpm), indicating that degradation processes occur. The reduction of intrinsic viscosity / molecular mass is especially evident in case of sample 0, which undergoes hydrolytic / thermal degradation to a much higher extent compared to sample 1 - torque increases from ~ 45 Nm (screws speed at loading - t_0, 30 rpm) to 75 Nm after a mixing time of 60 seconds at 110 rpm, and decreases progressively, although to a much lower extent than sample 0.

For samples 2 and 3, a torque increase from 60 Nm (t_0) to ~ 110 Nm after 70 seconds is observed, which indicates that the viscosity of the mixture increases. Viscosity also increases in samples 4 and 5, however, to a lesser extent than samples 2 and 3, indicating that the type of compatibilizer used influences the viscosity of the mixture and prevents degradation processes. Figure 2 shows that for sample 0 a higher mixing energy (90 kJ) is required in the first 240 sec. (4 min) compared to samples 1-5. However, for samples 2-5 containing compatibilizers, the energy required for mixing is much higher compared to samples 0 and 1 after a mixing period of 180 seconds, due to the increase and maintenance of a higher viscosity in the melt. These results demonstrate that degradation reactions responsible for viscosity reduction are significantly avoided by the addition of compatibilizers, observations confirmed by impact resistance tests. From the processed blends, test specimens with a length of 100 mm and a thickness of 4 mm were obtained in an electric press at a temperature of 243°C, pressing time of 7 minutes, pressure force 300 kN. The obtained specimens were used to determine Izod impact resistance and hardness. The morpho-structural analyses were performed in fracture, on the specimens obtained after Izod impact resistance tests.

Table 1. Formulations based on PETr / HDPE with / without compatibility

Samples/ Raw materials	0	1	2	3	4	5
PETr, g	280	168	168	168	168	168
HDPE, g	-	112	112	112	112	112
PE-g-AM, g	-	-	28	56	-	-
EVA, g	-	-	-	-	28	56
TOTAL, g	280	280	308	336	308	336
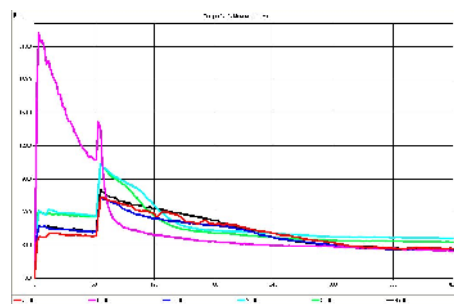
Figure 1. Variation of torque vs. time for samples 0-5, processed in Brabender
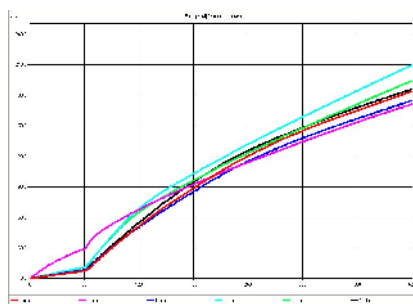
Figure 2. Variation of mixing required energy vs. time for samples 0-5, processed in Brabender

RESULTS AND DISCUSSION

Physico-Mechanical Tests

Izod Impact resistance recorded for samples 0-5 shows significant changes, induced by the type and amount of compatibility agents. Thus, for sample 0, impact resistance shows an extremely low value of only 1.2 kJ/m^2. Practically, these specimens are so

friable that they break when the notch is made. An improvement in friability can be seen in the case of the addition of HDPE - sample 1, although due to the incompatibility between the phases, impact resistance records a low value of only 1.83 kJ/m^2. Significant improvements could be seen with the addition of 10% PE-g-AM (Sample 2) and 20% PE-g-AM (Sample 3), the impact resistance being 7.93 and 12.91 kJ/m^2 respectively. This can be attributed to the fact that the addition of a higher amount of PE-g-AM improves the compatibility between the phases due to the reactions taking place between the various phase components, and prevents the degradation processes. In the case of 10% and 20% EVA addition, the impact resistance improves compared to samples 0 and 1 but to a much lower extent than samples 2 and 3. The obtained results are in very good concordance with the FTIR microscopy, which shows that the higher the compatibilizer quantity (20%), the more the degree of homogeneity of mixtures increases.
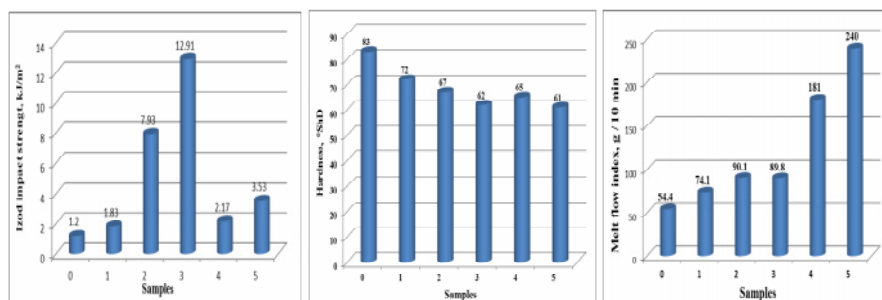
Figure 3. Physical-mechanical determinations and melt flow index of samples 0-5

Hardness of the mixtures decreases from 83°ShD for sample 0 to 72°ShD for sample 1 (PETr / HDPE). For mixtures containing EVA or PE-g-AM, a hardness drop is observed as the amount of compatibility increases.

Melt flow index was determined on samples 0-5 at 254°C and a 5 kg force. As can be seen from Figure 3, sample 0 - PETr has the lowest fluidity index of all the mixtures tested. This was to be expected because the higher the torque and the hardness the lower the fluidity index. Significant improvement in the indexes could be seen in samples 4 and 5, which shows that EVA improves flow properties. The samples containing 10 and 20% PE-g-AM (samples 2 and 3) shows a decrease of melt flow index up to 90.1 and 89.1 due to the increase in viscosity in the polymer melt (also highlighted by the torque / hardness tests). However, samples 2 and 3 did not raise processability issues, and the results obtained from physico-mechanical / morpho-structural tests showed that these mixtures have superior properties compared to other mixtures.

FTIR Microscopy

The FTIR microscopy was recorded on the fracture surface of the samples, and the maps recorded at the specific wavelengths of the components are presented in Figure 4.

PETr/HDPE/20%EVA   PETr/HDPE/20%PE-g-MA
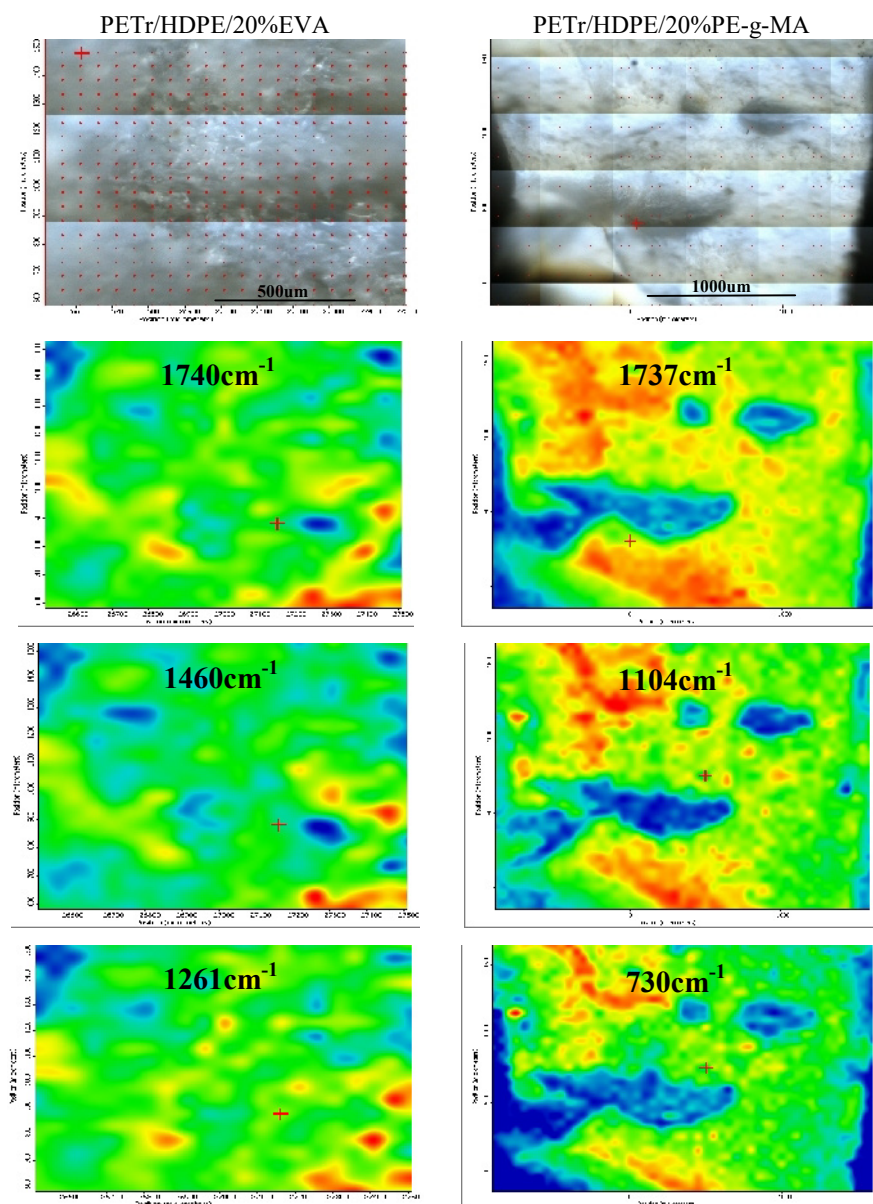
Figure 4. FTIR maps recorded at the specific wavelengths of the components

All the obtained samples were analyzed by FTIR microscopy and for all samples, good homogeneity was observed, being similar with the two examples provided in Figure 4. Based on the FTIR spectra of the samples it can conclude that the best peaks to monitor the distribution of PETr, HDPE and EVA are those centered at 1740, 1460 and 1261cm⁻¹ while for the PETr, HDPE and PE-g-AM the best peaks are 1737, 1104

and 730cm^{-1} (even if some peaks are overlapped, the distribution of the three components can be evaluated because the contribution of the overlapped peaks can be subtracted according to the intensity of other peaks) (Bui *et al.*, 2016).

CONCLUSIONS

Improving the adhesion, processability and physico-mechanical properties of the PETr / HDPE mixture is possible by the addition of suitable compatibilizers to limit the thermal or hydrolytic degradation processes, and the creation of optimal bonding at the polymer / polymer interfaces. The obtained results show that the PE-g-AM compatibilizer induces better properties to mixtures compared to EVA. Based on the FTIR data, it can be concluded that the use of PE-g-AM and EVA induces a very good compatibility between PETr and HDPE and this can be also highlighted in the fracture area.

REFERENCES

Bui, N.D. *et al*. (2016), "Effect of acetate group content in ethylene-vinyl acetate copolymer on properties of composite based on low density polyethylene and polyamide", *International Journal of Polymer Science*, 1-8, https://doi.org/10.1155/2016/3149815.

Chen, S.C. *et al*. (2018), "An Investigation and Comparison of the Blending of LDPE and PP with Different Intrinsic Viscosities of PET", *Polymers*, 147(10), 1-14.

Dimitrova, T.L. *et al*. (2000), "On the compatibilization of PET/HDPE blends through a new class of copolyesters", *Polymer*, 41(13), 4817–4824, https://doi.org/10.1016/S0032-3861(99)00709-0.

Dobrovszky, K. and Ronkay, F. (2016), "Influence of morphology and compatibilizer on burning behavior of PET/HDPE blend", *AIP Conference Proceedings*, Graz, American Institute of Physics, https://doi.org/10.1063/1.4965556.

Guessoum, M. *et al*. (2013), "Rheological and mechanical properties of recycled poly(ethylene terephtalate)/high density polyethylene blends", *MATEC Web of Conferences*, 5, 1-3. https://doi.org/10.1051/matecconf/20130504026.

Krehula, K.L. *et al*. (2015), "Study of masterbatch effect on miscibility and morphology in PET/HDPE blends", *Adhesion Science and Technology*, 29(2), 74–93, https://doi.org/10.1080/01694243.2014.975913.

Makkam, S. and Harnnarongchai, W. (2014), "Rheological and mechanical properties of recycled PET modified by reactive extrusion", *Energy Procedia*, 56, 547–553, https://doi.org/10.1016/j.egypro.2014.07.191

Pracella, M. *et al*. (2004), "Recycling of PET and polyolefin based packaging materials by reactive blending", *Polymer-Plastics Technology and Engineering*, 43(6), 1711-1722, https://doi.org/10.1081/PPT-200040075.

Taghavi, S.K. *et al*. (2017), "Detailed comparison of compatibilizers MAPE and SEBS-g-MA on the mechanical/thermal properties, and morphology in ternary blend of recycled PET/HDPE/MAPE and recycled PET/HDPE/SEBS-g-MA", *Journal of Elastomers & Plastics*, 50(1), 13-35, https://doi.org/10.1177/0095244317698738.

Todd, A.D. *et al*. (2016), "Reactive compatibilization of poly(ethylene terephtalate) and high density polyethylene using amino-telechelic polyethylene", *Macromolecules*, 49(23), 8988–8994, https://doi.org/10.1021/acs.macromol.6b02080.

UNDERGARMENT PPE WITH MODULAR STRUCTURE FOR STAFF WORKING IN THE NATIONAL DEFENSE, PUBLIC ORDER AND SECURITY SYSTEM

DOINA TOMA[1], ALINA POPESCU[1], CLAUDIA NICULESCU[1], GEORGETA POPESCU[1], ADRIAN SĂLIŞTEAN[1], MARCEL ISTRATE[2], MARIA BUZDUGAN[3], MARCELA RADU[3]

[1]*The National Research Development Institute for Textiles and Leather, 16 Lucretiu Patrascanu, 030508 Bucharest, Romania email: certex@certex.ro*

[2]*STIMPEX SA 46-48 Nicolae Teclu, 032368 Bucharest, Romania, email: marcel.istrate@stimpex.ro*

[3]*Magnum SX SRL 61 Ferdinand I, 021383 Bucharest, Romania, email: magsx2000@gmail.com*

The protection of operational staff from defense, public order, security structures, with a personal protective equipment system adequate to the conditions of execution of specific missions is a major desiderate for optimizing the efficiency of these formations. Reducing losses, increasing combativeness of fighters and the time actually dedicated to the mission are factors influenced by the quality of individual protection equipment. Underwear is the functional part of the military clothing system and it is affected by middle and outer clothing layers. Main function of the underwear is to maintain user's skin dry and improve thermal and moisture sensations on the skin. The aim of the project was to develop functional undergarment equipment, designed to be integrated in specialized protection equipment systems, in order to ensure the survival and resistance of operational staff from the defense, public order, security structures, in variable conditions of temperature, activity and weight levels of the equipment carried. The functional cellulose fibers (ex: Cell Solution Clima, Cell Solution Protection and Cell Solution Skin Care), blended with natural cellulosic fibres have been selected and used to accomplish the knitted fabrics. Prototypes of undergarment PPE which are integrated or non-integrated in specialized equipment of end users were evaluated and tested in real conditions of use.

Keywords: personal protective equipment, functional undergarment equipment, comfort

INTRODUCTION

Military activities and operations are intrinsically hazardous. Soldiers conducting full-spectrum operations must assume calculated risks every day, based on the significance of the mission, the operational requirement and opportunity.

The spectrum of hazards and threats facing dismounted soldiers include: man-made threats/ hazards: Improvised Explosive Devices, CBRNE effects, obstacles, mine fields, booby traps; operational hazards / threats: opposing military operations, insurgents, sympathizers, local population, fratricide; natural hazards / threats: weather, heat/cold, rain, sand/dust/wind, insects (Soldier Systems, 2011). Personal protective equipment (PPE) needs to remain effective and functional across a wide array of tactical requirements and operating environments - from arctic to desert temperatures, in high and low humidity, in urban, rural, forested, marine, or subterranean environments, and in almost every imaginable locations. PPE users also have a variety of mission profiles, from high visibility patrol to assault and covert operations, with the nature of threats and the acceptable risk in each scenario being varied as well. To respond to ever changing and varied threats that act on users and the variety of operating environments, PPEs need to be continually developed / upgraded.

The protection of operational staff from defense, public order, security structures, with a personal protective equipment system adequate to the conditions of execution of

specific missions is a major desiderate for optimizing the efficiency of these formations. Reducing losses, increasing combativeness of fighters and the time actually dedicated to the mission are factors influenced by the quality of PPE. Modular garment systems are generally designed around three primary layers: a base or next-to-skin layer that is designed to wick moisture away from the body; an insulation layer that provides volume and allows warm air to be trapped between the body and the outer garment; and the outer shell layer that protects the wearer from the elements. (Project Responder 4, 2014). Underwear is the functional part of the military clothing system and it is affected by middle and outer clothing layers. Main function of the underwear is to maintain user's skin dry and improve thermal and moisture sensations on the skin and, therefore, it may significantly affect comfort sensations.

The aim of the project was to develop functional undergarments equipment, designed to be integrated in specialized protection equipment systems, in order to ensure the survival and resistance of operational staff from the defense, public order, security structures, in variable conditions of temperature, activity and weight levels of the equipment carried.

EXPERIMENTAL PART

From the analysis of the types of aggression for which protection must be ensured there were identified the performance requirements imposed by the specific European standards that were translated into properties required for manufacturing materials and constructive design parameters of undergarment PPE with modular structure integrated into specialized PPE for use in military operations/ intervention actions: a multilayer structure: undergarment PPE (inner layer) – mainly taking over the sensorial and thermophysiological comfort functions; outer layer – having a barrier function for the risk factors in the work environment (heat and flame, cold, bad weather, mechanical aggression, etc.); intermediate layer - encompassing the system of enabling the thermal insulation function

Materials

Functional clothing by definition is user-requirement specific and designed or engineered to meet the performance requirements of the user under extreme conditions. Protective - functional represents the largest and most diverse segment of functional clothing (Gupta, 2011). Development of functional fibers is based on the process of incorporating active chemicals into de fiber in its manufacturing stage, and this technology is rather increasing today, mainly being supported by fiber manufacturers. The functionalized fibers developed by Smartpolymer GmbH AG (Germany), through ALCERU procedure (the active substance: Paraffin/ Permethrin/Tocopherol, is directly integrated into the cellulose matrix imparting a permanent function to the cellulose) mixed with cotton fibers and /or modal fibers have been used to accomplish knitted fabrics for undergarment PPE.

As part of the project there were used: a*) fibre Cell Solution CLIMA*, a PCM (Phase Change Material) micro composite of the latest fiber manufacturing generation with thermoregulating features. Via a patented spinning process, paraffin is embedded in crystalline and tear resistant functional Lyocell fibers (***Cell Solution Clima); b) *fibre Cell Solution PROTECTION* – are natural cellulosic manmade fibers provide effective and durable protection against insects-such as

ticks and mosquito. Via direct spinning, the insect repellent permethrin is embedded in the Cell Solution fiber core and migrates to the fiber surface in a tightly controlled manner (***Cell Solution Protection); c) *fibre Cell Solution SKIN CARE* – are Lyocell fibers with integrated natural oils and Vitamin E. By embedding a Vitamin E depot into the matrix structure a Cell Solution Skincare, the release of Vitamin E turns into a lifelong effect (*** Cell Solution Skin Care).

The knitted fabrics are made of different construction of yarns, as mentioned in table 1.

Table 1. Knitted fabrics yarns composition

Fabric code	Yarn count (Nm)	Yarn construction (%)	Yarn composition
T1	50/1	60/20/20	Cotton/ Modal/ Cell Solution PROTECTION
T2	50/1	60/20/20	Cotton/ Modal/ Cell Solution SKIN CARE
T3	50/1	70/30	Cotton / Cell Solution CLIMA

Interlock weft knitted fabrics were produced for this research on a E20 Uniplet circular knitting machine. The knitted fabrics were subjected to finishing procedures. The pretreatment, in a single "gentle" step with a chemical agent especially designed for a low temperature bleaching process based on synergistic mixtures of specific non-ionic surfactants with superior wetting, emulsifying and removal properties of grease impurities, oils, accidental pigments, was carried out at a lower temperature than the boiling point and a reduce duration of approx. 110 minute compared to the traditional pretreatment process in successive phases.

Table 2 shows the physical-mechanical and physical - chemical characteristics of the weft knitted fabrics produced.

Table 2. Characteristics of the knitted fabrics

Characteristics		Fabric code		
		T1	T2	T3
Weight, g/m^2		262	247	276
Density/10cm	course no/horizontal	151	146	140
	row no./vertical	152	141	161
Thickness, mm		0.99	0.98	1.21
Bursting strength, kPa		344	350	327
Bursting distension, mm		39	38	47
Abrasion resistance, cycles no.		50604	53543	44330
Air permeability, $l/m^2/s$		413.6	417.8	427.8
Water vapour resistance Ret, $m^2 Pa/W$		5.86	6.17	7.04
Thermal resistance Rct, $m^2 K/W$		0.0286	0.0255	0.0314

Physical - mechanical and physical - chemical characteristics have been made on knitted fabrics, as follows: weight (SR EN 12127:2003), density (SR EN 14971:2006), thickness (SR EN ISO 5084:2001), burst strength and burst distension (EN ISO 13938-2:2003), abrasion resistance – Martindale method (SR EN ISO 12947-2:2017), air permeability (SR EN ISO 9237:1999), water - vapour resistance and thermal resistance (SR EN ISO 11092:2015).

Prototype Design

There are a number of challenges for integration with respect to PPE: selecting and adapting materials for specific user and operational requirements; optimizing hybrid systems for protection, cost, weight, and human factors; developing concepts for mission – configurable systems; developing material system for multi- threat protection.

Principles that have been taken into account when designing an integrated prototype system of undergarments PPE are:

a) *establishing the operating environment and operational requirements*, which include identification of: clothing components (subsystems) of the PPE system; key performance parameters for each component garment (subsystem); any physical requirement for the component part of the PPE system or for the system; any requirement for interoperability and / or maintenance;

b) *integration of protection with other functions*: use of multifunctional materials, reducing weight and complexity of the PPE system through integration of functions;

c) *human factors* - factors that affect the comfort or effectiveness of the user and that have a critical effect on the performance of the wearer.

For undergarments PPE a two pieces garment configuration (long - sleeved shirt and full-length trousers; t-shirt and short trousers) was designed and manufactured (Figure 1).

Figure 1. Prototypes of undergarments PPE with modular structure

To ensure the performance requirements imposed there were considered the following technological design features of the PPE: a) use of technologies with fewer operations due to: fully tailored details; transfer of tucks into the constructive lines, providing also a degree of freedom in specific movements; b) selecting the correct fineness of sewing needles and thread depending on the structural features

of the knitted fabric and the type of ensemble; c) appropriate selection of the types of machinery and ensembles that would provide high standards on the stitch resistance.

RESULTS AND DISCUSSIONS

The analysis of the results obtained in performing specific laboratory tests for the knitted fabrics (T1,T2 and T3) of the undergarments PPE, highlights the following:

- bursting strengths with values of over 300 kPa combined with busting distension above 38 mm meet the minimum values required by the applicable product specifications in the military field (min. 160 kPa), respectively the minimum limits imposed by the PPE specific standards for knitted fabrics used as outer layer of the PPE (min. 200 kPa);
- air permeability has values above the minimum required by the technical product specifications applicable to defense / public order / security (min. 200 l/m^2/s);
- water - vapour resistance has comparable values between the knitted fabrics (5.86 - 7.04 m^{2}Pa/W), correlated with the percentage of functional fibers in the fiber mixture, meet the maximum imposed limit of 55 m^{2}Pa/W (for cold protective clothing) and maximum 30 m^{2}Pa/W for performance level 2 of firefighting clothing;
- good behavior in wearing appreciated through the abrasion resistance values of over 40000 cycles.

CONCLUSIONS

The aim of this research was to develop functional undergarments equipment, designed to be integrated in specialized protection equipment systems, in order to ensure the survival and resistance of operational staff from the defense, public order, security structures, in variable conditions of temperature, activity and weight levels of the equipment carried.

To meet this objective new textile knitted structures have been developed by using the functional cellulose fibers Cell Solution CLIMA, Cell Solution PROTECTION and Cell Solution SKIN CARE, mixed with cotton fibers and /or modal fibers being design and manufacture of undergarments PPE prototypes with modular structure.

The testing and evaluation process consisted of objective and subjective testing.

The objective laboratory testing of knitted fabrics validated the material performance and ensured compliance to standards requirements. However, laboratory data cannot accurately assess the operational suitability and effectiveness of a PPE system when used under operating conditions. Critical attributes, such as comfort, appearance, durability, freedom, and range of motion, could not fully evaluate under laboratory conditions.

The user's subjective perception for the operational suitability and effectiveness of the PPE system is determined by conducting a Wear Trial of the undergarments PPE which are integrated in specialized equipment. This subjective evaluation proves the essential difference of the performance of the various fabrics manufactured into the garments. Most importantly the operational assessment provide the feedback on the functionality of the PPE garment design.

REFERENCES

Gupta, D. (2011), "Functional clothing – Definition and classification", *Indian Journal of Fibre & Textile Research*, 36, 321-326.
Royal, M. and Jennings, D. (2014), "Project Responder 4 2014 National Technology Plan for Emergency Response to Catastrophic Incidents", Homeland Security Studies and Analysis Institute, RP13-17-02, 89-100.
*** Soldier Systems Technology Roadmap 2011–2025 (SSTRM) - Capstone Report and Action Plan, 2010.
*** http://www.cellsolution.eu/products/cell-solution-climafiber/
*** http://www.cellsolution.eu/products/cell-solution-protection/
*** http://www.cellsolution.eu/products/cell-solution-skin-care/

STUDY OF CENTER OF PRESSURE (COP) IN GAIT ANALYSIS OF ELDERLY WOMEN IN ROMANIA

ANA MARIA VASILESCU, MIRELA PANTAZI

INCDTP - Division Leather and Footwear Research Institute, 93 Ion Minulescu str., district 3, Bucharest, Romania, email: icpi@icpi.ro

The purpose of this study is to analyze the differences in the trajectory of the center of pressure, COP, in a group of 100 female volunteers aged 55 to 87, using the BioAnalysis software version 2.3.0 for data processing provided by AMTI's AccuGait System force plate. The trajectory of the COP during gait provides an additional tool in the assessment of foot pathology. Research has clarified the differences in trajectories of COP generated and controlled during locomotion, depending on the intensity of disturbances while walking. The aging process leads to a reduction of the movement capacity and the loss of balance, implicitly to a deviation of the center of pressure trajectory, leading to the clarification of a particular pathology. Evaluations of the centers of pressure trajectories of subjects participating in the study showed significant differences between normal and pathological gait. Research on the trajectory of the center of pressure is useful for human gait analysis and for a good understanding of the stability of subjects. In biomechanical evaluation by means of the inverse dynamics method, the force plate is a tool for assessing the interaction between the foot and the support surface, being an indispensable element. In the design of orthopedic footwear, biomechanical analysis is an essential element, so as to ensure a more efficient gait.

Keywords: center of pressure, gait, biomechanics

INTRODUCTION

According to the National Institute of Statistics of Romania (www.insee.ro), on January 1st, 2018 the demographic ageing phenomenon in Romania aggravated, the elderly population aged 65 and over exceeded the young population aged 0-14 by 350 thousand (3614 thousand compared to 3264 thousand persons). The demographic aging process deepened, compared with 2017, with an increase of 0.3 percentage points in the share of the elderly population (aged 65 and over) (Figure 1).
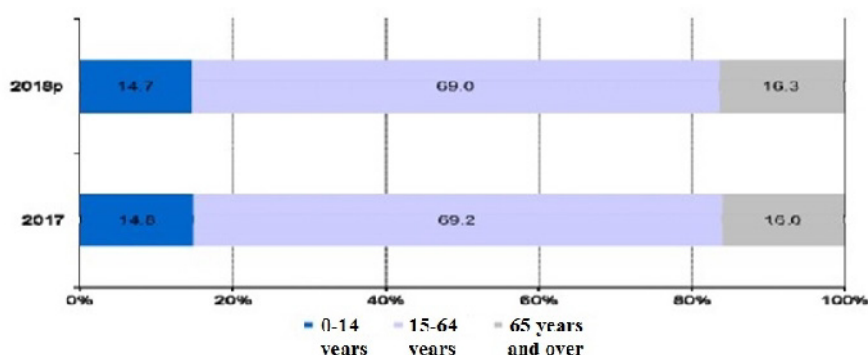
Figure 1. Structure of population per age groups, January 1st, 2018

As the body ages, it becomes less biomechanically active and the prevalence of gait dysfunction and postural balance is increased among the geriatric population. The

importance of the phenomenon results from its association with the increased risk of falling, immobilization, increased degree of dependency and lowered quality of life (Jahn, Zwergal and Schniepp, 2010; Stolze *et al*., 2004).

For many elderly subjects, the aging process is inevitably accompanied by a reduction in motion capacity and loss of balance (Woollacott, 1993), so the muscles responsible for movement become weaker by decreasing muscle mass and muscle volume, etc. The purpose of this study is to analyze the differences in the trajectory of the center of pressure, COP, in the gait of elderly women in Romania.

The center of pressure (COP) is the point where the resultant of all the ground reaction forces acts. For a normal subject, the center of pressure (COP) trajectory is shown in Figure 2 (Horak, 2006; Serban, 2011), which has the following characteristics in relation to the axis of the plantar surface:

- initial point situated center-lateral corresponding to the contact phase of the gait;
- the trajectory roughly parallel to the axis of the plantar surface for the unilateral support phase;
- medial deflection to the distal end of the hallux in the toe-off phase.
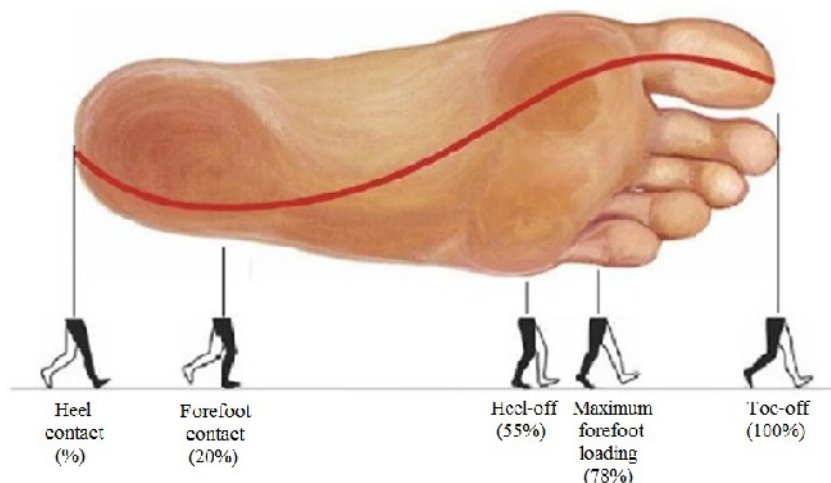
Figure 2. Normal trajectory of the COP (Horak, 2006; Serban, 2011)

Any deviation from this trajectory leads to the classification of a particular pathology or to a certain disturbance of the stable dynamic balance (Serban, 2011).

RESEARCH METHODOLOGY

The study followed biomechanical gait analysis by measuring ground reaction and, implicitly, the center of pressure (COP).

Data Collection

The trajectory of the center of pressure was determined using the BioAnalysis software version 2.3.0 for data processing provided by AMTI's AccuGait System (www.amti.biz).

The study included 100 elderly female volunteers, aged 55 to 87. The structure of the sample by age group is shown in Figure 3, most subjects were aged over 71 (34%), followed by subjects in the 60-64 age group (27%), then those aged 55-59 (26%), while the 65-70 age group consisted of only 13% (Vasilescu *et al*., 2016). They have given their prior consent to the participation of this experiment. The subjects walked on the track where the force plate was incorporated, and only the trials in which the right foot landed entirely on the plate were deemed valid.
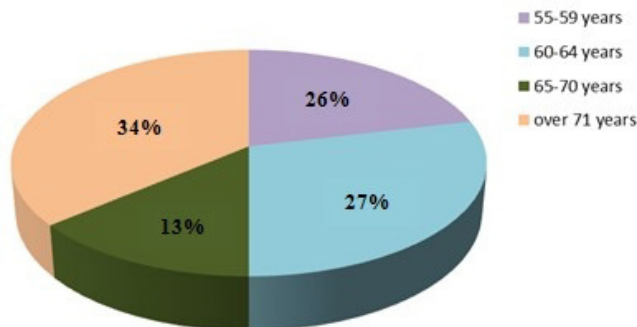
Figure 3. Structure of the age sample

Data Analysis and Interpretation

Normalized parameters provided by the force plate on the center of pressure are the following:
- COP:Heel Strike X (cm) - The X coordinate of the COP at Heel Strike, cm;
- COP:Heel Strike Y (cm) - The Y coordinate of the COP at Heel Strike, cm;
- COP: Toe Off X (cm) - The X coordinate of the COP at Toe Off, cm;
- COP: Toe Off Y (cm) - The Y coordinate of the COP at Toe Off, cm;
- COP: Excursion Along X-Axis,(cm) - The X coordinate of the COP at the maximum point along the X-Axis, cm;
- COP: Excursion along Y-Axis, (cm)- The Y coordinate of the COP at the maximum point along the Y-Axis, (cm);
- COP: Avg X (cm) - The COP's average distance in the X direction;
- COP: Avg Y (cm) - The COP's average distance in the Y direction;
- COP: Length (cm) - The length of the total distance traveled by the COP, (cm);
- COP: Max Velocity (cm/sec) - The maximum velocity traveled by the COP.

Determinations show significant differences between trajectories of the center of pressure of a normal foot and a pathological foot. Unlike the normal foot (Figure 4), the trajectory of the center of pressure for a pathological foot (Figure 5) shows the following characteristics:

- initial point situated center-medial corresponding to the contact phase of the gait;
- the trajectory curved outward during the unilateral support phase;
- lateral deflection to the end of the metatarsophalangeal joint, as a result of the inability to perform toe-off.
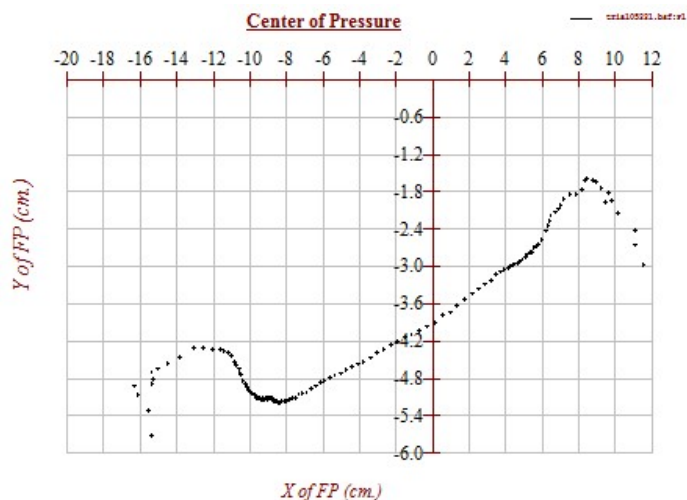
Figure 4. Graphical representation of the trajectory of the center of pressure, COP, for a normal foot (right foot)
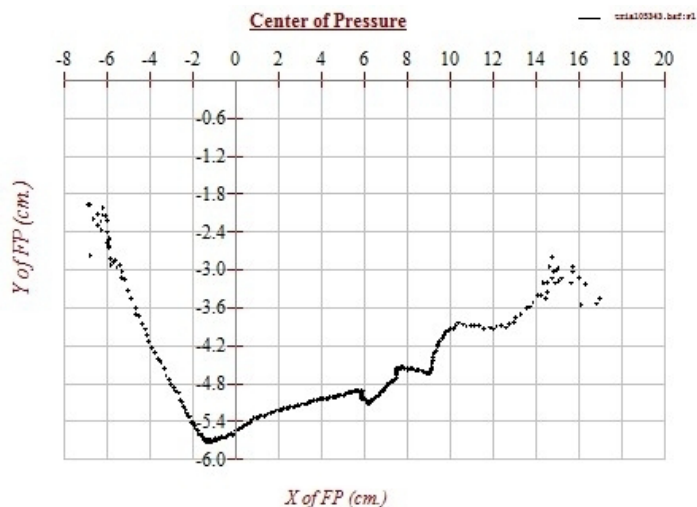
Figure 5. Graphical representation of the trajectory of the center of pressure, COP, for a pathological foot (right foot)

Each person responds to a task in different ways. For example, Figure 6 shows the comparative time variations of the center of pressure for several subjects participating in the study. There is a different evolution of biomechanical parameters depending on the walking style of each subject.
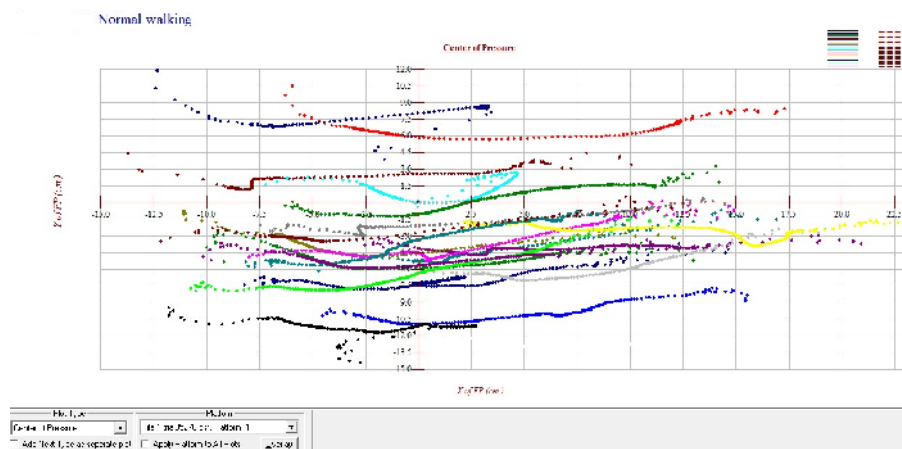
Figure 6. Evolution of the trajectory of the center of pressure over time for subjects participating in the study

CONCLUSIONS

The analysis of center of pressure trajectory is an essential element in designing and making orthopedic footwear so as to ensure a more efficient gait and so that the footwear functions would facilitate normal foot functions while walking for the purpose of successful day-to-day activities. The design of orthopedic footwear requires a good understanding of the normal and pathological gait biomechanics.

Acknowledgement

REFERENCES

Horak, F.B. (2006), "Postural orientation and equilibrium: what do we need to know about neural control of balance to prevent falls", *Age Ageing*, vol. 35, ii7- ii11
Jahn, K., Zwergal, A., Schniepp, R. (2010), "Gait Disturbances in Old Age, Classification, Diagnosis, and treatment From a Neurological Perspective", *Dtsch Arztebl Int*, 107(17), 306–316, published online 30 Apr 2010, https://doi.org/10.3238/arztebl.2010.0306.
Serban, I.I. (2011), "Studies and research on environmental influence on the stability and human locomotion", PhD thesis, Transilvania University of Brasov.
Stolze, H., Klebe, S., Zechlin, C. *et al*. (2004), "Falls in frequent neurological diseases - prevalence, risk factors and aetiology", *J Neurol*, 251, 79–84, https://doi.org/10.1007/s00415-004-0276-8.

Vasilescu, A.M., Deselnicu, D., Pantazi, M. *et al*. (2016), "Analysis of selected anthropometric parameters of elderly women", Proceedings of the 6th International Conference on Advanced Materials and Systems - ICAMS 2016, 429-434, https://doi.org/10.24264/icams-2016.III.19.
Woollacott, M.H. (1993), "Age-related changes in posture and movement", *J Gerontol*, 48, 56-60.
*** www.insee.ro

DEPOSITION OF METAL – NANOPARTICLES IN TEXTILE STRUCTURE BY CHEMICAL REDUCTION METHOD FOR UV-SHIELDING

VIKTORIIA VLASENKO[1], SVITLANA ARABULI[1], PETRO SMERTENKO[2]

[1]*Kyiv National University of Technologies and Design, N.-Danchenko srt. 2, 01011 Kyiv, Ukraine, e-mail: vlasenko@ekma.com.ua, arabuli.si@knutd.edu.ua*

[2]*V.E. Lashkaryov Institute of Semiconductor Physics, NAS of Ukraine, 41 pr. Nauki, 03028, Kyiv, Ukraine, e-mail: petrosmertenko@gmail.com*

Now mankind is exposed to danger of UV-radiation (UVR) for health and it is very important to create reliable ways for protection against it. For UVR impact reducing, various shielding materials are used. Special place are occupied by textile screens. Their advantages: flexibility, ability to form shields of various shapes, etc. One of main requirements to UV-screens is their electro-conductivity. To-day various methods of textile materials nano-modification are known (such as evaporation of metals in the electric arc, laser and magnetron sputtering of metals; deposition of nano-particles on the surface of textile materials). Each of methods, as a rule, complicates the technology of textile nano-modification; require high energy costs, lead to different environmental problems, and on synthetic textile materials such treatments cause polymer degradation. The purpose of this work: to elaborate the effective method of textiles modification to receive textiles with high level of protection against UV-radiation. We proposed the method of textile modification in Cu-sulfate solution with Cu-ion reduction for receiving of Cu nano-particles directly in porous textile structure. Textiles modified by using of this method have high degree of ultraviolet waves at wavelengths A (315-400nm) and B (315-280nm). The proposed method is simple, accessible and effective (cheap and accessible reagents; processing may be implemented on the equipment for dyeing).

Keywords: UV-shielding; textile modification.

INTRODUCTION

Even the weak energy impact of UV Radiation on the human body affects the resonant processes in various organs and systems of organs of a living organism.

The development of textiles for effective shielding from the action of UV is a task that has attracted attention medics and scientists for many years. All over the world the main requirement to UV-screens is their electro-conductivity (Prue, 2013; Holick, 2016, Juzeniene, 2011; Mikkelsen, 2015; Zaets, 2006).

At first, the textile material serves as a flexible two-dimensional substrate providing an effective surface for harvesting photons of light (Wilson, 2008; Singh, 2013; Vlasenko, 2016).

Secondly, the textile substrate is easier to apply functional nano-substances using different techniques (for example, from solutions, vacuum, laser, printing).

Modern trends in the world economic development of the textile industry and tough competition in the world textile industry market require the creation of innovative textile materials and products from them with a target set of properties. Nano-technologies play especial role in solving this problem. Their use makes it possible to create innovative textile materials with a given set of properties (Абдуллин, 2005; Горберг, 2003; Шаехов, 2006; Красина, 2011).

To-day various methods of textile materials nano-modification are known and used. There are such methods as evaporation of metals in the electric arc, laser and magnetron sputtering of metals and deposition of nano-particles on the surface of textile materials.

Each of these methods, as a rule, complicate the technology of textile nano-modification, require high energy costs; the special equipment must be used. Then these methods lead to different environmental problems. Besides it, vacuum metallization of textiles worsens its vapor and air permeability. Also, on synthetic textile materials such treatments cause polymer degradation.

In our work we have investigated and propose the method of textile nano-modification from metal salts solutions.

EXPERIMENTAL PART

Modification of the Textile Materials

In our day there is the great growing interest to fabrication and application of nano-materials in textile technologies. Nano-modification provides to textiles new very interesting and necessary properties.

As example, nano-modification with using some metals, provide antistatic, antimicrobial properties, electroconductivity, shielding against EM radiation in wide range of wavelength.

Among nano-articles, metallic cooper particles are interesting with its potential wide application, for example: electrical properties, catalytic activity, low cost, for heat transfer system and its antimicrobial, antiviral, antifungal properties and oth.

The method of modification by the nano-dispersed Cu-powder was performed in accordance with the patent (Vlasenko *et al.*, 2018). Transactions copper sulphate recovery process with glucose to form copper nano-powder are carried out in air at atmospheric pressure.

The sequence of stages of copper recovery process of sulfate glucose can be represented by the scheme:

$$CuSO_4 + (C_6H_{12}O_6 + NaOH) \rightarrow Cu_2O \qquad (1)$$

$$Cu_2O + NaOH \rightarrow Cu \qquad (2)$$

Copper sulfate was dissolved in 30% glucose solution at a temperature about 50-60°C. In this solution of the textile samples were placed. The solution was heated to 70°C. Samples were constantly agitated. To maintain the pH between 8-9 it was added sodium hydroxide – in 10, 20, 30 minutes. Under these conditions the reduction of copper oxide Cu_2O to copper Cu was completed. The reaction was ended after 60-70 minutes. The nano-particles of copper were formed both in the structure of the textile material and on its surface. Then the samples without pressing were dried in air.

We found that the nano-sized copper powder was formed not only in the internal structure of the textile web, but also deposited on both external surfaces of the modified material. To fix the surface deposited copper powder, we fixed a thin PET fabric (thickness of about 15-20 microns) on both outer surfaces of the modified fabric with the help of glue material "Sharnet" (f. Boostic, England).

Determination of UV Absorption by Textiles

To determine the extent of absorption of ultraviolet (UV) radiation was used UV dosimeter-radiometer Tensor-71. UV radiometer-dosimeter designed to measure the intensity of irradiation (radiation).

Irradiation of samples was carried out on the Fadometer mark LE-1 model KT7035.

The source of UV radiation is a xenon arc lamp, air-cooled with heat and light filters type OSRAM XENON SHORT ARC DISPLAY/OPTIC LAMP. XBOR XTREME LITE; wavelength range is 200-400nm (Vlasenko *et al*., 2017).

Textiles that are modified by metal nano-particles became also antistatic properties. The combination in one textile material of two fundamentally important health factors provide unique protective properties of textile products.

With the choice of soluble metal salts such as copper, iron, nickel and silver makes it possible to produce nano-modified textile materials for various purposes.

RESULTS OF RESEARCH

The results of UV-light absorption testing are summarized in Table 1. As we can see the modification by nano Cu-particles enhanced the protection properties both in A and in B range of UVR.

Table 1. The degree of ultraviolet light absorption by nano-Cu modified textile at wavelengths A (315-400nm) and B (315-280nm)

Characteristics of the sample	The degree of absorption in the range A,%	The degree of absorption in the range B,%
AS 703*, unmodified	91,8	94,4
AS 703*, modified by Cu	99,6	96,7
Cotton fabric bleached, unmodified	85,3	42,7
Cotton fabric bleached, modified by Cu	93,3	92,1

Note: * - AS 703 PET fabric includes conductive carbon fibers.

Advantage of the chemical method of textile nano-modification from salt solutions:
– simplicity of technology implementation;
– availability of initial reagents;
– low energy intensity of the process;
– the process of formation of nano-particles in micropores of textile material;
– the controlled size of the nano-particles of the metal (with a change of the solution concentration).

CONCLUSION

It was investigated the method of textiles nano-modification from metal-salt solution. It was established that nano-metal particles have deposited in porous textile structure and on its surface.

The developed method is simple, accessible and effective method of nano-sized copper particles obtaining directly in the textile structures. Insoluble nano-particles of copper are formed directly in the porous structure of the PET fibers.

This technique may be recommended for textile nano-modification with metals such as Cu, Ni, and Fe using their soluble salts.

Textiles that are modified by metal nano-particles became also antistatic properties. The combination in one textile material of two fundamentally important health factors provide unique protective properties of textile products.

The solving the problem of protection against UV radiation is the key for solving the problem of protection from electromagnetic radiation in a wide range of wavelengths.

Those innovative materials with multifunctional protective effects may have a wide range of applications (usual clothing, medical protective gown, hospital drapes, protective personal equipment for electricians, farmers, outdoor fabrics, etc.).

REFERENCES

Holick, M. (2016), "Biological Effects of Sunlight, Ultraviolet Radiation, Visible Light, Infrared Radiation and Vitamin D for Health", *Anticancer Research*, 36(3), 1345-1356.

Juzeniene, A. *et al*. (2011), "Solar radiation and human health", *Reports on Progress in Physics*, 74, 066701, p. 56.

Mikkelsen, S.H., Lassen, C. and Warming, M. (2015), "Survey and health assessment of UV filters", *Survey of chemical substances in consumer products*, 142, 81-113.

Prue, H. and Shelley, G. (2013), "Exposure to UV Wavelengths in Sunlight Suppresses Immunity. To What Extent is UV-induced Vitamin D3 the Mediator Responsible?", *Clin Biochem Rev*, 34(1), 3-13.

Singh, M.K. and Singh, A. (2013), "Ultraviolet protection by fabric engineering", *Journal of Textiles*, 16, 21-32.

Vlasenko, V. *et al*. (2017), "Synthesis of metals nano-particles in the porous structure of textiles for UV-shielding", *Vlakna a textil*, №4 (24), 30-33.

Vlasenko, V.I. *et al*. (2018), "Method for modified textile material obtaining", Patent of Ukraine for utility model, No. 125122, Bull No. 8.

Vlasenko, V.I. *et al*. (2016), "Rozrobka tekstylnykh kompozytsiynykh materialiv dlya zasobiv zakhystu vid elektromahnitnoho vyprominyuvannya", Shchorichna Naukova Konferentsiya "Intelektualnyy potentsial XXI veka", p.15-22.

Wong, W.Y. *et al*. (2016), "Influence of reactive dyes on ultraviolet protection of cotton knitted fabrics with different fabric constructions", *Textile research journal*, 86(5), 512-532, https://doi.org/10.1177/0040517515591776.

Wilson, C.A. *et al*. (2008), "Solar protection – Effect of selected fabric and use characteristics on ultraviolet transmission", *Textile Research Journal*, 78, 95–104.

Zaets, V.N. *et al*. (2006), "Molecular mechanisms of the repair of UV-induced damages of plant DNA", *Cytology and Genetics*, 40, 40-68.

Абдуллин, И.Ш., Хамматова, В.В., Кумпан, Е.В. (2005), "Плазменная обработка как метод повышения прочности тканей". *Прикладная физика*, №6, С. 92–94.

Горберг, Б.Л. (2003), "Современное состояние и перспективы использования плазмохимической технологии для обработки текстильных материалов". *Текстильная химия*, №1, С.59–68.

Красина, И.В. (2011), "Разработка и внедрение прорывных ресурсов материалов легкой промышленности". *Вестник Казанского технологического университета*, №5, С.288-290.

Шаехов, М.Ф. (2006), Физика высокочастотного разряда пониженного давления в процессах обработки капиллярно-пористых и волокнистых материалов, *Казань*, 452 с.

PHENOTYPIC CHARACTERIZATION AND ANTIBIOTIC SUSCEPTIBILITIES OF *EWINGELLA AMERICANA* AND *KLUYVERA INTERMEDIA* ISOLATED FROM SOAKED HIDES AND SKINS

EDA YAZICI[1]*, MERAL BIRBIR[2], PINAR CAGLAYAN[2]

[1]*Marmara University, Institute of Pure and Applied Sciences, Istanbul, Turkey,* *Corresponding Author: *eda.yazici@marun.edu.tr*

[2]*Marmara University, Faculty of Arts and Sciences, Biology Department, Istanbul, Turkey,*

Soaked hides and skins may contain different species of family Enterobacteriaceae, originating from animal's feces, soil, and water. Some species of this family may be pathogenic to humans and animals. Hence, phenotypic characteristics and antibiotic susceptibilities of Ewingella americana and Kluyvera intermedia belonging to Enterobacteriaceae were explained in this study. While Ewingella americana was isolated from only one soaked hide, Kluyvera intermedia was isolated from both soaked hide and skin. Phenotypic characterization of these isolates was performed using API 20E test kit. Antibiotic susceptibilities of these isolates were examined by Kirby Bauer Disc Diffusion Test using piperacillin/tazobactam (110μg), amoxicillin/clavulanate (30μg), ampicillin/sulbactam (20μg), amikacin (30μg), tobramycin (10μg), kanamycin (30μg), gentamicin (10μg), streptomycin (10μg), ampicillin (10μg), imipenem (10μg), meropenem (10μg), cefoxitin (30μg), cefuroxime sodium (30μg), ceftazidime (30μg), cephalothin (30μg), ceftriaxone (30μg), norfloxacin (10μg), nalidixic acid (30μg), ofloxacin (5μg), ciprofloxacin (10μg), sulfamethoxazole-trimethoprim (25μg), aztreonam (30μg), chloramphenicol (30μg), tetracyline (30μg). Ewingella americana was resistant against aztreonam, ceftazidime, ceftriaxone but this isolate was intermediate susceptible against cefuroxime sodium, ampicillin, nalidixic acid, tetracyline and chloramphenicol. Kluyvera intermedia was found to be resistant against streptomycin, cephalothin, aztreonam, and ampicillin but it was intermediate susceptible to amikacin, kanamycin, chloramphenicol, imipenem, ceftazidime, ceftriaxone, amoxicillin/clavulanate and ciprofloxacin. Moreover, both isolates were found to be susceptible to other antibiotics. Therefore, effective antibacterial applications should be applied to kill these antibiotic resistant bacteria.

Keywords: Ewingella americana, Kluyvera intermedia, antibiotics, soaked hides and skins

INTRODUCTION

Freshly slaughtered hides/skins may have different species of microorganisms which are related to normal bacterial flora of animal's skin and feces, soil, water and air (Birbir and Ilgaz, 1996; Aslan and Birbir, 2012; Birbir *et al*., 2016). To prevent bacterial growth and decomposition of hides/skins, moisture contents of these organic materials are reduced by drying, salt or brine curing until the beamhouse processes(Bailey, 2003). However, if the curing process has not performed adequately, salt tolerant bacteria, halophilic microorganisms and bacterial members of family *Enterobacteriaceae* may grow and damage to cured and soaked hides/skins (Bailey and Birbir, 1993; Bailey and Birbir, 1996; Birbir and Ilgaz, 1996; Berber and Birbir, 2010; Aslan and Birbir, 2012; Ulusoy and Birbir, 2015; Akpolat *et al*., 2015; Caglayan *et al*., 2017).

In soaking, the hides/skins are rehydrated and dirt, salt, blood, urine, manure, and interfibrillary material have been removed from the hides/skins. Long process duration, high organic content of soaking solution support growth and bacterial activities. Hence, antimicrobial agent is added into soaking solution but high organic content of soak liquor may adversely affect the efficiency of antimicrobial agent. In the study of Rangarajan *et al*. (2003), species of *Bacillus*, *Chromobacter*, *Pseudomonas*, *Clostridium*, *Lactobacillus* and *Serratia* were isolated from soak liquor. It was reported that bacterial populations in first soaking process decreased rapidly but tended to increase over time.

In another study, Pfleiderer *et al*. (1988) isolated bacterial species belonging to genera *Proteus*, *Pseudomonas*, *Bacillus*, *Corynebacterium*, *Clostridium*, *Chromobacter*, *Lactobacillus*, *Micrococcus*, *Sarcina*, *Staphylococcus* and *Serratia* from soak liquors. Moreover, bacterial species of genera *Citrobacter, Edwardsiella, Enterobacter, Escherichia, Hafnia, Klebsiella, Proteus, Salmonella, Serratia* and *Yersinia* belonging to family *Enterobacteriaceae* were isolated from ten salted cattle hides (Aslan and Birbir, 2012). Ulusoy and Birbir (2015) stated that total numbers of *Enterobacteriaceae*; total numbers of proteolytic *Enterobacteriaceae*; total numbers of lipolytic *Enterobacteriaceae* on salted hides and skins were found as between $1.7x10^4$ cfu/g-$4.5x10^5$ cfu/g and between $1.7x10^5$ cfu/g-$1.5x10^6$ cfu/g; between $9.1x10^3$ cfu/g-$3.9x10^5$ cfu/g and between $1.2x10^5$ cfu/g-$1.1x10^6$ cfu/g; between $6.0x10^2$ cfu/g-$3.7x10^5$ cfu/g and between $1.7x10^4$ cfu/g-$5.0x10^5$ cfu/g, respectively.

The family *Enterobacteriaceae* contains 56 genera (*Arsenophonus*, *Biostraticola*, *Brenneria*, *Buchnera*, *Budvicia*, *Buttiauxella*, *Dickeya*, *Calymmatobacterium*, *Cedecea*, *Citrobacter*, *Cosenzaea*, *Cronobacter*, *Sodalis*, *Pragia*, *Edwardsiella*, *Enterobacillus, Enterobacter*, *Erwinia*, *Escherichia*, *Ewingella*, *Franconibacter, Gibbsiella*, *Hafnia*, *Klebsiella*, *Kluyvera*, *Leclercia*, *Leminorella*, *Levinea*, *Lonsdalea*, *Mangrovibacter*, *Moellerella*, *Morganella*, *Obesumbacterium*, *Serratia*, *Pantoea*, *Pectobacterium*, *Phaseolibacter*, *Photorhabdus*, *Plesiomonas*, *Proteus*, *Providencia*, *Raoultella*, *Rouxiella*, *Saccharobacter*, *Salmonella*, *Samsonia*, *Shigella*, *Shimwellia*, *Tatumella*, *Thorsellia*, *Rahnella, Trabulsiella*, *Wigglesworthia*, *Xenorhabdus*, *Yersinia, Yokenella*) 454 named species (http://www.bacterio.net/-classifphyla.html#bacteria). All members of the family *Enterobacteriaceae* are facultative anaerobic, chemoorganotrophic, non-halophilic, non-sporulating, rod-shaped Gram-negative bacteria. Although most of the enteric bacteria may be motile by peritrichous flagella, a few of them are nonmotile. *Enterobacteriaceae* may be found in water, soil, animals and plants. Some species may be pathogenic to humans, animals, plants and insects. Most are oxidase negative, catalase positive and reduce nitrate to nitrite. Acid and gas are produced during fermentation of D-glucose, other carbohydrates and polyhydroxyl alcohols (Brenner and Farmer, 2005).

Newton *et al*. (1977) isolated *Enterobacter liquefaciens*, *Enterobacter aerogenes*, *Enterobacter cloacae*, *Klebsiella pneumoniae*, *Citrobacter* spp. and *Serratia* spp. from 85 hides. Oppong *et al*. (2006) isolated *Citrobacter freundii* and *Proteus vulgaris* from both raw and soaked hides. In the study of Shede *et al*. (2008), *Escherichia coli, Proteus mirabilis*, *Shigella boydii*, *Photorhabdus luminescens, Pantoea agglomerans* were isolated from raw buffalo hides.

Detection of *Ewingella* in vacuum-packaged meat, vegetables, molluscs, shiitake, button and oyster mushrooms, and some clinical specimens taken from blood, wounds, respiratory tracts was reported by the investigators (Muller et al.,1995; Hamilton-Miller and Shah, 2001; Reyes *et al*., 2004). *Ewingella americana* uncommonly causes infection in humans, is associated with nosocomial infections (Grimont *et al*., 1983; Farmer *et al*., 1985; Heizmann and Michel, 1991). *Kluyvera intermedia,* which is a potential pathogen, was isolated from potable water, surface water, soil, human samples such as stool, bile and gall blader (Pavan *et al*.,2005). This organism may cause blood infections, urinary tract and soft tissue infections and septic shock (Janda, 2006).

Antimicrobial agents are commonly used for human and animal health and welfare. Antimicrobial resistance influenced by widespread and inappropriate usage of antimicrobial agents in medicine, veterinary medicine and agriculture is a global public

and animal health concern (Madigan *et al.*, 2015; World Organization for Animal Health, 2015). Antibiotic resistance profiles of some members of Enterobacteriaceae isolated from salted hide and skin samples were examined in our previous study. In that study 70% of the hide and 68% of the sheep skin strains were found to be resistant to three or more of 24 antimicrobial agents. Resistance of the isolates to ampicillin (45%), cefoxitin (20%), kanamycin (9%), ceftriaxone (45%), meropenem (2%), aztreonam (71%), ceftazidime (33%), imipenem (4%), tetracycline (16%), amikacin (5%), ciprofloxacin (5%), cephalothin (16%), gentamicin (5%), amoxycillin-clavulanate (25%), tobramycin (13%), ampicillin-sulbactam (29%), piperacillin-tazobactam (38%), ofloxacin (2%), cefuroxime sodium (45%), chloramphenicol (35%),streptomycin(9%), sulfamethoxazole/trimethoprim (25%) and nalidixic-acid(42%) was detected (Ulusoy, 2014; Birbir *et al.*, 2016).

Although there are several studies on members of the family *Enterobacteriaceae,* antibiotic susceptibilities of *Ewingella americana* and *Kluyvera intermedia* isolated from soaked cattle hides and sheep skin samples treated with antimicrobial agent have not been examined yet. Hence, the goal of the study was to present phenotypic characteristics and antibiotic susceptibilities of *Ewingella americana* and *Kluyvera intermedia.*

MATERIAL AND METHOD

Test Isolates

The isolates were obtained from the soaked cattle hides and sheep skin samples using Eosin Methylene Blue Agar. Phenotypic characterization of these isolates were performed according to catalase and oxidase activities, reduction of nitrate to nitrite and API 20E test kit containing biochemical tests such as β-galactosidase, arginine dihydrolase, lysine decarboxylase, ornithine decarboxylase, utilization of citrate, production of H_2S, urease, tryptophan deaminase, production of indole from tryptophan, Voges-Proskauer, production of gelatinase, fermentation of glucose, mannose, inositol, sorbitol, rhamnose, sucrose, melibiose, amygdalin, arabinose (Yazici and Birbir, 2018).

Antibiotic Susceptibility Test

One isolate of *Ewingella americana* and two isolates of *Kluyvera intermedia* were grown on Mueller Hinton Agar at 37°C for 24 hours and the isolates were separately inoculated into Mueller Hinton Broth and incubated at 37°C for 24 hours. Then, the bacterial density of these isolates was adjusted to approximately $1x10^8$ cfu/mL. Disc diffusion susceptibility method was used to detect antibiotic susceptibilities of the isolates (CLSI, 2014; EUCAST, 2014). 24 antimicrobial agents belonging to 9 categories such as tetracyclines (tetracyline), carbapenems (imipenem, meropenem), aminoglycosides (amikacin, kanamycin, tobramycin, streptomycin, gentamicin), monobactams (aztreonam), penicillins (β-lactam/β-lactamase inhibitor combinations) (piperacillin/tazobactam, amoxicillin/clavulanate, ampicillin/sulbactam, ampicillin), cephalosporins I, II and III (cefoxitin, cefuroxime sodium, ceftazidime, cephalothin, ceftriaxone), quinolones and fluoroquinolones (norfloxacin, ofloxacin, nalidixic acid, ciprofloxacin), amphenicols (chloramphenicol) and sulfonamides, dihydrofolate reductase inhibitors combinations (sulfamethoxazole/trimethoprim), were utilized in the present study. The antimicrobial agents were placed on the Mueller Hinton Agar plate

inoculated with test isolate. After incubation at 37°C for 24 hours, the zones of growth inhibition around each of the test antibiotics were measured and the results were evaluated according to the criteria explained by the of Clinical and Laboratory Standards Institute (CLSI, 2014) and European Committee on Antimicrobial Susceptibiliy Testing (EUCAST, 2014). The test antimicrobial agents were purchased from Oxoid (Basingstoke, Hants, UK).

RESULTS AND DISCUSSION

While *Ewingella americana* was isolated from only soaked hide (CH10), *Kluyvera intermedia* was isolated from both soaked hide and skin samples (SS3 and CH1). Although *Ewingella americana* showed positive reactions of β-galactosidase, Voges-Proskauer, citrate utilization, catalase, nitrate reduction to nitrite, acid production from glucose and mannitol, negative reaction was detected in H$_2$S production, oxidase, urease, gelatinase, tryptophan deaminase, indol production, ornithine decarboxylase, lysine decarboxylase, arginine dihydrolase, acid production from inositol, sorbitol, rhamnose, sucrose, melibiose, amygdalin and arabinose (Yazici and Birbir, 2018). These biochemical test results were similar to the results mentioned in Janda (2006).

Ewingella americana was resistant to aztreonam, ceftazidime and ceftriaxone. While *Ewingella americana* was intermediate susceptible to cefuroxime sodium, ampicillin, nalidixic acid, tetracyline and chloramphenicol, this isolate was susceptible to tobramycin, gentamicin, kanamycin, streptomycin, amikacin, meropenem, imipenem, cephalothin, cefoxitin, ampicillin/sulbactam, amoxicillin/clavulanate, ciprofloxacin, piperacillin-tazobactam, sulfamethoxazole-trimethoprim, norfloxacin and ofloxacin in the present study. Bukhari and colleagues (2008) mentioned that *E. americana*, which was isolated from a patient, was resistant to ceftazidime and ceftriaxone. Our antibiotic results were similar to that study (Bukhari *et al*., 2008). Resistance of this isolate to ceftriaxone and aztreonam was stated by Pound *et al*. (2007). Moreover, Pound *et al*. (2007) detected that *E. americana*, isolated from a patient with a chronic pulmonary disease, was also resistant to amikacin, gentamicin, tobramycin, ampicillin, ampicillin/sulbactam, cefoxitin, ciprofloxacin, imipenem, and tetracycline. While the isolate was found to be intermediate susceptible to piperacillin/tazobactam, ceftazidime, susceptible to sulfamethoxazole/trimethoprim (Pound *et al*., 2007). In our study, the susceptibility of *E. americana* against aminoglycosides, carbapenems, fluoroquinolones, sulfamethoxazole/trimethoprim and cefoxitin were consistent with antibiotic test results of Stock *et al*. (2013). The researchers emphasized that *E. americana* has natural susceptibility to most antibiotics including aminoglycosides, aztreonam, cefepime, cefotaxime, trimethoprim/sulfamethoxazole, carbapenems, cefoxitin, fluoroquinolones, tetracyclines and chloramphenicol. In another study, all hide isolates of *Ewingella americana* were susceptible to tobramycin, gentamicin, kanamycin, streptomycin, amikacin, cefoxitin, imipenem, meropenem, piperacillin-tazobactam, ofloxacin, amoxicillin/clavulanate, norfloxacin, ciprofloxacin, cephalothin, ampicillin/sulbactam and sulfamethoxazole-trimethoprim, these isolates were detected as resistant to aztreonam, ceftazidime and ceftriaxone. *Ewingella americana* was found to be intermediate susceptible to tetracyline, nalidixic acid, ampicillin, cefuroxime sodium and chloramphenicol (Birbir *et al*., 2016). Although *Kluyvera intermedia* exhibited positive reactions of β-galactosidase, ornithine decarboxylase, catalase, nitrate reduction To nitrite, acid production from glucose, arabinose, amygdalin, mannitol, sorbitol and melibiose, negative reaction was detected in citrate utilization, H$_2$S production, oxidase,

urease, tryptophan deaminase, gelatinase, arginine dihydrolase, lysine decarboxylase, Voges-Proskauer, indol production, acid production from inositol and sucrose (Yazici and Birbir, 2018).

In this study, *Kluyvera intermedia* was resistant against streptomycin, cephalothin, aztreonam, ampicillin but susceptible against piperacillin-tazobactam, tobramycin, gentamicin, meropenem, cefoxitin, nalidixic acid, ampicillin/sulbactam, tetracyline, norfloxacin, ofloxacin, cefuroxime sodium, sulfamethoxazole-trimethoprim. This isolate was found to be intermediate susceptible to amikacin, kanamycin, chloramphenicol, amoxicillin/clavulanate, ceftriaxone, ciprofloxacin, imipenem and ceftazidime.

In another study, resistance of three *Kluyvera intermedia* strains*,* isolated from sink and distinct taps in an intensive care unit in Brazil, against meropenem, imipenem, ertapenem, doripenem was stated by Ribeiro *et al*. (2014). It was stated that two *Kluyvera intermedia* strains were susceptible against ceftriaxone, cefepime and aztreonam. In our study, resistance of *K. intermedia* against aztreonam, susceptibility to meropenem and intermediate susceptibility to imipenem and ceftriaxone were detected.

CONCLUSIONS

This is the first report that investigates antibiotic susceptibility profiles of *Ewingella americana* and *Kluyvera intermedia,* isolated from soaked cattle hides and sheep skins, against 24 different antimicrobial agents in leather industry. While *E. americana* was resistant against three antibiotics (aztreonam, ceftazidime and ceftriaxone), *K. intermedia* was resistant to four antibiotics (streptomycin, cephalothin, aztreonam, ampicillin). Due to resistance of these isolates against the antibiotics used in both human and veterinary medicine, we suggest effective antibacterial applications in leather industry to eradicate these antibiotic resistant microorganisms.

REFERENCES

Akpolat, C. *et al.* (2015), "Molecular Identification of Moderately Halophilic Bacteria and Extremely Halophilic Archaea Isolated From Salted Sheep Skins Containing Red and Yellow Discolorations", *JALCA*, 110(7), 211-220.

Aslan, E. and Birbir, M. (2012), "Examination of Gram Negative Bacteria on Salt-pack Cured Hides", *JALCA*, 107(4), 106-115.

Bailey, D.G. and Birbir, M. (1993), "A Study of the Extremely Halophilic Microorganisms Found on Commercially Brine-Cured Cattle Hides", *JALCA*, 88(8), 291-299.

Bailey, D.G. and Birbir, M. (1996), "The Impact of Halophilic Organisms on The Grain Quality of Brine Cured Hides", *JALCA,* 91(2), 47-51.

Bailey, D.G. (2003), "The Preservation of Hides and Skins", *JALCA*, 98,308-319.

Berber, D. and Birbir, M. (2010), "Examination of Bacterial Populations in Salt, Salted Hides, Soaked Hides and Soak Liquors", *JALCA*, 105(10), 320-326.

Birbir, M. and Ilgaz, A. (1996), "Isolation and Identification of Bacteria Adversely Affecting Hide and Leather Quality", *JSLTC,* 80(5), 147-153.

Birbir, M., Ulusoy, K. and Caglayan, P. (2016), "Examination of Multidrug-resistant *Enterobacteriaceae* Isolated from Salted Cattle Hides and Sheep Skins", *JALCA,* 111(9), 334-344.

Brenner, D.J. and Farmer, J.J. III. (2005), "Order XIII *Enterobacteriales,* Family I. *Enterobacteriaceae".* in: Brenner, D. J., Krieg, N. R., Staley, J. T and Garrity, G. M.(eds.), Bergey's Manual of Systematic

Bacteriology. The Proteobacteria, The Gammaproteobacteria, 2nd ed., Springer, East Lansing, 587-850, https://doi.org/10.1007/0-387-28022-7.

Bukhari, S.Z. *et al*. (2008), "Multi-drug Resistant *Ewingella americana*", *Saudi Med J.*, 29, 1051-1053.

Caglayan, P. *et al*. (2017), "Screening of Industrially Important Enzymes Produced by Moderately Halophilic Bacteria Isolated from Salted Sheep Skins of Diverse Origin", *JALCA*, 112(6), 207-216.

CLSI (Clinical and Laboratory Standards Institute) (2014), *Performance Standards for Antimicrobial Susceptibility Testing*; 24th Informational Supplement, CLSI document M100-S24.

EUCAST (The European Committee on Antimicrobial Susceptibility Testing) (2014), *Breakpoint Tables for Interpretation of MICs and Zone Diameters*, Version 4.0, www.eucast.org.

European Commission (2013), *Tanning of Hides and Skins*, Joint Research Centre, European Bureau.

Farmer J.J.III *et al.* (1985), "Biochemical Identification of New Species and Biogroups of *Enterobacteriaceae* Isolated from Clinical Specimen", *J Clin Microbiol.*, 21, 46-76.

Grimont, P.A.D. *et al*. (1983), "*Ewingella americana* gen. nov., sp. nov., A New *Enterobacteriaceae* Isolated from Clinical Specimens", *Ann Inst Pasteur Microbiol.*, 134, 39-52, https://doi.org/10.1016/0769-2609(83)90102-3.

Hamilton-Miller, J.M.T. and Shah, S. (2001), "Identity and Antibiotic Susceptibility of Enterobacterial Flora of Salad Vegetables", *Int J Antimicrob Agents*, 18, 81-83, https://doi.org/10.1016/S0924-8579(01)00353-3.

Heizmann, W.R. and Michel, R. (1991), "Isolation of *Ewingella americana* froma Patient with Conjunctivitis", *Eur J Clin Microbiol Infect Dis.* 10, 957-959, https://doi.org/10.1007/BF02005452.

Janda, J.M. (2006), "New Members of the Family *Enterobacteriaceae*", in: Dworkin, M., Falkow, S., Rosenberg, E., Schleifer, K. H., Stackebrandt, E. (eds) The Prokaryotes, A Handbook on the Biology of Bacteria, 3rd ed., Volume 6, Proteobacteria:Gamma Subclass, Springer, Minneapolis, 5-40.

Madigan, M.T. and Martinko, J.M. (2015), Brock Biology of Microorganisms, 14th ed., Pearson Education Limited, Edinburg Gate.

Muller, H.E., Fanning, G.R. and Brenner, D.J. (1995), "Isolation of *Ewingella americana* from Mollusks" *Curr Microbiol*. 31, 287-290, https://doi.org/10.1007/BF00314581.

Newton, K.G., Harrision, J.C.L and Smith, K.M. (1977), "Coliforms from Hides and Meat.", *Appl Environ Microbiol.,* 33,199-200.

Oppong, D. *et al*. (2006), "Application of Molecular Techniques to Identify Bacteria Isolated from the Leather Industry", *JALCA,*101, 140-145.

Pavan, M.E. *et al.* (2005), "Phylogenetic Relationships of the Genus *Kluyvera*: Transfer of *Enterobacter intermedius* Izard *et al*.1980 to the Genus *Kluyvera* as *Kluyvera intermedia* comb. nov. and Reclassification of *Kluyvera cochleae* as a Later Synonym of *K. intermedia*", *Int J Syst Evol Microbiol.*, 55, 437-442, https://doi.org/10.1099/ijs.0.63071-0.

Pfleiderer, E. and Reiner, R. (1988), "Microorganisms in Processing of Leather" in: *Biotechnology Vol 6b. Special Microbial Processes* H.J.Rehm (ed.), VCH, Weinheim, Germany, 730-739.

Pound, M.W., Tart, S.B. and Okoye, O. (2007), "Multidrug-resistant *Ewingella americana*: A Case Report and Review of The Literature", *Ann Pharmacother.*, 41, 2066-2070.

Rangarajan, R., Didato, T.D. and Bryant, S. (2003), "Measurement of Bacterial Populations in Typical Tannery Soak Solutions by Traditional and New Approaches", *JALCA,* 98, 477-485.

Reyes, J.E. *et al*. (2004), "Prevalence of *Ewingella americana* in Retail Fresh Cultivated Mushrooms (*Agaricus bisporus, Lentinula edodes* and *Pleurotus ostreatus*) in Zaragoza (Spain)", *FEMS Microbiol Ecol.*, 47(3), 291-296, https://doi.org/10.1016/S0168-6496(03)00283-6.

Ribeiro, V.B. *et al*. (2014), "Detection of blaGES-5 in Carbapenem-Resistant *Kluyvera intermedia* Isolates Recovered from the Hospital Environment", *Antimicrob Agents Chemother.*, 58(1), 622-623, https://doi.org/10.1128/AAC.02271-13.

Shede, P.N. *et al*. (2008), "Bacterial Succession on Raw Buffalo Hide and Their Degradative Activities Ambient Storage", *Int Biodeterior Biodegradation*, 62, 65-74, https://doi.org/10.1016/j.ibiod.2007.12.007.

Stock, I., Sherwood, K.J. and Wiedemann, B. (2003), "Natural Antibiotic Susceptibility of *Ewingella americana* Strains", *J Chemother.*, 15,428-41.

Ulusoy, K. (2014), "Isolation and Identification of Bacterial Species Belonging to Family *Enterobacteriaceae* on Salted Hides and Skin Samples and Determination of Their Antibiotic Resistance", Marmara University, Institute of Pure and Applied Sciences.

Ulusoy, K. and Birbir, M. (2015), "Identification and Metabolic Activities of Bacterial Species Belonging to the *Enterobacteriaceae* on Salted Cattle Hides and Sheep Skins", *JALCA*, 110(6), 186-199.

World Organization for Animal Health (OIE) (2015), *OIE List of Antimicrobial Agents of Veterinary Importance*, Geneva: World Health Organization.

Yazici, E. and Birbir, M. (2018), "Examination of Catabolic Activities of *Enterobacteriaceae* Isolated from Soaked SheepSkins and Cattle Hides", *JSLTC*, 102(3), 130-136.

***, http://www.bacterio.net/-classifphyla.html#bacteria, 21.06.2018.

VII.

MODELLING AND SIMULATION

THE FINITE ELEMENT ANALYSIS OF A POLYMER BASED TRIANGULAR CELL SANDWICH COMPOSITE

ION DURBACĂ[1], ADRIAN-COSTIN DURBACĂ[2]

[1] *„Politehnica" University of Bucharest, ion.durbaca@yahoo.com*
[2] *Richard Alan Engineering LTD, Dewsbury* (UK)*, costin.durbaca@yahoo.com*

Finite Element Analysis (FEA) method is used for analysing the mechanical behaviour of standardized tensile and bending (3-point) test specimens made from a multi-layered composite material with two outer polymer facesheets (synthetic glass / plexiglass) and a triangular cellular core. This analysis uses for design and modelling, the software Autodesk Inventor Professional, which will import later the model in the FEA analysis software - ANSYS 14.5. Highlighting the mechanical behaviour of the composite structure specific to the test specimens having cellular polymeric core (ABS, PLA, PC and CF triangular cells, with thicknesses 3 and 5 mm) and analysing the stress/strain state and specific deformations and correlating the FEA simulation results with the experimental tests lead to quasi-equivalent results under similar stress conditions until the specimen fails. Therefore, the FEA analysis of the mechanical assemblies is taking an important step forward in the modern design process, being one of the ways of identifying the von Mises equations and deformation fields in the composite above structures.

Keywords: test specimen, composite, sandwich, finite element analysis, cellular core, simulation.

INTRODUCTION

Because the highly complex analytical methods, it is almost impossible to apply them for a wide variety of mechanical structures. Therefore, many calculation of composite structures problems were solved with the use of numerical methods. It eliminates the need to write and solve complex equations with partial derivatives that characterize composite materials. Numerical calculation methods have the advantage of being applicable to more general classes of problems. Among the numerical methods, the finite element method (FEA) takes an important place in the analysis of structures made of composite materials, in general, or multi-layer materials, in particular (Durbacă, 2018).

The current development of sandwich composite structures makes it possible to use them with very good results in many industrial fields (aeronautics, aerospace, naval, motor, railway, industrial process equipment etc.), thus representing a scientific research direction in full progress. Cellular materials made from polymeric materials are now readily available, although prices are higher than standard products and they continue to have a massive market introduction as a result of the manufacturing process. Such materials are used in a variety of applications: sandwich panel cores, starting from simple and inexpensive parts to complex and advanced aerospace components (Syngellakis, 2016).

In literature, the cellular structure is referred to as the cellular core due to its positioning in a sandwich assembly comprising of two outer skins on the other side of the cellular core together with the joint attachment between the core and the outer shells (i.e. attaching with thin and ultra-adherent film coatings). This joining addition causes the cellular core and outer shells to behave as a continuous structure, thus transferring axial and transverse loads to and from the cellular core that provide sufficient rigidity to maintain equidistance between the outer skins. From a structural point of view (see Figure 1), the main function of the cell core is to stabilize the outer shells to avoid

buckling and deformation and to withstand the shear stresses along its thickness. The outer shells bear alongside some of the local stresses and tension and compression stresses, and their primary function is to provide the bend and shear stiffness of the sandwich assembly.

(a)   (b)
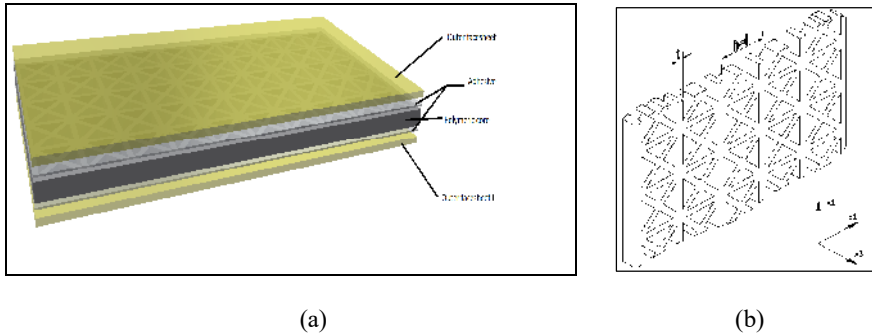
Figure 1. The main components of the sandwich composite structures (a) and the geometry of the cellular core (b)

The intense preoccupations in the international academic environment, demonstrated by the large number of scientific papers published in the field and supported by the results obtained in various industrial applications, reflect the practical importance of the finite element analysis of any composite layered structures (Itu, 2014).

Since many of the drawbacks found in the laboratory tests stem from their dependence on the prototype configuration, and the construction of an experimental prototype for each composite structure variant would sometimes be difficult to achieve in terms of execution, it is fully justified to apply the FEA as an innovative and of great interest for the future, both economically and in terms of simulation time.

Therefore, the use of modelling and simulation through the finite element analysis of the mechanical system components occupies an important place in the modern design process and is one of the ways to identify deformation fields and equivalent stresses within the analysed composite structures.

DESCRIPTION OF THE ANALYSIS MODEL WITH FINITE ELEMENT

The Finite Element Analysis Model with Triangular Cellular Polymer Layered Composite Specimens have been modelled and designed using 3D Autodesk Inventor, and imported in the FEA Analysis software, ANSYS 14.5 – Workbench (Durbacă and Durbacă, 2011).

The aim of the finite element analysis simulation is to highlight the mechanical behaviour of the composite structures specimens with cellular polymer core from ABS (acrylonitrile-butadiene-styrene), PC (Polycarbonate), PLA (polylactic acid) or CF (carbon fibre) having a thickness of 3 and 5 mm, which will study the stress and deformation conditions specific to the tensile and bending stresses (at 3 points) of the above structures.

If the results of the FEA analysis study reveal a good consistency with experimentally obtained results, it can be discarded in subsequent studies to use experimental tests, leading implicitly to direct economic effects.

Geometric Definition of the Model

Using the design drawings of standardized test specimens for tensile stress tests (EN ISO 527-1: 2012) and bending (EN ISO 14125: 2000), the model was designed and modelled using the Autodesk Inventor Professional software (see Figure 2).
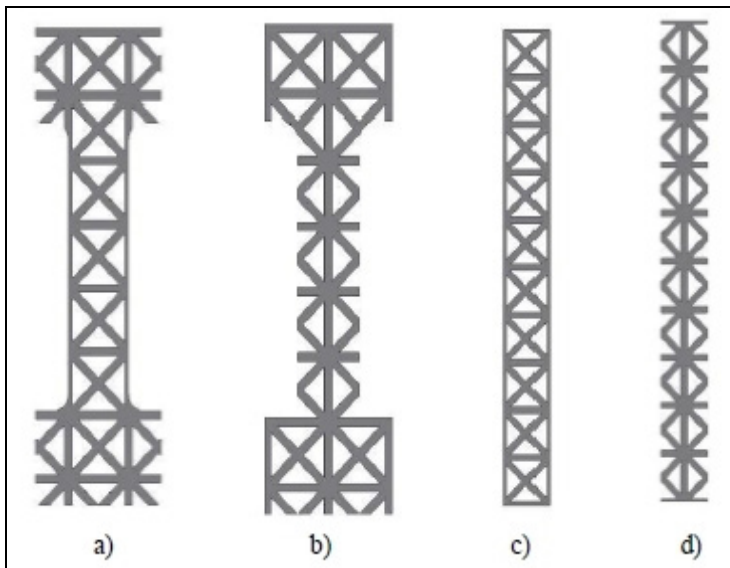
Figure 2. Representation of the 3D model made in Autodesk Inventor (Durbacă, 2018): a) closed cell tensile test specimen (type 1); b) open cell tensile test specimen (type 2); c) open cell bending test specimen (type 1); d) closed cell bending test specimen (type 2)

Meshing

By exporting the 3D models made in the Autodesk Inventor to the ANSYS software, the models were pre-processed: meshing and defining the boundary conditions specific to each type of specimen (ABS 3.1 / ABS 3.2, ABS 5.1 / ABS 5.2; PC 3.1 / CF 3.2; CF 5.1 / CF 5.2; PLA 3.1 / PLA 3.2; PLA 5.1 / PLA 5.1; CF 3.1 / CF 3.2; CF 5.1 / CF 5.2) Figures 3.

Each model was analysed separately using a static analysis, considering the nonlinear plastic characteristics of each material. It has been considered that the adhesive achieves perfect bonding of the layers (contact method between faces in ANSYS - "Bonded"). For meshing, I was considered an average size of the finite element of 1 mm and a Hex dominant method.
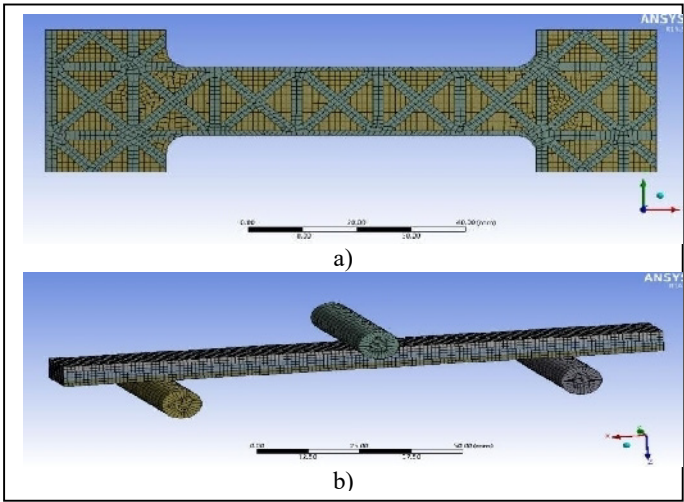
Figure 3. Pre-processing (meshing) of PLA3.1 specimen analysis on traction (a) and bending (b) (Durbacă, 2018)

Defining Structural Characteristics

The Finite Element Analysis requires knowledge of physical properties and mechanical behaviours for the calculation of stiffness matrices of finite elements. These can be grouped into geometric properties and material properties as shown in Table 1.

Table 1. Properties of polymer materials used in FEA analysis (Durbacă, 2018)

Property	PLA	PLA+40% carbon fibre	ABS	PC	PMMA
Density ρ [g/cm^3]	1.25	1.29	1.1	1.2	1.18
Elastic modulus E [GPa]	2.5	2.2	2.2	1.96	2.7
Elongation [%]	6	2	2.6	4	3
Yield strength [MPa]	40	48	42	50	50
Tensile strength [MPa]	45	52	49	55	60
Shear modulus g [GPa]	0.92	0.81	0.81	0.72	0.99
Poisson's ratio υ	0.36	0.36	0.35	0.37	0.37

In the case of the MEF analysis of the 16 types of specimens, 5 types of materials were considered. Thus, the superior faces are made of synthetic glass (PMMA or plexiglass), and the cellular core of ABS, PLA, CF and PC, having thicknesses of 3 mm and 5 mm.

RESULTS AND DISCUSSIONS

The post-processing of results aims to analyse the yield stresses and maximum deformation forces for each type of specimen and corresponding to each type of test. These are shown in Figures 4 ÷ 6, for the PLA cellular polymer specimens, and the maximum stresses were analysed based on the stress gradient.
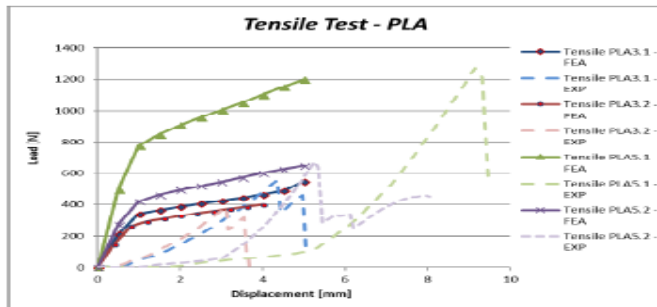
Figure 4. Deformation (elongation) force diagram for tensile stress simulations of composite material specimens having a PLA cellular polymer core of 3 mm thickness (PLA3.1, PLA3.2) and 5 mm (PLA5. 1; PLA5.2) (Durbacă, 2018)
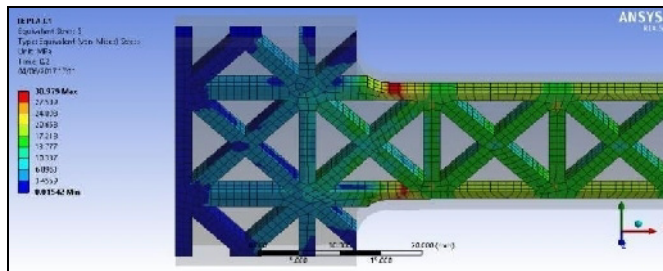
Figure 5. Maximum equivalent stresses in the PLA3.1 composite core [1]
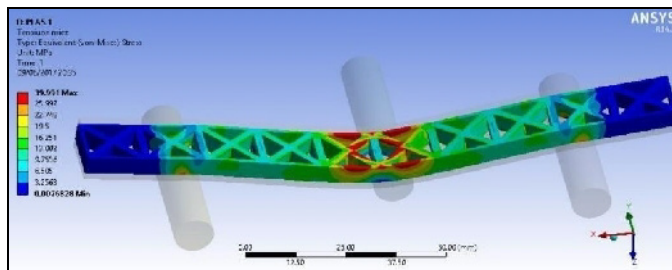
Figure 6. Maximum equivalent stresses in the composite core PLA5.1 (Durbacă, 2018)

For the other specimens having the ABS, CF and PC cellular core, the simulation results are analysed and presented in Durbacă, 2018.

CONCLUSIONS

The Finite Element method allows for a postcritical calculation of the structure in which damage has occurred, both in order to determine the load-bearing capacity of the structure and to observe how the material behaves under a certain damage (propagation of defects). The FEA analysis of mechanical system occupies an important place in the

modern design process, being one of the ways to identify deformation and stress fields in the structures in question.

Analysing the applied force - maximum strain diagrams for each type of simulated specimen in both cases, traction and 3 points bending, the following were observed:

- the differences between applied force values relative to the maximum deformations for each core configuration (closed cells "1" and open cells "2") are visible, resulting in higher resistances of closed cell specimens;
- due to the finite element analysis in the plastic field, the maximum forces are the cause of a single failure mode, namely the most vulnerable to the failure component, namely the upper / lower faces, which is not always the case for laminated composites in which yield mode is complex, and the yield curve can also be described by the later yield of the core;
- the differences in applied force values relative to the maximum deformations between closed cell specimens "1" and "2" open cells are 10-50%.

Using the finite element method, you can study several modifications, namely: changing load conditions, boundary conditions, and how to apply them to the virtual model; In this way you can choose the optimal version, the dimensions and the elastic characteristics of the materials.

Thanks to the FEA, there are advantages to comparing and verifying the strength of a material, measuring the stresses, deformations that may exist in the material, and whether they are within normal limits, so as to save a lot of time, much faster, reduce costs, to each part of the structure.

REFERENCES

Durbacă, A.C. (2018), "Cercetări teoretice și experimentale privind evaluarea caracteristicilor fizico – mecanice ale plăcilor polimerice de tip sandwich cu miez compus din celule triunghiulare", Teză de Doctorat, Universitatea POLITEHNICA din București.

Durbacă, A.C. *et al*. (2017), "Experimental research on the triangular lattce type polymer based composite structure for sandwich panel construction București", *Revista de Materiale Plastice*, 54(4), 639 – 644.

Durbacă, I. and Durbacă, A.C. (2011), "Injection moulding simulation of polymer structures modeled with finite element", *The Scientific Bulletin of Valahia University Materials and Mechanics*, no. 6 (year 9), p. 156 - 159.

Itu, C. (2014), "Contribuții privind îmbunătățirea plăcilor circulare realizate din materiale compozite stratificate", Teză de Doctorat, Universitatea "Transilvania" din Brașov.

Sorohan, S. (2015), *Practica modelării cu elemente finite - Note de curs*, Universitatea Politehnica din București.

Syngellakis, S. (2016), *Composites: Advances in Manufacture and Characterisation*, Wessex, UK: Wessex Institute of Technology, UK, ISBN 978-1-78466-167-0.

ESTABLISHING ANTHROPOMETRIC FOOT SIZES OF THE MALE POPULATION IN ROMANIA IN ORDER TO DEVELOP AN ORIGINAL ROMANIAN STANDARD

MIRELA PANTAZI, ANA MARIA VASILESCU

INCDTP - Division Leather and Footwear Research Institute, 93 Ion Minulescu St., Bucharest, Romania, email: icpi@icpi.ro

The purpose of this scientific paper is to present aspects related to a pre-project to develop an Original Romanian Standard by establishing anthropometric foot sizes of Romanian male population, specifying the size systems used in the design and development of lasts used to make shoes in the footwear industry. In the anthropometric survey conducted in Romania, the 3D shape of the foot in order to calculate anthropometric parameters was captured using the INFOOT USB system made up of the 3D scanner and the dedicated MEASURE 2.8 software. Anthropometric studies were conducted on a sample of 300 male subjects from three geographic regions of Romania: South (100 subjects), East (100 subjects) and Centre and West (100 subjects), aged between 24 and 72. Subjects with particular anthropometric features, including deformities and structural abnormalities of the foot, were excluded. Sizes obtained by processing are itemised in an individual anthropometric chart. A data base comprising 300 anthropometric charts was compiled. Values of each dimensional parameter were centralized in a table that constitutes a database. Anthropometric data were grouped for each foot size. The interdimensional interval was determined for each anthropometric size, for each size and standardized values were established.

Keywords: anthropometric parameter, size, foot.

INTRODUCTION

Making high quality footwear with an optimal comfort degree is conditioned by mastering processing techniques of anthropometric data from 3D foot scanning, by transposing anatomic-morphological and biomechanical information into design and modelling parameters for lasts and footwear models. Correlating the inner sizes of shoes with anthropometric foot sizes is particularly important in order to meet comfort conditions (Mochimaru *et al.*, 2000; Nácher *et al.*, 2006; Reel *et al.*, 2010). Building the anthropometric database and studying it will enable us to make anthropometric standards in accordance with the current sizes of the population.

MATERIALS AND METHODS

3D Image Capturing of the Foot and Processing Data Required to Make a Database for Anthropometric Parameters

In the anthropometric survey conducted in Romania, the 3D shape of the foot in order to calculate anthropometric parameters was captured using the INFOOT USB system (Fig. 1) made up of the 3D scanner and the dedicated MEASURE 2.8 software. The system enables scanning the foot shape and is intended for use in research, to design suitable footwear lasts (Sarghie, 2013).
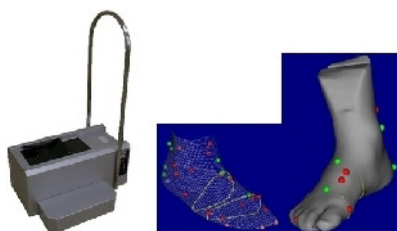
Figure 1. 3D Scanner (INFOOT) - Capturing foot sizes using the 3D scanner

As a result of foot shape scanning operations and placing anatomical points on the surface of the scanned foot shape, values are determined for 20 anthropometric parameters (Table 1).

Table 1. Anthropometric parameters of the foot

1.	Foot length	Lp	(mm)	11.	Toe 1 height	Hd1	(mm)
2.	Ball girth circumference	Pd	(mm)	12.	Toe 5 height	Hd5	(mm)
3.	Foot breadth	ld	(mm)	13.	Height of navicular	Hn	(mm)
4.	Instep circumference	Pr	(mm)	14.	Height of Sphyrion fibulare	Hsf	(mm)
5.	Heel breadth	lc	(mm)	15.	Height of Sphyrion	Hs	(mm)
6.	Instep length	Lr	(mm)	16.	Height of the most lateral point of lateral malleolus	Hme	(mm)
7.	Toe height	Hd	(mm)	17.	Height of the most medial point of medial malleolus	Hmi	(mm)
8.	Instep height	Hr	(mm)	18.	Heel angle	Uc	(°)
9.	Toe 1 angle	Ud1	(°)	19.	Heel girth	Pc	(mm)
10.	Toe 5 angle	Ud5	(°)	20.	Ankle girth	Pg	(mm)

Developing a Database of Anthropometric Foot Parameter Values of Adult Male Population in Romania

Anthropometric studies were conducted on a sample of 300 male subjects from three geographic regions of Romania: South (100 subjects), East (100 subjects) and Centre and West (100 subjects), aged between 24 and 72. Subjects with particular anthropometric features, including deformities and structural abnormalities of the foot, were excluded. Sizes obtained by processing are itemised in an individual anthropometric chart (Fig. 2). A data base comprising 300 anthropometric charts was compiled (Fig. 3).
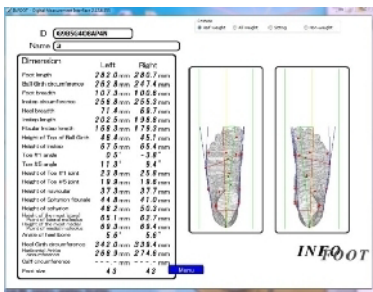
Figure 2. Individual anthropometric file   Figure 3. Database of anthropometric files
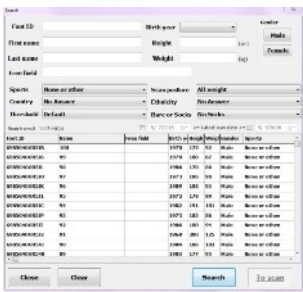
Statistical processing of data will enable the development of anthropometric standards in accordance with the current sizes of the population.

RESULTS AND DISCUSSIONS
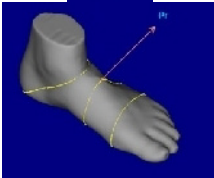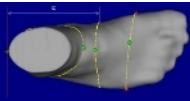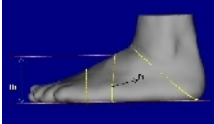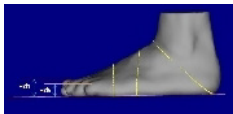
Pre-project for Developing an Original Romanian Standard
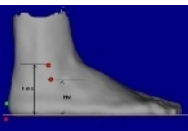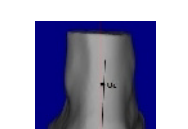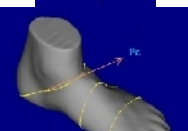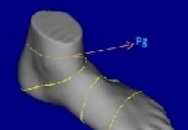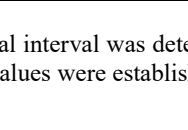
In order to establish anthropometric foot sizes of Romanian male population, the 20 anthropometric parameters are presented and described in Table 2.

Table 2. Anthropometric foot parameters of adult male population

No.	Anthropometric parameters		
	Name and u.m.	Image	Description
1	Foot length Lp (mm)		Distance measured in the horizontal plane, between the perpendiculars to the extremities of toe 2 and the most protruding part of the heel
2	Ball girth circumference Pd (mm)		The circumference of the foot measured through the points that mark toe 1 and toe 5

No.	Anthropometric parameters		
	Name and u.m.	Image	Description
3	Foot breadth ld (mm)		Projection on a horizontal plane of the toe circumference, which represents the horizontal distance between the perpendiculars in contact with the first and fifth metatarsophalangeal joints
4	Instep circumference Pr (mm)		The circumference of the foot measured through the point marking the instep
5	Heel breadth lc (mm)		Projection of heel girth on a horizontal plane
6	Instep length Lr (mm)		The distance measured horizontally between the perpendiculars passing through the point marking the instep and the most protruding part of the heel
7	Toe height Hd (mm)		The vertical distance measured between the highest point on the line marking the ball girth and the horizontal plane tangent to the plantar part of the foot
8	Instep height Hr (mm)		The distance measured vertically between the point marking the instep and the horizontal plane tangent to the plantar part of the foot
9	Toe 1 angle Ud1 o		The angles formed by the tangents in the vertical plane at the first and the fifth metatarsophalangeal joint and the lines joining the points marking the two joints with the ends of the heel width
10	Toe 5 angle Ud5 o		
11	Toe 1 height Hd1 (mm)		The measured vertical distance between the point marking the joint of toe 1 and the point marking the joint of toe 5 and the horizontal plane tangent to the plantar part of the foot
12	Toe 5 height Hd5 (mm)		

No.	Anthropometric parameters		
	Name and u.m.	Image	Description
13	Height of navicular Hn (mm)		The distance measured vertically between the point of the navicular and the horizontal plane tangent to the plantar part of the foot
14	Height of Sphyrion fibulare Hsf (mm)		The measured vertical distance between the lower point of the lateral malleolus and the horizontal plane tangential to the plantar part of the foot
15	Height of Sphyrion Hme (mm)		The measured vertical distance between the point marking the center of the lateral malleolus and the horizontal plane tangent to the plantar part of the foot
16	Height of the most lateral point of lateral malleolus Hs (mm)		The measured vertical distance between the lower point of the medial malleolus and the horizontal plane tangent to the plantar part of the foot
17	Height of the most medial point of medial malleolus Hmi (mm)		The distance measured vertically between the point marking the center of the medial malleolus and the horizontal plane tangent to the plantar part of the foot
18	Heel angle Uc o		The angle formed by the horizontal perpendicular through the most prominent part of the heel and the inclined axis of the foot
19	Heel girth Pc (mm)		The circumference of the foot measured through the junction and the extreme rear points of the foot
20	Ankle girth Pg (mm)		The circumference of the foot measured through the points marking the malleoli

The interdimensional interval was determined for each anthropometric size, for each size and standardized values were established.

Basic sizes required for making lasts are: foot length (Lp), ball girth (Pd), instep girth (Pr), ball width (ld) and heel width (lc). Standardized variants for these parameters, for each size are presented in Table 3.

Table 3. Standardized variants for basic parameters, for each size

Anthropometric parameter (u.m.)	Foot size							
	39	40	41	42	43	44	45	46
Lp (mm)	245	253	261	269	277	285	293	301
Pd (mm)	248	254	260	266	272	278	284	290
Pr (mm)	250	255	260	265	270	275	280	285
ld (mm)	102.3	104.5	106.7	108.9	111.1	113.3	115.5	117.7
lc (mm)	64.8	66.2	67.6	69	70.4	71.8	73.2	74.6

Limits of interdimensional intervals for parameters Lp and Pd are indicated in Tables 4 and 5.

Table 4. Limits of interdimensional intervals for foot length

Standardized value (mm)	Interdimensional interval (mm)	Standardized value (mm)	Interdimensional interval (mm)
245	241-248.9	277	273-280.9
253	249-256.9	285	281-288.9
261	257-264.9	293	289-296.9
269	265-272.9	301	297-304.9

Table 5. Limits of interdimensional intervals for ball girth

Standardized value (mm)	Interdimensional interval (mm)	Standardized value (mm)	Interdimensional interval (mm)
248	245-250.9	272	269-274.9
254	251-256.9	278	275-280.9
260	257-262.9	284	281-286.9
266	263-268.9	290	287-292.9

CONCLUSIONS

As a result of 3D scanning and processing anthropometric data, a database of anthropometric foot parameters of Romanian adult male population was developed. Statistical processing of data enabled the development of a pre-project for an Original Romanian Standard.

REFERENCES

Mochimaru, M., Kouchi, M. and Dohni, M. (2000), "Analysis of 3D human foot forms using the FFD method and its application in grading shoe last", *Ergonomics*, 43(9), 1301-1313, https://doi.org/10.1080/001401300421752.
Nácher, B., Aleman,y S., González, J. and Alcántara E. (2006), "A Footwear Fit Classification Model Based on Anthropometric Data", SAE Technical Paper, 2006-01-2356.
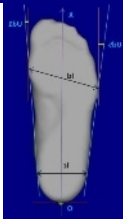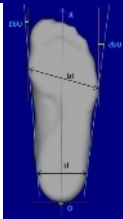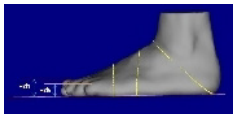Reel, S., Rouse, S., Vernon, W. and Doherty P. (2010), "Reliability of a two-dimensional footprint measurement approach", *Science & Justice*, 50(3), 113-118, https://doi.org/10.1016/j.scijus.2009.11.007.
Sarghie, B. (2013), "Software and equipment systems for measusing and analysing foot anthropometric and biomechanical characteristics for virtual modeling of custom footwear components", ERASMUS IP "Conducting interdisciplinary research in cross-cultural environment" No. 2012-1-LV1-ERA10-03686, Riga Technical University, Faculty of Engineering, Economics and Management, Riga, Latvia.

VIII.

MATERIALS CHARACTERIZATION

ESSENTIAL OIL COMPONENTS OF *Hypericum hircinum* subsp. *majus* (Aiton) N. Robson GROWING IN HATAY (TURKEY) FLORA

FILIZ AYANOĞLU, MUSA TÜRKMEN, DURMUŞ ALPASLAN KAYA

Hatay Mustafa Kemal University, Faculty of Agriculture, Field Crops Department, Turkey,
filizayanoglu@gmailcom; turkmenmusa@hotmail.com; alpaslankaya@yahoo.com

Essential oils obtained by hydrodistillation of *Hypericum hircinum* subsp. *majus* (Hypericaceae) from Hatay (Turkey), were analyzed by GC/MS. Fourty volatile components were identified in the oils, representing 93.95 % of the total oils. The major components were α-guaiene (43,23 %), ι-Gurjunene (8,77 %), β-Farnesene (4,59 %), Limonene (4,38 %), nonane (4,38 %) and Valencene (4,07 %).

Keywords: *Hypericum hircinum* subsp. *majus*, essential oils, GC/MS, Hatay

INTRODUCTION

Hypericum hircinum subsp. *majus* (Aiton) N. Robson, described as "Shrub form, 20-70 (-150) cm. Leaves 2-6.7(-7.5) cm, sessile or subsessile, narrowly lanceolate to broadly ovate, acute to rounded or apiculate, when crushed often smelling of goats. Sepals 3-7 mm, somewhat unequal, ovate-lanceolate to narrowly oblong, deciduous after flowering. Petals 15-25 mm, narrowly oblanceolate to narrowly obovate. Stamens exceeding petals. Styles 3-5 x longer than the ovary. Fruit capsular, 8-13 mm, ellipsoid to subcylindric, subcoriaceous, persistent. Damp, shady places often beside streams, 100-600 m and Mediterranean element" (Davis, 1967).

The Hypericum genus belongs to the Clusiaceae family and the Hypericaceae subfamily and covers about 400 species worldwide (Altan *et al*., 2015). Turkey is an important center for Hypericum species, having about 96 species from which 46 of them are endemic (Guner *et al*., 2012).

Hypericum species have been used for centuries as a healing herb in the relief of pain caused by nervous diseases, menstrual cramps, sciatica, joint inflammation and midwife disorders, and in the treatment of certain skin diseases (Cırak and Kevseroglu, 2004). Hypericum is considered a valuable herbal medicine by people.

The aims of this work were to investigate chemical composition of the *Hypericum hircinum* subsp. *majus* (Aiton) N. Robson essential oil growing in Hatay (Turkey).

MATERIALS AND METHODS

Plant Materials

Hypericum hircinum subsp. *majus* (Aiton) N. Robson plants were harvested in Hatay province of Turkey during the full bloom period (June), when the amount of active substance was most intense and then was dried in the shade at room temperature.

Preparation of Essential Oil

Plant material was weighted and placed in a round bottom flask with a volume of distilled water as extraction solvent; the herba-water mixture was refluxed about 2 h, after that the oil being collected in the side arm of the system. The installation was allowed to stand for about half of hour to prevent the oil to reach room temperature. The

oil was dried onto anhydrous sodium sulphate and then stored in dark color glass bottles and kept to refrigerator (about 4 °C) until its using to be analyzed.

GC/MS Analysis

Analysis of essential oil was performed using the Thermo Scientific Focus gas chromatograph equipped with a DSQ II single quadrupole mass spectrometer, Triplus autosampler and fused-silica capillary column TR-5MS (5% phenyl-polysilphenylene-siloxane, 30 m×0.25 mm inner diameter, film thickness 0.25 µm). The injection volume was 2 µL. The samples were injected with a split ratio of 250:1 by using helium (99.99%) as carrier gas, at a flow rate of 1 mL/min; ionization energy was 70 eV. The transfer line temperature of the mass spectrometer was 220°C, while the temperature of orifice injection was of 220°C. The temperature of oven was programmed in the range 50–220°C at a rate of 3°C/min. Data acquisition was made in the scanning mode. Identification was done on full scan mode in the m/z range of 50–650 a.m.u.

RESULTS

In this study we report the chemical composition of the essential oils hydrodistilled from *Hypericum hircinum* subsp. *majus* (Aiton) N. Robson plant that grown in Hatay flora in Turkey and analyzed by GC-MS. Forty volatile components were identified in the essential oils of *Hypericum hircinum* subsp. *majus* (Aiton) N. Robson (Figure 1, Table 1).

The components and component ratios of the essential oil obtained from the *Hypericum majus* plant naturally growing in Hatay are presented in Table 1. As evidenced in Table 1, the main component, α-Guaiene constitutes 43.23 % of the essential oil, and is followed by ι-Gurjunene with 8.77 %, β-Farnesene with % 4.59, Limonene (4,38 %), nonane (4,38 %) and Valencene (4,07 %).
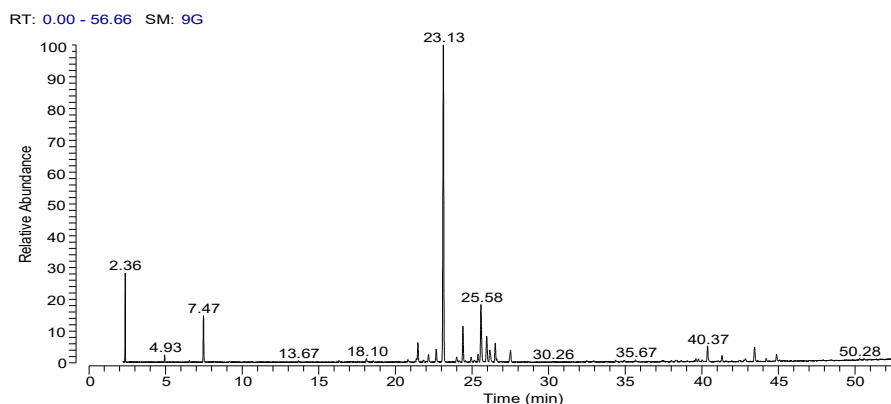
Figure 1. GC/MS chromatogram of *Hypericum hircinum* subsp. *majus* (Aiton) N. Robson

Table 1. Essential oil components of *Hypericum hircinum* subsp. *majus* (Aiton) N. Robson

RT	Compound Name	SI	RSI	Cas #	Area %
2,36	Nonane	981	985	111-84-2	4,38
4,93	Undecane	960	978	1120-21-4	0,55
7,47	Limonene	977	983	5989-54-8	4,38
13,67	3-Hexen-1-ol	865	923	928-96-1	0,22
16,31	2-Decen-1-ol	642	774	22104-80-9	0,26
18,10	Decanal	912	954	112-31-2	0,45
18,55	β-Bourbonene	679	803	5208-59-3	0,21
20,81	2-Pentadecyn-1-ol	777	868	2834-00-6	0,34
21,37	Elemene	911	930	515-13-9	0,38
21,47	trans-Caryophyllene	966	979	87-44-5	2,54
21,82	Aromadendrene	750	824	489-39-4	0,31
22,16	Eremophilene	878	894	10219-75-7	1,05
22,66	α-Ionol	807	864	25312-34-9	1,74
23,13	α-Guaiene	920	922	3691-12-1	43,23
24,00	Sativen	857	872	3650-28-0	0,79
24,41	β-Farnesene	939	958	502-60-3	4,59
24,94	Valencene	896	910	4630-07-3	0,71
25,15	Ledene	607	675	21747-46-6	0,29
25,39	β-Chamigrene	872	894	18431-82-8	1,10
25,58	ι-Gurjunene	977	981	489-40-7	8,77
25,96	Valencene	959	964	4630-07-3	4,07
26,16	α-helmiscapene	917	935	473-13-2	2,00
26,52	bicyclogermacrene	938	948	100762-46-7	2,61
26,62	trans-α-Bergamotene	807	908	17699-05-7	0,35
27,51	germacrene A	940	962	28387-44-2	1,89
34,92	Caryophyllene oxide	727	836	1139-30-6	0,27
35,67	spathulenol	532	657	77171-55-2	0,31
37,44	trans-β-Ionone	692	730	14901-07-6	0,27
38,29	Globulol	671	757	51371-47-2	0,29
38,64	Calarene	578	724	17334-55-3	0,24
39,61	Spathulenol	801	860	77171-55-2	0,40
39,77	3-Hexen-1-ol, benzoate	841	943	25152-85-6	0,36
40,01	Veridiflorol	614	690	552-02-3	0,27
42,74	β-Eudesmol	674	801	473-15-4	0,20
43,44	Ledol	895	901	552-02-3	2,39
44,19	Veridiflorol	728	798	552-02-3	0,48
50,28	Undecanoic acid	636	707	112-37-8	0,24
50,59	Docosane	543	572	629-97-0	0,24
53,19	Hexadecanoic acid, 2-hydroxy-1,3-propanediyl ester	546	592	502-52-3	0,26
55,75	Decyltetraglycol	646	765	NA	0,52

In previous research Maggi *et al.* (2010) studied the chemical composition and antimicrobial activity of *Hypericum hircinum* L. *subsp. majus*. In the study, they found that the major compounds of *Hypericum hircinum* L. *Subsp. majus* essential oil were cis-β-guaiene (23.25–41.23%) and -β-selinene (8.48–25.20%). Quassinti *et al.* (2012), when analyzed essential oil of *Hypericum hircinum L. subsp. majus* plant found that β-guaiene, δ-selinene and (E)-caryophyllene were the most representative. Our results varying according to the study conducted that previous studies.

DISCUSSION AND CONCLUSIONS

In our study; α-Guaiene constitutes, ι-Gurjunene and β-Farnesene were found to be the most abundant essential oil components. Different researchers have identified different components in the same plant species they collecting at different locations (Maggi *et al*., 2010; Quassinti *et al*., 2012). This means that different types of essential oil components can be found in the same species of plants in natural flora and that the essential oil components can be change at different locations.

REFERENCES

Altan, A. *et al*. (2015), "Effect of St. John's Wort (Hypericum Perforatum) on Wound Healing", *Archives Medical Review Journal*, 24(4), 578-591.

Cırak, C. and Kevseroglu, K. (2014), "Kantaron bitkisinin eski çağlardan günümüze kullanım şekilleri ile modern tıptaki yeri ve önemi", *OMÜ Ziraat Fakültesi Dergisi*, 19, 74-84.

Davis, P.H. (1967), *Flora of Turkey and the East Aegean Islands*, Edinburgh, Edinburgh University Press.

Güner, A. *et al*. (2012), Türkiye Bitkileri Listesi (Damarlı Bitkiler). Nezahat Gökyiğit Botanik Bahçesi ve Flora Araştırmaları Derneği Yayını. İstanbul.

Maggi, F. *et al*. (2010), "Chemical composition and antimicrobial activity of *hypericum hircinum* L*. subsp. majus* essential oil", *Chemistry of Natural Compounds*, 46(1).

Quassinti, L. *et al*. (2012), "Antioxidant and antiproliferative activity of *Hypericum hircinum* L. subsp. *majus* (Aiton) N. Robson essential oil", *Natural Product Research* (Formerly Natural Product Letters), 27(10).

THE ESSENTIAL OIL COMPONENTS OF MUSA SAGE (*Salvia tigrina* Hedge & Hub.-Mor.)

HAMİT AYANOĞLU[1], FİLİZ AYANOĞLU[2]

[1]*Ministry of Agriculture, Retired Undersecretary, Ankara, Turkey, hamitayanoglu@yahoo.com*

[2]*Hatay Mustafa Kemal University, Faculty of Agriculture, Field Crops Department, Turkey, filizayanoglu@gmail.com*

There are more than 100 species of Salvia genus distributed in the flora of Turkey, and 58 of them are endemic. 24 Salvia species are distributed in Hatay flora and 5 of them are endemic. *Salvia tigrina* Hedge & Hub.-Mor., named Musa Sage, because it is found in the Musa mountain in Hatay, is a species that attracts attention with its red-spotted flowers on yellow. In the study, which was the first study on the essential oil of Musa sage (*S. tigrina* Hedge & Hub.-Mor.), the essential oil components of leaf samples of plants collected from Musa Mountain were determined. Plant samples were dried and then hydrodistilled with neo-clevenger aparatus. Since the plant contained essential oil very low levels, hexane was used as solvent in the obtaining essential oil. As a result of the GCMS analysis 38 different compounds (98,64%) were analyzed in the essential oil of Musa sage (*S. tigrina* Hedge & Hub.-Mor.). The main compound of species was characterized by a high content of α-humulene ($C_{15}H_{24}$) with 17.52%, followed by 2,5,9-Trimethylcycloundeca-4,8-dienone ($C_{14}H_{22}O$), α-cadinol with 6,68% and α-cedrene with 5,92% respectively.

Keywords: *Salvia tigrina*, Musa sage, essential oil.

INTRODUCTION

Turkey is as an important center because of its rich biological diversity. The flora of Turkey has around 12000 taxa (species, subspecies, varieties) with 8988 native plant species and 2,991 endemic plant species (Ekim, 2000; Erik and Tarıkahya, 2004; Bayram *et al*., 2010; Tan, 2010). Hatay province where the study conducted especially with Amanos Mountains is one of the richest place among the location which is rich for their biological wellness in Turkey. There are more than 250 endemic species in this mountain region. Endemic plants are rare plants which are endangered (Erik and Tarıkahya, 2004; Çakan and Byfield, 2005; Vural and Aytaç 2005; Avcı, 2005). The area which is rich for their biological diversity is represented by 107 family, 520 cins and 1300 taxa (Anonymous, 2008).

With around 900 species of the genus salvia in the world, 96 in Turkey and 24 species are naturally found in Hatay (Davis, 1988; Kandemir, 2003; Demirci *et al*., 2002, Düzenli and Çakan, 2001; Turkmen and Düzenli, 1998; Ayanoğlu *et al*., 2017, Bahadırlı *et al*., 2017). Some of endemic ones of these species, endangered species (EN) group, some of them in vulnerable species (VU) group and one the other threatened with the lower risk (LR) species group. In addition, there are two species which are not endemic included in the vulnerable (VU) group (Ekim *et al*., 2000).

Salvia tigrina Hedge & Hub.-Mor. described as "a perennial herb. Endemic. East Mediterranean element. Stems erect, to 60 cm, unbranched, quadrangular, glabrous and glaucous below, glandular-villous above. Leaves pinnatisect, 8-11 x 5-7 cm and 2 pairs of smaller lateral segments, margins subentire; petiole c. 8 cm. Verticillasters 3-5-flowered, clearly distant. Bracts oblong, c. 4 mm. Pedicels 6-9 mm, erecto-patent. Calyx tubular-infun¬ dibular, 16-19 mm, glandular-villous; upper lip tridentate with c. 2 mm spinulose teeth. Corolla yellow with dark brown spots, 32-36 mm; tube straight, densely annulate c. 9 mm from base; upper lip ± straight, 8-10 mm. Stamens A. Nutlets ± ovate, smooth, c. 5x4 mm. Fl. 6. Hedges, c. 800 m. Known only from the type gathering.

Differing from *S. recognita* in the yellow corollas, longer pedicels and flowering calyces" (Davis, 1988).

Salvia essential oil has an important place in pharmacy, because it brings back the body lost energy, memory and strengthens the liver and also sage known to be used strengthening the nervous system. In addition to use for medical purposes, as well as cosmetics, food, tea, and there is also the use as an ornamental plant (Gurbuz, 1993; Demirci *at al*., 2002).

Studies on the essential oils of some species of sage that grows naturally in Anatolia, main components of *S. albimaculata*, *S. aucheri* var. *canescens*, *S. syriaca*, *S. potentillfolia*, *S. candissima* ssp. *occidentalis*, *S. macrochlamys*, *S. poculata*, *S. tomentosa*, *S. recognita*, *S. virgata*, *S. palaestina* and *S. ceratophylla* were idetified and it was determined that some of them has 14 monoterpenes and 13 oxidized monoterpene (Karaman, 2006; Tanker *et al*., 1985; Gören *et al*., 2006; İpek *et al*., 2008). The aim of the study is to determine the essential oil components of *S. tigrina* Hedge & Hub.-Mor. which is endemic to Turkey and grows naturally in the region. This is the first report on the essential oils of *S. tigrina* Hedge & Hub.-Mor.

MATERIALS AND METHODS

Plant Materials

S. tigrina Hedge & Hub.-Mor. grow naturally on the Musa Mountain which is part of The Amanous mountains in province of Hatay was used as material. Plants were harvested at the beginning of flowering period, when the amount of active substance was most intense and after being dried in the shade at room temperature. The following features of these examples were taken from the plants natural habitat environments.

Essential Oil

Dried leaves of *S. tigrina* Hedge & Hub.-Mor. were hydrodistilled for three hours and the essential oil ratio were determined volumetrically by using Neo-Clevenger apparatus.

GC/MS Analysis

Essential oil components were determined by using "Single quadrupole Thermo Scientific ISQ" gas chromatography and mass spectra with TR-5MS (5% Phenyl Polysilphenylene-siloxane, 0.25 mm x 30 m id, film thickness 0.25) column. 99.9% purity, helium as carrier gas of 1 mL / min was used. Ionization energy of 70 eV. Amu mass range 1.2-1100, MS transfer line temperature 250°C, ion source temperature 220°C, injection temperature 220°C is set to block. Samples were injected with 250 split ratio. Injection amount and oven temperature of 50°C to 220°C 1µl set to 3°C/min is set to increase. As a result of analysis of each component using the Xcalibur software library (Wiley and NIST) by comparing the automatically defined.

RESULTS

The results of analysis of the essential oils obtained by water distillation are shown in Table 2.

The results of analysis of the essential oils obtained by hydrodistillation are shown in Table 1 and chromatogram in Figure 1. Because the plant contain of essential oil has very low levels, hexane was used as solvent in the obtaining essential oil.
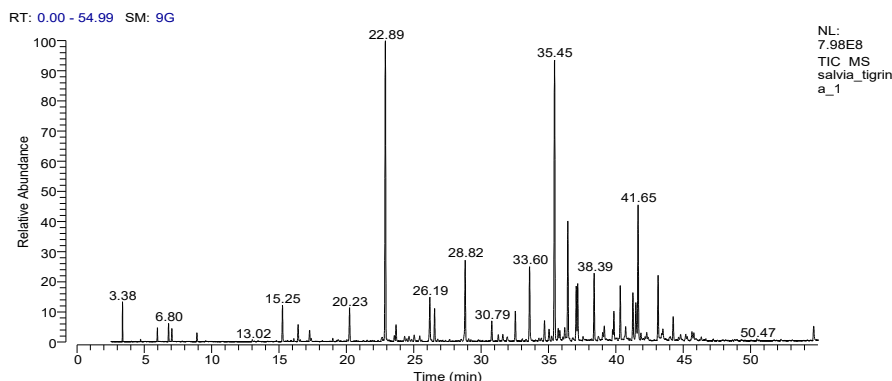
Figure 1. GC/MS chromatogram of *Salvia tigrina* Hedge & Hub.-Mor.

Table 1. Essential oil components of *Salvia tigrina* Hedge & Hub.-Mor.

RT	Compound Name	SI	RSI	Cas #	%
3,38	α-pinene	992	995	80-56-8	0,94
5,97	β-myrcene	974	986	123-35-3	0,43
6,80	l-limonene	976	993	5989-54-8	0,62
7,04	β-phellandrene	981	988	555-10-2	0,47
8,90	P-cymene	956	960	99-87-6	0,34
15,25	α-cubebene	970	979	17699-14-8	1,51
16,41	α-copaene	961	978	3856-25-5	0,79
17,27	Camphor	971	981	76-22-2	0,60
20,23	trans-caryophyllene	991	994	87-44-5	1,62
22,89	α-humulene	991	995	6753-98-6	17,52
23,68	α-muurolene	961	983	31983-22-9	1,25
26,19	δ-cadinene	962	987	483-76-1	2,17
26,54	Neryl acetate	989	990	141-12-8	1,54
28,82	Calamenene	972	989	483-77-2	4,12
30,79	Junipene	869	875	475-20-7	1,02
31,27	Geranyl Butyrate	888	963	106-29-6	0,34
31,61	Naphthalene, 1,2-dihydro-1,5,8-trimethyl	785	824	4506-36-9	0,37
32,54	Ledene	884	889	21747-46-6	1,40
33,60	Caryophyllene oxide	973	982	1139-30-6	8,75
35,45	2,5,9-Trimethylcycloundeca-4,8-dienone	866	868	NA	16,35
35,72	Bicyclogermacrene	860	899	100762-46-7	0,58
36,21	Junipene	878	880	475-20-7	0,57
36,43	α-cedrene	877	880	469-61-4	5,92
37,06	Veridiflorol	934	967	552-02-3	2,64
37,17	Elemol	971	972	639-99-6	2,65

RT	Compound Name	SI	RSI	Cas #	%
38,39	Spathulenol	973	974	77171-55-2	3,35
39,02	Ledene	853	857	21747-46-6	0,37
39,14	Alloaromadendrene oxide	851	878	NA	0,79
39,76	Guaiol	920	924	489-86-1	0,49
39,85	δ-cadinol	947	947	36564-42-8	4,75
41,27	Azulene, 1,4-dimethyl-7-(1-methylethyl)	701	976	489-84-9	2,42
41,48	β-cudesmol	893	944	473-15-4	1,84
41,65	α-cadinol	963	981	481-34-5	6,68
44,26	2H-Pyran, 2-(7-heptadecynyloxy)tetrahydro-	853	853	56599-50-9	1,28
44,81	1-Naphthol, 1,2,3,4-tetrahydro-4,5,7-trimethyl-	700	775	32281-79-1	0,43
45,19	Neocloven oxid-alcohol	886	911	NA	0,37
45,65	Isolongifolene, 4,5,9,10-dehydro-	760	792	156747-45-4	0,52
54,69	Phenethyl benzoate	952	986	94-47-3	0,84

DISCUSSION AND CONCLUSION

Thirty eight compounds were determined in the oil of *S. tigrina* Hedge & Hub.-Mor. representing 98.64% of the total oil. The main compound of species was characterized by a high content of α-humulene ($C_{15}H_{24}$) with 17.52%, followed by 2,5,9-trimethylcycloundeca-4,8-dienone ($C_{14}H_{22}O$) with 16.35%, caryophyllene oxide with 8.75%, α-cadinol with 6.68% and α-cedrene with 5.92%, respectively. GCMS analyzes show that *S. tigrina* Hedge & Hub.-Mor. essential oil consists of mainly sesquiterpenes.

REFERENCES

Avcı, M. (2005), "Çeşitlilik ve endemizm açısından Türkiye'nin bitki örtüsü", *Coğrafya Dergisi*, Sayı 13.

Ayanoglu, F. *et al*. (2017), "Variations of essential oil contents and components of 16 wild Salvia species and propagated clones", *Nat Vol Essent Oils*, 4(3), 72.

Bahadirli, N.P. *et al*. (2017), "Molecular characterization of some Sage species (Salvia spp.) with microsatellite markers in flora of Hatay, Turkey", *Nat Vol Essent Oils*, 4(2), 18.

Bayram, E. et al. (2010), "Tıbbi ve Aromatik Bitkiler Üretiminin Arttırılması Olanakları", Türkiye Ziraat Mühendisliği VII.Teknik Kongresi Bildiriler Kitabı, 11-15 Ocak, ANKARA, 437-456.

Çakan, H. and Byfield, A. (2005), *Amanos Dağları, Türkiye'nin Önemli Bitki Alanı* (Ed. N.Özhatay, A.Byfield ve S.Atay), WWF Türkiye yayını, İstanbul, s. 254-257.

Davis, P.H. *et al*. (1988), "Salvia L.", *Flora of Turkey and the East Aegean Islands*, Vol.7. Edinburgh: Edinburgh Univ. Press.

Demirci, B. *et al*. (2002), "Composition of the essential oil of *Salvia aramiensis* Rech. Fil. growing in Turkey", *J Flav Fragr*, 17, 23-25, https://doi.org/10.1002/ffj.1027.

Düzenli, A. and Çakan, H. (2001), "Flora of Mount Musa (Hatay-Turkey)", *Turkish Journal of Botany*, 25(2001): 285-309.

Ekim, T. *et al*. (2000), *Türkiye Bitkileri Kırmızı Kitabı (Red Data Book of Turkish Plants)*, Türkiye Tabiatını Koruma Derneği ve Van Yüzüncü Yıl Üniversitesi, Barışcan Ofset, Ankara.

Erik, S. and Tarıkahya, B. (2004), "Türkiye florası üzerine", *Kebikeç insan kaynakları araştırmaları dergisi*, 17, 139-163.

Gören, A.C. *et al*. (2006), "Chemotaxonomic evaluation of Turkish species of *Salvia*: fatty acid compositions of seed oils", *Biochemical Systematics and Ecology*, 34, 160–164, https://doi.org/10.1016/j.bse.2005.09.002.

Gürbüz, B. (1993), "Türkiye'de Tıbbi Adaçayı (Salvia officinalis L.) Yetiştirme Çalışmaları", *Tarım ve Köy Dergisi*, 93, 51-52.

İpek, A. *et al*. (2008), "Essential oil composition of *Salvia aucheri* Bentham var. *canescens* Boiss.& Heldr. described endemic species from Turkey", *Journal of Applied Biological Sciences*, 2(2), 99–101.

Kandemir, N. (2003), "The morphological, anatomical and karyological properties of endemic *Salvia hypargeia* Fich. & Mey. in Turkey", *Pak J Bot*, 35(2), 219–236.

Karaman, Ş. (2006), Morphogenetic Variation for Essential Oils in *Salvia palaestina* Bentham Levaves and Bracts from Turkey, *Pakistan Journal of Biological Sciences*, 9, 2720-2722, https://doi.org/10.3923/pjbs.2006.2720.2722.

Tan, A. (2010), *State of Plant Genetic Resources for Food and Agriculture. Second Report of Turkey on Conservation and Sustainable Utilization of Plant Genetic Resources for Food and Agriculture*, Meta Basım, Bornova (Turkish and English), ETAE Yayin No: 142, ISBN 978-975-407-292-1.

Tanker, N. *et al*. (1985), "On the Essential Oils of Some Salvia Species Growing in S. Anatolia", *DOĞA*, Seri A2, 9(2), 358-362.

Türkmen, N. and Düzenli, A. (1998), "The Flora of Dörtyol and Erzin District of Hatay Province in Turkey", *Turk J Bot*, 22, 121-141.

Vural, C. and Aytaç, Z. (2005), "The Flora of Erciyes Dağı (Kayseri, Turkey)", *Turkish Journal of Botany*, 29, 185-236.

WORLD RAW HIDE AND SKIN EXPORTS AND SOME MICROBIOLOGICAL PROBLEMS DURING EXPORTATION

ESER EKE BAYRAMOĞLU[1], SEVİM YILMAZ[2], SULTAN ÇİVİ[1]

[1]*Ege University, Engineering Faculty, Leather Engineering Department, Izmir, Turkıye, e-mail: eserekebay@gmail.com*

[2]*Pamukkale University, Denizli Technical Vocational School of Higher Education, Denizli, Turkıye, e-mail: sevimy@pau.edu.tr*

Nowadays the biggest countries that produce raw hides are China, India, Brazil and the USA; and major tanning companies are in Argentina, Brazil, China, India, Italy, South Korea, Mexico, Pakistan, Russia, Spain, Turkey and the USA. The top exporter of raw hides and skins is the USA. During exportation many microbes especially bacteria and archaea can damage the raw hides and skins. In this study, some information is given about some microbiological problems during exportation of raw hides and skins.

Keywords: Raw hides, Skins, Microorganisms, Bacteria

INTRODUCTION

The raw and processed leather industry (including tanneries and leather fashion industries) as well as leather product manufacturers are the majorly found in countries where meat consumption is high and growing. The biggest countries that produce raw hides are China, India, Brazil and the USA. Major tanning countries are – Argentina, Brazil, China, India, Italy, South Korea, Mexico, Pakistan, Russia, Spain, Turkey and the USA (https://blog.go4worldbusiness.com/2017/05/03/top-10-raw-processed-leather-suppliers-and-raw-leather-manufacturers).

The countries that produce raw hides and skins have to export them in case they cannot process all of the raw material. However, it is very natural that the organic structure of raw hide and skin is faced with many microbial problems during transportation. The best way to reduce microbiological damage of the hide and skin is to process them immediately after slaughtering of the animal, but unfortunately, it is not possible sometimes.

After slaughter of the animal in 5-6 hours period the autolitic destruction starts (Kanagaraj *et al*., 2004; Vankar and Dwivedi, 2009). This deterioration is probably due to the presence of proteolytic enzymes produced by microorganisms growing on the hide or skin. Conservation is made to eliminate the destruction of the skin or hide. Conservation is the process which contains chemicals, biosidal and physical operations. 40-50% salt is generally used for conservation during the export of raw hide and skin in the world. Salt has two functions at this step; it dehydrates the raw material and has the bacteriostatic effect (Kanagaraj *et al*., 2004; Vankar and Dwivedi, 2009). Some researchers reported that when they use 400 kg of salt, this amount dehydrates 270 kg of water (Kannan, 2010).

Even salt is used for conservation many microbes can grow on the skin and hides. These microorganisms are generally halophile or halotolerant microorganisms (Bayramoglu and Civi, 2012).

In this study, after giving brief information about the world export of the raw hides, some information about microorganisms and microbiological events that may develop during the export will be given.

RAW HIDES AND SKINS EXPORT IN THE WORLD

The USA takes the first place in the export of raw hides. In 2000, approximately one third of the world's 4.6 billion dollars' worth of raw hide exports is made by this country. The USA is followed by Australia and France with a 7.4 percent share of world raw hide exports. The total amount of raw hide exports of these three countries is close to half of the world raw hide exports. The raw hides and skins export amount of the ten raw hides and skins exporters in 2000 was 73.5 percent of the world's raw hides and skins export amount (Ozcorekci and Ongut, 2005).

Other countries that export animal hides or skins are England, New Zealand and Russian Federation. Among these countries, the export of hides from England has been negatively influenced by mad cow disease (Bovine Spongiform Encephalopathy-BSE) in the late 1990s.

Microbiological diseases seen in animals may cause the formation and spread of very dangerous diseases and outbreaks by microorganism genus and species. For this reason, cutting of healthy animals and processing of their skin are extremely important. In some diseases, such as anthrax, the animal should not even be cut. It is very dangerous and forbidden.. It is inevitable to spread the deadly anthrax by slaughtering and floating such an animal. The issue of export of diseased animal hides or skins is very important and should be discussed carefully.

The hide or skin cut from the animal is not sterile even if it is undergoing a conservation process. The presence of microorganisms on the hide or skin is extremely normal and this is admissible for healthy animals as well. When the animal is alive, there is a microbiological load on its hide or skin called normal flora; however, these microorganisms begin to damage the hide or skin when the animal is dead and its immune system disappeared. In fact, microbial load is exported together with the raw hide or skin.

MICROORGANISMS AND MICROBIOLOGICAL EVENTS IN THE SALT CONSERVED LEATHERS

In the world raw hides or skins exports, mostly the hides preserved with salt are sold. Since there is no prohibition on the use of salt in the hide or skin, it can be considered as the safest substance in conservation. However, when it is actually investigated, it will be seen that there are different points of this issue. In that salt is ideal environment for some microorganisms.

The microbes which require the salt in order to grow are called as Halophile (the suffix phile means 'loving'). Halotolerant microorganisms tolerate high salt medium and have ability to live in the medium without salt. Haloversatile (euryhaline) means the microorganisms grow maximum in salty medium (Kushner, 1978; Kahraman, 2008).

Extremophiles kind of halophile prokaryotes could be present in Archaea, Bacteria or Eucarya domains (Kahraman, 2008; Horikoshi and Grant, 1998). They naturally live in salt lakes. The most common eucaryotic halophiles are *Dunaliella*, *Artemia salina* and *Ephydra*. *Salinibacter ruber* is the most extremly halophylic bacteria. The genus of *Halobacterium*, *Haloarcula* and *Haloferax* can live in the medium with high concentration of the salt (Kushner, 1978; Kahraman, 2008).

Halophilic bacteria could be present in both Bacteria and Archaea domains. It was reported that halophilic archaea are prokaryotic, but are not classified as bacteria (Shand and Perez, 1999). The identification of halophilic microorganisms can be performed by

comparing the 16S rRNA sequences of pure cultures or mixed cultures with specific archaea and bacteria primers as well as physiological tests (Kahraman, 2008; Galinski, 1995).

The animal's hide has 60-65% moisture after cutting and the moisture content of the hide can be reduced to 35-40% by salting. Although this may limit bacterial development, it does not provide adequate protection. In some researches, it has been expressed that the sea and lake waters contain halophile bacteria and the conservation process of hide or skin cannot be carried out as desired by the use of the salts obtained from these waters (Birbir and Ilgaz, 1996, Birbir *et al.*, 2002). Although it is possible to control mesophilic bacteria that are not tolerant to salt, it is stated that halophile bacteria are developed and they can grow on the hide by passing to it during the protection process (Degirmenci, 2006; Bailey and Birbir, 1993). In addition, it is known that the salt used has negative effects on the environment.

It has been reported that dried salts contain 10^5-10^6 CFU/g halophilic bacteria, these bacteria can live under storage conditions and that salt lakes contain 10^7-10^9 CFU/ml halophilic bacteria (Bilgi, 2007; Mitchel, 1987). In a study on the salt quality in Şereflikoçfisar salt lake, the maximum number of halophilic bacteria in salt water was 10^5 CFU/ml, and the number of halophilic bacteria in the salt crystals taken from the lake was 10^5-10^7 CFU/g (Birbir and Ilgaz, 1996; Bilgi 2007).

Bacterial attack in raw hide causes redness, decay odor, hair loss, staling and deterioration of collagen tissue. This situation can be seen as grain loss, pinhole (pit-like pits), loss of epidermis, blistering and peeling, hollow structure and holes in the manufactured leathers (Mitchel, 1987). Among the halophilic bacteria the most active in the deterioration of gelatin are middle halophils, halophils and proteolytic excess halophilic bacteria (Birbir and Ilgaz, 1996; Hendry *et al.*, 1971).

The purpose of salt curing in skin or hide preservation is to prevent bacteria from damaging them and to protect them until the first process. In a study, however, it was found that most of the 94 excess halophilic bacteria isolated from the salts obtained from various sources had digested collagen and lipids. If the untreated salt taken from the salt mines or salt lakes is used to protect the hide or skin directly without any treatment, these microorganisms will reduce their quality by digesting the collagen. Therefore, in order to prevent hide or skin damage in the conservation, the salt should be checked for halophilic bacterial population and their proteolytic and lipolytic activities before being used directly (Birbir *et al.*, 2002).

Bailey and Birbir indicated that in the skins protected by the salt containing blood, fertilizers and organic matter the number of excess halophile bacteria are increased (Degirmenci, 2006; Bailey and Birbir, 1993). If the salt used in the conservation is contaminated with proteolytic excess halophilic bacteria, leather grain may be damaged significantly due to the high temperature during storage (Bailey and Birbir, 1996). Proteolytic bacteria in salt can settle into the hair follicles and develop here, causing the formation of holes on the entire leather grain (Didato *et al.*, 1999).

The event, which is seen as red spots on the flesh side of the skin, is called as red heat and it especially increases during the summer months. This is due to the development of halophilic bacteria. The bacteria isolated from these spots were generally *Micrococcus roseus*, *M. luteus*, *M. morhuae*. It is stated that the skins containing halophilic bacteria have a similar odor as the smelting fish (Birbir and Ilgaz, 1996; Madigan *et al.*, 1997).

In the researches, it was reported that excess halophilic bacteria can be developed and cause damage of the skins stored in high temperature and humid atmosphere; and

that they will not be damaged if they are preserved with salts that do not contain these bacteria and they are stored at the refrigerator temperature (Bailey and Birbir, 1996).

Halobacteriacea members usually have resistance against specific antibiotics such as penicillin, ampicillin, cycloserine, kanamycin, neomycin, polymyxin and streptomycin (Rakesh *et al.*, 2010; Boleno *et al.*, 1984). Most of them are sensitive to novobiocin and bacitine. The transcriptional induction of the purple membrane (bob gene) and the gas vesicle synthesis (gvpA gene) are blocked by novobiosine in the *Halobacterium salinarum*, a major halophilic strain located on the skin surface (Yang and Das Sarma, 1990).

The most common problem observed in the export of raw hides is the reddish-purple color. The hides can be felt warm when handled. The main reason for this is the development of microorganisms on them. Halobacteria are red in color due to the C_{50} carotenoids which protect the cell from radiation, temperature and salt evaporation. White, opaque or pink pigmented halobacteria are also presented with colorless gas vesicles. Those appearing as purple are halobacteria with purple membranes of bacteriorhodopsin (Oren, 2002).

CONCLUSION

In the international raw hides or skins export, the hides are usually transported with salt which is generally used in the conservation process in order to protect them from microorganisms. In this review, it has been tried to explain that salt used in skin or hide conservation actually creates the ideal living environment for many microorganisms. This property of salt used for the control of microorganisms in the leather industry is often overlooked by conservationists. It should be kept in mind that raw hide is not sterile in the world leather trade, and although salt has some protective effects, it provides an ideal environment for some microorganisms and may pave the way for some unwanted microbiological events. Since it is very important that the salt used in the leather industry should not contain microorganisms, the salt used should never be used again, and the salt to be used for the first time should be free of microbial load. If an antimicrobial agent is used next to or apart from the salt, it is important to note that the main active substance of it should not be a banned compound in export.

REFERENCES

Bailey, D.G. and Birbir, M. (1993), "A Study of the Extremely Halophilic Microorganisms Found on Commercially Brine-cured Cattle Hides", *Journal of American Leather Chemists Association*, 88, 285-293.

Bailey, D.G. and Birbir, M. (1996), "The Impact of Halophilic Organisms on the Grain Quality of Brine Cured Hides", *Journal of American Leather Chemists Association*, 91, 47- 51.

Bayramoglu, E.E. and Civi, S. (2012), "Deri Sanayiinde Koruyucu Olarak Tuz ve Tuzda Gelisen Mikroorganizmalar", *Elektronik Mikrobiyoloji Dergisi TR*, 10/2, 13-26.

Bilgi, S.T. (2007), "Tabaklama Öncesi islemlerde Bakteri ve Fungus Sayısının Belirlenmesi Üzerine Bir Arastırma", Çanakkale Onsekiz Mart Üniversitesi, Fen Bilimleri Enstitüsü, Yüksek Lisans Tezi.

Birbir, M. (2004), "Examination of Amylase, Caseinase and Cellulase Enzymes Production of Extremely Halophilic Strains Isolated from Tuz Lake, Kaldırım and Kayacık Salterns and Tuzköy Salt Mine", *Marine Bacteriology Congress Proceedings*, Istanbul, 25-28.

Birbir, M. and Ilgaz, A. (1996), "Isolation and Identification of Bacteria Adversely Affecting Hide and Leather Quality", *Journal of Society of Leather Technologists and Chemists*, 80, 147-153.

Birbir, M., Kalli, N. and Johannson, C. (2002), "Examination of Salt Quality of Sereflikockisar Lake Used in Turkish Leather Industry", *Journal of Society of Leather Technologists and Chemists*, 86, 112-117.

Boleno, G. et al. (1984), "The Sensitivity of Halobacteria to Antibiotics", *FEMS Microbiol Lett*, 21, 341-345, https://doi.org/10.1111/j.1574-6968.1984.tb00333.x.

Degirmenci, D. (2006), "Derilerin Korunmasında Kullanılan Tuzların _çindeki Asırı Halofil Bakterilerin Üzerine Dogru Elektrik Akımının Etkileri", Marmara Üniversitesi Fen Bilimleri Enstitüsü, Biyoloji Anabilim Dalı Biyoloji Programı Yüksek Lisans Tezi.

Didato, D., Browen, J. and Hurlow, E. (1999), "Microorganism Control During Leather Manufacture", *Leather Technologists Pocket Book*, Chapter 20. (M.K. Leafeed.), The Society of Leather Technologists and Chemists, East Yorkshire, England, 339-352.

Galinski, E.A. (1995), "Osmoadaptation in bacteria", *Adv. Microb. Physiol.*, 37, 272- 328, https://doi.org/10.1016/S0065-2911(08)60148-4.

Hendry, M.F., Cooperand, D.R. and Woods, D.R. (1971), "The Microbiology Curing and Tanning Process, Part IV, The Laboratory Screening of Antiseptics", *Journal of American Leather Chemists Association*, 66-31.

Horikoshi, K. and Grant, W.D. (1998), *Ekstremophiles: Microbial Life in Extreme Environments*, New York, 93-133.

Kahraman, Ö. (2008), "Halofilik mikroorganizmaların izolasyonu, identifikasyonu ve biyoteknolojik öneme sahip ekstraselüler enzimlerin arastırılması", Ege Üniversitesi, Fen bilimleri Enstitüsü, Yüksek Lisans Tezi.

Kanagaraj, J. *et al*. (2004), "Alternatives to sodium chloride in prevention of skin protein degradation - a case study", *Journal of Cleaner Production*, 13, 825-831.

Kannan, K.C. *et al*. (2010), "A Novel Approach Towards Preservation of Skin", *Journal of American Leather Chemists Association*, 105, 360-368.

Kushner, D.J. (1978), Life in High salt and solute concentrations: halophilic bacteria, Microbial Life in Extreme Environments, Academic Press, London, 317-368.

Madigan, M.T., Martinko, J.M. and Parker, J. (1997), "Microbial Growth", in *Brock Biology of Microorganisms* (8th. Ed.), Prentice Hall International, Inc. 149-172.

Mitchel, J.W. (1987), "Prevention of Bacterial Damage on Brine Cured and Fresh Cattlehides", *Journal of American Leather Chemists Association*, 82, 372- 383.

Oren, A. (2002), *Halophilic Microorganism and Their Enviroments*, Kluwer Academic Publishers, Dordrect, The Netherlands, 211, 575.

Özçörekçi, M. and Öngüt, E. (2005), *Dünya'da ve Türkiye'de Deri ve Deri Ürünleri Sanayiinin Gelişme Eğilimleri ve Geleceği*, DPT, yayın no: 2685.

Rakesh, G. *et al*. (2010), "Antibiotic Resistance Profile of The Halophilic Microorganisms Isolated From Tannery Effluent", *Indian Journal of Biotechnology*, 9, 80-86.

Shand, R.F. and Perez, A.M. (1999), "Haloarcheal Growth Physiology", in: J. Seckbah(Ed.), *Enigmatic Microorganisms and Life in Extreme Environments*, Kluwer Academic Publisher Dordrecht, 414-424.

Vankar, P.S. and Dwivedi, A.K. (2009), "Raw skin preservation through sodium salts - A comparative analysis", *Desalination*, 249, 158-162, https://doi.org/10.1016/j.desal.2008.08.011.

Yang, C.F. and Das Sarma, S. (1990), "Transcriptional Induction of Purple Membrane and Gas Vescile Synthesis in The Archebacterium, Halobacterium halobium Is Blocked by a DNA Gyrator Inhibitor, *J Bacteriol*, 172, 4118-4123, https://doi.org/10.1128/jb.172.7.4118-4121.1990.

***, https://blog.go4worldbusiness.com/2017/05/03/top-10-raw-processed-leather-suppliers-and-raw-leather-manufacturers/

A SURVEY STUDY TO DETECT PROBLEMS ON SALTED HIDES AND SKINS

PINAR CAGLAYAN[1], MERAL BIRBIR[1], ANTONIO VENTOSA[2]

[1]*Marmara University, Faculty of Arts and Sciences, Biology Department, Istanbul,Turkey,*
pinar.caglayan@marmara.edu.tr

[2]*University of Sevilla, Pharmacy Faculty, Microbiology and Parasitology Department, Spain*

Some problems originated from raw hides/skins can not be recovered by other steps in leather processing and affect adversely quality of leather. To detect these problems, a questionnaire containing 14 questions was prepared and applied to 15 leather technicians working in different tanneries of Tuzla and Corlu Leather Industrial Zones, Turkey. According to questionnaire results, numbers of tanneries used cattle hides were higher than those of goat and sheep skins. Hides/skins cured in different countries were used in leather industry. Storage period of salted hides/skins was not long and most of samples were processed between one and six months. Storage temperature of tanneries were ranged from 0oC to 30°C. Dry salting was used mostly by tanneries. Fairly high percentage of tanneries used only salt in preservation of hides/skins. Problems such as hair loosening, bacterial and fungal growth, bad odor, red heat, holes, stains on hides/skins and loss of hide/skin elasticity were reported by technicians. Most of problems encountered in leather industry were related to bacterial and fungal growth and their activities. Our microbiological studies results supported that presence of red heat, bad odor, hair slip, stains, holes on the hides/skins and loss of leather elasticity was closely related to microbial growth and activities.

Keywords: Leather industry, tanneries, questionnaire

INTRODUCTION

Raw hides and skins, which are the most valuable by-product of meat industry, are cured with salt after the animal is slaughtered (Vankar and Dwivedi, 2009). As known, animals contain normal flora of microorganisms and contaminant microorganisms found in the air, soil, water, animal feeds, dust, barn, pasture and feces (Birbir and Ilgaz, 1996; Birbir *et al*., 2016; Oppong *et al*., 2006). When the animal is alive, most of these microorganisms have little effect on hides and skins, but after flaying process these microorganisms use proteins, fats and carbohydrates to grow rapidly and digest hide and skin substances. Traditionally, sodium chloride is used for preservation of animal hides and skins as a curing agent which is routinely applied in leather industry (Vankar and Dwivedi, 2009). In this method, fresh hides and skins are cured with 40-50% concentration of sodium chloride, and the moisture content of hides and skins is reduced to 40-48% (Bienkiewickz, 1983; Kanagaraj *et al*., 2001; Bailey, 2003). Although salt is used for curing process, the experimental results of other investigations showed that it contaminates hides and skins with halotolerant microorganisms, slightly halophilic bacteria, moderately halophilic bacteria, extremely halophilic archaea and fungi. The salt samples obtained from Sereflikochisar Salt Lake, which is used in leather industry for curing hides and skins, were examined by Birbir *et al*. (2002). The researchers determined diverse halophilic bacterial and archaeal communities in the curing salt (Birbir *et al*., 2002). In the study of Berber *et al*. (2010), archaeal and bacterial populations were detected on curing salt samples, salted hides, soaked hides, soaking liquors. In another study, various Gram-positive and Gram-negative bacterial species were isolated from salted hides by Aslan and Birbir (2011, 2012). Moreover, moderately halophilic bacteria and extremely halophilic archaea were isolated from salted sheep and goat skins by the researchers (Akpolat *et al*., 2015; Caglayan *et al*.,

2015). In addition to bacterial species, fungal species were detected in the curing salt samples collected from Tuz Lake. Experimental results showed that preservation salt samples contained different fungal species (Ozyaral and Birbir, 2005). While bacterial and archaeal species may cause cream, yellow, white, pink, red discolorations, slimy layer, bad odor, hair slip, pin pricks, entire degradation of hair follicle, holes in grain surface, grain peeling, distruption of collagen fibers on the salted hides and skins (Anderson, 1954; Haines, 1984; Kallenberger, 1985; Birbir and Ilgaz, 1996; Berber and Birbir, 2010; Aslan and Birbir, 2011; Akpolat *et al*., 2015), fungal species may cause yellow, green, white, black discolorations, unpleasant musty odors, surface roughness, loss of physical and mechanical resistance on salted hides and chrome-tanned hides (Birbir *et al*.,1994; Karaboz *et al*., 2003; Fontoura *et al*., 2016).

Although there are several studies about the microorganisms and their adverse effects on the leather quality, there is no information about the quality problems of hides and skins and the factors affecting leather mentioned by leather technicians. Hence, the goal of the study was to collect data on the problems encountered in leather industry from the leather technicians.

MATERIAL AND METHODS

The questionnaire containing 14 questions was applied to leather technicians working in 15 different tanneries found in tanneries in Tuzla and Corlu Leather Industrial Zones, Turkey in 2015. Eight tanneries in Tuzla and seven tanneries in Corlu participated in the following questionnaire:

1. Which type of animal hides/skins do you process?
2. Do you process imported leather?
3. How long do you store the hides/skins before tanning process?
4. What is the storage temperature of hides/skins?
5. Which method do you use to preserve raw hides/skins?
6. Where do you get salt used in the preservation of hides/skins?
7. Do you utilize the used salt again?
8. Do you use antimicrobials during the curing of hides/skins? If you use, could you please write the names and content of antimicrobial?
9. Do you apply the salting method to the hides/skins or do you buy salted hides/skins?
10. How much salt do you use in salting process? (kg/per skin)
11. What are the defects observed on the salted hides/skins?
12. How long does it take for effective curing process of hides/skins?
13. Have you noticed bad odor in the stacked salted hides/skins?
14. What are the other issues that are not included in this survey?

RESULTS AND DISCUSSION

According to questionnaire results, only sheep skins, goat skins or cattle hides, both cattle hides and goat/sheep skins, both sheep and goat skins are processed by the Turkish tanneries (Figure 1). Questionnaire results indicated that the numbers of tanneries used cattle hides were higher than those of goat and sheep skins. These raw materials were belong to Australia, Bulgaria, Israel, South Africa, Russia, China, Turkey, France, Greece, U.S.A., Dubai, and Kuwait. Fifty-three percent, 27%, 20% of

the tanneries processed imported, domestic, both domestic and imported hides/skins, respectively.

Storage periods of salted hides/skins were not long. According to questionnaire results, 46.6%, 6.7%, 33.3%, 6.7%, 6.7% of the tanneries stored salted hides/skins at one month, 1-3 months, 3-6 months, 6-12 months, more than 12 months, respectively. More than half of the tanneries stored salted hides/skins more than one month. When the storage period is longer, the microorganisms can grow and the microbial damage can be more worse.

Storage temperatures of the hides/skins were between 0-10°C, 10-20°C, 20-30°C for 33.3%, 46.6%, 6.7% of the tanneries, respectively. Two tanneries (13.4%) could not give a definite answer about the storage temperature. It was reported that the moderately halophilic bacteria isolated from salted skins and hides could be able to grow 4-45°C (optimally 37°C) (Birbir *et al*., 2015; Caglayan, 2015). In addition fungi can grow at room temperatures. To prevent microbial growth and damage, salted hides/skins should be stored at 5°C.

While 86.6% of the tanneries apply salt curing method, 13.4% of the tanneries apply brine curing method. As known, most of the hides/skins cured in different countries were processed in Turkey. However, all Turkish hides/skins were cured using salt obtained from Tuz Lake. It was determined that most of the tanneries (93%) used only salt for curing process, one tannery (7%) used the mixture of boric acid and salt in curing process. In the tanneries, 1-12 kg of salt were used per skin and hide during curing process. This amount varied according to the size and type of the animal. Raw salt obtained from salt lake and salterns contain microorganisms. In the study carried out with 40 curing salt samples, archaeal counts were found as between 10^2-10^4 CFU/g (Berber and Birbir, 2010). In that study, proteolytic and lipolytic extremely halophilic archaea were detected in the most salt samples. Therefore, the preservation salts should be treated with antimicrobial applications.
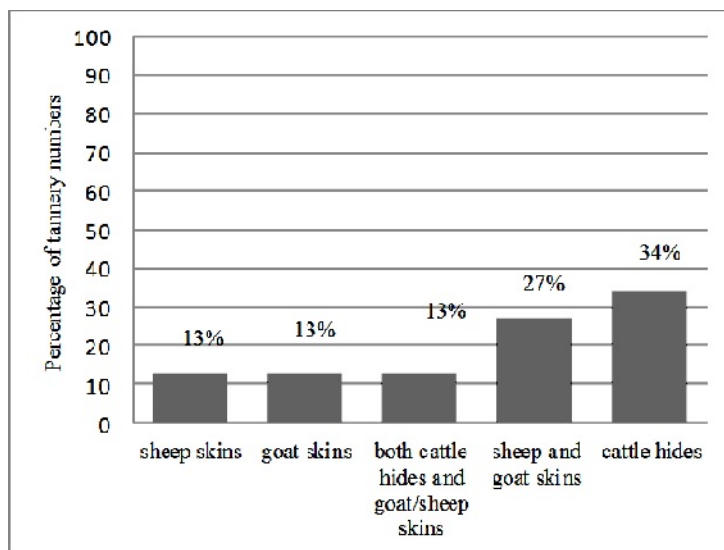
Figure 1. Types of hides and skins processed

Leather technicians emphasized that red heat, bad odor, hair slip, stains, loss of leather elasticity, holes, bacterial, fungal growth, staining differences were among the important problems observed on the hides and skins. We think that these problems were closely correlated with the previous studies' results. In the study of Berber and Birbir (2010), the bacterial counts were found as 10^2-10^6 CFU/g in 36 salted hides collected from different tanneries in Tuzla, Turkey. It was also stated that proteolytic and lipolytic extremely halophilic archaea were observed in salted hides. In addition, the numbers of proteolytic and lipolytic extremely halophilic archaea were respectively 10^2-10^6 CFU/g, on the salted hides (Berber and Birbir, 2010). In our study carried out with 25 salt-cured sheep skins and 25 salt-cured goat skins, non-halophilic bacteria (10^3-10^7; 10^3-10^7 CFU/g), moderately halophilic bacteria (10^3-10^7; 10^3-10^7 CFU/g) and extremely halophilic archaea (10^3-10^7; 10^4-10^7 CFU/g) were isolated from the samples. Proteolytic non-halophilic bacteria (10^2-10^6; 10^2-10^6 CFU/g), proteolytic moderately halophilic bacteria (10^2-10^6; 10^2-10^6 CFU/g) and proteolytic extremely halophilic archaea (10^2-10^6; 10^2-10^6 CFU/g) were detected on all salted sheep and goat skins. Moreover, we found lipolytic non-halophilic bacteria (10^2-10^6; 10^2-10^6 CFU/g), lipolytic moderately halophilic bacteria (10^2-10^6; 10^2-10^6 CFU/g) and lipolytic extremely halophilic archaea (10^2-10^6; 10^2-10^6 CFU/g) on both salted sheep and goat skins (Caglayan *et al*., 2018). These isolates were white, cream, pink, yellow pigmented. The growth of these bacteria may cause stains on the hide/skin surface. Moreover, extremely halophilic archaea produce red, orange and pink coloured colonies due to the presence of C50 carotenoids (Akpolat *et al*., 2015). It is known that the growth of extremely halophilic archaea cause red discolorations on the salted hides and skins (Grant *et al*., 2001). Furthermore, the hides/skins were preserved with curing salt for one month, three months, 6 months, more than six months by 33.3%, 33.3%, 20%, 13.4% of the tanneries, respectively.

Figure 2. The problems encountered in the tanneries

When we combine our experimental results with the results of questionnaires applied to leather technicians, we concluded that the aforementioned problems may be caused as a result of metabolic activities of proteolytic and lipolytic bacterial and archaeal microorganisms found on the hides and skins.

CONCLUSIONS

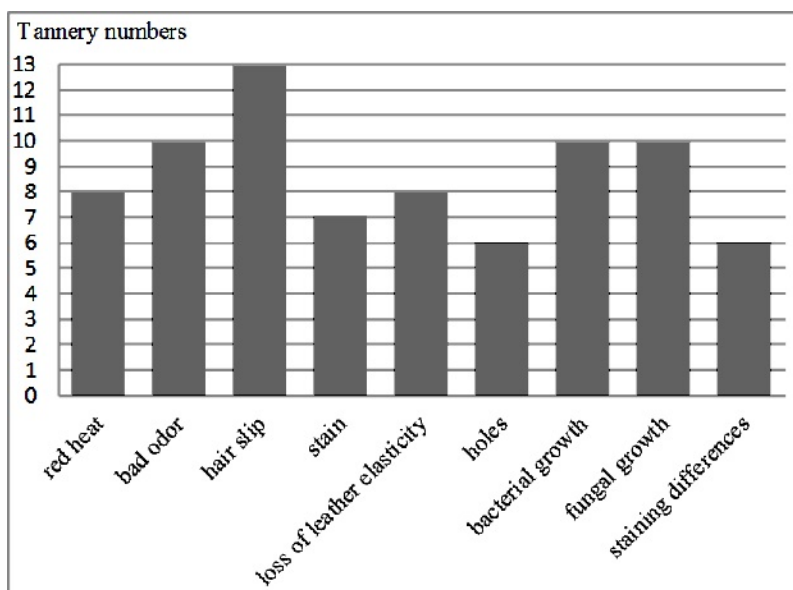Our survey study results showed that most of the problems encountered in the leather industry were related to microbial activities. Our microbiological studies' results supported that presence of red heat, bad odor, hair slip, stains, loss of leather elasticity, holes on the hides/skins were closely related to microbial growth and activities. Most of tannery technicians reported that bacterial and fungal growth were also common problems on the hides/skins. Hence, the storage temperature should be decreased to prevent microbial growth.

REFERENCES

Akpolat, C. *et al*. (2015), "Molecular Identification of Moderately Halophilic Bacteria and Extremely Halophilic Archaea Isolated from Salted Sheep Skins Containing Red and Yellow Discoloratios", *The Journal of the American Leather Chemists Association*, 110, 211-220.

Anderson, H. (1954), "The Reddening of Salted Hides and Fish", *Applied and Environmental Microbiology*, 2, 64-69.

Aslan, E. and Birbir, M. (2011), "Examination of Gram-Positive Bacteria on Salt-Pack Cured Hides", *The Journal of the American Leather Chemists Association*, 12(106), 372-380.

Aslan, E. and Birbir, M. (2012), "Examination of Gram-Negative Bacteria on Salt-Pack Cured Hides", *The Journal of the American Leather Chemists Association*, 4(107), 106-115.

Bailey, D.G. (2003), "The Preservation of Hides and Skins", *The Journal of the American Leather Chemists Association*, 98, 308-319.

Berber, D., Birbir, M. and Mertoğlu, B. (2010), "Examination of Bacterial and Archaeal Populations in Salt, Salted and Soaked Hide and Soak Liquors via Fluorescent In Situ Hybridization", *Journal of the Society of Leather Technologists and Chemists*, 6(94), 259-261.

Berber, D. and Birbir, M. (2010), "Examination of Bacterial Populations in Salt, Salted Hides, Soaked Hides and Soak Liquors", *The Journal of the American Leather Chemists Association*, 105, 320-326.

Bienkiewickz, K. (1983), "Physical Chemistry of Leather Manufacture", Florida, Krieger Publishing Company, Volume 33.

Birbir, M. *et al*. (1994), "Mold Strains Isolated from Unfinished and Finished Leather Goods and Shoes", *The Journal of the American Leather Chemists Association*, 89, 14-19.

Birbir, M. and Ilgaz, A. (1996), "Isolation and Identification of Bacteria Adversely Affecting Hide and Leather Quality", *Journal of the Society of Leather Technologists and Chemists*, 80, 147-153.

Birbir, M., Kalli, N. and Johansson, C. (2002), "The Examination of Salt Quality of Şereflikoçhisar Lake Used in Turkish Leather Industry", *Journal of the Society of Leather Technologists and Chemists*, 86(3), 112-117.

Birbir, M., Ventosa, A. and Caglayan, P. (2015), "Characterization of Moderately Halophilic Bacteria Found on the Sheep and Goat Skins", The Scientific Research Project Commission of Marmara University, Project number FEN-C-DRP-040712-0281.

Birbir, M., Ulusoy, K. and Caglayan, P. (2016), "Examination of Multidrug resistant *Enterobacteriaceae* Isolated from Salted Cattle Hides and Sheep Skins", *Journal of the American Leather Chemists Association*, 111, 334-344.

Caglayan, P. (2015), "Characterization of Moderately Halophilic Bacteria Found on the Sheep and Goat Skins", PhD Thesis, Marmara University.

Caglayan, P. *et al*. (2015), "Characterization of Moderately Halophilic Bacteria from the Salt-pack Cured Hides", *Journal of the Society of Leather Technologists and Chemists*, 5, 250-254.

Caglayan, P. *et al*. (2018), "Investigation of Moderately Halophilic Bacteria Causing Deterioration of the Salted Sheep and Goat Skins and Their Extermination via Electric Current Applications", *Journal of the American Leather Chemists Association*, 113, 41-52.

Fontoura, J.T., Ody, D. and Gutteres, M. (2016), "Performance of Antimicrobial Agents for the Preservation of Chrome Leather", *The Journal of the American Leather Chemists Association*, 111(6), 221-229.

Grant, W.D. *et al*. (2001), "Phylum All. Euryarchaeota phy. nov., Class III. Halobacteria, Order I. Halobacteriales", in *Bergey's Manual of Systematic Bacteriology: The Archaea and the Deeply Branching and Phototrophic Bacteria*, 2nd Edn., eds. D. R. Boone, R. W. Castenholz and G. M. Garrity, Springer-Verlag, New York, USA, 2001, Vol. 1, 294-333.

Haines, M.B. (1984), "Quality Rawstock", *The Journal of the American Leather Chemists Association*, 66, 164-173.

Kallenberger, W.E. (1985), "Halophilic Bacteria in Hide Curing", *Ph.D. Thesis*, Division of Graduate Studies and Research of the University of Cincinati, Department of Basic Science Tanning Research of The Collage of Arts and Science.

Kanagaraj, J. *et al*. (2001), "Cleaner Techniques for the Preservation of Raw Goat Skins", *Journal of Cleaner Production*, 9, 261-268, https://doi.org/10.1016/S0959-6526(00)00060-3.

Karaboz, I., Gülümser, G. and Bayramoğlu Eke, E. (2003), "Tabakhanelerde Depolama Sırasında Gelişen Bazı Fungusların Koruma Piklesi ve Kromla Tabaklama Aşamasında Deride Oluşturdukları Pigmentasyonun İncelenmesi", *Ege Üniversitesi Ziraat Fakültesi Dergisi*, 40(3), 129-136.

Oppong, D. *et al*. (2006), "Application of Molecular Techniques to Identify Bacteria Isolated From the Leather Industry", *The Journal of the American Leather Chemists Association*, 101, 140-145.

Ozyaral, O. and Birbir, M. (2005). "Examination of the Fungal Community on Salt Used in the Turkish Leather Industry", *Journal of the Society of Leather Technologists and Chemists*, 89, 237-241.

Vankar, P.S. and Dwivedi, A.K. (2009), "Raw Skin Preservation Through Sodium Salts-A Comparative Analysis", *Desalination*, 249, 158-162, https://doi.org/10.1016/j.desal.2008.08.011.

ANTIBACTERIAL AND UV PROTECTIVE EFFECTS OF COTTON FABRICS DYED WITH BRASI-COLOR EXTRACT

IULIANA DUMITRESCU[1], RODICA CONSTANTINESCU[1], ELENA-CORNELIA MITRAN[1], ELENA PERDUM[1], LAURA CHIRILĂ[1], OVIDIU GEORGE IORDACHE[1], DANA ŞTEFĂNESCU[2], MARIANA PÎSLARU[2], IULIAN MANCAŞI[3]

[1]*The National Research Development Institute for Textiles and Leather, Bucharest, Romania, Str. Lucretiu Patrascanu nr. 16, sector 3, 30508, Bucharest, Romania, E-Mail: iuliana.dumitrescu@certex.ro*

[2]*SC Tanex SRL, Sos. Bucuresti - Magurele, nr. 47B, 051432, Bucharest, Romania, E-Mail: dana.stefanescu@tanex.ro*

[3]*SC Majutex SRL, Bîrnova, Jud. Iaşi, 707035, Romania, e-mail: majutex@yahoo.com*

The wood of the *Caesalpinia sappan* species is the main source of red dyes used for dyeing textiles and paper, stain biological samples, metals identification, as anti-convulsant, immunosuppressant, anti-inflammatory, anti-bacterial and cancer drug. The main component, brazilin is colorless and to obtain a functional dye, it is oxidized to brazilein. The experimental work consisted in dyeing pre-mordanted cotton knit with Brasi-Color, a dyestuff extract of brazilwood. The aim of this research was to evaluate the effectiveness of mimosa tannin and aluminum potassium sulfate on dye exhaustion, the dyeing fastness, the antibacterial efficiency and UV protective effects of pre-mordanted and dyed cotton fabrics. The dyeing fastness is modest and need to be further optimized. The UV-Vis spectra demonstrated the presence of brazilein (λmax: 445nm and 542nm) as the main compound of the dye solution. The highest degree of dye exhaustion was obtained at the lowest concentration of mimosa tannin and alum. All the fabrics show an excellent ultraviolet protection factor (UPF>50+). The fabric pre-mordanted with 2% mimosa/4% alum and dyed with Brasi-Color transmits the lowest amount of UV rays on both UVA and UVB domains. All the dyed fabrics show a good antibacterial effect against *S. Aureus*.

Keywords: Brasi-Color, UV protection, *S. Aureus*

INTRODUCTION

Both acute and low-dose UV radiation exposure has immunosuppressive effect increasing the risk of infection with viral, bacterial, parasitic or fungal infections, cataracts, photokeratitis and photoconjunctivitis, skin cancer (http://www.who.int/ uv/health/uv_health2/en/). In 2012, 100339 persons were diagnosed in EU with skin cancer, the mortality rate being of 2.3 (Ferlay *et al*., 2013). The clothes could avoid at least a part of these harmful effects if they have a specific structure, design and are dyed in certain colors. In the last decade, natural dyes are preferred instead synthetic dyes due to their multiple valences: pharmacological effects, UV blocking, renewability. Numerous natural dyes were tested for their biological and UV protection such as eucalyptus (Hussein and Elhassaneen, 2014), red onion peel, madder, chamomile (Gawiash *et al*., 2016). Most of the natural dyes such as indigo, annatto, gardenia, and cochineal absorb about 80% of the ultraviolet rays (Gogoi and Gogoi, 2016). The extract from *Caesalpinia sappan* L. was used in food, as dye, and medicines (antioxidant, antibacterial, anti-inflammatory, anti-photoaging, hepatoprotective) (Nilesh *et al*., 2015) and protects the human epidermal keratinocytes exposed to UVA irradiation (Hyung and Joong, 2018). The aim of this research was the evaluation of mimosa tannin and aluminum potassium sulfate effectiveness on Brasi-Color exhaustion, the dyeing fastness, the antibacterial efficiency and UV protective effects of pre-mordanted and dyed cotton fabrics.

EXPERIMENTAL

Materials

Brasi-Color: dyestuff extracts of brazilwood, kindly provided by NIG Nahrungs - Ingenieurtechnik GmbH, Austria;
Cotton knit, 165 g/m^2, chemically bleached.
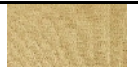
Methods

Pre-mordanting: the fabrics were pre-mordanted with 2% and 8% mimosa tannin, 2% mimosa and 4% alum, 8% mimosa and 15% alum at 30-40^{0}C for 60 minutes at a liquor ratio of 1:60. After that, the fabrics were maintained at room temperature for 3 hours, washed 3 times with hot, warm and cold water, squeezed and freely dried.

Dyeing: the pre-mordanted fabrics were dyed with Brasi-Color solution (4% o.w.f) in a liquor ratio of 1:60, at 80^{0}C for 1 hour. The squeezed fabric was immersed in 20g/L NaCl and maintained at 40^{0}C for 30 minutes. Then, the fabric was rinsed 3 times with hot, warm and cold tap water, squeezed and dried at room temperature.

The appearance of dyed fabrics is displayed in the table 1.

Table 1. The appearance of the fabrics mordanted with mimosa/alum and dyed with Brasi-Color

2% Mimosa	8% Mimosa	2% Mimosa 4% alum	8% Mimosa 15% alum
Brasi-Color 2% Mimosa	Brasi-Color 8% Mimosa	Brasi-Color 2% Mimosa 4% alum	Brasi-Color 8% Mimosa 15% alum

Characterisation

The maximum absorption and the degree of exhaustion of Brasi-Color dyestuff were measured by UV-Vis spectroscopy (Lambda 950, Perkin Elmer, USA). Ultraviolet Protection Factor (UPF) was evaluated on UV-Vis spectrophotometer (Cary 50, Varian, Australia) according to standard AS/NZ 4399:1996. Fabrics are rated as providing an "Excellent UV Protection" if UPF value is 40 or greater, "Good UV Protection" if UPF values are between 25 and 39 and as having "Good UV Protection" if UPF value is in the range 15 – 24 (Hatch, 2003). The samples were tested for microbial activity against *Staphylococcus aureus* according to SR EN ISO 20645/2005. The dyeing fastness was evaluated according the ISO standards with grey scale values (rating 1 to 5: 1-poor and 5 = excellent) for washing, perspiration and rubbing fastness and the blue scale values for light fastness evaluation (rating 1-8: 1=poor, 8=excellent).

RESULTS

UV-Visible Spectra

The recorded UV-VIS spectra of Brasi-Color dyestuff and mimosa tannin are presented in the Fig.1.
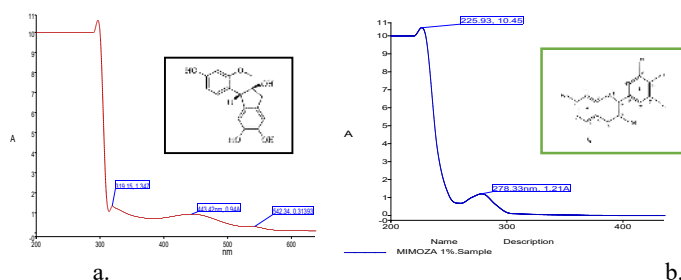
Figure 1. UV-VIS spectrum: a. Brasi-Color; b. mimosa tannin

Except the very broad and intensive band in 200-280nm region, the Brasi-Color solution shows 3 peaks, situated at 319nm, 443nm and 542nm. The result is in accordance the data reported (Lee *et al*., 2008) for sappan wood extract having the maximum absorption wavelength at 447 and 538 nm, specific for yellow and red components. The absorption at 254 and 280 nm are characteristic for phenolic compounds (brazilin) while the absorption at 445 nm and 540nm are attributed to the protonated form of brazilein (Kim *et al*., 1997). Mimosa having the maxima absorption at 226nm and 279nm doesn't interfere with Brasi-Color spectra.

Degree of Dye Exhaustion

To quantify the dye concentration, a calibration curve (Fig. 2) was plotted at 443 nm in five points using 0.1g/L, 0.3 g/L, 0.4g/L, 0.5 g/L, 0.7g/L dye solutions.
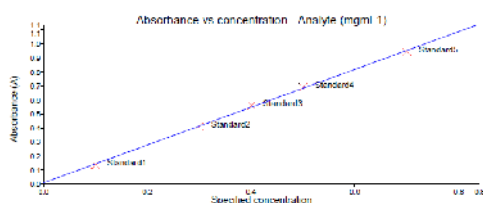
Figure 2. Calibration curve of Dyestuff extract of Brasi Color at 443nm (r2 =0.9996)

The initial and final concentrations of dye baths were determinate based on calibration curve by recording the absorption of diluted solutions (dilution factor: 6:1).

The degree of exhaustion was calculated according to equation (1):

$$\% \, E = 100(\, C_i - C_f)/C_f \tag{1}$$

where C_i: the initial concentration; C_f = the final concentration of the dye.

The exhaustion degree of premordanted and dyed cotton fabrics are shown in table 2.

Table 2. The exhaustion degree of the Brasi-Color (BC) initial and final dye baths, $\lambda = 443$ nm

Sample	C_i	C_f	E, %
BC, 2 % mimosa	0.2120	0.1974	6.88
BC, 8 % mimosa	0.2425	0.2789	-15.01
BC, 2% mimosa 4% alum	0.3060	0.2459	19.64
BC, 8% mimosa 15% alum	0.2888	0.2657	7.99

As the results show, a high content of mimosa tannin negatively influenced the dye bath exhaustion, probably due to the saturation of the cotton knit with tannin and low bonding between the fibers and dye. The hypothesis is confirmed by the lower degree of dyebath exhaustion when a higher amount of mimosa tannin (8%) and alum (15%) is used. The optimum condition for the highest diffusion of dye into cotton fabric was obtained at 2% mimosa/4% alum. The red color could indicate an absorption shift to longer wavelengths due to complex formed with Al ions. Some authors suggested that the ionized hydroxyl group and carbonyl oxygen of brazilein are coordinated to Al^{3+} which with two water molecules form an octahedral configuration (Wongsooksin, 2008).

The Colour Fastness Evaluation of the Fabrics Dyed with Brasi-Color

The colour fastness of the fabrics dyed with Brasi-Color are shown in table 3.

Tabel 3. Colour fastness of the fabrics mordanted and dyed with Brasi-Color (BC)

Colour fastness to/Sample		BC + 2% Mimosa	BC + 8% Mimosa	BC +2% Mimosa + 4% alum	BC + 8% Mimosa + 15% alum
Washing		1-2	2	1	1
Acid perspiration		1-2*	1-2*	1-2*	2*
Alkaline perspiration		2	2-3	2	2-3
Rubbing	dry	4-5	4-5	4	4
	wet	2-3	3	2	2-3
Light fastness		2-3	2-3	3	3

Exposure time: * 7 hours, the colour is modified

Except the fastness to the dry rubbing which could be considered good, all the other tests demonstrate a poor fastness to washing, perspiration, artificial light.

Assessment of the Ultra-violet Protection Factor (UPF)

The UPF values of the fabrics pre-mordanted with mimosa tannin and dyed with Brasi-Color are shown in the table 4.

Table 4. UPF values of the fabrics pre-mordanted and dyed with Brasi-Color (BC)

Sample	Mean UPF	Mean UVA Transmission	Mean UVB Transmission	UPF calculate	UPF rating
untreated	15.698	11.807	5.289	13.498	**10**
2% mimosa	136.207	1.345	0.669	114.127	**50+**
8% mimosa	232.204	0.752	0.377	207.556	**50+**
2% mimosa/ 4% alum	187.415	0.849	0.445	157.032	**50+**
8% mimosa/15% alum	189.435	1.084	0.443	154.351	**50+**
2% mimosa /BC	209.370	0.308	0.437	195.458	**50+**
8% mimosa /BC	175.413	0.461	0.536	145.199	**50+**
2% mimosa/ 4% alum /BC	572.350	0.073	0.202	293.592	**50+**
8% mimosa/15% alum /BC	472.271	0.406	0.210	325.778	**50+**

While the white, untreated fabric shows a high transmission of UV rays, a very small amount of UV rays penetrates through the mordanted and dyed samples on both UVA and UVB domains. The lowest transmission, so the highest UV protective effect is recorded for the knit pre-mordanted with 2% mimosa/ 4% alum and further dyed with Brasi-Color.

Antibacterial Activity of Knitted Fabrics Mordanted and Dyed with Reseda Luteola

The cotton fabrics mordanted and dyed were tested against *S. aureus* and the results were compared with control (table 5).

Table 5. Antibacterial effect of mordanted and dyed fabrics
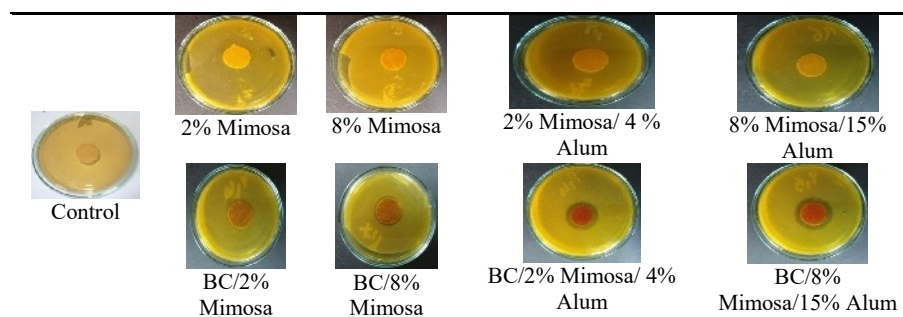
The control fabric presents a moderate growth of *S. aureus*. The materials mordanted with mimosa and mimosa/alum are classified as having a satisfactory effect, the inhibition zone being zero and some restricted bacterial colonies are seen on their surface. Instead, the dyed fabrics do not allow the growth of *S. aureus* colonies, the antibacterial efficiency being higher as the amount of mordant is larger. The most effective activity is shown by the material treated with 8% Mimosa / 15% Alum.

The improved efficiency could be attributed to the dye if we consider the limited efficacy of the fabrics mordanted with the same mordants.

CONCLUSIONS

The highest dye exhaustion is attained for the cotton pre-mordanted with 2% mimosa 4% alum. All the mordanted and dyed materials have a high UV protection on both UVA and UVB regions. The material dyed with Brasi-Color presents a good antibacterial efficiency against *S. aureus*.

REFERENCES

Ferlay, J. *et al*. (2013), "Cancer incidence and mortality patterns in Europe: estimates for 40 countries in 2012", *Eur J Cancer*, 49(6), 1374-403, https://doi.org/10.1016/j.ejca.2012.12.027.

Gawish, S.M. *et al*. (2016), "UV Protection Properties of Cotton, Wool, Silk and Nylon Fabrics Dyed with Red Onion Peel, Madder and Chamomile Extracts", *Textile Sci Eng*, 6, 4, https://doi.org/10.4172/2165-8064.1000266.

Gogoi, M. and Gogoi, A. (2016), "UV ray protection property and natural dye", *Internat J Appl Home Sci*, 3 (3 & 4), 159-164.

Hatch, K.L. (2003), "Making a claim that a garment is UV protective", *AATCC Review*, 3, 23-26.

Hussein, A. and Elhassaneen, Y. (2014), "Natural dye from red onion skins and applied in dyeing cotton fabrics for the production of women's headwear resistance to ultraviolet radiation (UVR)", *J American Sci*, 10, 129-139.

Hyung, S.H. and Joong, H.S. (2018), "Brasilin and Caesalpinia Sappan L. extract protect epidermal keratinocytes from oxidative stress by inducing the expression of GPX7", *Chinese Journal of Natural Medicines*, 16(3), 203-209, https://doi.org/10.1016/S1875-5364(18)30048-7.

Kim, D.S. *et al*. (1997), "NMR assignment of brazilein", *Phytochemistry*, 46, 177–178, https://doi.org/10.1016/S0031-9422(96)00874-6.

Lee, D.K. *et al*. (2008), "Fabrication of nontoxic natural dye from sappan wood", *Korean J Chem Eng*, 25(2), 354-358, https://doi.org/10.1007/s11814-008-0058-6.

Nilesh, P.N. *et al*. (2015), "Brazilin from Caesalpinia sappan heartwood and its pharmacological activities: A review", *Asian Pacific Journal of Tropical Medicine*, 8(6), 421–430, https://doi.org/10.1016/j.apjtm.2015.05.014.

Wongsooksin, K. (2008), "Study of an Al(III) complex with the plant dye brazilein from Ceasalpinia sappan Linn", *Suranaree J Sci Technol*, 15(2), 159-165.

*** http://www.who.int/uv/health/uv_health2/en/, accessed 14.04.2018.

ANTIBACTERIAL AND UV PROTECTIVE EFFECTS OF COTTON FABRICS DYED WITH RESEDA LUTEOLA EXTRACT

IULIANA DUMITRESCU[1], RODICA CONSTANTINESCU[1], ELENA-CORNELIA MITRAN[1], ELENA PERDUM[1], LAURA CHIRILĂ[1], OVIDIU GEORGE IORDACHE[1], DANA ŞTEFĂNESCU[2], MARIANA PÎSLARU[2], IULIAN MANCAŞI[3]

[1]*The National Research Development Institute for Textiles and Leather, Bucharest, Romania, Str. Lucretiu Patrascanu nr. 16, sector 3, 30508, Bucharest, Romania, E-Mail: iuliana.dumitrescu@certex.ro*

[2]*SC Tanex SRL, Sos. Bucuresti - Magurele, nr. 47B, 051432, Bucharest, Romania, E-Mail: dana.stefanescu@tanex.ro*

[3]*SC Majutex SRL, Bîrnova, Jud. Iaşi, 707035, Romania, e-mail: majutex@yahoo.com*

Reseda luteola (Weld) extracts were used to dye textiles and decorate medieval manuscripts. The main components are luteolin and apigenin in the form of β-glucosides, having an important role in plant UV protection, coloration and defense. Luteolin and apigenin have anti-oxidant, anti-carcinogenic, anti-inflammatory and anti-bacterial properties. The present study investigates the degree of exhaust of dyestuff extract of Weld in the dyeing process of cotton fabrics pre-mordanted with mimosa tannin and tannin/alum, the antibacterial and UV protective effects of dyed fabrics. The UV-Vis spectra of the dye solution demonstrated the presence of luteolin-7, 3'-di-O'-glucoside as the main compound. The highest dye exhaustion in the dye bath is attained for the cotton pre-mordanted with 8% Mimosa and 15% Alum, probably due to the complex formed between the flavonoids components and Al^{3+} ions. While the ultraviolet protection factor (UPF) for the untreated cotton knit is 10, indicating the lack of protection against UV radiation, all the mordanted and dyed fabrics show an excellent protection (UPF >50+) due to the UV high absorbance of tannins and Reseda luteola components. The only samples demonstrating a satisfactory antibacterial effect against *S. Aureus* are the fabrics pre-mordanted with mimosa tannin and alum and dyed with Reseda luteola extract.

Keywords: dyer's weld, UPF, exhaustion degree.

INTRODUCTION

Reseda luteola L., known as dyer's weld, was used to produce a yellow mordant dye, especially for dyeing wool and silk, as weld lake and for decorating medieval manuscripts (Angelini *et al*., 2003). The main components responsible for the yellow color are luteolin and apigenin. Other components are luteolin glycosides (luteolin 3',7-O-diglucoside, luteolin-7-glucoside, luteolin 4'-O-glucoside), apigenin 7-O-glucoside, kaempferol, quercetin, chrysoeriol (Gaspar *et al*., 2009). Most of the flavonoids are in the form of their β-glucosides, and have an important role in plant UV protection, flower coloration and defense (Schmidt *et al*., 2011). Luteolin and apigenin have anti-allergic, anti-oxidant, anti-carcinogenic, anti-inflammatory and anti-bacterial (Funakoshi-Tago *et al*., 2011; Shukla and Gupta, 2010). The Weld dyestuff (flavonoids) being a mordant dye needs mordants to be fixed on the fiber. The color depends on the metal salts: a lemon yellow is obtained with alum, greenish yellow with copper and olive with iron, deep yellow with slightly hard water or adding sodium carbonate or calcium carbonate to the dyeing bath (Vankar and Shukla, 2018). The present study was carried out to investigate the degree of exhaust of dyestuff extract of Weld (Reseda Luteola) in dyeing process of cotton fabrics pre-mordanted with mimosa tannin and mimosa tannin/alum, the antibacterial and UV protective effects of dyed fabrics.

EXPERIMENTAL

Materials

Reseda Luteola: Wau-Color - Dyestuff extract of Weld (Reseda Luteola), Dye content: 236g/Kg, kindly provided by NIG Nahrungs- Ingenieurtechnik GmbH, Austria; Cotton knit, 165 g/m^2, 0.79mm thick, chemically bleached.

Methods

Pre-mordanting: the bleached cotton fabric was pre-mordanted with 2% and 8% mimosa tannin, 2% mimosa and 4% alum, 8% mimosa and 15% alum at 30-40°C for 60 minutes in a liquor ratio of 1:60. After that, the fabrics were maintained at room temperature for 3 hours, washed 3 times with hot, warm and cold water, squeezed and freely dried.

Dyeing: the pre-mordanted fabric was dyed with Reseda Luteola solution (4% o.w.f) in a liquor ratio of 1:60, at 80°C for 1 hour. The squeezed fabric was immersed in 20g/L NaCl and maintained at 40°C for 30 minutes. Then, the fabric was rinsed 3 times with hot, warm and cold tap water, squeezed and dried at room temperature.

The appearance of dyed fabrics is displayed in the table 1.

Table 1. The appearance of the fabrics mordanted with mimosa/alum and dyed with Reseda Luteola

2% Mimosa	8% Mimosa	2% Mimosa 4% alum	8% Mimosa 15% alum
Reseda Luteola 2% Mimosa	Reseda Luteola 8% Mimosa	Reseda Luteola 2% Mimosa 4% alum	Reseda Luteola 8% Mimosa 15% alum

Characterisation

UV-Vis spectroscopy (Lambda 950, Perkin Elmer, USA) was used to determine the maximum absorption of weld dye and evaluate the degree of exhaustion representing the amount of dyestuff or mordant diffused in the fibers. Ultraviolet Protection Factor (UPF) was measured on UV-Vis spectrophotometer (Cary 50, Varian, Australia) according to standard AS/NZ 4399:1996. Fabrics are rated as providing an "Excellent UV Protection" if UPF value is 40 or greater, "Good UV Protection" if UPF values are between 25 and 39 and as having "Good UV Protection" if UPF value is in the range 15 – 24 (Hatch, 2003). The samples were tested for microbial activity in *Staphylococcus aureus* according to SR EN ISO 20645/2005. The dyeing fastness was evaluated according the ISO standards, respectively: ISO 105 C06 (washing; ISO 105-E04:2013-(perspiration), ISO 105-X12 (rubbing), ISO 105 B02 (light).

RESULTS

UV-Visible Spectra

The UV-VIS spectrum of Reseda Luteola and mimosa tannin (fig. 1) was recorded to determine the maximum wavelengths absorption.
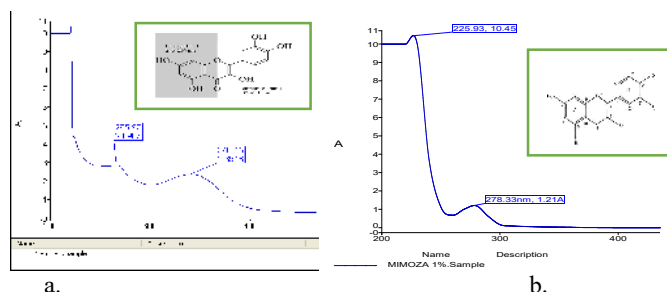
Figure 1. UV-VIS spectrum: a. Reseda Luteola; b. mimosa tannin

The aqueous solution of Reseda Luteola shows 2 absorption bands, situated at 266nm and 340nm, the first being specific for the benzoyl ring and the 2nd for the cinnamoyl structure (Boots *et al*., 2007). By comparisons with literature data, the detected compound belongs to the group of flavonoids and could be luteolin-7,3'-di-O'-glucoside, λmax = 269, 339 nm) (Troalen, 2013) or its mixture with apigenin (λmax = 267, 300, 338 nm). The high solubility in water is another argument for this component knowing that flavonoid glycosylation enhances solubility compared to the corresponding aglycones. 1% Mimosa tannin solution has two maxima absorption, situated at 226nm and 279nm specific for $\pi \rightarrow \pi^*$ transitions in the benzene ring system conjugated with carbonyl group, double bond, or hetero atom (Barnum, 1977).

Degree of Dye Exhaustion

To quantify the dye concentration, a calibration curve (figure 2) was plotted at 340 nm in five points using 0.1g/L, 0.3 g/L, 0.4g/L, 0.5 g/L, 0.7g/L dye solutions.
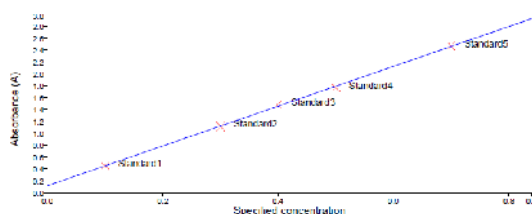
Figure 2. Calibration curve of Dyestuff extract of Weld at 340nm (r^2 =0.9997)

The initial and final concentrations of dye baths were determinate based on calibration curve by recording the absorption of diluted solutions.

The degree of exhaustion was calculated according to equation (1):

% E = 100(C_i- C_f)/C_f (1)

where C_i: the initial concentration; C_f = the final concentration of the dye.

The exhaustion degree of premordanted and dyed cotton fabrics are shown in table 2.

Table 2. The exhaustion degree of the initial and final dye baths, λ =340 nm

Sample	Ci	Cf	Degree of exhaustion, %
4% R. Luteola, 2% Mimosa	0.6273	1.3614	-117.025
4% R. Luteola, 8% Mimosa	0.7158	1.3941	-94.761
4% R. Luteola, 2% Mimosa, 4% Alum	0.993	0.5622	43.383
4% R. Luteola, 8% Mimosa, 15% Alum	1.1136	0.5901	47.009

The negative degree of exhaustion in the case of dyebath used to dye the cotton pre-mordanted with 2% and 8% mimosa tannin demonstrates the low diffusion of dye into fabrics, probably due to saturation of the material with tannin. Additionally, both tannin and flavonoid compounds have similar structures and functional groups, creating an electrostatic repulsion between them. In the case of mordanting with tannin and alum, the exhaustion degree increases, the more the amount of alum is higher. This demonstrates that the agent causing the dye to fix on the material is alum and less, or not at all, tannin. During dyeing, it is possible that the glycosidic compounds are hydrolyzed to parent aglycones (Halpine, 1996). As studies demonstrated both apigenin and luteolin form complex with Al^{3+}, depending on metal ion concentration. Luteolin forms a 2 : 1 complex at low Al^{3+} concentration, a 1 : 1 complex at higher concentration, and a 1 : 2 complex which is in Al^{3+} binds to the 3′,4′-dihydroxyl moiety (Kasprzak et al., 2015).

The Colour Fastness Evaluation of the Fabrics Dyed with Reseda Luteola

The colour fastness of the fabrics dyed with Reseda Luteola are shown in table 3.

Tabel 3. Colour fastness of the fabrics mordanted and dyed with Reseda Luteola (RL)

Colour fastness to/Sample	RL + 2% Mimosa	RL + 8% Mimosa	RL + 2% Mimosa + 4% alum	RL + 8% Mimosa + 15% alum
Washing	2	2	1	1
Acid perspiration	2	2	1-2	1-2
Alkaline perspiration	2-3	3	3	3-4
Rubbing dry	4-5	4-5	4-5	4-5
wet	4	4	3-4	3-4
Light fastness	3*	3*	3**	3**

Exposure time: * 26 hours; ** 7 hours

The color change to washing and acid perspiration is very poor, the worst results being recorded for the fabrics mordanted with mimosa and alum. Instead, the fastness to alkaline perspiration is better for the fabrics pre-mordanted with larger amount of mordants, especially with 8% Mimosa + 15% alum. The color change for the dry rubbing is excellent while for wet rubbing is good mainly for the fabric pre-mordanted with 2 and 8% mimosa tannin. The light fastness is moderate.

Assessment of the Ultra-violet Protection Factor (UPF)

The UPF values of the fabrics pre-mordanted with mimosa tannin and dyed with Reseda Luteola are shown in the table 4.

Table 4. UPF values of the fabrics pre-mordanted and dyed with Reseda Luteola (RL)

Sample	Mean UPF	Mean UVA Transmission	Mean UVB Transmission	UPF calculate	UPF rating
untreated	15.698	11.807	5.289	13.498	10
2% mimosa	136.207	1.345	0.669	114.127	**50+**
8% mimosa	232.204	0.752	0.377	207.556	**50+**
2% mimosa/ 4% alum	187.415	0.849	0.445	157.032	**50+**
8% mimosa/15% alum	189.435	1.084	0.443	154.351	**50+**
2% mimosa /RL	221.794	0.451	0.432	205.066	**50+**
8% mimosa /RL	174.423	0.606	0.559	151.332	**50+**
2% mimosa/ 4% alum / RL	613.328	0.048	0.208	347.282	**50+**
8% mimosa/15% alum / RL	426.001	0.429	0.229	335.383	**50+**

The UPF value for the untreated white cotton knit is 10, indicating the lack of protection against UV radiation. All the treated fabrics provide a protection factor of 50+, ensuring an excellent protection of the human body against harmful UV radiation.

A higher quantity of mimosa tannin lets to pass a smaller amount of UV rays than fabrics mordanted with mimosa/alum. The dyeing further decreases the UVB and transmission UVA through the fabrics, the lowest transmission being ensured by the knit mordanted with 2% mimosa + 4% alum and then dyed with Reseda Luteola.

Antibacterial Activity of Knitted Fabrics Mordanted and Dyed with Reseda Luteola

The cotton fabrics mordanted and dyed were tested against *S. aureus* and the results were compared with control (table 5).

Table 5. Antibacterial effect of mordanted and dyed fabrics

| Control | 2% Mimosa | 8% Mimosa | 2% Mimosa/ 4 % Alum | 8% Mimosa/15% Alum |
| | RL/2% Mimosa | RL /8% Mimosa | RL/2% Mimosa/ 4% Alum | RL/8% Mimosa/15% Alum |
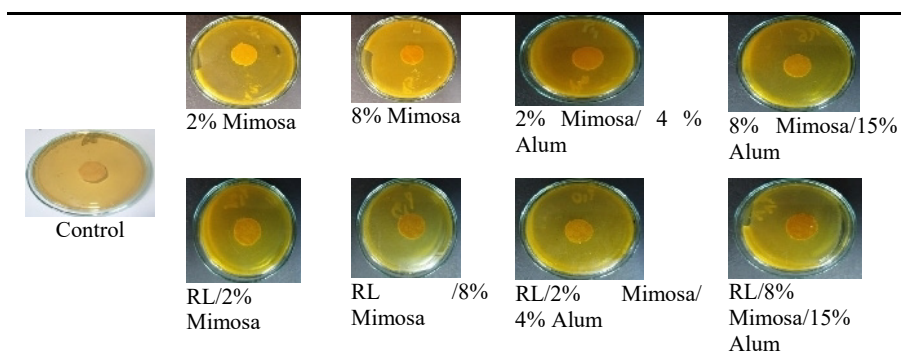
According to EN ISO 20645:2004 standard, the treatment is considered effective if the inhibition zone is ≥1-0 mm and no growth under specimen is detected, whereas 0 mm inhibition zone and slight growth is evaluated as limited effect. The results show

the absence of inhibition zone for all the samples. The untreated cotton fabric presents a moderate multiplication of *S. aureus* colonies while the mordanted fabrics and those mordanted with mimosa and dyed show some restricted colonies growth on their surface. The only samples demonstrating a satisfactory antibacterial effect against *S. Aureus* are the fabrics pre-mordanted with 2% Mimosa/ 4% Alum and 8% Mimosa/ 15% Alum and dyed with Reseda Luteola. The improved efficiency could be attributed to the dye if we consider the limited efficacy of the fabrics mordanted with the same mordants.

CONCLUSIONS

The highest dye exhaustion in the dye bath is attained for the cotton pre-mordanted with 8% Mimosa and 15% Alum due to the complex formed between the flavonoids components and Al^{3+} ions. The fabric excellent UV protection is due to the UV high absorbance of tannins and Reseda Luteola components. The low content of dyestuffs on the fabrics decreases the antibacterial efficiency of textiles dyed with Reseda luteola.

Acknowledgments

REFERENCES

Angelini, L.G. *et al*. (2003), "Agronomic potential of Reseda luteola L. as new crop for natural dyes in textiles production", *Ind Crops Prod*, 17, 199–207, https://doi.org/10.1016/S0926-6690(02)00099-7.

Barnum, D.W. (1977), "Spectrophotometric determination of catechol, epinephrine, dopa, dopamine and other aromatic vic-diols", *Anal Chim Acta*, 89(1), 157-66, https://doi.org/10.1016/S0003-2670(01)83081-6.

Boots, A.W. *et al*. (2007), "The quercetin paradox", *Toxicol Appl Pharmacol*, 222, 89–96, https://doi.org/10.1016/j.taap.2007.04.004.

Funakoshi-Tago, M. *et al*. (2011), "Anti-inflammatory activity of structurally related flavonoids, apigenin, luteolin and fisetin", *Int. Immunopharmacol*, 11, 1150–1159, https://doi.org/10.1016/j.intimp.2011.03.012.

Gaspar, H. *et al*. (2009), "Influence of soil fertility on dye flavonoids production in weld (Reseda luteola L.) accessions from Portugal", *J Sep Sci*, 32(23−24), 4234−4240, https://doi.org/10.1002/jssc.200900425.

Halpine, S.M. (1996), "An improved dye and lake pigment analysis method for high-performance liquid chromatography and diode-array detector", *Stud Conserv*, 41, 76–94, https://doi.org/10.1179/sic.1996.41.2.76.

Hatch, K.L. (2003), "Making a claim that a garment is UV protective", *AATCC Review*, 3, 23-26.

Kasprzak, M.M. *et al*. (2015), "Properties and applications of flavonoid metal complexes", *SC Adv*, 5, 45853-45877.

Schmidt, S. *et al*. (2011), "Identification of a *Saccharomyces cerevisiae* Glucosidase That Hydrolyzes Flavonoid Glucosides", *Appl Environ Microbiol*, 77(5), 1751-1757, https://doi.org/10.1128/AEM.01125-10.

Shukla, S. and Gupta, S. (2010), "Apigenin: A promising molecule for cancer prevention", *Pharm Res*, 27, 962–978, https://doi.org/10.1007/s11095-010-0089-7.

Troalen, L.G. (2013), "Historical dye analysis: Method development and new application in cultural heritage", Doctoral thesis, School of Chemistry, The University of Edinburgh.

Vankar, P.S. and Shukla. D. (2018), "Spectrum of colors from reseda luteola and other natural yellow dyes", *J Textile Eng Fashion Technol*, 4(2), 107-120, https://doi.org/10.15406/jteft.2018.04.00127.

EVALUATION OF THE COMPLEXITY OF RESEARCH PROJECTS BY MULTI-CRITERAL DECISION METHODOLOGIES

MARGARETA-STELA FLORESCU[1], GHEORGHE COARA[2]

[1]*The Bucharest University of Economic Studies, margareta.florescu@ari.ase.ro*

[2]*INCDTP - Division: Leather and Footwear Research Institute, 93 Ion Minulescu st., Bucharest, Romania*

The complexity of the projects is in constant ascent thus be understood, analyzed and measured as well using modern project management. The major objective of this article is to define a measure of the complexity of the projects in order to be used in decision-making, especially when looking at a portfolio with several projects, or when studying different parts of a project. The purpose of this paper is to identify the relative factors relative to the four sizes, which are representative of the construction of the complexity framework of a project, and to identify the multiple criteria in the multi-criterion decision-making methodology for assessing the complexity of the project. These tools will allow for a relative measure of the complexity of the project, which may be part of the decision-making process.

Keywords: decision-making methodology, evaluation, research project

INTRODUCTION

A project represents a unique but temporary effort to achieve technical, scientific results. These results can be reflected in changing the partner or coordinating organization in projects in: processes, performance, products and services. In this sense, human resources, time and financial resources are allocated to generate the results, which can be produced, and / or improved and / or improved, new skills and new knowledge in the field of project management. Every project is unique because it always represents one of the following parameters that changes: objectives, resources and the environment.

Consequently, project management was created as a structured and formal methodology. The complexity of the project is reflected in the failures and mistakes of a project management. In other words, the growing complexity of the project is a source of continuous growth in the risks of its implementation. Identifying sources of complexity and complexity levels of the project has become a crucial issue in order to practice a modern project management.

The complexity of the project in terms of the system complexity of the project and not the algorithmic complexity in solving project management problems as well as problem programming was discussed in the research by Edmonds (1999), Latva Koivisto (2001) and Nassar and Hegab (2006), researches that were crucial sources in generating this list of 40 measurable indicators of the complexity of a project.

A project can undoubtedly be considered a system. A project exists in a specific environment that aims to achieve context-specific objectives (the teleological aspect). A project must carry out a set of activities using methods and methodologies (the functional aspect). A project has an internal structure composed of human resources, materials, suppliers, tasks, IT systems, etc. (ontological aspect). Finally, a project develops over time by consuming resources, delivering the product, changing members and gaining experience without losing its own identity (genetic aspect). In the view of thinking systems, the evolution of the project system is considered to be a presumption

of the future underlying perpetuation (Prigogine, 1996), which excludes the use of analytical tools.

The complexity of the project is the property of a project that makes it difficult to understand, predict and control its overall behavior even when there is reasonable overall information about the project system. The determining factors are the ones that define the size of the project, its variety, the interdependence of the project and the context of the project. In other words, the complexity of the project is the property that makes it difficult to understand, to anticipate and to keep under control each of these aspects.

There are two main scientific approaches to complexity (Schlindwein and Ison, 2005):

- The first approach, often known as the descriptive domain of complexity, considers complexity as an intrinsic property of the system, a vision that has induced researchers to try to quantify or measure it.
- A second approach is the perception of complexity, which presents subjectively complexity, because the complexity of a system is improperly understood in the perception of an observer.

Both approaches can be applied to the complexity of the project and the complexity of project management.

Thus, corroborating the information from the literature, we can identify a large number of important factors of the complexity of the project using an approach based on the four main aspects of the thinking systems (Vidal and Marle, 2008).
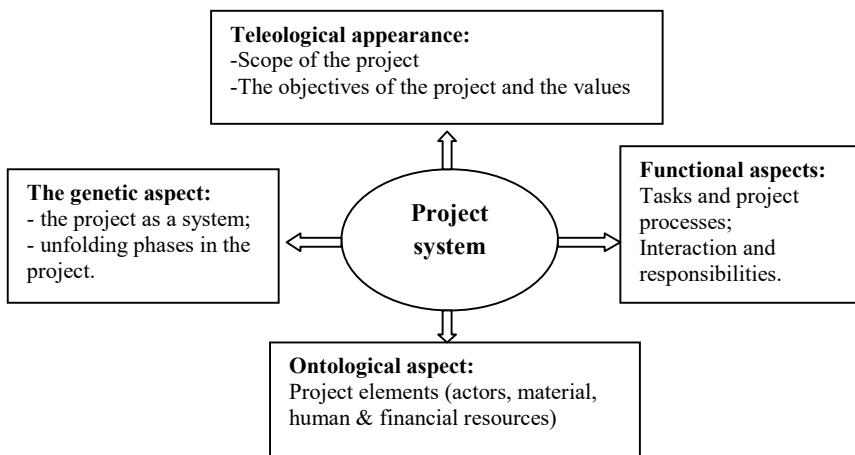
Figure 1. An approach based on systems thinking to describe projects. Source: Vidal, L.A. and Marle, F. (2008), Understanding project complexity: Implications on project management, *Kybernetes*, 37(8), 1094-1110

The first group brings together the factors that are relative to the size of the project system, the second group brings together those relative factors to the variety of the project system. These two first groups correspond globally to the ontological aspect of the project system. The third gathers those that are relative through interdependencies and intercorrelations within the project system, which corresponds to some extensions of

the functional aspects of the project system. Finally, the fourth one functions in a contextual dependence of the complexity of the project, which corresponds mainly to the teleological and genetic aspects of the project system.

The contextual dependence of the complexity of the project was also emphasized by Koivu, Nummelin, Tukiainen, Tainio and Atkin (2004), who insisted on the fact that "the practice and the context applied to a project are not directly transferable to other projects with other institutional and cultural configurations must be taken into account in the project management and leadership processes."

RESEARCH METHODOLOGY

To draw up a set of relative factors, we aim to follow this methodology:
• Identifying the relative factors relative to the 4 sizes that are representative of the construction of the complexity framework of a project
• Identifying the criteria in the multi-criterion decision methodology for assessing the complexity of the project

Conceptual Presentation of the Relative Factors in Constructing the Working Framework of the Project Complexity

This concept requires that any project manager identify and characterize a descriptive vision of complexity for all practical purposes. Moreover, it should be remembered that this framework of work is a consensual form of project complexity and that this complexity can not be essentially driven by a generic consensus. This framework should be considered as a starting point for better understanding of complex projects and for identifying the main sources of complexity within a project. To build a framework for the complexity of a project by identifying a set of relative factors means to "stream" the conversion of a flow of processes from a project consisting of activities, information transfer, know-how, material and cost flows, programming limited resources in the project, etc. Nassar and Hegab (2006) defined a measure for the activities covered by the project plans. This measure of complexity is presented with the formula below for an activity in the project network:

$$C_n = 100 * (\text{Log}(a/(n-1))/\text{Log}[(n^2-1)/4(n-1)])\% \; \textit{if } n \textit{ is unknown}$$
$$C_n = 100 * (\text{Log}(a/(n-1))/\text{Log}[n^2/4(n-1)])\% \tag{1}$$

But this formula also has a number of disadvantages due to certain reasons. First of all, some limits have highlighted the safety of these measures is that these measures mainly refer to one complex aspect of the project, notable in terms of interdependence. These mathematical formulas can not refer to factors of the complexity of the project in reality: the identification of sources of complexity of the project and the possible actions for control / reduction of complexity are not facilitated. Moreover, such measures are difficult to calculate for unknown users, which further complicates their implementation and analysis.

A project can be designed, modeled using different WBS (Work Breakdown Structure) maps, PERT networks or GANT graphics, depending on the level of detail, the wishes of the project manager, etc. Consequently, to prevent the disadvantages of these measures, this article aims to establish a framework of project complexity able to point sources of complexity of the project when building measure, so that the user can

analyze more accurately the complexity of the project and they make decisions with a vision good on the problem.

Identifying Multiple Criteria in the Multi-Criteria Decision Methodology for Assessing the Complexity of the Project

Decision-making, even within project management, is the study of identifying and choosing alternatives based on the values and preferences of the decision-maker. Adopting a decision implies that more alternatives have to be considered and only one will best fit the goals, goals, wishes and values of the problem. Gerhson (1981), Deason (1984) and Tecle (1988) show that the problem of selecting the most appropriate method seems to be a multi-criterion itself: in the case of evaluating the complexity of the project, these multiple criteria are proposed in Table 1.

The multi-criteria methods identified are elementary methods, multi-criteria optimization methods, classification methods, or simple methods of approaching the synthesis criterion. They have been checked by corroborating the information in the literature on the identified requirements. The first criteria are evaluated on the Boolean scale, which makes it possible to assert that these criteria are respected by the method or not. Consequently, when a method is tested with 0 for one of these criteria, the next evaluation of the method is no longer executed, and the method is eliminated. Then the set of the last criteria is evaluated on the fifth level of the Likert scale. The assessment of the criteria (adapted to the environment of the project) is based considerably on the information and scientific surveys to test the use of these methods in the project management literature. A difference is found as a comparison in absolute values with the ideal method that would be marked with the 5th mark on each criterion in this set.

Table 1. Identify multiple criteria in multi-criteria decision making methodology for project complexity assessment

Criteria	Description of requirements
Multi-criteria	The method should be able to compare alternatives on multiple criteria of natural differences.
Identification of qualitative criteria	The method should also be able to handle the qualitative criteria, in addition to the quantitative ones.
Criteria prioritization	The method should be able to determine the user to prioritize the criteria, because they may have different influences.
The evaluation of a set of discrete alternatives	The method should be able to look for the best alternative in a discrete alternative sett known initially.
Classification of alternatives	The method should not only provide the most complex project in the portfolio but also prioritize the functions of the projects according to their level of complexity.
Classification of alternatives according to the cardinal scale	The method should classify alternatives according to the cardinal scale. This scale is used after building a cardinal relative complexity measures we have proposed it.
Safety	The method should provide a safe result for being eligible in decision-making support.
Registration	The method should be recorded to make rapid calculations on computers
Easy interface	The method should have an easy interface; this includes two aspects, namely not requiring special skills to run the processes and

Criteria	Description of requirements
	the results to be easy to understand and manage.
Autonomy	Users (mainly project managers) should be autonomous and should be able to make changes.
Evolution	Changes need to be easy to implement
Adaptation to the project environment	The method should be adapted to decision-making processes in the project environment and take into account project characteristics (limitations, abilities, information systems, need for networking, etc.)

Regarding the problem of evaluating the complexity of the project, it is preferable to use the analytical method (AHP), due to the numerous applications within the context of the project management. According to Al-Harbi, 2001 "AHP has a flexible and repetitive assessment procedure that can be easily understood by which decision-maker in selecting the right software tool for project management." This analytical method is also used for analyzing and evaluating project risks, assuming the project's risks are more important. AHP allows integration of both qualitative and quantitative aspects of decision making, making it more effective and efficient in more complex contexts.

If we consider alternatives: projects, or possible future projects compared to the initial ones, the stages of a given project or possible future project scenarios in a mono-project environment, and to be the score of the priority A_i alternatives obtained due to calculations of the AHP analytical method ($0 \leq S_i \leq 1$), we propose that the relative complexity of the A_i alternatives, given the specific context of the set of alternatives, can be expressed under the following ratio:

$$CI_i = \frac{S(i)}{\max\{S(i)\}} \rightarrow 0 \leqslant CI_i \leqslant 1 \tag{2}$$

A relative scale of the complexity of the project between 0 and 1 can thus be built due to this method. This index allows the classification of projects / scenarios of projects / phases of a project according to the main sources of complexity of the project. This scale allows us to provide a relatively complex indicator of the project, because it is closely related to the initial set of alternatives. But this indicator does not depend on the project models, but only on the evaluation of the expert in projects related to the evaluation criteria. The sub-scales can be defined in the same way to focus on the specific aspects of project complexity and to highlight how a project is complex in terms of interdependence or scientific or technical context.

CONCLUSIONS

This paper elaborates a methodology based on an analytical hierarchical process and the measure of evaluating the relative complexity of a project. Of the project models that are used for project management (WBS, PERT networks, Gantt diagrams, risk lists, etc.), none of these models are needed as a reference to evaluate the complexity of the project. The ability to highlight the sources of complexity of the project when building scale and complexity subscales, these scales allow the user to address more issues in terms of decision-making and project complexity.

In project management, in addition to its performance, out-of-the-out terms, intermediate results, a correct assessment of project complexity - is one of the criteria to

be considered before deciding on project management. Some aspects of the complexity of the project are very present or specific to any area of project activity.

Another conclusion is that it is important to prioritize projects within a project portfolio in order to focus on the most complex projects (those where more than complex management methods and tools are needed). Project managers should pay special attention to the complexity of the project to get the best relative score. On the contrary, some aspects of the complexity of the project (low scores) can potentially be neglected at first glance. This set of information allows managers to focus more effectively on the main complexity factors of the project according to the project environment. Future research will explore the possibility of extending this conceptual model to assess the complexity of a project through an ANA (Process Analytic Network) model. Building an NAP network structure to assess the complexity of the project may be interesting because it includes interdependence and feedback.

REFERENCES

Al-Harbi, K.M.A.S. (2001), "Application of the AHP in project management", *International Journal of Project Management*, 19(1), 19–27. 9.

Bryant, D.L. and Abkowitz, M.D. (2007), "Estimation of chemical spill risk factors using a modified Delphi approach", *Journal of Environmental Management*, 85(1),112–120.

Deason, J. (1984), "A multi-objective decision support system for water project portfolio selection", Ph.D. Dissertation, University of Virginia.

Edmonds, B. (1999), "Syntactic measures of complexity", Thesis of the University of Manchester for the degree of doctor of philosophy in the faculty of arts.

Gershon, M. (1981), 'Model choice in multi-objective decision making in natural resource systems", Ph.D. Dissertation, University of Arizona.

Koivu, T. *et al*. (2004), "Institutional complexity affecting the outcomes of global projects", Published by VTT, *VTT Working Papers*, 14, ISSN 1459-7683, http://www.vtt.fi/inf/pdf.

Latva-Koivisto, A. (2001), "Finding a complexity measure for business process models", Research report Helsinki University of Technology, Systems Analysis Laboratory 5404   L.-A. Vidal *et al*. / Expert Systems with Applications, 38 (2011) 5388–5405.

Nassar, K.M. and Hegab, M.Y. (2006), "Developing a complexity measure for schedules", *Journal of Construction Engineering and Management*, 132(6), 554–561.

Prigogine, I. (1996), *La fin des certitudes*, Odile Jacob.

Schlindwein, S. and Ison, R. (2005), "Human knowing and perceived complexity: implications for systems practice", *Emergence: Complexity and Organisation*, 6(3),19–24.

Tecle, A. (1988), "A decision methodology for the resource utilization of rangeland watersheds", Ph.D. Thesis. School of Renewable Natural Resources, University of Arizona.

Vidal, L.A., Marle, F. and Bocquet, J.C. (2007), "Modelling project complexity", *International conference on engineering design, ICED'07*, Paris, France.

Vidal, L.A. and Marle, F. (2008), "Understanding project complexity: Implications on project management", *Kybernetes*, 37(8), 1094–1110.

FT-IR ANALYSIS OF *FUSARIUM OXYSPORUM* GROWN MYCO-COMPOSITE

OVIDIU IORDACHE[1], IULIANA DUMITRESCU[1], CIPRIAN CHELARU[1],
ELENA PERDUM[1], CORNELIA MITRAN[1,2], ANDREEA CHIVU[1],
IRINA-MARIANA SĂNDULACHE[1]

[1]*The National Research Development Institute for Textiles and Leather, 16 Lucretiu Patrascanu, 030508, Bucharest, Romania*

[2]*Politehnica University of Bucharest, 1-7 Polizu Street, Bucharest, Romania*

Present study was focused on obtaining a novel biocomposite obtained from a plant pathogenic strain, *Fusarium oxysporum*, on wastes from renewable sources, and assessment of microbial development on both the substrate surface and inside the aerial structure, by FT-IR analysis. Fourier Transform Infrared (FTIR) spectroscopy was successfully used for recording of infrared spectra specific to various components of microbial biomass of *Fusarium oxysporum*, grown on an alternative substrate composed of recycled shredded paper and worn coffee. FT-IR analysis allowed highlighting of various functional groups, specific of constituents of microbial biofilm and hyphae: C–H asymmetric and symmetric stretching of CH, $-CH_2$, and $-CH_3$ highlighted at 2923 and 2857cm^{-1} which were indicators of the microbial cell fatty acids component, C=O stretching at 1631cm^{-1} of amide I of protein β-turns, N–H and C–N stretching at 1542cm^{-1} of amide II from α-helix of proteins, polysaccharide components, as a major constituent of the fungal biofilm, was confirmed by FT-IR bands at 1380cm^{-1}, 1195cm^{-1} and 1029.8 cm^{-1}. The verso side of the composite showed similar absorption values as the paper, but with higher intensity peaks, which indicated substrate degradation. Therefore, FT-IR analysis made possible the assessment of existence in the developed biocomposite of various biomolecules such as proteins, lipids, polysaccharides.

Keywords: FTIR, biofilm, fungi, *Fusarium oxysporum*

INTRODUCTION

Microorganisms derived biomaterials have lately enjoyed great attention, as self-growing natural composites, based on fungal mycelium, represent the latest trend in the biocomposites market. Innovative biotechnological processing for transforming and improving exploitation of waste and by-products from household waste, agricultural waste, fruits and vegetables processing industries, plastic and textile industries, will reduce the environmental impact of wastes, will enhance the sustainable management of organic as it can be used as feedstock for value-added bio-based materials. The production of packaging materials with the use of fungal strains and organic waste uses 12% of the energy normally required in the manufacture of traditional plastic packaging and can reduce carbon emissions by up to 90%. Various patents have explored the use of filamentous fungi strains for obtaining mycelium-derived biocomposites, with the aid of *Pleurotus djamor, Pleurotus eryngii, Pleurotus ostreatus, Pleurotus ostreatus* var. *columbines, Grifola frondosa, Ganoderma lucidum, Ganoderma oregonense, Lentinula edodes, Agrocybe aegerita*, or *Coprinus Comatus* (U.S. 2011/0306107 A1 and U.S. 8283153 B2). Patent U.S. 2011/8001719 B2 provides the method of growing Basidiomycetes and Ascomycetes fungal fruiting bodies into a low density, chitinous material that can replace balsa, bass, other woods, and also many foamed plastics. Patent U.S. 5854056 discloses a process for the production of "phylum fungal pulp" but the method is optimized for *Neurospora crassa* as the filamentous fungus that can be used in the production of paper products and textiles. Patent U.S. 2015/0342138 provides a method for producing dehydrated mycelium which can be re-

hydrated and rapidly re-formed into many different shapes, such as bricks, blocks, pellets and the like elements wherein the adhesion of the elements is achieved through "re-animation" of a fungal organism which grows the elements together.

The main challenge in this novel class of biomaterials remains the high heterogeneity of the mixture components with different structures which makes difficult the uniform growth of the mycelium mass (Zeller *et al.*, 2012).

MATERIALS AND METHODS

Biotechnological Process

Plant pathogen *Fusarium oxysporum* (obtained from Politehnica University of Bucharest strains collection) was used in the present experiment. Fresh culture was firstly grown on Potato-Dextrose-Agar media (Scharlau) (Fig. 1) and incubated at 28°C for 14 days. After the incubation period, small biomass samples were further passed in Potato Dextrose nutritive broth (100mL volume) and incubated for 10 days at 28°C.
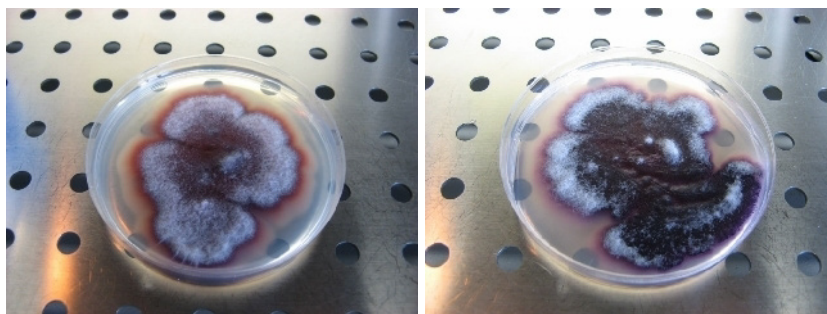
Figure 1. *Fusarium oxysporum* growth on solid media

Furthermore, flask obtained biomass was used for inoculation of an alternative substrate, composed of shredded recycled paper and worn coffee, mixed in a ratio of 10:1 grams, and 0.5g of anhydrous D(+)-Glucose (Scharlau). All the substrate ingredients were thoroughly mixed, hydrated with sterile water, left at rest for 3hours, at room temperature (28°C) for the water to drain, and then sterilized at 121°C for 15 minutes. After sterilization, the substrate was inoculated with the microbial strain by mixing the substrate volume with only the microbial biomass (approximately 4 grams of biomass) and thoroughly mixed in order to obtain a highly homogenized mix (Figure 2). The biocomposites was then incubated for 14 days, in the dark, at 28°C. Following incubation period, the composite was inactivated by sterilization at 130°C for 3 hours.

Figure 2. Mix of microbial strain, shredded paper and grown coffee

Optical Microscopy Analysis

Specific surface biofilm morphology assessment was carried out on an Olympus SZX7 stereomicroscope, with 7:1 zoom ratio, built-in electrostatic discharge protection, and advanced Galilean optical system for highly resolved images. For assessment of surface biofilm morphological structure analysis was carried out on at a magnification level of 0.67x from two different sites of the surface.

FT-IR Analysis

The FT-IR spectroscopy analysis was carried out on a Jasco FT/IR-4700 spectrometer, with max resolution of $0.5cm^{-1}$ and S/N ratio of 30,000:1, and Specac Golden Gate ATR accessory, with single reflection monolithic diamond ATR sampling accessory, featuring a Type IIIA diamond ATR element metal-bonded into a tungsten carbide mount. Spectrometer parameters were set to: measuring range: $4000-600cm^{-1}$; readings/specter: Auto; resolution: $16cm^{-1}$; type of measurement: Abs. For FT-IR analysis, the biocomposite material was dried at 105°C for 3 hours, for components moisture reduction. Composite was analyzed on both surfaces, by depositing a small quantity on the sensor, for ATR analysis.

RESULTS AND DISCUSSIONS

Fusarium oxysporum strain is an abundant and active soil saprophyte, with some specific pathogenic forms of the plant, the strain being part of the Eukaryotes (Smith *et al.*, 1988). The saprophytic capacity allows the strain to survive in the soil between harvest cycles of infected plant remains. The fungus can survive either as a mycelium or as any of the three different types of spores it can produce.

The strain presented a fast growing rate on the alternative substrate used, allowing development of a microbial biofilm on the surface of the substrate (Figure 3a). Further analysis of the microbial biofilm was conducted by stereomicroscopy analysis, which highlighted the homogenous growth of the biofilm (Figure 3b-c)

a   *b*   *c*
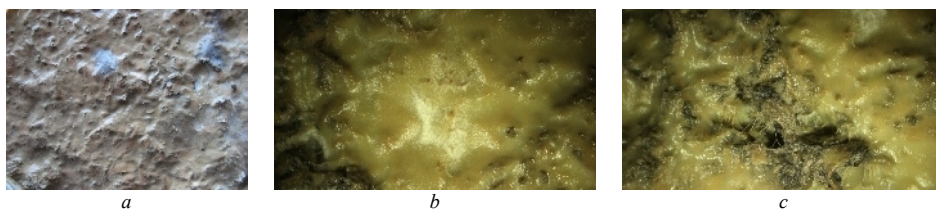
Figure 3. Biofilm structure formed at the surface of the alternative substrate

Significant microbial growth could be best highlighted on the surface of the substrate, which may be due to too high humidity in the initial substrate, which did not allowed sufficient penetration by microbial hyphae, thus colonizing the most accessible portion as a nutrient substrate, respectively the surface of the alternative substrate. Final biocomposite material had a thickness of approximately 1.5cm, with increased rigidity and microbial biofilm developed at the interface substrate-air (Figure 4).

Biofilm detail (front)   *Back detail (verso)*

Section detail

Figure 4. Final biocomposite version

FT-IR analysis was conducted on three component parts of the composite: biofilm surface (composite face), back of the biofilm that was in close contact with the recycled paper and worn coffee (composite verso) and the recycled shredded paper. Obtained spectra for all components were then overlapped for a better visualization of bands distribution in the 4000-600cm^{-1} range (Figure 5).
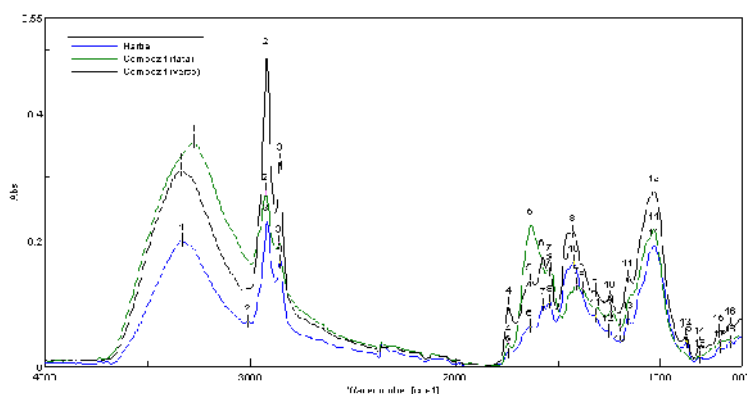
Figure 5. Biocomposite components FT-IR spectra overlapping

The FT-IR spectrum of the **composite front (biofilm)** shows modified positions and intensities of the peaks compared with feeding substrate and verso side of the composite. The broad band between 3600- 3000cm^{-1} with a maximum situated at 3274 cm^{-1} is attributed to the stretching vibrations of hydrogen bonded O-H coming from H_2O or bonded N-H (Gupta *et al*., 2015). The sharp and intensive peak at 2923cm^{-1} accompanied by the less intensive peak at 2857cm^{-1} are specific for C–H asymmetric and symmetric stretching of CH, $–CH_2$, and $–CH_3$ from the fatty acids produced in fungal cells (Diehl *et al*., 2003). All these bands and the small peak at 1743cm^{-1} attributed to the ester C=O stretching vibration are similar with those found by other authors for lipids (Muhammad *et al*., 2017) of the biofilm grown on cellulose substrates. Phospholipids could be characterized by the peak situated at 1238cm^{-1} (Wang *et al*., 1997), and the cell lipids by the band at 1407cm^{-1} (C=O symmetric stretching of COO groups) (Gupta *et al*., 2015).

Except few bands (3012, 1454, 1029cm^{-1}), **the verso side of the composite** absorbs at almost the same wavenumbers as the paper but the intensities of the peaks are highly increased indicating the substrate degradation. More than that, the band at 3332cm^{-1}, becomes broader demonstrating that the -OH groups of cellulose are largely affected by the fungal growth. Furthermore, the bands situated at 2919 and 2854cm^{-1}, assigned to CH_2 asymmetric and symmetric stretching vibrations are sharper and show a significant increment probably due to the mycelia fibers formed on the feeding substrate. The hypothesis is confirmed by the increase of the peaks intensities absorption in the 1538-600cm^{-1} domain and the absence of specific cellulose bands situated at 1454 and 1029cm^{-1}.

The FT-IR results of **paper used as substrate** for fungal growth show absorbance at the following wavenumbers: 3332cm^{-1} (OH stretching), 3012cm^{-1}, 2919cm^{-1} (C-H asymmetric stretching, CH_2 group), 2854cm^{-1} (C–H symmetrical stretching in methylene groups), 1739cm^{-1} (C=O stretching vibration), 1635cm^{-1} (OH bending of absorbed water), 1569cm^{-1} (C-H bending), 1538 cm^{-1} (C=C), 1454cm^{-1} (C=C), 1423 cm^{-1} (HCH and OCH in plane bending), 1319 cm^{-1} (CH2 rocking vibration at C6), 1253 cm^{-1} (G ring stretching), 1157 cm^{-1} (C-O-C asymmetrical stretching), 1029 cm^{-1} (C-C, C-OH, C-H ring and side group vibrations), 871 cm^{-1} (COC,CCO and CCH deformation and stretching), 806 cm^{-1} (glucosidic bond), 709 cm^{-1} and 659 cm^{-1} (C-OH out-of-plane bending) (Mizi *et al*., 2012).

The bands situated at 1631cm^{-1} (C=O stretching, amide I of protein β-turns) (Hu *et al.*, 2006) and 1542cm^{-1} (N–H and C–N stretching, amide II from α-helix of proteins) are characteristic for proteins (amide I at 1700–1600cm^{-1}, amide II and III at 1575–1300 cm^{-1}). The presence of polysaccharides is indicated by the bands situated at 1380cm^{-1}, 1195cm^{-1} and 1029.8 cm^{-1}.

As the results demonstrate, **the composite front** is composed entirely from biomolecules characteristic for fungal mycelia (lipids, proteins, nucleic acids and polysaccharides).

CONCLUSIONS

Despite the massive work already done by the scientific community, biotechnologies based on fungi are not mature for full scale application in packaging systems. Present work has successfully obtained a novel biocomposite from *Fusarium oxysporum* plant pathogen fungal strain grown on alternative nutritive substrate composed of recycled shredded paper and worn coffee, as source of cell grow nutrients and carbon source. Fourier Transform Infrared analysis stands out as a highly versatile analysis tool for monitoring in situ components of various biomolecules, constituents of both microbial biomass and hydrolyzed substrate, and allowed identification of functional groups stretching and vibrations specific to microbial hyphae developed within the aerial structure of the substrate and biofilm formed at the interface air-substrate surface, such as polysaccharides, proteins, fatty acids etc.

Acknowledgments

REFERENCES

Diehl, S.V. *et al*. (2003), "Use of fatty acid profiles to identify white-rot wood decay fungi", in B. Goodell, D. D. Nicholas, and T. P. Schultz, Eds., *Wood Deterioration and Preservation—Advances in Our Changing World*, p. 313, American Chemical Society, Washington, DC, USA.

Gupta, B.S. *et al*. (2011), "Characterization of wood mould fungi by FTIR—a valuable step for prediction of initiation of decay", *Proceedings of the 12th DBMC International Conference on Durability of Building Materials and Components*, Porto, Portugal, April 2011.

Gupta, B.S. *et al*. (2015), "Application of ATR-FTIR Spectroscopy to Compare the Cell Materials of Wood Decay Fungi with Wood Mould Fungi", International Journal of Spectroscopy, Volume 2015, Article ID 521938, 7 pages, https://doi.org/10.1155/2015/521938.

Hu, X. *et al*. (2006), "Determining beta-sheet crystallinity in fibrous proteins by thermal analysis and infrared spectroscopy", *Macromolecules*, 39, 6161–6170, https://doi.org/10.1021/ma0610109.

Mizi, F. *et al*. (2012), "Fourier Transform Infrared Spectroscopy for Natural Fibres", in Dr Salih Salih (Ed.), *Fourier Transform - Materials Analysis*, IntechOpen, Open access peer-reviewed chapter.

Muhammad, H. *et al*. (2017), "Advanced Materials From Fungal Mycelium: Fabrication and Tuning of Physical Properties", *Scientific Reports*, 7, 41292, https://doi.org/10.1038/srep41292.

Smith, I.M. *et al*. (1988), *European handbook of plant diseases*, Blackwell Scientific Publications: Oxford, 583pp.

Wang, H.P. *et al*. (1997), "Microscopic FTIR studies of lung cancer cells in pleural fluid", *Science of the Total Environment*, 204(3), 283–287, https://doi.org/10.1016/S0048-9697(97)00180-0.

Zeller, P. and Zocher, D. (2012), "Ecovative's Breakthrough Biomaterials", *Fungi Magazine*, 5, 51–56.

ANTIFUNGAL ACTIVITY OF *Nigella sativa* L. AND *Thymbra spicata* L. ESSENTIAL OILS AGAINST *Tricophyton rubrum*

DURMU ALPASLAN KAYA[1], N ZAM DURAN[2]

[1]*Hatay Mustafa Kemal University, Faculty of Agriculture, Field Crops Department, Turkey,*
alpaslankaya@yahoo.com

[2]*Microbiology & Clinical Microbiology Department, Medical Faculty, Hatay Mustafa Kemal University, Turkey, nizamduran@hotmail.com*

In this study, we aimed to investigate components and the antifungal activity of *Nigella sativa* L. and *Thymbra spicata* L. essential oils against *Tricophyton rubrum.* Thirty-nine essential oil components, representing 99,69 %, were detected in the essential oil of *Thymbra spicata* L. The major essential oil constituents were carvacrol (58,32 %), -terpinene(28,53 %),o-cymene (5,20 %) and -terpinene (2,03 %). Twenty-four essential oil components, representing 98,39 %, were detected in the essential oil of *Nigella sativa* L. The major essential oil constituents were anethole (22.97 %), thymoquinone (21.36 %), -thujene (6.22 %), longifolene (5.76 %), trans-isoeugenol (3.55 %) and carvacrol (2.23 %). Antifungal activity of the essential oils of *Nigella Sativa* and *Thymbra spicata* was evaluated microdilution method. Fluconazole was selected as the standard antifungal drug. The activity of *Nigella sativa* L. and *Thymbra spicata* L. essential oils against *T. rubrum* was quite high. While *Nigella sativa* L. essential oils had MIC and MBC values of 1 and 2, *Thymbra spicata* L. essential oils were remarkable against *T. rubrum*. *Thymbra spicata* L. essential oils had the best MIC and MBC values (6.25 and 12.5 mg/ml). In our study, the efficacy of *Thymbra spicata* L. essential oils against *Tricophyton rubrum* was found higher. It seems that the essential oils of *Nigella sativa* L. and *Thymbra spicata* L. contain active components against rubrum, which is an important effect of superficial fungal infections.

Keywords: *Nigella Sativa* and *Thymbra spicata* essential oils against *T. rubrum* Candida, antifungal

INTRODUCTION

Dermatophyte infections are common as a result of the use of topical or systemic corticosteroids. It is characterized by diffuse, erythematous or hyperpigmented lesions in the body. *Tricophyton rubrum* (*T. rubrum*) is the first cause of *Tinea corporis* cases. Inflammatory lesions can develop when local or systemic immunity is suppressed. Tinea corporis infections can also be seen in healthy individuals. Tinea corporis can also cause general health problems in patients with such as leukemia, diabetes mellitus, atopic dermatitis, AIDS and Cushing's syndrome (Kick and Korting, 2001).

T. rubrum is an anthropophilic dermatophyte seen all over the world. Infection usually has a low inflammation and causes mild lesions. This fungal infection is often seen in the deep keratinized epithelial layer (Kick and Korting, 2001; Jacobs *et al*., 2001).

In this study, we aimed to investigate the antifungal activity of *Nigella Sativa* and *Thymbra spicata* essential oils against *Tricophyton rubrum.*

MATERIALS AND METHODS

Clinical *T. rubrum* isolates were used in the study. A total of eighteen *T. rubrum* isolates were selected. *T. rubrum* strains were isolated from samples sent to routine mycology laboratory from various clinical specimens. Isolated strains were inoculated into Sabouraud-dextrose-agar media for identification and incubated at 37 °C for 48 hours. For typing, isolates were evaluated in terms of germ tube test, hif formation in

corn flour aged with Tween 80, pseudo-hif formation, blastospor and chlamydospor formation properties. When needed, automated culture systems (Vitek-2, BioMerieux France) were utilized for typing.

Plant Materials

Nigella sativa L. and *Thymbra spicata* L. plants were harvested in Hatay province of Turkey during the full bloom period, which the amount of active substance was most intense and after being dried in the shade at room temperature.

Preparation of Plant Extracts

Plant material was weighted and placed in a round bottom flask with a volume of distilled water as extraction solvent; the herba-water mixture was refluxed about 2 h, during which the oil was collected in the side arm of the system. The installation was allowed to stand for about half an hour to prevent the oil to reach room temperature. The oil was dried over anhydrous sodium sulphate and then stored in dark color glass bottles and keep to refrigerator (about 4°C) until use for analysis.

GC/MS Analysis

Analysis of essential oil was performed using the Thermo Scientific Focusgas chromatograph equipped with a DSQ II single quadrupole mass spectrometer, Triplus autosampler and fused-silica capillary columnTR-5MS (5% phenyl-polysilphenylene-siloxane, 30 m×0.25 mm inner diameter, film thickness 0.25 µm). The injection volume was 2 µL. The samples were injected with a split ratio of 250:1 by using helium (99.99%) as carrier gas, at a flow rate of 1 mL/min; ionization energy was 70 eV. The transfer line temperature of the mass spectrometer was 220°C, while the temperature of orifice injection was of 220°C. The temperature of oven was programmed in the range 50–220°C at a rate of 3°C/min. Data acquisition was made in the scanning mode. Identification was done on full scan mode in the m/z range of 50–650 a.m.u.

Determination of MIC (Minimal Inhibitory Concentration) and MFC (Minimal Fungicidal Concentration)

The isolates were identified using conventional methods. For quality control *T. rubrum* standard strains was also included to the experiments. Fluconazole (Fako Co. Istanbul, Turkey) was used as a control drug. The Clinical and Laboratory Standards Institute (CLSI, M27-A2) microdilution broth method was used to determine the MICs of this fungus *Nigella Sativa* and *Thymbra spicata* essential oils against *Tricophyton rubrum* diluted in DMSO. Fluconazole was prepared in sterile distilled water. Final drug concentrations in the microdilution plates ranged from 256-0.25 µg/ml for Fluconazole. The microdilution tubes were prepared by using the Saboraud Dextroz Broths medium (Sigma). The cell suspensions for spectrophotometric measurements were prepared after vortexing and adjusting to a 0.5 Mc Farland standards. The final inoculum density was adjusted $1x \ 10^3$ cells/ml. Its confirmation was made by performing colony counts on SDA plates. MIC values were evaluated at the end of 48 hours of incubation at 35 ºC. The last tube which absence of growth was accepted as the MIC value. he broth microdilution tests were performed according to the NCCLS guidelines. National Committee for Clinical Laboratory Standards.

MFC Determination

The *in-vitro* fungicidal activities were determined as previously describe (Espinel-Ingroff, 2001).

RESULTS

Thirty-nine essential oil components, representing 99,69 %, were detected in the essential oil of *Thymbra spicata* L. (Table 1). The major essential oil constituents were carvacrol (58,32 %), -terpinene(28,53 %),o-cymene (5,20 %) and -terpinene (2,03 %). Twenty-four essential oil components, representing 98,39 %, were detected in the essential oil of *Nigella sativa* L. (Table 2). The major essential oil constituents were anethole (22.97 %), thymoquinone (21.36 %), -thujene (6.22 %), longifolene (5.76 %), trans-isoeugenol (3.55 %) and carvacrol (2.23 %).

Table 1. Essential oil components of *Thymbra spicata* L.

RT	Compound Name	SI	RSI	Cas #	%
3,42	-Pinene	988	992	80-56-8	0,30
3,48	-Thujene	976	981	2867-05-2	1,05
4,06	Camphene	958	981	79-92-5	0,05
4,30	Diethylmethylcarbinyl chloride	745	865	918-84-3	0,01
4,79	-Pinene	942	966	127-91-3	0,08
5,07	Sabinene	973	988	3387-41-5	0,11
5,65	3-Carene	929	966	13466-78-9	0,05
6,05	-Myrcene	977	985	123-35-3	0,96
6,40	-Terpinene	975	983	99-86-5	2,03
6,88	Limonene	976	992	5989-54-8	0,14
7,07	Eucalyptol	960	987	470-82-6	0,06
7,13	-Phellandrene	969	978	555-10-2	0,11
8,23	-Terpinene	986	991	99-85-4	28,53
8,47	Ocimene	919	956	502-99-8	0,04
9,01	o-Cymene	969	970	527-84-4	5,20
9,36	2-Carene	860	942	554-61-0	0,03
9,60	Cyclohexanone	857	965	108-94-1	0,03
13,31	3-Octanol	896	980	589-98-0	0,03
13,50	Cyclohexanol	811	943	108-93-0	0,02
15,43	1-Octen-3-ol	946	983	3391-86-4	0,07
15,81	Cis Sabinene hydrate	929	972	17699-16-0	0,05
17,46	2-Caren-4-ol	784	871	6617-35-2	0,04
18,91	trans Sabinene hydrate	918	977	17699-16-0	0,06
19,12	Linalool	897	923	78-70-6	0,04
20,39	trans-Caryophyllene	969	988	87-44-5	1,26
20,90	Terpinen-4-ol	953	976	562-74-3	0,11
21,64	Dihydrocarvone	632	741	7764-50-3	0,01
23,03	Humulene	860	907	6753-98-6	0,04
24,46	L- -Terpineol	837	860	10482-56-1	0,08
25,06	Ascaridole	672	733	512-85-6	0,02
25,38	bicyclogermacrene	677	796	100762-46-7	0,01
25,52	Carvone	870	960	99-49-0	0,03
33,75	Caryophyllene oxide	965	976	1139-30-6	0,23
38,54	Spathulenol	927	969	77171-55-2	0,23
39,73	Sulfabenzamide	567	584	127-71-9	0,01

RT	Compound Name	SI	RSI	Cas #	%
40,92	Thymol	925	950	89-83-8	0,12
41,70	Carvacrol	972	972	89-83-8	58,32
50,56	3,5-Heptadienal, 2-ethylidene-6-methyl-	758	784	99172-18-6	0,08
51,13	Caryophyllene oxide	734	783	1139-30-6	0,05

Table 2. Essential oil components of *Nigella sativa* L.

RT	Compound Name	Cas #	%
3,48	-Thujene	2867-05-2	6,22
3,65	-Pinene	80-56-8	3,71
4,06	Camphene	79-92-5	0,93
5,06	Sabinene	3387-41-5	1,83
5,19	-Pinene	127-91-3	1,46
6,56	-Myrcene	123-35-3	0,43
6,88	Limonene	138-86-3	4,55
7,06	Eucalyptol	470-82-6	0,74
7,12	-Phellandrene	555-10-2	0,13
8,21	-Terpinene	99-85-4	0,44
9,15	p-Cymene	99-87-6	17,16
18,89	trans-Sabinene hydrate	17699-16-0	0,31
19,36	Linalyl acetate	115-95-7	0,22
19,94	Endobornyl acetate	76-49-3	0,96
20,38	Caryophyllene	87-44-5	0,67
20,89	Terpinen-4-ol	562-74-3	0,3
25,38	-Bisabolene	495-61-4	0,21
29,03	Anethole	4180-23-8	22,97
29,90	p-Cymenol	1197-01-9	0,86
36,65	Thymoquinone	490-91-5	21,36
40,09	trans-Isoeugenol	5932-68-3	3,55
41,68	Carvacrol	499-75-2	2,23
43,22	Longifolene	475-20-7	5,76
44,65	Longifolenaldehyde	19890-84-7	1,39

The MIC value of *Nigella sativa* essential oils against *T. rubrum* was found to be 32 µg/ml, while the MFC value was found to be 64 µg/ml. MIC value of *Thymbra spicata* was 16 µg/ml, while the MFC value was found as 32 µg/ml. Clearly, it has been determined that *Thymbra spicata* essential oils were more potent against *T. rubrum* (Figure 1).
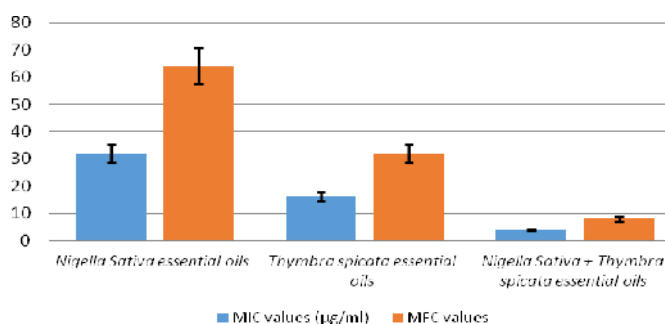
Figure 1. MIC and MFC values of *Nigella Sativa* L. and *Thymbra spicata* L. essential oils against *Tricophyton rubrum*

In addition, it was determined that the combined use of essential oils of *Nigella sativa* with *Thymbra spicata* resulted in a statistically significant decrease in both MIC and MFC values. Briefly, the combined use of the oils of these two plants showed a stronger effect against *T. rubrum*. In the study, the MIC and MFC values of the standard drug fluconazole showed that the combined use of the essential oils of these two plants was how strongly effective (Figure 2,3).
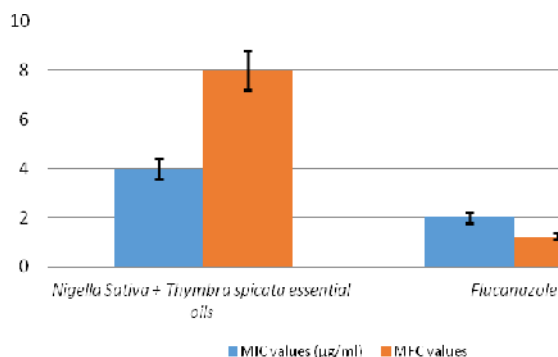
Figure 2. Comparing the MIC and MFC values of *Nigella Sativa* and *Thymbra spicata* essential oils with Fluconazole against *Tricophyton rubrum*
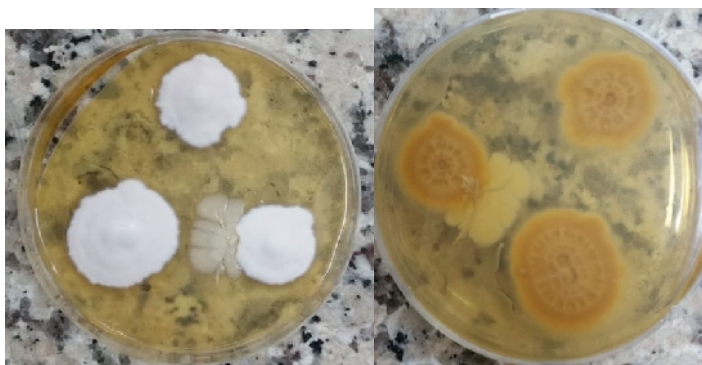
Figure 3. *Trichophyton rubrum* from Saboraud dextroz agar culture

DISCUSSION AND CONCLUSION

It has been found that *Nigella sativa* L. and *Thymbra spicata* L. essential oils have a strong effect against one of the most common dermatophyte infections, *Tricophyton rubrum*. In particular, it has been found that the essential oils of these two plants show a stronger antifungal effect. We think that these plants may be effective in the treatment and protection of superficial fungal infections caused by *Tricophyton rubrum*.

REFERENCES

Espinel-Ingroff, A. (2001), "In vitro fungicidal activities of voriconazole, itraconazole, and amphotericin B against opportunistic moniliaceous and dematiaceous fungi", *J Clin Microbiol*, 39, 954-958, https://doi.org/10.1128/JCM.39.3.954-958.2001.

Jacobs, J.A. *et al*. (2001), "Tinea incognito due to Trichophyton rubrum after local steroid therapy", *Clin Infect Dis*, 33, 142-144, https://doi.org/10.1086/338023.

Kick, G. and Korting, H. (2001), "The definition of Trichophyton rubrum syndrome", *Mycoses*, 44, 167-171, https://doi.org/10.1046/j.1439-0507.2001.00640.x.

ANTIMICROBIAL EFFICACY OF *Origanum syriacum* L. AND *Origanum onites* L. ESSENTIAL OILS AGAINST *Pseudomonas aeruginosa* AND THEIR EFFECTS ON BIOFILM FORMATION

SUPHI BAYRAKTAR, N ZAM DURAN

Microbiology & Clinical Microbiology Department, Medical Faculty, Hatay Mustafa Kemal University, Turkey, nizamduran@hotmail.com

In this study, we aimed to search the components and antimicrobial activity of *Origanum syriacum* and *Origanum onites* essential oils against *Pseudomonas aeruginosa* and also investigated the effects of these two plants essential oils on biofilm formation of *Pseudomonas aeruginosa*. Seventeen essential oil components, representing 98,76 %, were detected in the essential oil of *Origanum syriacum* L. and the major essential oil constituents were thymol (42,18 %), carvacrol (33,95 %), cymene (8,87 %) and -terpinene (8,21%). Thirty-four essential oil components, representing 98,62 %, were detected in the essential oil of *Origanum onites* L. with major essential oil constituents were thymol (68,28 %), -terpinene (5,50 %), p-cymene (5,47 %) and linalool (4,40%). In the study, *Origanum onites* essential oils were found to be more effective against both amikacin-resistant *Pseudomonas aeruginosa* strains and amikacin susceptible strains. In addition, the combination of *Origanum syriacum* and *Origanum onites* essential oils showed stronger efficacy against both amikacin-resistant and susceptible strains of *Pseudomonas aeruginosa*. The combined use of *Origanum syriacum* and *Origanum onites* essential oils showed stronger biofilm inhibition activity in all Pseudomonas strains. In the present study, the remarkable efficacy of *Origanum syriacum* and *Origanum onites* essential oils against both drug-resistant and drug-sensitive *Pseudomonas aeruginosa* strains was determined. More importantly, it has been found that the ability of these bacteria to form biofilms was inhibited by increasing concentrations of essential oils of these plants.

Keywords: Candida, *Origanum syriacum*, *Origanum onites,* essential oils, drug, resistant, sensitive *Pseudomonas aeruginosa*

INTRODUCTION

Hospital infections is an important health problem in our country as it is in the world because of its high economic cost, morbidity and mortality rates. Pseudomonas aeruginosa is reported to be responsible for 10-25% of hospital infections (Fidan *et al*., 2005).

P. aeruginosa is widely found in nature. It's also present as a saprophytic in healthy humans. *Pseudomonas aeruginosa* is a microorganism that can easily colonized in patients with intensive care units, burn units, mechanical ventilators, cancer chemotherapy or broad-spectrum antibiotics, which predispose to invasive infections. It leads to hospital infections. It is the fifth most common cause of hospital infection. *Pseudomonas aeruginoa* is one of the most important nosocomial infections. It is the fifth most common cause of hospital infection (Pier and Ramphal, 2005). It contains various virulence factors. It is also a microorganism that is naturally resistant to some antimicrobials and can easily develop resistance to antimicrobials (Horan *et al*., 2008).

In this study, we aimed to investigate the antimicrobial activity of *Origanum syriacum* and *Origanum onites* essential oils against *Pseudomonas aeruginosa* and also investigated the effects of these two plants essential oils on biofilm formation of *Pseudomonas aeruginosa*.

MATERIALS AND METHODS

Plant Materials

Origanum syriacum L. and *Origanum onites* L. plants were harvested in Hatay province of Turkey during the full bloom period, which the amount of active substance was most intense and after being dried in the shade at room temperature.

Preparation of Plant Extracts

Plant material was weighted and placed in a round bottom flask with a volume of distilled water as extraction solvent; the herba-water mixture was refluxed about 2 h, during which the oil was collected in the side arm of the system. The installation was allowed to stand for about half an hour to prevent the oil to reach room temperature. The oil was dried over anhydrous sodium sulphate and then stored in dark color glass bottles and keep to refrigerator (about 4 °C) until use for analysis.

GC/MS Analysis

Analysis of essential oil was performed using the Thermo Scientific Focus gas chromatograph equipped with a DSQ II single quadrupole mass spectrometer, Triplus autosampler and fused-silica capillary columnTR-5MS (5% phenyl-polysilphenylene-siloxane, 30 m×0.25 mm inner diameter, film thickness 0.25 µm). The injection volume was 2 µL. The samples were injected with a split ratio of 250:1 by using helium (99.99 %) as carrier gas, at a flow rate of 1 mL/min; ionization energy was 70 eV. The transfer line temperature of the mass spectrometer was 220°C, while the temperature of orifice injection was of 220°C. The temperature of oven was programmed in the range 50–220°C at a rate of 3°C/min. Data acquisition was made in the scanning mode. Identification was done on full scan mode in the m/z range of 50–650 a.m.u.

Bacterial Isolates

Laboratory isolates and clinical bacterial strains were used in the study. 12 amikacin resistant isolates and 12 amikacin sensitive *P. aeruginosa* strains were selected in the study. *Pseudomonas aeruginosa* (ATTC27853) was used as the standard strain. Amikacin was selected as the control drug in the study. All bacterial isolates were cultured on Mueller-Hinton agar for 24 hours at 37°C. Standard culture methods and techniques were used for isolation. Bacterial identification was performed using conventional techniques.

Determination of the Minimum Inhibitory Concentration (MIC)

The MIC of the essential oils was evaluated on ten concentrations, 1.56, 3.12, 6.25, 12.5, 25, 50, 100 and 200 µg/ml were tested. Briefly, the stock solutions of essential oils were diluted with DMSO. a stock solution was prepared by dissolving 200 mg of each extract in one ml of the solvent containing dimethyl sulfoxide and water in a ratio of 2:4 v/v, respectively. 100µl of nutrient broth medium was dispensed into one well for each treatment to be a first control. The second control consists of other well contained only 100 µl of the extract. Another 100 µl of stock solution was transferred to a third well. The serial dilutions were performed by taking 100 µl from the third well to the fourth well and this procedure was repeated with other 5 wells until reaching the desired concentration, i.e. (6.25 mg/ml). Aliquot of 100 µl of previously prepared bacterial

broth were added to each well except the control well. All the plates were incubated at 37°C for 24 hr. The MIC value was accepted by the lack of turbidity in the tubes.

Biofilm Formation Assay

The formation of biofilm in *Pseudomonas aeruginosa* strains was performed as described by Mashhady *et al*., 2016.

RESULTS

Seventeen essential oil components, representing 98,76 %, were detected in the essential oil of *Origanum syriacum* L. (Figure 1, Table 1). The major essential oil constituents were thymol (42,18%), carvacrol (33,95%), cymene (8,87%) and -terpinene (8,21%).
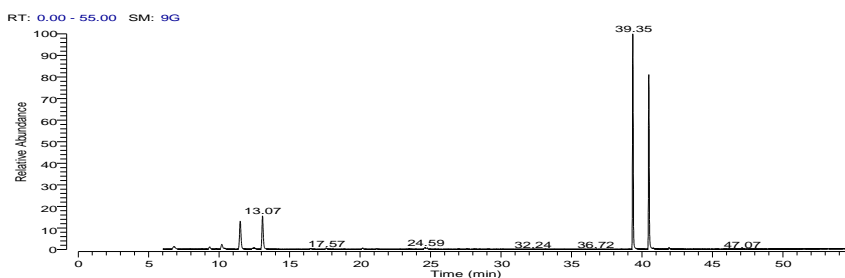
Figure 1. GC/MS chromatogram of *Origanum syriacum* L.

Table 1. The main essential oil components of *Origanum syriacum* L.

RT	Compound Name	SI	RSI	Cas #	%
6,78	-Pinene	942	969	80-56-8	1,02
10,19	-Terpinene	962	979	99-86-5	1,40
11,49	-Terpinene	988	992	99-85-4	8,21
13,07	Cymene	984	995	25155-15-1	8,87
39,35	Thymol	970	982	89-83-8	42,18
40,48	Carvacrol	966	966	499-75-2	33,95

Thirty-four essential oil components, representing 98,62%, were detected in the essential oil of *Origanum onites* L. (Figure 2, Table 2). The major essential oil constituents were thymol (68,28%), -terpinene (5,50%), p-cymene (5,47%) and linalool (4,40%).
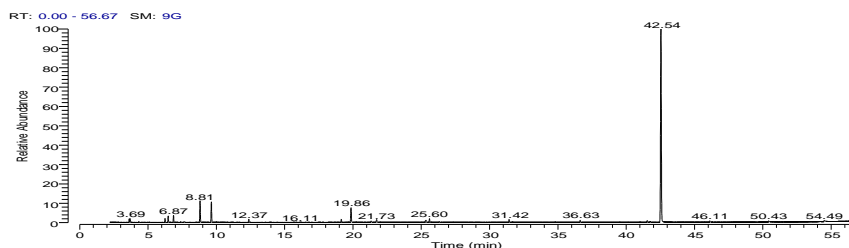

Figure 2. GC/MS chromatogram of *Origanum onites* L.

Table 2. Essential oil components of *Origanum onites* L.

RT	Compound Name	SI	RSI	Cas #	%
6,48	-Myrcene	969	974	123-35-3	1,47
6,87	-Terpinene	974	983	99-86-5	1,64
8,81	-Terpinene	989	993	99-85-4	5,50
9,64	p-Cymene	975	975	99-87-6	5,47
19,86	Linalool	994	995	78-70-6	4,40
42,54	Thymol	969	969	89-83-8	68,28

In the study, *Origanum onites* L. essential oils were found to be more effective against both amikacin-resistant *Pseudomonas aeruginosa* strains and amikacin susceptible strains (Figure 3). In addition, the combination of *Origanum Syriacum* L. and *Origanum onites* L. essential oils showed stronger efficacy against both amikacin-resistant and susceptible strains of *Pseudomonas aeruginosa* (Figure 4).

Figure 3. MIC values of *Origanum syriacum* L. and *Origanum onites* L. essential oils against *Pseudomonas aeruginosa* strains

In addition, it has been shown that these two plant essential oils were also effective on the biofilm formation properties of *Pseudomonas aeruginosa* strains. All bacterial strains were found to be capable of biofilm formation, when *Origanum syriacum* essential oils were used at the concentration of 50 µg/ml. In amikacin susceptible strains, it was determined that the concentration of 12.5 µg/ml of essential oils inhibited biofilm formation in all strains (Table 3). The biofilm formation inhibition capacity of *Origanum onites* essential oils was found to be stronger than that of *Origanum syriacum* L. essential oils (Table 4).

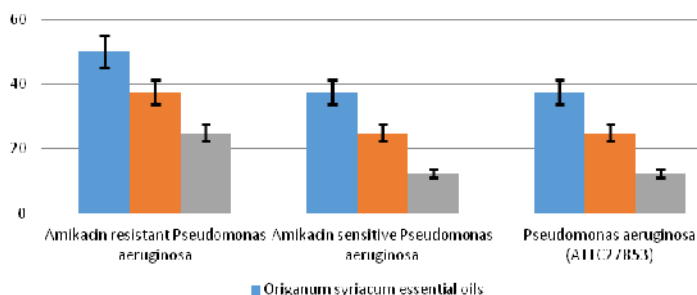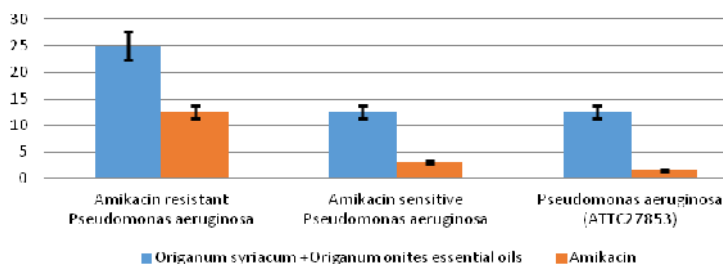Figure 4. Comparing the MIC values of *Origanum syriacum* L. and *Origanum onites* L. essential oils with Amikacin *Pseudomonas aeruginosa* strains

Table 3. Effects of *Origanum syriacum* essential oils on biofilm formation of pseudomonas strains

Biofilm Formation	1.56 µg/ml	3.12 µg/ml	6.25 µg/ml	12.5 µg/ml	25 µg/ml	50 µg/ml	100 µg/ml	200 µg/ml
Amikacin resistant Pseudomonas aeruginosa	12	12	12	9	3	0	0	0
Amikacin sensitive Pseudomonas aeruginosa	12	6	1	0	0	0	0	0
Pseudomonas aeruginosa (ATTC27853)	+	+	+	-	-	-	-	-

Table 4. Effects of *Origanum onites* essential oils on biofilm formation of pseudomonas strains

Biofilm Formation	1.56 µg/ml	3.12 µg/ml	6.25 µg/ml	12.5 µg/ml	25 µg/ml	50 µg/ml	100 µg/ml	200 µg/ml
Amikacin resistant Pseudomonas aeruginosa	12	12	8	6	0	0	0	0
Amikacin sensitive Pseudomonas aeruginosa	12	4	1	0	0	0	0	0
Pseudomonas aeruginosa (ATTC27853)	+	+	+	-	-	-	-	-

These two plant essential oils seem to be effective on biofilm formation of *Pseudomonas aeruginosa* strains. *Origanum syriacum* L. essential oils were found to inhibit the ability of all *Pseudomonas aeruginosa* strains to form biofilms at the concentration of 50 µg/ml. In amikacin susceptible strains, it was determined that the concentration of 12.5 µg/ml of essential oils prevented biofilm formation in all strains. In addition, the combined use of *Origanum syriacum* L. and *Origanum onites* L. essential oils showed stronger biofilm inhibition activity in all Pseudomonas strains (Table 5).

Table 5. Effects of combined use of essential oils of *Origanum syriacum* L. and *Origanum onites* L. on biofilm formation on *Pseudomonas* strains

Biofilm Formation	1.56 µg/ml	3.12 µg/ml	6.25 µg/ml	12.5 µg/ml	25 µg/ml	50 µg/ml	100 µg/ml	200 µg/ml
Amikacin resistant Pseudomonas aeruginosa	12	9	5	0	0	0	0	0

Biofilm Formation	1.56 µg/ml	3.12 µg/ml	6.25 µg/ml	12.5 µg/ml	25 µg/ml	50 µg/ml	100 µg/ml	200 µg/ml
Amikacin sensitive Pseudomonas aeruginosa	11	3	0	0	0	0	0	0
Pseudomonas aeruginosa (ATTC27853)	+	+	+	-	-	-	-	-

DISCUSSION AND CONCLUSION

In our study, amikacin resistant and amikacin susceptible strains of *Pseudomonas aeruginosa* were used. Today, antibiotic resistance is a serious problem. *Pseudomonas aeruginosa* is one of the most important nosocomial infections. In addition, this bacterium gains resistance quite easily. Furthermore, it is also known that this bacterium produces biofilms, which make it easier to obtain resistance to antibiotics and detergents (Ahmed *et al*., 2012; Sharma and Srivastava, 2016).

In the present study, the remarkable efficacy of *Origanum syriacum* L. and *Origanum onites* L. essential oils against both drug-resistant and drug-sensitive *Pseudomonas aeruginosa* strains was determined. More importantly, it has been found that the ability of these bacteria to form biofilms was inhibited by increasing concentrations of essential oils of these plants (Chisti *et al*., 2013).

In the last years when drug resistance has become a global problem, these essential oils have been found promising for the discovery of a new antimicrobial agent.

REFERENCES

Ahmed, S.M. *et al*. (2012), "An emerging multi-drug resistance pathogen in a tertiary care centre in North Kerala", *Ann Biol Res*, 3, 2794-2799.

Chishti, S. *et al*. (2013), "Medicinal importance of genus Origanum: A review", *Journal of Pharmacognosy and Phytotherapy*, 5(10), 170-177, https://doi.org/10.5897/JPP2013.0285.

CLSI (2014), "Performance standards for antimicrobial susceptibility testing twenty-fourth informational supplement", CLSI document M100-s24, Clinical Laboratory Standard Institute, Wayne, PA. Franco, B.E., Martinez, M.A.

Fidan, I. *et al*. (2005), "Pseudomonas aeruginosa su larında antibiyotik direnci ve metallo-beta-laktamaz sıklı ı", *ANKEM Derg*, 19(2), 68-70.

Horan, T.C. *et al*. (2008), "CDC/NHSN surveillance definition of health care–associated infection and criteria for specific types of infections in the acute care setting", *Am J Infect Control*, 36(5), 309-32, https://doi.org/10.1016/j.ajic.2008.03.002.

Mashhady, M.A. *et al*. (2016), "Inhibitory Effects of Plant Extracts on Pseudomonas aeruginosa Biofilm Formation", *Int J Infect*, 3(4), e38199, https://doi.org/10.17795/iji.38199.

Pier, G.B. and Ramphal, R. (2005), "Pseudomonas aeruginosa", in Mandell GL, Bennett JE, Dolin R (eds): *Principles and Practice of Infectious Diseases*, 6th Edition, 2587-615, Churchill Livingstone, New York.

Sharma, S. and Srivastava, P. (2016), "Resistance of Antimicrobial in Pseudomonas aeruginosa", *Int J Curr Microbiol App Sci*, (3), 121-128.

PATRIMONY TEXTILE MATERIALS SHORT CHARACTERIZATION

ELENA-CORNELIA MITRAN[1,2], GABRIEL-LUCIAN RADU[2], ELENA PERDUM[1], IULIANA DUMITRESCU[1], OVIDIU-GEORGE IORDACHE[1], IRINA-MARIANA SĂNDULACHE[1], ANA-MARIA ANDREEA CHIVU[1]

[1]*The National Research Development Institute for Textiles and Leather, 16 Lucretiu Patrascanu, 030508, Bucharest, Romania*

[2]*Politehnica University of Bucharest, 1-7 Polizu Street, Bucharest, Romania,* cornelia.mitran@certex.ro

In this paper we aimed to characterize heritage samples trough different analyses such as physicochemical and microbiological bioburden assessment analyses. The characterization was made on two types of textile materials coming from a private collection: the 1st was from the beginning and the second one from the end of the 20th century. Micro-destructive methods (such as SEM and optical microscopy) and macro-destructive methods (by use of chemical reagents for fibers solubilization) were used to identify and quantify the fibrous composition of the samples. The Differential Scanning Calorimetry (DSC) technique was successfully applied to confirm the fibrous composition. The microbiological bioburden of the samples was evaluated by isolation on two semy-synthetic media: Czapek-Dox and Potato-Dextrose-Agar supplemented with Chloramphenicol. Thus, we have realized a primary characterization of the samples with desire to continue the future studies with focusing on the evaluation of the classes of dyes used for dyeing the samples and the use of micro- or non-destructive methods to obtain more information that could give us a better view of the realization and application of archaeological textile materials. The results showed that the studied textiles were composed from natural yarns (wool and cellulose), unevenness damaged (holes, creases) due to conservation conditions and, in a lesser extent, to the microbiological activity of the specific strains present on the surface of the textiles.

Keywords: micro-destructive method, heritage sample, SEM, textile.

INTRODUCTION

Natural fibers such as cotton, wool, hemp, flax and silk are used since the beginning of human kind. In the 20th century there was a tendency to increase the production of synthetic fibers to the detriment of natural fibers, until highlighting of pollution impact that these synthetic fibers have on the human health and environment (Monteiro *et al*., 2012). But, as we can see, there is a trend to go back in the past and learn about how the human lived healthier and without affecting the environment too much. Because of the amount of textile samples that can be found in different places of the world and the big impact that they have on our history, in recent years, there has been an increasing need for the development of micro and non-destructive analyses of historical samples characterization. These characterizations methods can provide useful information for improving the methods of preserving and restoring historical textiles and give us more information about how the people that didn't have so much technology, that exist in our days, were able to create so complex, resistant and beautiful textiles.

Unfortunately, the materials deterioration due to the storage conditions, the complex composition, the unknown dyeing and finishing processes make difficult an accurate analysis of heritage samples. More than that, the microbiological degradation due to enzymatic activity of various fungi strains or pests aggravates the problems.

This study aims to highlight some of the heritage materials characteristics through physical, chemical and microbiological methods.

MATERIALS AND METHODS

Samples

Two samples were evaluated in this study. First sample, abbreviated A, is from the beginning of the 20th century and it is a belt form Susag - Miercurea Sibiului area, while the second sample, abbreviated B, is a textile material from the end of the 20th century, both originating from a private collection.
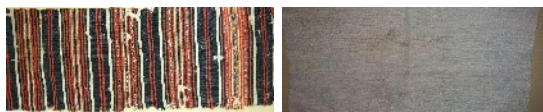

Figure 1. Left: sample from the beginning of the 20th century (A); right: sample from the end of 20th century (B)

Methods

Two types of microscopes were used for evaluating the particularity of the samples, namely the Scanning Electron Microscopy (Quanta 200, FEI, Netherlands) and an Optical Microscope (Olympus BX41, Japan). SEM analysis is widely used for the examination of patrimony textiles because of its micro-destructive properties (Peceliunaite-Baziene, 2002). Optical microscopy gave us information about the type of fiber components and also a better view of the level of degradation of the two samples.

The fibrous composition was investigated based on SR 13231-95 and the UE Regulation 1007/2011 standardized methods. The main disadvantage of this method is its destructive character.

The thermal behavior of the samples was assessed by Differential Scanning Calorimetry - DSC (Perkin Elmer, USA) by using only a few milligrams of fibers. The fibers were placed in closed aluminum crucibles and a similar empty crucible was used as reference. The temperature program was started from $35°C$ (held for 1 minute) to $500°C$ (held for 1 minute) with a heating temperature of $10°C$ per minute. Nitrogen with a flow rate of $10mL/min^{-1}$ was purged in the DSC oven. Beside SEM and optical microscopy analyzes, DSC is one of the most used techniques due to its advantages such as: any form and type of material may be tested, short time for investigations, small quantities of sample, micro-destructive analysis (Shafizadeh, 1985; Calamari *et al*., 1990; Dong *et al*., 2015; Ferrero *et al*., 1998).

To deeply investigate the causes of deterioration, microbiological analyzes were carried out to isolate the eventually microorganisms present on the samples. Two different nutritive media were used in this procedure: Czapek-Dox –CD (Scharlau, Spain) a semi-synthetic media usually frequently used for isolation of fungal species such as *Aspergillus, Penicillium*, *Paecilomyces*, *Saccharomyces* etc. and a second nutritive media, Potato-Dextrose-Agar (Scharlau, Spain) supplemented with 250mg of Cloramfenicol antibiotic (250mg/400mL of PDA media) for inhibition of certain bacterial species (species of *Staphylococcus*, *Streptococcus*, *Escherichia* etc.). Chopped samples were put in sterile jars in 60 mL of sterile deionized water and agitated for 2h at 185 rpm. Afterwards, 300µL from each samples were plated in duplicates on each nutritive media and incubated for 7 days at $28°C$.

RESULTS AND DISSCUSION

Physical-Chemical Evaluation

The fibrous composition of the samples is shown in Table 1. While the sample A is composed from a mixture of cotton and wool, the sample B is based on a complex mixture of cellulose yarns (cotton, flax, hemp).

Table 1. Fibrous composition identification

Sample	Nature of raw material SR 13231:1995	Fibrous composition UE Regulation 1007/2011
A	Cotton + Wool	23.7% cotton + 76.3% wool
B	Cellulosic fibers (Cotton, Flax and Hemp)	100% cellulosic fibers

The results presented above are confirmed by SEM (Figure 2) and optical microscopy images (Figure 3). We can see in the pictures bellow the visual characteristics of the constituent fibers. The images give us information about the degradation of the fibers, as it can be seen that sample A is more degraded than sample B. The extended degradation of sample B is caused by longer exposure to environmental physical and chemical factors, like light, dust, organic and inorganic pollutants, temperature and humidity variations.
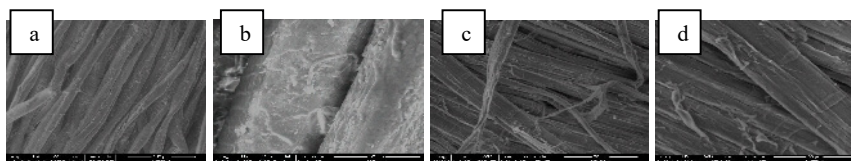

Figure 2. SEM images of: Sample A- a) cotton fibers (100 μm); b) wool fibers (30 μm);Sample B- c) cotton fibers (50 μm); d) hemp and flax fibers (30 μm);
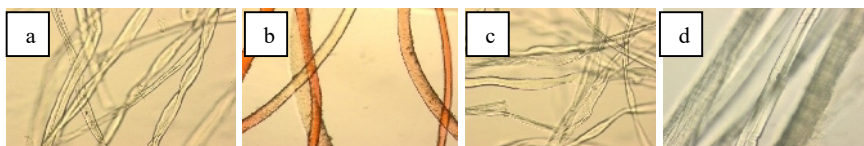
Figure 3. Optical microscope images of: Sample A- a) cotton fibers(10x); b) wool fibers (10x); Sample B- c) cotton fibers (20x); d) hemp and flax fibers (20x)

Thermal behavior
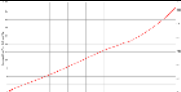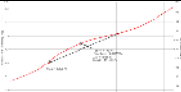
In order to identify different textile fibers we have used DSC as an alternative qualitative method. DSC analysis is useful to distinguish different types of fibers and their differences after exposure to bleaching, descaling or other treatment processes (Tonetti *et al*., 2015). Thermal behavior of samples A and B is presented in Table 2 and 3.

Table 2. Thermodynamic parameters for sample A and B

Thread	Weight sample [mg]	Onset temperature [°C]	Peak temperature [°C]	Delta H [J/g]
A: gray- transverse	5.9	350.78	357.43	13.1499
A: black	6.1	223.17	238.72	223.2328 J/g
B: white- peak 1	4.8	259.99	299.20	335.8923
B: white- peak 2		345.56	350.04	25.2335

Table 3. Thermogram for sample A and B

Thread	Thermogram
A: gray- transverse	
A: black	
B: white	

Sample A: The DSC results obtained for sample B are correlated with those obtained from the assessment of fibrous composition, namely 23.7% Cotton and 76.3% Woo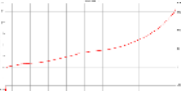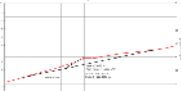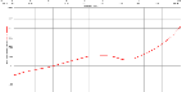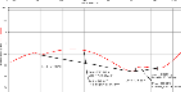l. As can be seen in Table 3, the transverse gray yarn shows a broad endotherm peak at a temperature of 357.43°C, corresponding to the partially crystallized cellulose decomposition (Macsim *et al.*, 2011). In oxygen atmosphere, this peak is shifted to lower values (346.2°C) due to cotton pyrolysis followed by oxidation of the resulted compound by oxygen (Macsim *et al.*, 2011). Theoretically, cotton cellulose is characterized by three regions, located between 60-150°C, 150-250°C and 250-500°C, corresponding to water loss, non-cellulosic volatile components (waxes, acids, esters) and decomposition of cellulosic components (proteins, pectins and hemicellulose) and cellulose / chemical decomposition (cleavage of glyosidic linkages with levoglucose formation) (Ciolacu *et al.*, 2011).

In the case of the black thread, it is noticeable an endotherm peak that starts from 223°C with the maximum at 238°C. This peak it is attributed to the cleavage of the crystal structure due to the melting and degradation of the various morphological components that form the complex hierarchical structure of the wool chain (Giuliano *et al.*, 2003; Jinan, 1997).

In the case of sample B, 2 peaks are detected: a large one with a maximum temperature of 299°C and a second small peak with maximum located at 350°C. As literature data show (Albano *et al.*, 1999) for the flax yarns, the thermal depolymerization of hemicellulose and glycosidic bonds takes place at about 340-370°C. At the same time, hemp shows a two-step degradation process: the first at 225-275°C corresponding to the decomposition of hemicellulose and the second at 325-360°C attributed to lignin decomposition (Pracella *et al.*, 2006). Under nitrogen atmosphere, an endothermic peak around 345°C is observed for the cellulose decomposition in cotton, the temperature being strongly affected by multiple factors as

contaminants, molecular weight, dyes, finishing agents etc. (Ibrahim, 2011; Ciolacu *et al*., 2011; Xia *et al*., 2016). Corroborating all the obtained data, we could affirm that the third component of sample B is cotton.

Bioburden

Microbial deterioration can affect historic and culturally important artefacts, by specific mechanisms, such as enzymatic activity on the substrate, biofilm formation attached to materials' surface (polymer matrix formation). After samples were placed in sterile jars (Figure 4), aliquots were plated on semi-synthetic nutritive media (spread with a Drigalski rod) (Figure 5).

Figure 4. Left- Sample A, Right- Sample B
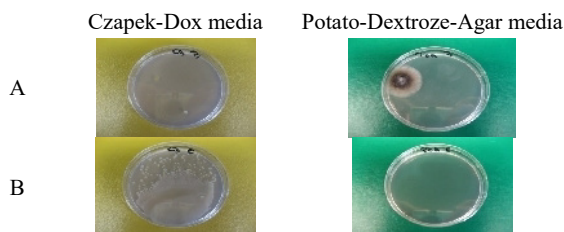
Figure 5. Sample A and B on Czapek-Dox and Potato-Dextrose-Agar media

Following incubation period (28°C for 7 days), strains were visualized on an Olympus SZ 61 stereomicroscope, at magnification levels of 0.67x and 3x (Figure 6).
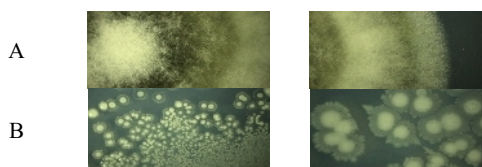
Figure 6. Sample A (left- 0.67x, right- 3x) (PDA media); Sample B (left- 0.67x, right- 3x) (Czapek-Dox media)

Microbial growth highlighting on Petri dishes show no biomass development on sample A plate, on Czapek-Dox media, compared to a filamentous structure developed on PDA media. Furthermore, sample B showed microbial development on Czapek-Dox plate, which can be highlighted as a yeast-like structure, and no development on the PDA plate. Also, it can be seen the lack of bacteria-like specific structures, both on Czapek-Dox media, which is a low nutritive value substrate, and on PDA media, that although it possesses high enough nutritive value for bacterial development, the presence of chloramphenicol in the media inhibited bacterial growth.

CONCLUSIONS

In the present work two different samples have been investigated using electronic and optical microscopy, standardized chemical methods, DSC and microbiological procedures. The used methods allowed the identification of the fibrous composition and the stage of the samples degradation. As the results demonstrated, the sample A is more degraded than sample B. Also we can correlate the obtained results with the ones existing in the literature. The future studies will be focused on the evaluating the classes of dyes or other type of compounds used in these samples manufacturing.

REFERENCES

Albano, C. *et al*. (1999), "Thermal Stability of Blends of Polyolefins and Sisal Fiber", *Polymer Degradation and Stability*, 66,179-190, https://doi.org/10.1016/S0141-3910(99)00064-6.

Calamari, T.A. *et al*. (1990), "Distinguishing weathered from unweathered cotton by thermal analysis", *American Dyestuff Reporter*, 79, 42-47.

Ciolacu, D. *et al*. (2011), "Amorphous cellulose- structure and characterization", *Cellulose Chemistry and Technology*, 45, pp. 13-21.

Dong, Z. *et al*. (2015), "Thermal properties of flax fiber scoured by different methods", *Thermal Science*, 19, 939-945, https://doi.org/10.2298/TSCI130329005Z.

Ferrero, F. *et al*. (1998), "Thermal degradation of linen textiles: the effect of ageing and cleaning", *Journal of the Textile Institute*, 89, 562-569, https://doi.org/10.1080/00405009808658642.

Giuliano, F. *et al*. (2003), "Physical properties of wool fibers modified with isocyanate compounds", *Journal of Applied Science*, 89, 1390-1396, https://doi.org/10.1002/app.12271.

Ibrahim, S.F. (2011), "Thermal Analysis and Characterization of Some Cellulosic Fabrics Dyed by a New Natural Dye and Mordanted with Different Mordants", *International Journal of Chemistry*, 3, 40-54, https://doi.org/10.5539/ijc.v3n2p40.

Jinan, C. (1997), "Origin of the bimodal "melting" endotherm of α-form crystallites in wool keratin", *Journal of Applied Science*, 63, 411-415, https://doi.org/10.1002/(SICI)1097-4628(19970124)63:4%3C411::AID-APP1%3E3.0.CO;2-U.

Kazayawoko, M. *et al*. (1997), "Diffuse Reflectance Fourier Transform Infrared Spectra of Wood Fibers Treated with Maleated Polypropylenes", *Journal of Applied Polymer Science*, 66, 1163-1173, https://doi.org/10.1002/(SICI)1097-4628(19971107)66:6%3C1163::AID-APP16%3E3.0.CO;2-2.

Macsim, M. *et al*. (2011), "Investigation of dyeing effect on the morphology of cotton fibre and cotton/PES blend by thermal analysis", *Buletinul Institutului Politehnic din Iasi*, Tomul LVII (LXI), Fasc. 1, 53-61.

Monteiro, S.N. *et al*. (2012), "Thermogravimetric Stability Behavior of Less Common Lignocellulosic Fibers – a Review", *Journal of Materials Research and Technology*, 1, 189-199, https://doi.org/10.1016/S2238-7854(12)70032-7.

Parvinzadeh, G.M. and Elahi, A., (2013), "UV Radiation Inducing Succinic Acid/Silica-Kaolinite Network on Cellulose Fiber to Improve the Functionality", *Composites Part B: Engineering*, 48, 158-166, https://doi.org/10.1016/j.compositesb.2012.12.002.

Peceliunaite-Baziene, E. (2004), "Archaeological Textiles of 2/2 Diagonal Twill Found in the Coastal Cemeteries of the 1st – 12th Centuries", *Lithuania Archaeologia Lituana*, 5, 66 – 77.

Pracella, M. *et al*. (2006), "Functionalization, compatibilization and properties of polypropylene composites with Hemp fibres", *Composites Science and Technology*, 66, 2218-2230, https://doi.org/10.1016/j.compscitech.2005.12.006.

Shafizadeh, F. (1985), "Thermal Degradation of Cellulose", *Cellulose Chemistry and its Application*, 266-289.

Tonetti, C. *et al*. (2015), "Differential scanning calorimetry for the identification of animal hair fibres", *Journal of Thermal Analysis and Calorimetry*, 119, 1445-1451, https://doi.org/10.1007/s10973-014-4247-8.

Xia, Z. *et al*. (2016), "Comparative study of cotton, ramie and wool fiber bundles' thermal and dynamic mechanical thermal properties", *Textile Research Journal*, 88, 856-867, https://doi.org/10.1177/0040517515596937.

SYNTHETIC PYRETHROIDS DETERMINATION FROM FUNCTIONALIZED TEXTILE MATERIALS - PERMETHRIN

ELENA PERDUM, DOINA TOMA, IULIANA DUMITRESCU, CORNELIA-ELENA MITRAN, IRINA-MARIANA SĂNDULACHE, OVIDIU-GEORGE IORDACHE

The National Research Development Institute for Textiles and Leather, 16 Lucretiu Patrascanu, 030508, Bucharest, Romania, E-mail: elena.varzaru@certex.ro.

Cell Solution® Protection fibers are natural cellulosic manmade fibers and provide effective and durable protection against insects - such as ticks and mosquitoes. Cell Solution® Protection fibers can be easily processed into textiles and have consistent dyeability whan following the recommended processing/finishing method. Permethrin is a chemical categorized in the pyrethroid, insecticide group. Permethrin is used as an insecticide in agriculture or as a personal protective measure (cloth impregnant, used primarily for US military uniforms and mosquito nets). The objective of this work was the determination of Permethrin from functionalized textile materials. Permethrin has four stereoisomers (two enantiomeric pairs), arising from the two stereocenters in the cyclopropane ring. (1R,3S)-trans and (1R,3R)-cis enantiomers are responsible for the insecticidal properties of permethrin. We performed the extraction of Permethrin from textile materials using accelerated solvent extraction (ASE), followed by identification of permethrin and cuantification by liquid chromatography with spectrophotometric detection (HPLC-MWD) and we confirmed the results by gas chromatography with mass spectrometric detection (GC-MS). Both analytical methods have contributed to determination of trans and cis-permethrin.

Keywords: Permethrin-impregnated clothing, Cell Solution® Protection Fibers, chromatography

INTRODUCTION

Permethrin is an insecticide in the Pyrethroid family, which are synthetic chemicals that act like natural extracts from the chrysanthemum flower. Clothing, shoes, bed nets, and camping gear can be treated with a pesticide called permethrin to kill or repel insects such as mosquitoes and ticks. Clothing and other products can be purchased pre-treated, or products can be treated using EPA-registered products. The U.S. Military has been using permethrin to treat combat uniforms for over 20 years to protect soldiers from diseases carried by insects. Permethrin is the only pesticide approved by the EPA for these uses. When it is applied properly, permethrin binds tightly to the fabrics, resulting in little loss during washing and minimal transfer to the skin. Permethrin is poorly absorbed through the skin, although sunscreens and other products may increase the rate of skin absorption (http://npic.orst.edu/pest/mosquito/ptc.html). Personal protective measures against hematophagous vectors constitute the first line of defense against arthropod-borne diseases. In this regard, a major advance has been the development of residual insecticides that can be impregnated into clothing (Faulde *et al.*, 2016). Cell Solution® Protection fibers provide effective and durable protection against insects - such as ticks and mosquitoes. Via direct spinning, the insect repellent permethrin is embedded in the Cell Solution® fiber core and migrates to the fiber surface in a tightly controlled manner. The patented technology ensures that a small, but just enough amount of permethrin is diffused from the inner of the Protection fiber to the surface. The direct contact with high concentration of active ingredients for example. in a coating, is avoided because the stored permethrin from the interior of the Cell Solution® Protection fiber is resupplied in small doses. Due to the limited availability of the active substance at the fiber's surface it is avoided that the active

substance is lost rapidly by environmental influences. Impregnation by dipping, spraying or even covering of polymer-insecticide blends on the fabric's surface give long-term permanent anti-insecticide activity at very high concentration only.

Our study was focused on the extraction of Permethrin from textile materials using accelerated solvent extraction (ASE), followed by identification of permethrin and cuantification by two chromatographyic methods, HPLC-MWD and GC-MS.

EXPERIMENTAL

We used 3 textile materials in our study: Raw Cell Solution Protection knit, Bleached Cell Solution Protection knit and Dyed Cell Solution Protection knit.

The three test specimens were subjected to accelerated solvent extraction. Approximately 1 g of material was weighed out of each sample. These were cut into pieces and introduced into extraction cells (22 mL volume) which were filled with diatomaceous earth and subjected to methanol-accelerated extraction.

Extraction Method

The condition of the extraction method are the following:
Solvent: Methanol;
Preheat time: 5 min;
Analysis time: 40 min;
Extraction cycles: 3;
Temperature: 80°C;
Washing: 60% with methanol

After extraction, the resulting solutions were allowed to cool and subsequently filtered through 0.45 μm PTFE filters and transferred to vials for further analysis by HPLC-MWD and GC-MS. For the quantification of permethrin in the textile samples a calibration curve was made by diluting stock solution of permethrin to the following concentrations: 2400 ppm, 1800 ppm, 1200 ppm, 600 ppm and 300 ppm.

Liquid Chromatography with Spectrophotometric Detection (HPLC-Equipment Agilent Technologies 1100 series MWD)

Conditions of the detection method used are the following:
Eluent: Acetonitrile / HOH: 90/10, isocratic
Stationary phase: Zorbax Eclipse XDB C18 column (3.5 μm); (150 x 4.6) mm
Flow rate: 0.5 mL / min
Column temperature: 32°C
Volume injected: 10 μl
Detection: MWD (spectrophotometer) at 275 nm.

Gas Chromatographic Method Coupled with Mass Spectrometry (GC-MS 6890N / 5793 Agilent Technologies)

Capillary column: DB-35MS (J & W) ®, length: 35 m, inside diameter 0.25 mm
Injection system: splitless; Injector temperature: 250°C;
Carrier gas: helium;
Flow rate: 1.24 mL / min

Temp. program: Initial temp.: 70°C (1min), Heating rate: 25°C/min., Final temp.: 280°C (8min);

Injection volume: 1 μl; Detector: MS (mass spectrometer)

RESULTS AND DISCUSSIONS

Sample Raw Cell Solution Protection Knit

Figure 1. HPLC chromatogram of sample Raw Cell Solution Protection Knit
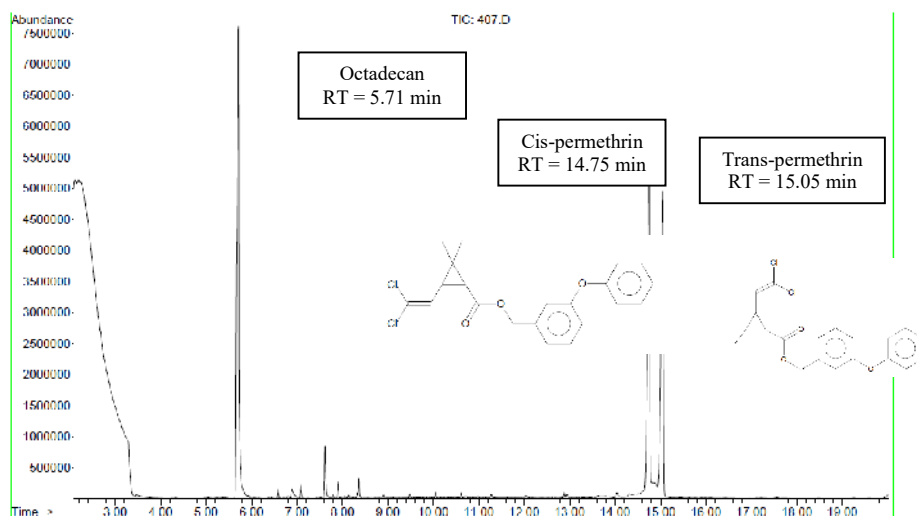
Figure 2. GC chromatogram of sample Raw Cell Solution Protection Knit

Bleached Cell Solution Protection knit

Figure 3. HPLC chromatogram of sample Bleached Cell Solution Protection Knit
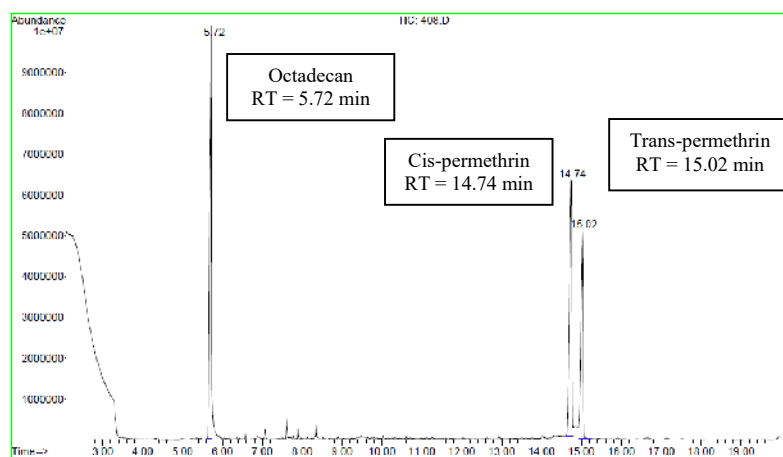
Figure 4. GC chromatogram of sample Bleached Cell Solution Protection Knit
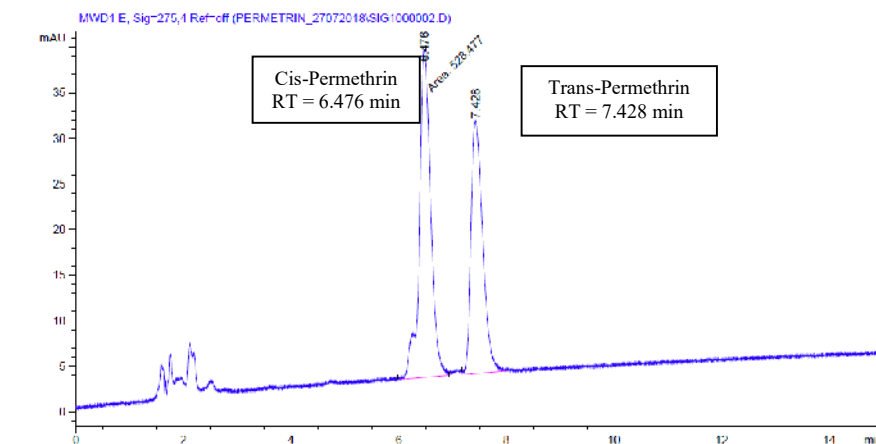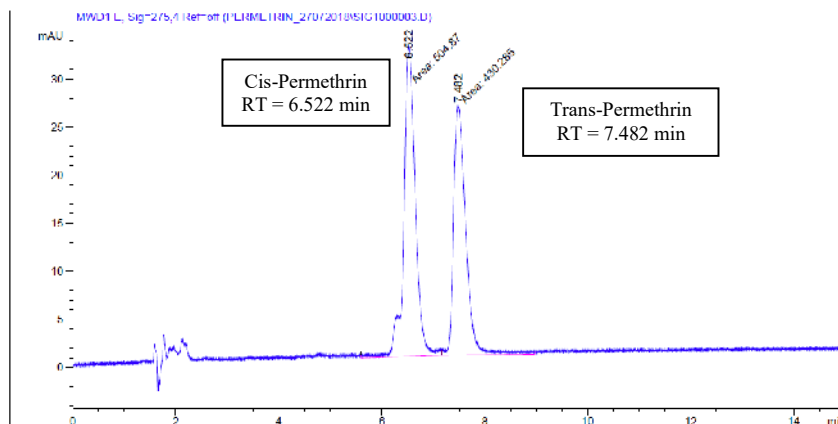
Dyed Cell Solution Protection knit
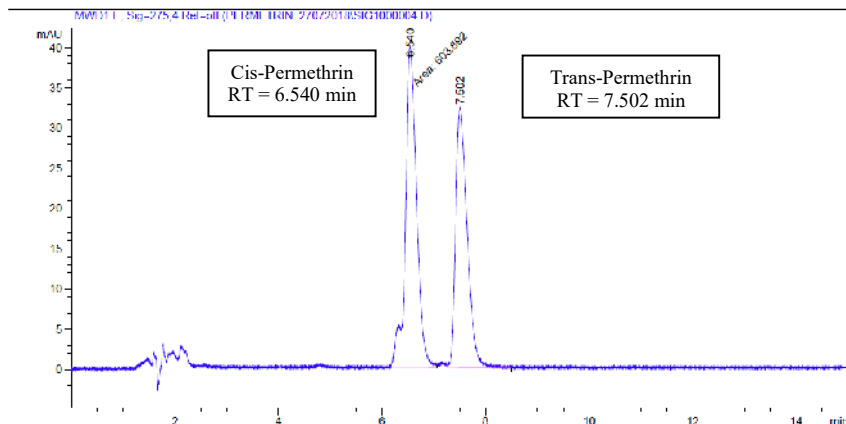
Figure 5. HPLC chromatogram of sample Dyed Cell Solution Protection Knit
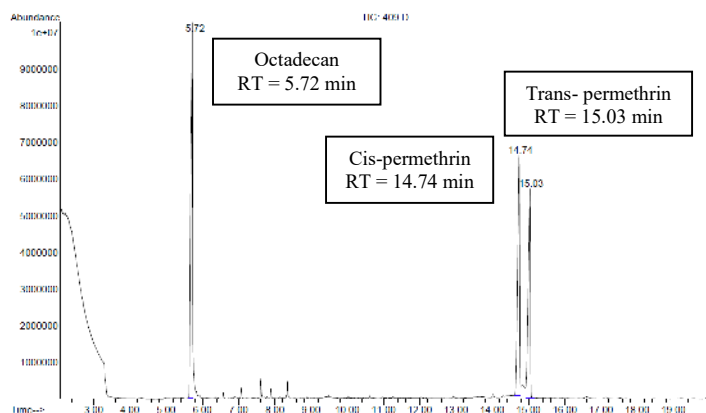
Figure 6. GC chromatogram of sample Dyed Cell Solution Protection Knit
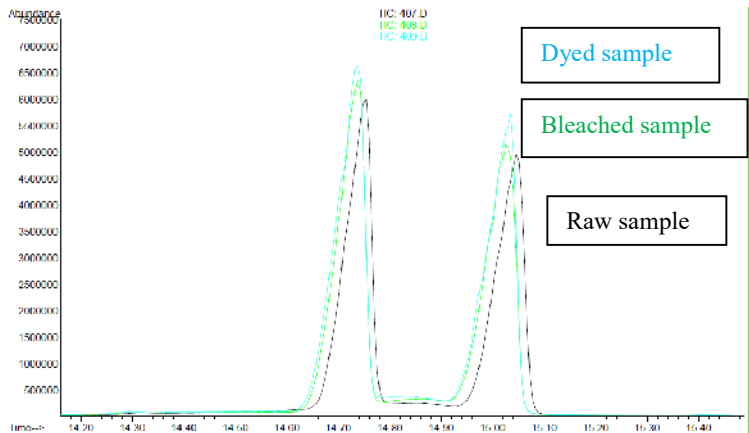
Figure 7. Overlaid GC chromatogram of the three sample: dyed, bleached and raw
textile materials

Permethrin Quantification

Table 1. Quantification of permethrin in the textile samples

	Raw sample	Bleached sample	Dyed sample
Permethrin	595.68 µg/mL	592.26 µg/mL	702.59 µg/mL

CONCLUSIONS

As we can see in Figures 1-7, both Cis-permethrin and Trans-permethrin have been extracted and detected in the textile samples; HPLC method was useful in quantification of permethrin based on a calibration curve, and GC method confirmed the presence of both isomers. The highest quantity of permethrin was found in dyed sample, probably due to the fact that including the insecticide in the Cell solution fiber core followed by dyeing of textile materials ensures a better fixation of the protective agents against insects, thus resulting a greater amount of insecticide extracted from sample.

REFERENCES

Faulde, M.K., Pages, F. and Uedelhoven, W. (2016), "Bioactivity and laundering resistance of five commercially available, factory-treated permethrin-impregnated fabrics for the prevention of mosquito-borne diseases: the need for a standardized testing and licensing procedure", *Parasitology Research*, 115(4), 1573–1582, https://doi.org/10.1007/s00436-015-4892-2.
*** http://npic.orst.edu/pest/mosquito/ptc.html

SELF-CLEANING PROPERTIES OF COTTON GAUZES IMPREGNATED WITH CALCIUM ALGINATE/TiO2-Ag/REDUCED GRAPHENE OXIDE COMPOSITE

MARCELA-CORINA ROŞU[1], CRINA SOCACI[1], ALIN-SEBASTIAN PORAV[1], ALEXANDRU TURZA[1], LAURA CHIRILĂ[2]*, CARMEN GAIDĂU[2], DANIEL TÎMPU[3], ALICE-ORTANSA MATEESCU[4], IOANA-RODICA STĂNCULESCU[4]

[1]National Institute for Research and Development of Isotopic and Molecular Technologies, 67-103 Donat Street, 400293, Cluj-Napoca, Romania, email: marcela.rosu@itim-cj.ro

[2] The National Research Development Institute for Textiles and Leather, 16 Lucretiu Patrascanu Street, 030508, district 3, Bucharest, Romania, *Corresponding author email: chirila_laura@yahoo.com

[3]"Petru Poni" Institute of Macromolecular Chemistry, 41A Grigore Ghica Voda Alley, 700487 Iasi, Romania, email: dtimpu@icmpp.ro

[4]"Horia Hulubei" National Institute for Research and Development in Physics and Nuclear Engineering, 30 Reactorului Street, 077125, Magurele, Romania, email:amateescu@niham.nipne.ro

Nano-modified fabrics using photocatalytic materials have a vast potential for the development of new products from self-cleaning fabrics for consumer to filter membranes for separation field and/or photocatalytic degradation of various dyes from wastewater. The aim of this study was to obtain TiO2-Ag/reduced graphene oxide-treated cotton gauzes impregnated in calcium alginate matrix with self-cleaning properties. The morphological and structural properties of prepared materials were investigated by X-ray diffraction, FTIR spectroscopy and SEM analysis. Self-cleaning tests were performed by evaluation of the photodegradation of amaranth dye solution. Samples were exposed to sun light in March at Cluj-Napoca, Romania (latitude: 47°N; longitude: 24°E; altitude: 354 m) for 2 hours. No noticeable discoloration of dye was observed when the untreated cotton sample was used. TiO2-Ag composite-treated cotton gauzes display self-cleaning properties. By using TiO2-Ag/reduced graphene oxide composite, an increase in self-cleaning efficiency based on the photocatalytic amaranth degradation was obtained. The photocatalytic activity under natural environmental conditions indicates that the prepared composite has practical application to develop textile materials with self-cleaning properties.

Keywords: TiO_2-Ag/reduced graphene oxide, photocatalytic materials, amaranth degradation

INTRODUCTION

Treatment of fabrics with various additives (organic or inorganic nano-structured materials) shows a growing interest for domestic and industrial use due to self-cleaning, antimicrobial and anti-pollution characteristics (Wang *et al*., 2014). TiO_2-based materials are a reliable choice to provide photocatalytic properties considering the special properties of TiO_2 (such as, chemical and photo stability, non-toxicity, lower cost, etc.) (Katoueizadeh *et al*., 2017). An interesting perspective is created by using graphene derivatives for uniform coating the cotton fibers that confer them special properties, such as good electric conductivity, tensile strength, flexibility etc. As a result, smart multifunctional fabrics could appear on market making life safer, healthier, and more comfortable (Kowalczyk *et al*., 2017; Karim *et al*., 2017).

In this study, TiO_2-Ag and TiO_2-Ag/reduced graphene oxide (TiO_2-Ag/RGO) composites were prepared and coated over cotton gauzes specimens impregnated in calcium alginate matrix in order to develop fabrics with self-cleaning properties.

EXPERIMENTAL

Materials

Sodium alginate was purchased from Sigma Aldrich, United Kingdom, calcium chloride ($CaCl_2$) was obtained from Alfa Aesar, Germany. Conventional cotton gauze fabric was used. TiO_2-Ag and TiO_2-Ag/reduced graphene oxide (TiO_2-Ag/RGO) composites were prepared according to the previously described procedure (Rosu *et al.*, 2016).

Preparation of Composite-Treated Cotton Gauzes

The composite powders (TiO_2-Ag and TiO_2-Ag/RGO) were dispersed into a 2% aqueous solution of sodium alginate (8 mg/ml) and were sonicated for 15 min. The cotton gauze specimens (2cm x 3cm 6-fold 1 sheets) were impregnated with these two prepared dispersions (4 ml/each piece of cotton gauze). Thereafter, the specimens were immersed in 4% $CaCl_2$ aqueous solution for cross-linking and thus, obtaining insoluble Ca-alginate with TiO_2 immobilized on them. After one day, all gauze cotton specimens were removed from $CaCl_2$ aqueous solution and were dried at 25°C in an oven for 24 h. The resulting materials were denoted as CaAlg/TiO₂-Ag/CG and CaAlg/TiO₂-Ag/RGO/CG. A cotton gauze specimen impregnated with calcium alginate matrix without composites was prepared as control specimen (CaAlg/CG).

Characterization of Composite-Treated Cotton Gauzes

The X-ray diffraction (XRD) patterns of the specimens were measured with a BRUKER D8 Advance X-ray diffractometer using CuK_α radiation (λ =1.54056 Å). The functional groups of the specimens were investigated with a JASCO FTIR-6100 Instrument. The morphology of the composite-treated cotton gauzes was studied by scanning electron microscope (SEM) using an SU-8230 operated at 30 kV (Hitachi, Japan) . Energy dispersive X-ray (EDX) spectroscopy was used for elemental analysis. An UV-VIS Jasco Spectrophotometer (Japan) was used for recording the absorbance spectrum of amaranth dye solutions.

Photocatalytic Experiments

The photocatalytic experiments were carried outside the laboratory based on the degradation of amaranth dye (AM) in an aqueous solution under sun light radiation. The composite-treated cotton gauzes were placed in 20 ml of 2×10^{-5}M amaranth aqueous solution. After irradiation of sun light at fixed intervals of time, the dye concentration was determined based on UV-VIS spectroscopy measurements and AM calibration curve (λ_{max} = 520 nm). The AM degradation percentage was calculated as:

degradation efficiency (%) = (1-C₀/Cₜ) x 100,　　　　　　　　　　　　　(1)

where C_0 and C_t are the concentrations of the dye at the initial time and at time *t*, respectively.

RESULTS AND DISCUSSION

The morpho-structural characterization of TiO_2-Ag and TiO_2-Ag/RGO composites was previously reported (Rosu *et al*., 2016). The XRD patterns of composite-treated cotton gauzes were presented in Figure 1. X-ray diffraction studies showed the typical of cellulosic materials peaks at 2θ = 14.8°, 16.2°, 22.5°, and 34.0° related to (101), (101), (002) and (040) reflections of cellulose I (natural cellulose) (Liu *et al*., 2012; Mikhalovska *et al*., 2012). The peaks at 2θ = 25.1°, 37.5°, 47.8°, 53.8°, 54.8° correspond to crystal planes (011), (004), (020), (015), (121) of tetragonal TiO_2 anatase phase (PDF Form 99-100-9413). No TiO_2 rutile phase was detected. No typical peaks of silver were found. The broad and low intensity XRD peak of (002) reduced graphene oxide at $2\theta \approx 25°$ was not observed.
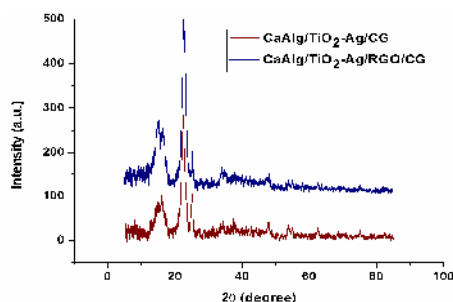
Figure 1. X-ray diffraction profiles of CaAlg/TiO_2-Ag/CG and CaAlg/TiO_2-Ag/RGO/CG

Infrared spectra of composite-treated cotton gauzes (Figure 2) are typical of natural cellulosic fibres. The main absorption bands were noted at 3400 cm^{-1}, 2900 cm^{-1}, 1650 cm^{-1}, 1151 cm^{-1}, 1100 cm^{-1} attributed to vibration of functional groups of cellulose: -OH stretching, -CH stretching, HOH bending of adsorbed water/C=O stretching, C-O-C stretching and C-O stretching (Liu *et al*., 2012; Mikhalovska *et al*., 2012).
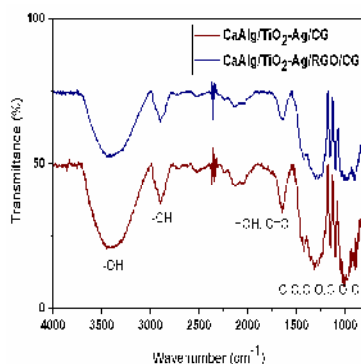
Figure 2. FTIR spectra of CaAlg/TiO_2-Ag/CG and CaAlg/TiO_2-Ag/RGO/CG

The SEM images (Figure 3) showed a surface discontinuity of cotton gauze coated with CaAlg/TiO$_2$-Ag. On the other hand, the treatment of cotton gauze using CaAlg/TiO$_2$-Ag/RGO resulted in a smoother and more homogeneous surface than that CaAlg/TiO$_2$-Ag-treated one suggesting a good adhesion bonding between composite and cotton fibers.
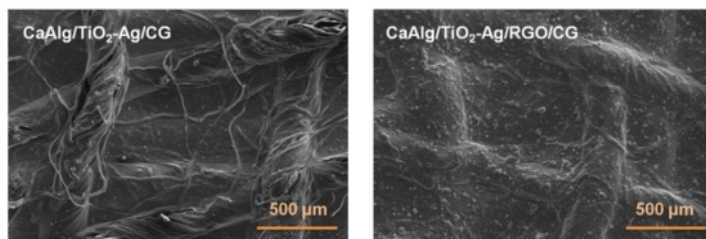
Figure 3. SEM image of composite-treated cotton gauzes

EDX analysis (Figure 4) reveals the presence of C, O, Ti, Ag, Ca and Cl elements in the CaAlg/TiO$_2$-Ag/RGO/CG specimen. The presence of Cl element is caused by cotton gauze immersion into CaCl$_2$ aqueous solution for cross-linking. The EDX mapping image of CaAlg/TiO$_2$-Ag/CG is not shown.
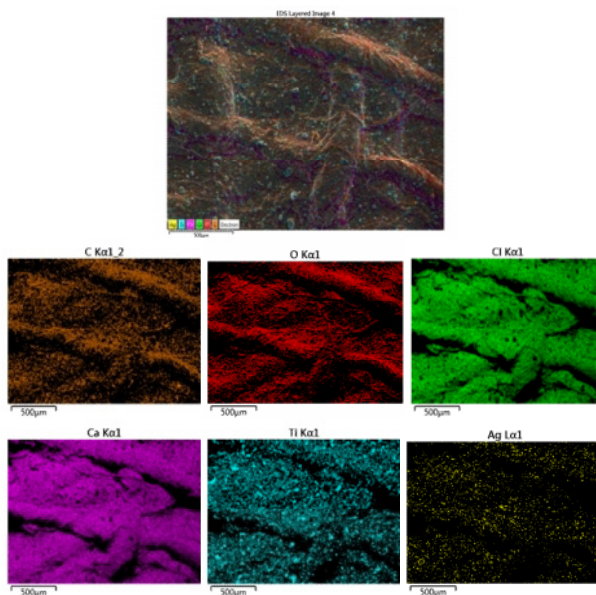
Figure 4. Elements mapping of CaAlg/TiO$_2$-Ag/RGO/CG specimen surface

The photocatalytic behavior of the composite-treated cotton gauzes was evaluated by photodegradation of amaranth dye solution under sun light exposure. Figure 5 shows the UV-VIS spectra of composite-treated cotton gauzes in comparison with amaranth

dye solution spectrum. The intensity of the adsorption peaks diminished in order: CaAlg/CG > CaAlg/TiO$_2$-Ag/CG > CaAlg/TiO$_2$-Ag/RGO/CG.
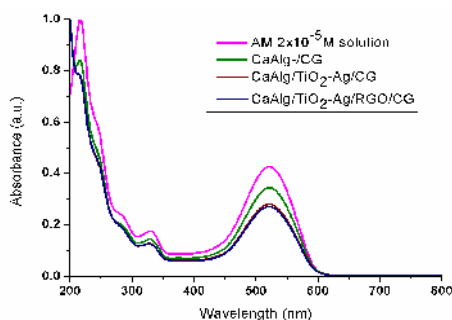
Figure 5. Comparative UV-VIS spectra of composite-treated cotton gauzes after 2 h of sun light exposure

As can be seen from Figure 6, the CaAlg/TiO$_2$-Ag/CG and CaAlg/TiO$_2$-Ag/RGO/CG rapidly degrade AM under sun light irradiation with a slight increasing degradation efficiency of specimens containing reduced graphene oxide.
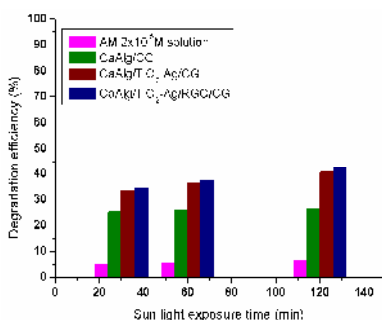
Figure 6. Comparative degradation efficiency of composite-treated cotton gauzes after 2 h of sun light exposure

CONCLUSION

The TiO$_2$-Ag and TiO$_2$-Ag/RGO-treated cotton gauzes impregnated in calcium alginate matrix have been prepared to compare their photodegradation efficiencies. The photodegradation of amaranth dye over TiO$_2$-based composite treated cotton gauzes is improved under exposure of sun light. This result highlights the potential of obtained composites to use in the development of self-cleaning photocatalytic cotton fabrics. Further experimental studies will be considered in order to determine the optimum conditions for maximizing amaranth dye degradation using the TiO$_2$-Ag/RGO based composites.

REFERENCES

Karim, N. *et al*., (2017), "Scalable production of graphene-based wearable e-textiles", *ACSNano*, 11, 12266−12275, https://doi.org/10.1021/acsnano.7b05921.

Katoueizadeh, E. *et al*. (2017), "Synthesis and enhanced visible-light activity of N-doped TiO₂ nano-additives applied over cotton textiles", *J Mater Res Technol*, https://doi.org/10.1016/j.jmrt.2017.05.011.

Kowalczyk, D. *et al*. (2017), "Modification of cotton fabric with graphene and reduced graphene oxide using sol–gel method", *Cellulose*, 24, 4057–4068, https://doi.org/10.1007/s10570-017-1389-4

Liu, Y. *et al*. (2012), "Comparative investigation of Fourier Transform Infrared (FT-IR) Spectroscopy and X-ray Diffraction (XRD) in the determination of cotton fiber crystallinity", *Appl Spectrosc*, 8(66), 983-986, https://doi.org/10.1366/12-06611.

Mikhalovska, L.I. *et al*. (2012), "Cottonised flax fibres vs. cotton fibres: structural, textural and adsorption characteristics", *RSC Adv*, 2, 2032–2042, https://doi.org/10.1039/C2RA00725H.

Rosu, M.C. *et al*. (2016), "Photocatalytic performance of graphene/TiO₂-Ag composites on amaranth dye degradation", *Mat Chem* Phys, 179, 232-241, https://doi.org/10.1016/j.matchemphys.2016.05.035.

Wang, J. *et al*. (2014), "A review on the application of photocatalytic materials on textiles", *Text Res J*, 0(00) 1–15, https://doi.org/10.1177/0040517514559583.

PHYSICAL AND CHEMICAL ASSESSMENT OF A PATRIMONY SAMPLE

IRINA-MARIANA SĂNDULACHE[1,2], ELENA-CORNELIA MITRAN[1,2], ELENA PERDUM[1], OVIDIU-GEORGE IORDACHE[1], ANA-MARIA ANDREEA CHIVU[1]

[1]*The National Research Development Institute for Textiles and Leather, 16 Lucretiu Patrascanu, 030508, Bucharest, Romania*

[2]*Politehnica University of Bucharest, 1-7 Polizu Street, Bucharest, Romania,* *irina.sandulache@certex.ro*

The objective of this paper was to investigate the physical and chemical properties of a sample from a national heritage private collection from the beginning of the 20th century. The fibrous composition was determined by using Scanning Electron Microscopy (SEM) and also Optical Microscopy, these methods also providing an insight on the level of degradation of the sample. Physical and mechanical analysis methods were performed on yarns extracted from the sample with the purpose of gathering informations about the way the textile fabric was produced. The thermal behavior of the extracted yarns was assessed by using Differential Scanning Calorimetry (DSC). This way it could be determined the level of humidity which was present in the yarns, the melting temperature of the crystalline areas in the fibers, the enthalpy of melting and the temperature of thermal destruction of the sample. Although DSC is a destructive analysis, the main advantage of this method is the necessity of a very small amount of sample. According to the results, the sample's composition was 100% wool and it had some level of damage due to environmental factors, considering its old age. DSC analysis indicated a low level of humidity and also confirms the composition of the material as being indeed wool.

Keywords: wool, fiber, DSC

INTRODUCTION

Although the increasing use of synthetic fibers (polyesters, polyamides, polyacrylates) in all domains and industries, natural fibers – animal or plant derived still play a significant role in everyone's lives. The main advantage of using natural fibers over synthetic fibers is the lower rate of pollution with fiber waste, but also the sustainability of raw materials used to produce natural fibers. Textile fabrics that have historical significance must be studied in ways in which their integrity is preserved as much as possible. Non-destructive and micro-destructive analytical methods can be used to provide information about the deterioration of these historical fabrics and also about ways in which they can be restored to almost their initial condition. However, sometimes, the level of degradation can affect the results of the analyzes end can even make some analytical methods impossible to perform.

This particular research highlights the way in which a historical textile sample has been affected by environmental factors, and also provides information about the sample's fibrous composition and its thermal behavior.

MATERIALS AND CHARACTERIZATION METHODS

Materials

The present study was performed using a textile sample. The textile sample is a narrow girdle which was selected from a private collection from the beginning of the 20th century from Radosi – Gorj area.

Figure 1. Sample – narrow girdle

Characterization Methods

The qualitative analyzes for investigating the fibrous composition of the sample were performed by using Scanning Electron Microscopy – SEM (apparatus: Quanta 200, FEI, Netherlands) and Optical Microscopy (apparatus: Olympus BX41, Japan). SEM could be used for identifying the fiber composition of the national heritage samples because the original textile material has not been widely damaged. The only drawback of this method was the necessity of coating the textile sample with an electrically conductive material in order for them to be examined using SEM. Optical Microscopy was also used for the qualitative analysis of the sample with the main purpose of assessing the exfoliation of the fibers and thus the overall level of degradation.

Physical–mechanical properties of the textile yarns extracted from the sample were also assessed within this study in order to provide a better understanding of the material that was analyzed. The following determinations were made: linear density, twisting in yarns and the direction of the twist in yarns.

Differential Scanning Calorimetry - DSC (apparatus: Perkin Elmer, USA) was performed on a yarn sample to investigate the glass transition temperature - Tg, the crystallization temperature, the thermal destruction temperature and enthalpies of transitions (O'Neill, 1964). The sample was placed in a crucible made from aluminium which was then closed. The reference used for the DSC analysis was made from indium. The heating program started at 35°C and this temperature was maintained for 1 minute, then the temperature range was from 35 to 500°C at a heating rate of 10°C/min. When the temperature reached 500°C it was maintained for 1 minute.

RESULTS AND DISSCUSION

Fibrous Composition Determination

The fibrous composition of the sample is shown in Table 1.

Table 1. Fibrous composition identification

Nature of the raw material (SR 13231:1995)	Fibrous composition (EU Regulation 1007/2011)
Wool	100% Wool

The wool fiber consists of a multitude of cortical cells and flaky cells which are held together by a cell membrane complex, representing the continuous phase in the wool fiber (Wilkie *et al*., 2016). In the SEM micrograph (Figure 2-a) and in the Optical Microscope image (Figure 2-b) presented below it can be observed that there is a slight exfoliation at the surface of some of the wool fibers which indicates that the material most likely has been subjected to various mechanical and environmental factors such as UV radiation, variations in humidity or microorganisms.
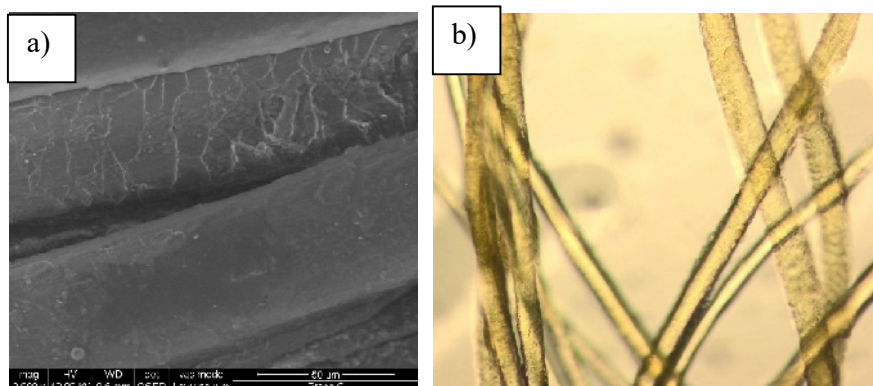
Figure 2. a) SEM micrograph of wool fibers (50 μm); b) Optical Microscope image of wool fibers (20x)

Physical–Mechanical Properties

Linear density represents the mass of a yarn per unit length. The twisting in yarn represents the number of rotations around its own axis per nominal length between the clamps before the de-twisting of the yarn. Most fibers have either an S twist or a Z twist. S-twist yarns are spun counter-clockwise, in other words, if the yarn is held in a vertical position, the spirals created by the fibers around their own axis are inclined in the same direction as the diagonal segment of the letter S. Z-twist yarns are spun clockwise and the fibers mentioned previously are inclined in the same direction as the diagonal segment of the letter Z.

Table 2. Physical–mechanical properties of the yarns extracted from the sample

Analysis name				Results	Standard Regulation
Linear density	Tex (Nm)	Warp	Beige yarn	127,3x1 (7,86/1)	SR EN 7271:2008
			Brown yarn	140,7x1 (7,11/1)	
			Red yarn	182,9x1 (5,47/1)	
		Weft		124,1x2 (8,06/2)	
Direction of the twist		Warp		S	ISO 2/ 1973
		Weft		-	
Twist	t/m	Warp	Beige yarn	111,7	SR EN ISO 2061:2015

Analysis name		Results	Standard Regulation
Brown yarn		110,0	
Red yarn		123,3	
Weft		-	

In the warp of the sample there have been identified three types of yarns, each one having S-twist direction, as shown in Table 2. The direction of the twist of the yarns extracted from the weft could not be determined due to the degradation of the sample and the impossibility of extracting yarns with a sufficient length.

Thermal Properties

DSC was used to confirm the fibrous composition of the sample and also to provide information regarding the crystallinity of the fibers (keratin in particular), the glass transition temperature of the macromolecular components found in the sample, the thermal destruction temperature and the enthalpy of transition.

Table 3. DSC thermograms for the sample

Thread	Thermograms
Dark brown	
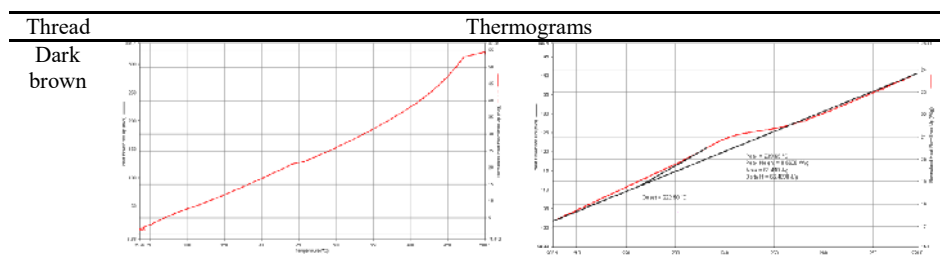
Table 4. Thermodynamic parameters for the sample

Thread	Sample weight [mg]	Onset temperature [°C]	Peak temperature [°C]	Delta H [J/g]
Dark brown	5.9	222.50	239.65	66.4098

In wool threads, the glass transition temperature depends on the humidity content of the sample (Phillips, 1985). By increasing the water content, the width of the endotherm peak and the glass transition temperature decrease. These effects occur due to the breakdown of the polar networks in the amorphous regions of the keratin (Phillips, 1985). In other words, water can act as a plasticizer in wool fibers (Wortman *et al*., 1984).

The first thermogram presented above shows a slight peak at 90-100°C, which corresponds to the vaporization of the water present in the sample. The broad and barely noticeable peak can suggest that water was present in the sample, but in very low quantity. The glass transition temperature could not be identified within this study because the peak most likely corresponds with the one of the water vaporization. According to a study of Phillips, D.G., the glass transition temperature of wool is approximately 85°C. This confirms the difficulty of identifying the glass transition

temperature in a wool sample which contains moisture. The endotherm peak which begins at 222,5°C, with a maximum at 239,65°C represents the melting of the crystalline areas in the fibers. This peak can be correlated with the degree of crystallinity in the material. A higher melting temperature is associated with a higher crystallinity degree. At 350-430°C there is a peak which is slightly noticeable, corresponding to the decomposition of the macromolecular chains by carbonization and thermolysis (Wortmann and Deutz, 1998), with the release of carbon dioxide, sulfur dioxide, nitrogen dioxide, nitrogen monoxide, methane, butane (Xia *et al*., 2016).

CONCLUSIONS

In this paper, a textile sample from a national heritage collection was analyzed using SEM and Optical Microscopy, standardized physical-mechanical methods and DSC. These analysis methods provided information regarding the composition of the material and its level of degradation. The assessment of these properties could be performed by correlating the results with those existing in the literature. The results show some level of degradation of the fabric, but overall the condition of the material is satisfying.

Acknowledgement

REFERENCES

O'Neill, M.J. (1964), "The Analysis of a Temperature-Controlled Scanning Calorimeter", *Analytical Chemistry*, 36, 7, 1238-1340, https://doi.org/10.1021/ac60213a020.

Phillips, D.G. (1985), "Detecting a Glass Transition in Wool by Differential Scanning Calorimetry", *Textile Research Journal*, 55, 171-174, https://doi.org/10.1177%2F004051758505500306.

Wilkie, C.A. *et al*. (2016), *Handbook of Research on Functional Materials: Principles, Capabilities and Limitations*, Apple Academic Press, 1, 58-61, ISBN 9781482221640.

Wortmann, F.J. and Deutz, H. (1998), "Thermal analysis of ortho and para- cortical cells isolated from wool fibers", *Journal of Applied Polymer Science*, 68, 1991-1995.

Wortmann, F.J. *et al*. (1984), "Glass Transition Temperature of Wool as a Function of Regain", *Textile Research Journal*, 54, 6-8, https://doi.org/10.1177/004051758405400102.

Xia, Z. *et al*. (2015), "Comparative study of cotton, ramie and wool fiber bundles' thermal and dynamic mechanical thermal properties", *Textile Research Journal*, 86, 8, 856-867, https://doi.org/10.1177%2F0040517515596937.

Xu, W.L., Guo, W.Q. and Li, W.B. (2003), "Thermal analysis of ultrafine wool powder", *Journal of Applied Polymer Science*, 87, 2372–2376.

BIODEGRADABILITY OF HAIR AS A WASTE OF LEATHER INDUSTRY

VIRGILIJUS VALEIKA[1], VIRGINIJA JANKAUSKAITĖ[2], KĘSTUTIS BELEŠKA[3], VIOLETA VALEIKIENĖ[3]

[1]Kaunas University of Technology, Physical and Inorganic Chemistry Department, Radvilėnų pl. 19, 50254, Kaunas, Lithuania, virgilijus.valeika@ktu.lt

[2]Kaunas University of Technology, Production Engineering Department, Studentų g. 56-142, Kaunas, 51424, Kaunas, Lithuania, virginija.jankauskaite@ktu.lt

[3]Kaunas University of Technology, Polymer Chemistry and Technology Department, Radvilėnų pl. 19, 50254, Kaunas, Lithuania, kestutis.beleska@ktu.lt, violeta.valeikiene@ktu.lt

Leather industry is one of the sources, which releases keratin-containing wastes. Still now, most of the tanneries are following hair-burning process, which contribute high amount of COD, BOD, TDS etc., to the effluent. This is a reason why numerous investigations are done reaching to replace the hair burning process by hair save unhairing: enzymatic or unhairing with hair immunization. The aim of the study was to investigate the biodegradability peculiarities of native hair, hair after enzymatic unhairing and hair obtained by unhairing with immunization effect. The soil burial test was carried out and the biodegradability of the wool was estimated. The biodegradability of the wool was estimated analysing their mass loss and fungal colonization. It was established that hair samples behave differently during the exposition in the soil: there were determined different species of fungi after 3-month exposition. The mass loss was different as well. Accordingly, the hair obtained after different method of unhairing are different in their properties as well. The different properties should mean different behaviour of the hair during biodegradation.

Keywords: unhairing, hair wastes, biodegradability.

INTRODUCTION

Leather industry is one of the sources, which releases keratin-containing wastes. Still now, most of the tanneries are following hair-burning process, which contribute high amount of COD, BOD, TDS etc., to the effluent. This is a reason why numerous investigations are done reaching to replace the hair burning process by hair save unhairing: enzymatic or unhairing with hair immunization. It is a paradox that the application of the hair save methods will lead to formation of huge amount of hair waste. It is known fact that hair/wool covering constitutes no less than 2 % of hide/skin mass. Compendium of Food and Agriculture Organization of the United Nations (2013) presented data which showed that during 2012 year about 7.2 billion ton of hides/skins (generally bovine, sheep, lamb and goat hides/skins) were processed into leather. Taking into account both facts, we can calculate that about 143 thousands ton (practically not less than amount of feather wastes: about 156000 ton annually as report Prasanti *et al.* (2016)) of hair/wool wastes in degraded form will not pass with tanneries wastewaters into environment, but it must be utilized in other way.

Despite the fact, that keratins find applications in cosmetic (Villa *et al.*, 2013; Sharma and Gupta, 2016), feedstuff (Martínez-Alvarez *et al.*, 2015), composites (Prochon *et al.*, 2016), pharmaceutical (Rouse and Van Dyke, 2010), fertilizer (Vasileva-Tonkova *et al.* 2009), sorbents (Wang *et al.*, 2016) industry etc., Tesfaye *et al.* propose that only small amounts of feather are processed into valuable products such as feather meal and fertilisers.

Unfortunately, the investigations related with the treatment of hair covering removed from hide/skin by enzymatic or immunization unhairing process are not

numerous. Here could be mentioned investigations of Barrena *et al*. (2007) devoted for composting of hair obtained using immunization unhairing method from bovine hide. Onyuka *et al*. (2012) present a study of a development of conditions favorable for the degradation of shaved form bovine hair (native hair) in a composting environment. Catalan *et al*. (2017) proposed two ways of utilization of hair obtained by enzymatic unhairing: composting and solid-state fermentation (SSF) for protease production. To similar investigations can be attributed research of Laba *et al*. (2017) describing process of bioconversion of pig bristle waste, after thermo-chemical pretreatment with sulfite, using keratinolytic enzymes of Bacillus cereus PCM 2849, and efforts of Prochon and Ntumba (2015) to use the cattle hair keratin derived from tanning industry wastes as fillers for Carboxylated Nitrile Rubber.

There are presented in a literature base few research works associated with the utilization of wool (mainly native wool) wastes obtained from leather and fur industry as well turning the waste wool into amendment-fertilizers (Zoccola *et al*., 2015); to use the wool waste as the main medium for growing of a keratin-degrading strain (Fang *et al*., 2013), or direct use of uncomposted native wool wastes as nutrient source and growth medium constituent for plants (Zheljazkov *et al*., 2009; Gorecki and Gorecki, 2010).

Thus, the utilization of keratin wastes from leather industry is somewhat studied but not enough thinking about possible amount of such wastes in future. Herewith, the researches, who investigate utilization of hair/wool obtained as waste after unhairing process, practically do not pay any attention to the method of unhairing while the unhairing method has vast influence on properties of keratin in the obtained hair/wool.

The aim of current research is to investigate an influence of unhairing method on biodegradability of the hair after unhairing process.

EXPERIMENTAL

Preparations of Hair Samples

Three pieces (20x20 cm) were cut from merino sheepskin (with medium wool) preserved by salting. The pieces were soaked under conditions: H_2O 1000%, sodium fluorosilicate 1 g/l, temperature 30°C, duration 6 h, run continuously, draining. The soaked samples were degreased: H_2O 1000%, sodium alkansulfonate „Volgonat" (Chimprom, Russia) 7 g/l, alkyl sulphate „Novost" (Chimprom, Russia) 5 g/l, temperature 42°C, duration 1 h, run continuously (draining at the end of process), and washed three times: H_2O 1000%, temperature 42°C, duration 20 min. Afterwards, the wool was cut from first piece, dried at ambient temperature and used for experiments as native wool (wool 1).

Second piece was unhaired according to enzymatic method: H_2O – 200%, temperature 25°C, enzyme preparation (EP) NovoBate WB (Novo Nordisk, Denmark) – 0.6 %, CH_3COONa – 2%, CH_3COOH – 0.3%, duration 6 hours (Valeika *et al*., 2012). After the process the wool was removed from the skin sample using blunt knife, washed three times: H_2O 1000%, temperature 42°C, duration 20 min., dried at ambient temperature and used as enzymatically unhaired wool (wool 2).

Third piece was unhaired according to immunization method: H_2O 150%, temperature 20°C, Na_2SiO_3 2%, duration 2 h (immunization stage), Na_2S (100%) 0.9%, duration 2 h (unhairing stage) (Valeika *et al*., 2015). After the process the wool was

removed from the skin sample using blunt knife, washed three times: H_2O 1000%, temperature 42°C, duration 20 min., dried at ambient temperature and used as immunised wool (wool 3).

The chemicals used for the technological processes were of analytical grade and of commercial grade as well.

Soil Burial Test

Wool specimens of three different kinds were dried to a constant weight at 105°C temperature. The wool specimens (0.1g) were put into 50×60 mm bags of polyvinyl chloride with 0.05 mm mesh diameter buried into the soil in 5 L volume desiccators and incubated at 26±2°C temperature. The soil was from organic farming: sandy loam Haplic Luvisol; the moisture content 20–30%; pH 5.8; the soil activity was 30% after 3 months (estimated by cotton wool mass loss). Monthly the specimens were removed from the soil and were analysed regarding their mass loss and fungal colonization. The specimens were rinsed with sterile water and their replicas were made on Malt Extract Agar with chloramphenicol (50mg/L) to stop bacterium growth. The isolated fungi were purified and identified according to the morphological and cultural features (Domsch, 1980). The biodegradability of the wool was estimated according to their relative weight loss $(a - b) / a \times 100\%$, where a is the initial weight of the specimen (g); b is the specimen weight after incubation. The wool specimens were weighted by means of an analytical balance with high precision (±0.001).

RESULTS AND DISCUSSION

The wool biodegradability test showed the decrease of all specimens during three exposition months in the soil (Fig. 1).
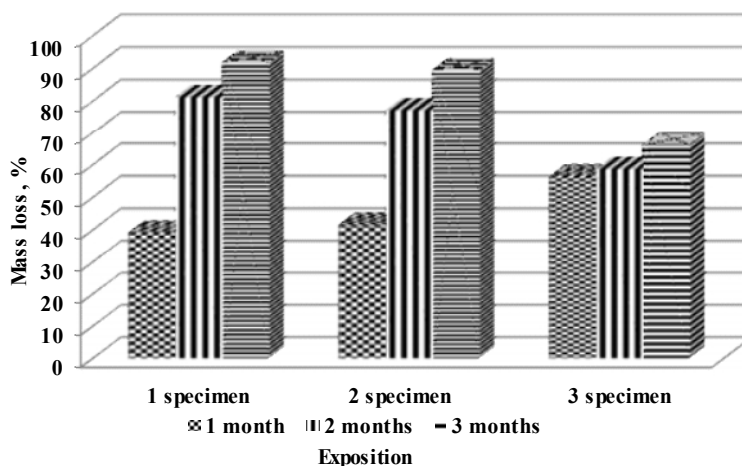

Figure 1. Wool biodegradability in soil during 3-month exposition

The mass loss of the wool 1 and 2 was alike: their weight decrease made up 39.17 and 41.60%, respectively, after first month of the exposition, and after 3 month – 91.82 and 89.46%, respectively. However, after first exposition month the weight of the wool

3 decreased 1.4 times more than the wool 1 and 2, at the end of the experiment it was 1.4 times less degraded than the wool 1 and 2. Fungi from six different genera that likely took part in the wool decomposition were isolated from the specimens (Table 1). Fungi from *Trichoderma* genus were most often detected on the buried specimens.

Table 1. Fungi isolated from wool 1, 2 and 3 after month exposition in soil

Specimen	Exposition		
	1 month	2 month	3 month
1	*Aspergillus ustus* *Fusarium sp.* *Mucor sp.* *Trichoderma spp.*	*Aspergillus ustus* *Fusarium sp.* *Trichoderma spp.*	*Aspergillus ustus* *Fusarium sp.* *Trichoderma spp.*
2	*Trichoderma spp.*	*Aspergillus ustus* *Fusarium sp.* *Trichoderma sp.*	*Cunninghamella elegans* *Fusarium sp.* *Trichoderma spp.*
3	*Fusarium sp.* *Penicillium sp.* *Trichoderma spp.*	*Aspergillus ustus* *Trichoderma spp.*	*Aspergillus ustus* *Fusarium sp.* *Trichoderma spp.*

According to the results obtained, the wool 1 was the most degradable among tested wools and the wool 3 was decomposed at the least in natural environment during three-month exposition.

The results obtained from this test were somewhat surprising. It was expected, that mostly degraded wool should be after enzymatic unhairing process. The reason for such presumption is the damage of keratin by keratinolytic enzymes during the unhairing. Through the work of Lange *et al*. (2016), evidence was provided for the need for a combination of endoprotease, exoproteases, and oligopeptidase to bring about keratin degradation. Of course, one enzyme preparation acts as endoprotease or exoproteases, or oligopeptidase but not like all three sorts simultaneously. Thus, usually one enzyme preparation affects only one segment in macromolecule of keratin. Herewith, the conditions of the unhairing process are significantly milder comparing with conditions of complete hydrolysis of keratin. Accordingly, although the wool after the enzymatic unhairing visually seems not affected, nonetheless it is affected in macromolecular level somewhat.

The biodegradability test has shown (Fig. 1.) that wool after enzymatic unhairing is more stable than native wool independently on duration of exposition in soil. The mostly stable wool (as it was expected) was immunized one (wool 3). As is mentioned in literature, during immunization keratin becomes more resistant against action of reducers and enzymes (Heidemann, 1993). Therefore, the immunised wool becomes more stable against action of enzymes of microorganisms in soil during 3-month exposition.

On the other hand, the change of mass of the wool 3 in soil exhibits by odd character. The main loss of mass is on during first month of exposition. Further, the mass loss increases but negligible.

Six sorts of fungi were isolated from wool during the exposition in soil. There are reports that some species from *Aspergillus, Fusarium, Mucor* and *Trichoderma* develop on keratin and fat substrates and produce keratinaze (Singh, 2014; Kim, 2003). The utilised experiment approved the mentioned proposition, and mainly *Aspergillus,*

Fusarium and *Trichoderma* species were detected on wool samples after 3-month exposition. By the way, there were determined different species of fungi after 3-month expositions as well: only on wool 2 specimen was detected fungi *Cunninghamella elegans*. The appearance of fungi *Cunninghamella elegans* is not surprising, because it is known as keratinophilic fungi (Fujii *et al.*, 2013).

CONCLUSION

The test has shown that each wool sample is characterised by different behaviour during the exposition in soil, and the behaviour depends on the method of unhairing. Accordingly, deterioration of any sort of waste keratin should be investigated thoroughly before the utilization by burial in landfills.

REFERENCES

Barrena, R., Pagans, E., Artola, A., Vazquez, F. and Sanchez, A. (2007), "Co-composting of hair waste from the tanning industry with de-inking and municipal wastewater sludges", *Biodegradation*, 18, 257-268, https://doi.org/10.1007/s10532-006-9060-z.

Catalan, E., Komilis, D. and Sanchez, A. (2017), "Solid-state fermentation and composting as alternatives to treat hair waste: A life-cycle assessment comparative approach", *Waste Management and Research*, 35, 786-790, https://doi.org/10.1177/0734242X17709909.

Domsch, K.H., Gams, W. and Anderson, T.H. (1980), *Compendium of Soil Fungi*, Vol. 1-2, Academic Press, London.

Fang, Z., Zhang, J., Liu, B.H., Du, G.C. and Chen, J. (2013), "Biodegradation of wool waste and keratinase production in scale-up fermenter with different strategies by Stenotrophomonas maltophilia BBE11-1", *Bioresource Technology*, 140, 286-291, https://doi.org/10.1016/j.biortech.2013.04.091.

Fujii, K., Kai, Y., Matsunobu, S., Sato, H. and Mikami, A. (2013), "Isolation of digested sludge-assimilating fungal strains and their potential applications", *Journal of Applied Microbiology*, 115, 718-726, https://doi.org/10.1111/jam.12266.

Gorecki, R.S. and Gorecki, M.T. (2010), "Utilization of Waste Wool as Substrate Amendment in Pot Cultivation of Tomato, Sweet Pepper, and Eggplant", *Polish Journal of Environmental Studies*, 19, 1083-1087.

Heidemann, E. (1993), *Fundamentals of leather manufacture*, Eduard Roether KG, Darmstadt.

Kim, J.-D. (2003), "Keratinolytic activity of five *Aspergillus* species isolated from poultry farming soil in Korea", *Mycobiology*, 31, 157-161, https://doi.org/10.4489/MYCO.2003.31.3.157.

Laba, W., Chorazyk, D., Pudlo, A., Trojan-Piegza, J., Piegza, M., Kancelista, A., Kurzawa, A., Zuk, I. and Kopec, W. (2017), "Enzymatic Degradation of Pretreated Pig Bristles with Crude Keratinase of Bacillus cereus PCM 2849", *Waste and Biomass Valorization,* 8, 527-537, https://doi.org/10.1007/s12649-016-9603-4.

Lange, L., Huang, Y.H. and Busk, P.K. (2016), "Microbial decomposition of keratin in nature-a new hypothesis of industrial relevance", *Applied Microbiology and Biotechnology*, 100, 2083-2096, https://doi.org/10.1007/s00253-015-7262-1.

Martínez-Alvarez, O., Chamorro, S. and Brenes, A. (2015), "Protein hydrolysates from animal processing by-products as a source of bioactive molecules with interest in animal feeding: A review", *Food Research International*, 73, 204–212.

Onyuka, A.S., Bates, M., Attenburrow, G., Covington, A.D. and Antunes, A.P.M. (2012), "Parameters for Composting Tannery Hair Waste", Journal of American Leather Chemists Association, 107, 159-166.

Prasanthi, N., Bhargavi, S. and Machiraju, P.V.S. (2016), "Chicken Feather Waste – A Threat to the Environment", *International Journal of Innovative Research in Science, Engineering and Technology*, 5, 16759-16764, https://doi.org/10.15680/IJIRSET.2016.0509188.

Prochon, M. and Ntumba, Y.H.T. (2015), "Effects of biopolymer keratin waste sources in XNBR compounds", *Rubber Chemistry and Technology*, 88, 258-275, https://doi.org/10.5254/rct.15.85948.

Prochon, M., Przepiorkowska, A., Yves-Herve, Y. and Ntumba, (2016), "A New Generation of Elastomers Containing Innovative Biopolymers", *Journal of the Society of Leather Technologists and Chemists*, 100, 8-18.

Rouse, J.G. and Van Dyke, M.E. (2010), "A Review of Keratin-Based Biomaterials for Biomedical Applications", *Materials*, 3, 999-1014, https://doi.org/10.3390/ma3020999.

Sharma, S. and Gupta, A. (2016), "Sustainable Management of Keratin Waste Biomass: Applications and Future Perspectives", *Brazilian Archives of Biology and Technology*, 59, 1-14, e16150684.

Singh, I. (2014), "Extracellular keratinase of some dermatophytes, their telemorphs and related keratinolytic fungi", *European Journal of Experimental Biology*, 4, 57–60.

Valeika, V., Beleska, K. and Sirvaityte, J. (2012), "Alkaline-free method of hide preparation to tanning", *Brazilian Journal of Chemical Engineering*, 29, 315-323.

Valeika, V., Beleska, K., Sirvaityte, J., Alaburdaite, R. and Valeikiene, V. (2015), "Immunization action of sodium silicate on hair", *Journal of the Society of Leather Technologists and Chemists*, 99, 223-230.

Vasileva-Tonkova, E., Gousterova, A. and Neshev, G. (2009), "Ecologically safe method for improved feather wastes biodegradation", *International Biodeterioration and Biodegradation,* 63, 1008-1012, https://doi.org/10.1016/j.ibiod.2009.07.003.

Villa, A.L.V., Aragão, M.R.S., dos Santos, E.P., Mazotto, A.M., Zingali R.B., de Souza, E.P. and Vermelho, A.B. (2013), "Feather keratin hydrolysates obtained from microbial keratinases: Effect on hair fiber", *BMC Biotechnology*, 13, 13:15, (18), https://doi.org/10.1186/1472-6750-13-15.

Wang, H., Jin, X.Y. and Wu, H.B. (2016), "Adsorption and desorption properties of modified feather and feather/polypropylene melt-blown filter cartridge of lead ion (Pb^{2+})", *Journal of Industrial Textiles*, 46, 852-867.

World Statistical Compendium for raw hides and skins, leather and leather footwear 1993-2012, Trade and Markets Division, Food and Agriculture Organization of the United Nations, 2013, http://www.fao.org/fileadmin/templates/est/COMM_MARKETS_MONITORING/Hides_Skins/Documents/COMPENDIUM2013.pdf

Zheljazkov, V.D., Stratton, G.W., Pincock, J., Butler, S., Jeliazkova, E.A., Nedkov, N.K. and Gerard, P.D. (2009), "Wool-waste as organic nutrient source for container-grown plants", *Waste Management*, 29, 2160-2164, https://doi.org/10.1016/j.wasman.2009.03.009.

Zoccola, M., Montarsolo, A., Mossotti, R., Patrucco, A. and Tonin, C. (2015), "Green Hydrolysis as an Emerging Technology to Turn Wool Waste into Organic Nitrogen Fertilizer", *Waste and Biomass valorization*, 6, 891-897, https://doi.org/10.1007/s12649-015-9393-0.

IX.

NON-DESTRUCTIVE TESTING

IN-SITU MODIFIED ANTIMONY-FILM GLASSY CARBON ELECTRODE FOR METAL TRACE ANALYSIS

KLODIAN XHANARI[1,2], ALJAŽ RAMOT[1], BARBARA PETOVAR[1], MATJAŽ FINŠGAR[1]

[1]*University of Maribor, Faculty of Chemistry and Chemical Engineering, Smetanova ulica 17, 2000 Maribor, Slovenia*

[2]*University of Tirana, Faculty of Natural Sciences, Boulevard "Zogu I", 1001 Tirana, Albania, klodian.xhanari@fshn.edu.al*

Glassy carbon electrodes (GCE) have been extensively employed for the determination of trace amounts of heavy metals. Lately, modifications of GCE are currently being sought. One way of obtaining better analytical performance compared to GCE is the employment of an *in situ* prepared antimony-film glassy carbon electrode (SbFE). This combination is especially attractive in anodic stripping voltammetry technique which uses square wave excitation signal. This work will report on the optimization of the *in situ* prepared SbFE by employing different deposition potentials. Furthermore, a preliminary study using electrochemical impedance spectroscopy (EIS) was performed at different deposition and measured potentials in order to understand the mechanism of SbFE sensor performance.

Keywords: heavy metal analysis; antimony film electrode; square wave anodic stripping voltammetry.

INTRODUCTION

A growing interest has been shown in the last years on the determination of heavy metals as they are present in different environmental systems as micropollutants (Bansod *et al*., 2017; Tchounwou *et al*., 2012). Apart from their natural occurrence in the earth crust as elements the main sources of heavy metals contamination are related among others to industrial applications and waste, mining, atmospheric deposition, cosmetics, agricultural and metal-containing products (Bansod *et al*., 2017; Tchounwou *et al*., 2012; Roy, 2010; He *et al*., 2005; Callender, 2003; Nriagu, 1989). Lead (Pb), chromium (Cr), cadmium (Cd), mercury (Hg) and arsenic (As) are known for their high toxicity. The exposure to even low concentrations (ppb range) can be dangerous not only to the environment, but to the human health as well, leading to multiple organ damage (Cui *et al*., 2015; Tchounwou *et al*., 2003; Yedjou and Tchounwou, 2007; Gumpu *et al*., 2015; WHO, 1996). The high toxicity of these elements combined with the fact that their ions are non-biodegradable further increase the concern on their impact (Bansod *et al*., 2017; Tchounwou *et al*., 2012). On the other hand, some heavy metals (like Cu, Fe, Mg, Ni and Zn) are essential to the functioning of the human body (WHO, 1996).

Square wave anodic stripping voltammetry (SWASV) is among the most used electroanalytical techniques in the determination of trace heavy metals (Bansod *et al*., 2017; Lu *et al*., 2018). Glassy carbon electrodes (GCE) have presented an excellent alternative to the mercury drop electrodes. The latter's use is restricted due to high mercury toxicity concerns (Lu *et al*., 2018). In the last years the focus of the research community has been on the modification of the GCE using among others nanomaterials, organic molecules and biomolecules (Bansod *et al*., 2017; Cui *et al*., 2015; Lee *et al*., 2016; Zinoubi *et al*., 2017; Dahaghin *et al*., 2018; Sadok and Tyszczuk-Rotko, 2018; Lee *et al*., 2015; Ariño *et al*., 2017). Film electrodes, *in situ* or *ex situ* prepared with mainly bismuth, but also of copper, lead and tin, have been also explored (Ariño *et al*., 2017; Jovanovski *et al*., 2015, 2017; Economou, 2005; Petovar *et al*., 2018; Czop, 2011; Korolczuk *et al*., 2005). Several research groups have also reported on the use of *in situ* and *ex situ* prepared antimony film electrodes (SbFE) for trace heavy metal determination (Serrano *et al*., 2016) in either 0.01 M HCl solution (Hocevar *et al*., 2007; Bassie *et al*., 2013; Ashrafi and Vytřas, 2012; Vasko and Bozidar, 2009) or in 0.1 M acetate buffer (Bassie *et al*., 2013; Arancibia *et al*., 2013; Maczuga *et al*., 2013).

In this work we first discuss the analytical performance of the antimony film electrode (SbFE) that was formed *in situ* in 0.01 M HCl containing 0.5 ppm of Sb(III), in the

determination of Pb(II) and Cd(II) using the SWASV technique. Next, electrochemical impedance spectroscopy (EIS) measurements for the studied systems were performed at different deposition and measured potentials and the response of the bare GCE was compared with SbFE with and without additions of the tested analytes. Finally, based on the preliminary EIS results the SbFE performance is discussed.

EXPERIMENTAL

The electrochemical measurements were performed in a three-electrode electrochemical cell using GCE (Cat. No.6.1204.300) as working electrode, Ag/AgCl(saturated KCl) as reference electrode, and a Pt counter electrode. All potentials in this work refer to Ag/AgCl (saturated KCl) reference electrode. These electrodes and the electrochemical cell were provided by Metrohm (Herisau, Switzerland). Before the measurements the working electrode was polished using Al_2O_3 powder (Buehler, Illinois, USA) and thoroughly washed with ultrapure water. Then the electrode was also cleaned under the ultrasound for 5 minutes in ultrapure water.

A system containing 10 mM potassium hexacyanoferrate(III) (Sigma Aldrich, St. Louis, Missouri, USA) in 1.0 M KCl solution was used to test the electrode reversibility. The tests were performed using cyclic voltammetry at different sweep rates, where the electrode response needed to fit into specific criteria. HCl and KCl were supplied by Carlo Erba Reagents (Val de Reuil, France). The atomic absorption standard stock solutions (1000 mg L^{-1}) of Cd(II), Pb(II) and Sb(III) were purchased from Merck (Darmstadt, Germany). These standards were diluted as required. All the solutions were prepared using ultrapure water with a resistivity of 18.2 MΩ cm that was obtained with a Milli-Q system (Millipore Corporation, Massachusetts, USA).

The *in situ* SbFE was formed in 0.01 M HCl where 0.5 mg/L of Sb(III) alongside the Pb(II) and Cd(II) analytes were present. SWASV was performed at different deposition potentials, *i.e.* –1.2, –1.1, and –1.0 V *vs*. Ag/AgCl. These are sufficiently negative deposition potential that three elements deposit on the surface – analytes preconcentration step alongside SbFE formation. All the methods were performed at 60 s deposition time. Before and after the measurement the electrode was electrochemically cleaned by applying a potential of 0.3 V *vs*. Ag/AgCl for 30 s. This potential is positive enough to oxidize all the employed metals. Before the measurements a period of 15 s equilibration time was employed. The measurements were performed with SW excitation signal with positive-going potential scan between –1.2 V (or –1.1 V or –1.0 V) and 0.6 V *vs*. Ag/AgCl. During the preconcentration step the solution was stirred at about 300 rpm, whereas during the equilibration and measurement steps the solution was not stirred.

EIS measurements were performed with the same electrodes as used for the method validation procedure and the same 60 s preconcentration step was used. The EIS response was obtained at two different potentials, *i.e.* E_{meas} and E_{oc} (open circuit potential). Measurements were performed in the $5 \cdot 10^4$–0.05 Hz frequency range, with 5 points per decade and 10 mV amplitude of the excitation signal. All the electrochemical measurements were performed with a PalmSens3 EIS potentiostat/galvanostat controlled by PSTrace 4.7 software (PalmSens, Houten, the Netherlands).

RESULTS AND DISCUSSION

Analytical Performance of the SbFE

In order to evaluate the analytical performance of the prepared SbFE first the selectivity of the method was proven. Then, the linearity of the method was determined, followed by the determination of the accuracy and the precision of the method.

Selectivity of the Method

Fig. 1 shows voltammograms measured after the preconcentration step at three different deposition potentials, *i.e.* –1.2, –1.1, and –1.0 V *vs*. Ag/AgCl. The stripping signals for Cd(II), Pb(II) and Sb(III) are located at approximately –0.75, 0.50, and 0.00 V *vs*. Ag/AgCl, respectively. The peaks are well separated indicating method selectivity towards Pb(II), Cd(II), and Sb(III).
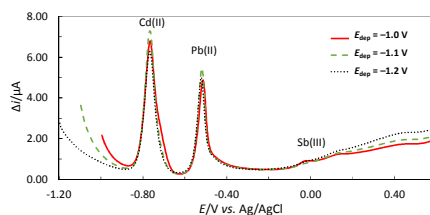
Figure 1. Voltammograms measured at three different deposition potentials using SbFE in 0.01 M HCl

Linearity of the Method

The method linearity was determined at three different deposition potentials, *i.e.* at –1.2, –1.1, and –1.0 V *vs*. Ag/AgCl respectively, as shown in Fig. 2. The current response Δi *vs*. mass concentration γ was fitted using a least squares linear regression. Method linearity was accepted when the square of the correlation coefficient was higher than 0.99 ($R^2 > 0.99$). The linearity of the method for Cd(II) determination was found to be in the concentration range from 14.6 to 100.0 µg/L, using all three deposition potentials (Fig. 2a–c). On the other hand, in the case of Pb(II) determination at the same deposition potentials, the method was found to be linear in the mass concentration range from 24.4 to 100.0 µg/L (Fig. 2d–f).

Accuracy and Precision

The accuracy of the method was evaluated based on the calculated recovery value as shown in equation 1:

$$\text{recovery [\%]} = \frac{\text{(determined concentration)}}{\text{(theoretical concentration)}} \cdot 100 \qquad (1)$$

The accuracy was tested at four different concentrations of Pb(II) and Cd(II), *i.e.* 15 and 40 µg/L. The method was considered accurate when the recovery was in the range from 80.0 to 120.0%.

Figure 2. Linearity of the method for (a, b, c) Cd(II) and (d, e, f) Pb(II) determination at different deposition potentials. The accumulation time was 60 s.

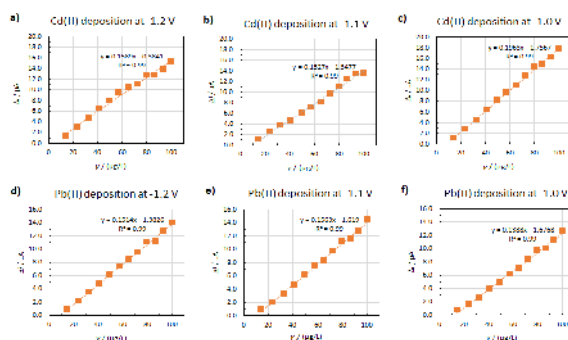Two distinguished patterns of the EIS measurements can be observed from Fig. 3 and 4. First, the EIS measurements obtained at more negative potentials (*i.e.* at –1.1 and –0.9 V *vs*. Ag/AgCl), independently of the addition of the analytes, present depressed semi-circular shape indicating charge-transfer-controlled reaction (kinetic control). However, it can be seen in Fig. 3 and 4 that the impedance of both the bare GCE and the SbFE increases with the presence and concentration of the analytes. The EIS response of the SbFE measured at E_{dep} is an exception from the above mentioned observation. Meanwhile at more positive potentials (*i.e.* at –0.6 and –0.3 V *vs*. Ag/AgCl) the measured curve in the Nyquist spectrum deviates from the Z_{real} axis indicating diffusion-controlled reaction. Second, in all the studied systems the impedance is found to be significantly reduced when moving towards more negative potentials. The lower the polarisation resistance the higher the sensitivity of the method (Petovar *et al*., 2018). Fig. 3 and 4 show no significant change in the impedance of the bare GCE and the SbFE at –1.1 V *vs*. Ag/AgCl.

CONLUSIONS

In this work the analytical performance of an *in situ* antimony-modified glassy carbon electrode in 0.01 M HCl solution containing 0.5 mg/L Sb(III), is presented. In addition a preliminary electrochemical impedance spectroscopy (EIS) study was performed at different deposition and measured potentials with and without additions of analytes, *i.e.* 15 and 40 µg/L of Pb(II) and Cd(II).

It was shown that at deposition potentials of –1.2, –1.1, and –1.0 *vs*. Ag/AgCl, for the determination of Pb(II) the method linearity was in the range from 24.4 to 100.0 µg/L, while for Cd(II) determination in the range from 14.6 to 100.0 µg/L. The accuracy and precision of the measurements was proven as shown by the recovery and relative standard deviation (RSD) values.

A preliminary EIS study indicated that at –1.1 and –0.9 V *vs*. Ag/AgCl the system is under kinetic control, while at more positive potentials (*i.e.* at –0.6 and –0.3 V *vs*. Ag/AgCl) the system is under both kinetic and diffusion control.

REFERENCES

Arancibia, V. *et al*. (2013), "Ex situ prepared nafion-coated antimony film electrode for adsorptive stripping voltammetry of model metal ions in the presence of pyrogallol red", *Sensors and Actuators B: Chemical*, 182, 368-373, https://doi.org/10.1016/j.snb.2013.03.014.

Ariño, C. *et al*. (2017), "Voltammetric determination of metal ions beyond mercury electrodes. A review", *Analytica Chimica Acta*, 990, 11-53, https://doi.org/10.1016/j.aca.2017.07.069.

Ashrafi, A.M. and Vytřas, K. (2012), "New procedures for voltammetric determination of copper (II) using antimony film-coated carbon paste electrodes", *Electrochimica Acta*, 73, 112-117, https://doi.org/10.1016/j.electacta.2011.12.042.

Bansod, B. *et al*. (2017), "A review on various electrochemical techniques for heavy metal ions detection with different sensing platforms", *Biosensors and Bioelectronics*, 94, 443-455, https://doi.org/10.1016/j.bios.2017.03.031.

Bassie, T., Siraj, K. and Tesema, T.E. (2013), "Determination of Heavy Metal Ions on Glassy Carbon Electrode Modified with Antimony", *Advanced Science, Engineering and Medicine*, 5(3), 275-284, https://doi.org/10.1166/asem.2013.1251.

Callender, E. (2003), "Heavy metals in the environment—Historical trends", in *Treatise on Geochemistry*, H.D. Holland and K.K. Turekian, Eds., Pergamon: Oxford, 67-105, https://doi.org/10.1016/B0-08-043751-6/09161-1.

Cui, L., Wu, J. and Ju, H. (2015), "Electrochemical sensing of heavy metal ions with inorganic, organic and bio-materials", *Biosensors and Bioelectronics*, 63, 276-286, https://doi.org/10.1016/j.bios.2014.07.052.

Czop, E., Economou, A. and Bobrowski, A. (2011), "A study of in situ plated tin-film electrodes for the determination of trace metals by means of square-wave anodic stripping voltammetry", *Electrochimica Acta*, 56(5), 2206-2212, https://doi.org/10.1016/j.electacta.2010.12.017.

Dahaghin, Z., Kilmartin, P.A. and Mousavi, H.Z. (2018), "Determination of cadmium(II) using a glassy carbon electrode modified with a Cd-ion imprinted polymer", *Journal of Electroanalytical Chemistry*, 810, 185-190, https://doi.org/10.1016/j.jelechem.2018.01.014.

Economou, A. (2005), "Bismuth-film electrodes: recent developments and potentialities for electroanalysis", *TrAC Trends in Analytical Chemistry*, 24(4), 334-340, https://doi.org/10.1016/j.trac.2004.11.006.

Gumpu, M.B. *et al*. (2015), "A review on detection of heavy metal ions in water – An electrochemical approach", *Sensors and Actuators B: Chemical*, 213, 515-533, https://doi.org/10.1016/j.snb.2015.02.122.

He, Z.L., Yang, X.E. and Stoffella, P.J. (2005), "Trace elements in agroecosystems and impacts on the environment", *Journal of Trace Elements in Medicine and Biology*, 19(2), 125-140, https://doi.org/10.1016/j.jtemb.2005.02.010.

Hocevar, S.B. *et al*. (2007), "Antimony film electrode for electrochemical stripping analysis", *Analytical Chemistry*, 79(22), 8639-8643, https://doi.org/10.1021/ac070478m.

Jovanovski, V., Hočevar, S.B. and Ogorevc, B. (2017), "Bismuth electrodes in contemporary electroanalysis", *Current Opinion in Electrochemistry*, 3(1), 114-122, https://doi.org/10.1016/j.coelec.2017.07.008.

Jovanovski, V., Hrastnik, N.I. and Hočevar, S.B. (2015), "Copper film electrode for anodic stripping voltammetric determination of trace mercury and lead", *Electrochemistry Communications*, 57, 1-4, https://doi.org/10.1016/j.elecom.2015.04.018.

Korolczuk, M., Tyszczuk, K. and Grabarczyk, M. (2005), "Adsorptive stripping voltammetry of nickel and cobalt at in situ plated lead film electrode", *Electrochemistry Communications*, 7(12), 1185-1189, https://doi.org/10.1016/j.elecom.2005.08.022.

Lee, P.M. *et al*. (2015), "Glassy carbon electrode modified by graphene–gold nanocomposite coating for detection of trace lead ions in acetate buffer solution", Thin Solid Films, 584, 85-89, https://doi.org/10.1016/j.tsf.2015.03.017.

Lee, S. *et al*. (2016), "Voltammetric determination of trace heavy metals using an electrochemically deposited graphene/bismuth nanocomposite film-modified glassy carbon electrode", *Journal of Electroanalytical Chemistry*, 766, 120-127, https://doi.org/10.1016/j.jelechem.2016.02.003.

Lu, Y. *et al*. (2018), "A review of the identification and detection of heavy metal ions in the environment by voltammetry", *Talanta*, 178, 324-338, https://doi.org/10.1016/j.talanta.2017.08.033.

Maczuga, M. *et al*. (2013), "Novel screen-printed antimony and tin voltammetric sensors for anodic stripping detection of Pb(II) and Cd(II)", *Electrochimica Acta*, 114, 758-765, https://doi.org/10.1016/j.electacta.2013.10.075.

Nriagu, J.O. (1989), "A global assessment of natural sources of atmospheric trace metals", *Nature*, 338, 47-49, https://doi.org/10.1038/338047a0.

Petovar, B., Xhanari, K. and Finšgar, M. (2018), "A detailed electrochemical impedance spectroscopy study of a bismuth-film glassy carbon electrode for trace metal analysis", *Analytica Chimica Acta*, 1004, 10-21, https://doi.org/10.1016/j.aca.2017.12.020.

Roy, S.P. (2010), "Overview of heavy metals and aquatic environment with note on their recovery", *The Ecoscan*, 4(2&3), 235-240.

Sadok, I. and Tyszczuk-Rotko, K. (2018), "Ultra-trace determination of silver using lead nanoparticles-modified thiol functionalized polysiloxane film glassy carbon electrode", *Journal of Electroanalytical Chemistry*, 808, 204-210, https://doi.org/10.1016/j.jelechem.2017.12.010.

Serrano, N. *et al*. (2016), "Antimony-based electrodes for analytical determinations", *TrAC Trends in Analytical Chemistry*, 77, 203-213, https://doi.org/10.1016/j.trac.2016.01.011.

Tchounwou, P.B. *et al*. (2012), "Heavy metals toxicity and the environment", *EXS*, 101, 133-164, https://doi.org/10.1007/978-3-7643-8340-4_6.

Tchounwou, P.B., Patlolla, A.K. and Centeno, J.A. (2003), "Carcinogenic and systemic health effects associated with arsenic exposure—A critical review", *Toxicologic Pathology*, 31(6), 575-588, https://doi.org/10.1080/01926230390242007.

Vasko, J., Hocevar, S.B. and Bozidar, O. (2009), "Ex Situ Prepared Antimony Film Electrode for Electrochemical Stripping Measurement of Heavy Metal Ions", *Electroanalysis*, 21(21), 2321-2324, https://doi.org/10.1002/elan.200904692.

World Health Organization (1996), Trace elements in human nutrition and health, Geneva.

Yedjou, C.G. and Tchounwou, P.B. (2007), "N-Acetyl-L-cysteine affords protection against lead-induced cytotoxicity and oxidative stress in human liver carcinoma (HepG(2)) cells", *International Journal of Environmental Research and Public Health*, 4(2), 132-137, https://doi.org/10.3390/ijerph2007040007.

Zinoubi, K. *et al*. (2017), "Determination of trace heavy metal ions by anodic stripping voltammetry using nanofibrillated cellulose modified electrode", *Journal of Electroanalytical Chemistry*, 799, 70-77, https://doi.org/10.1016/j.jelechem.2017.05.039.

VALIDATION AND OPTIMIZATION OF AN *IN-SITU* COPPER-MODIFIED GLASSY CARBON ELECTRODE

KLODIAN XHANARI[1,2], ŽAN ŠAŠEK[1], BARBARA PETOVAR[1], MATJAŽ FINŠGAR[1]

[1]*University of Maribor, Faculty of Chemistry and Chemical Engineering, Smetanova ulica 17, 2000 Maribor, Slovenia*

[2]*University of Tirana, Faculty of Natural Sciences, Boulevard "Zogu I", 1001 Tirana, Albania*

Square wave anodic stripping voltammetry (SWASV) technique is one of the most used electrochemical techniques in the determination of the trace amounts of heavy metals in different environments. This is due among other reasons to the fact that this method offers low detection limit, high selectivity and precision at relatively low cost. Modified film electrodes have been found as good replacement to the mercury electrodes. In this work different deposition potentials have been used to optimize an in situ-prepared copper-film glassy carbon electrode (CuFE). In addition, a preliminary study using electrochemical impedance spectroscopy (EIS) was performed to investigate the characteristics of the CuFE sensor.

Keywords: heavy metal analysis; copper film electrode; square wave anodic stripping voltammetry.

INTRODUCTION

The determination of trace amounts of heavy metals in different systems has always been of great interest for the research community due to their high toxicity and ability to bioaccumulate. Moreover, their impact is not only on the environment, but it is also closely connected to the human health. The exposure to the heavy metals is mainly through the alimentary chain (Gumpu *et al*., 2015; Bansod *et al*., 2017). Several possible mechanisms (depending also on the specific heavy metal) have been proposed on how these elements affect the human health (Gumpu *et al*., 2015; Tchounwou *et al*., 2012). The generation of the DNA leading to its damaging, depletion of protein sulfhydryl and lipid peroxidation are among few of the known effects of these metals (Gumpu *et al*., 2015; Tchounwou *et al*., 2012; Valko *et al*., 2005; Labuda *et al*., 2005).

Different techniques have been employed to determine the concentration of the heavy metals in different matrixes including soil, air, water and biological samples. The selection of the method is closely dependent on the concentration of these elements (in the ppb range) which in response requires high sensitivity and selectivity of the method (Bansod *et al*., 2017). Spectroscopic techniques, including atomic absorption spectroscopy (AAS), inductively coupled plasma mass spectrometry (ICP-MS), X-ray fluorescence spectrometry (XRF) and inductively coupled plasma-optical emission spectrometry (ICP-OES) have been extensively used in the determination of the heavy metals in different matrixes (Pohl, 2009; Silva *et al*., 2009; Sitko *et al*., 2015; Losev *et al*., 2015). Electrochemical techniques have also found a wide range of applications in trace heavy metals determination. Based on the change of different electrical signals caused by the presence of these elements several techniques have been developed (Bansod *et al*., 2017; Lu *et al*., 2018; Ariño *et al.*, 2017; Alves *et al*., 2017; Cui *et al*., 2015; Yasri *et al*., 2011; Town *et al*., 2001; Gao *et al*., 2013). The square wave anodic stripping voltammetry (SWASV) is an affordable (low cost) technique that offers low detection limit, high selectivity, accuracy and precision (Gumpu *et al*., 2015; Bansod *et al*., 2017; Lu *et al*., 2018).

A large number of materials has been employed as the working electrode in the electrochemical techniques, trying to restrict the use of mercury drop electrodes (Ariño *et al.*, 2017). Film electrodes, prepared from the electrodeposition of different elements,

like Bi, Sb and Pb, on the surface of a glassy carbon electrode are among the most commonly used (Korolczuk *et al*., 2005; Petovar *et al*., 2018; Makombe *et al*., 2016). Only a few research groups have reported on the use of copper film electrodes (CuFE) for trace heavy metal determination. Jovanovski *et al*. (2015) reported on the preparation of an *in situ* CuFE for the determination of Hg(II) and Pb(II) using the SWASV technique and 120 s accumulation time. The determination of trace levels of Zn(II) in blood serum was also reported by Pei *et al*. (2014) using a disposable copper-based electrochemical sensor. In this work copper was used not only as working electrode, but as counter and reference (Cu/CuCl$_2$) electrode as well.

In this work we report on the *in situ* preparation and validation of a copper modified film electrode, in 0.1 M HCl and 0.4 M NaCl containing 0.5 mg/L Cu(II) in the determination of Pb(II). The accumulation time was 60 s. The linear range of the method at three different potentials (*i.e.* at –0.8, –0.7 and –0.6 V) is given and the accuracy and precision of the obtained results is proven. Electrochemical impedance spectroscopy was used to understand the performance of CuFE, with and without additions of 15 and 40 µg/L Pb(II). The results were compared with the bare GCE.

EXPERIMENTAL

A PalmSens3 EIS potentiostat/galvanostat controlled by PSTrace 5.4 software (PalmSens, Houten, the Netherlands) was employed to perform all the electrochemical measurements at room temperature. The three-electrode electrochemical cell and the working (GCE, Cat. No.6.1204.300), reference (Ag/AgCl filled with saturated KCl) and counter (Pt wire) electrodes were all provided by Metrohm (Herisau, Switzerland). Al$_2$O$_3$ powder (Buehler, Illinois, USA) was used to polish the working electrode surface prior to the electrochemical measurements. All the potentials mentioned in this work are given in reference to the Ag/AgCl(saturated KCl) electrode.

KCl provided by Carlo Erba Reagents (Val de Reuil, France) and K$_3$[Fe(CN)$_6$] purchased from Sigma Aldrich (St. Louis, Missouri, USA) were employed to test the reversibility of the working electrode. Cyclic voltammetry measurements at different sweep rates were performed in 1.0 M KCl solution containing 10 mM K$_3$[Fe(CN)$_6$].

Ultrapure water (resistivity of 18.2 MΩ) obtained with a Milli-Q system (Millipore Corporation, Massachusetts, USA), was used to dilute all the solutions. The atomic absorption standard stock solutions (1000 mg L^{-1}) of Pb(II) and Cu(II) were provided by Merck (Darmstadt, Germany). HCl was provided by Carlo Erba Reagents (Val de Reuil, France).

A 0.1 M HCl and 0.4 M NaCl solution containing 0.5 mg/L of Cu(II) with and without additions of the analyte, *i.e.* Pb(II), was used to prepare the *in situ* CuFE.

The application of a potential of 0.3 V *vs*. Ag/AgCl for 30 s prior and after the SWASV measurements assured the electrochemical cleaning of the electrode through oxidation of all the employed metals. The preconcentration step was performed at –0.8 or –0.7 or –0.6 V *vs*. Ag/AgCl deposition potential. The accumulation was performed for 60 s. The solution was stirred during the preconcentration step at approximately 300 rpm, but not during the measurement and equilibration step. The latter lasted 15 s. Analysis was performed with a SW excitation signal after the preconcentration and equilibration step at three different potentials, *i.e.* –0.8 or –0.7 or –0.6 V *vs*. Ag/AgCl. The EIS measurements were carried out at the same potential as the deposition potential ($E_{meas} = E_{dep}$) and at the open circuit potential ($E_{meas} = E_{ocp}$), preserving also the preconcetration step used during the method validation procedure. A signal with 10 mV amplitude and 5 point per decade was used to record the EIS response in the frequency range from 50 kHz to 50 mHz.

RESULTS AND DISCUSSION

Analytical Performance of CuFE

Limit of Quantification

The limit of quantification (LOQ) was determined based on the signal-to-noise ratio (S/N) as a Pb(II) concentration at which S/N ≥ 10. This was repeated for three deposition potentials, *i.e.* –0.8, –0.7, and –0.6 V *vs.* Ag/AgCl. The determined LOQ for all three deposition potentials used was found to be 2.00 µg/L.

Selectivity of the Method

Figure 1 shows a voltammogram measured using CuFE. The peak for Pb(II) develops at approximately –0.4 V *vs.* Ag/AgCl. The stripping signal of Cu is represented by two peaks located at approximately –0.2 and 0.25 V *vs.* Ag/AgCl. On that basis, we can conclude that the method is selective towards Pb(II) and Cu(II). An intensive hydrogen evolution starts at approximately –0.7 V *vs.* Ag/AgCl as seen in Figure 1.
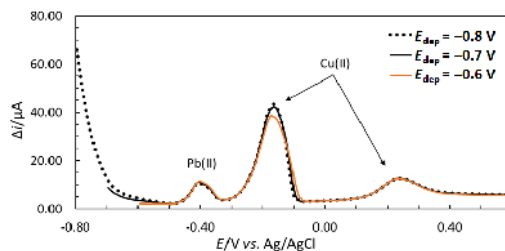
Figure 1. Voltammograms measured at three different deposition potentials using CuFE in 0.1 M HCl and 0.4 M NaCl containing 38.5 µg/L Pb(II).

Linearity of the Method

Figure 2 presents the linear ranges by employing different deposition potentials. The method showed linear response in the mass concentration range from 2.0 to 38.5 µg/L for the –0.6 V *vs.* Ag/AgCl deposition potential. A wider mass concentration range was determined when the deposition potential of –0.7 and –0.8 V *vs.* Ag/AgCl was employed. The linear range in this case was found to be from 2.0 to 56.6 µg/L. The linearity was accepted when the correlation coefficient R^2 was higher than 0.99 ($R^2 > 0.99$).
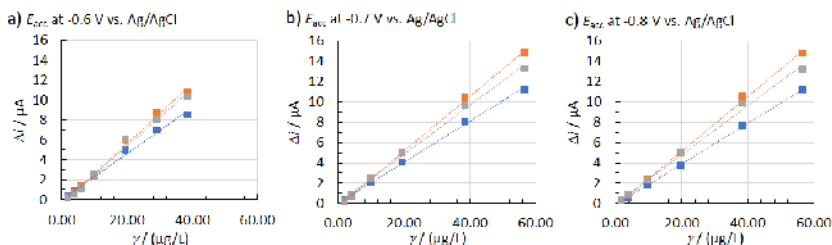
Figure 2. Linearity of the method for Pb(II) determination at different deposition potentials using an *in situ*-prepared CuFE.

Accuracy and Precision

Accuracy and precision were evaluated based on the recovery and relative standard deviation (RSD) values, respectively. The 0.1 M HCl and 0.4 M NaCl was spiked with certain Pb(II) concentration and the analysis using CuFE was repeated at least 6 times. An average recovery value and RSD was calculated. All three methods showed accurate (recovery in the range of 80.0–120.0%) and precise (RSD ≤ 20.0%) results.

Electrochemical Impedance Spectroscopy (EIS) Measurements

The Nyquist plots showing the EIS response of the CuFE in 0.1 M HCl and 0.4 M NaCl, containing 0.5 mg/L Cu(II), measured either at the same potential as the deposition potential ($E_{meas} = E_{dep}$) or at the open circuit potential ($E_{meas} = E_{oc}$), are given in Figures 3a–c and 4a–c, respectively. In order to understand the performance of CuFE, the EIS spectra of the bare GCE in the same electrolyte, with and without additions of the analyte, for measurements performed at E_{dep} and E_{oc} (Figure 3d–f and Figure 4d–f) are also given. In all cases the EIS spectra were recorded at –0.8, –0.6 and –0.3 V *vs.* Ag/AgCl, with or without addition of 15 and 40 µg/L Pb(II).

As seen in Figures 3 and 4 the EIS response obtained at –0.6 and –0.8 V *vs.* Ag/AgCl, independently of the addition of analyte, is presented as depressed semicircles. This indicates that the system is under kinetic control. The same behaviour is not seen in the case of the bare GCE measured at E_{dep}, without addition of Pb(II) (Figure 3f) and with 15 µg/L Pb(II) (Figure 3d).

The real part of impedance (Z_{real}) of all the CuFE systems (with or without addition of the analyte) measured at E_{dep} (Figure 3) decreased at the most negative potential (*i.e.* at –0.8 V *vs.* Ag/AgCl) compared with that of the bare GCE at the same conditions. This decrease is even more pronounced in the case of the measurements performed at E_{oc} (Figure 4) where it can be observed also for measurements performed at –0.6 V *vs.* Ag/AgCl. It is important to notice that on one hand the real part of impedance contributes to the polarization resistance of these systems. On the other hand, the sensitivity of the method is inverse proportional to the polarization resistance (Petovar *et al*., 2017). This implies that the sensitivity of the method at the most negative potential increased when using CuFE.

No clear influence of the concentrations of the analyte on the impedance values can be observed for all the studied systems (Figures 3 and 4) independently if measured at E_{dep} or E_{oc}.
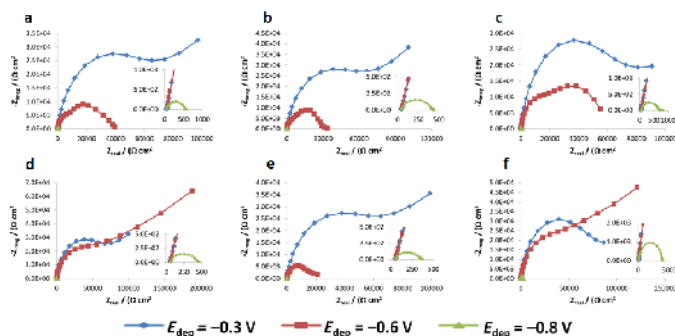
Figure 3. The Nyquist plots of the CuFE (a–c) and bare GCE (d–f), recorded in 0.1 M HCl and 0.4 M NaCl at the same potential as the deposition potential, with (a, d) 15 µg/L, (b, e) 40 µg/L and (c, f) without additions of Pb(II).
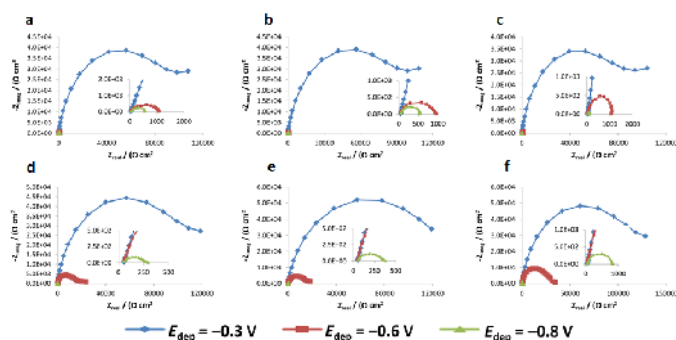
Figure 4. The Nyquist plots of the CuFE (a–c) and bare GCE (d–f), recorded in 0.1 M HCl and 0.4 M NaCl measured at open circuit potential, with (a, d) 15 µg/L, (b, e) 40 µg/L and (c, f) without additions of Pb(II)

Figure 4 shows that for measurements performed at E_{oc}, the impedance of all the systems (with or without addition of Pb(II), bare GCE or CuFE) it is significantly decreasing when the measured potential shifts towards more negative values. The decrease of the impedance measured at the most positive potential (*i.e.* at –0.3 V *vs.* Ag/AgCl) and at the most negative potential (*i.e.* at –0.8 V *vs.* Ag/AgCl) it is of approximately three orders of magnitude. A similar behaviour of the EIS response with the change in value of the measured potential is generally seen also in the case when measurements were performed at E_{dep} (Figure 3) for both the bare GCE and the CuFE. However, the EIS spectra of the bare GCE with no additions of Pb(II) (Figure 3f) and with 15 µg/L Pb(II) (Figure 3d) did not follow the above mentioned trend.

CONCLUSIONS

This work presents the validation and optimization of a *in situ*-modified copper glassy carbon electrode used for the determination of Pb(II). The CuFE was prepared 0.1 M HCl and 0.4 M NaCl solution containing 0.5 mg/L of Cu(II) and used for the determination of two different concentrations of Pb(II), *i.e.* 15 and 40 µg/L.

The results obtained from the square wave anodic stripping voltammetry (SWASV) measurements performed at three different potentials (*i.e.* at –0.8, –0.7 and –0.6 V *vs.* Ag/AgCl) showed that the method was linear in the range 2.0–38.5 µg/L for the –0.6 V vs. Ag/AgCl deposition potential, but the linearity at –0.7 and –0.8 V *vs.* Ag/AgCl was found to be from 2.0 to 56.6 µg/L. The limit of quantification at all three potentials was determined to be 2.00 µg/L. The accuracy and precision of the obtained results was also confirmed.

Preliminary electrochemical impedance spectroscopy (EIS) measurements performed at –0.8, –0.6 and –0.3 V *vs.* Ag/AgCl showed that the systems are under kinetic control for measurements performed at the most negative potentials.

REFERENCES

Alves, G.M.S. *et al.* (2017), "Multi-element determination of metals and metalloids in waters and wastewaters, at trace concentration level, using electroanalytical stripping methods with environmentally friendly mercury free-electrodes: A review", *Talanta*, 175(Supplement C), 53-68, https://doi.org/10.1016/j.talanta.2017.06.077.

Ariño, C. *et al.* (2017), "Voltammetric determination of metal ions beyond mercury electrodes. A review", *Analytica Chimica Acta*, 990(Supplement C), 11-53, https://doi.org/10.1016/j.aca.2017.07.069.

Bansod, B. *et al.* (2017), "A review on various electrochemical techniques for heavy metal ions detection with different sensing platforms", *Biosensors and Bioelectronics*, 94, 443-455, https://doi.org/10.1016/j.bios.2017.03.031.

Cui, L. *et al.* (2015), "Electrochemical sensing of heavy metal ions with inorganic, organic and bio-materials", *Biosensors and Bioelectronics*, 63, 276-286, https://doi.org/10.1016/j.bios.2014.07.052.

Gao, A. *et al.* (2013), "Electrochemiluminescent lead biosensor based on GR-5 lead-dependent DNAzyme for Ru(phen)32+ intercalation and lead recognition", *Analyst*, 138(1), 263-268, https://doi.org/10.1039/C2AN36398D.

Gumpu, M.B. *et al.* (2015), "A review on detection of heavy metal ions in water – An electrochemical approach", *Sensors and Actuators B: Chemical*, 213, 515-533, https://doi.org/10.1016/j.snb.2015.02.122.

Jovanovski, V. *et al.* (2015), "Copper film electrode for anodic stripping voltammetric determination of trace mercury and lead", *Electrochemistry Communications*, 57, 1-4, https://doi.org/10.1016/j.elecom.2015.04.018.

Korolczuk, M. *et al.* (2005), "Adsorptive stripping voltammetry of nickel and cobalt at in situ plated lead film electrode", *Electrochemistry Communications*, 7(12), 1185-1189, https://doi.org/10.1016/j.elecom.2005.08.022.

Labuda, J. *et al.* (2005), "Voltammetric detection of damage to DNA by arsenic compounds at a DNA biosensor", *Sensors*, 5(6), 411, https://doi.org/10.3390/s5060411.

Losev, V.N. *et al.* (2015), "Silica sequentially modified with polyhexamethylene guanidine and Arsenazo I for preconcentration and ICP–OES determination of metals in natural waters", *Microchemical Journal*, 123, 84-89, https://doi.org/10.1016/j.microc.2015.05.022.

Lu, Y. *et al.* (2018), "A review of the identification and detection of heavy metal ions in the environment by voltammetry", *Talanta*, 178(Supplement C), 324-338, https://doi.org/10.1016/j.talanta.2017.08.033.

Makombe, M. *et al.* (2016), "Antimony film sensor for sensitive rare earth metal analysis in environmental samples", *Journal of Environmental Science and Health, Part A*, 51(8), 597-606, https://doi.org/10.1080/10934529.2016.1159857.

Pei, X. *et al.* (2014), "Disposable copper-based electrochemical sensor for anodic stripping voltammetry", *Analytical Chemistry*, 86(10), 4893-4900, https://doi.org/10.1021/ac500277j.

Petovar, B. *et al.* (2018), "A detailed electrochemical impedance spectroscopy study of a bismuth-film glassy carbon electrode for trace metal analysis", *Analytica Chimica Acta*, 1004, 10-21, https://doi.org/10.1016/j.aca.2017.12.020.

Pohl, P. (2009), "Determination of metal content in honey by atomic absorption and emission spectrometries", *TrAC Trends in Analytical Chemistry*, 28(1), 117-128, https://doi.org/10.1016/j.trac.2008.09.015.

Silva, E.L. *et al.* (2009), "Simultaneous preconcentration of copper, zinc, cadmium, and nickel in water samples by cloud point extraction using 4-(2-pyridylazo)-resorcinol and their determination by inductively coupled plasma optic emission spectrometry", *Journal of Hazardous Materials*, 171(1), 1133-1138, https://doi.org/10.1016/j.jhazmat.2009.06.127.

Sitko, R. *et al.* (2015), "Green Approach for Ultratrace Determination of Divalent Metal Ions and Arsenic Species Using Total-Reflection X-ray Fluorescence Spectrometry and Mercapto-Modified Graphene Oxide Nanosheets as a Novel Adsorbent", Analytical Chemistry, 87(6), 3535-3542, https://doi.org/10.1021/acs.analchem.5b00283.

Tchounwou, P.B. *et al.* (2012), "Heavy metals toxicity and the environment", EXS, 101, 133-164, https://doi.org/10.1007/978-3-7643-8340-4_6.

Town, R.M. and van Leeuwen, H.P. (2001), "Fundamental features of metal ion determination by stripping chronopotentiometry", *Journal of Electroanalytical Chemistry*, 509(1), 58-65, https://doi.org/10.1016/S0022-0728(01)00420-X.

Valko, M. *et al.* (2005), "Metals, toxicity and oxidative stress", *Current Medicinal Chemistry*, 12(10), 1161-1208, https://doi.org/10.2174/0929867053764635.

Yasri, N.G. *et al.* (2011), "Chronoamperometric determination of lead ions using PEDOT:PSS modified carbon electrodes", *Talanta*, 85(5), 2528-2533, https://doi.org/10.1016/j.talanta.2011.08.013.

X.

ADVANCED MATERIALS & SYSTEMS INNOVATION

BIOTECHNOLOGY FOR OBTAINING A RETANNING AGENT FROM FLESHINGS

RODICA ROXANA CONSTANTINESCU, GABRIEL ZĂINESCU,
GHEORGHE BOSTACA

INCDTP - Division: Leather and Footwear Research Institute, 93 Ion Minulescu st., 031215, Bucharest, Romania e-mail: icpi@icpi.ro

Currently, the leather industry has to deal with very high costs for waste treatment and disposal. As a result, it is recommended to subject the organic protein waste from tanning to biochemical treatments for recycling in the industry. The degree of novelty lies primarily in the fact that the starting point of the promoted technologies is obtaining new complex products by processing organic waste and using it in tanneries. The lime fleshings resulting from the hide fleshing operation represents the highest amount of reusable leather material of approx. 15%. This paper presents an innovative process for the biochemical degradation of hide waste resulting from hide fleshing in order to obtain a retanning/filling agent used in leather processing, which was characterization by chemical and FT-IR Analysis.

Keywords: hide waste (fleshings), conversion, retanning/filling agent

INTRODUCTION

Leather industry generates huge amount of fleshing waste, which is rich in proteins and lipids that have potential for various applications (Kamini *et al*., 1999). From every ton of hide about 10 kg of fleshing waste is engendered accounting to the production of 700,000 tons of fleshings worldwide every year. Fleshings are considered as hazardous due to content of sodium sulfide, a corrosive and an asphyxiating chemical and need to be disposed of securely (Saravanan *et al*., 2014). Therefore, it is essential to utilize the waste for preparation of various value added products thereby making the environment clean. The protein part of fleshings has been utilized for various applications (Kumar *et al*., 2008; Renitha *et al*., 2015). The lipid content of tannery fleshing waste is remarkable and suitable methods have not been reported for the recovery of lipids.

The non-edible and low cost lipids could be used as a feedstock for biodiesel production (Bala *et al*., 2015; Bokhari *et al*., 2016) and the lipids could be extracted from biomass using Bligh and Dyer [B & D], Folch and Soxhlet extraction methods (Perez-Palacios *et al*., 2008). The extraction efficiency could be improved by disrupting the biomass prior to extraction by autoclaving, sonication, micro-wave irradiation, surfactants and enzymes (Lai *et al*., 2016). Therefore, a viable tissue disruption method is essential for optimal recovery of lipids from fleshing waste, in order to develop a green and cost effective.

All waste treatments are mainly aimed at substantially reducing environmental pollution. For this purpose, unprocessed hide waste (fleshings, pelt splits and trimmings, as well as protein from the ash exhaust solution) is best suited for processing into protein form with different degrees of denaturation and purity.

Current technologies are primarily intended for untanned hide waste and generally aim to extract the collagen protein, the basic leather component, in the form of short fibers or dissolved, for the highest yield that can be used as a protein binder, such as a source of collagen in the pharmaceutical and cosmetic industry, the footwear industry in manufacturing insoles obtained from tanned (chrome) leather, or for the production of fertilizers.

Following the hydrolysis of fleshings, the surface fat will be separated by the steam and will be sold as a byproduct for processing into soap or biodiesel.

This paper presents an innovative process for the biochemical degradation of hide waste resulting from hide fleshing in order to obtain a retanning/filling agent used in leather processing, which was characterization by chemical and FT-IR Analysis.

EXPERIMENTAL PART

Materials

Untanned waste (fleshing) was obtained from SC Pielorex Jilava, Ilfov County, and were kept at room temperature and analyzed to determine pH, humidity, ash, total Kjeldahl nitrogen (TKN) using standardized methods. Moisture was determined by heating the sample at 110°C for 12 hours. Ash from dry products was determined by heating the sample at 600°C for 4 hours. TKN was determined by the semi-micro Kjeldahl method.

The chemical characteristics of hide waste (fleshings) used in experiments are presented in Table 1.

Table 1. Chemical characteristics of hide waste (fleshings)

No.	Characteristics / UM	Determined values	*uncertainty	Method standard
1.	Volatile matter, %	89.30	± 0,42	SRENISO 4648-2006
2.	Ash, %	12.52	±0,27	SRENISO 4047-2002
3.	Total nitrogen, %	10.93	±0,66	SR ISO 5397-1996
4.	Dermal substance, %	61.43	±2,26	SR ISO 5397-1996
5.	pH of aqueous extract	9.00	±0,10	SRENISO 4045-2008
6.	Fatty substances, %	41.59		STAS 145/20-1988
7.	Metal oxides, %	12.52		ICPI method

Obtaining of hydrolysate

The proposed procedure for the valorization of hide waste (fleshings) into high added value by-products is the following: 5 kg of hide waste (fleshings) are weighed and washed with running water at a temperature of 20-25°C in a drum, for 1-3 hours and decalcified with 2.5-3.5% ammonium sulfate for 2-3.5 hours; waste is shredded with a TC 32 grinder (double knife) from SAP-Italy. Hydrolysis occurs in two stages: the first stage is done at a temperature of 35-40°C with the addition of concentrated proteolytic enzyme product containing 30,000 units/g of lipase; 900 units/g cellulase; 1,200 units/g amylase and 10,000 units/g protease for 1.8-3.5 hours, then temperature is raised to 90-100°C and 1-1.3% H_2SO_4 is added continuous. The hydrolysate preparation equipment is shown in Figure 1.

Figure 1. Hydrolysis equipment (grinder for pelt waste and autoclave)

Biochemical treatment consists in processing hide waste (fleshings) with a set of enzymes, coenzymes and natural improvers with "starter" fluids, which modify the toxic reactions of the protein hydrolysate with a corresponding elimination of hydrogen sulphide, mercaptans, ammoniacal odours and other specific odours. The product used is commercially known as Dekosinth and is produced in Switzerland.

Obtaining of Retanning Agent

In order to obtain the leather retanning/filling agent, complexing agents (dicarboxylic acids, metal oxides based on titanium or sodium tripolyphosphate) are introduced into the collagen matrix. This filler compared to other similar products has the advantage of eliminating some additional technological operations in the retanning process (salt purification), therefore it presents an economical advantage and is a natural biopolymer based on collagen, it is ecologic (formaldehyde-, phenol- and chromium-free), and it is suitable for making a wide range of leather assortments.

These leather wastes were treated by chemical-enzymatic hydrolysis. Thus, a quantity of hide waste (fleshings), then mixed with water (50%) and hydrochloric acid in concentration of 6...8% for 4-6 h. The mixture is hydrolysed in a 50 l autoclave with double jacket and stirrer, adding dicarboxylic acids in concentration 0,8-1% at a temperature of 90-98°C for 1 hour.

RESULTS AND DISCUSSIONS

The retanning agent obtained according to the framework technological process was analyzed physico-chemically with the following characteristics (Table 2):

Table 2. Physical-chemical characteristics of the retanning/filling agent obtained

No.	Characteristics, UM	Determined values	Test method standard number
1.	Volatile matter, %	84,04	SR EN ISO 4684 -2006
2.	Extractible substances, %	undetectable	SRENISO 4048 - 2008
3.	Total ash, %	9,41	SR EN ISO 4047 - 2002
4.	Total nitrogen, %	7,58	SR ISO 5397-1996
5.	Dermal substance, %	42,61	SR ISO 5397 - 1996
6.	Metal oxides	5,41	ICPI method
7.	pH of aqueous extract	3,5	SRENISO 4045 -2008

IR spectra were measured with a range of 7800-350 cm^{-1}; optical system - monobeam; resolution 0.2-16 cm^{-1}; that can measure spectra in transmission, reflection and absorption. Infrared Spectroscopy (IR) is the most appropriate method of identifying the presence of polar functional groups in the structure of molecules of organic compounds. Depending on the wave number, the bands can be assigned to the specific functional groups of finishing compounds and collagen processed in tanneries (Figure 2).
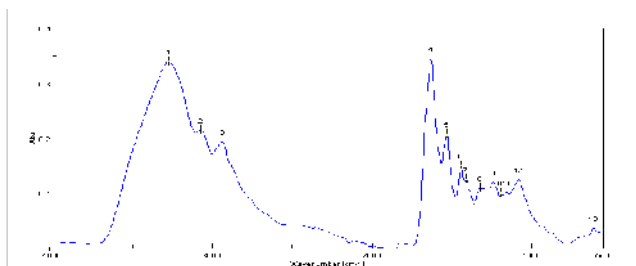
Figure 2. FT-IR spectrum for tanned agent

According to spectral assignments, the bands corresponding to the amide groups ($\nu_{C=O}$ at 1636cm^{-1}, δ_{NH} and ν_{C-N} at 1549cm^{-1}) were observed for the retanning agent. Also, signals characteristic of NH groups are present at 1345 cm^{-1}. The OH groups in the hydroxyproline units give a signal at 1081 cm^{-1}. The amide absorption band II is given by N-H deformation and C-N stretching modes. The absorption bands for amide III are attributed to several stretching vibrations: C-N and C-O but also deformation vibrations: N-H and O=C-N.

CONCLUSIONS

The paper presents a biotechnology for obtaining a retanning agent from hide fleshings. The composition presented in the paper is obtained by the biochemical degradation of hide waste from leather tanning in order to make a retanning/filling agent which will provide leather with the following characteristics: increased wear resistance, reduced water absorption, softness, greater or less flexibility depending on the assortment.

The degree of novelty lies primarily in the fact that the starting point of the promoted technologies is obtaining new complex products by processing organic waste and using it in tanneries.

REFERENCES

Bala, D.D. *et al.* (2015), "Conversion of a variety of high free fatty acid containing feedstock to biodiesel using solid acid supported catalyst", *J Clean Prod*, 104, 273-281, https://doi.org/10.1016/j.jclepro.2015.05.035.

https://doi.org/10.24264/icams-2018.X.1

Christie, W.W. (2003), "Preparation of derivatives of fatty acids", in: Christie, W.W. (Ed.), *Lipid Analysis: Isolation, Separation and Structural Analysis of Lipids*, J. Barnes and Associates, 205-225.

Dang, Y. *et al*. (2016), "Value-added conversion of waste cooking oil and post-consumer PET bottles into biodiesel and polyurethane foams", *Waste Manag*, 52, 360-366, https://doi.org/10.1016/j.wasman.2016.03.054.

Kumar, A.G. *et al*. (2008), "Production of alkaline protease by *Pseudomonous aeruginosa* using proteinaceous solid waste generated from leather manufacturing industries, *Bioresource Technology*, 99, 1935–1939.

Kamini, N.R. *et al*. (1999), "Microbial enzyme technology as an alternative to conventional chemicals in leather industry", *Curr Sci*, 77, 80-86.

Lai, Y.S. et al. (2016), "Improving lipid recovery from Scenedesmus wet biomass by surfactant-assisted disruption", *Green Chem*, 18, 1319-1326, https://doi.org/10.1039/C5GC02159F.

Renitha, T.S. et al. (2015), "Wealth from waste-beef extract for microbiological media from tannery solid waste", *Rsc Adv*, 5, 9891-9897, https://doi.org/10.1039/C4RA13811B.

Saravanan, P. *et al*. (2014), "Understanding the chemical free enzyme based cleaner unhairing process in leather manufacturing", *J Clean Prod*, 79, 258-264, https://doi.org/10.1016/j.jclepro.2014.05.022.

TREATMENT AND PROCESSING OF LEATHER MATERIALS USING GAMMA RADIATION

COSMIN HERMAN[1], OVIDIU CĂPRARU[1], BOGDAN LUNGU[1], IOANA STĂNCULESCU[1,2], MARIA STANCA[3], CARMEN GAIDĂU[3]

[1]*Horia Hulubei National Institute for Physics and Nuclear Engineering, Dept. IRASM, 30 Reactorului Str, 077125 Magurele, Ilfov, Romania*

[2]*University of Bucharest Dept. of Physical Chemistry, Regina Elisabeta Bld 4-12, 030018 Bucharest, Romania, istanculescu@nipne.ro*

[3]*INCDTP - Division: Leather and Footwear Research Institute, 93 Ion Minulescu st., Sector 3, 031215 Bucharest, Romania*

This paper presents a review on the functionalization methods of leather materials using gamma radiation. There are few studies regarding the effects of gamma irradiation on leather materials while the majority of studies are on the irradiation of collagen for medical purposes, decontamination and preservation of heritage leather objects and parchment documents. Recent studies on leather and parchment treated with bigger doses then the sterilization or decontamination doses and on gamma irradiated collagen, new information about the solubility of collagen, crystalline structure, shrinkage temperature and mechanical properties were obtained. The relation between the shrinkage temperature and the gamma radiation dose absorbed by the material were investigated with the MHT (Micro Hot Table) method. Evidences of cross-linking of the collagen were found at doses up to 25 kGy while for doses of 50 kGy and more the principal process was the scission of the peptide chains. The mechanical properties of tanned leather and parchment such as tensile strength and elongation at break were studied. The parchment tensile strength decreases with the increase of absorbed dose, for doses bigger than 10 kGy. The behaviour of tanned leather is different, an increase in the tensile strength at doses up to 25 kGy which can be a threshold for collagen cross-linking. More evidence of cross–linking of the collagen fibrils in leather materials were shown with the SEM-EDX and TG investigations. There were no substantial modifications in the structure of collagen for doses of 5, 10 and 15 kGy as shown by the SEM and TG analysis, but a slightly smaller loss of mass in the case of the dose of 25 kGy which can prove the cross-linking of collagen in the tanned leather material. Based on literature review a conceptual application model for gamma irradiation on leather materials was elaborated.

Keywords: leather, gamma irradiation, collagen

INTRODUCTION

Leather clothing, footwear, upholstery and other leather goods manufactured from animal hides and skins are subject to complex chemical processes which are under continuously ecological attention. From salt preservation of the animal hides in the purpose of preventing the decomposition to chromium salts tanning and biocide treatment of the wet blue leather against fungi, leather processing consists in many time and chemical consuming steps (Mesquita, 2013; Wu, 2009). This implies high costs and time consuming processing of the leather materials and residues and that is why innovative processes based on green technologies have to be developed.

Introducing gamma radiation as a treatment method to the leather industry is a new approach; few studies were conducted on leather materials, mostly in cross-linking of collagen chains (Guererro *et al*., 2017). Other applications were found in medicine, in the purpose of sterilization or decontamination of medical collagen for different uses (Takitoh *et al*., 2015). Gamma radiation was also used in cultural heritage conservation

and restoration, as a nondestructive method of decontamination, and preservation of artifacts (IAEA, 2017; Vujčić et al., 2017).

Also, gamma irradiation can be used in leather industry for treatment of the leather materials in view of cross-linking activation of different polymeric substances to improve certain characteristic of the finished product (Catalina et al., 2010; Demeter et al., 2018).

Mechanical properties and elemental analysis showed evidence of cross-linking of the collagen for doses up to 25 kGy, and scission of the peptide chains for bigger doses, indicating a recommended dose for treatments on leather materials.

Processing of leather materials using gamma radiation to substitute steps in manufacturing and functionalization using different types of polymers can be cost effective and environmentally friendly and will be envisaged in the conceptual application model developed.

GAMMA IRRADIATION OF COLLAGEN BASED MATERIALS - STATE OF THE ART

Gamma Irradiation of Leather

Gamma radiation effects on leather materials were analysed on different hides and skins, vegetable tanned with extracts of quebracho, mimosa and with chromium salts (Carsote et al., 2016; Misra et al., 2018). The effects of gamma irradiation on the hides tanned with these commercial tanning agents have indicated supplementary cross-linking as a primary effect for doses up to 25 kGy, the material showing an increase in tensile strength, elongation at break and a smaller loss of mass according to thermogravimetric analysis. For bigger doses the main process is scission of the peptide chain, with evidence in shrinkage temperature and tensile strength decrease (Lungu et al., 2014; Sendrea et al., 2017). The four studies showed in Table 1 share the same conclusion.

Table 1. Studies on gamma radiation effect on tanned leather with a ^{60}Co gamma rays source

References	Material	Tanning agent	Analysed properties	Dose (kGy)
C. Sendrea et al., 2017	Calf leathers Sheep skins Goat skins	Quebracho extract Mimosa extract	Shrinkage temperature and intervals	10, 25, 50, 100
C. Sendrea et al., 2015	Calf leather	Quebracho and Mimosa extracts	Spin-lattice and spin-spin proton relaxation time	10,25 ,50, 100
Kovacheva et al., 2017	Calf leather Calf suede Pig skin	Not specified Chromium salts	Leather morphology and thermal decomposition	5, 10, 15
Lungu et al., 2014	Kid skin Sheep skin	Mimosa extract Quebracho extract	Tensile strength and elongation at break	10, 25, 50

Gamma Irradiation of Parchment

Gamma radiation is used in decontamination and sterilization of parchment documents, for its non-destructivity and efficiency. Parchment documents were made usually from goat and sheep skins stretched and polished with calcium carbonate ($CaCO_3$) to achieve the white surface.

The dose of 30 kGy was proposed as a maximum dose of decontamination for parchment artifacts, indicating no changes in structural composition, colour and texture, as can be seen in Table 2 (Nunes *et al*., 2012). All small deviations in the measured properties were associated to structural diversity and different tanning methods (Nunes *et al*., 2012). For doses up to 10 kGy more recent studies showed cross-linking of the collagen fibrils, and deterioration for bigger doses applied on new parchment experimental models (Lungu *et al*., 2014). The tensile strength of the parchment documents decreased with the absorbed dose.

Table 2. Gamma irradiation of parchment documents with ^{60}Co gamma rays source

References	Material	Analysed properties	Dose (kGy)
Lungu *et al*., 2014	Goat parchment Kid parchment	Tensile strength and elongation at break	5, 10 ,15
Nunes *et al*., 2012	XV century parchment XVI century parchment XVII century parchment	Colour, texture and elasticity	10, 19, 22, 30

Gamma Irradiation of Collagen

Native and tanned collagen were irradiated with gamma rays from a ^{60}Co source, and the Electron Paramagnetic Resonance (EPR) spectrum was correlated with the absorbed dose, indicating different sensibility of collagen to gamma radiation due to the tanning process and tanning agent in comparison with native collagen, as can be seen in Table 3 (Duliu *et al*., 2001). Also, using gamma irradiation a stable hydrogel was obtained from an aqueous solution. The hydrogel that received a bigger dose of radiation revealed better mechanical properties, indicating cross-linking of collagen chains. At low doses, although chemical cross-links have been observed, the structure of the gelatine has not been significantly altered (Cataldo *et al*., 2007; Leontiu *et al*., 1993).

Table 3. Effects of gamma irradiation of collagen with a ^{60}Co gamma rays source

References	Material	Preparation method and irradiation	Analysis	Doses (kGy)
Catalado *et al*., 2008	Gelatine from porcine skin	Gelatine dissolved in demineralized water resulting in 28 ml homogeneous solution and irradiated in absence of air	Polarimetric measurements, FT-IR, spectra of electronic absorption, differential scanning calorimetry (DSC), thermogravimetric analysis with simultaneous differential thermal analysis (TGA-DTA)	12, 25, 50, 100, 150, 200

References	Material	Preparation method and irradiation	Analysis	Doses (kGy)
Duliu *et al*., 2001	Tanned collagen membranes	1% Fibrous collagen gel in HCL solution 1% Fibrous collagen gel in HCL solution + formaldehyde 1% Fibrous collagen gel in HCL solution + $Cr(OH)(SO_4)_2$ 1% Fibrous collagen gel in HCL solution + $Al(OH)(SO_4)_2$	EPR spectroscopy	1, 3, 7, 11, 15
Maslennikova *et al*., 2015	Rat tail collagen	Rat tails dissected after 24 h, 7 days, 1, 2 and 3 months	Laser scanning microscopy, cross-polarization optical coherence tomography, differential scanning calorimetry	2, 4, 6, 8, 10 20, 30, 40
Grant *et al*., 1973	Rat tail collagen	Washed in saline solution and dried pre-irradiation Washed in saline solution and irradiated in saline solution Washed in saline solution and cross-linked with 5% glutaraldehyde	Electron microscopy, amino acid analysis, histology, solubility, enzyme reaction	From 50 to 1000
Gotoh *et al*., 1977	Dry collagen film	Regenerated with electrochemical method before irradiation	Elemental analysis, thickness, mass and tensile strength	40, 80, 100
	Wet collagen film	Regenerated with electrochemical method before irradiation		20, 40, 50
	Collagen film	Regenerated with electrochemical method under gamma irradiation		10, 20, 25

Gamma radiation was found to be useful for tannery wastewater harmful substances decomposition (Iqbal *et al*., 2015).

Conceptual Model for Leather Treatment with Gamma Radiation-a "Green Chemistry" Tool

As gamma irradiation equipments are more and more accessible and gamma radiation represents an ecological and effective alternative for chemical preservation, sterilization and cross-linking, the application in leather industry needs only advanced knowledge and economical approaching.

Based on the state of the art of the gamma irradiation applications in the field of collagen based materials processing a conceptual model is proposed in view of further developments (Fig. 2):
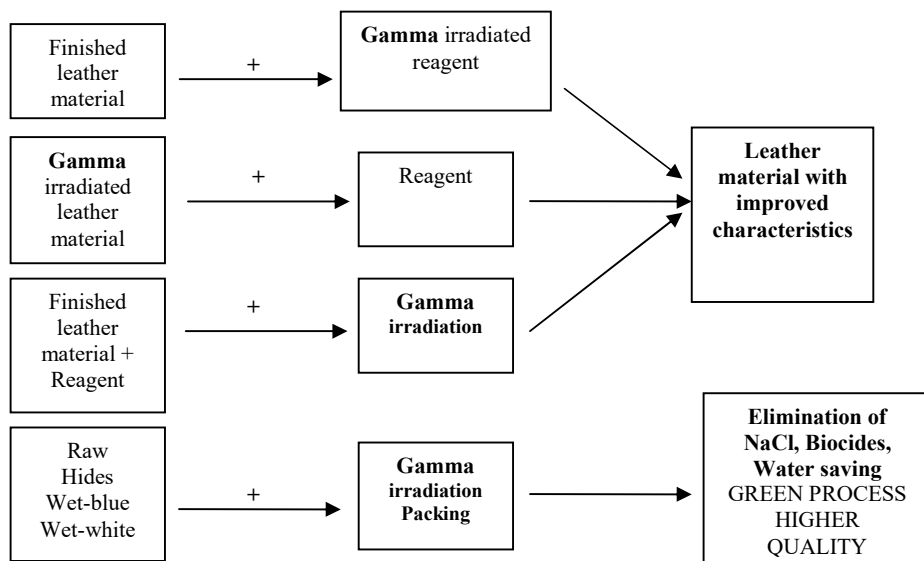
Figure 2. Conceptual model for leather processing by gamma irradiation

CONCLUSIONS

The application of gamma irradiation in leather industry represents an ecological approach for chemical and water saving with potential impact on leather quality improving. The knowledge in the area of gamma radiation application on collagen based materials are few and needs research efforts for innovative methods development.

Acknowledgement

REFERENCES

Carşote, C. *et al*. (2016), "Study of the effect of tannins and animal species on the thermal stability of vegetable leather by differential scanning calorimetry", *Journal of Thermal Analysis and Calorimetry*, 124(3), 1255-1266, https://doi.org/10.1007/s10973-016-5344-7.
Cataldo, F. *et al*. (2007), "Radiation-induced crosslinking of collagen gelatin into a stable hydrogel, *Journal of Radioanalytical and Nuclear Chemistry*, 275(1), 125-131, https://doi.org/10.1007/s10967-007-7003-8.
Catalina, M. *et al*. (2010), "Influence of crosslinkers and crosslinking method on the properties of gelatin films extracted from leather solid waste, *Journal of Applied Polymer Science*, 119(4), 2105-2111, https://doi.org/10.1002/app.32932.
Cox, R., Grant, R. and Horne, R. (1967), "The structure and assembly of collagen fibrils*: I. Native-collagen fibrils and their formation from tropocollagen, *Journal of the Royal Microscopical Society*, 87(1), 123-142, https://doi.org/10.1111/j.1365-2818.1967.tb04498.x.

Demeter, M. *et al*. (2018), "Network structure studies on γ–irradiated collagen–PVP superabsorbent hydrogels", *Radiation Physics and Chemistry*, 131, 51-59, https://doi.org/10.1016/j.radphyschem.2016.09.029.

Duliu, O., Epuras, M. and Trandafir, V. (2001), "EPR investigation of the gamma-ray-irradiated natural and tanned collagen", *Applied Radiation and Isotopes*, 54(6), 887-891.

Gotoh, T., Itoh, M. and Okuda, T. (1977), "The changes of electrochemical and mechanical properties through gamma irradiation of a collagen aqueous solution", *The International Journal of Applied Radiation and Isotopes*, 28(12), 933-937, https://doi.org/10.1016/0020-708X(77)90057-6.

Grant, R., Cox, R. and Horne, R. (1967), "The structure and assembly of collagen fibrils*: II. An electron-microscope study of cross-linked collagen", *Journal of the Royal Microscopical Society*, 87(1), 143-155, https://doi.org/10.1111/j.1365-2818.1967.tb04499.x.

Grant, R.A. *et al*. (1973), "The effects of gamma irradiation on the structure and reactivity of native and cross-linked collagen fibers, *J. Anat.*, 115, 1, 29-43.

Guerrero, L. and Camacho, B. (2017), "Comparison of different skin preservation methods with gamma irradiation", *Burns*, 43(4), 804-811, https://doi.org/10.1016/j.burns.2017.01.003.

Hedberg, Y., Lidén, C. and Odnevall Wallinder, I. (2018), "Correlation between bulk- and surface chemistry of Cr-tanned leather and the release of Cr(III) and Cr(VI)", *Journal of Hazardous Materials*, 280, 654-661 https://doi.org/10.1016/j.jhazmat.2014.08.061.

IAEA (International Atomic Energy Agency) (2017), "Uses of ionizing radiation for conservation of tangible cultural heritage", *Radiation Technology Series*, No. 6. STI/PUB/1747, Vienna: IAEA, 244 p.

Iqbal, M. *et al*. (2015), "Tannery wastewater treatment using gamma radiation: Kasur tanneries waste management agency, Pakistan", *Physical Chemistry*, 17(1), 41-46.

Kovacheva, P., Boshnakova, N. and Zhekov, D. (2017), "Studying Side-Effects of Gamma-Irradiation Processing of Leather Materials", *Industry 4.0*, 2(5), 228-231.

Leontiou, I. *et al*. (1993), "The effect of gamma irradiation on collagen fibril structure", *Micron*, 24(1), 13-16, https://doi.org/10.1016/0968-4328(93)90010-X.

Lungu, I.B. *et al*. (2014), "Study on mechanical proprieties of gamma irradiated leather and parchment", *Proceedings of the 5th ICAMS 2014*, 23-25 October 2014, 527-532.

Maslennikova, A. *et al*. (2015), "Effects of gamma irradiation on collagen damage and remodeling", *International Journal of Radiation Biology*, 91(3), 240-247, https://doi.org/10.3109/09553002.2014.969848.

Mesquita, N. *et al*. (2013), "Flow cytometry as a tool to assess the effects of gamma radiation on the viability, growth and metabolic activity of fungal spores", *International Biodeterioration & Biodegradation*, 84, 250-257, https://doi.org/10.1016/j.ibiod.2012.05.008.

Misra, N. *et al*. (2018), "Mitigation of Cr(VI) toxicity using Pd-nanoparticles immobilized catalytic reactor (Pd-NICaR) fabricated via plasma and gamma radiation", *Environmental Science and Pollution Research*, 25(16), 16101-16110, https://doi.org/10.1007/s11356-018-1709-8.

Nunes, I. *et al*. (2012), "Gamma radiation effects on physical properties of parchment documents: Assessment of Dmax", *Radiation Physics and Chemistry*, 81(12), 1943-1946, https://doi.org/10.1016/j.radphyschem.2012.07.016.

Sendrea, C. *et al*. (2015), "Dose-Dependent Effects of Gamma Irradiation on Collagen in Vegetable Tanned Leather by Mobile NMR Spectroscopy", *Leather and Footwear Journal*, 15(3), 139-150, https://doi.org/10.24264/lfj.15.3.1.

Sendrea, C. *et al*. (2017), "The Effect of Gamma Irradiation on Shrinkage Activity of Collagen in Vegetable Tanned Leather", *Revista de Chimie*, 68(7), 1535-1538.

Takitoh, T. *et al*. (2015), "Gamma-cross-linked nonfibrillar collagen gel as a scaffold for osteogenic differentiation of mesenchymal stem cells", *Journal of Bioscience and Bioengineering*, 119(2), 217-225, https://doi.org/10.1016/j.jbiosc.2014.07.008.

Vujčić, I. *et al*. (2017), "Gamma Irradiation Of Leather Gloves In Terms Of Cultural Heritage Preservation, *XXV International Conference "ECOLOGICAL TRUTH" ECO-IST'17*, 12-15 June 2017, Serbia, 531-535.

Wu, B. *et al*. (2009), "Effects of Cr3+on the Structure of Collagen Fiber", *Langmuir*, 25(19), 11905-11910, https://doi.org/10.1021/la901577j 11905.

A CLOUD SYSTEM UTILIZED FOR DIABETIC FOOT MANAGEMENT

MINGYU HU[1], QUTING HUANG[1], BO XU[1], WUYONG CHEN[1], JIANXIN WU[2], JIN ZHOU[1,2*]

[1]*Sichuan University, National Engineering Laboratory for Clean Technology of Leather Manufacture; Chengdu 610065, P. R. China*

[2]*Science Lab, Zhejiang Red Dragonfly Footwear Co., LTD., Zhejiang Province, Wenzhou 325100, P. R. China, *corresponding author email: zj_scu@scu.edu.cn*

Diabetic foot is one of the major chronic complications of diabetes mellitus, where foot infection, deep tissue destruction due to local nerve abnormalities and peripheral vascular lesions in the distal extremity of the lower limbs are usually found. Those feet lesions are also assumed as main reasons to cause the ulceration, amputees, or even the death of patients. Appropriate intervention is helpful in the daily care of diabetic feet. However, current approaches only considered one or several foot conditions through routine inspection, such as diabetic peripheral index (DPI) or MICHIGAN test etc., an overall evaluation for the diabetic feet were lacking. Therefore, the purpose of this study was aimed to establish a cloud system for diabetic feet management, where we can quantify the diabetic feet according to an algorithm designed to overall evaluation. Those data were transferred into digital format and saved in the cloud platform, where remote accessing is available. In our system, we included examination of peripheral neuropathy, foot deformities and plantar pressure of the patient and this system could be applied for both the management of diabetic feet and used for early warning in order to prevent feet ulcerations.

Keywords: diabetes foot management system; algorithm to evaluate the risk of ulceration; diabetic peripheral neuropathy.

INTRODUCTION

Diabetic foot (DF) is one of the major chronic complications of diabetes mellitus. Appropriate intervention is helpful in daily care of diabetic feet, which will not only help patients avoid amputates, but also alleviate a lot of financial burden (Boulton *et al*., 2005). However, proper prevention of DF requires accurate evaluation. Key factors have been reported that lead to DF and they were Diabetic Peripheral Neuropathy (DPN), Peripheral Vascular Lesions (PVD), Foot Infection, Ulcers and Deep tissue destruction (van Netten *et al*., 2016). Accordingly, methods are established for assessment, such as Neuropathy Impairment Score in the Lower Limbs (NIS-LL), Michigan Neuropathy Screening Instrument (MNSI), Michigan Diabetic Neuropathy Score (MDNS), Neurological Disability Score (NDS), Neurological Symptom Score (NSS) and Toronto Clinical Scoring System (TCSS) (Bril, 1999; Ohnishi *et al*., 1999; Bril and Perkins, 2002; Dias *et al*., 2015; Nisansala and Wimalasekera, 2015; Wei, 2018). Physical protocols such as Semmes-Weinstein Monofilament Examination (SWME), Tuning Fork, and Vibration Perception Thresholds (VPT) are also widely used due to their low cost of tools (Lavery and Armstrong, 2012; Bagherzadeh Cham *et al*., 2016). Other clinical detective devices liking Quantitative Sensory, Electromyogram and Electrocardiograph, Ergograph, Force Plate, and Plantar Pressure Plate are also used for DPN's evaluate (Lavery *et al*., 2002; Turgut *et al*., 2009; Kuhn *et al*., 2017). Moreover, in terms of quantification of PVD, Color Doppler Flow Imaging, Digital Subtraction Angiography, Transcutaneous Oxygen Pressure and other medical equipment are adopted (Goebel *et al*., 1995; Chen *et al*., 2008; Reichelta *et al*., 2009; Gastroenterology *et al*., 2010). Unfortunately, some protocols are too expensive for either medical institutions or patients in their DF assessment.

Current literatures were widely reported concerning on the DF assessment. Meggitt and Wagner had first divided the DF into six level marked as 0 to 5 to help doctor to determine whether patients need amputation (Wagner, 1981). To add the infection and ischemia symptoms. After that Lavery *et al*. (Armstrong, 1996) created the Texas method on the basis of Wagner, that can be used to predict the healing time of patients. Macfarlane had also put forward a new method to describe DF in 1999, S(AD)SAD classification (Macfarlane and Jeffcoate, 1999). This method enables the ordinary to distinguish the pathological state of patients and was more suitable for statistic research than Texas method. In 2004, a DEPA scoring system which Unprecedented contained the score, grade, predict prognosis, treatment of patients was developed by Foot Hospital of Jordan University (Younes and Albsoul, 2004). At the same, the International Working Group of the DF (IWGDF) launched the PEDIS classification system (Schaper, 2004), which was objective and accurate in description of infection and ischemia, but no description of the size of ulcers. Then in the year 2005, Strauss and Akenov used Strauss classification to differentiate the wound of foot (Strauss and Aksenov, 2005). Next year, Beckert from German provided the DUSS (Diabetic Ulcer Severity Score) (Beckert *et al*., 2006), which was the first to apart the ulcerations from the location in toe or foot, single or multiple ulcers. Furthermore, new classifications such as SINBAD Scoring system, MAID Scoring system and SEWSS Scoring system were separately improved from S(AD)SAD classification, DUSS system and PEDIS system (Schaper, 2004; Ince *et al*., 2008; Beckert *et al*., 2009). All of the approaches had a different degree of improvement. But now no classification system could perfectly evaluate diabetic foot. Thus, doctors need to choose the method considering the balance of advantages and limitation. Previous studies only evaluated the DB in a single level, which cause the incomplete in the assessment process; moreover, results of those approaches could not be compared since no standards were regulated. Those two reasons make it hard to comprehensively judge the DB.

Therefore, the purpose of this study was aimed to establish a cloud system for diabetic feet management, where we can quantify the diabetic feet according to algorithm designed to overall evaluation for those inspection data which were transferred into digital format and saved in the cloud platform.

METHODS

Subjects

In our system, patients with DB were recruited by the guidance of doctors in the hospital. Doctors would introduce the system to patients and give advice for patients about the acquisition frequency.

Data Collection of DF

DPN, foot deformities and plantar pressure of the patient were detected as the input data of the system. Their processes were as follows:

In the DPN detection process, we first chose the Michigan patient's self-rating scale to obtain the subjective score of patients. This scale includes twelve questions that reflects the symptoms of DPN of the foot. Then 10 g nylon wire stimulation, 128Hz tuning fork and percussion hammer conditioned reflex were adopted (Malik *et al*., 2003). Toe and thumb of foot were simulated by the Nylon wire and fork respectively,

and the hammer was used to test knee reflex. In the self-test report, each question equals 1 point, and the feeling of physical test can be calculated as: 0 for normal feel, 1 for disappeared feel and 0.5 for the weakened feel. Then, the score of self-test and physical test were uploaded to cloud.

Foot deformities were evaluated using Static three-dimensional foot scanner (LSF350-AM, 3DOEsolution Int., China). Through three laser cameras, the transverse section of the foot is scanned at the frequency of 50Hz from three vertical angles. The data collected will be fitted into the three-dimensional entity by the software, and the static foot image will be obtained. In the scanning process, patients stand statically with their both feet separate naturally. Data of this section can be used to identify the foot deformities. Strephenopodia or arch collapse, mallet or overlapping toes and hallux valgus. The number of deformities would be counted.

Plantar pressure was tested by Footscan Pressure Plate System (one-meter plate, RSscan Int., Belgium), with scanning frequency of 250Hz (Birch *et al*., 1998). Distribution of the plantar pressure and the peak pressure can be recorded during the statistic stand and walking period of our test. Plantar was divided into six parts as follows: interior forefoot, medial forefoot, lateral forefoot, midfoot, lateral and external heel. Pressure, impulse and contact area were counted and normalized to relative values by their weight and total contact area. Then the above factors were compared with a criterion, which was made calculated of a group of healthy participants (Liu *et al*., 2017).

Point of DPN, level of foot deformities and pressure distribution of patients were uploaded to our cloud server. Then the collection step had already finished.

Data Processing

All the data in the cloud system were visualized and the expert could read the report of patients. The self-test point and total physical point will both directly send to doctor. Number of deformities also be distinguished as: Mild (no or one deformities), Moderate (two deformities), Severe (multiple deformities). As for plantar plate force, pressure that in, at the edge and beyond the criterion would be marked as green, yellow and red color on the report of cloud. Experts would give a diagnosis based on the report.

Report of a Case

Report of one participant was shown in Figure 1, patients could follow the advice of doctor to make better prevention of his foot.
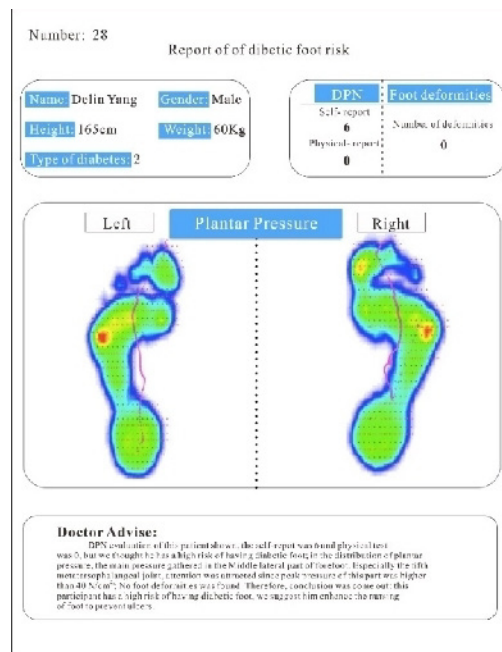
Figure 1. A case of the report. Left part of the figure shown the information of the patients, and the right part contains the point of DPN and number of foot deformities. Mid part of picture is the plantar pressure of the patients, green, yellow and red are separately resemble normal, warning and severe degrees of pressure value. Doctor advise were given at bottom of the picture, in this case, doctor suggested the patients to enhance the nursing of his foot.

RESULTS AND DISCUSSION

System was put into used on 24 January 2017, 1168 patients have registered and uploaded their information to the system, few of them keep the collection as a habit. Data and diagnostic report can provide the information of patients, and the longitudinal detection of patients could provide more information in evaluating the pathological stage in DF.

Advantages of the system are the data could be upload to the cloud system. This feature enables the doctors the ability to achieve access the information and remote diagnosis. Since the low cost of detection equipment, detection point could be sited to remote countryside, patients lived far from city can also uploaded their information to doctor immediately. Longitudinal data acquisition enables patients have their individual electronic medical records and the service of obtaining long-term tracking data.

As for the data we collect, since DPN can be detected in a low-cost way, and some other factors can be detected by inspection. Longitudinal followed up need to set up a number of detection site, and we focused on the big sample of the patients. So, through the comprehensive consideration of the cost and our goals, we detect the DPN, foot deformities and plantar pressure of the patient for medical examination of diabetic feet

and those data were saved in the cloud server. In current stage, we fulfilled the process of cloud system establishment and more and more inspection data from diabetic patients were adding to this system. Our system would be applied for early warning and strategy making of clinical intervention for diabetic feet, in order to avoid the occurrence of foot ulcerations.

CONCLUSION

In our system, key factors of patients could be recorded, doctors could evaluate condition of the patients remotely. Longitudinal followed up could be easily achieved in our system. More and more people participant and record their information of DF in our cloud system. Now this system enables doctors to achieve remote diagnose.

REFERENCES

Armstrong, D.G. (1996), "The University of Texas Diabetic Foot Classification System", *Ostomy/wound Management*, 42(8), 60-1.

Bagherzadeh Cham, M. *et al*. (2016), "Reliability of Semmes-Weinstein Monofilaments and tuning fork on pressure and vibration sensation measurement in diabetic patients", *Iranian Journal of Rehabilitation*.

Beckert, S. *et al*. (2006), "A new wound-based severity score for diabetic foot ulcers: A prospective analysis of 1,000 patients", *Diabetes Care*, 29(5), 988.

Beckert, S. *et al*. (2009), "M.A.I.D.: A prognostic score estimating probability of healing in chronic lower extremity wounds", *Annals of Surgery*, 249(4), 677, https://doi.org/10.1097/SLA.0b013e31819eda06.

Birch, I. *et al*. (1998), "Foot pressure measurement and diabetes: Where we are now?", *Diabetic Foot*, 1, 28-32.

Boulton, A.J. *et al*. (1987), "The natural history of foot pressure abnormalities in neuropathic diabetic subjects", *Diabetes Research*, 5(2), 73, https://doi.org/10.1016/S0140-6736(05)67698-2.

Boulton, A.J. *et al*. (2005), "The global burden of diabetic foot disease", *The Lancet*, 366(9498), 1719-1724.

Bril, V. (1999), "NIS-LL: The Primary Measurement Scale for Clinical Trial Endpoints in Diabetic Peripheral Neuropathy", *European Neurology*, 41(Suppl.1), 8-13.

Bril, V. and Perkins, B.A. (2002), "Validation of the Toronto Clinical Scoring System for Diabetic Polyneuropathy", *Diabetes Care*, 25(11), 2048, https://doi.org/10.1159/000052074.

Chen, X. *et al*. (2008), "Danshen Tablet on TNF-α, hs-CRP and 6-MWT in Patients with Diabetes and Heart Failure", *Chinese Journal of Integrative Medicine on Cardio-/Cerebrovascular Disease*, 1.

Dias, L.S. *et al*. (2015), "Sensitivity and specificity of neuropathy diabetes score, neuropathy symptoms score, diabetic neuropathy score and esthesiometry compared with the gold standards Michigan neuropathy screening instrument (MNSI) and Beck depression inventory (BDI)", *Diabetology & Metabolic Syndrome*, 7(S1), 1-2, https://doi.org/10.1186/1758-5996-7-S1-A199.

Goebel, W. *et al*. (1995), "Color Doppler imaging: a new technique to assess orbital blood flow in patients with diabetic retinopathy", *Invest Ophthalmol Vis Sci*, 36(5), 864-70.

Gonzalez, J.A. (1989), "Artificial intelligence: expert systems", *Isa Transactions*, 28(1), 1.

Ince, P. *et al*. (2008), "Use of the SINBAD Classification System and Score in Comparing Outcome of Foot Ulcer Management on Three Continents", *Diabetes Care*, 31(5), 964, https://doi.org/10.2337/dc07-2367.

Kuhn, B. *et al*. (2017), "(438) Quantitative sensory testing (QST) and diabetes risk: are abnormalities in small diameter afferents present in healthy persons at high risk for diabetes?", *Journal of Pain*, 18(4), S83, https://doi.org/10.1016/j.jpain.2017.02.288.

Lavery, L.A. and Armstrong, D.G. (2012), *Clinical Examination and Risk Classification of the Diabetic Foot*, Humana Press.

Lavery, L.A. *et al*. (2002), "Ankle equinus deformity and its relationship to high plantar pressure in a large population with diabetes mellitus", *Journal of the American Podiatric Medical Association*, 92(9), 479-82, https://doi.org/10.7547/87507315-92-9-479.

Liu, J. *et al*. (2017), "Classification of Diabetic Feet in Terms of Risk of Ulceration", *Leather and Footwear Journal*, 17(3), 129-134, https://doi.org/10.24264/lfj.17.3.2.

Macfarlane, R.M. and Jeffcoate, W.J. (1999), "Classification of diabetic foot ulcers: The S(AD) SAD system", *The Diabetic Foot*, 2(4), 123-131.

Malik, R.A. *et al*. (2003), "Corneal confocal microscopy: a non-invasive surrogate of nerve fibre damage and repair in diabetic patients", *Diabetologia*, 46(5), 683-688, https://doi.org/10.1007/s00125-003-1086-8.

Nisansala, M.W.N. and Wimalasekera, S.W. (2015), "Usefulness of Michigan Neuropathy Screening Instrument (MNSI) in diagnosis of diabetic neuropathy in a Sri Lankan diabetic clinic", *Proceedings of the Scientific Sessions of the Faculty of Medical Sciences*, University of Sri Jayewardenepura, Nugegoda.

Ohnishi, A. *et al*. (1999), "[A family of hereditary motor and sensory neuropathy type 1B showing a marked difference of neurological disability score among affected family members]", *Journal of Uoeh*, 21(2), 149, https://doi.org/10.7888/juoeh.21.149.

Reichelta, A. *et al*. (2009), "Chronic thromboembolic pulmonary hypertension: Evaluation with 64-detector row CT versus digital substraction angiography", *European Journal of Radiology*, 71(1), 49-54, https://doi.org/10.1016/j.ejrad.2008.03.016.

Schaper, N.C. (2004), "Diabetic foot ulcer classification system for research purposes: a progress report on criteria for including patients in research studies", *Diabetes/metabolism Research & Reviews*, 20, S90, https://doi.org/10.1002/dmrr.464.

Strauss, M.B. and Aksenov, I.V. (2005), "Evaluation of diabetic wound classifications and a new wound score", *Clin Orthop Relat Res*, 439(439), 79-86, https://doi.org/10.1097/01.blo.0000182393.31978.c3.

Turgut, N.L. *et al*. (2009), "Comparative Neurophysiological Study for the Diagnosis of Mild Polyneuropathy in Patients with Diabetes Mellitus and Glucose Intolerance", *International Journal of Neuroscience*, 116(6), 745-759, https://doi.org/10.1080/00207450600675340.

van Netten, J.J. *et al*. (2016), "Prevention of foot ulcers in the at-risk patient with diabetes: a systematic review", *Diabetes/Metabolism Research and Reviews*, 32, 84-98, https://doi.org/10.1002/dmrr.2701.

Wagner, F.W., Jr. (1981), "The dysvascular foot: a system for diagnosis and treatment", *Foot & Ankle*, 2(2), 64, https://doi.org/10.1177/107110078100200202.

Wei, Y. (2018), "The analysis of the symptom score, neurological function and quality of life of the patients with cerebral infarction treated by fuqi tongluo decoction", *Contemporary Medicine*.

Younes, N.A. and Albsoul, A.M. (2004), "The DEPA scoring system and its correlation with the healing rate of diabetic foot ulcers", *Journal of Foot & Ankle Surgery*, 43(4), 209-213, https://doi.org/10.1053/j.jfas.2004.05.003.

CENTER OF MASS MOVEMENT OF PRESCHOOLER DURING OBSTACLE-CROSSING WALKING

QUTING HUANG[1], MINGYU HU[1], BO XU[1], WUYONG CHEN[1], JIANXIN WU[2], JIN ZHOU[1,2]*

[1]*Sichuan University, National Engineering Laboratory for Clean Technology of Leather Manufacture; Chengdu 610065, P. R. China*

[2]*Science Lab, Zhejiang Red Dragonfly Footwear Co., LTD., Zhejiang Province, Wenzhou 325100, P. R. China, *Corresponding author email: zj-scu@scu.edu.cn*

Obstacle-crossing walking (OW) activated a specify compensation strategy in motion, which was indicator to children's development. Therefore, we aimed to comprehend features of center of mass (COM) of preschooler crossing over obstacles, so as to explicit their compensation strategies in motion. The COM of ten healthy preschoolers aged 3-6 and nine adults were recruited and their straight and obstacle-crossing walking was measured by Codamotion system, where four markers being set on the pelvis. Trajectory, range of motion (ROM) and Time to peak value (TPV) of COM were calculated and used for further analysis. One sample T test was applied to explore the distinctions between preschoolers and adults. Significant group differences were found in medio-lateral (M/L) and vertical motion of the COM. Preschoolers demonstrated significantly greater motion of the COM when crossing obstacle, and their TPV advanced in both sagittal and coronal planes, which indicates efforts made by them to finish the task and maintain balance. Overall, distinctions found between preschoolers and adults demonstrated compensative strategies in motion of those children required further development to the level of adult-like style.

Keywords: center of mass, obstacle crossing, compensative strategies

INTRODUCTION

Obstacle-crossing walking (OW) is often required in our daily activity. It demands precise postural and balance control (Deconinck *et al*., 2010) and activates a specify compensation strategy in motion, while little is known about whether preschoolers' can make successful gait adjustments to safely stride over the obstacle. In this study, we compared the obstacle crossing behavior between a group of typically developing preschoolers and a group of healthy adults. The motion of the center of mass (COM) during OW can demonstrate their compensation strategies. We believe that an adult-like compensation strategy could be regarded as one of the references to normal development of preschoolers and provide a basis for assessing the development of them.

Obstacle-crossing gait of physically or mentally injured crowd was widely reported this few years. Some diseases involved in the literature such as Parkinson's disease (PD) (Galna *et al*., 2010) and Paralytic stroke (Said *et al*., 2008) are commonly find in elderly crowd while some others like Developmental Coordination Disorder (DCD) (Deconinck *et al*., 2010), Cerebral Palsy (CP) (Malone *et al*., 2016) or Down syndrome (DS) (Chen *et al*., 2015) are more common among children. These researches do help the protection and treatment of the related patients. In addition, studies on the healthy crowd have also gone very far. Both Hahn & Chou (2004) and Chou *et al*. (2003) studied the center of mass motion in sagittal plane during obstacle crossing. Likewise, Huang *et al*. (2008) investigated the influence of age and obstacle height on the center of mass of during obstacle-crossing. They mainly targeted at elderly person over the age of 65 as they are usual victims of accidental fall (Hahn & Chou, 2004).

Throughout the researches above, few studies aimed at preschoolers, studies carried out on children mainly focused on those who aged over 6 year old (Boonyong *et al*.,

2012) or suffering from DCD, CP or DS. However, on the other side, it is also necessary to learn obstacle-crossing gait of healthy preschoolers as they are at a critical period of growth (Bosch *et al.* 2010). The study can help us comprehend how compensation strategies of average children developed and matured, so as to sum up the common regularity which may become an indicator to children's development.

In summary, the purpose of current study was to investigate the motion of COM of preschoolers in both sagittal plane and coronal plane during OW. It was hypothesized that there would be age-related differences between the patterns of COM and energy of preschoolers and adults. Furthermore, preschoolers may have preliminarily mastered the gait of OW and their compensation strategies are close to those of adult.

METHOD

Ten healthy preschoolers (5 male/5 female, age:6.0(0.0) years, weight:19.0(4.2)kg, height: 112.5(8)cm, leg length:59.3(7.8)cm) and nine healthy adults(5 male/4 female, age 34.6(11.0) years, weight 58.3(21.8)kg, height: 166.4(1.0)cm, leg length 84.5(8.5)cm) as control group were recruited for this study. Before the test, the experimental procedures were explained to all Participants/Guardians, and then verbal and written approvals were obtained.

Subjects were asked to walk at their self-selected speed for obstacle-crossing task along a 6-m walking track (Fig. 1). According to the leg length(LL) measured during the subject's enrollment process, an obstacle at a height of 24 cm (40%LL) was set for preschooler, while 33 cm (40%LL) were set for adults respectively. Straight Walking (SW) and Obstacle-crossing Walking (OW) were each measured randomly. For each subject, a complete crossing stride in each OW was required. The crossing stride was defined as the heel-strike of the right/leading limb before the obstacle to the heel-strike of the same limb after clearing the obstacle. At least five successful trails were obtained in each task.
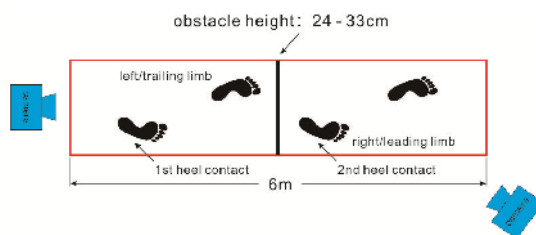

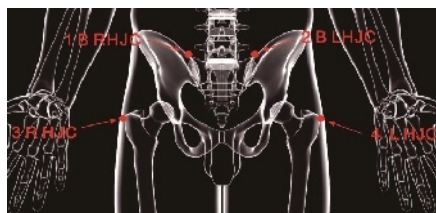Figure 1. Illustration of Obstacle-crossing Walking

Figure 2. Demonstration of Markers' Installation

Motion data of COM was collected using a two camera Coda Motion System (Coda Motion cx1, Charnwood Dynamics Ltd., United Kingdom), two collectors were aligned on the two sides of the walking track, facing at an angle of 120 degrees. The COM was defined as the central point of the pelvic model consisting of four markers (Fig.2, marker1: the posterior right of pelvic; marker2: the posterior left of pelvic; marker3: anterior right of pelvic; marker4: the anterior left of pelvic).

A low-pass filtered with the cutoff frequency set at 6 Hz on the Three-dimensional marker trajectory data of COM was applied. Tempero-spatial parameters were first considered, then M/L(X) and vertical(Z) displacement of the COM, velocities of the COM, as well as the range of motion (ROM) and time to peak value (TPV) in the crossing stride were calculated. A normalization procedure was executed in order to achieve a comparable result: X and Z displacement of COM was divided by leg length of each subject and transfer into X-rel and Z-rel variables (Scrutton, 1969). Gait cycle of each test was also normalized into 100 points (%GC).

All statistical models were executed under SPSS 22 with a significance level of 0.05 and a confidence interval of 95%.

RESULT

All subjects were able to complete the obstacle-crossing task without tripping. In contrast with FW, both preschoolers and adults decreased their stance phase ($p < 0.001$) and increased their swing phase ($p < 0.001$) in OW. Further, they prolonged their time of gait cycle ($p < 0.001$) and step length ($p = 0.364$), and lowered walking speed ($p = 0.434$). During OW, significant group difference was found only in step length ($p < 0.001$). Stride time ($p = 0.301$), step length ($p < 0.003$) and frond number ($p = 0.226$) of preschoolers were smaller than that of adults. The ratio for stance phase of children was greater than that of adults ($p = 0.021$) and the ratio for swing phase was smaller ($p = 0.022$).

Table 1. Tempero-spatial Parameters during SW and OW

	SW		OW		p-values	
	Preschooler	Adult	Preschooler	Adult	Pg*	Pt*
Stride Time (s)	0.97(0.11)	1.09(0.10)	1.26(0.19)	1.31(0.27)	0.301	0.000
Step Length (m)	0.71(0.10)	1.03(0.13)	0.78(0.11)	1.07(0.05)	0.003	0.364
Frond Number*	0.15(0.03)	0.20(0.02)	0.18(0.04)	0.21(0.05)	0.226	0.434
Stance Phase	56.7(5.5%)	54.4(3.0%)	43.2(3.9%)	40.2(2.9%)	0.021	0.000
Swing Phase	43.3(5.5%)	45.6(3.0%)	56.8(3.9%)	59.8(3.9%)	0.022	0.000

*Frond Number is used to characterize walking velocity ($Fr = V^2/gL$, V represents walking velocity, L represent leg length). *Pg represents group effect in OW, Pt represents gait type effect

When stepping over obstacles, M/L ROM of the COM in both preschooler and adult groups decreased, however, vertical ROM of both two groups increased. In Coronal plane, obstacle-crossing condition advanced the first TPV in both preschooler (the peak of SW is 28%GC, OW is 19% GC) and adult (the peak of SW is 40%GC, OW is 29% GC) groups; such regularity was also found in sagittal plane where the first TPV in preschooler was advanced from 28%GC to 24% GC for preschoolers and from 30%GC to 24% GC for adults; further, the second TPV were also both advanced (the 2nd peak of SW is 77%GC, OW is 70% GC for preschoolers, the 2nd peak of SW is 77%GC, OW is 74% GC for adults.)

Moreover, similar COM trajectory of the two groups in M/L direction was found for OW, as well as ROM and TPV of the COM, totally adults showed larger ROM and displacement than children. In terms of sagittal plane, compared with adult group, amplitude of COM, as well as its ROM were smaller in preschoolers while TPV was nearly the same.
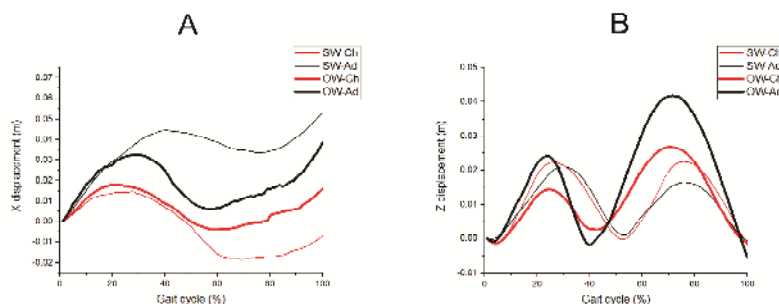

Figure 3. Trajectory of the COM during SW and OW in (A) M/L and (B) vertical direction

DISCUSSION

Current study investigated the trajectory of COM in sagittal and coronal plane during OW. Results from this study revealed that when coping with the obstacle-crossing task, preschoolers would prolong their movement time, lengthen their stride and decrease their speed. Moreover, their M/L and vertical ROM of the COM changed and their TPV advanced, which is similar to that of adult. Such result supported our hypotheses that preschoolers have preliminary mastered the gait of OW. Those findings were helpful for us to comprehend the mechanism of gait adjustment in children, so as to understand their development in motion.

The result of spatiotemporal parameters showed preschoolers' adjustment of gait in order to trip over the obstacle. Such result was similar to previous studies (Chou *et al.*, 2001; Austin *et al.*, 1999). The prolonged time of gait and step length revealed their awareness and effort to cross the obstacle. In contrast with adults, spatiotemporal parameters of preschoolers changed much greater, which demonstrated that the obstacle-crossing task has led to trouble for them. That is to say their compensation strategy in OW is not fully mature yet.

The present study found that the M/L and vertical trajectory of the COM was affected by obstacle-crossing task. In general, at the beginning of a gait cycle, the leading leg was contacting with the ground and trailing leg went forward, so COM showed a tendency towards the right side (leading leg), and it reversed following the toe-off of the leading leg. When tripping over the obstacle, this process was advance for an early preparation for the obstacle (Fig. 3A). Whereafter, an additional stretch of leg was required to cross over the obstacle so as to increase the height of COM (Fig. 3B). While we can see from Fig. 3 that adults had an earlier TPV in M/L direction and a higher vertical displacement which means their compensation strategies in OW is more perfect than preschoolers. The above findings suggested that an adult-like compensation strategy in motion have not completely mastered in preschoolers and it was consistent

with Beerse *et al*. (2005) and Jianhua *et al*. (2009), who reported that children's motion ability is still developing after the age of 5 and 10 more years was need for them to gain an adult like variability-partitioning capability.

In terms of ROM of the COM, M/L ROM was slightly affected, which indicated that preschoolers succeed to maintain balance and gait stability during OW. Similar result was reported by Chou *et al*. (2001), they summarized that slight changes in COM M/L displacement and the M/L distance between the COM and the corresponding during OW may represent a successful effort to maintain the line of progression within the base of support and to avoid imbalance.

CONCLUSION

When tripping over an obstacle, COM of healthy preschoolers in either cornel and sagittal plane showed partly similar to those of adult. But some distinctions existed which indicated that compensative strategies of those children were still developing.

REFERENCES

Austin, G.P. *et al*. (1999), "Kinematic analysis of obstacle clearance during locomotion", *Gait & Posture*, 10(2), 109-20, https://doi.org/10.1016/S0966-6362(99)00022-3.

Bennett, B.C. *et al*. (2005), "Center of mass movement and energy transfer during walking in children with cerebral palsy", *Archives of Physical Medicine & Rehabilitation*, 86(11), 2189, https://doi.org/10.1016/j.apmr.2005.05.012.

Boonyong, S. *et al*. (2012), "Development of Postural Control during Gait in Typically Developing Children: The Effects of Dual-task Conditions", *Gait & Posture*, 35(3), 428-434, https://doi.org/10.1016/j.gaitpost.2011.11.002.

Bosch, K. *et al*. (2010), "Development of healthy children's feet--nine-year results of a longitudinal investigation of plantar loading patterns", *Gait & Posture*, 32(4), 564, https://doi.org/10.1016/j.gaitpost.2010.08.003.

Chen, H.L. *et al*. (2015), "Obstacle crossing in 7-9-year-old children with Down syndrome", *Research in Developmental Disabilities*, 48, 202, https://doi.org/10.1016/j.ridd.2015.11.004.

Chou, L.S. *et al*. (2001), "Motion of the whole body's center of mass when stepping over obstacles of different heights", Gait & Posture, 13(1), 17-26, https://doi.org/10.1016/S0966-6362(00)00087-4.

Chou, L.S. *et al*. (2003), "Medio-lateral motion of the center of mass during obstacle crossing distinguishes elderly individuals with imbalance", *Gait & Posture*, 18(3), 125, https://doi.org/10.1016/S0966-6362(02)00067-X.

Deconinck, F.J. *et al*. (2010), "Balance problems during obstacle crossing in children with Developmental Coordination Disorder", *Gait & Posture*, 32(3), 327-331, https://doi.org/10.1016/j.gaitpost.2010.05.018.

Galna, B. *et al*. (2010), "Obstacle crossing in people with Parkinson's disease: foot clearance and Tempero-spatial deficits", *Human Movement Science*, 29(5), 843-852, https://doi.org/10.1016/j.humov.2009.09.006.

Hahn, M.E. and Chou, L.S. (2004), "Age-related reduction in sagittal plane center of mass motion during obstacle crossing", *Journal of Biomechanics*, 37(6), 837, https://doi.org/10.1016/j.jbiomech.2003.11.010.

Huang, S.C. *et al*. (2008), "Age and height effects on the center of mass and center of pressure inclination angles during obstacle-crossing", *Medical Engineering & Physics*, 30(8), 968, https://doi.org/10.1016/j.medengphy.2007.12.005.

Kim, H.D. and Brunt, D. (2007), "The Effect of a Dual-Task on Obstacle Crossing in Healthy Elderly and Young Adults", *Archives of Physical Medicine & Rehabilitation*, 88(10), 1309-1313, https://doi.org/10.1016/j.apmr.2007.07.001.

Malone, A. *et al*. (2016), "Obstacle Crossing During Gait in Children With Cerebral Palsy: Cross-Sectional Study With Kinematic Analysis of Dynamic Balance and Trunk Control", *Physical Therapy*, 96(8), 1208-1215, https://doi.org/10.2522/ptj.20150360.

Said, C. *et al*. (2008), "Balance during obstacle crossing following stroke", *Gait & Posture*, 27(1), 23-30, https://doi.org/10.1016/j.gaitpost.2006.12.009.

Scrutton, D.R. (1969), "Footprint sequences of normal children under five years old", *Developmental Medicine & Child Neurology*, 11(1), 44, https://doi.org/10.1111/j.1469-8749.1969.tb01394.x.

Wu, J. *et al*. (2009), "Center of mass control and multi-segment coordination in children during quiet stance", *Experimental Brain Research*, 196(3), 329-339, https://doi.org/10.1007/s00221-009-1852-z.

USING A SOFTWARE APPLICATION TOOL TO IMPROVE MARKETING ACTIVITIES

GHEORGHE MILITARU, DANA CORINA DESELNICU, IUSTINA-CRISTINA COSTEA-MARCU

University Politehnica of Bucharest, Splaiul Independenței 313, ghmilitaru.militaru@gmail.com, d_deselnicu@yahoo.com, costeamarcuiustina@gmail.com

Merchants need to know how elastic the demand is for a price change. The higher the elasticity, the higher the volume resulting from the one-percent drop in price. It is proposed to develop an IT application to improve marketing activities by analyzing the variations in percentage of sales, sales revenue, average price and number of units sold. The application is addressed to any company that has multiple sales points and companies that own a wide range of products that make a difference in turnover. A case study has been carried out for several products within a chain of stores by processing the data obtained from the company. A chart was created using the IT tool which identifies the variations in sales and sales revenue and a chart which indicates variations of the average price and number of units sold. By analyzing these charts, it can be concluded about the amount of attention that needs to be given to a product.

Keywords: elastic demand, inelastic demand, software application.

THE INFLUENCE OF THE DEMAND ELASTICITY

It is important for an economist to master concepts such as demand curve and demand elasticity. The way that supply and demand interact helps to determine the size and price level of a market (Perreault and McCarthy, 2002).

Elasticity measures the willingness and ability of buyers and sellers to change their behavior based on economic changes. Companies are trying to estimate price elasticity of demand for their products (McEachern, 2016).

The demand curve shows the potential purchase volume of the market at alternative rates. This summarizes the reaction of many individuals with different sensitivity to price. The first step estimating demand is understanding the factors that affect price sensitivity. In general, the customers have a lower sensitivity to cheap or rarely purchased products. They are also less price sensitive when: *the number of available substitutes and competitors is limited, do not recognize easily higher prices, being slow changeing their buying habits, thinking that higher prices are justified, the price is only a small part of the total cost of obtaining, operating and selling the product*.

Price elasticity depends on the magnitude and direction of the reference in the price changing. This may be negligible at a small price change or , on the contrary , a big change. It may vary a lot for a price drop compared to a price increase, but there may be alo an indifference interval where the price changes have a small or no effect (Kotler and Keller, 2012).

The following table highlights the effects of a 10% rise in price.

Table 1. The effects of a 10% rise in price

Demand elasticity by price	Type of request	Change the required quantity	Change in total revenue
$E_{cp} = 0$	Perfectly inelastic	No changes	Increase by 10%
$E_{cp} < 1$	Inelastic	Decreases by 10 %	Increase with less than 10%

Demand elasticity by price	Type of request	Change the required quantity	Change in total revenue
$E_{cp} = 1$	Uniform elasticity	Decreases by10 %	No changes
$E_{cp} > 1$	Elastic	Decrease by more than 10%	Decrease by 10 %
$E_{cp} = \infty$	Perfectly elastic	It drops to 0	It drops to 0

Source: adaptation after McEachern, 2016, p. 98.

Develop an IT Application in order to Identify the Type of Product Elasticity

In order to improve the marketing activities and the management of the company's products, an application can be developed for any company that has several outlets. In the same time, the application may be implemented for companies that have a wide range of product, which make different contributions to turnover. This will have the following advantages:

- Products monitoring tool
- A tool for improving decision-making as it is used in defining the marketing strategy.
- No human resource training is required to use the application.
- Accessible from anywhere - requires just user and password.
- It helps to standardize the format for data collection and interpretation.
- Evaluation tool for elasticity products and percentage changes in sales revenue.
- Collecting data - creating databases for storing or updating data.
- Updates data in real time.
- Helps identify percentage variations on: sales share, sales income, average price, and unit sold.
- Helps identify elasticity based on average price variations and unit sales.
- Graphic representation of:
  - ➢ the percentage change in the share of sales
  - ➢ the percentage change in sales revenue
  - ➢ percentage change in average price
  - ➢ the percentage change in the number of units.
- Possibility to save the graphic image as PNG image, JPEG image, PDF document, SVG vector image and helps to make reports easy.

Application Working Scenario

I. The person employed by the firm logs into the application through a username and password.

II. After login, the person can choose certain activities, depending on the purpose of the operation. The operation are:

    2.1. Inserting data on the share of sales and sales revenue;

    2.2. Inserting average price data and number of units sold

    2.3. Updating sales and sales revenue share data

    2.4. Updating data on average price and number of units;

    2.5. Analysis of the percentage change in the share of sales in total revenue and percentage change in revenue;

    2.6. Analysis of price elasticity of demand.

2.1. Inserting into the database the sales of share data and sales revenue data.

For this stage, create a table specifying:
- The category of the product
- Product name
- The percentage of sales in year *n-1*, for the product chosen, of the total turnover achieved by the store.
- The percentage of sales in year *n*, for the chosen product, of the total turnover achieved by the store.
- Income earned by the company in year *n-1.*
- Income earned by the company in year *n.*

2.1.1. inserting into database (I)
- Calculation of the change in the share of sales and percentage change in revenue.
- Inserts data from step 2.1 into the database. and the results of the calculations.

At this stage, the following formulas are used:

To determine **the weight variation** bad **sales:**

To determine the percentage change in revenue:

$$\frac{Share\ of\ sales\ n - Share\ of\ sales\ (n-1)}{Share\ of\ sales\ (n-1)} \tag{1}$$

To determine the **percentage change in revenue**:

$$\frac{Revenue\ n - Revenue\ (n-1)}{Revenue\ (n-1)} \tag{2}$$

2.2. Inserting into the database the data on the average price and the number of units sold

For this stage, a table will be created specifying:
- The category of the product
- Product name
- Average price in year **n-1** for the product chosen
- Average price in year **n** for the product chosen
- Number of units sold in year **n-1**, on the product chosen
- Number of units sold in year **n** on the product chosen.

2.2.1. inserting into the database (II)
- Calculation of the percentage change in the average price and the percentage change in the number of units.
- Makes the data in step 2.2 entered into the database. and the results of the calculations.

At this stage, the following formulas were used:

To determine the **percentage change in average price**:

$$\frac{Medium\ price\ n - Medium\ price\ (n-1)}{Medium\ price(n-1)} \tag{3}$$

To determine the percentage change in the number of units :

$$\frac{Number\ of\ units\ n - Number\ of\ units\ (n-1)}{Number\ of\ units\ (n-1)} \tag{4}$$

2.3. Updating share of sales and sales revenue data
2.4. Updating average price and number of units data
2.5. Analysis of the percentage change in the share of sales in total revenue and percentage change in revenue
2.5.1. Choosing products to analyze sales and sales revenue

For this stage there will be a table listing ten products. With the *Step 2.5.2. Forming the sales and revenue analysis charts*, the products listed in the table will be read from the database.

2.5.2. Forming the sales and revenue analysis charts

At this stage:

- are read from the database - "graph_1" - the products that were selected in the table in step 2.5.
- Depending on the products read from the database, the following charts are generated:
  - the chart represent sales for their chosen products;
  - the chart represent the income for their chosen products;
  - the chart represent sales and revenue for products they have chosen.

In the "graph_1" the data about:
  - the percentage of sales in years n-1 and n for each product
  - sales share variation for each product
  - revenue in years n-1 and n for each product
  - the percentage change in revenue for each product.

2.6. Analysis of price elasticity of demand

2.6.1. Choice of products for price elasticity analysis

For this stage there will be a table listing ten products.

With the *Step 2.6.2. Developing graphs for demand elasticity analysis based on price*, the products listed in the table will be read from the database.

2.6.2. Developing graphs for demand elasticity analysis based on price

At this stage:

- read from the database, in the table "graphic_2", the products that were selected in the table in step 2.6.
- Depending on the products read from the database, it generates:
  - the graphical representation of the percentage change in average price and the percentage change in the number of units
  - representation of the type of elasticity for each product.

In the graph "2" the data about:

  - average price for each product in years **n-1** and **n**
  - the percentage change in the average price for each product
  - number of units sold in **n-1** and **n years** , for each product
  - the percentage change in the number of units per product.

For products with a large variation on the number of units sold, the stock needs to be analyzed, as there is a risk of stagnation.

CASE STUDY FOR THE PRODUCTS OF THE INMEDIO STORE

Comparative Presentation of the Percentage Change in the Share of Sales in Total Revenue and Percentage Change in Revenue

Figure 1 shows the chart which highlight a comparison between the percentage change in sales of share and the percentage change in sales revenue.
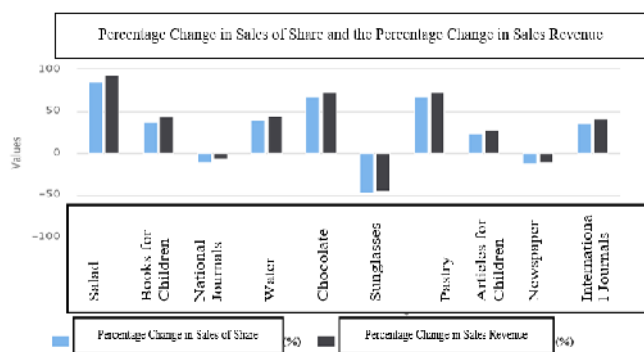
Figure 1. Comparative presentation of the two variables analyzed

It is noticed that no significant imbalance is identified for the analyzed products. The change in sales of shares and the percentage change in sales revenue are positively correlated, both changing in the same sense. In case of:

- ⬆ increase revenue and ⬇ decrease sales of share→ the product has a small impact on turnover

- ⬇ decrease revenue and ⬆ increase sales share → the product requires increased attention from the company that can decide to change marketing strategies.

- ⬆ increase revenue and ⬆ increase sales share → the product is very important, the company will take action to stimulate this trend.

- ⬇ decrease revenue and ⬇ decrease sales share → product elimination, if you can not find a way to increase revenue.

Analysis of Demand Elasticity Depending on the Price

Processing data for ten products, related to the percentage variation of the average price and the percentage change in the number of units sold, the following results are obtained:
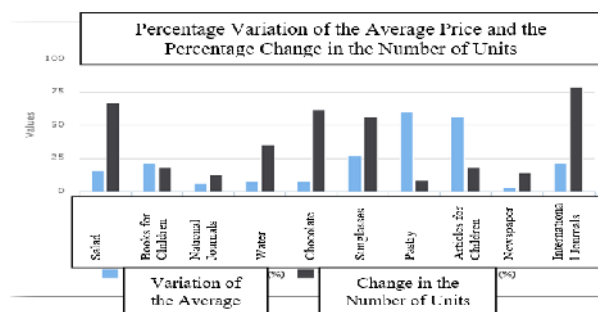

Figure 2. Comparative representation of price variations and number of units

For products with a large variation, on the number of units sold (such as chocolate or salad), the stock needs to be analyzed, as there is a risk of being out of stock.

The application provides results which highlights the type of demand - next to each product is mentioned whether the demand is elastic or inelastic.

Interpretation of Results

1. It can be seen that the *salad has* a strong **elastic** demand . A price variation has a large impact on the required quantity, the percentage change in the number of units of 67% exceeding the percentage change in the average price of 16%.
2. *Pastry* products have a strong **inelastic** demand **.** This is due to the percentage change in the average price which has a small effect on the percentage change in the number of units so that the percentage variation of the required quantity (the percentage change in the number of units of 8%) is less than the percentage change in the average price of 60%.
3. The **strong elasticity** of the ten analyzed products is for *international magazines.* This indicates that a 21% price drop has a relatively large effect on the quantity required, so that the percentage change in the quantity requested (the number of units = 79%) exceeds the percentage change in the average price.

CONCLUSION

The evaluation of the elasticity function allows a more complex analysis of the consumer's purchasing behavior as opposed to the single income / sales evaluation.

A modeling of ten products randomly selected has been carried out after the implementation of the IT application for improving marketing activities and efficient product management. After the application run, we identified: the change in sales share, the variation in sales revenue, the variation in the average price and the change in the number of units. At the same time, the application identifies the type of elasticity of demand in terms of price for each product.

REFERENCES

Kotler, P., Keller, K.L. (2012), *Marketing Management,* Prentice Hall, p.392.
McEachern, W.A. (2016), *Microeconomics: A Contemporary Introduction,* Cengage Learning, p.111.
Perreault, W.D., Jr. and McCarthy, E.J. (2002), *Basic Marketing - A Global-Managerial Approach,* McGraw-Hill, p.49.

PILOT SCALE TRIALS FOR HIGHER EXHAUSTING CHROMIUM TANNING

HASAN ÖZGÜNAY[1], MEHMET METE MUTLU[1], CEMILE CEREN TOSUN[2], ÖZGÜR DEMIRCI[2], ONUR ABALI[2], YIGIT KAMAN[2], TALIP SEPICI[2]

[1]*Ege University, Engineering Faculty, Faculty of Leather Engineering, Bornova, İzmir, Turkiye, Phone: +90 232 311 26 44, e-mail: hasan.ozgunay@ege.edu.tr*

[2]*Sepiciler Caybasi Leather Company , Mustafa Kemal Atatürk Mah. Izmir - Aydın Asfalti Cad. No: 110 Torbalı - Izmir 35860, Turkiye, Phone: +90 232 850 50 00*

Chromium tanning is a matter of high concern due to chromium containing effluents and wastes. More ecologic systems with less chromium usage or chrome-free production systems are subject of studies in recent years. One of the approaches in this concern is to use non-pickling systems and higher initial pH to increase exhaustion in chromium tanning. However adopting this system in leather industry has some challenges like to assure the same quality. In a project with one of the leading companies in Turkish Leather Industry, higher exhausting chromium tanning system has been planned to be tried in laboratory, pilot and industrial scales respectively with various pH and pre-tanning agent parameter changes. In the present stage (pilot scale trials) of the project, best resulting formulations from the laboratory scale trials were carried out to pilot scale (500kg batches) by expanding the trials with additional pre-tanning agents. From the results, it was seen that chromium remaining in the baths were varying between 325 - 875 mg/L. Which means amount of chromium remaining in residual baths could be reduced up to 78.87 % to 92.15% comparing to conventional tanning while 2.9-4.7% of Cr_2O_3 bound to the leathers depending on the type of system used in pilot scale trials.

Keywords: Leather, Chromium Tannage, High Exhaustion

INTRODUCTION

Due to the excellent properties of chrome as a tanning agent, a majority of leathers are produced by chrome tanning method (Sundar *et al*., 2002) but 90% of chrome tanned leathers shows only a 60-70% uptake of chrome (Cui, 2017).

Chromium tanning is followed closely due to chromium containing effluents and wastes. More ecologic systems with less chromium usage or chrome-free production systems are subject of studies in recent years. One of the approaches in this concern is to use non-pickling systems and higher initial pH to increase exhaustion in chromium tanning. However adopting this system in leather industry has some challenges like to assure the same quality.

Kumar *et al*. (2011) have evaluated chrome tanning process for its "greenness" by using a prominent tool named atom economy (the conversion efficiency of a chemical process in terms of all atoms involved) for four types of chrome tanning processes: direct chrome liquor recycle, ethanol-amine assisted, pickleless chrome tanning and conventional chrome tanning. Among the four improved methods of chrome tanning evaluated, the pickles chrome tanning method provided the maximum atom economy.

In this project namely "Environmentally Friendly Chromium Tanning Technology" the higher exhausting chromium tanning system has been tried to be adopted with one of the leading companies in Turkish Leather Industry in three stages: 1-Laboratory trials at the stage of transition from concept to design, 2-Pilot scale trials at the stage of design development and verification works and 3-Industrial scale trials at the stage of experimental production and reporting. In first stage, laboratory based trials (50kg batches) were done with 3 pre-tanning agents, 2 chromium tanning agents and 2

different pHs. The results of the first stage was given in ICAMS 2016 (Ozgunay *et al*., 2016). In second stage of the project, best resulting formulations from laboratory scale trials were carried out to pilot scale (500kg batches) by expanding the trials with additional pre-tanning agents. In this paper the results of stage 2: pilot scale trials will be discussed.

MATERIAL AND METHOD

Lime split domestic pelts (to be approx. 500 kg per each trial) which were conventionally processed were used as material. They were delimed and bated according to company's production route. As blank, the first trial was performed according to company's conventional chromium tanning system with pickling. Other trials were performed without pickling and the necessary pH values depending on the pre-tanning agents were adjusted by using non-swelling acids.

From the evaluations of stage 1 (laboratory scale); considering both physical and chemical data and committee's remarks it was concluded that best results were obtained from Cr_Aldehyde, Cr_Sulphonylchloryde, Cr_Syntan-1(F90), LBCr_Syntan-1(F90) trials conducted at pH 5-5.5 (Ozgunay *et al*., 2016). It was decided to make further studies to improve and verify these process designs in higher batches at pH 5.5-6.0. Additionally the committee offered to include 2 more synthetic tannins ((Syntan-2(HS) and Syntan-3(CAT)) to the trials considering the promising results of Syntan-1(F90). So an aldehyde, a sulphonylchloride and 3 syntans which are available in the market were selected to be used as pre-tanning agents.

After pre-tanning stage, the pH of the pelts were adjusted to 5.5-6.0 and chromium tanning was performed by using 5% standard basic chromium sulphate and 6% of a commercial chromium tanning agent having lower basicity and Cr_2O_3. The trial scheme is given in Fig.1.

In residual tanning baths total chromium and COD values were determined according to SM 3120 B (2005) and SM 5220 (2005) standard methods. Cr_2O_3 contents (ISO 5398-1:2007), shrinkage temperatures (ISO 3380:2015), tensile strengths and percentage extensions (ISO 3376:2011), and tear loads (ISO 3377-2:2016.) of the produced leathers were determined according to related standards.
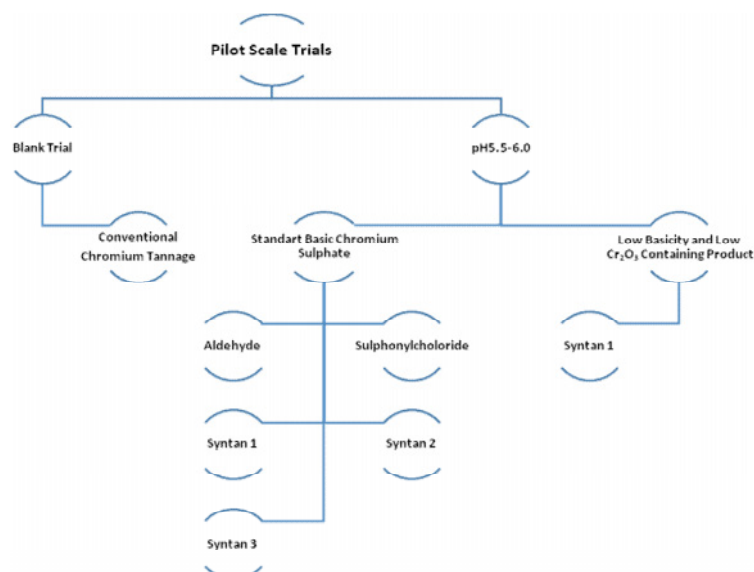
Figure 1. Pilot Scale Trial Scheme

RESULTS AND DISCUSSION

In Table 1 & Table 2, parameters of residual baths and properties of obtained leathers belonging to trials are given. When Table 1 is investigated, it is seen that chromium in the remaining baths were varying between 325 - 875 mg/L (Table 1). Which means amount of chromium remaining in residual baths could be reduced up to 78.87 % to 92.15% comparing to conventional tanning while 2.9-4.7% of Cr_2O_3 bound to the leathers depending on the type of system used in pilot scale trials as presented in Fig.2. Accordingly, with the increased consumption, COD values of residual baths decreased noticeably comparing with conventional chromium tanning system. Furthermore, regarding homogeneity parameter, the distribution of chromium through cross-section was found homogen for all samples by increasing mechanical effect and by the pH shift. Thus, homogeneity problem, which was a bothering issue in laboratory scale trials was, overcome (Ozgunay et al., 2016).

Table 1. Residual bath and leather parameters of tanning trials

| pH | Trials | Leather Parameters | | | Residual Bath | |
		Homogeneity	Thickness (mm)	Cr_2O_3 (%)	Cr (mg/L)	COD (mg/L)
-	Blank	Homogen	1.25	4.07	4142	15000
5.5-6.0	Cr_ Aldehyde	Homogen	1.65	4.50	325	4800
5.5-6.0	Cr_ Sulphonylchloryde	Homogen	1.61	4.70	383	5200
5.5-6.0	Cr_ Syntan-1(F90)	Homogen	1.62	4.10	520	6880
5.5-6.0	Cr_ Syntan-2(HS)	Homogen	1.53	3.40	875	11500
5.5-6.0	Cr_ Syntan-3(CAT)	Homogen	1.57	4.10	400	8400
5.5-6.0	LBCr_Syntan-1(F90)	Homogen	1.53	2.90	405	8006
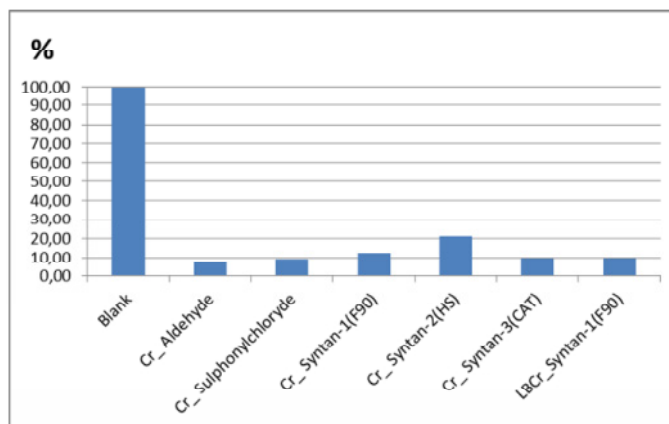
Figure 2. Comparison of mg/L chromium in residual baths of pilot scale trials

From the evaluation and comparison of the physical test results of the pilot scale trials' leather samples with conventional produced leather samples it was seen that most of the physical properties were found better or comparable but a few exceptions in shrinkage temperature (Table 2). Considering shrinkage temperatures of trials, only Cr_ Syntan-3(CAT) sample gave noticeable lower shrinkage temperature (101°C) than the Blank. However, the increment in Double Edge Tear values of this higher exhaustion system was remarkable.

Table 2. Physical properties of the final leather products of pilot scale trials

pH	Trials	Leather Parameters			
		T_s (°C)	Tensile Strength (N/mm^2)	Elongation (%)	Double Edge Tear (N/mm)
-	Blank	110	11.9	51.6	46.0
5.5-6.0	Cr_Aldehyde	124	13.9	50.3	108.4
5.5-6.0	Cr_Sulphonylchloryde	118	15.2	45.8	95.9
5.5-6.0	Cr_ Syntan-1(F90)	121	18.4	50.2	111.5
5.5-6.0	Cr_ Syntan-2(HS)	108	12.3	45.2	77.3
5.5-6.0	Cr_ Syntan-3(CAT)	101	15.5	45.3	100.0
5.5-6.0	LBCr_Syntan-1(F90)	109	20.5	50.9	119.4

CONCLUSION

In leather production, scaling up the laboratory trials to industrial scale may be problematic due to varying process conditions and the results may vary extremely. For this reason pilot scale trials at the stage of design development and verification works are necessary. In the present of the project, the trials giving the best results in laboratory scale were verified and improved

From the results, it was seen that chromium remaining baths were varying between 325 - 875 mg/L, which means amount of chromium remaining in residual baths could be reduced up to 78.87 % to 92.15% comparing to conventional tanning system. Accordingly, COD values of residual baths were also decreased noticeably.

The homogeneity problem, which was a bothering issue in laboratory scale trials was, overcome in pilot scale trials.

From the evaluation and comparison of the physical test results of the pilot scale trials' leather samples with conventional produced leather samples it was seen that most of the physical properties were found better or comparable

The results of pilot scale trials of this higher exhausting chromium tanning system were found to be promising to be used in industrial scale trials at the stage of experimental production.

Acknowledgements

REFERENCES

American Water Works Association (2005), Standard Methods for Examinations of Water and Wastewater. Metals by plasma emission spectrometry, SM 3120 B:2005.
American Water Works Association (2005), Chemical Oxygen Demand (COD), Opened Reflux-Closed Reflux, Titrimetric Method, SM 5220 B:2005.
Cui, L. *et al*. (2017), "A Cleaner Method for Low-Chrome Tanning with No-Salt Pickling", *JSLTC,* 101, 219-226.
International Organization for Standardization (2007), Chemical determination of chromic oxide content -- Part 1: Quantification by titration, ISO 5398-1:2007.
International Organization for Standardization (2015), Determination of shrinkage temperature, ISO 3380:2015.
International Organization for Standardization (2011), Determination of tensile strength and percentage extension, ISO 3376:2011.
International Organization for Standardization (2016), Determination of tear load -- Part 2: Double edge tear, 3377-2:2016.
Pradeep Kumar, M. *et al*. (2011), "Green Chemistry Approach in Leather Processing: A Case of Chrome Tanning", *JALCA*, 106, 113-120.
Ozgunay, H. *et al*. (2016), "Industrial Trials For a More Ecological Chromium Tanning", *Proceedings of the 6th International Conference on Advanced Materials and Systems*, ICAMS 2016, Bucharest-Romania, https://doi.org/10.24264/icams-2016.IV.9.
Sundar, V.J. *et al*. (2002), "Cleaner Chrome Tanning Emerging Options.", *J. Clean. Prod.*, 10, 69, https://doi.org/10.1016/S0959-6526(01)00015-4.

DESIGN AND PRODUCTION OF UNIQUE DRESS COLLECTION FOR SUMMER FROM KIZILCABOLUK "PESHTAMAL'S" AS A PART OF EDUCATION

SEVIM YILMAZ

Pamukkale University, Denizli Technical Vocational School of Higher Education, Denizli, Turkıye, e-mail:sevim71@gmail.com

When it is thought that women that indigenize freedom, modernity and naturalness as a lifestyle look for light and unique clothing; it is possible to see the value of the local fabrics. It can easily be said that the Kizilcaboluk cotton made fabrics are free, comfortable and useful for clothing. The clothes designed in the present study were selected to be suitable for the "Nature" theme from the breechcloth made of Kizilcaboluk fabrics. By keeping the size and patterns, looseness, thickness, wrinkling of the cloths in mind, and by foregrounding comfort and aesthetics, designs were done by the students at the Cloth Design class under the title "Nature". Among these, one design from each which is suitable for production was selected. The technical details of the designs were analyzed by the researcher considering the sewing technique and pattern features, trying to make them suitable for boutique production, and to let the least fabric waste. As the target audience, the customers that like to wear expensive and unique clothes were considered. It is believed that if the cloth collection produced is marketed well, Kizilcaboluk fabrics will be known not only in the country but all around the world.

Keywords: Cloth design, Kizilcaboluk fabrics, comfort

INTRODUCTION

It is said that the hand loom in Kizilcaboluk date back about 500 years ago. Besides being used for cloth designs, today, Kizilcaboluk fabrics are especially used for home textile.

Through a study, the 100% plain weave and the Kizilcaboluk weaving fabrics that were weaved at a textile factory at Denizli Organized Industrial Zone, were compared in terms of their wrinkle resistance. The wrinkle resistances of Kızılcabölük fabrics were found out to be lower than other similar fabrics (Can and Akaydin, 2008).

When it is thought that women that indigenize freedom, modernity and naturalness as a lifestyle look for light and unique clothing; it is possible to see the value of the local fabrics. It can easily be said that the Kizilcaboluk fabrics are free, comfortable and useful for clothing. In addition, when they are used as evening dresses, they have an elegant and chic tissue. Even the American film stars try to show their beauty at their film premieres through the evening dresses made from fabric that is similar to Kizilcaboluk weaves. For instance, Catherine Zeta Jones had a chic and authentic style through her one shoulder dress made of a fabric that is made from Kizilcaboluk fabric at her "Death Defying Acts" film premiere (Yilmaz and Bayramoglu, 2008).

The clothes designed in the present study were selected to be suitable for nature theme from the breechcloth made of fabrics.

DESIGN PROCESS OF UNIQUE DRESS COLLECTION FOR SUMMER FROM KIZILCABOLUK "PESHTAMAL'S

The Importance of Local Fabrics for Fashion

When the culture of past meets today's fashion, a perfect match is met for Kızılcabölük fabrics. When the 2015-2017 summer fashion is checked, it is seen that there is a theme with the dominance of naturality, the different shades of yellow, brown, green, red, and pink coming from the sunburn dried flowers, grass, and falling leaves.

Vogue generally express the change. Mostly seeing equal as clothing, fashion is fact which include all areas about the man (Ertürk, 2011).

This collection is done in accordance to fashion trends for 2015-2017 years, but will be suitable for 2018-2020 years because nature theme is mostly actual.

According to Turkish dictionary meaning of "peshtamal" is wide and long woven fabric, which is belt on waist in Turkish bath and work place (Demiray *et al.,* 1981).

The simple "peshtamal" whish was used in dress production for Kizilcaboluk Fest collection was demonstrated in Picture 1.This product is made from %100 bamboo yarn. Mostly Kizilcaboluk "peshtamal's" are produced from natural yarns which consists of more than % 70 cotton fibre and some of them in small amount may contain polyester ore viscose fibre.

Picture 1. Simple "peshtamal" which was used in dress production for Kizilcaboluk Fest collection

Cloth Design

By keeping the size and patterns, looseness, thickness, wrinkling of the cloths in mind, and by foregrounding comfort and aesthetics, designs were done by the students at the Cloth Design class under the title "Nature". Among these, one design from each, which is suitable for production was selected. The technical details of the designs were analyzed by the researcher considering the sewing technique and pattern features, trying to make them suitable for boutique production, and to let the least fabric waste. For each cloth, was been done the ¼ scale laying plans and fabric wastes in accordance with the peshtamal sizes.

The Production of the Collection

Patterns of all models were made according to a size of 38 and the height of 172 cm, and then one prototype for each model has been produced with cheaper but similar fabrics to test the patterns size and the sewing method. They were tested on the models to be used at the fashion show and the size and pattern adjustments were done. With the justified patterns, the laying plans, cutting and sewing processes were done. The bead ornamentations on the models were done especially on the tasselled parts after the sewing was finished. Among the products that were found to be successful concerning their sewing and ornamentation, 30 products were handed in to the Kizilcaboluk Wakf to be presented at the Kizilcaboluk Fest in May 2015. Only a part of the products done according to unique designs (Picture 2, Picture 3, Picture 4, Picture 5) is presented in the present article.

Picture 2. a) Front view of dress model 1; b) Back view dress of model 1

Picture 3. a) Front view of dress model 2; b) Profile view of dress model 2

Picture 4. a) Front view of dress model 3; b) Profile view of dress model 3

Picture 5. a) Front view of dress model 4; b) Profile view of dress model 4

CONCLUSION

In this collection as shown in pictures are used sometimes very basic similar patterns as in dress model 3 but mostly difficult patterns with big labourer cost, like in dress models 1 and 4. The creation of different designer were original one on her behalf and it was difficult to put theme in one collection, that's why some very unique models were not preferred from researcher to be produced. This collection is suitable for boutique production only, because consists of handmade fabrics and special laying plans suitable for peshtamals sizes.

It is believed that if the unique cloth collection produced is marketed well, Kızılcabölük fabrics will be known not only in the country but all around the world and will bring to producers good income.

Acknowledgement

REFERENCES

Can, Y. and Akaydin M. (2008), "Kızılcabölük Dokuma Kumaşların Buruşma Dayanımlarının İncelenmesi", *Kızılcabölük Geleneksel Dokumalar Sempozyumu*, Mayıs.
Demiray, K. *et al*. (1981), *Türkçe Sözlük*, Türk tarih Kurumu Basımevi, Ankara.
Ertürk, N. (2011), "Moda Kavramı, Moda Kuramları ve Güncel Moda Eğilimi Çalışmaları", *Süleyman Demirel Üniversitesi Güzel Sanatlar Fakültesi Hakemli Dergisi*, Mayıs.

Yılmaz, S. and Bayramoğlu, E.E. (2008), "Kızılcabölük Kumaşlarıyla Deriyi, Ahilik Felsefesi Işığında Bayan 2009 İlkbahar-Yaz Modasına Uygun Abiye Giysi Kolleksiyonunda Buluşturma", *Kızılcabölük Geleneksel Dokumalar Sempozyumu*, Mayıs.

UTILIZATION OF SLUDGE FROM LEATHER TANNING RESIDUAL BATHS AS ADDITIVE IN MORTARS

GABRIEL ZĂINESCU[1], VIORICA DESELNICU[1], XIAOYAN PANG[3],
ROXANA CONSTANTINESCU[1], LUMINIȚA ALBU[1], DANA DESELNICU[2]

[1]*National R&D Institute for Textiles and Leather - Division: Leather and Footwear Research Institute, 93 Ion Minulescu str., 031215, Bucharest, Romania e-mail: icpi@icpi.ro*

[2]*University Politehnica Bucharest, email: d_deselnicu@yahoo.com*

[3]*China Leather and Footwear Research Institute Co Ltd., Beijing, China*

In tanneries, one of the environmental issues is the removal of trivalent Chromium from residual leather tanning floats. In this paper we have experimented separation of floats from leather tanning process and the precipitation of trivalent Chromium by flocculation with synthetic polymers. The method presents the following advantages: on one hand the trivalent Chromium can be extracted from sludge and re-use in tanning process; on the other hand, the sludge containing trivalent Chromium and synthetic polymers (polyacrylamide) can be used in the construction industry, as a binder with cement to obtain mortars. The freeze-thaw resistance of the mortar containing "polymer-sludge" addition, compared to the control subjected to 15-25 freeze-thaw cycles was greatly improved.

Keywords: tanning floats, sludge, polymers, mortar

INTRODUCTION

Wastewaters from tanneries are highly polluted with chemicals such as: sodium chloride (preservative), lime, sodium sulphide, protein hydrolysates, vegetable and synthetic tanning agents, mineral tanning agents, dyes, surfactants, grease, solvents (Zainescu *et al*., 2005).

There are a large number of studies concerning the elimination, through precipitation of chromium salts from tannery's wastewaters; due to the incomplete exhaustion of the chromium salts was proposed its utilization after a concentration in Cr_2O_3. After each utilization, wastewaters are enriched in neutral salts so, they couldn't be used for more times in tanning process; for this reason, was proposed chromium recovery from these waters. Usually, after tanning process results exhausted tanning solutions with variable concentration of chromium salts, in the range of 3…9 g Cr_2O_3/l; also, washing waters before the neutralization contain 2…3 g Cr_2O_3/l (Panagiotakis *et al*., 2015).

In scientific papers there were presented some methods used for chrome recovery from exhausted baths, specially using the chrome precipitation as chromium hydroxide that is then transformed in basic salt of chromium sulfate or sodium bichromate (Vollpracht *et al*., 2016). For the chrome precipitation as chromium hydroxide there are using alkaline substances like: sodium hydroxide, sodium carbonate, ammonium hydroxide, calcium hydroxide, magnesium oxide, etc. The use of hydroxide sodium or soda salt may create some problems due to the sodium sulphate (Bulijan and Kral, 2018). It is known that sodium sulphate as well as sodium chlorides couldn't be removed from the wastewaters by the traditional treatment methods and that is why, it is recommended to avoid their introduction into the treatment floats.

Nowadays, the using of synthetic polyelectrolytes presents some advantages as: the reducing quantity of inorganic coagulants, the increasing of treatment efficiency and

rate sedimentation of wastewaters, reducing in the same time the dimensions of equipments and treatment costs, also.

In this work it was proposed a precipitation system using lime (calcium hydroxide), flocculation system with polyelectrolytes and filtration system of chrome hydroxide on a rotary filter, on blankness. Through this method, the basis chrome solution is treated with calcium hydroxide and, after the reaction, results a precipitate composed by chrome hydroxide and lime sulphate (Zainescu *et al*., 2008). The pH value of 8.2… 8.5 allows a complete precipitation of chrome without the risk of formatting the chromite (pH >9.5).

The chemical physical analysis, have shown that in the wastewater samples from the hide tannage process, with an initial content of Cr_2O_3 of 5,2..5,5 g/l, had finally resulted a content of Cr_2O_3 between 10...25mg/l, after the treatment through the precipitation system, using the system calcium hydroxide polyelectrolyte.

There are two possibilities for utilization of "polymer-sludge" obtained by this method:

   a) The precipitate is treated with sulphuric acid of high concentration with the aim to convert the chrome hydroxide into the chrome sulphate (the idea is to be used again at the hides tannage). In order to increase the reaction speed, it could be added the sulphuric acid in excess. It results chromium sulphate which pass into solution, the sulphuric acid which did not participate in the reaction and lime sulphate a precipitate.
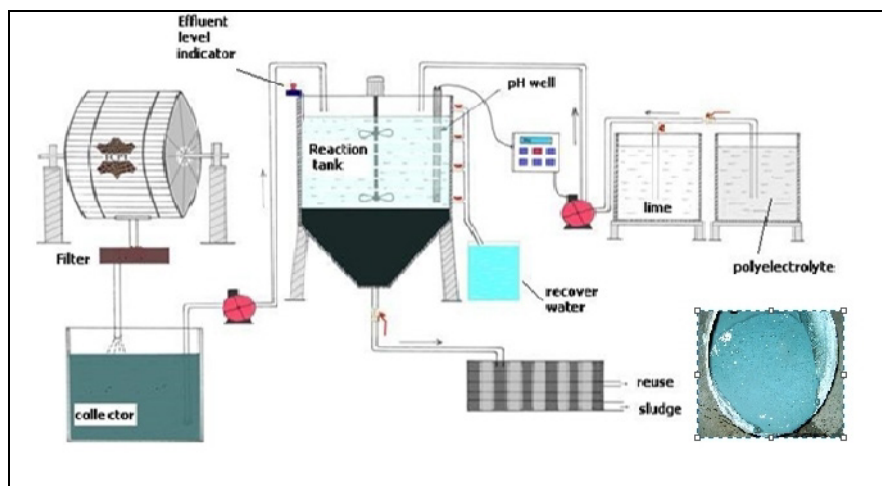
Scheme 1. Installation for obtaining polymer-sludge from tannery wastewater

   b) The "polymer-sludge" containing calcium hydroxide combined with synthetic polymers and Cr^{3+} can be used in obtaining construction materials.

In this paper is proposed a method for valorization of "polymer-sludge" as construction materials, e.g. mortars or concrete, that are suitable for use in various frost-thaw phenomena.

EXPERIMENTAL

Materials and Methods

Obtaining of "Polymer-Sludge"

The experiments using synthetic polymers have been realized within two bovine hides tanneries, with a water consumption of 63 m^3/hide tons, respectively of 37 m^3/hide tons. The wastewaters resulted from the tanning stage, are collected in a tank first, where are homogenized. In that tank, it is introduced lime milk for neutralization at pH 8,3…8,5, where all the heavy metals in the water are quantitatively precipitated as hydroxides. The modified polyelectrolyte to this treated effluent is added, while stirring. By this way, it is produced the flocculation and coagulation phenomenon, decantation taking place in the secondary basin the purified waters go to the sewage.

Obtaining of Mortars Containing Polymer-Sludge

The sludge containing trivalent chromium and synthetic polymers (polyacrylamide) was used in the construction industry. The sludge was tested as binder with cement to obtain mortars.

The composition for mortars or concrete, based on cement as binder, natural aggregates of maximum 3 mm and water, is characterized by the fact that the binder consists of a compound from cement and dry or wet sludge with calcium and chromium content resulting from the treatment of wastewater from leather tanning.

The mortar composition was made in two variants: N_1 (containing 9% dry sludge from the total binder) and N_2 (containing wet sludge in a proportion of 9% of the total binder), which comprises a cement compound and dry or wet sludge with calcium and chromium content as a binder. These compositions were compared to a sludge-free composition (M).

To make mortars, natural aggregates of (0 ÷ 3) mm and two CEM II/B-M (21...35)% composite Portland cements were used. Assays for aggregate and cement characterization were performed according to STAS 4606-1980 "Heavy natural aggregates for concrete and mortar with mineral binders. Test methods", and SR EN 196-1: 1995 "Test methods for cements. Determination of mechanical strengths", respectively.

RESULTS AND DISCUSSION

The study of dry and wet sludge mortar characteristics resulting from treatment of waste water from tanning process has included laboratory tests on mortars prepared with the two types of sludge and characterization of their behavior for up to 30 days.

Compressive Strength of Mortars

The compressive strength of the mortars was determined by tests after 7 and 28 days. The results of mortars resistance are presented in comparison with the resistance values of the control mortars containing only cement. The mortar series N_1, The compressive strengths of the N_1 mortar series are superior to those of control sludge-free mortar M: after 7 days they are +60% higher and after 28 days +66% higher. The increase in compression strength of N1 mortar over time is +46% from 7 to 28 days.

The compressive strength of the N_2 mortar series is higher than that of the control mortar M: after 7 days +31% higher, after 28 days +43% higher.

Frost-Thaw Behavior of Mortars

The compressive strengths of the N_2 mortar series have an increase of +53% from 7 to 28 days. The freeze-thaw resistance is expressed by the loss of compressive strength of sludge mortars subjected to 15 and 25 freeze-thaw cycles compared to the sludge-free mortar specimens having the same compositions but which have been kept in water between 28 days and the age of the compression resistance test of mortar specimens subjected to freeze-thaw. The loss of compressive strength of sludge mortars subjected to 15 and 25 freeze-thaw cycles is presented compared to the loss of compressive strength of sludge-free mortars subjected to the same number of freeze-thaw cycles.

The loss of compressive strength of the N_1 mortar series after 15 freeze-thaw cycles is 2%. After 25 freeze-thaw cycles the loss of compressive strength is 3.56%.

The loss of compressive strength of the M mortar series after 15 freeze-thaw cycles is 3.01%. After 25 freeze-thaw cycles the loss of compressive strength is 10.07%.

The experiments show that the compressive strength of mortars with sludge is much higher than the strength of control samples (7%).

CONCLUSIONS

It has been proposed a process which allows the Cr^{3+} precipitation, by using as additives the polyelectrolytes. This process presents the following economic and environmental advantages:

a) tannery waste waters decontamination from leather tanning process and the obtaining of chromium (III) solution being able to be recycled for leather tanning or for use in other industries, for ex. additives in footwear adhesives. By this method, the final sludge can be used in agriculture as fertilizer, because do not content chromium.

b) the "polymer-sludge" resulting by precipitation with polyelectrolytes has been experienced in mortars' compositions for construction industry; the freeze-thaw resistance of the mortar with "polymer-sludge" addition compared to the control subjected to 15-25 freeze-thaw cycles was greatly improved.

Acknowledgement

REFERENCES

Bulijan, J. and Kral, I. (2018), The framework for sustainable leather manufacture, UNIDO.
Vollpracht, A. and Brameshuber, W. (2016), "Binding and leaching of trace elements in Portland cement pastes", *Cem. Concr. Res.*, 79, 76–92.
Zainescu, G. *et al*. (2005), "Using sludges from tannery wastewaters decontamination", *15th Annual West Coast Conference on Soils, Sediments, and Water*, San Diego, USA.
Zainescu, G. *et al*. (2018), "New concept of bioconversion of tanned leather fibres with applications in the construction industry", *4th International Congress, Water, Waste and Energy Management*, Madrid, Spain, 18-20 July, p. 55, ISBN 978-84-09-032389.
Zainescu, G. *et al*. (2008), "The Recovery and Reutilization of the Sludge from the Tanneries Wastewaters", *ECSM'08 European Conference on Sludge Management*, Liege, Belgium.

SPECIAL SESSION

TOWARDS A CIRCULAR ECONOMY

LIFE CYCLE INVENTORY ANALYSIS FOR CONDUCTIVE TEXTILE BASED ON HYDROPHOBIC AND HYDROPHILIC SURFACES

RALUCA MARIA AILENI, LAURA CHIRIAC, RĂZVAN RĂDULESCU

National Research & Development Institute for Textiles and Leather (INCDTP), Lucretiu Patrascanu 16, Bucharest, 030508, raluca.aileni@certex.ro

In this work, we present some aspects regarding the life cycle inventory for textile surfaces with hydrophobic character required by conductive textiles with different surface resistance. There is already a few researches that deals with the aspects of conductive property influenced by hydrophobic or hydrophilic substrate, such as perfluorodecyltriethoxysilane to increase the durability of electrically conductive fabric obtained by polypyrolle treatment. In this paper, we investigated the life cycle inventory of the processes involved in obtaining the conductive textile using a hydrophobic substrate obtained by classical technology (padding/ coating) or advanced RF plasma technology (plasma hydrophobization/coating).

Keywords: hydrophobic, metallic, conductive textiles, life cycle inventory

INTRODUCTION

The scientific literature shows great concerns in the use of the advanced processes for obtain a hydrophobic effect for conductive textiles.

For the evaluation of the life cycle for conductive textiles obtained by classical finishing method and by RF plasma method, we consider the following steps:

-evaluation of the constraints in the system (CS);

-data collection of the inventory (ICV);

-calculation of the resources used in the manufacturing processes.

LIFE CYCLE INVENTORY ANALYSIS AND DISCUSSIONS

In our research we consider two technological flows, the first one is based on classical technology (padding) and the second one is based on plasma RF hydrophobisation.

The composite technological flows are the following:

- **Technological flow 1:** Boiling ➔ Bleaching ➔ Drying ➔ Padding ➔ Coating ➔ Drying ➔ Crosslinking
- **Technological flow 2:** Boiling ➔ Bleaching ➔ Drying ➔ RF plasma hydrophobization ➔ Coating ➔ Drying ➔ Crosslinking

In the fig.1 is presented the process of obtaining the conductive textile using a textile hydrophobic substrate obtained by classical method and in figure 2 is presented the composite process based on hydrophobic textile obtained by RF plasma.

Data required for the inventory of the life cycle (ICV) was collected by classical method (machine specification, laboratory tests) and using the program SimaPro.

The quantification of the environmental impact for the textile processes, using the method ECO-Indicator 99 (carcinogenic, inorganic and organic substances, climatic changes, radiation, ozone layer, eco-toxicity, acidification /Eutrophication, land-use, fossil fuels).

For comparing the two technological flows and analysis, we generate, by SIMAPRO, the characterization (figure 3), normalization (figure 4), Single Score (figure 5), weighting (figure 6) diagrams and process trees for classical method (figure 7) and for RF plasma hydrophobization (figure 8). From figure 1 and 2 it is evident that in the classical process a

major impact has the energy consumption for drying, approximately 48% in technological flow 1 in comparison with 34% energy consumption for technological flow 2.

In figure 7 is presented the process tree for the technological flow based on classical hydrophobization treatment and in figure 8 is presented the process tree for the technological flow based on advanced technology -RF plasma based on fluorocarbons gases. The process trees (figure 7), of the technological flow 1 and technological flow 2 (figure 8), shows that the classic process (hydrophobization) involves 50.8% energy for drying and the hydrophobization based on RF plasma process involves a reduction with 17.8% of the energy consumption on comparison with classical process and also a reduction of the time allocated for hydrophobization.
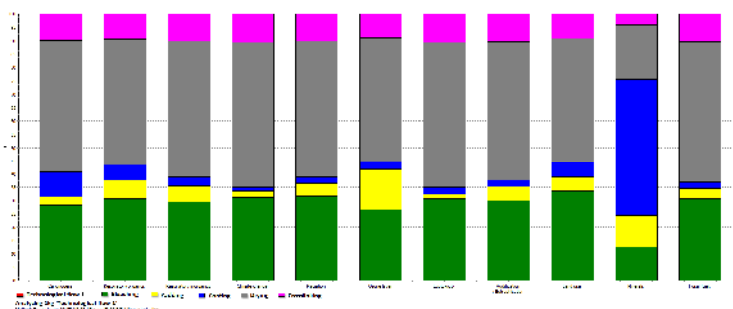

Figure 1. Composite process for conductive textile based on hydrophobic textile
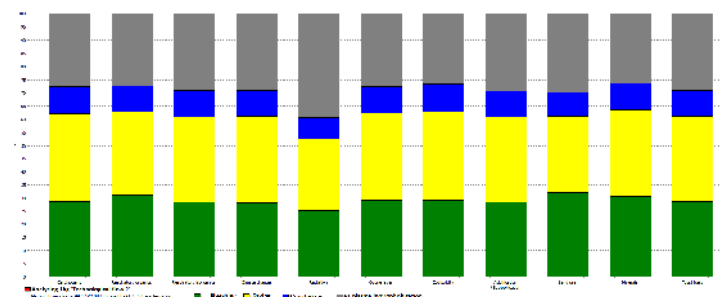obtained by classical method

Figure 2. Composite process for conductive textile based on hydrophobic textile
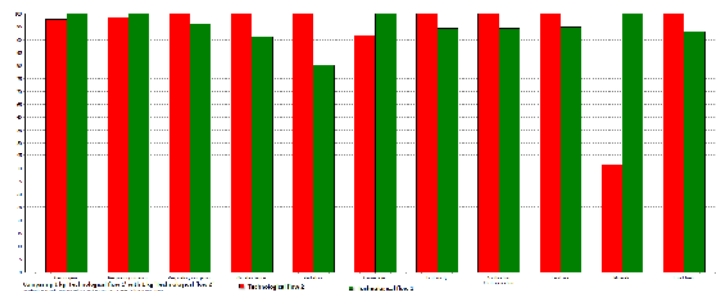obtained by RF plasma

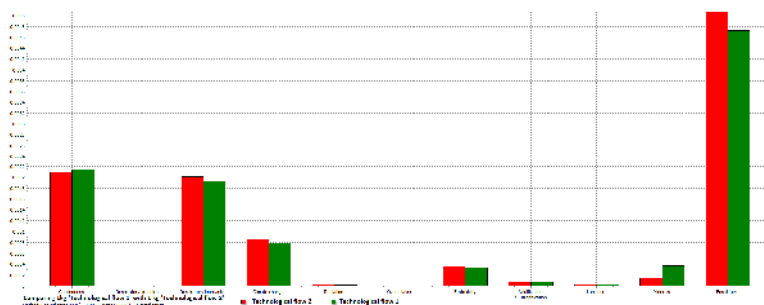Figure 3. Characterization diagram – technological flow 1 vs. technological flow 2

Figure 4. Normalization diagram - technological flow 1 vs. technological flow 2
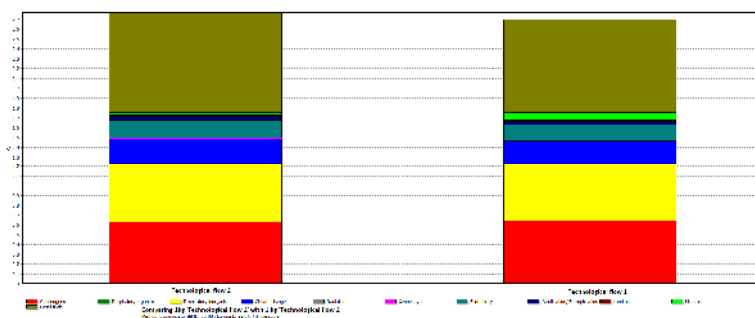

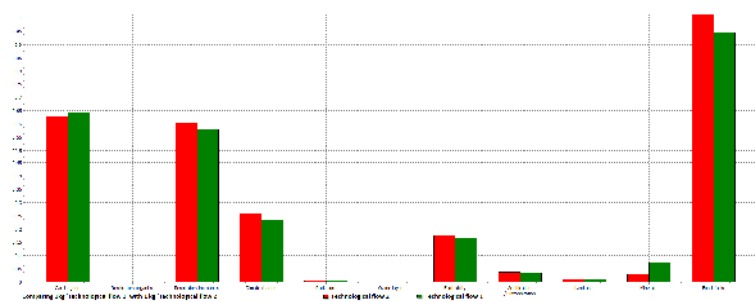Figure 5. Single Score diagram - technological flow 1 vs. technological flow 2

Figure 6. Weighting diagram - technological flow 1 vs. technological flow 2

The impact diagrams (figures 3-6) shows that the advanced technologies (RF plasma) has a strong impact by respiratory inorganics, climate change, radiation, eco-toxicity/acidification, land use and fossil fuel (lignite) consumption.
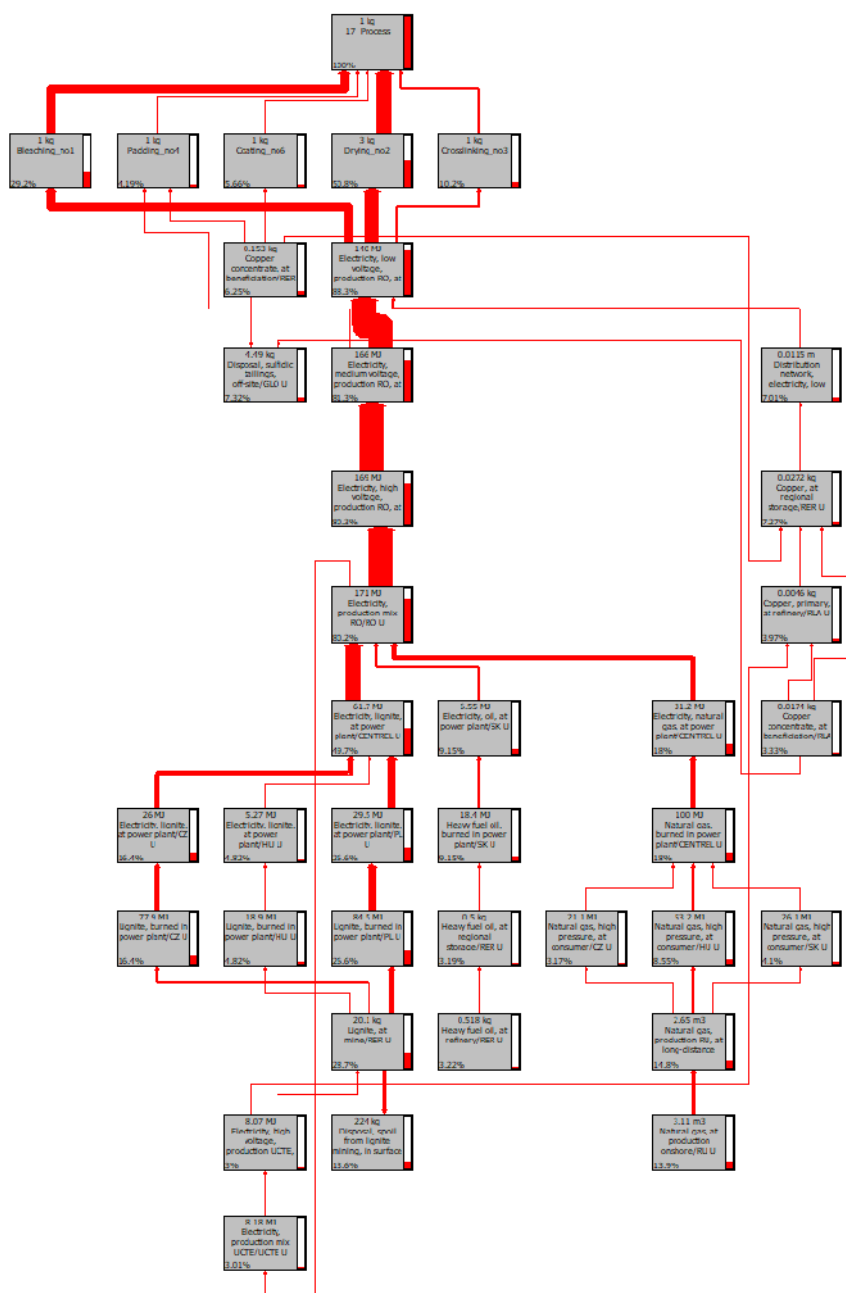
Figure 7. Process tree- technological flow 1 (Metallic coating on hydrophobic textile surface obtained by classical treatment)
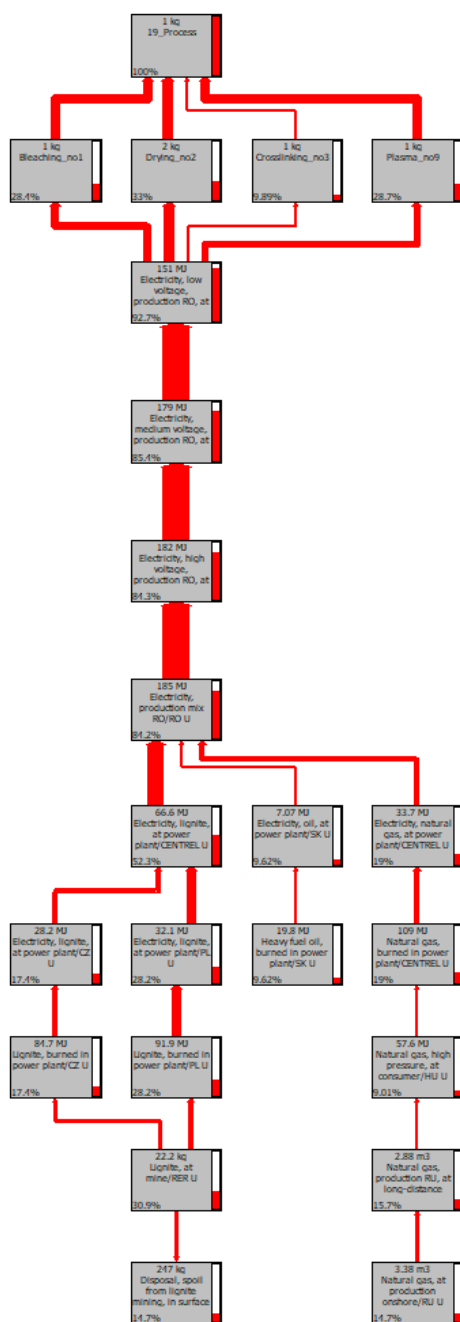
Figure 8. Process tree- technological flow 1 (Metallic coating on hydrophobic textile surface obtained by RF plasma PTFE treatment)

CONCLUSIONS

The environmental impact analysis by SimaPro shows a reduction of inputs in terms of energy consumption and time for advanced technology (RF plasma based on fluorocarbons).

Comparing the first and second technological flow is evident that the RF plasma technology output generates a negative impact through radiation, emissions of inorganics with harmful effect by respiration.

On the other hand, the classical method (technological flow 1) has a major impact on inputs by fossil fuel consumption for production of the electrical energy.

REFERENCES

Das, A. *et al*. (2011), "Design and synthesis of superhydrophobic carbon nanofiber composite coatings for terahertz frequency shielding and attenuation", *Applied Physics Letter*, 98, 174101, https://doi.org/10.1063/1.3583523.

Kowalczyk, D. *et al*. (2015), "Conductive hydrophobic hybrid textiles modified with carbon nanotubes", *Applied Surface Science*, 357, 1007-1014, https://doi.org/10.1016/j.apsusc.2015.09.132.

Lee, S.J., Yun, C. and Park, C.H. (2018), "Electrically conductive and superhydrophobic textiles via pyrrole polymerization and surface hydrophobization after alkaline hydrolysis", *Textile Research Journal*, https://doi.org/10.1177/0040517518773371.

Mittal, K.L. and Bahners, T. (Eds.) (2017), *Textile Finishing: Recent Developments and Future Trends*, John Wiley & Sons, https://doi.org/10.1002/9781119426790.

Nateghi, M.R., Dehghan, S. and Shateri-Khalilabad, M. (2013), "A facile route for fabrication of conductive hydrophobic textile materials using N-octyl/N-perfluorohexyl substituted polypyrrole", *International Journal of Polymeric Materials and Polymeric Biomaterials*, 62(12), 648-652, https://doi.org/10.1080/00914037.2013.769167.

Samanta, K.K., Jassal, M. and Agrawal, A.K. (2010), "Antistatic effect of atmospheric pressure glow discharge cold plasma treatment on textile substrates", *Fibers and Polymers*, 11(3), 431-437 https://doi.org/10.1007/s12221-010-0431-z.

Schutzius, T.M. *et al*. (2011), "High strain sustaining, nitrile rubber based, large-area, superhydrophobic, nanostructured composite coatings", *Composites,* Part A 42, 979–985, https://doi.org/10.1016/j.compositesa.2011.03.026.

Shateri-Khalilabad, M. and Yazdanshenas, M.E. (2013), "Preparation of superhydrophobic electroconductive graphene-coated cotton cellulose", *Cellulose*, 20(2), 963-972, https://doi.org/10.1007/s10570-013-9873-y.

Textor, T. and Mahltig, B. (2010), "A sol–gel based surface treatment for preparation of water repellent antistatic textiles" *Applied Surface Science*, 256(6), 1668-1674, https://doi.org/10.1016/j.apsusc.2009.09.091.

Ul-Islam, S. and Butola, B.S. (2018), *Advanced Textile Engineering Materials,* John Wiley & Sons, USA, https://doi.org/10.1002/9781119488101.

Vosgueritchian, M., Lipomi, D.J. and Bao, Z. (2012), "Highly conductive and transparent PEDOT:PSS films with a fluorosurfactant for stretchable and flexible transparent electrodes", *Adv. Funct. Mater.*, 22, 421–428.

Yang, K. *et al*. (2013), "Waterproof and durable screen printed silver conductive tracks on textiles", *Textile Research Journal*, 83(19), 2023-2031, https://doi.org/10.1177/0040517513490063.

THE INVENTORY OF THE LIFE CYCLE FOR TEXTILE PROCESSES INVOLVED IN OBTAINING ANTISTATIC SURFACE

RALUCA MARIA AILENI, RĂZVAN RĂDULESCU, LAURA CHIRIAC, LILIOARA SURDU

National Research & Development Institute for Textiles and Leather (INCDTP), Lucretiu Patrascanu 16, Bucharest, 030508, raluca.aileni@certex.ro

This paper presents several aspects regarding life cycle inventory for processes involved in obtaining antistatic effect for textile surfaces made by synthetic fibers. The objective of use antistatic is to reduce or eliminate static electricity that is generated by triboelectric effect. The static electricity can be reduced if is used an antistatic agent for treatment in order to obtain a slightly conductive surface, a conductive surface or a hydrophilic surface in order to absorb moisture from air. For a long-term protection are used conductive agents such as carbon black, conductive fibers and conducting polymer nanofibers. The synthetic fibers in general have a very small electrical conductivity and electrostatic charges. In our paper, we present the comparative analyses (process trees and diagrams) of the inventory of the life cycle for finishing processes (classical and advanced) required in obtaining the textiles with antistatic effect. Synthetic fibers in general have a very small electrical conductivity and electrostatic charges. This fact is because they have a low hygroscopic/ hydrophilic character and the absence of water absorbed allows the build-up of static electricity. In our work, we present the process tree and several comparisons between classical process used for textile clean and plasma processes.

Keywords: antistatic, textile, life cycle inventory, conductive

INTRODUCTION

The inventory of the life cycle involves data collection about water, energy and chemical substances necessary to obtain textiles for antistatic effect. For the evaluation of the life cycle for textiles, products finished using traditional and advanced processes and technologies we consider the following inputs and outputs (figure 1):
-inputs: energy, water, chemical substances (acquisition➔production➔usage)
-outputs: waste, wastewater, emissions (recycling/reuse)
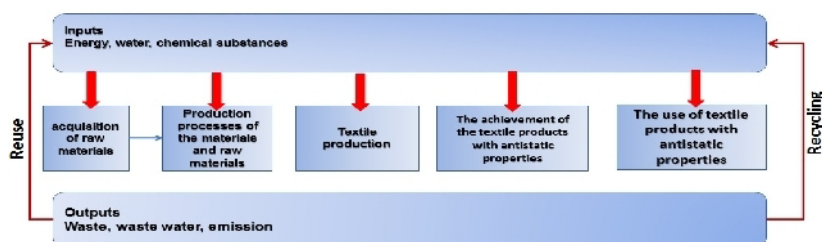

Figure 1. The inventory of the life cycle - the principle diagram

DATA PROCESSING BY INFORMATION TECHNOLOGY

For comparison, we consider two technological flows, the first one contains the advanced technology RF plasma and the second one was based on classical technologies. The technological flows are described in the following lines:
- **Technological flow 1**: Boiling ➔ Bleaching ➔ Drying ➔ Thin film deposition (Tubicoat 41 + Tubivis DL 650 + Cu) ➔ Drying ➔ Crosslinking
- **Technological flow 2**: RF O2 plasma treatment ➔ Thin film deposition (Tubicoat 41 + Tubivis DL 650 + Cu)➔ Drying ➔ Crosslinking

For textile processes involved in obtaining textile surfaces with antistatic properties has been carried out the inventory of the life cycle (ICV) using the program SimaPro. The quantification of the environmental impact for the textile processes has been carried out using the method ECO-Indicator 99 (Curran, 2012; Sanfwon and Huppes, 2005; http://www.ecoinvent.org). Method ECO-Indicator 99 provides for the analysis of the impact several categories of distinct impact (http://esu-services.ch/ourservices/lci/), such as carcinogenic, inorganic and organic substances, climatic changes caused by the substances with the greenhouse effect, radiation protection, the changes that take place at the level of the ozone layer, ecotoxicity, acidification /Eutrophication, land-use, minerals and consume fossil fuels for power generation (http://esu-services.ch/ourservices/lci/; International Energy Agency, 2015).

Using SimaPro software, we used the following types of diagrams:

- Normalization diagram that allows the elimination of marginal impact that contribute to the pollution of the environment in the region concerned (Klopffer and Grahl, 2014; Werner, 2005; Steward and Weidema, 2004).

- Weighting diagram allows the results adjustment by multiplication (Steward and Weidema, 2004).

- Single Score diagram that require knowledge concerning the correlation between the emissions into the environment according in the environment and potential impact of such emissions and extractions (Suh, 2003; Nakamura and Kondo, 2009).

By comparing technological flow 1 and technological flow 2 (figures 2-5), it should be noted that the flow of technology 2 (classical processes) has the greatest impact on the environment (100% for all categories of impact), followed by the technological flow 2 that is influencing 75% by harmful substances through breathing and with 100% by ionized radiation resulting.

The energy consumption necessary to obtain textile surfaces with antistatic properties is presented by process tree method (Jolliet *et al*., 2016).

In figure 6 is presented the process tree for the technological flow based on RF oxygen and in figure 7 is presented the process tree for the technological flow based on classical technologies. The process tree (figure 6), for the technological flow 2 –RF oxygen plasma, highlights the possibility of replacing the classic processes (cleaning, whitening) by RF plasma oxygen process and the reduction of the energy consumption with 4% and the duration of the process with 96%.
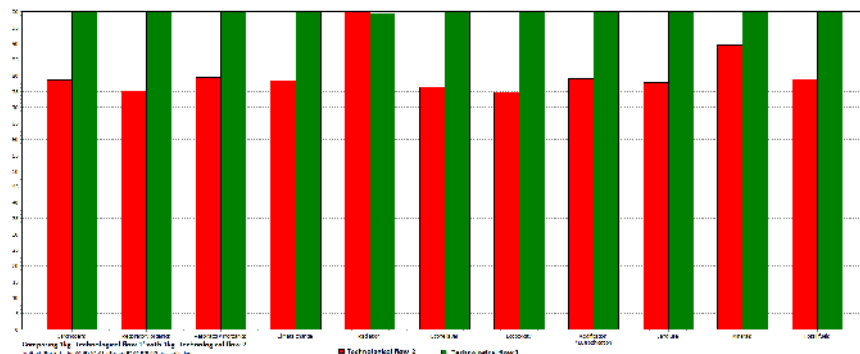

Figure 2. Characterization method - comparing technological flow 1 with technological flow 2

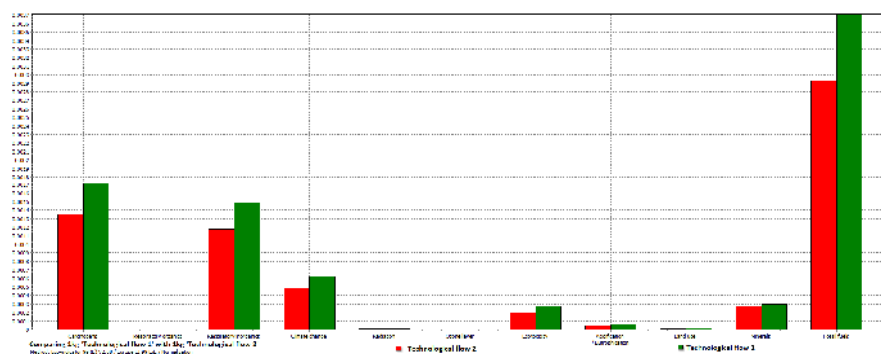Figure 3. Normalization method - comparing technological flow 1 with technological flow 2
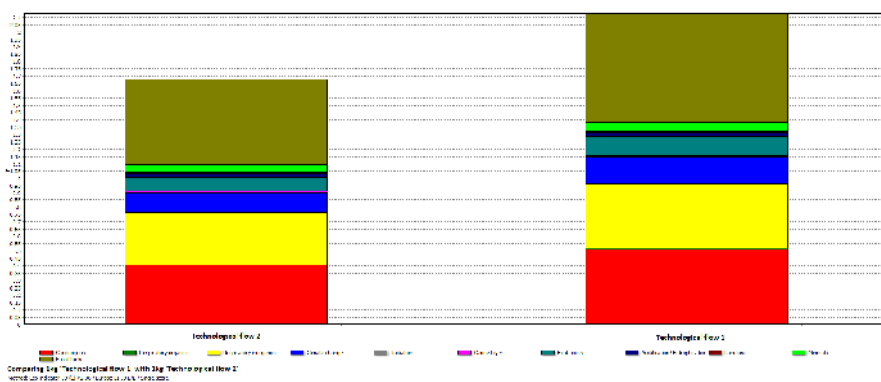

Figure 4. Single score method - comparing technological flow 1 with technological flow 2
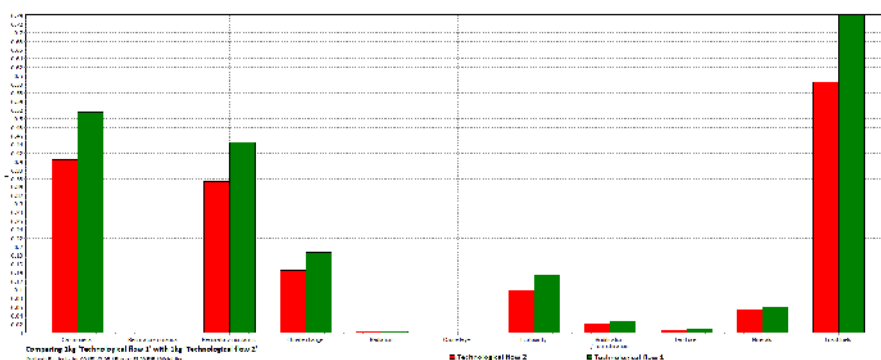

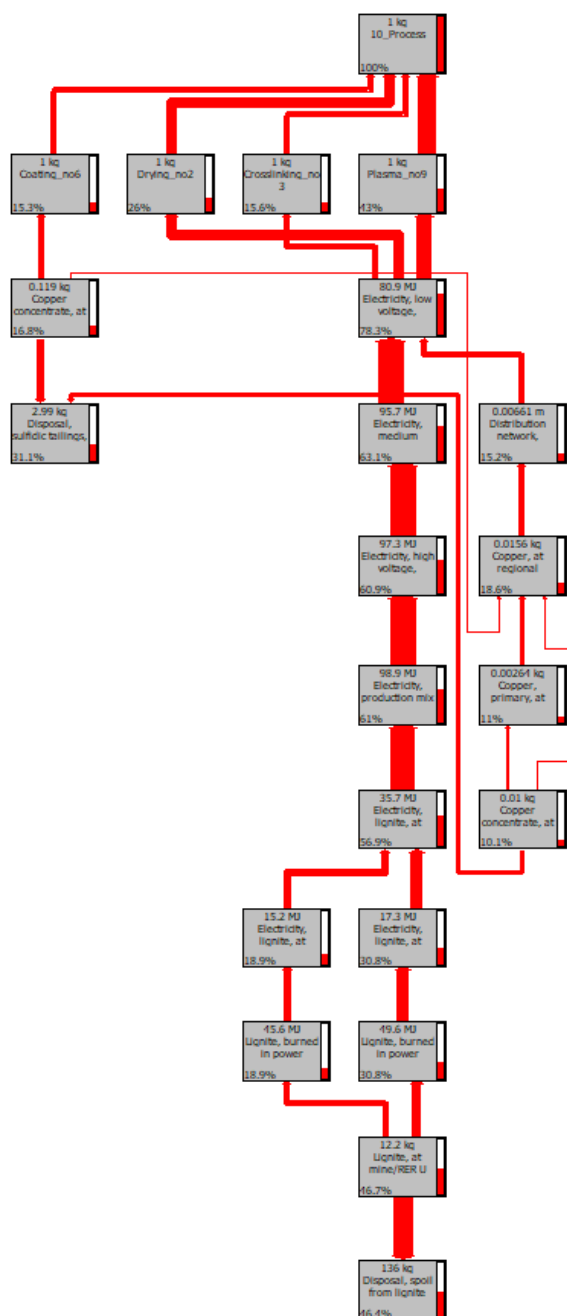Figure 5. Weighting method - comparing technological flow 1 with technological flow 2

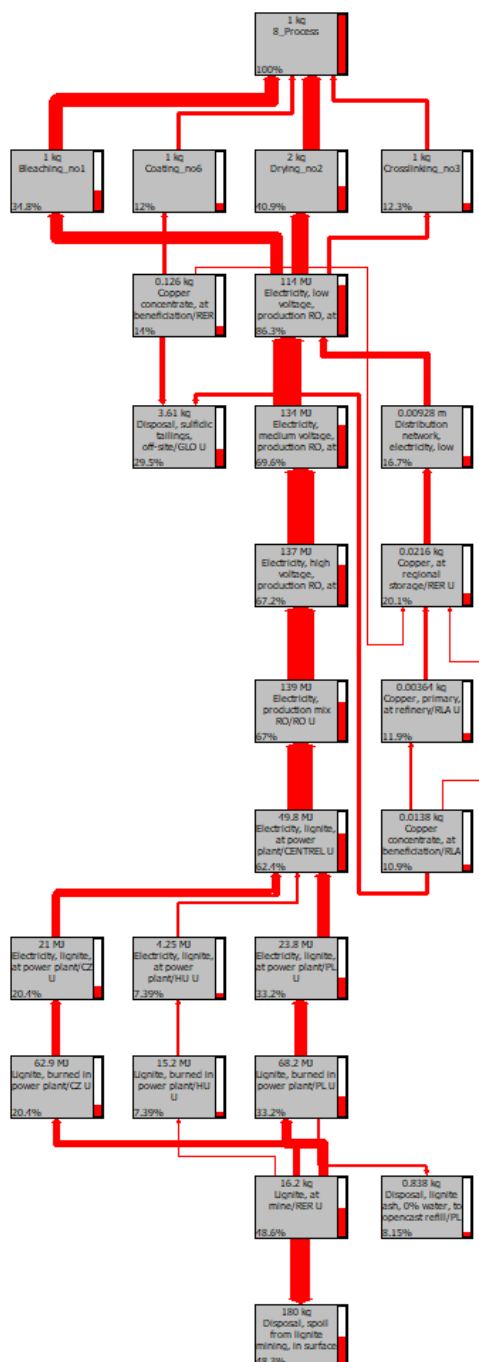Figure 6. Process Tree - Technological flow based on RF oxygen plasma

Figure 7. Process tree - Technological flow for classical technologies

CONCLUSIONS

The investigation of the environmental impact by process trees and the diagrams (normalization, Single Score, Characterization, Weighting) on different categories of impact

(Eco-Indicator Method 99) is an important step in choosing the best technology flow (reduced time, tending to zero emissions and product quality), before final decision and industrial manufacturing.

In all diagrams, we can observe a significant impact of the classic technologies on fossil fuels consumption and on releasing the carcinogen and inorganics that are harmful if they enter into the respiratory system.

REFERENCES

Curran, M.A. (2012), *Life Cycle Assessment Handbook,* Wiley Publishing, USA.
International Energy Agency (2015), Life Cycle Inventories and Life Cycle Assessments of Photovoltaic Systems, Report IEA-PVPS T12-04:2015.
Jolliet, O. *et al*. (2016), *Environmental life cycle assessment*, CRC Press.
Klopffer, W. and Grahl, B. (2014), *Life Cycle Assessment (LCA),* Wiley.
Nakamura, S. and Kondo, Y. (2009), *Waste Input-Output Analysis*, Springer.
Sanfwon, S. and Huppes, G. (2005), "Methods for Life Cycle Inventory of a product", *Journal of Cleaner Production*, 13(7), 687–697, https://doi.org/10.1016/j.jclepro.2003.04.001.
Steward, M. and Weidema, B. (2004), "A consistent framework for assessing the impacts from resource use. A focus on resource functionality", *Int. J. Life Cycle Assess*, 10(4), 240–247, https://doi.org/10.1065/lca2004.10.184.
Suh, S. (2003), "Input-output and hybrid life cycle assessment", *Int. J. Life Cycle Assess*, 8(5), 257.
Werner, F. (2005), *Ambiguities in decision-oriented life cycle inventories*, Springer.
***, http://esu-services.ch/ourservices/lci/
***, http://www.ecoinvent.org/

SUSTAINABLE DEVELOPMENT IN THE FRAME OF THE 7th ENVIRONMENT ACTION PROGRAMME

DANA CORINA DESELNICU[1], GHEORGHE MILITARU[1], VIORICA DESELNICU[2], GABRIEL ZĂINESCU[2], LUMINIȚA ALBU[2]

[1]*University POLITEHNICA of Bucharest, 313 Splaiul Independentei, sector 6, Bucharest, Romania, dana.deselnicu@upb.ro*

[2]*INCDTP - Division: Leather and Footwear Research Institute Bucharest, 93 Ion Minulescu st., sector 3, RO- 031215 Bucharest, viorica.deselnicu@icpi.ro*

This paper presents the 7th EAP — the new general Union Environment Action Programme to 2020. Through this Programme, the EU has agreed to step up its efforts to protect our natural capital, stimulate resource-efficient, low-carbon growth and innovation, and safeguard people's health and wellbeing – while respecting the Earth's natural limits. It's a common strategy that should guide future action by the EU institutions and the Member States, who share responsibility for its implementation and the achievement of its priority objectives. It identifies three key objectives: a) to protect, conserve and enhance the Union's natural capital; b) to turn the Union into a resource-efficient, green, and competitive low-carbon economy; c) to safeguard the Union's citizens from environment-related pressures and risks to health and wellbeing.

Keywords: sustainability, resource-efficient, natural capital, low-carbon economy, wellbeing

INTRODUCTION

The term "sustainable development" first appeared in a document signed by 33 African countries in 1969, under the auspices of the International Union for Conservation of Nature (IUCN). In the same year, the Environmental Protection Agency was set up in the US; its guidelines have had a huge impact on developing theories and practice in global environmental policies.These two aspects are what characterized "the Brundtland Report", which was produced by a commission led by Dr. Gro Harlem Brundtland and published in 1987.

The Report defines sustainable development as meeting: *"the needs of the present without compromising the ability of future generations to meet their own needs"* (World Commission on Environment and Development, United Nations, 1987).

In the book "The limits to growth", D.H. Meadows *et al.* (1987) present the need for sustainable development (Figure 1):
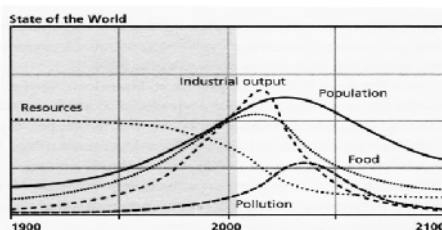

Figure 1. The need for sustainable development (Meadows *et al.*, 1987)

Sustainable development should be viewed from three different angles: economic activity, ecological factors and social responsibility (Schmel, 2015) (Figure 2):

• **Economic**: An economically sustainable system must be able to produce goods and to avoid extreme sectoral imbalances which damage agricultural or industrial production.

• **Environmental**: An environmentally sustainable system must maintain a stable resource base, avoiding over-exploitation of renewable resource systems or environmental sink functions, and depleting non-renewable resources only to the extent that investment is made in adequate substitutes. This includes maintenance of biodiversity, atmospheric stability, and other ecosystem functions not ordinarily classed as economic resources.

• **Social:** A socially sustainable system must achieve distributional equity, adequate provision of social services including health and education, gender equity, and political accountability and participation.
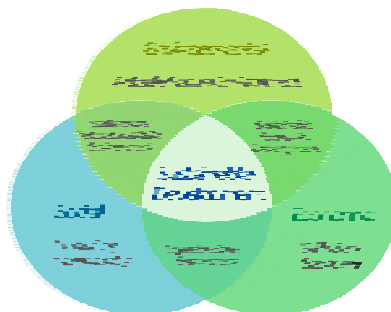
Figure 2. Correlation among key components of sustainable development (Schmel, 2015)

There are many models for the sustainable development system.

The "Daly Rules" approach (Womersley, 2002) is a closed thermodynamic system in which economic systems sit inside of social systems, both of which are inside of our one environment; this means that sustainable development must involve the health of all three systems. (Figure 3 and 4):
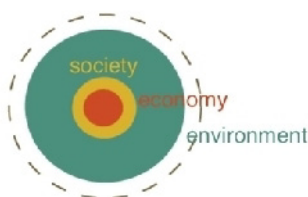
Figure 3. Closed thermodynamic system
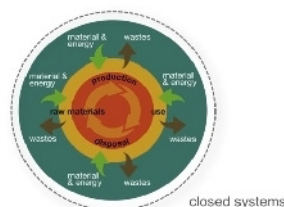
Figure 4. "Daly Rules" for sustainability of natural resources

The Herman E. Daly (possibly founded on ecological/thermodynamic principles) suggests the following criteria of sustainability:

- **Renewable resources** (e.g. fish, soil, groundwater) must be used no faster than the rate at which they regenerate.
- **Non-renewable resources** (e.g. minerals, fossil fuels) must be used no faster than renewable substitutes for them can be put into place.

- **Pollution and wastes** must be emitted no faster than natural systems can absorb them, recycle them, or render them harmless.
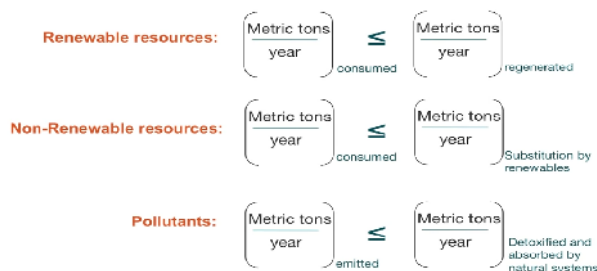
Figure 5. Criteria of sustainability suggested by Herman E. Daly (Womersley, 2002)

Some other authors suggest that sustainability indicators should be holistic in nature, measuring sufficiency of well-being for all, sustainability of natural resources and efficiency (https://www.youtube.com/watch?v=RCN6it0LZvY; https://www.youtube.com/watch?v=-jnH9o8Ajd0; https://www.youtube.com/watch?v=Q3tJL4JRgnA).

THE 7TH EAP — THE NEW GENERAL UNION ENVIRONMENT ACTION PROGRAMME TO 2020

Since the mid-1970s, EU environment policy has been guided by action programmes defining priority objectives to be achieved over a period of years. The 7th EAP was adopted by the European Parliament and the Council of the European Union in November 2013 and covers the period up to 2020.

The new programme includes an "enabling framework" with the next four priority objectives to help Europe deliver on these goals: better implementation of legislation, better information by improving the knowledge base, more and wiser investment for the environment, and full integration of environmental requirements and considerations into other policies.

"In 2050, we live well, within the planet's ecological limits. Our prosperity and healthy environment stem from an innovative, circular economy where nothing is wasted and where natural resources are managed sustainably, and biodiversity is protected, valued and restored in ways that enhance our society's resilience. Our low-carbon growth has long been decoupled from resource use, setting the pace for a safe and sustainable global society".

Figure 6. The long-term vision of the 7th EAP (http://ec.europa.eu/environment/action-programme/)

Priority objectives and what the EU needs to do to achieve them by 2020 (http://ec.europa.eu/environment/action-programme/):

- to protect, conserve and enhance the Union's natural capital;
- to turn the Union into a resource-efficient, green, and competitive low-carbon economy;
- to safeguard the Union's citizens from environment-related pressures and risks to health and wellbeing;
- to maximise the benefits of the Union's environment legislation by improving implementation;
- to increase knowledge about the environment and widen the evidence base for policy;
- to secure investment for environment and climate policy and account for the environmental costs of any societal activities;
- to better integrate environmental concerns into other policy areas and ensure coherence when creating new policy;
- to make the Union's cities more sustainable;
- to help the Union address international environmental and climate challenges more effectively.

Thematic Priorities

The programme identifies three priority areas where more action is needed to protect nature and strengthen ecological resilience, boost resource-efficient, low-carbon growth, and reduce threats to human health and wellbeing linked to pollution, chemical substances, and the impacts of climate change (http://ec.europa.eu/environment/pubs/pdf/factsheets/7eap/en.pdf).

1. The first action area is linked to **"natural capital"** –from fertile soil and productive land and seas to fresh water and clean air – as well as the biodiversity that supports it. Natural capital includes vital services such as pollination of plants, natural protection against flooding, and the regulation of our climate. The Union has made commitments to halt biodiversity loss and achieve good status for Europe's waters and marine environment. Moreover, it has put in place the means to achieve this, with legally-binding commitments including the Water Framework Directive, the Air Quality Directive, and the Habitats and Birds Directives, together with financial and technical support.

2. The second action area concerns the conditions that will help transform the EU into a **resource-efficient, low-carbon economy**. This requires: a) full delivery of the climate and energy package to achieve the 20-20-20 targets and agreement on the next steps for climate policy beyond 2020; b) significant improvements to the environmental performance of products over their life cycle; c) reductions in the environmental impact of consumption, including issues such as cutting food waste and using biomass in a sustainable way. There is a special focus on turning waste into a resource, with more prevention, re-use and recycling, and phasing out wasteful and damaging practices like landfilling. Water stress is increasingly affecting more parts of Europe – not least because of climate change – and the need for further action towards more efficient use of water is highlighted.

In the context of rising natural resource prices, scarcity and dependency on imports, Europe's competitiveness and capacity for sustainable growth will depend on improving resource efficiency across the economy. The EAP calls for indicators and targets for resource efficiency to be established, to guide public and private decision-makers.

The benefits of a resource-efficient economy are being felt in many sectors. Environmental technologies and services are a major success story, with employment growing at 3 % per annum. The global market for eco-industries, currently valued at a trillion euros, is forecast to double over the next 10 years.

3. The third key action area covers challenges to **human health and wellbeing**, such as air and water pollution, excessive noise, and toxic chemicals. According to the World Health Organisation, environmental factors could be responsible for up to 20 % of all deaths in Europe. Europe already has high standards for air quality, but in many cities, pollution remains above acceptable levels. The EAP sets out commitments to improve implementation of existing legislation, and to secure further reductions in air and noise pollution. The EAP also sets out a long-term vision of a non-toxic environment and proposes to address risks associated with the use of chemicals in products and chemical mixtures, especially those that interfere with the endocrine system. In parallel, a more predictable framework combined with more investment in knowledge is intended to encourage innovation and the development of more sustainable solutions.

4. Better implementation of existing legislation will bring numerous benefits. A study prepared for the Commission in 2012 estimated that full implementation of EU waste legislation would save €72 billion a year, increase the annual turnover of the EU waste management and recycling sector by €42 billion and create over 400,000 new jobs by 2020. If properly implemented, EU environment legislation creates a level playing-field and opportunities in the single market for sustainable investments, in addition to environmental benefits.

5. Scientific research, monitoring and reporting environmental developments mean that our understanding of the environment is constantly increasing. This knowledge base should be made more accessible to citizens and policymakers to ensure policy continues to draw on a sound understanding of the state of the environment. The EAP aims to address these challenges by improving the way data and other information is collected, managed and used across the EU, investing in research to fill knowledge gaps, and developing a more systematic approach to new and emerging risks.

6. Adequate investments and innovation in products, services and public policies will be needed from public and private sources, in order to achieve the objectives set out in the programme. This can only happen if impacts on the environment are properly accounted for and if market signals also reflect the true costs to the environment. This involves applying the polluter-pays principle more systematically, phasing out environmentally harmful subsidies, shifting taxation from labour towards pollution, and expanding markets for environmental goods and services. As a concrete example, the EAP calls for a minimum 20 % share of the EU budget 2014-2020 to be devoted to climate change mitigation and adaptation. Companies increasingly see advantages in expanding eco-innovation and taking up new technologies, in measuring the environmental impact of their businesses and disclosing to their investors and customers environmental information in their annual reporting. The EAP sets out some ways in which this can be further developed.

7. The fourth enabling condition in the programme is **better integration of environmental concerns into other policy areas**, such as regional policy, agriculture, fisheries, energy and transport. Systematically assessing the environmental, social and economic impacts of policy initiatives and full implementation of Environmental Impact Assessment legislation will ensure better decision-making and coherent policy approaches that deliver multiple benefits.

8. The first is to help **cities become more sustainable**. Europe is densely populated and 80 % of its citizens are likely to live in or near a city by 2020. Cities often share a common set of problems such as poor air quality, high levels of noise, greenhouse gas emissions, water scarcity, and waste. The aim is to ensure that by 2020, most cities in the EU are implementing policies for sustainable urban planning and design, and are using the EU funding available for this purpose.

9. The final priority concerns wider **global challenges**. Many of the priority objectives in the EAP can only be achieved in cooperation with partner countries or as part of a global approach. The EU and its Member States are committed to engage more effectively in working with international partners towards the adoption of Sustainable Development Goals as a follow-up to the Rio+20 conference. The EAP also proposes to explore further steps that could be taken to reduce impacts on the environment beyond EU borders. **«Living well, within the limits of our planet»** is a global aim.

CONCLUSION

Through the Environment Action Programme (EAP), the EU has agreed to step up its efforts to protect our natural capital, stimulate resource-efficient, low-carbon growth and innovation, and safeguard people's health and wellbeing – while respecting the Earth's natural limits.

The new programme includes an "enabling framework" with the next four priority objectives to help Europe deliver on these goals: better implementation of legislation, better information by improving the knowledge base, more and wiser investment for the environment, and full integration of environmental requirements and considerations into other policies.

It's a common strategy that should guide future action by the EU institutions and the Member States, who share responsibility for its implementation and the achievement of its priority objectives.

Acknowledgements

REFERENCES

Meadows, D.H. *et al*. (1972), The limit to growth, Universe Books, New York.
Schmel, F. (2015), *Sustainable Development Goals*, UNIDO, SDG.
Womersley, M. (2002), "A Peculiarly American Green: Religion and Environmental Policy in the United States", Dissertation, University of Maryland School of Public Policy, 19-21.
World Commission on Environment and Development, United Nations (1987), *Our Common Future*.
***, 7th EU action plan, http://ec.europa.eu/environment/pubs/pdf/factsheets/7eap/en.pdf
***, http://ec.europa.eu/environment/action-programme/
***, http://ec.europa.eu/environment/resource_efficiency/about/index_en.htm
***, https://www.youtube.com/watch?v=-jnH9o8Ajd0
***, https://www.youtube.com/watch?v=Q3tJL4JRgnA
***, https://www.youtube.com/watch?v=RCN6it0LZvY

TOWARDS A CIRCULAR ECONOMY– A ZERO WASTE PROGRAMME FOR EUROPE

DANA CORINA DESELNICU[1], GHEORGHE MILITARU[1], VIORICA DESELNICU[2], GABRIEL ZĂINESCU[2], LUMINIȚA ALBU[2]

[1]University POLITEHNICA of Bucharest, 313 Splaiul Independentei, sector 6, Bucharest, Romania, dana.deselnicu@upb.ro

[2]INCDTP - Division: Leather and Footwear Research Institute Bucharest, 93 Ion Minulescu str., sector 3, RO- 031215 Bucharest, viorica.deselnicu@icpi.ro

This paper presents key elements of the revised waste proposals. From the new waste proposals will benefits the economy, citizens and the environment. Clear rules, common standards and support for the use of more secondary raw materials will create a safe and sustainable supply of raw materials to the industry. This helps create new jobs, supports innovation and boosts competitiveness. Improved waste management rules will reduce landfill and tipping fees. Smarter use of resources is not only good for business, but will also help protect the environment preserve essential resources for current and future generations, and create synergies for industries which most depend on it – such as tourism, agriculture and food manufacturing.

Keywords: circular economy, waste management, secondary raw materials, recycling materials

INTRODUCTION

Circular economy systems (http://ec.europa.eu/environment/circular-economy/index_en.htm) keep the added value in products for as long as possible and eliminate waste. They keep resources within the economy when a product has reached the end of its life, so that they can be productively used again and again and hence create further value. Transition to a more circular economy requires changes throughout value chains, from product design to new business and market models, from new ways of turning waste into a resource to new models of consumer behaviour.

Waste management plays a central role in the circular economy: it determines how the EU waste hierarchy is put into practice. The waste hierarchy establishes a priority order from prevention, preparation for reuse, recycling and energy recovery through to disposal, such as landfilling. This principle aims to encourage the options that deliver the best overall environmental outcome.
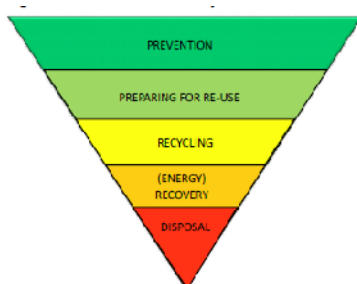
Source: European Commission.

Figure 1. The waste hierarchy

The Circular Economy package includes **specific proposals to amend the EU's waste legislation**, seeking to improve waste management practices, stimulate recycling and innovation in materials management, and limit the use of landfilling. The proposals will provide a clear and stable policy to allow long-term investment strategies focusing on prevention, reuse and recycling.

The aim of the paper is to present key elements of the revised waste proposal.

KEY ELEMENTS OF THE REVISED WASTE PROPOSAL (EUROPEAN COMMISSION, 2015a, b)

In order to boost the economic, social and environmental benefits gained from the better management of municipal waste, the Commission proposes **to ban the landfilling** of recyclable plastics, metals, glass, paper and cardboard, leather and biodegradable waste by 2025, while Member States should endeavour to virtually eliminate landfill by 2030. Industry already recognises the strong business case for improving resource productivity. It is estimated that resource efficiency improvements all along the value chains could reduce material inputs needs by 17%-24% by 2030 (Meyer *et al*., 2011) and a better use of resources could represent an overall savings potential of €630 billion per year for European industry (Europe INNOVA, 2012). Business driven studies based on product-level modelling demonstrate significant material cost saving opportunities for EU industry from circular economy approaches and a potential to boost EU GDP by up to 3.9% (Ellen MacArthur Foundation, 2012) by creating new markets and new products and creating value for business. It is not surprising therefore that companies are continually working to improve resource management, but they are held back by a range of market barriers.

The European Integrated Pollution Prevention and Control (IPPC) Bureau produces reference documents on Best Available Techniques, the so-called BREFs, which are used by competent authorities in EU Member States when issuing operating permits. BREFs incorporate best practices with regard to the resource use, residues and by-product' reuse and recycling as well as waste generation and management, therefore contributing to the EU initiatives on Circular Economy.

Targets (European Commission, 2015a)

Turning waste into a resource is an essential part of increasing resource efficiency and closing the loop in a circular economy. Europe currently loses around 600 million tonnes of waste materials, which could potentially be recycled or reused. Only around 40% of the waste produced by EU households is recycled, with recycling rates as high as 80% in some areas, and lower than 5% in others. The proposal reflects a high level of ambition while taking account of the different realities and performance levels across the EU:

- a common EU target for recycling municipal waste of 65% by 2030;
- a common EU target for recycling packaging waste of 75% by 2030.
- material-specific targets for different packaging materials;
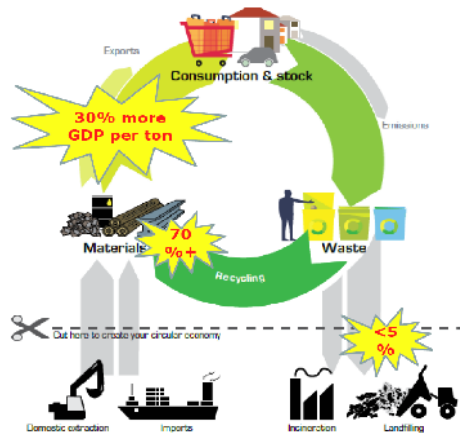- a binding landfill reduction target of 10% by 2030.

Figure 2. Targets for reduction of waste by 2030
(http://ec.europa.eu/environment/circular-economy/index_en.htm)

Measurements

- simplification and harmonisation of definitions and calculation methods to ensure comparable, high quality statistics across the EU;
- special rules for Member States facing the biggest implementation challenges;
- simplification of reporting obligations and alleviating obligations faced by SMEs;
- introduction of an Early Warning System for monitoring compliance with targets;
- steering Member States towards greater use of economic instruments (such as a landfill tax) to incentivise the application of waste hierarchy, to prioritise prevention, reuse and recycling, with disposal as the last resort.

Incentives

- concrete measures to boost reuse activities, including a clearer definition and rules that expand the scope of reuse activities rewarded under the EU targets;
- general requirements for the operation of Extended Producer Responsibility (EPR) schemes – meaning a producer's responsibility for a product is extended to the post-consumer stage of a product's life cycle, aimed at improving their performance and transparency, including direct financial incentives for greener product design;
- clearer rules on by-products and end-of-waste criteria to stimulate the sharing of by-product resources among industries and markets for recycled materials;
- new measures to promote prevention, including for food waste and marine litter, and reuse;
- provisions to improve the traceability of hazardous waste.

The Benefits to the Economy, Citizens and the Environment of the New Waste Proposals

These proposals will secure Europe's **access to high quality and affordable raw materials**, making the economy more competitive in the context of volatile resource

prices, political instability, resource scarcity, and increasing global competition concerning the access to raw materials.

Sustainable growth will boost job creation, with more than 170,000 direct jobs potentially being created in Europe by 2030. A reduction in the total materials requirement of around 20 % can lead to an estimated 3 % boost in GDP. Measures such as better ecodesign, waste prevention and reuse could bring net savings to businesses in the EU of up to €600 billion or 8% of their annual turnover.

The proposals will contribute to **reducing greenhouse gas emissions**. More than 500 million tons of greenhouse gas could be avoided between 2015 and 2035, directly by cutting emissions from landfills and indirectly by recycling materials which would otherwise be extracted and processed. The proposals will reduce landfills, and their associated pollution.

The proposals will **reduce the administrative burden**, in particular **for SMEs**, as well as for public administrations, by improving definitions and simplifying reporting requirements.

FROM WASTE TO RESOURCES

Recycling is a precondition for a circular economy – resources and materials can be recycled, returned back to the economy and used again. What was once considered as waste can become a valuable resource. To realise the potential of these so called secondary raw materials, we have to remove the existing barriers to their trade, improve the waste management practices and guarantee high quality standards. Only then can industry make full use of secondary raw materials and help ensure their secure supply.

Recovering and Recycling Materials

In a circular economy, materials from products at the end of their lifecycle should be recovered through dismantling and recycling. Re-injecting these materials into the beginning of the product lifecycle reduces environmental impact and costs of production. We are proposing a number of tools to encourage and help this process.

Trading in Secondary Raw Materials

The market and the EU single market for recovered and waste materials are still underdeveloped. While 45% of waste material from large companies is resold, this figure falls to only 25% for SMEs. We want to create common standards and market tools to improve this.

As an example, alongside the prevention and recycling of waste, an important pillar of **FCC Environment CEE** waste management approach is treating waste as a valuable resource. Using modern technologies, they are able to recover renewable energy from non-hazardous waste collected through our business and municipal waste operations. (Founded in Austria in 1988 **FCC Environment CEE** (formerly A.S.A. Group) is one of Europe's leading **waste and resource management** companies, **operating in eight countries in the CEE region** and employing a workforce of 4.300 international **experts**) (https://www.fcc-group.eu/en/fcc-cee-group/about-us.html).

Handling more than 1/2 million tonnes of secondary raw materials per year, extracting value and minimizing waste sent to landfill, they contribute to reducing environmental burdens for future generations and help save natural resources (https://www.fcc-group.eu/en/fcc-cee-group/about-us.html).

Figure 3. FCC Environment CEE waste management
(https://www.fcc-group.eu/en/fcc-cee-group/about-us.html)

KEY COMMISSION PROPOSALS

Quality standards – the lack of adequate tools to ensure the quality of secondary raw materials is a barrier to their take-up in the EU economy. Common standards are needed to build and support trade. The Commission will develop such standards where needed.

Common rules on fertilizers – diverging rules and standards hamper the manufacturing of organic and waste-based fertilisers from inputs such as food waste, sewage sludge or manure. The Commission will revise the EU regulation on fertilizers to help develop an EU-wide market for bio-nutrients while ensuring safety and quality of the EU Fertilisers.

Using water again – reuse of treated wastewater is a promising and under-exploited option in Europe. This can alleviate pressure on natural resources that are already scarce, and the reuse of water in agriculture also contributes to nutrients recycling. The Commission will take a series of actions to encourage the reuse of treated waste water, including legislation on minimum requirements for water reuse.

Plastic as a recyclable resource – smart design and proper sorting can increase the recycling rates of plastics and avoid landfilling, incineration and use of virgin materials. The Commission will elaborate a strategy addressing issues such as recyclability, biodegradability, the presence of hazardous substances of concern in certain plastics, and marine litter.

Use of chemicals fitting the circular model – to increase safety, facilitate recycling and improve the trust in and uptake of secondary raw materials, the Commission will promote nontoxic material cycles involving less and better traced chemicals of concern. The Commission will also examine how chemicals, products and waste legislation can best work together, including proposals to improve the tracking of chemicals of concern in products.

Cross-border trade – to facilitate the cross-border circulation of secondary raw materials, the Commission will simplify cross-border formalities through the use of electronic data exchange. It will also support an EU-wide research on raw material flows through the Raw Materials Information System.

CONCLUSION

Clear rules, common standards and support for the use of more secondary raw materials will create a safe and sustainable supply of raw materials to the industry. This helps create new jobs, supports innovation and boosts competitiveness. Improved waste

management rules will reduce landfill and tipping fees. Smarter use of resources is not only good for business, but will also help protect the environment preserve essential resources for current and future generations, and create synergies for industries which most depend on it – such as tourism, agriculture and food manufacturing.

Acknowledgements

REFERENCES

Ellen MacArthur Foundation (2012), Towards the Circular Economy: Economic and business rationale for an accelerated transition, available at https://www.ellenmacarthurfoundation.org/assets/downloads/publications/Ellen-MacArthur-Foundation-Towards-the-Circular-Economy-vol.1.pdf.

Europe INNOVA (2012), Guide to resource efficiency in manufacturing: Experiences from improving resource efficiency in manufacturing companies, available at https://www.greenovate-europe.eu/sites/default/files/publications/REMake_Greenovate%21Europe%20-%20Guide%20to%20resource%20efficient%20manufacturing%20%282012%29.pdf.

European Commission (2015a), Proposal for a Directive of the European Parliament and of the Council amending Directive 2008/98/EC on waste, https://eur-lex.europa.eu/resource.html?uri=cellar:c2b5929d-999e-11e5-b3b7-01aa75ed71a1.0018.02/DOC_1&format=PDF.

European Commission (2015b), Annex to the Proposal for a Directive of the European Parliament and of the Council amending Directive 2008/98/EC on waste, https://eur-lex.europa.eu/resource.html?uri=cellar:c2b5929d-999e-11e5-b3b7-01aa75ed71a1.0018.02/DOC_2&format=PDF.

Meyer, B. *et al*. (2011), *Macroeconomic modelling of sustainable development and the links between the economy and the environment. Final report*, available at http://ec.europa.eu/environment/enveco/studies_modelling/pdf/report_macroeconomic.pdf.

***, http://ec.europa.eu/environment/circular-economy/index_en.htm.

***, http://ec.europa.eu/environment/circulareconomy/index_en.htm.

***, https://www.fcc-group.eu/en/fcc-cee-group/about-us.html.

CIRCULAR ECONOMY – AN INNOVATIVE AND CREATIVE PRODUCTION MODEL

VIORICA DESELNICU[1], GABRIEL ZĂINESCU[1], LUMINIȚA ALBU[1],
DANA CORINA DESELNICU[2], GHEORGHE MILITARU[2], XIAOYAN PANG[3]

[1]*INCDTP - Division: Leather and Footwear Research Institute Bucharest, 93 Ion Minulescu str., sector 3, RO- 031215 Bucharest, viorica.deselnicu@icpi.ro*

[2]*University POLITEHNICA Bucharest, 313 Splaiul Independentei, sector 6, Bucharest, Romania, dana.deselnicu@upb.ro,*

[3]*China Leather and Footwear Institute Co Ltd., Beijing, China*

This paper presents circular economy concept - one of the most innovative and creative production models around. The European Commission is supporting the EU's transition to a Circular Economy with a broad set of measures to maintain the value of products, materials and resources for as long as possible, while minimising the generation of waste. The aim of the package is to give clear signals to economic operators and society on the way forward. Action at EU level can drive investments, create a level playing field, and remove obstacles in the single market. The Circular economy offers an opportunity to reinvent the economy, making it more sustainable and competitive. This will bring benefits for European businesses, industries, and citizens alike.

Keywords: circular economy, production, consumption, waste management, innovation.

INTRODUCTION

Policy Context

In a changing world, the EU's economy needs innovation to become **smarter, more sustainable and more inclusive** (https://www.eumonitor.eu/9353000/1/j9vvik7m1c3gyxp/vimh9eb5oozb).

– **Smart growth:** developing an economy based on knowledge and innovation.

– **Sustainable growth:** promoting a more resource efficient, greener and more competitive economy.

– **Inclusive growth**: fostering a high-employment economy delivering social and territorial cohesion.

Along with its growth strategy **EU 2020**, the EU has launched the **Innovation Union** and **Resource Efficient Europe flagship initiatives** aimed to help all EU countries to provide their citizens with a more competitive economy, more and better jobs and a better quality of life.

The Innovation Union Initiative (https://ec.europa.eu/research/innovation-union/pdf/innovation-union-communication-brochure_en.pdf) addresses the challenges and opportunities of Europe in key areas where urgent need for sustained efforts to create an Innovation Union, contributing to the achievement of their objectives "*An industrial policy for the Globalisation era*" to improve the business environment, especially SMEs. It aims is to improve conditions and access to finance for research and innovation, to ensure that innovative ideas can be turned into products and services that create growth and jobs.

Natural resources underpin the functioning of the European and global economy and our quality of life. These resources include raw materials such as fuels, minerals and metals but also food, soil, water, air, biomass and ecosystems. The pressures on resources are increasing. If current trends continue, by 2050, the global population is expected to have grown by 30% to around 9 billion and people in developing and emerging economies will legitimately aspire to the welfare and consumption levels of

developed countries. As we have seen in recent decades, intensive use of the world's resources puts pressure on our planet and threatens the security of supply. Continuing our current patterns of resource use is not an option.

A number of measures have already been identified in **Efficient Europe flagship initiatives**   (https://www.eumonitor.eu/9353000/1/j9vvik7m1c3gyxp/vimh9eb5oozb). These include: A strategy to make the EU a **'circular economy',** based on a recycling society with the aim of reducing waste generation and using waste as a resource; to create a **low-carbon economy** in 2050, cutting greenhouse gas emissions by 80-95%, as part of global efforts to fight climate change, while improving energy security and promoting sustainable growth and jobs.

European Resource Efficiency Platform (EREP), 2014 stated: "secure at least a doubling of resource productivity as compared with the pre-crisis trend … equivalent to an increase of well over 30% by 2030" (http://ec.europa.eu/environment/ resource_efficiency/re_platform/index_en.htm).

In this policy context will take place a transition from a **Linear Economy** - which means from raw materials – production- distribution- consumption-waste- to a **Circular Economy** in which waste can be used as raw material.
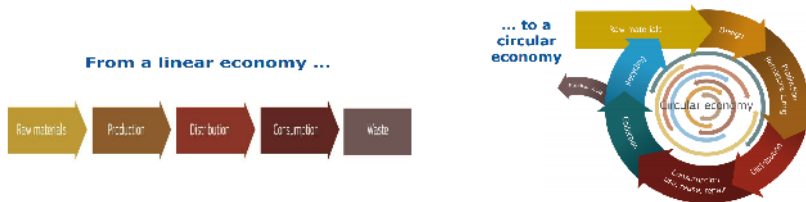
Figure 1. From a linear economy to a circular economy
(https://www.oecd.org/env/outreach/EC-Circular-econonomy.pdf)

What is a Circular Economy?

In a circular economy (EPRS, 2016), products and the materials they contain are valued highly, unlike in the traditional, linear economic model, based on a 'take-make-consume-throw away' pattern. In practice, a circular economy implies **reducing waste to a minimum** as well as re-using, repairing, refurbishing and recycling existing materials and products. What used to be considered as 'waste' can be turned into a valuable resource.

Moving towards a more circular economy could deliver **benefits**, among which reduced pressures on the environment, enhanced security of supply of raw materials, increased competitiveness, innovation, and growth and jobs. However, it would also face **challenges**, among which finance, key economic enablers, skills, consumer behaviour and business models, and multi-level governance.

The aim of this work is to present the concept of **Circular Economy** - **closing the loop,** an innovative and creative production model.

CIRCULAR ECONOMY PACKAGE

The European Commission adopted an ambitious Circular Economy Package (EPRS, 2016), which includes measures that will help stimulate Europe's transition towards a circular economy, boost global competitiveness, foster sustainable economic growth and generate new jobs.

Objectives

- Synergies between **environment and business agendas**
    - Preserve resources while creating business opportunities
    - Closer links to other key EU priorities (climate and energy, jobs and growth, investment, innovation, social, industrial competitiveness)
- Propose **concrete and ambitious action** where EU intervention has **high added value** e.g. long-term signals on waste management; internal market; barriers linked to existing EU legislation; enforcement issues.

Circular Economy Action Plan

The Action Plan aims to stimulate Europe's transition towards a circular economy to boost global competitiveness, foster sustainable economic growth and generate new jobs. It gives a clear signal to economic operators that the EU is using all the tools available to transform its economy, opening the way to new business opportunities and boosting competitiveness. The proposed actions will contribute to **"closing the loop" of product lifecycles through sustainable consumption and production and sound waste management, including greater recycling and re-use, also by creating a market for secondary raw materials. This will bring benefits for the environment, the economy and the society**.

Figure 2. Circular Economy

Diversity of Actions and Priority Sectors

There are 5 main area of actions: Production, Consumption, Waste management, Secondary raw materials, Innovation & Investment. A number of sectors face specific challenges in the context of the circular economy, because of the specificities of their products or value-chains, their environmental footprint or dependency on material from outside Europe. The priority sectors are: plastics, Food waste, Critical raw materials, Construction & Demolation, Biomass & Bio-based products.
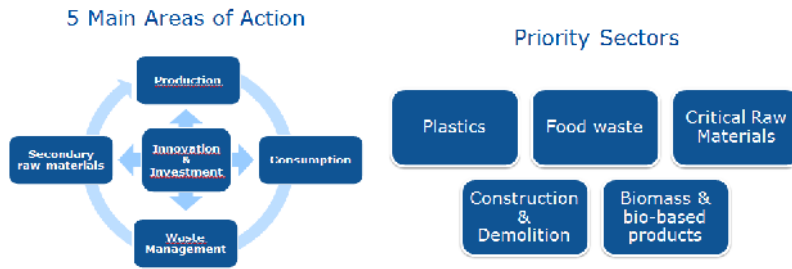
Figure 3. Diversity of actions and priority sectors

Production

A circular economy starts at the very beginning of a product's life. Both the design phase and production processes have an impact on sourcing, resource use and waste generation throughout a product's life.

- **Product design -** Better design can make products more durable or easier to repair, upgrade or remanufacture. It can help recyclers to disassemble products in order to recover valuable materials and components. Overall, it can help to save precious resources.

   The Commission will promote the reparability, upgradability, durability, and recyclability of products by developing product requirements relevant to the circular economy in its future work under the Ecodesign Directive, as appropriate and taking into account the specificities of different product groups.

- **Production processes**

   Even for products or materials designed in a smart way, inefficient use of resources in production processes can lead to lost business opportunities and significant waste generation.

Consumption

The choices made by millions of consumers can support or hamper the circular economy. These choices are shaped by the information to which consumers have access, the range and prices of existing products, and the regulatory framework. This phase is also crucial for preventing and reducing the generation of household waste.

-Once a product has been purchased, its lifetime can be extended through reuse and repair, hence avoiding wastage. The reuse and repairs sectors are labour-intensive and therefore contribute to the EU's jobs and social agenda.

-Other actions can be taken to reduce the amount of household waste.

-Innovative forms of consumption can also support the development of the circular economy, e.g. sharing products or infrastructure (collaborative economy), consuming services rather than products, or using IT or digital platforms.

Waste Management

Waste management plays a central role in the circular economy: it determines how the EU waste hierarchy is put into practice. The waste hierarchy establishes a priority order from prevention, preparation for reuse, recycling and energy recovery through to

disposal, such as landfilling. This principle aims to encourage the options that deliver the best overall environmental outcome.

Turning waste into a resource is an essential part of increasing resource efficiency and closing the loop in a circular economy. Europe currently loses around 600 million tonnes of waste materials, which could potentially be recycled or reused. Only around 40% of the waste produced by EU households is recycled, with recycling rates as high as 80% in some areas, and lower than 5% in others. The proposal reflects a high level of ambition while taking account of the different realities and performance levels across the EU.

Market for Secondary Raw Materials

In a circular economy, materials that can be recycled are injected back into the economy as new raw materials thus increasing the security of supply. These "secondary raw materials" can be traded and shipped just like primary raw materials from traditional extractive resources.

- Recycled nutrients are a distinct and important category of secondary raw materials, for which the development of quality standards is necessary. They are present in organic waste material, for example, and can be returned to soils as fertilisers.

- The promotion of non-toxic material cycles and better tracking of chemicals of concern in products will facilitate recycling and improve the uptake of secondary raw materials.

- Water scarcity has worsened in some parts of the EU in recent decades, with damaging effects on our environment and economy. In addition to water-efficiency measures, the reuse of treated wastewater in safe and cost-effective conditions is a valuable but under-used means of increasing water supply and alleviating pressure on over-exploited water resources in the EU.

Innovation & Investment

The transition to a circular economy is a systemic change.

Innovation will play a key part in this systemic change. In order to rethink our ways of producing and consuming, and to transform waste into high value-added products, we will need new technologies, processes, services and business models which will shape the future of our economy and society. Hence, support of research and innovation will be a major factor in encouraging the transition; it will also contribute to the competitiveness and modernisation of EU industry.

The Horizon 2020 programmes support innovative projects relevant to the circular economy, in fields such as waste prevention and management, food waste, remanufacturing, sustainable process industry, industrial symbiosis, and the bioeconomy.

Benefits of the Circular Economy Package

The Circular economy offers an opportunity to reinvent the economy, making it more sustainable and competitive. This will bring benefits for European businesses, industries, and citizens alike. With this new plan to make Europe's economy more sustainable and more competitive, the Commission is delivering ambitious measures to cut resource use, reduce waste and boost recycling:

- will preserve resources that are increasingly scarce and subject to mounting environmental pressure or volatile prices, and reduce costs for European industries
- will support a new generation of European businesses which make and export more efficient and sustainable products and services around the globe, and create

innovative, more resource efficient ways to provide services or products to customers;

- will help to create jobs for European citizens and opportunities for social integration and cohesion;
- will create more than 170,000 direct jobs by 2035 through the measures on waste management alone;
- will provid consumers with more durable, sustainable and less toxic products that save money and their increase quality of life;
- will continue to deliver ambitious energy efficiency for products, which by 2020 will bring savings of 465 EUR per year per household on their energy bills;
- will contribute to preserving the environment and our planet, bring a substantial cut in carbon emissions and preserve threatened resources;
- will take measures which can reduce greenhouse gas emissions by more than 500 million tons between 2015 and 2035;
- will increase the competitiveness of key industry sectors including manufacturing, waste management and recycling, as well as reducing the dependency of the EU on raw material imports.

Through long terms targets on waste and landfill, backed by clear supportive measures, we create incentives for action by Member States and investment certainty for businesses.

CONCLUSION

The Circular economy offers an opportunity to reinvent the economy, making it more sustainable and competitive. This will bring benefits for European businesses, industries, and citizens alike.

The proposed actions support the circular economy at each step of the value chain – from production to consumption, repair and remanufacturing, waste management, and secondary raw materials that are fed back into the economy.

Action on the circular economy ties in closely with a number of other EU priorities, including jobs and growth, the investment agenda, climate and energy, the social agenda, industrial innovation and with global efforts to secure sustainable development.

The Circular Economy is a win-win situation:
- o Savings of €600 billion for EU businesses, equivalent to 8% of their annual turnover;
- o Creation of 580,000 jobs;
- o Reduction of EU carbon emissions by 450 million tonnes by 2030.

REFERENCES

EPRS (2016), Circular economy package, available at http://www.europarl.europa.eu/EPRS/EPRS-Briefing-573936-Circular-economy-package-FINAL.pdf.
***, http://ec.europa.eu/environment/resource_efficiency/re_platform/index_en.htm
***, http://eur-lex.europa.eu/LexUriServ/LexUriServ.do?uri=COM:2010:2020:FIN:EN:PDF
***, https://ec.europa.eu/research/innovation-union/pdf/innovation-union-communication-brochure_en.pdf
***, https://www.eumonitor.eu/9353000/1/j9vvik7m1c3gyxp/vimh9eb5oozb
***, https://www.oecd.org/env/outreach/EC-Circular-econonomy.pdf

LIFE CYCLE ASSESSMENT OF TWO ALTERNATIVE END-OF-LIFE SCENARIOS FOR LEATHER SAFETY SHOES

ALEXANDRA LUCA[1], DAVID SANCHEZ DOMENE[2], FRANCISCA ARAN AIS[2]

[1] *"Gheorghe Asachi" Technical University of Iasi, Faculty of Textile – Leather and Industrial Management, 28 D. Mangeron, Iasi, Romania, alexandra.luca@tuiasi.ro*

[2] *INESCOP, Centre for Technology and Innovation, Elda (Alicante), Spain, d.sanchez@fundaficia.org, aran@inescop.es*

This paper provides a brief overview of the environmental impact of footwear industry and the end of life solutions. Nowadays almost 23 billion pairs of shoes are produced worldwide every year and most of them are landfilled after their use. Currently the lifetime of a pair of shoes is falling because of the customer preferences and the fast fashion trend at market and fashion industry. As a result, huge amounts of wastes are being landfilled. The aim of this paper is to analyses the environmental implications of shoes landfilling and incineration end-of-life scenarios. To achieve it, these two scenarios were applied in a life cycle assessment of a pair of shoes performed for this study.

Keywords: end-of-life, sustainable footwear, landfilling, incineration, life cycle assessment

INTRODUCTION

In the last years the footwear industry is trying to become more sustainable, improving the energy and material consumption and eliminating the hazardous substances from the production phase (Staikos, 2006). The fast fashion trend creates new challenges to footwear companies; they have to adapt to the market changes in order to satisfy the consumers.

Less than 5% of 20 billion pairs of shoes produced per year are recycled or reused, and the rest goes to landfill or are stocked in the wardrobes for years (Lee and Rahimifard, 2012). But, in the last years, the number of footwear produced worldwide has increased, reaching 23 billion pairs in 2017 (World Footwear, 2017).

Because of the diversity of materials, not all shoes collected can be recycled, most of them are made from a mix of materials such as leather, polyurethanes, textiles, adhesives, polymers, rubber, which are difficult to separate.

Environmental Impact of Footwear Industry

The highest environmental impact of footwear industry, according to Haworth *et al*., 2006 is the end-of-life phase because of the huge quantity of waste generated. This fact can be explained because the majority of the shoes worldwide are discarded in landfills which lead to groundwater, surface, and soil contamination.

If in the design phase is taking into consideration the end-of-life scenarios it can offer the possibilities to integrate the distinct elements of circular economy (White *et al*., 2013). Basically the design of a product decides the waste management approach.

The nature and the quantity of waste generated by the footwear industry can be classified in two groups:
   a. The type of the materials (leather, polyurethane, foam, rubber, plastic);
   b. The type of assembling technology (bonding, direct moulding, stitching).

Waste management options for shoes at the end of their life use are (Staikos, 2006): Reusing, extending the lifespan of the shoes; Recycling – down-cycling; Energy recovery – incineration, gasification, pyrolysis; Landfill.

The EU Landfill Directive has an important role, developing the waste management policies, landfill restrictions. The Landfill Directive also defines the waste categories (municipal waste, hazardous waste, non-hazardous waste and inert waste) and presents the legislation and procedure for the acceptance of waste in a landfill.

The EU Waste Incineration Directive is establishing the emission limit values for incineration and co-incineration plants and is monitoring the requirements for pollutants to air such as sulphur dioxide (SO_2), hydrogen chloride (HCl), dust, nitrogen oxides (NOx) or heavy metals.

RESEARCH METHODOLOGY

To analyses the environmental implications of shoes landfilling and incineration end-of-life scenarios, these two scenarios were applied in a life cycle assessment of a pair of shoes performed for this study. Life cycle assessment is a method for evaluating the environmental impact of a product or an activity over its life cycle. The LCA asses only the environmental impact of a product without taking into consideration economic or politic aspects (LCA Compendium, 2017).

For this study it was applied "cradle to grave" approach, this refers to the activities involved in the life cycle of a product, presented in figure 1, starting from the raw materials extraction, manufacturing, use, maintenance and, in the end, disposal.

Figure 1. Footwear life cycle phases

Inventory Data

Several sets of data were required to assess the environmental implications of shoes landfilling and incineration end-of-life scenarios. Life cycle assessment was applied to a pair of safety boots, for men, size EU 42 with its primary packaging. Shoe materials are classified in three main components: upper, sole and packaging. In the upper it was used bovine leather, polyurethane, and textile. The sole is separated in outsole and midsole, both made of polyurethane.

The background inventory data was obtained from Ecoinvent database, version 3.4. The manufacturing and assembling of safety footwear includes several processes: cutting, stitching the parts for upper and injection for outsole and midsole.

Impact Assessment

The impact was determined using Global Warming Potential (GWP) where the contribution of emissions to the global warming for 100 year period are calculated according to the values of Intergovernmental Panel on Climate Change (IPCC, 2007).

The impact of greenhouse gas emissions were measured as relative carbon dioxide and are expressed in terms of an equivalent mass of carbon dioxide (kg CO_2eq).

The Life cycle analyses were conducted using SimaPro software.

RESULTS AND DISCUSSION

The majority of the used shoes are landfilled or incinerated (depending on the legislation of the country, for example in Romania there is no municipal incineration plant). The recycling process is not involved in this study therefore there is no material recovery.

Landfilling Scenarios

According to the report Diverting waste from landfill – effectiveness of waste management policies in the European Union (EEA report, 2009) there are three scenarios for the end of life of professional footwear, presented in table 1.

Table 1. Scenarios for the end of life of professional footwear

	Percentage
Average landfilling in weight for professional footwear	79,2%
Average incineration in weight for professional footwear	19,8%
Average recycling in weight for professional footwear	1,0%

To estimate the GWP of the analysed shoes in landfill is was used SimaPro software. The total emissions associated with the end of life treatment of professional footwear are small. At the end of their life use, in the first scenarios (figure 2), it was assumed that they are landfilled and this emits 0.0996 kg CO_2 –eq per pair resulting from emissions of methane during anaerobic decomposition of organic matter in landfills. The total emissions are only 0.554% of the total life cycle impact of the analysed product.
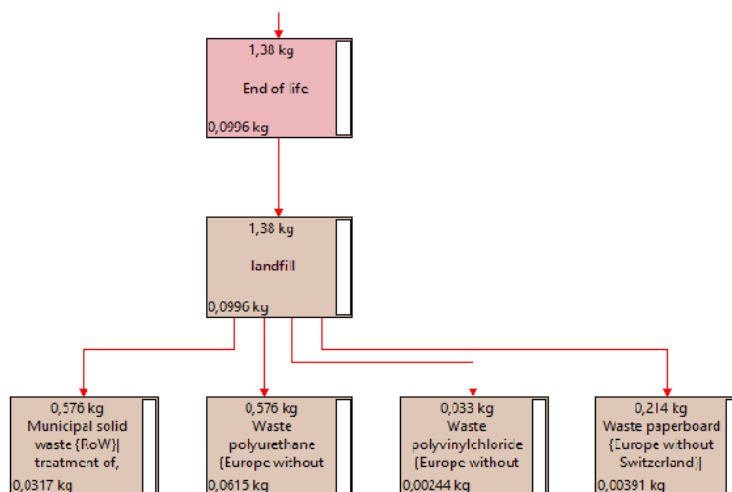

Figure 2. Waste generated from landfill

The value can be explained by the fact that, the method used, Global Warming Potential, is taking into consideration the impact of emissions for a period of 100 years.

In this time the materials used are not degraded, some of them have a faster degradability than others, that is the reason why the CO_2 emissions have a small value (i.e. a midsole made of EVA can last up to 1000 years on landfill (Lippa *et al*., 2016)).

The consequence of the anaerobic conditions that exist in landfills is the release of biogas, especially methane (CH_4). Methane have a radiative forcing 21 times greater than CO_2 (Simple Shoes Report, 2008).

Incineration Scenarios

Energy Recovery at Municipal Incineration Plants

In the case of leather the advantages are: substitution of fossil fuels and reduction of CO_2 emissions. The biggest concern, in a classic process of incineration, is the conversion of chromium III to chromium VI (Lety, 2018).

Polyurethane, as well as other plastics, is a good material to recover energy from, because, according to Thompson and Thompson (2014), has a high energy content.

The main disadvantages of municipal incineration plants are: harmful air emissions and is not accepted in all European countries.

At the end of their life use, in the second scenarios, it was assumed that the shoes are incinerated. The end of life emissions are 1.86 kg CO_2 –eq or 9.48 % of the total life cycle impact. The emissions are higher to incineration compared to landfill because all the components of the shoes are destroyed at the same time and the CO_2 is release immediately.
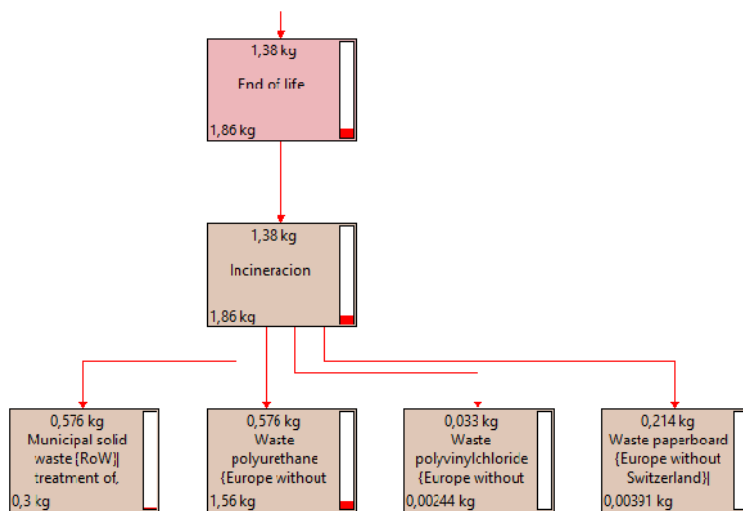
Figure 3. Waste generated from incineration

Figure 3 illustrates the waste that is sent to a municipal incinerator. Polyurethane have the most significant impact on the environment, 1.56 kgCO_2 –eq per pair.

As a result of this analysis, the use of polyurethane in a shoe represents a hotspot of carbon impact, this means that shoe designers should focus on other materials in order to reduce the material impact (recycled materials, biodegradable).

Alternatives Scenario for the End of Life of Shoes

Recycling

A recycled material can be uncycled or downcycled. The recycled materials recovered from a shoe and their applications are considered as downcycling, but it is better compared to the disposal to landfill (James and Rahimifard, 2012).

If the components of a shoe are separated, there are several recycling options used nowadays in order to add value to the materials instead of landfilling or incineration. From a quantitative point of view this method cannot be used on a scale mass. The SOEX company and its partners developed an industrial-scale footwear recycling plant. This plant is able to recycle all types of shoes and to separate the different components such as leather, rubber, foam, metal.

The recycling process is presented in figure 4, first step is shredder the shoes (all types it is not necessary to sort them) after that the materials are separated (metals, non-metals, textiles, rubber, foam, leather) and in the end they are granulated. The new raw materials derived are leather fibres, foam granules, rubber granules. An example of reusing these materials is creating soles and floor mats from rubber granules, or production of inner soles, floor covering from foam granules. The amount of shoes passing through the system is 2000 pairs per shift, the waste reduction per shoe is up to 70%, the daily waste reduction of shoes is up to 45% (SOEX Footwear Recycling).
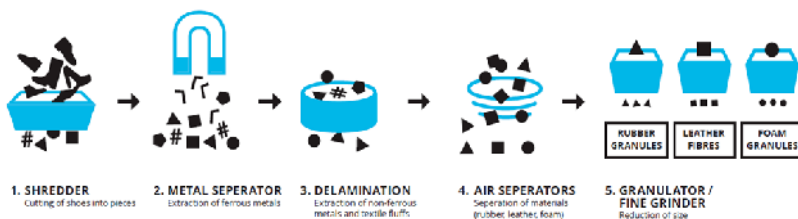

Figure 4. Recycling process for footwear (source SOEX Footwear Recycling)

CONCLUSION

The purpose of the study was to determine environmental implications of shoes landfilling and incineration end-of-life scenarios. For this, these two scenarios were applied in a life cycle assessment of a pair of safety shoes.

Based on literature, the end-of-life phase is considered to have the significant environmental impact because of the huge quantity of waste generated. The majority of the used shoes are landfilled or incinerated.

The results indicate that for the disposal of mixed materials in a sanitary landfill, ecoinvent 3.4. estimates the environmental impact at 0.0996 kgCO_2-eq per pair waste disposed. For waste that is sent to a municipal incinerator plant, the impact is higher at 1.86 kg CO_2-eq per pair.

In the first scenario, landfilling, the total emissions represents 0.554% of the total life cycle impact (GWP 100 years). In the second scenario, the used shoes are incinerated and the emissions associated are 9.48 % of the total life cycle impact of the product.

REFERENCES

Albers, K., Canepa, P. and Miller, J. (2008), *Analysing the Environmental Impacts of Simple Shoes*, Donald Bren School of Environmental Science & Management, 63-64.

Curran, M.A. (2017), *LCA Compendium – The Complete World of Life Cycle Assessment*, Springer, Rock Hill, SC, USA, ISBN 978-94-024-0855-3 (eBook), https://doi.org/10.1007/978-94-024-0855-3.

Haworth, B. *et al*. (2006), "End-of-Life Management of Shoes and the Role of Biodegradable Materials", in W.S. Engineering (Ed.), *13th CIRP International Conference on Life Cycle Engineering*, 497-502, Loughborough University, UK. Retrieved from http://www.mech. kuleuven.be/lce2006/177.pdf.

Intergovernmental Panel on Climate Change (2007), https://www.ipcc.ch/publications_and_data/publications_ipcc_fourth_assessment_report_synthesis_report.htm

Lee, M.J. and Rahimifard, S. (2012), "An Air-Based Automated Material Recycling System for Postconsumer Footwear Products", *Resources, Conservation and Recycling*, 69, 90-99, https://doi.org/10.1016/j.resconrec.2012.09.008.

Lety, R. (2018), *A sustainable solution for the 23 billion pairs of used shoes?*, 20th UITIC International Technical Footwear Congress, Porto, Portugal.

Lippa, N.M. *et al*. (2016), "Biofidelic mechanical ageing of ethylene vinyl acetate running footwear midsole foam", *Sports Engineering and Technology*, 1-11.

Rahimifard, S. and Staikos, T. (2006), "Post-consumer waste management issues in the footwear industry", *Proceedings of the Institution of Mechanical Engineers, Part B: Journal of Engineering Manufacture*, 221(2), 363-368.

Staikos, T. *et al*. (2006), "End-of-Life Management of Shoes and the Role of Biodegradable Materials", *13th CIRP International Conference on Life cycle Engineering*, 497-502.

Thompson, R. and Thompson, M. (2014), *Manufacturing Processes for Textile and Fashion Design Professionals* (01 edition ed.), Thames and Hudson Ltd.

White, P., St. Pierre, L. and Belletire, S. (2013), *Okala Practitioner - Integrated Ecological Design*. Phoenix: Okala Team.

World Footwear Yearbook (2017), https://www.worldfootwear.com/yearbook/the-world-footwear-2017-Yearbook/209.html.

*** EU Landfill Directive, http://ec.europa.eu/environment/waste/landfill/useful-information.htm

*** EU Waste Incineration Directive, http://ec.europa.eu/environment/archives/air/stationary/wid/legislation.htm

*** European Environment Agency (2009), *Diverting waste from landfill - Effectiveness of waste-management policies in the European Union,* Copenhagen, Denmark, ISBN 978-92-9167-998-0, ISSN 1725-9177, https://doi.org/10.2800/10886.

*** SOEX Footwear Recycling (2016), https://footwear-recycling.com/en/

PORTAL OF CLUSTERS AND COMPETITIVENESS POLES IN THE TEXTILE-CLOTHING SECTOR

SABINA OLARU, CĂTĂLIN GROSU, EFTALEA CĂRPUȘ, CARMEN GHIȚULEASA

The National Research Development Institute for Textiles and Leather, 16 Lucretiu Patrascanu, 030508, Bucharest, Romania, sabina.olaru@certex.ro

The remarkable advances in technological development and innovation, which have taken place in the last few years, have influenced the organization and business strategies. The knowledge revolution was identified, a complex process of transition from the physical to knowledge-based economy, in which intangible intellectual resources, knowledge packages and informational capital play an essential strategic role, being the engine of competitiveness. In order to support the members of the national textile-clothing clusters, the members of the competitiveness pole in the related fields, the stakeholders, a portal of competitiveness clusters and poles in the textile – clothing industry was created and developed. The portal functions as a common platform that concentrates information on the activity of clusters and competitiveness poles in the T&C sector, in order to facilitate the effective interaction and collaboration of actors in the sector. The main goal of this portal is to support the competitiveness of the Romanian clusters in the T&C industry, by increasing their visibility on the national market. Through this approach, it is intended to promote a development based on cooperation among cluster members and a relational system between both cluster members and stakeholders.

Keywords: cluster, textile-clothing, portal, competitiveness

INTRODUCTION

The remarkable advances in technological development and innovation, which have taken place in the last few years, have influenced the organization and business strategies. The knowledge revolution was identified, a complex process of transition from the physical to knowledge-based economy, in which intangible intellectual resources, knowledge packages and informational capital play an essential strategic role, being the engine of competitiveness (Lut, 2012).

Ensuring social well-being and added value is possible through a systematic generation and efficient use of knowledge. Thus, among developed countries, the trend is the development of national systems with complex international interactions, called by specialists: "triangles of knowledge". "The triangle of knowledge" consists of education, research and innovation and is realized through cooperation between education institutions, research organizations and the business environment (Dan, 2012; Irecson, 2009). Among these, the greatest degree of complexity that raises the most problems (specific policies, well-prepared human resources, financial resources to be allocated) is innovation. Innovation is a function of many variables due to the role it plays as a link element (bridge between research and industry). The innovative process does not end with the implementation of new products and services in the industry, but it is continuously developing in order to improve these products and services to be competitive.

The ultimate consumer, through his needs, changing with astonishing dynamics, demands the acceleration of the innovative process. Reducing development time in innovative products and services, implemented in industry, leads to the acceleration of the economic circuit and thus to the increase of final consumer satisfaction (European Commission, 2010).
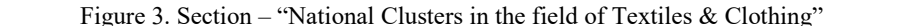
THE PORTAL ARCHITECTURE OF CLUSTERS AND POLES OF COMPETITIVENESS FROM TEXTILE & CLOTHING FIELD

In order to support the final users: members of the national textile-clothing clusters, members of the competitiveness poles in the related fields, stakeholders, a portal of competitiveness clusters and poles in the textile – clothing industry was created and developed. The portal functions as a common platform that concentrates information on the activity of clusters and competitiveness poles in the T&C sector, in order to facilitate the effective interaction and collaboration of actors in the sector.

The main goal of this portal is to support the competitiveness of the Romanian clusters in the T&C industry, by increasing their visibility on the national market.

The portal is a vector for the development of the Romanian clusters and competitiveness poles.

Through this approach, it is intended to promote a development based on cooperation among cluster members and a relational system between both cluster members and stakeholders by promoting the textile industry and increasing the visibility of Romanian textiles on the national and European market.

The portal functions as a platform that can be upgraded and expanded with up-to-date information. The user of the portal must find the right information in a minimum search time. Thus, designing a user-friendly platform has been a very important goal of this phase. The portal was designed and built in Romanian. To achieve the site a WYSIWYG program (What You See Is What You Get), Joomla! 3.8.0 - toolkit for building a professional site has been used. Joomla is a PHP Content Management System (CMS) designed to publish content locally or online through SQL databases. Joomla offers the ability to build complex web sites and applications (Figure 1).

Figure 1. Joomla articles manager

The portal, accessible on the website of the National Research & Development Institute for Textiles and Leather, from Bucharest, at http://www.certex.ro/cluster/, comprises 11 sections, which focus on:
- Definition of the cluster, the innovation cluster and the competitiveness pole;

information on the role and effects of each actor in a cluster / competitiveness pole, namely the policy and strategy of clusters / competitiveness poles (section - Home) (Figure 2) (Coşniţă and Bucur, 2013);

Figure 2. "Home" section

- The short history, in which are presented: the main events that marked the textile industry in Romania; data on the economic situation of textile & clothing field in 2015 (section - Textile & Clothing Industry in Romania);

- The charts with updated information on cluster activity: general information (logo; name; year of establishment; contact person; telephone / fax; headquarters address; e-mail; website; management team; excellence label; participation in other networks / partnerships); field of activity (areas of specialization, domains targeted for inter-sectoral collaborations); members (total number, total number of SMEs, SME identification data, universities, research institutes, public authorities, catalysts, others); cluster / pole strategy (missions, general objectives, specific objectives); the main products / services / projects offered (products, services, projects, main markets, international collaborations, industry turnover - 2015, industry turnover - 2016, 2015, number of employees in 2016). All this information was centralized for the 4 national clusters of the textile & clothing: Romanian Textile Concept, Bucharest; Traditions Manufacture Future, Focsani, Vrancea; Transylvania Textile & Fashion Sfântu Gheorghe Covasna; ASTRICO N-E, Săvineşti, Neamţ and Noatex - meta cluster that reunites the four clusters mentioned above. (Section - National Clusters of the Textile & Clothing) (Figure 3);

- The general information on mission of the main Textile & Clothing European and international clusters and contact data of these clusters (Section – International Clusters of Clusters of the Textile & Clothing);

- Up-to-date information on the activity of the Romanian Poles of Competitiveness: Southwest Automotive Oltenia, Ind-Agro-Pol and Ro-Health, where INCDTP has membership (general information; mission; field of activity; members; contact data;) (Section - Poles of Competitiveness in related fields);

- The information on funding opportunities for clusters under specific programs such

as: Eureka Cluster - PNIII program, P3: European and International Cooperation: Subprogram 3.5: Other European and International Initiatives and Programs: EUREKA Traditional (Network), EUREKA Cluster, EUROSTARS; "Cluster Organization and Development - Innovative Cluster" (Section - Financing possibilities);

- The brief information on Romanian university level education (Section - Pre-university and university education in the field of textile & clothing, in Romania);

- Section designed for the experts (specialists) in the field of textiles & clothing, at national level (Section – Romanian specialists in the field);

- Presentation of Romanian and international publications that define clusters and poles of competitiveness, strategies, economic measures on increasing internationalization process, intelligent recommendations on clusters, etc. (Section - Supporting Documents) (Pavelkova et al., 2016);

- The main institutions, organizations and platforms that provide a mapping of European clusters, statistical data, analysis, favoring the implementation of EU policies at regional level; a short description of the two textile and clothing journals in Romania: "Industria Textilă" and "Dialog Textil" (section - Useful Links).

- Up-to-date information that helps better dissemination amongst the clusters and poles of the competitiveness of the events and news in the sector (section - News and Events).

Figure 3. Section – "National Clusters in the field of Textiles & Clothing"

CONCLUSIONS

The paper presents the portal architecture of the clusters and poles of competitiveness in the textile & clothing industry. The content of the portal is structured into 11 sections, whose information is addressed to industry actors, universities, research institutes, local and regional public authorities, catalysts and other stakeholders.

According to the strategic objectives and the Romanian and European action directions in the field of clusters, the portal leads to the increase of the competitiveness of clusters in the textile & clothing industry.

The Romanian cluster structure, "Four clover" type, is fully found in the four Romanian textile clusters: Romanian Textile Concept, Bucharest; Traditions Manufacture Future, Focsani, Vrancea; Transylvania Textile & Fashion Sfântu Gheorghe Covasna; ASTRICO N-E, Săvineşti, Neamţ, so that the synergy between the constituent actors will lead to positive results.

REFERENCES

Coşniţă, D. and Bucur, D. (2013), "Clusterization in textile and clothing industry", *Proceedings of 6th TEXTEH International Conference*, Bucharest, Romania, 274-288.

Dan, M.C. (2012), "Clusterele inovative: o solutie pentru dezvoltarea economica a Romaniei", *Economie teoretica si aplicata*, vol. XIX, no. 9(574), 3-14.

European Commission (2010), "EUROPE 2020: A strategy for smart, sustainable and inclusive growth", Brussels.

Irecson (2009), "Ghid pentru implementarea in Romania a conceptului de cluster inovativ", Bucharest, http://www.inma-ita.ro/clustere/Ghid.pdfhttp://www.nwtexnet.co.uk/

Lut, D. (2012), "The role and importance of clusters in the context of the knowledge economy", Timisoara, "Dimitrie Cantemir" Christian University, available at: http://www.quaestus.ro/wp-content/uploads/2012/03/D.-Lut.pdf.

Pavelkova, D. *et al*. (2016), *Internationalization of Cluster Organizations: Strategy, Policy and Competitiveness*, Cambridge Scholar Publishing.

Porter, M.E. (1985), *The Competitive Advantage: Creating and Sustaining Superior Performance*, Free Press, New York.

UTILIZATION POSSIBILITIES OF TIMBER WASTES IN LEATHER MANUFACTURING

CIGDEM KILICARISLAN OZKAN, SINA POURRASOUL SARDROUDI, ARIFE CANDAS ADIGUZEL ZENGIN[*], GOKHAN ZENGIN, HUSEYİN ATA KARAVANA, BEHZAT ORAL BITLISLI

Ege University, Faculty of Engineering, Leather Engineering Department, 35100, Bornova, Izmir/Turkey, cigdem.kilicarislan@ege.edu.tr, pourrasoul9984@gmail.com, gokhan.zengin@ege.edu.tr, huseyin.ata.karavana@ege.edu.tr, oral.bitlisli@ege.edu.tr

*Corresponding Author E-mail: candas.adiguzel@ege.edu.tr

In timber production, only the 24% of trees could be turned into timber and used as an end product, while the rest becomes the waste of forest goods. Although it is known that the wastes of timbers are utilized in different fields such as energy and composites production in general, their use in the leather industry as a tanning material is seemed to be a new concept. For this purpose, the usage possibilities of the timber wastes of red and black pine in the form of sawdust and bark were aimed to investigate for the leather manufacturing. The red and black pine wastes were extracted at Koch extractor at 90°C for 8 h and the tannin contents, influences on the shrinkage temperature, filling properties and final physical characteristics of the leathers such as tensile strength, elongation at break, tear strength and color measurements were investigated. The results revealed that the red pine barks (*Pinus resinosa* L.) could be an alternative source of vegetable tannins compared to other timber wastes for the leather industry due to the better extraction yield and tannin content. Besides similar results in terms of tanning properties were obtained with the commonly used vegetable tannins such as valonea and mimosa.

Keywords: timber waste, red pine, leather tanning

INTRODUCTION

Timber wood wastes are disposed of directly to landfill due to the lack of processing and this amount is approximately reached to two-third of the timber production (Taylor and Warnken, 2008). Solid forest wastes that create pollution are tree barks, chip and sawdust as well as sludge and coal ash. The forest industry wastes in general are organic and they can be used as a raw material in the field of energy (fuel), agriculture and composites production (Engür and Kartal, 2001).

The wood wastes have phenolic compounds and polymers which release bio-inhibitory phenols, terpenes and tannins during decomposition (Martin, 1998). In the view of these findings, the phenolic compounds in wood-based wastes seem to be an alternative source of vegetable tannins for the leather manufacturing depending on their tannin contents and extraction yields. Although there are several vegetable tannins having polyphenolic characteristics used in tanning and retanning processes in leather production, mimosa, quebracho, sumac, tara, valonea and chestnut are the most important tannins that are commercially available for the leather industry (Kilicarislan *et al.*, 2015).

In this study, the utilization possibilities of the timber wastes of red and black pine in the form of sawdust and bark were aimed to investigate for leather manufacturing. After the extraction of red and black pine wastes at Koch extractor at 90°C for 8h, the tannin contents, extraction yields and tanning properties of the extracts were determined. The pickled sheep skins were used for the tanning operation and the shrinkage temperatures, filling coefficients and physical properties of the leathers were investigated.

MATERIALS AND METHODS

Materials

The sawdust and barks of red and black pine were obtained from timber companies in Izmir/Turkey. The barks of red and black pine were crushed to 5-10mm pieces before extraction process to ensure an increase in the extraction yields.

Pickled sheep skins used in tanning trials were supplied from Tezcan Leather Company in Uşak/Turkey. The conventional chemicals were used in the leather production. Commercially available mimosa and valonea were used as the control tannins.

Methods

Determination of the Moisture Content

The moisture contents of the timber wastes were determined according to SLC 113. All experiments were carried out in triplicates and the results were given as an average value.

Extraction of Timber Wastes

Timber wastes (100g) were soaked in 700 ml distilled water in a clean glass beaker and maintained for one day to make the soaking easier. Then, timber wastes were subjected to extraction process at 90ºC for 8h at Koch extractor. High extraction temperature and long extraction time were preferred to obtain higher extraction yields. The yield of extraction was calculated according to Equation (1).

Yield= [(Extract obtained (g) / Amount of gallnuts used (g)] x 100   (1)

Tannin Analysis of the Extracts

The total solid matters, total soluble matters, non-tannin constituents and tannin matters absorbable by hide powder of extracts were determined according to SLC 114, 115, 116 and 117, respectively. Triplicate analyses were performed and the results were given as a mean value.

Tanning Procedure

After the tannin content determination of the extract solutions, the sheep skins were tanned with the extract solutions that contain 13% of active matter. The extract solutions were introduced to pelts in three batches according to the recipe given in Table 1. The vegetable tanning by the use of valonea and mimosa were similarly performed for the control group. The powder forms of mimosa and valonea with the active tanning matter of 13% were selected.

Table 1. Tanning procedure

Process	Amount(%)	Product	Temp(°C)	Time(Min.)	pH
Depickle	300	Water 7-8 °Be	28-30	10	
	1	HCOONa		30(15*2)	
	x	NaHCO$_3$		90	4.5-5

Process	Amount(%)	Product	Temp(°C)	Time(Min.)	pH
Bating	100	Water	35	30	
	1	Acidic bating enzyme			
Washing	100	Water	25-28	15	
Degreasing	3	Degreasing agent	30-35	30	
Washing	100	Water 3°Be		10	
Washing	100	Water 3°Be		10	
Washing	100	Water 3°Be		10	
Tanning	2	Dispersing syntan	30	20	
	x	Extract solution		30	
	1	Synthetic fatliquor		20	
	x	Extract solution		30	
	1	Synthetic fatliquor		20	
	x	Extract solution		30	
	1	Dispersing syntan		20	
	1	Synthetic fatliquor		20	
	1	Combination of Sulfochlorinated Synthetic Paraffin and Emulsifiers		15	
	0.2	Fungicide		20	
Fixation	1.2	HCOOH		60	3.5
		Washing & Draining			
Neutralization	150	Water	30-35		
	1	HCOONa		30	
	x	NaHCO$_3$		60	5-5.5
Fatliquoring	80-100	Water	40-45		
	2	Synthetic fatliquor			
	1	Sulphited fish oil			
	2	Synthetic sulphonated fatliquor		60	
	x	HCOOH		30-45	3.8-4

Determination of Shrinkage Temperature and Filling Coefficient of the Leathers

The tanning properties of the leathers were evaluated according to the shrinkage temperatures and filling coefficients. In order to investigate the filling properties of the tannins, the thicknesses of de-pickled pelts (T_i) and tanned leathers (T_e) were measured in the wet form by using a thickness gauge. Filling coefficients were calculated according to the following Equation (2).

$$\text{Filling coefficient \%} = ((T_e-T_i)/T_i)\text{x}100 \qquad (2)$$

The shrinkage temperatures of the leathers were determined according to IUP 16.

Determination of the Physical Properties

The leathers were conditioned before physical tests at 23±2°C and 50±5% relative humidity for 48 h according to TS EN ISO 2419.

The thicknesses of the leathers were measured with SATRA Thickness Gauge according to TS EN ISO 2589.

The tensile strength and percentage of elongation at break of the leathers were tested according to TS EN ISO 3376. The tear load of leathers was determined according to TS EN ISO 3377-1 Part 1: Single edge tear and TS EN ISO 3377-2 Part 2: Double edge

tear standard methods. All physical tests were performed by Shimadzu AG-IS Tensile Tester and Trapezium-2 software. Three horizontal and vertical samples were tested and the results were given as an average value.

Color Measurements

The color of the leathers was evaluated by Minolta Spherical spectrophotometer by the use of CIE*Lab system. 20 different measurements were performed for the each leather sample and the results were given as a mean value.

RESULTS AND DISCUSSIONS

Moisture Content of Timber Wastes

Average moisture contents of red and black pine sawdust were found to be 5.72% and 15.03%, while the mean moisture values of their barks were determined as 14.12% and 11.31%, respectively.

Extraction Yields and Tannin Contents of Timber Wastes

Extraction yield represents the percentage of obtained total solid matter at the end of extraction process and it is a crucial parameter as well as the tannin contents of the extracts. Because the low-yielded extract solution with high tannin content does not seem to be efficient in the use of tanning process. The extraction yields and tannin contents of the timber wastes are given in Table 2.

Table 2. The extraction yields and tannin contents of the timber wastes

		Extraction Yields (%)	Tannin Contents (%)
Red pine	Sawdust	1.91	50.21
	Bark	25.14	60.47
Black Pine	Sawdust	2.22	39.37
	Bark	1.94	7.82

The results of tannin analysis showed that the barks of red pine had higher extraction yield and tannin content as 25.14% and 60.47% respectively.

Although the tannin contents of red and black pine sawdust were relatively high, the extraction yields were found considerable low. These results indicate that the extraction process must be repeated for many times in the use of tanning operation in addition to high energy, source and time consumption. Therefore only the extract of red pine barks was found favorable for the tanning experiments.

Tanning Properties of the Leathers

The shrinkage temperatures and filling coefficients of the leathers are given in Table 3. Considering the results of filling coefficient, it was observed that the fullness properties of the leathers tanned with extract solution were appropriate. The shrinkage temperature of the leathers tanned with extract solution was found lower than the control leathers, although it is very common shrinkage temperature of the vegetable leathers (75-85°C).

Table 3. Filling coefficients and shrinkage temperatures of the leathers

	Filling Coefficients (%)	Shrinkage temperatures (°C)
Red pine bark extract	30.4	75.1
Valonea	26.9	83.3
Mimosa	58.5	85.0

Physical Strengths of Tanned Leathers

The physical strengths of leathers are given in Table 4. The percentage of elongation results were found similar, but the tensile strength of the leathers tanned with red pine bark extract was found appreciably higher than the control leathers. The single and double edge tear strength results showed that the leathers tanned with red pine bark extract and mimosa were gave similar characteristics in contrast to leathers tanned with valonea. The tensile and tear strength properties of the leathers were found adequate in accordance with UNIDO acceptable leather qualities.

Table 4. Physical test results of the leathers

	Tensile strength (N/mm^2)	Elongation (%)	Single edge tear strength/ thickness (N)/(mm)	Double edge tear strength/ thickness (N)/(mm)
Red pine bark	23.8	73.8	28.5/0.98	66.7/1.04
Valonea	18.0	72.7	22.1/0.82	46.8/0.87
Mimosa	14.8	73.4	29.9/1.65	60.8/1.65

Color Measurements of the Leathers

The color difference between the leathers was determined by calculating ΔE value (Equation 3).

$$\Delta E^2 = (\Delta L)^2 + (\Delta a)^2 + (\Delta b)^2 \tag{3}$$

The increase in ΔE indicates an increase in color difference. The L, a, b values are shown in Table 5.

Table 5. Color measurement values of the leathers

	L	a	b	dL	da	db	dE
Red pine bark	63.99	12.96	26.79	-34.92	13.07	27.14	46.22
Valonea	63.09	5.95	22.63	-35.81	6.06	22.97	43.07
Mimosa	60.00	10.87	17.64	-38.91	10.98	17.99	44.35

The ΔE results of the leathers revealed that there is a color difference due to the different characteristics of the vegetable tannins. A and b values (represent the red and yellow color respectively) of the leathers tanned with red pine bark extract are determined higher than the valonea and mimosa tanned leathers. Although red pine extract and valonea gave similar lightness value, mimosa tanned leathers lead to a slight decrease in lightness value.

CONCLUSION

In the present study, the utilization possibilities of the timber wastes of red and black pine in the form of sawdust and bark were aimed to investigate and following conclusions have been drawn;

    a. Only the extract of red pine bark had sufficient extraction yield and tannin content.

    b. The extract of red pine bark gave higher filling properties than valonea, but mimosa had the highest value.

    c. The similar and higher shrinkage temperature values were obtained from the leathers tanned with valonea and mimosa.

    d. The red pine bark extract provided higher physical characteristics to leathers.

    e. Consequently, it can be revealed that the extract of red pine barks can be used as a tanning agent in leather industry.

REFERENCES

Engür, M.O. and Kartal, S.N. (2001), "Orman Ürünleri Endüstrisinde Çevre Kirliligi ve Kontrolü", *İstanbul Üniversitesi Orman Fakültesi Dergisi*, 51(2), 43-52.

Kilicarislan Ozkan, C., Ozgunay, H. and Kalender, D. (2015), "Determination of Antioxidant Properties of Commonly Used Vegetable Tannins and Their Effects on Prevention of Cr(VI) Formation", *Journal of the Society of Leather Technologists and Chemists*, 99(5), 245-249.

Martin, A.M. (1998), "Bioconversion of Waste Materials to Industrial Products", in: Martin A.M. (ed), Springer Science +Business Media, LLC, 160, https://doi.org/10.1007/978-1-4615-5821-7.

Taylor, J. and Warnken, M. (2008), "Wood Recovery and Recycling: A Source Book for Australia", *Forest & Wood Products Australia*, 11.

Official Methods and Analysis (1996), SLC-113 Determination of Moisture, Society of Leather Technologists and Chemists.

Official Methods of Analysis (1996), SLC-114 Determination of Total Solids, Society of Leather Technologists and Chemists.

Official Methods of Analysis (1996), SLC-115 Determination of Total Solubles, Society of Leather Technologists and Chemists.

Official Methods of Analysis (1996), SLC-116 Determination of Non-Tannin Constituents, Society of Leather Technologists and Chemists.

Official Methods of Analysis (1996), SLC-117 Determination of Tannin Matter Absorbable By Hide Powder, Society of Leather Technologists and Chemists.

Official Methods and Analysis (2002), IUP 16, Measurement of Shrinkage Temperature up to 100°C.

TS EN ISO 2419 (2012), Leather - Physical and mechanical tests - Sample preparation and conditioning.

TS EN ISO 2589 (2016), Leather - Physical and mechanical tests - Determination of thickness.

TS EN ISO 3376 (2012), Leather - Physical and mechanical tests - Determination of tensile strength and percentage extension.

TS EN ISO 3377-1 (2012), Leather - Physical and mechanical tests - Determination of tear load - Part 1: Single edge tear.

TS EN ISO 3377-2 (2016), Leather - Physical and mechanical tests - Determination of tear load - Part 2: Double edge tear.

UNIDO (1996), Acceptable Quality Standards in the Leather and Footwear Industry. Vienna, Austria: United Nations Industrial Development Organization.

COMPOSITE STRUCTURES CONTAINING LEATHER FIBERS WITH APPLICATIONS IN CONSTRUCTIONS INDUSTRY

GABRIEL ZĂINESCU, VIORICA DESELNICU, ROXANA CONSTANTINESCU

INCDTP - Division: Leather and Footwear Research Institute, 93 Ion Minulescu st., 031215, Bucharest, Romania e-mail: icpi@icpi.ro

In tanneries, only approx. one-third of the total mass of raw hides and skins is converted to finished leather, while two-thirds become either dissolved or solid waste. Leather waste, especially leather fibers belonging to the category of natural materials, can play a fundamental role in obtaining materials for the construction. This paper presents the production of composite structures containing leather fibers obtained from leather waste (leather shavings). The new composite structures based on leather fibers (paving blocks) were analyzed for physical – mechanical characteristics and by SEM-EDAX. Physical – mechanical characteristics of paving blocks correspond standard SR EN 1338: 2004 – Paving blocks; SEM-EDAX analysis reveled a large number of portlandite plates, reducing the amount of silicon crystals and consequently decreasing the compressive strength and mechanical strength, but also increasing the tensile strength - a main characteristic of concrete paving blocks.
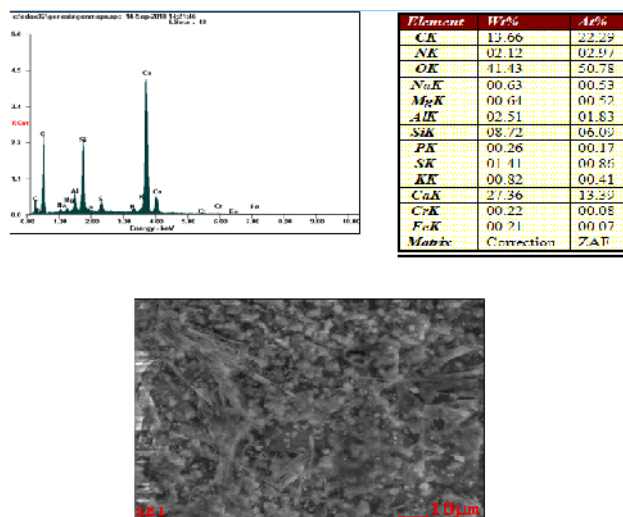
Keywords: leather shavings, composites, paving blocks

INTRODUCTION

In order to reduce waste, new technological solutions have recently been developed resulting in rubber materials and innovative building materials to reduce natural resources (Vlachovicova *et al*., 2007; Hansen *et al*., 2007; Trezza, M.A. *et al*., 2007).

Thus, the concept of "green" materials involved both natural fibers and a large amount of waste. Natural fibers are used to improve the mechanical performance of cement and rubber composites (Cao, 2007; Chiu *et al*., 2007) instead of synthetic ones (e.g. PVA or polypropylene) as it provides greater tensile strength and splitting resistance, higher elasticity and post-cracking behavior (Wu *et al*., 2006; Wu *et al*., 2007) and at the same time they are increasingly applied due to low price, health benefits and recyclability.

The main objective of this paper is to re-evaluate leather waste from the tanning industry by turning it into value-added raw materials and use it in the construction materials industry by developing new technologies.

The possibility of using tanned leather fibers in combination with Portland cement to obtain paving blocks for pedestrian use has been studied.

EXPERIMENTAL

Materials

Portland II / A-LL cement used has a specific surface area of 0.93 m^2/g and its specific weight is 3.11 kg/dm^3. The sand has a specific surface area of 0.68 m^2/g and its specific weight is 2.7 kg/dm^3.

The leather shavings used in this work are obtained from Pielorex-SA Jilava-Ilfov tannery (Figure 1).

Figure 1. Leather waste: a) Leather shavings; b) Finished Leather waste

Preparation of Leather Fibers

The leather waste were cut using a knife mill equipped with a metal sieve with meshes of 6-9 mm in diameter, resulting in pieces of waste with a surface area of max. 0.5-0.6 cm^2, transported to the storage room, where they are loaded into bags. The leather wastes before grinding were hand-picked with a permanent magnet. An amount of 420-1200 g of leather fibers was subjected to hydrolysis with a concentrated sulfuric acid solution with 1-2% based on the weight of the leather fibers at a temperature of 30-50^{0}C for 60 minutes, obtaining leather fibers treated with acid (FPA). Then a 0.4-0.9% organic polymer binder used in the field of synthetic foil and fiber is poured over FPA fibers. This polymer has the role of encapsulating the fibers of cover leather fibers in a polymeric "shirt".

Table 1 presents physical- chemical characteristics of leather fibers treated with acid.

Table 1. Physical-chemical characteristics of leather fibers treated with acid

Characteristics	UM	FPA	Standard Method
Dry substance	%	8,53	SR EN ISO 4684 : 2006
Ashes	%	18,29	SR EN ISO 4047 : 2002
Total nitrogen	%	12,66	SR ISO 5397 : 1996
Dermal substance	%	71,15	SR ISO 5397 : 1996
Chromium oxide	%	5,16	SR EN ISO 5398/1 :2008
pH	Unit.pH	1,78	STAS 8619/3 :1990
Calcium Oxide	%	0,23	

Values for ash, total nitrogen and dermal substance are reported as free from volatile matter

Production of Paving Blocks

Paving blocks for use in pedestrian paving have been obtained by blending 1% of treated leather fibers (FPA) with conventional Portland cement - commercially known as Structo Plus®.

Recipe Used for the Production of Paving Blocks

A) Wear layer (I)
- Washed sand, grain size 0-3 mm = 60Kg

- Cement II / A-LL reference 42.5 = 200Kg
- Master Glenium Sky 578 superplastifying additive, 150-200ml solution from BASF
- Additive 280 l / mc (cubic meter of prepared concrete)
- Master Aire 9060 from BASF was used to remove the air from the mortar
- Dye 4% related to the amount of cement, 2 kg of dye per 50 Kg cement bag
- Leather waste 1% related to cement = 2Kg

B) Resistance layer (II)
- Washed sand, grain size 0-3 mm = 70Kg
- gravel, grain size 4-8mm = 70Kg
- Master Glenium Sky 578 superplastifying additive, 150-200ml/42.5Kg cement bag
- Cement II / A-LL (freeze-thaw resistant) = 50Kg
- Dye 0.200Kg

The wear layer (A) is first prepared respecting the proportion in the composition depending on the concrete mixer size.

Firstly, water is added in the rotating mixer, where 1% of leather fibers are added relative to the amount of cement. Then it is stirred for about 8-10 minutes and then sand, dye, additive and cement are added and further stirred for 10-15 minutes. The mixture is poured in a bowl and layer II is prepared. For the second resistance layer the following are added to the concrete mixer in the following order: gravel, sand, dye, water with additive and cement. The mixture is stirred for 5-10 minutes and poured in another pot. The amount required for the second layer is about 6-9 times the quantity required for the first layer, for paving block thickness of 4.5-8 cm.

The paving blocks are spray coated with a release agent (best using a compressed air gun) and stacked face down. The paving block mould is placed on the vibrating table, the wear layer and then layer II are placed and vibration is continued. Layer II should be softer so as to vibrate for 10-18 seconds until "boiling", i.e. air is removed from the mortar.

The moulds are placed on Euro-pallets, covered with plastic foil and transported to the place of drying.

The paving blocks are removed from the moulds after 24 h or 48 h.

Physical - Mechanical Characterization of Paving Blocks

Physical - mechanical characterization of paving blocks was performed following standard SR EN 1338: 2004 – Paving blocks.

Microstructural Characterization of Paving Blocks

Microstructural characterization was performed by SEM-EDAX scanning electron microscopy. The samples were analyzed at the "Petru Poni" Molecular Institute in Iasi using a Zeiss DSM 940-A electronic scanning microscope, with a voltage of 25 kV and a distance of 15 mm.

RESULTS AND DISCUSSIONS

$10m^2$ of paving blocks containing 1% leather fibers (Figure 2) were made at the S.C. PAV-Consult SRL-Glina-Popesti Leordeni factory, and were analyzed according to the

standards in force for physical and mechanical characteristics (Table 2) and for microstructural characterization.

Figure 2. Paving blocks with leather fibers

Physical and Mechanical Characteristics

Table 2. Physical-mechanical characteristics of paving blocks with leather fibers

Characteristics	Test standard	Standard provisions	Results
Dimensions	SR EN 1338:2004	Deviations allowed ±2,5mm	Corresponds
Visual aspect	SR EN 1338:2004	No cracks, no fissures	Corresponds
Thickness of surface layer	SR EN 1338:2004	No textured surface	Corresponds
Tensile strength	SR EN 1338:2004	Min 3,6 MPa	4,1-47 MPa
Loading	SR EN 1338:2004	Min 250 N/mm	286-20,2 N/mm
Water absorption	SR EN 1338:2004	≤ 6%	5,7-5,9%

The product is certified with SR EN 1338: 2004 – Paving blocks. Tensile strength values correspond to the average of 5 values for each block and were obtained with a universal INSTrum 5500R tester, and a weight of 1.5 mm/min.

Microstructural Characterization

Images of the surface of Portland cement mortar with leather fibers show a structure with portlandite plates whose EDAX analysis shows the main components (silicon and calcium). A large number of portlandite plates can be seen in the image, reducing the amount of silicon crystals and consequently decreasing the compressive strength and mechanical strength, but also increasing the tensile strength - a main characteristic of concrete paving blocks (Figure 3).

Element	Wt%	At%
CK	13.66	22.29
NK	02.12	02.97
OK	41.43	50.78
NaK	00.63	00.53
MgK	00.64	00.52
AlK	02.51	01.83
SiK	08.72	06.09
PK	00.26	00.17
SK	01.41	00.86
KK	00.82	00.41
CaK	27.36	13.39
CrK	00.22	00.08
FeK	00.21	00.07
Matrix	Correction	ZAF

Figure 3. SEM-EDAX images of the surface of Portland cement mortars containing 1% leather fibers

CONCLUSIONS

In the paper were studied the possibilities of using leather fibers (leather shavings) in obtaining Portland cement paving blocks.

10m^2 of paving blocks were obtained using a recipe for paving block production, replacing cement with 1% leather fibers by weight.

Paving blocks were characterized physical-mechanically and the results were within the limits provided by the standards in force.

Paving blocks were also structurally characterized by SEM-EDAX electron scanning microscopy obtaining information on elemental composition and on the presence of portlandite plates.

This research can contributes to the management and reuse of leather fiber waste, focusing on the possibility of using leather fibers in the production of paving blocks.

REFERENCES

Hansen, K.R. *et al*. (2000), "Current and future uses of non-bituminous components of bituminous paving mixtures", *Transportation in the New Millennium*, TRB A2D02, Washington, USA.

Trezza, M.A. and Scian, A.N. (2007), "Waste with chrome in the Portland cement clinker production", *J Hazard Mater*, https://doi.org/10.1016/j.jhazmat.2006.12.082.

Vlachovicova, Z. *et al*. (2007), "Creep characteristics of asphalt modified by radial styrene–butadiene–styrene copolymer", *Constr Build Mater*, 21, 567–77, https://doi.org/10.1016/j.conbuildmat.2005.09.006.

Wu *et al*. (2006), "Effect of fiber types on relevant properties of porous asphalt", *Trans Nonferrous Met Soc China*, 16, 791–5, https://doi.org/10.1016/S1003-6326(06)60302-6.

Wu *et al*. (2007), "Investigation of rheological and fatigue properties of asphalt mixtures containing polyester fibers", *Constr Build Mater*, http://dx.doi.org/10.1016/j.conbuildmat.2007.07.018.

INDEX OF AUTHORS

LEATHER ENGINEERING DEPARTMENT EGE UNIVERSITY, TURKEY

EAST SIBERIA STATE UNIVERSITY OF TECHNOLOGY & MANAGEMENT, ULAN-UDE, RUSSIA

MUSTAFA KEMAL UNIVERSITY, TURKEY

CHINA LEATHER & FOOTWEAR RESEARCH INSTITUTE Co. Ltd., CHINA

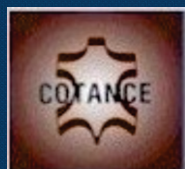**"POLITEHNICA" UNIVERSITY BUCHAREST, ROMANIA**

"GH. ASACHI" TECHNICAL UNIVERSITY OF IASI, ROMANIA

BUCHAREST ACADEMY OF ECONOMIC STUDIES, ROMANIA

ITA TEXCONF ROMANIAN ENTITY WITHIN INNOVATION & LEATHER TECHNOLOGICAL TRANSFER

CONFEDERATION OF NATIONAL ASSOCIATIONS OF TANNERS AND DRESSERS OF THE EUROPEAN COMMUNITY

ROMANIAN LEATHER & FUR PRODUCERS ASSOCIATION

SFERA FACTOR THE ROMANIAN LEATHER MANUFACTURERS ORGANIZATION